CELLULAR DELIVERY OF HAMMERHEAD RIBOZYMES

ANDREW JOHN HUDSON

Doctor of Philosophy

ASTON UNIVERSITY

September 1997

ASTON UNIVERSITY

CELLULAR DELIVERY OF HAMMERHEAD RIBOZYMES

ANDREW JOHN HUDSON

Doctor of Philosophy

1997

SUMMARY

Hammerhead ribozymes are potent RNA molecules which have the potential to specifically inhibit gene expression by catalysing the *trans*-cleavage of mRNAs. However, they are unstable in biological fluids and cellular delivery poses a problem. Site-specific chemical modification of hammerhead ribozymes was evaluated as a means of enhancing biological stability. Chimeric, 2'-O-methylated ribozymes, containing only five unmodified ribonucleotides, were catalytically active *in vitro* (k_{cat} = 1.46 min^{-1}) and were significantly more stable in serum and lysosomal enzymes than unmodified (all-RNA) counterparts. Furthermore, they remained undegraded in cell-containing media for up to 8 hours. Stability enhancement allowed cellular uptake properties of radiolabelled ribozymes to be assessed following exogenous delivery. Studies in vulval and glial cell lines indicated that chimeric ribozymes became cell-associated via an inefficient process, which was energy and concentration dependant. A considerable proportion of ribozymes remained bound to cell-surface components, however, a small proportion (<1%) were internalised via mechanisms of adsorptive and / or receptor mediated endocytosis. Fluorescent microscopy indicated that ribozymes were localised within endosomal / lysosomal vesicles following cell entry. This was confirmed by immuno-electron microscopy, which allowed the detection of biotin-labelled ribozymes within the cell ultrastructure. Despite the predominant localisation within endocytic vesicles, a small proportion of internalised ribozymes appeared able to exit these compartments and penetrate target sites within the nucleus and cytoplasm.

The ribozymes designed in this report were directed against the epidermal growth factor receptor mRNA, which is over-expressed in a malignant brain disease called glioblastoma multiforme. In order to examine the fate of ribozymes in the brain, the distribution of FITC-labelled ribozymes was examined following intra-cerebro ventricular injection to mice. FITC-ribozymes demonstrated a highly punctate pattern of distribution within the striatum and cortex, which appeared to represent localisation within cell bodies and dendritic processes. This suggested that delivery to glial cells *in vivo* may be possible. Finally, strategies were investigated to enhance the cellular delivery of ribozymes. Conjugation of ribozymes to anti-transferrin receptor antibodies improved cellular uptake 3-fold as a result of a specific interaction with transferrin receptors. Complexation with cationic liposomes also significantly improved cell association, however, some toxicity was observed and this could be a limitation to their use. Overall, it would appear that hammerhead ribozymes can be chemically stabilised to allow direct exogenous administration *in vivo*. However, additional delivery strategies are probably required to improve cellular uptake, and thus, allow ribozymes to achieve their full potential as pharmaceutical agents.

KEYWORDS: Catalytic RNA, hammerhead, stability, uptake, cellular delivery.

ACKNOWLEDGEMENTS

The work in this thesis was jointly funded by a case award from the Biotechnology & Biological Sciences Research Council (BBSRC) and Cruachem Ltd. Consumables were partly funded by Aston University and The Cancer Research Campaign (CRC).

I gratefully acknowledge my supervisors at Aston; Saghir Akhtar and Bill Irwin, for their guidance and encouragement during my studies. I would also like to thank my external supervisors at Cruachem Ltd; Dr. John Ackroyd and Dr. Vaman Rao, for their technical advice and financial support.

The following people are kindly acknowledged for their advice and assistance with experimental techniques used during this thesis: Leslie Tompkins and Dr. Paul Monaghan (immuno-electron microscopy), Dr. Sheila Handley (animal studies), Dr. Glynn Woodward and Dr. Ken Price (cryo-sectioning), Dr. Ruth Duncan (preparation of tritosome extract), Kenny McFarlane (RNA synthesis and HPLC), Dr. Nadia Normand (conjugate synthesis) and last but by no means least, Chris Bache for performing minor miracles whenever laboratory equipment required repair.

I would like to thank Ram Patel, Patricia Fell and Ian Baxter for all their help and good humour over the past 3 years.

Finally, I would like to thank my parents for all the support they have given me throughout my six years of undergraduate and postgraduate study at Aston University.

LIST OF CONTENTS

LIST OF FIGURES

LIST OF TABLES

LIST OF ABBREVIATIONS

2-O-Me	2'-O-methylated
A, G, C, T, U	adenine, guanine, cytidine, thymidine, uridine
Ab	antibody
AE	adsorptive endocytosis
AIDS	acquired immune deficiency syndrome
ATP	adenosine tri-phosphate
AP	alkaline phosphatase
°C	degrees Celcius
cm, mm, μm, nm	centimetre, millimetre, micrometre, nanometre
BSA	bovine serum albumin
CO_2	carbon dioxide
CPG	controlled pore glass
cpm	counts per minute
CSF	cerebro-spinal fluid
DABCO	diazobicyclo [2,2,2] octane
DCA	dichloroacetic acid
ddCTP	di-deoxy cytosine tri-phosphate
DEPC	diethyl pyrocarbon
DMEM	Dulbecco's Modified Eagle's medium
DMSO	dimethyl sulphoxide
DMT(r)	dimethoxytrityl-
DNA	deoxyribonucleic acid
DOPE	dioleoyl phosphatidylethanolamine
DOSPA	N-[2-({2,5-bis[(3-aminopropyl)amino]-1-oxypentyl}amino)ethyl]-N,N-dimethyl-2,3-bis(9-octadecenyloxy)-1-propanaminium triflouroacetate
DOTAP	N-(1-(2,3-dioleoyloxy)propyl)-N,N,N-trimethylammoniummethylsulphate
DOTMA	N-[1-(2,3-dioleyloxy)propyl]-N,N,N-trimethylammonium chloride
DTT	dithiothreitol
ECACC	European collection of animal cell cultures
EDTA	ethylenediamine tetra-acetic acid
EGFr	epidermal growth factor receptor

EGS	external guide sequence
Er	endoplasmic reticulum
FBS	foetal bovine serum
FCS	foetal calf serum
FITC	flourescein isothiocyanate
FPE	fluid-phase endocytosis
Fpmp	1-(2-fluorophenyl)-4-methoxypiperidin-4-yl
ΔG	energy of formation of lowest energy structure
GBM	glioblastoma multiforme
HBSS	Hanks' balanced salt solution
HDV	hepatitis delta virus
HEPES	(N-2-hydroxymethylpiperazine)-N'-2-ethanesulfonic acid
HIV	human immunodeficiency virus
HPLC	high-performance liquid chromatography
ICV	intra-cerebroventricular
i.p.	intra-peritoneal
kcal / mol	kilocalories per mole
kDa	kilo Daltons
Mag	Objective Lens Magnification
MES	(2-[N-morpholine]-ethanesulfonic acid
mL, μL	millilitres, microlitres
μCi	micro Curies
mol. wt.	molecular weight
MP	methylphosphonate
Mt	mitochondria
Mvb	multi-vesicular bodies
Nu	nucleotide (or cell nucleus where applicable)
OD	optical density
ODN	oligodeoxynucleotide
ON	oligonucleotide
ORN	oligoribonucleotide
PAGE	polyacrylamide gel electrophoresis
PBS	phosphate buffered saline
PCR	polymerase chain reaction
PLA	poly-(L-lactic acid)
PLT	progressive lowering of temperature
pm	plasma membrane (cell membrane)
PO	phosphodiester

PS	phosphorothioate
®	registered trade mark
RITC	rhodamine isothiocyanate
RME	receptor-mediated endocytosis
RNA	ribonucleic acid
RNase H	ribonuclease H
RNase P	ribonuclease P
rRNA	ribosomal RNA
rpm	revolutions per minute
sd / SD	standard deviation
SDS	sodium dodecyl sulphate
$t_{\frac{1}{2}}$	half life
TBDMS	2'-O-t-butyldimethylsilyl
TBE	tris-borate EDTA buffer
TCA	trichloroacetic acid
TEMED	N,N,N',N'-trimethylethylenediamine
TETD	triethylthiuram disulphide
TFO	triplex-forming oligonucleotide
TRA	anti-transferrin receptor antibody
UTR	un-translated region
UV	ultraviolet light
v/v	volume per volume
w/v	weight per volume
w/w	weight per weight

CHAPTER ONE

INTRODUCTION

1.1. THE REQUIREMENT FOR DRUG THERAPIES WHICH CAN MODULATE GENE EXPRESSION.

The function of living cells is essentially governed by the sum of the activities of protein molecules within them. Protein molecules within cells are present in a wide variety of different forms, such as enzymes, hormones or receptors. All proteins are synthesised from unique mRNA sequences, which carry a specific 'blueprint' for the protein from the chromosomal DNA to the sites of protein synthesis (for a detailed description of the protein translation process see Alberts *et al*, 1989). If a cell produces too much or too little of a specific protein, the activity of the cell will be different from that of cells with the normal amount of the protein. Variations in the expression of particular proteins between cells are often the basis of disease (Bradley *et al*, 1992). Another possible cause of disease is damage (or mutation) to the genetic 'blueprint' (the chromosomal DNA) which encodes a particular protein. This can result in the production of defective proteins which, in turn, can disrupt normal cell function.

There are two crucial considerations in designing a drug to treat a disease state. The first is the identification of an appropriate target in the disease process. The second is finding an appropriate molecule that has specific recognition and affinity for the target and can thereby interfere with the disease process (Agrawal, 1996a). Most of the targets employed by traditional drugs are protein molecules such as enzymes or hormones. The traditional method of drug discovery in the pharmaceutical industry has been to identify a protein target and then screen thousands of potential drug candidates that might inhibit or stimulate that protein (Bradley *et al*, 1992). Consequently, many of the drugs discovered to date recognise their protein targets by mechanisms which are not well defined and the knowledge gained via their discovery cannot be generalised for rational drug design (Agrawal, 1996a). Furthermore, many drugs are relatively small (low molecular weight) molecules which often lack specificity. This lack of specificity may arise because there is not sufficient information in the relatively simple structure of a small drug molecule to define the three-dimensional space surrounding the active site of a target protein (Bradley *et al*, 1992). Hence, many drugs tend to bind to sites in other proteins which can result in

unwanted side effects and toxicity (i.e. the drug interacts with proteins which are not the intended target). The conventional drug therapies for conditions such as neoplastic and viral diseases are particularly fraught with systemic toxicity (Rojanasakul, 1996). As a result of the lack of selectivity demonstrated by many conventional drugs, a great deal of attention has been focused on the design of new agents which can modulate gene expression, rather than interact with the protein molecules which the genes encode.

The concept of 'gene therapy' has been widely investigated in recent years (for a comprehensive review see Sokol and Gewirtz, 1996). The gene therapy approach involves the permanent insertion or replacement of a complete functional gene within a cell. Once inserted, the 'new' gene is endogenously expressed within the 'host' cell leading to the synthesis of specific proteins. Gene therapy utilises a vector system to introduce the 'new' gene into the cell, along with a 'promoter' gene which influences its expression once it has been incorporated into the host genome (Bunnell and Morgan, 1996). Viral vectors, such as modified retroviruses are the most widely used agents for inserting genes into cells (Sokol and Gewirtz, 1996). However the use of viral vectors is often limited by the random integration of delivered genes into the host cell genome (this is discussed further in Section 1.4.1). This represents a potentially dangerous intervention into the genetic structure of the recipient cell (Marschall *et al*, 1994).

The overall goal of gene therapy can vary, but has included the correction of inherited genetic defects, such as cystic fibrosis (Zabner *et al*, 1994). In addition new traits have been engineered into cells, such as diminished chemo-sensitivity in the case of bone marrow cells (Mickisch and Shroeder, 1994). Since gene therapy involves the permanent modification of the cell genome, both its intended effects and any undesirable effects would theoretically last for the entire lifetime of a 'host' cell (i.e. any toxicity could be potentially irreversible). Consequently, alternative strategies involving the exogenous delivery of novel agents, which can temporarily modulate gene expression, may have advantages (Kregnow *et al*, 1995). The effects of such agents, likes those of many conventional drugs, could possibly be reversed by simply withdrawing their administration. On the other hand, the requirement for the repeated administration of such agents could be a potential drawback. One strategy, based on this approach, which has been widely investigated over the past decade is the use of antisense oligonucleotides.

1.1.1. Modulation of Gene Expression with Antisense Oligonucleotides.

For some years, relatively short sequences of synthetic, single-stranded DNA called oligodeoxynucleotides (ODNs) have been reported to inhibit gene expression in living cells (Belikova *et al*, 1967, Miller *et al*, 1977). Nevertheless, it was not until the pioneering work of Zamecnik and Stephenson (1978) that it became widely accepted that synthetic ODNs were able to cross the external membrane of eukaryotic cells and exert a specific, inhibitory effect on gene expression. Since this discovery, a large number of studies have demonstrated that ODNs, and a variety of chemically related oligonucleotide (ON) analogues, can specifically inhibit gene expression both *in vitro* and *in vivo* (for comprehensive reviews see Erickson and Izant, 1992, Stein and Cheng, 1993, Wagner, 1994, Akhtar, 1995, Agrawal, 1996b).

The inhibition of gene expression exhibited by certain ONs has been termed an 'antisense' effect because these molecules owe their specificity of action to the fact that they are complementary (antisense) to specific nucleotide sequences within regions of 'target' mRNAs (Akhtar and Juliano, 1991). Antisense ONs anneal to their complementary sequences via Watson-Crick base pairing to form (anti-parallel) antisense / mRNA duplexes (Gibson, 1994). Since the specificity of antisense ONs is governed primarily by the sequence of the target mRNA, the principles learned from working with one genetic target can theoretically be applied to an indefinite number of genetic targets (Agrawal, 1996a). Therefore the antisense strategy allows a more rational approach to drug design than the traditional 'blanket screening' of drug candidates against (often poorly defined) protein targets.

The precise mechanism of 'antisense action' remains a matter of debate although it is known to be dependant upon the type of ON analogue used. (The structure of ONs and chemical modifications are discussed in more detail within later sections of this report (see Section 1.2.4 and Figure 1.7) and have been reviewed in detail by Milligan *et al* (1993), Scanlon *et al*, (1995) and Wickstrom (1992 & 1995)). Antisense ON analogues can be placed into two broad groups with regard to their mechanism of action: One group, which includes unmodified phosphodiester (PO) ODNs and those containing phosphorothioate (PS) inter-nucleotide bonds, are thought to inhibit mRNA translation by facilitating the destruction of antisense / mRNA duplexes by ribonuclease H (Tidd, 1996, Akhtar and Agrawal, 1997). Ribonuclease H (RNase H) is a ubiquitous intracellular enzyme which cleaves the RNA portion of RNA / DNA duplex hybrids (Helene and Toulme, 1990). The second group of analogues, which includes ODNs containing methylphosphonate inter-nucleotide linkages (MP-ODNs) and oligoribonucleotides (ORNs), form antisense / mRNA duplexes which are more

RNase H resistant (Kole *et al*, 1991). Nevertheless they are still able to down-regulate protein translation (Wickstrom *et al*, 1992, Krystal, 1992). Hence, physical blocking of mRNA translation at the ribosomes offers a likely explanation for the mechanism by which this second group of ONs exert their effects (Akhtar, 1991, Krystal, 1992, Rossi, 1995).

The ability of all ONs to exert their biological effects in cells is governed by their ability to interact with genes located within the nucleus or cytoplasm (Gibson, 1994). Therefore, ONs must remain stable in biological environments, be imported into the appropriate cells and localised to specific intracellular sites in order to exert their activity (Kregnow *et al*, 1995, Rojanasakul, 1996). Furthermore, once antisense ONs have been delivered to intra-cellular regions containing their mRNA targets, the target (sense) sequence itself must be accessible to binding (hybridisation). The accessibility of target sequences in cells is a function of mRNA physical structure, which is dictated, in turn, by the internal base composition of the mRNA and any associated protein molecules (Gewirtz *et al*, 1996).

Since unmodified ODNs and ORNs are unstable towards nucleases which are present in biological fluids (Wickstrom ,1986, Akhtar *et al*, 1991b), chemical modified analogues have been designed with improved biological stability (for reviews see Milligan *et al*, 1993, Wickstrom 1992 & 1995, Rojanasakul, 1996). Chemical modification of ONs is discussed later in this chapter (see Section 1.2.4).

The mechanism(s) of cellular entry and sub-cellular distribution of antisense ONs has also been investigated and this aspect is discussed in detail throughout this thesis (see Sections 1.4.2, Section 4.1, Section 5.1 and Figure 1.10) and has been reviewed elsewhere (Akhtar and Juliano, 1992, Rojanasakul, 1996). Briefly, the exact mechanism of ON uptake remains a matter of debate, although it is widely considered that ONs enter cells via active, endocytic processes (see Section 1.4.2 and Figure 1.10) which are extremely inefficient (Wickstrom et al, 1988, Wu-Pong et al, 1992). This results in the initial localisation of ONs in endosomal / lysosomal vesicles (Tonkinson and Stein, 1994, Tarrason *et al*, 1995, Beltinger *et al*, 1995), from which their exit is necessary for biological activity (Akhtar *et al*, 1995).

Since the uptake of ONs following exogenous delivery is highly inefficient and leads to inappropriate sub-cellular localisation, a means of delivery enhancement is thought to be required if antisense ONs are to realise their full potential as therapeutic agents (Akhtar *et al*, 1992). Despite the difficulties involved delivering antisense ONs (see Section 1.2.4), several recent reports suggest that they can be effective at inhibiting

the expression of undesirable genes both *in vitro* and *in vivo* (for recent review see Akhtar and Agrawal, 1997). Indeed, a number of different antisense ODNs are currently under investigation in human clinical trials (Agrawal, 1996).

Variations on the antisense ON strategy have also been attempted, which can target alternative points in the expression of a chromosomal gene into a protein (Akhtar and Juliano, 1991). For example, antisense ONs have been targeted to pre-mRNAs and this has been shown to specifically down-regulate gene expression *ex vivo* (for review see Kole *et al*, 1991). Pre-mRNAs are the products of chromosomal DNA transcription, which undergo splicing to yield mature mRNAs (Alberts *et al*, 1989).

Alternatively, ODNs have been targeted to the chromosomal DNA itself, since it has been demonstrated that homopurine / homopyrimidine ODNs can form a local triple helix ('triplex') with purine rich strands within double-stranded DNAs (for review see Sun and Helene, 1993). Triplex forming ODNs (TFOs) bind to chromosomal DNA via the formation of Hoogsteen hydrogen bonds rather than via Watson-Crick base pairing. The formation of the ODN / DNA triplex can prevent the transcription of specific genes into mRNAs (or more specifically pre-mRNAs) by blocking the binding of transcription factors or restriction enzymes (Okada *et al*, 1994, Scanlon *et al*, 1995, Porumb *et al*, 1996). The advantage of utilising TFOs is that they act at the transcriptional level, which is the first step in the intermediary metabolism of RNA, and therefore only a few molecules of TFO may be required to exert a gene inhibitory effect (Scanlon *et al*, 1995). However, there are considerable limitations to the use of TFOs since potential targets are limited to regions which are homopurine in one strand of the chromosomal DNA target. Furthermore there are concerns regarding the affinity of TFOs for their targets since non-specific effects have been reported *in vitro* (Ebbinghaus *et al*, 1993).

The main focus of attention during this thesis concerns a more recent innovation which can be classified as a variation to the antisense ON approach. This involves this use of ORN-based molecules which have catalytic properties and have been termed 'ribozymes'. The word ribozyme is derived from "ribonucleic acid" and "enzyme" and was used to describe small, naturally occurring RNA molecules capable of demonstrating catalytic activity, in the absence of proteins. Prior to the discovery of naturally occurring ribozymes (see Section 1.2.1), protein enzymes were considered to be the only macromolecules capable of performing catalytic processing within cells (Cech, 1993).

In nature most ribozymes are involved in intra-molecular (*cis*) reactions which cleave a specific region of their own RNA sequence (see Section 1.2.1). However, most ribozymes can be engineered such that they can act in *trans*. The term *'trans*-acting' describes a ribozyme molecule capable of intermolecular cleavage, at a specific site within an entirely separate RNA molecule, rather than at a site within a region of its own RNA sequence (Zaug *et al*, 1986). This allows a *trans*-acting ribozymes to theoretically be targeted to cleave mRNA sequences.

A *trans*-acting ribozyme can be considered to be an ORN sequence which combines an antisense component, in the form of 'base-pairing regions' which are complementary to a target RNA, and a catalytic component which is involved in the catalytic cleavage of the target. *Trans*-acting ribozymes share several characteristics with antisense ONs: Firstly, their specificity is governed primarily by the sequence of their target RNA (or mRNA), which they anneal to via Watson-Crick base-pairing. In addition they are polar, high molecular weight molecules which probably share similar obstacles to their effective use as therapeutic agents (Rossi, 1995). This includes the requirement for delivery to specific sites within cells and the accessibility of sites within target mRNA molecules (Akhtar *et al*, 1995).

However because of their catalytic power, *trans*-acting ribozymes are expected to be more efficient inhibitors of gene expression than antisense ONs (Woolf, 1995). The ribozyme and antisense ON strategies are further compared and contrasted in Section 1.3, but first the concept of ribozymes is introduced in more detail.

Compared to antisense ON technology, the therapeutic application of ribozymes remains in its infancy. The most widely studied ribozyme with regard to therapeutic applications is probably the hammerhead ribozyme. Nevertheless its chemical stabilisation has proved problematic and very little is known with regard to its cellular uptake and sub-cellular localisation following exogenous delivery (Bratty et al, 1993, Elkins and Rossi, 1995). Hence during this thesis, these properties and methods to enhance hammerhead ribozyme delivery have been investigated. The ultimate goal of this research group is to design therapies which are able to modulate the expression of specific genes involved in the progression of a malignant form of brain cancer called glioblastoma multiforme. Therefore, hammerhead ribozymes which can potentially cleave mRNA targets involved in the progression of this disease have been studied during this thesis.

1.2 THE HAMMERHEAD RIBOZYME.

1.2.1. A Historical Overview.

In the early 1980's, the Nobel Prize winning discovery of ribozymes, by research groups led by Tom Cech (Cech *et al*, 1981) and Sydney Altman (Guerrier-Takada *et al*, 1983), fundamentally changed accepted opinions with regard to the function of RNA within living cells.

Originally, two different naturally occurring ribozymes were discovered almost in parallel: Intra-molecular catalytic activity was identified within the Group I intron of *Tetrahymena thermophila* RNA (Cech *et al*, 1981 and for review see Cech and Bass, 1986). A short time later, Altman's group (Guerrier-Takada *et al*, 1983) discovered that an RNA subunit of the enzyme Ribonuclease P was capable of inter-molecular catalytic cleavage in *Escherichia coli* (Guerrier-Takada *et al*, 1983). Subsequently five more naturally occurring examples of ribozymes have been identified (See Section 1.2.2 for a further details and for general reviews see Symons, 1992, Symons, 1994, Usman and McSwiggen, 1995). These have generally been named according to their supposed secondary structure. Amongst these is the 'hammerhead' ribozyme which was first detected as a structural motif within certain types of plant pathogen; called satellite viruses, viroids and virusoids (Prody *et al*, 1986, Buzayan *et al*, 1986, Hutchins *et al*, 1986, Forster and Symons, 1987). All of the ribozyme motifs which have been discovered to date, have in common the ability to splice or cleave RNA molecules in a highly sequence-specific manner. This sequence specificity is a result of the base-pairing of ribozymes with nucleotides adjacent to the actual cleavage site (Symons, 1992). Another feature common to all ribozymes is that their catalytic activity is dependant upon the presence of divalent metal ions, such as magnesium or manganese (see Section 1.3). Thus ribozymes are considered to be analogous to protein metalloenzymes (Bratty *et al*, 1993).

In nature most ribozymes, with the exception of Ribonuclease P (Kiehntopf *et al*, 1995), are involved in intra-molecular (*cis*) reactions (see Section 1.1.1): For example the hammerhead ribozyme motif was discovered due to its role in the replication of the linear plus-strand of the tobacco ringspot virus satellite RNA (Prody *et al*, 1986). This satellite RNA consists of a 359 nucleotide monomer which is produced by the cleavage of a much larger RNA polymer (Prody *et al*, 1986). Generation of the monomeric products involves a highly specific cleavage reaction via a 'rolling circle' mechanism (Foster and Symons, 1987). Similar cleavage mechanisms, catalysed by

hammerhead structures, have since been shown to be involved in the replication of a variety of other plant pathogens (for review see Symons, 1992).

Following the discovery of the naturally occurring *cis*-acting ribozymes, attempts were made to produce *trans*-acting ribozyme motifs based on their structures (Cech, 1992). Since in theory, these could be designed to cleave any target RNA 'substrate' molecule, such as a mRNA, in a sequence-specific manner. *Trans*-acting motifs also have the potential to exhibit multiple-turnover, (i.e. repeatedly cleaving substrate molecules) in the manner of a classical protein enzyme (Haseloff and Gerlach, 1988, Sarver *et al*, 1990, Sullenger and Cech, 1993). With regard to the hammerhead ribozyme, the development of a *trans*-acting motif was considered to be a particularly interesting prospect because the hammerhead, at around 30-35 nucleotide bases, is the smallest ribozyme structure (Symons, 1992). Therefore its size makes the molecule more amenable to mechanistic investigation and allows preparation via automated, solid-phase chemical synthesis (Reese *et al*, 1991, Wincott *et al*, 1995, Wahl *et al*, 1996).

Figure 1.1. The Consensus Sequence of the Hammerhead as Proposed by Forster and Symons (1987). [The arrow indicates the site of catalytic cleavage, the large Roman numerals label the helices. In all naturally occurring examples two of the helical stems are closed by loops. Invariant nucleotides found in natural hammerheads are identified, all others are identified by 'N'].

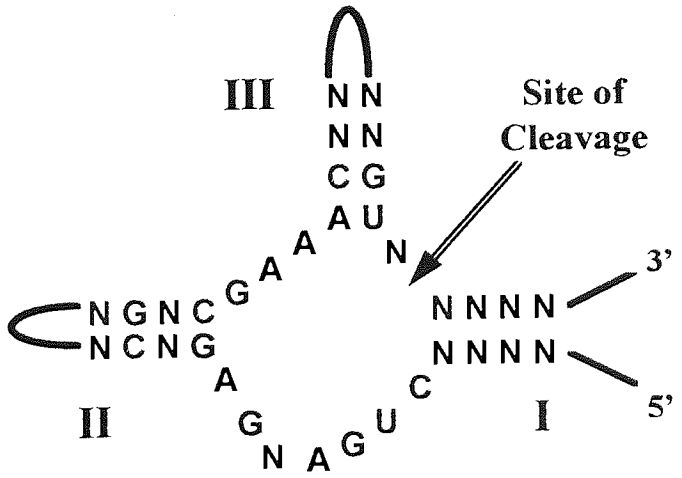

The potential for preparing a *trans*-acting hammerhead motif was first proposed when it was noticed that regions surrounding the cleavage sites within the RNA of a variety of viroids and virusoids could be folded into a strikingly similar structure (Hutchins *et al*, 1986, Forster and Symons, 1987). In its two-dimensional representation the appearance of the consensus domain actually gave rise to the term 'hammerhead'

because the molecule appeared to consist of three Watson-Crick base-paired helices, radiating from a central catalytic core (See Figure 1.1). However the actual three-dimensional structure of this molecule (prior to catalytic cleavage), as predicted by recent X-ray analyses (Pley et al, 1994, Scott et al, 1995 & 1996), is not so much a 'hammerhead' as a 'wishbone' structure (see Section 1.2.3.3).

Uhlenbeck (1987) was the first to synthesise a *trans*-acting form of the hammerhead when he separately synthesised the top and bottom halves of a ribozyme based upon the consensus RNA sequence shown in Figure 1.1. The lower half of the structure was able to cleave multiple copies of the top half in the presence of magnesium ions at 55°C *in vitro*. The kinetic parameter K_{cat} (see Section 1.3) calculated for this reaction was 0.5 min^{-1}, which was several orders of magnitude lower than those observed with most protein enzymes (Symons, 1992).

The *trans*-acting hammerhead motif was further refined by Haseloff and Gerlach (1988) when they designed a molecule based upon the self-cleaving domain of the tobacco ringspot virus satellite RNA. Their basic concept was to construct a ribozyme which could cleave any 'substrate' RNA provided that it contained only a GUC triplet of nucleotides within its sequence (see Figure 1.2).

Figure 1.2. The *Trans*-Acting Hammerhead Structure of Haseloff and Gerlach (1988). The numbering System of Hertel *et al* (1992) has been used to label specific nucleotides. [The 13 conserved nucleotides are boxed. The cleavage site is indicated by an arrow. N represents any base nucleotide].

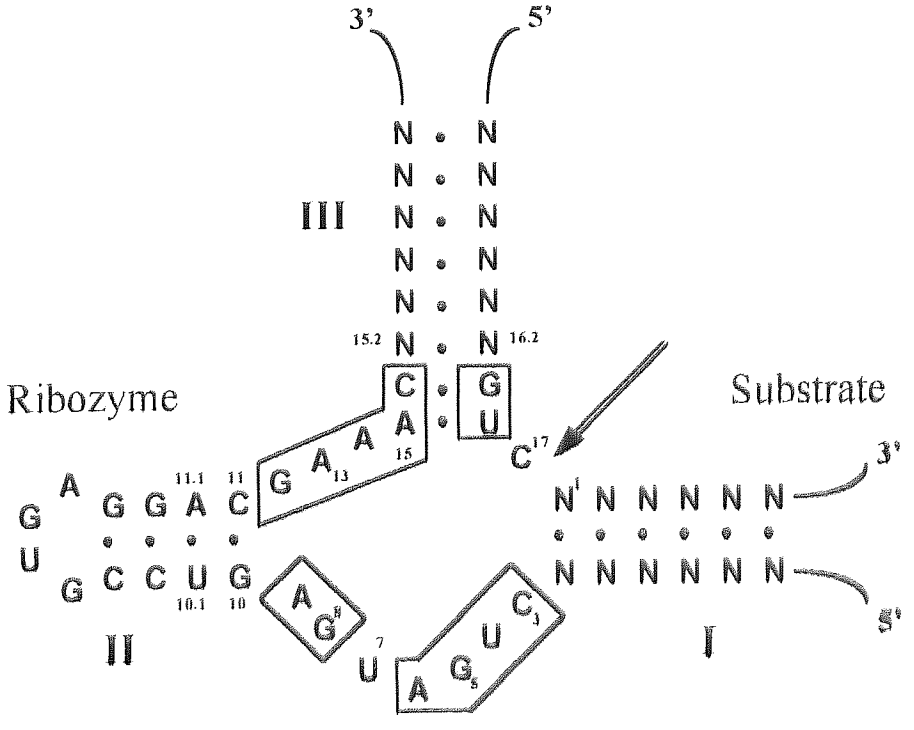

The consensus nucleotides observed by Forster and Symons (1987) were maintained in this motif. The composition of the remaining nucleotides within the ribozyme was determined by the requirements for Watson-Crick base pairing to complete stems I and III (see Figure 1.2). The catalytic ability of the *trans*-acting hammerhead was demonstrated *in vitro*, via the cleavage of an 835 nucleotide transcript (present at molar excess) from a cloned bacterial chloramphenicol acetyl transferase gene. Kinetic parameters such as K_{cat} (see Section 1.3) were not determined in this study. However the authors concluded that each ribozyme was capable of cleaving more than 10 substrate molecules within 75 minutes *in vitro*. This was the first demonstration that a *trans*-acting hammerhead motif could indeed cleave a target RNA molecule, entirely unrelated to its natural substrate. This finding fuelled a great deal of interest with regard to the potential applications of hammerhead ribozymes for therapeutic uses. The *trans*-acting motif, first described by Haseloff and Gerlach (1988) has since been widely adopted by investigators and a standard numbering system has been adopted for the nucleotide bases within this structure (Hertel *et al*, 1992, see Figure 1.2).

1.2.2. Other Ribozyme Motifs.

Since the experimental studies outlined later in this report are focused on the hammerhead ribozyme, this chapter is mainly centered upon this motif and only a brief overview of the other known ribozyme motifs is included here (for further reviews see Symons, 1992, Symons, 1994, Usman and McSwiggen, 1995). New ribozyme motifs may be isolated in future because at least three other RNA-protein complexes are currently suspected of harbouring ribozymes: Noller *et al* (1992) suggested the involvement of a catalytic RNA component within the 23S ribosomal RNA subunit of the thermophillic eubacterium *Thermus aquaticus*. Sharp (1991) suggested that the amino acid transferase activity of ribosomal RNAs and the splicing of pre-mRNA by small nuclear RNAs could also involve catalytic RNA components. Furthermore, a technique called '*in vitro* selection' has be used to identify new catalytic motifs which may not be present in nature (Santoro and Joyce, 1997). This technique has allowed 'DNA enzymes', composed entirely of ODNs, to be isolated. The sequences of these DNA enzymes differ from those of the known ribozyme motifs but they are, nevertheless, able to cleave RNA substrates in *trans* (see Santoro and Joyce, 1997).

The ribozymes discovered to date have all been modified in some way to allow investigators to study their mechanism of action (Symons, 1994). However the smaller motifs, which include the hammerhead, hairpin and hepatitis delta ribozyme, are considered to offer the greatest potential with regard to therapeutic applications.

This is because their size permits direct automated synthesis and allows chemical modifications to be made which can enhance nuclease stability. Their size also makes exogenous cellular delivery more convenient, whereas the larger ribozymes would currently require vector-mediated delivery to cells (Usman and McSwiggen, 1996).

1.2.2.1. Group I & Group II Intron Ribozymes.

The first ribozyme to be described was the 413 nucleotide, Group I intervening sequence in the nuclear ribosomal RNA (rRNA) precursor of the protozoa; *Tetrahymena thermophila* (Cech *et al*, 1981). The natural role of the Group I intron ribozyme is to excise the intervening sequence of the rRNA precursor, in a two step transesterification reaction which requires the presence of divalent metal ions and a guanosine co-factor (Cech and Bass, 1986). Since its discovery, a lengthy series of conserved nucleotides involved in the Group I intron reaction have been identified in *Tetrahymena* and in other species (Burke *et al*, 1987). A small group of mitochondrial pre-mRNA intervening sequences, distinctly different to the Group I introns, were subsequently identified in certain yeast species. These intervening sequences, termed Group II introns, have also been shown to contain large conserved sequences which are capable of self-splicing (Cech and Bass, 1986). Again, a two step transesterification reaction is catalysed which requires a divalent metal ion. However there is no requirement for guanosine in the Group II intron splicing reaction (Cech and Bass, 1986).

Mechanistic studies have demonstrated that the reactions catalysed by Group I and Group II introns yield cleaved products with 2', 3'-hydroxyl groups and a 5'-phosphate at their termini (Symons, 1994). Such products are similar to those produced by the reaction of Ribonuclease P (see Section 1.2.2.2) but are distinctly different to the products of the hammerhead ribozyme reaction (see Section 1.2.3). Although a large number of mechanistic studies have been performed with the Tetrahymena Group I and Group II ribozymes, their large size (generally >300 nucleotide bases) has limited their use in therapeutic applications. However these larger motifs may prove useful in the search for more efficient ribozyme therapies via the developing technique of *in vitro* selection (Usman and McSwiggen, 1996).

1.2.2.2. The Catalytic RNA Component of Ribonuclease P.

Ribonuclease P (RNase P) is a two component endoribonuclease which generates the mature 5'-end of transfer RNAs (tRNAs) by endonucleocatalytic cleavage of precursor transcripts (Guerrier-Takada *et al*, 1983). The M1-RNA component of the

enzyme, derived from eubacterial sources, demonstrates catalytic activity similar to that of a true enzyme *in vitro* (Guerrier-Takada *et al*, 1983). In nature, the M1-RNA component cleaves tRNA precursors at specific sites, which are 3' to 'UUC' triplet codons. These triplet codons are cleaved when they are located at sites which are 5' to double-stranded aminoacyl stems (for a diagram of this structure see Symons, 1994). It is the only naturally occurring ribozyme which is known to catalyse RNA cleavage in *trans*, with multiple turnover, via a hydrolytic reaction mechanism (Symons, 1994, Kiehntopf *et al*, 1995).

Although a great deal of mechanistic study has taken place with this ribozyme motif (see Karwan, 1993), only Altman's group have investigated its potential therapeutic applications (Guerrier-Takada *et al*, 1995). For example, the M1-RNA component of RNase P, from *E. coli*, has been converted to an endoribonuclease that can specifically cleave the thymidine kinase mRNA of herpes simplex virus-1 (Liu and Altman, 1995). This was achieved via the attachment of an antisense ORN 'external guide sequence' (EGS) to the 3' end of the M1-RNA. The EGS was complementary to the herpes thymidine kinase mRNA, at a site which was 3' to a 'UUC' triplet codon. Binding of the EGS to the mRNA formed an aminoacyl stem structure, similar to that of a tRNA which, in turn, allowed specific cleavage of the mRNA by the M1-RNA. The catalytic construct was endogenously expressed in mouse embryo fibroblasts, which were subsequently infected with herpes simplex-1. Levels of viral thymidine kinase mRNA were reduced by 80% in these cells, compared with cells that either did not express the construct, or expressed a catalytically inactive construct (Liu and Altman, 1995). More recently, a similar approach, involving the use of antisense EGS's, has been used to direct endogenous RNase P to cleave mRNAs in *E. coli*. This strategy allowed the specific cleavage of bacterial mRNAs involved in antibiotic drug resistance (Guerrier-Takada *et al*, 1997). The exploitation of endogenous RNase P in *E.coli*, may prove to be particularly useful tool in combating drug resistance in this bacterium. Especially since some other ribozyme motifs, such as the hammerhead, have been ineffective when directed against mRNA targets in *E.coli* (Guerrier-Takada *et al*, 1995).

1.2.2.3. The Hairpin Ribozyme.

The hairpin ribozyme, like the hammerhead, is a catalytic motif which occurs naturally within RNA replicons associated with plant viruses (Hampel and Tritz, 1989). However the hairpin motif is only present within a limited number of viral satellite RNAs which utilise a minus-strand of RNA in their replication cycle (Rubino *et al*, 1990). The hairpin ribozyme is capable of both the site-specific cleavage and ligation

of its single stranded RNA substrate, in the presence of divalent metal ions. It is unique in its absolute requirement for a guanosine residue immediately to the 3' side of the cleavage / ligation site (Chowrira *et al*, 1991). Although the products of the cleavage reaction, like those of the hammerhead cleavage reaction (see Section 1.2.3), bear 5'-hydoxyl and 2',3'-cyclic phosphate groups at their termini.

Figure 1.3. The Consensus Structure of the Hairpin Ribozyme, Derived from Mutation and *In Vitro* Selection Analysis (Berzal-Herranz *et al*, 1993, Anderson *et al*, 1994). [Arrow indicates cleavage site. Conserved nucleotides are shown, N represents any nucleotide].

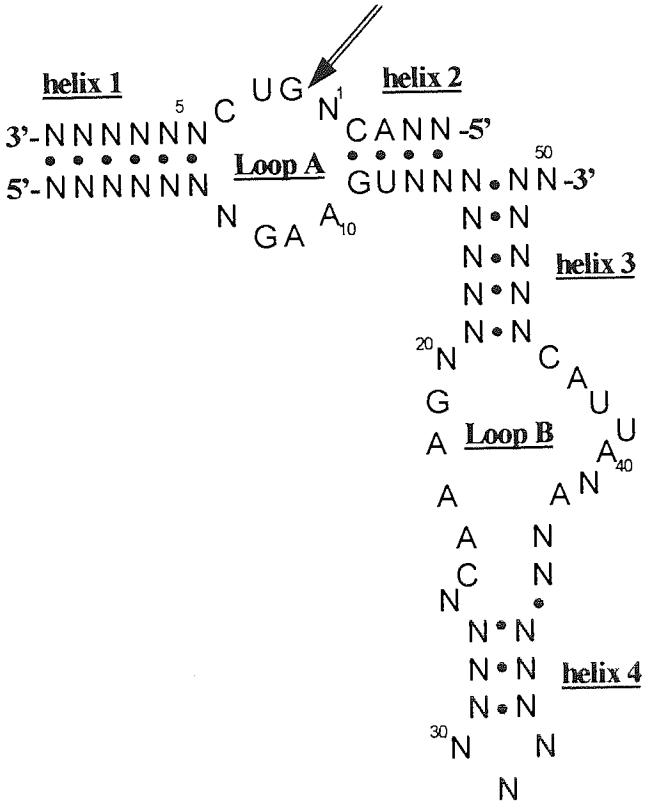

The majority of studies involving hairpin ribozymes have utilised *trans*-acting derivatives of the naturally occurring forms to determine mechanistic and structural properties (for review see Burke, 1996). For example the consensus sequence of the hairpin (see Figure 1.3) has been determined via mutational (Anderson *et al*, 1994) and *in vitro*-selection analysis (Berzal-Herranz *et al*, 1993).

The *trans*-acting motif can be reduced to around 50 nucleotides in length and consists of four helical elements and two internal loops (Burke, 1996), the composition of which can vary widely (see Figure 1.3). The ribozyme binds the substrate using a 14 nucleotide substrate binding sequence located at the 5'-end of the ribozyme (Anderson *et al*, 1994).

Kinetic analyses have shown that substrate binding and cleavage by the hairpin are superficially similar to that of the hammerhead (see Section 1.2.3); after binding to the substrate, cleavage usually occurs much more rapidly than substrate dissociation (Hampel and Tritz, 1989). However recent studies have shown that the rate of the ligation reaction (the reverse of the cleavage reaction) is actually up to ten times higher than that of cleavage (Hegg and Fedor, 1995). Which is in stark contrast to the hammerhead reaction where ligation occurs more slowly than cleavage (Hertel *et al*, 1994).

Although the hairpin has not received as much interest as the hammerhead with regard to therapeutic applications, significant progress has been made in the use of *trans*-acting hairpin ribozymes for the inhibition of HIV-1 replication. Successful inhibition of viral replication has been reported with hairpin ribozymes in several *ex vivo* studies (Ojwang *et al*, 1992, Joseph and Burke, 1993, Yu *et al*, 1993, Yamada *et al*, 1994, Burke, 1996). Perhaps the most promising studies, to date, with the hairpin are those by Wong-Staal and co-workers at the University of California in San Diego: This group has demonstrated that anti-HIV-1 hairpin ribozymes, endogenously expressed via a murine retroviral vector, can completely inhibit viral replication in $CD4^+$ lymphocytes obtained from (non-infected) patients (Leavitt *et al*, 1994, Yu *et al*, 1993 & 1994). The inhibitory effect was thought to be cleavage dependant because a catalytically inactive (control) ribozyme was much less effective (10% effective) in reducing viral replication (Yu *et al*, 1993). Therefore it is possible that $CD4^+$ lymphocytes derived from HIV-positive patients can be immunised against viral infection and then re-infused. Human clinical trials were planned to investigate the benefits of such an approach in infected patients (Yu *et al*, 1995). However, the regulatory approval for these trials is still awaited because of problems with the use of the retroviral expression system in patient-derived cells (personal communication; Dr. Saghir Akhtar, Aston University).

Another recent innovation has been the incorporation of protein-binding domains into the structure of the hairpin ribozyme to yield ribonucleoprotein (RNP) enzymes (Burke, 1996). For example, helix 4 of a hairpin ribozyme (see Figure 1.3) has been extended to accommodate a binding site for phage R17 coat protein (an RNA binding protein) (Sargueil *et al*, 1995). This binding protein remained attached to the hairpin ribozyme throughout the catalytic cycle. Furthermore it increased the catalytic efficiency of the ribozyme *in vitro* because it stabilised the helical secondary structure (Sargueil *et al*, 1995). In future, the binding of cellular proteins to hairpin ribozymes could possibly be used to influence the subcellular localisation of the ribozyme following exogenous delivery to cells (Burke, 1996).

1.2.2.4. The Hepatitis Delta Virus (HDV) Ribozyme.

The genome of hepatitis delta, which is considered to be a satellite RNA of the human hepatitis B virus, contains both genomic and antigenomic regions which are capable of auto-catalytic cleavage (Lee *et al*, 1993). Sequence and structural analysis have revealed the boundaries of these catalytic domains, and have shown that the sequences of both the genomic and antigenomic RNAs are highly homologous and distinctly different to those of any of the other ribozyme (Young-Ah *et al*, 1993).

The cleavage mechanism of the HDV ribozyme bears several similarities to that of the hammerhead domain (see Section 1.2.3) in that the products of cleavage bear 2',3'-cyclic phosphate and 5'-hydroxyl groups at their termini (Wu *et al*, 1993). Also, the catalytic reaction requires the presence of magnesium, or possibly other divalent cations, at millimolar concentrations (Lee *et al*, 1993). However a comprehensive investigation of the cation requirements of the HDV ribozyme reaction has not yet been performed.

The exact nature of the secondary structure of the HDV ribozyme motif is still uncertain. Debate continues as to whether the secondary structure conforms to either a 'pseudo-knot' model or an 'axehead' structure and further investigation is ongoing (for review see Thill *et al*, 1993).

Despite the fact that the HDV ribozyme has been engineered into a *trans*-acting motif, capable of cleaving an RNA substrate (derived from human 7SL RNA) *in vitro* (Lai *et al*, 1991). There has been little utilisation of the HDV ribozyme for potential therapeutic applications to date. The main source of therapeutic interest surrounding the HDV ribozyme appears to be in its involvement in the life cycle of the Hepatitis virus itself and the possibility, therefore, that it could be targeted to prevent replication of the hepatitis virus in humans (Taira and Nishikawa, 1992).

1.2.2.5. Catalytic RNA within Fungi (*Neurospora*).

Autocatalytic activity has also been observed within a 154 nucleotide sequence of circular RNA derived from the mitochondrial plasmid of *Neurospora* species (Collins and Olive, 1992). Although its base composition is distinctly different to that of the other ribozyme motifs, the mechanism of cleavage is similar to that of the hammerhead in that it generates the same phosphate substitution in its products (Collins and Olive, 1992). However, computer analyses have predicted that its secondary structure may be similar to that of the hairpin ribozyme (Symons, 1994).

As yet there are no published data regarding therapeutic applications of this motif. Interestingly, with the exception of the hammerhead motif which was discovered within the satellite RNA of the newt (Epstein and Gall, 1987), the *Neurospora* ribozyme is the only self-cleaving motif which does not occur naturally within a pathogenic organism (Symons, 1994).

1.2.3. Catalytic Cleavage By The Hammerhead Ribozyme.

1.2.3.1. Sequence Requirements for Efficient Cleavage by *Trans*-Acting Hammerhead Ribozymes.

As discussed in section 1.2.1, following the discovery of naturally occurring hammerhead ribozymes; the consensus sequence of the catalytic motif along with a proposed secondary structure was derived from phylogenetic comparison of self-cleaving plant virus satellite RNAs (see Figure 1.2 and Forster and Symons, 1987). In naturally occurring examples, ribozyme cleavage usually occurs after a GUC triplet sequence within the RNA 'substrate'. Although examples of cleavage after GUA (Forster and Symons, 1987) and AUA triplets (Miller *et al*, 1991) have subsequently been observed in nature but occur much less frequently.

Extensive mutagenesis studies with *trans*-acting derivatives based upon the hammerhead design of Haseloff and Gerlach (1988) have further elucidated sequence and structural requirements for efficient cleavage by the hammerhead: Some studies appear to indicate that any triplet sequence of nucleotides within a substrate RNA, of the form NUX (where N = any nucleotide and X = A, U or C) can be cleaved (Usman *et al*, 1996). However the efficiency of cleavage varies widely depending upon the exact composition of the target triplet (Shimayama *et al*, 1995, Zoumadakis and Tabler, 1995). For example, the catalytic efficiency of *trans*-acting hammerhead ribozymes targeted to different triplets, at non-saturating concentrations, has been estimated to decrease in the following order: GUC > CUC > UUC > GUU, AUA, AUC > GUA, UUU, UUA, CUA > AUU, CUU (Shimayama *et al*, 1995).

In general, the conclusions of Bratty *et al* (1993) appear to hold true in that hammerhead ribozymes are usually successful in cleaving the 'wild type' triplet (GUC) in most instances. The triplets CUC, GUA and UUC are also usually suitable as targets, provided that incompatible secondary structures do not form because of the influence of neighbouring nucleotides.

Any alterations to the non-paired nucleotides, present with the catalytic core of the ribozyme, are poorly tolerated and result in a drastic reduction in catalytic activity (Ruffner *et al*, 1990). The only exception is nucleotide 7 where changes are usually tolerated and have less effect on catalysis (Sheldon and Symons, 1989). The highest cleavage rates have been observed with U at position 7, followed by G, A and C which have 60%, 50% and 20% of the activity, respectively (Ruffner *et al*, 1990).

The composition of the nucleotides in stems I and III is determined by the requirement for complementary Watson-Crick base pairing with the substrate molecule. Base mismatches in these substrate binding stems result in a substantial reduction in both substrate binding and catalytic cleavage rates (Werner and Uhlenbeck, 1995, Hertel *et al*, 1996). The actual number of base pairing nucleotides in stems I and III (i.e. the length of the 'substrate binding arms') is also important for efficient catalysis and this aspect is further discussed in Section 1.2.3.2. Generally as few as 5 base pairs on each side of the cleavage site are thought to be required to achieve proper substrate binding (Usman *et al*, 1996).

With regard to the composition of stem II, the nucleotides at the base of this stem and the adjacent nucleotides within the catalytic core of the ribozyme appear to co-ordinate the association of a divalent metal ion (Scott *et al*, 1996). The association of the divalent ion is thought stabilise the secondary structure of the ribozyme / substrate complex, thus allowing cleavage to be initiated (see Section 1.2.3.3). Studies indicate that the minimum requirements for efficient catalysis are two base pairs in stem II and the first pair must be $G_{10.1}$ and $C_{11.1}$. However the neighbouring bases in stem II can be composed of any Watson-Crick pairing nucleotides (Tuschl and Eckstein, 1993). Two or more base pairs are essential to compensate for the helix destabilising effect of the terminal hairpin loop at the end of stem II. However the extension of stem II beyond four base pairing nucleotides does not enhance catalytic activity (Homann *et al*, 1994). The composition of nucleotides within the hairpin loop at the end of stem II (often referred to as Loop II) can vary without any significant effect upon catalytic activity (Thomson *et al*, 1993). The overall sequence requirements for efficient catalytic activity of the all-RNA hammerhead ribozyme are summarised in Figure 1.4. The structure demonstrates the minimum sequence requirements based on the findings of all of the studies described above.

Figure 1.4. Usual Sequence Requirements of the all-RNA Catalytic Core of the Hammerhead Ribozyme. [N = any nucleotide, Large Arrow indicates site of catalytic cleavage, X = A, U or C. The Numbering System of Hertel *et al*, 1992 has been used].

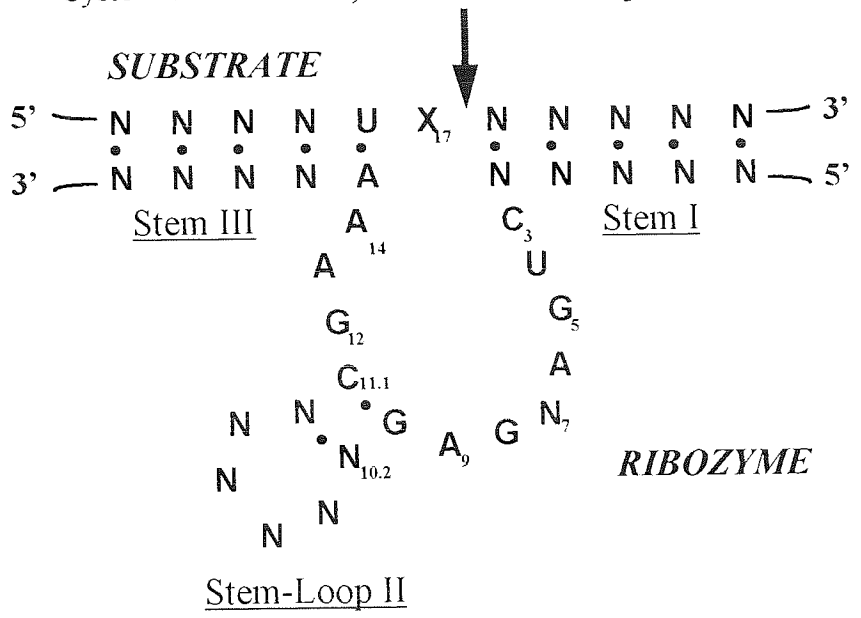

1.2.3.2. The Reaction Mechanism of *Trans*-Acting Hammerhead Ribozymes.

Following the advent of *trans*-acting hammerhead ribozyme motifs (Haseloff and Gerlach, 1988) which behave in a similar manner to true enzymes, Michaelis-Menton parameters (see Figure 1.5) were established for the cleavage reaction of the ribozyme (Fedor and Uhlenbeck, 1992). The individual rate constants for the various steps involved in the reaction have been examined by *in vitro* kinetic analysis (Hertel *et al*, 1994) under both single and multiple turnover conditions.

Figure 1.5. Minimal Kinetic description (Michaelis-Menton Equation) for Hammerhead Ribozyme Catalysis in *Trans*. [E represents the ribozyme, S represent substrate, P_1 and P_2 represent the two cleavage products].

$$E + S \underset{k_{association}}{\rightleftharpoons} E{:}S \underset{k_{cleavage}}{\rightleftharpoons} E{:}P_1P_2 \underset{k_{dissociation}}{\rightleftharpoons} E + P_1 + P_2$$

The term k_{cat} can be used to define the number of substrate molecules which can be converted to products per unit time. It can often be simplified to reflect the rate of the slowest step in the Michaelis-Menton reaction (see Figure 1.5), which in theory can be the formation of the ribozyme / substrate complex ($k_{association}$), the chemical cleavage ($k_{cleavage}$) step or product release ($k_{dissociation}$) (Fersht, 1977). However

in some circumstances, reaction kinetics are more complex and the rate of each step will influence k_{cat} to some extent (Fersht, 1977). In the hammerhead ribozyme reaction, the reaction rates of the individual steps are greatly influenced by the length and nucleotide sequence of the base pairing arms (stems I and III) of the ribozyme (Hertel *et al*, 1994 & 1996, Tabler *et al*, 1994).

1.2.3.2.1. Association with the Target Substrate Molecule.

The first step of the catalytic reaction involves the formation of a reactive complex in which stems I and III of the ribozyme become paired with the RNA substrate molecule and a divalent metal ion (such as magnesium) is bound to the ribozyme molecule (Bratty *et al*, 1993). In theory, the rate of association of any given ribozyme and its complementary substrate should be unaffected by the length or particular sequence involved, as predicted for the association of simple RNA duplexes (Birikh *et al*, 1997b). In practice, this holds true for ribozymes with short base pairing arms (<8 base pairs), directed against (short) substrate sequences *in vitro*. These generally demonstrate rapid association rates which are rarely rate limiting under either multiple or single-turnover conditions (Fedor and Uhlenbeck, 1992). For example the association of a 17 nucleotide substrate to a fully complementary ribozyme was demonstrated to occur at a rate of 2×10^{-7} min^{-1} (Hertel *et al*, 1994). However, the association rates can be slowed when ribozymes are targeted to long substrates due to the formation of non-binding secondary structures within the substrate sequence (Tuschl *et al*, 1995). As a result, when ribozymes have been designed to cleave long substrate sequences *in vitro,* cleavage has sometimes been several orders of magnitude lower than that of short substrates (Birikh *et al*, 1997b). Under these circumstances the rate of association appears to be no longer independent of the length or sequence of the binding arms and increasing their length may improve association rates. However, elongation of the ribozyme arms can also increase the probability that non-base-pairing, self-complementary structures will form within the ribozyme itself and this can reduce rates of association (Clouet-D'Orval and Uhlenbeck, 1996).

1.2.3.2.2. The Cleavage / Ligation Reaction.

Once bound, the ribozyme cleaves a specific phosphodiester bond within the substrate molecule via a transesterification reaction to yield two product fragments, one bearing a 5'-hydroxyl group, the other a 2',3'-cyclic phosphate (Uhlenbeck, 1987). A simplified version of the reaction mechanism is depicted in Figure 1.6.

The reaction is pH dependant and is thought to be initiated by the de-protonation of the 2'-sugar residue of the nucleotide positioned at the 3'-side of the cleavage site (Cech and Uhlenbeck, 1994). As the cleavage mechanism has been shown to proceed with the inversion of the stereochemical configuration about the phosphorus atom (Slim and Gait, 1991), an 'in-line' nucleophilic substitution (S_N2) reaction is implied. This is thought to proceed via a transition state in which the attacking 2'-oxygen is on one apex of a trigonal bipyramid and the leaving 5'-oxygen is on the opposite apex (Cech and Uhlenbeck, 1994).

Figure 1.6. The Hammerhead Ribozyme Catalytic Cleavage Mechanism, derived from Dahm and Uhlenbeck, 1993. [N represents any base nucleotide, X represents the nucleotides A, U or C and M represents a divalent metal ion such as magnesium].

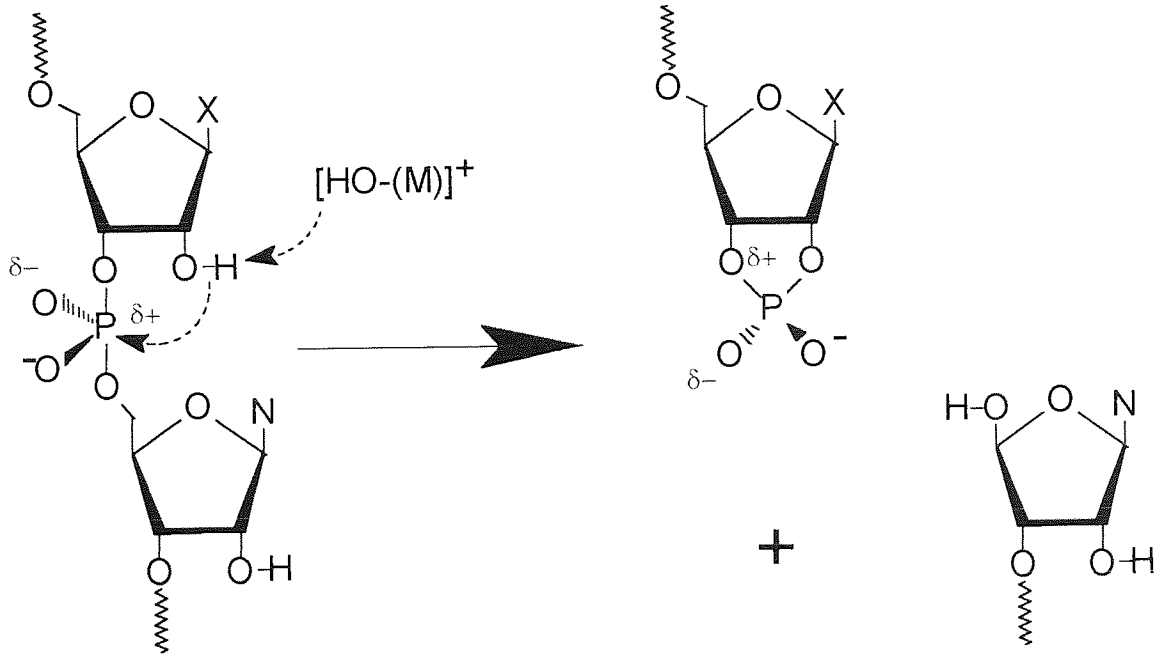

Kinetic analyses have indicated that rate of the cleavage step ($k_{cleavage}$) appears to be independent of the length of stable substrate binding helices (Fedor and Uhlenbeck, 1992, Hertel *et al*, 1994). Under multiple turnover conditions *in vitro*, for ribozymes with short base pairing arms (6 to 7 base pairs or less), the substrate binding and product release steps in the Michaelis-Menton reaction occur extremely rapidly (Hertel *et al*, 1994, Hendry and McCall, 1996). Hence calculated k_{cat} values represent the rate of phosphodiester bond cleavage ($k_{cleavage}$), which is the rate limiting step. Under such conditions, values of k_{cat} have been calculated to range from 1-2 min^{-1} when 'standard' conditions were used (25°C, 10mM $MgCl_2$, pH 7.5) (Hertel *et al*, 1994). However varying the pH, temperature, metal ion concentration or the degree of substrate saturation can affect the rate of reaction (Tuschl and

Eckstein, 1993). For example, k_{cat} values, determined for a hammerhead ribozyme *in vitro*, increased in a linear manner as the reaction temperature was increased from 25°C to 50°C (Takagi and Taira, 1995). Interestingly, k_{cat} values determined at 37°C (human body temperature) were almost 2-fold higher than those at 25°C.

Elongation of the substrate binding arms of the hammerhead increases the stability of helix formation with the substrate and drastically reduces the rate of product dissociation ($k_{dissociation}$). Hence product release becomes the rate limiting step and has the greatest influence on k_{cat} values (Fedor and Uhlenbeck, 1992). For example a hammerhead containing eight nucleotides in stems I and III had a k_{cat} of only 0.008 min^{-1}, under the 'standard' conditions described above. This compared with values greater than 1.0 min^{-1} when ribozymes of a similar sequence but with shorter base pairing arms, were examined (Hertel *et al*, 1994).

The hammerhead cleavage reaction is actually reversible (i.e. a ligation reaction can occur). However the rate of this ligation reaction has been estimated to be at least three orders of magnitude lower than the cleavage reaction under similar conditions, hence the hammerhead ribozyme strongly favours cleavage (Hertel *et al*, 1994). This is in contrast to the ligation reaction of the hairpin ribozyme which has been estimated in one study to be ten times higher than that of cleavage (Hegg and Fedor, 1995).

1.2.3.2.3. Product Release / Dissociation.

In the final reaction step the cleaved substrate fragments dissociate, thus liberating the ribozyme which can proceed in further catalytic events. As discussed in section 1.2.3.2.2, product release is not usually rate limiting under multiple turnover conditions *in vitro*, for hammerheads with fewer than 8 nucleotides in the base pairing arms (Hertel *et al*, 1994). However as the length of stems I and III is increased, the helices formed with the corresponding substrate become more stable. The dissociation rate generally decreases exponentially with increasing stability of the substrate binding arms (Fedor and Uhlenbeck, 1992). This implies that for efficient multiple-turnover catalysis (*in vitro*), ribozymes with greater than 7 nucleotides in each substrate binding arm are unsuitable candidates because product dissociation will become rate-limiting (Hertel *et al*, 1994). This appears to hold true when short substrate sequences are used *in vitro*. However, when longer, structured substrates are targeted, the situation often changes because the formation of non-binding secondary structures within the long substrates can often cause the association step to become rate limiting (see Section 1.2.3.2.1). Under such circumstances, elongation of the binding arms can

have a beneficial effect on substrate binding, which outweighs any effect of decreased dissociation rates (Birikh *et al*, 1997b).

1.2.3.2.4. The Requirement for a Divalent Metal Cation.

Early studies with the naturally occurring *cis*-acting forms of the hammerhead indicated that a range of divalent metal cations and polyamines were able to act as co-factors in the cleavage reaction (Prody *et al*, 1986). However subsequent mechanistic studies with *trans*-acting motifs have indicated that agents such as spermidine, Pb^{2+} and Zn^{2+} are only capable of stabilising the folded structure of the ribozyme (Dahm and Uhlenbeck, 1991). For actual cleavage to take place, specific divalent metal ions (namely; Mg^{2+}, Mn^{2+}, Ca^{2+}, Co^{2+}, or Cd^{2+}) are required at millimolar concentrations. The minimum concentration required for efficient catalysis is thought to be at least 10mM *in vitro* (Dahm and Uhlenbeck, 1991).

It is thought that a divalent ion / hydroxo complex (see Figure 1.6) is formed which is responsible for the proton abstraction of the attacking 2'-hydroxyl group during the cleavage mechanism (Dahm *et al*, 1993). Therefore reducing the metal ion concentration would be expected to affect the actual chemical cleavage step, rather than substrate binding or product dissociation.

1.2.3.3. The Three Dimensional Structure of the Hammerhead Ribozyme.

The detailed X-ray crystal structures of two hammerhead ribozymes in their 'ground-states' (i.e. prior to catalytic cleavage) were originally solved, in the presence of millimolar concentrations of divalent metal ions, using substrate sequences which were chemically modified to prevent catalytic cleavage (Pley *et al*, 1994, Scott *et al*, 1995). More recently, this 'ground-state' conformation has been verified using an all-RNA substrate sequence, in the absence of divalent cations (Scott *et al*, 1996). As a result of these studies and the use of other techniques, a consistent picture of the three dimensional structure of the hammerhead ribozyme in its 'ground-state' has emerged (for detailed reviews with graphical representations of the structures see Cech and Uhlenbeck, 1994, Tuschl *et al*, 1995, McKay, 1996). The appearance of the ribozyme in its three dimensional 'ground state' appears to be not so much a 'hammerhead' as a 'wishbone' structure. Stems I and II diverge from the core at an acute angle, while stem III points in the opposite direction (Cech and Uhlenbeck, 1994). Within the catalytic core, stems II and III form a near continuous helix via the continual right handed helical path of nucleotides G_{12} to A_{14} and N_7 to A_9. This is thought to form a divalent-ion binding domain in the ground-state structure, which has been described as

a 'basket' for the divalent ion (Pley *et al*, 1994). The 3'-end of stem I is connected to this continuous helix via a 'uridine turn' within nucleotides C_3 to A_6. This thought to form a 'catalytic pocket', in which the nucleotide at the cleavage site (C_{17}) forms a hydrogen bond with C_3 (Scott *et al*, 1995) The 5'-end of stem III is connected to the continuous helix through the scissile phosphate, by disruption of helical winding (Tuschl *et al*, 1995).

Recently, the use of time-resolved crystallography, has allowed the direct observation of an all-RNA hammerhead (i.e. using a 'cleavable' substrate), not only in its ground state, but also in a transition state thought to exist immediately prior to catalytic cleavage (Scott *et al*, 1996). Observation of this structure revealed that the only significant conformational change occurred in the immediate vicinity of the cleavage site, whereas the remainder of the 'ground-state' structure remained essentially unchanged (Scott *et al*, 1996). The main features of this conformational change were that C_{17} (and hence the adjacent scissile bond) moved away from the 'catalytic pocket' observed in the 'ground-state' structure. Hence C_{17} no longer hydrogen-bonded to C_3 but instead formed a hydrogen-bond with $U_{16.1}$. An additional metal-ion also appeared to be bound to an oxygen atom adjacent to the scissile bond. This metal ion binding site appears to be much more relevant to the catalytic cleavage mechanism (see Figure 1.6) than the metal ion site observed in the previous ground-state structures (see above). The authors concluded that the binding of a divalent metal ion to the oxygen (adjacent to the scissile bond), induces the conformational change required for 'in-line' attack at the cleavage site by the 2'-oxygen (see Section 1.2.3.2.2. and Figure 1.6). In this scenario the same metal ion which binds to the oxygen atom also provides the hydroxide which initiates the base-catalysed, de-protonation of the 2'-sugar residue (Scott *et al*, 1996).

When combined with other methods of investigation, X-ray crystallography studies have provided an insight into structural and functional properties of the ribozyme, such as inter-helical cross linking and the stabilising influence of Stem II on the catalytic core (for review see McKay, 1996). However the most important application arising from the solving of the crystal structures, may be the information that this data can provide regarding hydrogen bonding interactions within the catalytic core. Such information, when compared with the results of kinetic studies, can be used to predict sites at which chemical modifications can be tolerated (see Section 1.2.4).

Kinetic studies involving the deletion or replacement of functional groups have identified several phosphate oxygens, 2'-hydroxyl groups and nucleobase functional groups which are vital for catalytic activity (for reviews see Bratty *et al*, 1993, Usman

et al, 1996. Also see section 1.2.4). X-ray crystallography data generally confirm the findings of the kinetic studies but some contradictions are also noted: For example, kinetic studies suggest that nucleotide G_5 is vital for catalysis but even in the most recent crystal structures (Scott *et al*, 1996) it does not appear to be involved in any important hydrogen bonding interactions, which suggests it may not be directly involved in catalysis (Pley *et al*, 1994).

1.2.3.4. The Implications of Kinetic Studies *In Vitro* for the Design of *Trans*-Acting Hammerhead Ribozymes.

When designing hammerhead ribozymes, two particularly important properties are the catalytic turnover (the ribozyme's ability to cleave multiple substrate strands) and its specificity (the ability to cleave at a unique site). These properties are affected by the characteristics of the substrate binding arms (stems I and III). For hammerhead ribozymes to exhibit multiple-turnover *in vitro*, the rate limiting step should ideally be the cleavage step rather than product dissociation (Birikh *et al*, 1997b). The rate of product dissociation in the cleavage reaction is dependant upon the length of Stems I and III, but this is not usually rate limiting until the length of these stems increases to 8 nucleotides or more (Hertel *et al*, 1994). Elongation of stems I and III also increases the probability that a ribozyme will fold into non-binding (self-complimentary) secondary structures. Computer-based folding algorithms (Denman, 1993) can be used to eliminate ribozyme candidates which are likely to adopt these non-binding structures, However, there is no guarantee that the use of such algorithms will predict ribozyme structures which possess potent catalytic activity. An additional consideration is that approximately 5 bases are thought to be required in each of the substrate binding arms for proper substrate binding (Usman et al, 1996). Therefore, many investigators have tended to use hammerheads with 6 or 7 base pairing nucleotides in stems I and III when targeting short substrate sequences *in vitro*.

Some studies have shown that hammerheads with 6 to 8 base pairing nucleotides are optimal for the *ex vivo* cleavage of specific substrate targets (Lieber and Strauss, 1995, Bertrand *et al*, 1994). However other studies have shown that kinetic data obtained *in vitro* with small ribozyme constructs does not translate to the *ex vivo* situation (Crisell *et al*, 1993, Tsuchihashi *et al*, 1993, Rossi et al, 1994, Heidenreich *et al*, 1994, Beck and Nassal, 1995). This contradiction probably reflects the different accessibilities of the cleavage sites targeted in these studies (Birikh et al, 1997b), but several other factors may influence the activity of ribozymes directed against targets *ex vivo* (or *in vivo*) and these are discussed further in Section 1.3.2.

Specificity is an important consideration when designing ribozymes for applications such as inhibition of gene expression in cells. In these situations the ribozyme must recognise a unique, complementary cleavage site and be able to differentiate between the desired substrate and alternative substrates. One might think that elongated binding arms would improve cleavage specificity, but in reality the situation is not that simple (Birikh et al, 1997b). Recent kinetic studies have shown that in order to exploit the difference in binding affinity between matched and mismatched targets, the dissociation rate should ideally be slightly faster than the chemical cleavage step (Hertel *et al*, 1996). This indicates that the specificity of hammerhead ribozymes can be improved by the incorporation of features which increase product dissociation. Alternatively the introduction of features which reduce (slow) the rate of the cleavage step, relative to dissociation, may also improve specificity (Birikh *et al*, 1997b). Unlike antisense ONs, exceptionally strong binding of a ribozyme to a target RNA (via the introduction of elongated (antisense) binding arms), therefore, appears to be neither desirable or essential in improving the potential activity of these molecules as therapeutic agents (Usman *et al*, 1996).

1.2.4. Chemical Modification of Hammerhead Ribozymes.

1.2.4.1. Improving the Stability of Ribozymes in Biological Environments.

A major obstacle to the development of ribozyme based strategies for therapeutic purposes is their instability in biological fluids (Heidenreich *et al*, 1996). RNA molecules, such as all-RNA ribozymes, are extremely susceptible to degradation by nucleases and 2'-hydroxyl-dependant ribonucleases present in both the intra- and extra-cellular environments (Usman and McSwiggen, 1995).

Two main types of nuclease exist; exonucleases which digest RNA molecules starting from either the 3'- or 5'-terminus of the sequence, and endonucleases which generally digest RNA molecules at sites which are 3' to pyrimidine residues (Alberts *et al*, 1989). In nature RNA molecules, such as mRNAs, are protected against intracellular nuclease activity because they possess a 5'-cap structure and a 3'-poly A tail (Beelman and Parker, 1995).

Ribozymes expressed in cells endogenously, following vector-mediated delivery (described later in Section 1.4.1), are able to evade extracellular nucleases but remain susceptible to intracellular populations of these enzymes. Stability problems arising during endogenous expression have been addressed by embedding ribozymes within

'natural' RNA molecules such as tRNA constructs (Thomson *et al*, 1995), or by adding hairpin loops to the termini of ribozyme molecules (Sioud *et al*, 1992). However these strategies can only protect the ribozyme molecule from the action of exonucleases.

Exogenous delivery strategies may be preferable for the administration of ribozymes for therapeutic purposes (Akhtar *et al*, 1995) since this approach does not require any alteration to the genetic make-up of target cells (see Section 1.4.1). Therefore the problem of instability in biological fluids must be addressed for such an approach to be successful.

Antisense ODNs (see Section 1.1.1) also demonstrate poor nuclease stability in biological fluids (Wickstrom, 1986). Extensive modifications to either the phosphate backbone or the 2'-sugar residue of antisense molecules have been made during chemical synthesis (for reviews see Milligan *et al*, 1993, Wickstrom, 1995). These chemical modifications can enhance nuclease stability and improve cellular uptake, therefore improving exogenous delivery of intact antisense ODNs (for a recent review see Agrawal, 1996b).

More recently, improvements in the chemical synthesis of RNA have offered the opportunity of introducing site-specific chemical modifications into small RNA molecules such as hammerhead ribozymes (Scaringe *et al*, 1990, Reese *et al*, 1991, Wincott *et al*, 1995, Rao *et al*, 1995). These developments have considerably enhanced the available options for producing stabilised ribozymes because existing methods of *in vitro* RNA synthesis, such as transcription with T7 RNA polymerase, do not allow site-specific chemical modifications (Usman *et al*, 1996). Several functional groups within oligoribonucleotide molecules can be chemically modified (see Figure 1.7); namely the phosphodiester linkage, the 2'-sugar residue and the base moiety itself. Specific examples of these types of modification and their effects on catalysis and nuclease resistance are described in Sections 1.2.4.2 to 1.2.4.4.

Chemical modification of hammerhead ribozymes is a considerably more challenging concept than the modification of an antisense oligoribonucleotides because any beneficial effects upon stability which result from such modifications often have to be balanced against the detrimental effects this will have upon the catalytic activity of the ribozyme (Usman and Cedergren, 1992). Contrary to classical mutagenesis studies in which simple nucleotide substitution is employed (see section 1.2.3.1), the use of modified nucleotides often elicits more subtle changes in the structure and function of the hammerhead (Bratty *et al*, 1993). Therefore, the identification of functional

groups within the catalytic core which can accept chemical modifications without affecting catalysis, has been critical to the notable advances made in this area in recent times.

Figure 1.7. Schematic Diagram of the Structure of Oligoribonucleotides and Examples of Potential Sites for Chemical Modification. ['Base' represents either A, C, G or T. 'Z' represents the 2'-sugar residue, 'X' represents an oxygen atom at the Phosphodiester Inter-nucleotide Linkage].

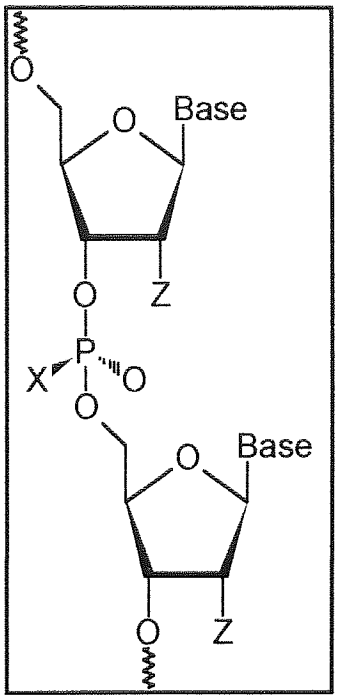

Some Potential Structural Modifications:

$X = O^-$,	$Z = OH$	(RNA oligoribonucleotide)
$X = O^-$,	$Z = H$	(DNA oligodeoxynucleotide)
$X = P^-$,	$Z = OH$	(Phosphorothioate RNA)
$X = CH_3$,	$Z = H$	(Methylphosphonate DNA)
$X = O^-$,	$Z = OCH_3$	(2'-O-methyl RNA)
$X = O^-$,	$Z = NH_2$	(2'-amino RNA)
$X = O^-$,	$Z = F$	(2'-fluoro RNA)
$X = O^-$,	$Z = CH_2CHCH_2$	(2'-C-allyl RNA)

1.2.4.2. Modifications to the Phosphodiester Linkage.

The inter-nucleotide phosphate linkage is a structural feature common to both oligoribonucleotides (RNA) and oligodeoxynucleotides (DNA). It is the target for the action of nucleases and ribonucleases, as well as a variety of other enzymes such as those present in spliceosomes and therefore, it seems logical to modify this site to prevent digestion (Heidenreich *et al*, 1994).

The most common modification at this site in the field of antisense ON technology, has been the replacement of a non-bridging oxygen atom within this linkage with a sulphur atom, to yield a phosphorothioate oligodeoxynucleotide (PS ODN). Like their unmodified phosphodiester counterparts, PS ODNs are water soluble, polyanionic compounds (For review see Zon and Stec, 1991). The increased stability which this modification confers towards nucleases present in cellular extracts and sera has been well documented (Akhtar *et al*, 1991, Stein and Cheng, 1993), with some studies

reporting a 100-fold increase in nuclease stability following complete PS substitution of an antisense ODN (Stein *et al*, 1988). In addition, PS modifications have been shown to improve the cellular uptake profiles of antisense constructs (see Stein *et al*, 1988, Beck *et al* 1996, Rojanasakul, 1996 and for further discussion see Section 4.1).

Methods for automated chemical synthesis of phosphorothioates have long been available (See Section 2.1 and Zon and Stec, 1991) and yield a racemic mixture of diastereoisomers about the phosphorus atom in the PS linkage known as the Sp and Rp isomers respectively. Studies with antisense ODNs indicate that the Sp stereoisomer is more stable and shows better hybridisation properties (Cohen, 1993).

Initial mechanistic studies indicated that complete sulphurisation of all phosphodiester linkages within trans-acting hammerheads or their substrates resulted in a total loss of catalytic activity (Ruffner and Uhlenbeck, 1990). However 'pinpoint' modification of phosphodiester linkages within the catalytic core of the hammerhead complex revealed four phosphodiester linkages at sites 5' to A_9, G_{12}, A_{13} and $N_{1.1}$ (i.e. the cleavage site, see Figure 1.2 for nomenclature) which were critical for catalysis (Buzayan ,1990, Ruffner and Uhlenbeck, 1990 & 1991, Slim and Gait, 1991). Further studies assessed the effects of partial PS substitution on nuclease stability (Shimayama *et al*, 1993). Initially, PS ODNs were substituted for ribonucleotides at non-catalytic core residues within stems I, II and III. This modification did not impair catalysis but the ribozyme construct was rapidly degraded by pyrimidine-specific endonucleases present in serum. The introduction of additional PS linkages at sites 3' to the pyrimidine residues at U_7, U_4 and C_3 (i.e. the principle sites of endonuclease digestion) increased the stability of the ribozyme 100-fold compared with an unmodified ribozyme. However the catalytic ability of this construct was significantly impaired (10-fold reduction in k_{cat}) when compared with an unmodified ribozyme (Shimayama *et al*, 1993).

The most successful application of PS modifications to date, in terms of the stabilisation of a highly active hammerhead construct, has been their use in combination with 2'-sugar modifications (Heidenreich *et al*, 1994 & 1996). Ribozymes containing 2'-fluoro-pyrimidines, with 2'-amino modified residues at positions U_4 and U_7, in conjunction with PS modifications at non-catalytic core linkages within stems I, II and III, were examined in these studies. Catalytic activity was improved and nuclease stability was considerably enhanced as a result of these modifications (Heidenreich *et al*, 1994). Protection from exonucleases offered by the 3'- and 5'- terminal PS linkages was considered to be a major factor in the stability enhancement. Ribozyme constructs bearing terminal phosphorothioates were able to

remain undegraded for over 2 hours in cell nuclei suspensions, whereas hammerheads not possessing these modifications were 50% degraded within 5 minutes (Heidenreich *et al*, 1996).

However it appears that some investigators are becoming slightly wary of using PS modifications in ODN constructs designed for therapeutic purposes (see Krieg and Stein, 1995). Non-sequence specific and anti-protein effects of PS ODNs have been reported (Krieg and Stein, 1995, Coulson *et al*, 1996) and it is therefore uncertain whether these compounds will demonstrate toxicity profiles which permit administration to humans. The potential problems regarding the clinical use of phosphorothioates were highlighted recently when GEM91, a PS ODN complementary to the *gag* gene of HIV-1 (Agrawal, 1996), was withdrawn from human clinical trials due to toxicity problems (personal communication Dr. Saghir Akhtar).

1.2.4.3. Modifications to the 2'-Ribose Sugar Moiety.

The first functional group to undergo extensive substitution within the hammerhead was the 2'-hydroxyl group of the ribose sugar. This moiety represents the difference between ribonucleotides (RNA) and deoxyribonucleotides (DNA) (Bratty *et al*, 1993), the latter being slightly more stable in biological fluids (Milligan *et al*, 1993). Replacement of all 2'-hydroxyl moieties with hydrogen atoms (i.e. the synthesis of a 'DNA hammerhead ribozyme'), resulted in a total loss of catalytic activity (Perreault *et al*, 1990). The loss of the 2'-hydroxyl moiety from nucleotides within the catalytic core prevents the participation of these nucleotides in hydrogen bonding interactions which are vital in the formation of secondary and tertiary structures (Bratty *et al*, 1993). However, chimeric DNA / RNA constructs, with deoxyribonucleotides in the substrate binding arms only, have demonstrated enhanced catalytic activity and improved intracellular stability following liposome mediated delivery (Taylor *et al*, 1992).

Most investigators have utilised 2'-amino, 2'-fluoro or 2'-O-alkyl substitutions, since these are considered less likely to perturb the overall structure of the ribozyme and are more easily introduced than most backbone modifications (Beigelman *et al*, 1995). Pieken *et al* (1991) were the first investigators to utilise 2'-amino and 2'-fluoro modifications within the hammerhead motif. They used these substitutions at all pyrimidine nucleotides (i.e. all uridines and cytosines) in the hammerhead, in an attempt to improve endonuclease stability. Their modified constructs showed a 1200-fold increase in stability in rabbit serum, but disappointingly a 25-50-fold decrease in

catalytic activity (*in vitro*) was also observed when compared with an unmodified ribozyme (Pieken *et al*, 1991). Further studies confirmed the importance of modifying the pyrimidine nucleotides, especially at sites within Stem Loop II, in order to prevent endonuclease digestion (Heidenreich *et al*, 1993). By comparison, mechanistic studies showed that substitution of specific purine nucleotides (G_5 and G_8) within the catalytic core of the ribozyme, with 2'-amino or 2'-fluoro analogues, was not a viable prospect because catalytic activity was completely eradicated (Williams *et al*, 1992).

Considerable progress was made when a combination of 2'-fluoro and 2'-amino modifications were used, in conjunction with 3' and 5' terminal PS modifications which afforded protection from exonucleases (Heidenreich *et al*, 1994). All pyrimidine residues within a hammerhead were 2'-fluoro modified, with the exception of the nucleotides at U_4 and U_7 which were 2'-amino modified. The 2'-fluoro modification was thought to offer the best nuclease protection, however the 2'-amino modification was used at these specific sites because this modification did not have an adverse effect upon hydrogen bonding interactions in the catalytic core (Heidenreich *et al*, 1994). These subtle changes to the previous designs of Pieken *et al* (1991), not only produced further improvements in the nuclease stability of the hammerhead (typical half life in human serum was > 4 hours), but also slightly improved the catalytic efficiency of this construct when compared to an unmodified control (Heidenreich *et al*, 1994).

With regard to 2'-O-alkyl modifications; Goodchild *et al* (1992) were the first to introduce these into the hammerhead structure when they demonstrated that 2'-O-methyl substitution in the base pairing arms did not impair ribozyme catalysis, nevertheless nuclease stability was not significantly improved. Yang *et al* (1992) demonstrated that 2'-O-methyl modification at all positions in a hammerhead ribozyme, with the exception of G_5, G_8, A_9, $A_{15.1}$ and $G_{15.2}$, resulted in a 1000-fold increase in stability in yeast extract but this modification significantly reduced catalytic activity (0.3% of 'wild type' activity). In contrast, Paolella *et al*, (1992) synthesised ribozymes containing either 2'-O-methyl or 2'-O-allyl modifications at all nucleotides except for U_4, G_5, A_6, G_8, G_{12} and $A_{15.1}$ within the catalytic core. The catalytic activity of these constructs was only slightly impaired (20% of 'wild type' activity). However improvements in nuclease stability (100-fold compared with an unmodified control) were relatively more modest (Paolella *et al*, 1992). This indicates that the effects of 2'-O-alkyl substitution within the hammerhead can be unpredictable (Beigelman *et al*, 1995).

Recently a key study has pooled the findings described above. This resulted in the preparation of a range of generic, nuclease stable hammerhead motifs that retained only five unmodified purine residues (G_5, A_6, G_8, G_{12}, $A_{15.1}$) within the catalytic core (Beigelman *et al*, 1995):

Beigelman *et al* (1995) synthesised ribozymes (with unmodified purines as described above) in which nucleotides at positions U_4 and U_7, were modified with a variety of different 2'-substituents. Based on the findings of previous reports (Yang *et al*, 1992, Paolella *et al*, 1992), the 2'-O-methyl modification was chosen to modify all of the remaining nucleotides in these constructs (Beigelman *et al*, 1995). This was because the 2'-O-methyl modification maintains the structure of the hammerhead, is more nuclease stable than 2'-fluoro or 2'-amino analogues, is easily synthesised and would potentially be less toxicity *in vivo* because it is a naturally occurring moiety (Beigelman *et al*, 1995). The *in vitro* catalytic activity (under single turnover conditions) and serum stability of these hammerhead constructs was examined (see Table 1.1) and compared to that of an unmodified all-RNA control ribozyme (Beigelman *et al*, 1995).

Table 1.1. The Cleavage Activity and Nuclease Resistance of Some Chimeric Hammerhead Constructs Developed by Beigelman *et al*, 1995. (See text for a further description of this study. Modifications at sites U4 and U7 are indicated. Single turnover catalytic activity was determined *in vitro* using a 17-mer all-RNA substrate).

2'-Modification at Positions U4 / U7	Catalytic Activity (Substrate half life *in vitro*) [minutes]	Stability (Half Life in Human Serum) [minutes]	Relative Stability / Activity
-OH / -OH (RNA control)	1	0.1	1
-O-Me / -O-Me	4	260	650
- NH_2 / NH_2	2	300	1500
-C-allyl / -OMe	3	>500	>1700

Initially, 2'-O-methyl substitutions were introduced at positions U_4 and U_7 and this considerably enhanced the stability of the hammerhead in human serum (>2000 fold increase), however the catalytic activity of this construct was impaired (by approximately 25%) compared with the control (Beigelman *et al*, 1995). Subsequently, a variety of 2'-substitutions were introduced at positions U_4 and U_7.

The most notable were 2'-amino modifications and a 2'-C-allyl modification (a design patented by this group) which further enhanced serum stability but had a less detrimental effect upon catalytic activity (see Table 1.1) than 2'-O-methyl modification (Beigelman *et al*, 1995). The authors compared the relative activity / stability of all their hammerhead constructs with an all-RNA ribozyme control, by using the following formula (their results are indicated in Table 1.1);

$$\text{Relative Stability / Activity Compared with Control} = \frac{\text{Catalytic Activity } (t_{1/2}) \text{ / Stability } (t_{1/2})}{\text{Control Activity / Control Stability}}$$

Although the catalytic activity of all the modified constructs used in this study was slightly impaired compared with the all-RNA control ribozyme *in vitro* (Beigelman *et al*, 1995) The dramatic increases seen in serum stability (see Table 1.1) indicate that the modified constructs would be superior at cleaving target sites *in vivo* because, unlike their unmodified counterparts, they would probably be able to survive for a sufficient period to cleave their target sequences in biological fluids. This lead the authors to conclude that their findings demonstrated that a suitable balance could be found between nuclease resistance and catalytic activity when designing hammerhead constructs. Therefore, the potential use of hammerhead ribozymes in therapeutic applications was no longer limited by their poor biological stability (Usman *et al*, 1996).

In addition to the above findings, Beigelman *et al* (1995) also noted that the main source of degradation of their constructs was 3'-exonuclease activity, since the action of (pyrimidine specific) endonucleases had been largely neutralised by their 2'-modifications. Therefore they added a base modification (a 3'-3'-linked inverted dT nucleoside, see Section 1.2.4.4) to the 3'-terminus of their hammerhead constructs. This had no effect upon catalysis but further increased the half life of these hammerheads to over 260 hours in human serum (Beigelman *et al*, 1995).

1.2.4.4. Base Modifications.

Fewer studies have focused upon modifications to nucleotide bases within the catalytic core of the hammerhead. Although more interest in the function of certain bases has developed since X-ray crystal structure analyses indicated that not all core bases are involved in hydrogen-bonding interactions, therefore not all of these bases may be essential for catalysis (Pley *et al*, 1994, Scott *et al*, 1995 & 1996).

Mechanistic studies, involving modifications to purine bases within the catalytic core (such as replacement with inosine), have shown the importance of maintaining bases G_{12}, G_8 (Grasby *et al*, 1993, Tuschl *et al*, 1993) and A_8 (Fu and McLaughlin, 1992) in their unmodified form. The crystal structures supported these findings because they indicated the involvement of these bases in important hydrogen-bonding interactions (Pley *et al*, 1994, Scott *et al*, 1995 & 1996). However mechanistic studies also indicate that base modifications at position G_5 are poorly tolerated (Grasby *et al*, 1993, Tuschl *et al*, 1993). Whereas X-ray analyses (Pley *et al*, 1994, Scott *et al*, 1995 & 1996) do not appear to predict a key role for this base in hydrogen-bonding interactions.

Other mechanistic studies have identified the effect of base modifications to certain pyrimidine bases within the catalytic core. For example, abasic modifications to positions C_3 (Adams *et al*, 1994) and U_4 (Beigelman *et al*, 1995b) result in a significant reduction in catalytic activity. It would appear that modifications to these bases interferes with the formation of the 'uridine turn' predicted by the X-ray crystal structures (see Section 1.2.3.3). Although there have been relatively few investigations into the effects of base modifications on hammerhead ribozyme catalysis, such modifications may allow further advances in the design of chimeric hammerhead constructs with both improved catalytic activity and nuclease stability in future (Usman *et al*, 1996).

So far, chemical modifications to hammerhead ribozymes have almost universally resulted in some decrease in catalytic activity (*in vitro*). However a recent study has shown that a 'pyrimidine-4-one' base modification at position U_7 can actually increase the catalytic activity of the hammerhead (Usman *et al*, 1996). In addition there have been recent advances in the use of base modifications to enhance biological stability. For example a 3'-3'-linked, inverted deoxy-thymidine base modification at the 3'-terminus of chimeric hammerhead constructs afforded protection from 3'-exonucleases (see also Section 1.2.4.3 and Beigelman *et al*, 1995).

Although the full extent to which ribozymes can be chemically modified is yet to be determined, some substituents have been identified which are known to be critical for the catalytic action of the hammerhead. These are depicted in schematic form in Figure 1.8 and are further summarised in a recent review (see Usman *et al*, 1996). In summarising all the studies to date, this figure highlights the functional groups, which when modified chemically, have resulted in at least a 10-fold reduction in catalytic efficiency. This does not mean that all of the other sites within the molecule can be universally modified without any effect upon catalytic activity. Instead Figure 1.8

merely indicates sites within the catalytic core of the hammerhead which almost certainly cannot be modified if catalytic activity is to be maintained (N.B. The minimum base sequence requirements for hammerhead ribozyme-mediated catalysis were demonstrated in Figure 1.4).

Figure 1.8. Diagram Showing the Critical Substituents within the *Trans*-acting Hammerhead Catalytic Domain (Adapted from Usman *et al*, 1996). Point substitutions to critical bases (shaded rectangles), phosphate linkages (shaded circles) and 2'-sugar residues (shaded hexagons) which yield more than a 10-fold reduction in catalytic activity are indicated. 3'-oxygens have been omitted for clarity. 'N' represents any base nucleotide. For further nomenclature refer to Figure 1.4.

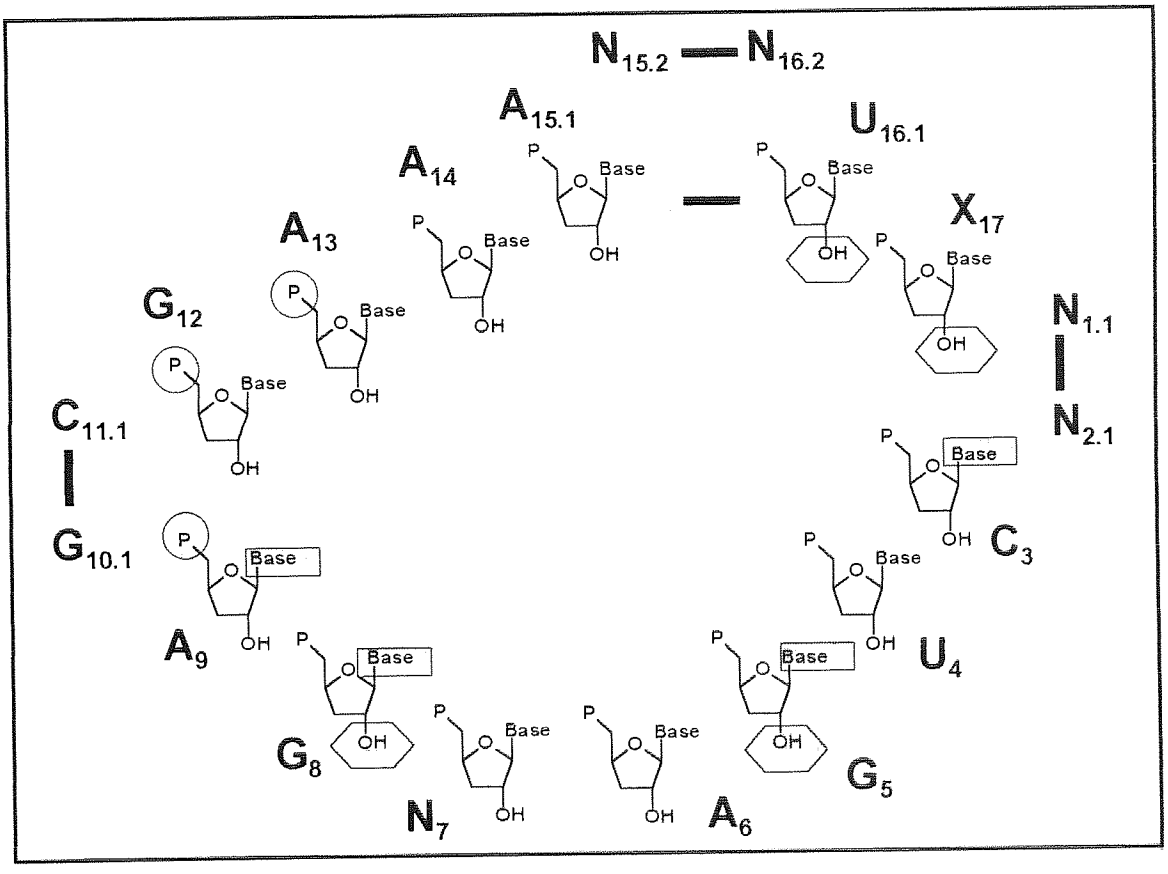

1.3. DESIGNING HAMMERHEAD RIBOZYMES TO INHIBIT mRNA EXPRESSION *IN VIVO*.

1.3.1. A Comparison of the Antisense and Ribozyme-Based Strategies.

Antisense ONs have been widely studies over the past decade due to their potential in inhibiting gene expression (see Section 1.1.1). By comparison the therapeutic application of ribozymes remains in its infancy. Although ribozymes and antisense ONs share several properties and obstacles to their use (see Section 1.1.1), the

ribozyme-based strategy may prove to be more effective in controlling gene expression for a variety of reasons:

The selectivity of the antisense strategy relies entirely upon the discrimination between perfect and partially mismatched sequences if it is to specifically inhibit gene expression. The length of an antisense construct would usually have to be in the range of 11 to 20 nucleotide bases in order to maintain such discrimination (Gibson, 1994) and to allow stable duplex formation with the target mRNA (Frier *et al*, 1992). By comparison a hammerhead ribozyme construct would probably need to be larger (in excess of 30 nucleotide bases in length) because non-binding nucleotides involved in catalysis are required, in addition to those which bind to the target. However the specificity of ribozyme action is not only dependant upon RNA binding but also upon the cleavage after a specific triplet of nucleotides (see Hertel *et al*, 1996 and Section 1.2.3) within the target sequence (i.e. ribozymes demonstrate two levels of specificity). In addition kinetic studies (see Section 1.2.3.4) have indicated that exceptionally strong binding of target RNAs, using ribozymes with long substrate binding arms, is neither desirable nor essential (Usman *et al*, 1996).

Another factor to consider is the mechanism by which antisense constructs disrupt gene expression after annealing to their specific, complementary target (see Figure 1.9 and Section 1.1.1). Antisense ONs inhibit mRNA expression either by physical prevention of mRNA translation at the ribosomes (Akhtar, 1991, Rossi, 1995) or by destruction of antisense / mRNA duplexes by intracellular enzymes such as ribonuclease H (Tidd, 1996, Akhtar and Agrawal, 1997) as described in Section 1.1.1. In theory, ribozymes can also inhibit gene expression by physically preventing mRNA translation at the ribosomes (i.e. they can potentially exhibit an 'antisense effect'). More importantly, however, ribozymes have the ability to actually cleave and destroy the target mRNA molecule (Woolf, 1995). Furthermore, they can potentially exhibit multiple turnover catalysis (Haseloff and Gerlach, 1988), where a single ribozyme molecule can theoretically act upon multiple mRNA substrate molecules, resulting in a more effective inhibition of gene expression. (Cech, 1993). Ribozyme based therapeutics are, therefore, not reliant upon 'passive' mechanisms such as physical prevention of mRNA translation or the action of host cell enzymes, which are known to vary in concentration (Gibson, 1994). Indeed, antisense strategies have proved ineffective in certain circumstances in the past and varying levels of intracellular enzymes such as Ribonuclease H have been implicated as the cause (Kerr *et al*, 1988).

Figure 1.9. Schematic Diagram Comparing the Antisense and Ribozyme Mediated Strategies for the Inhibition of mRNA Expression, Adapted from Rossi, 1995. (In [A] the mRNA base pairs with the antisense construct, in [B] with the ribozyme. See text for further details of each mechanism).

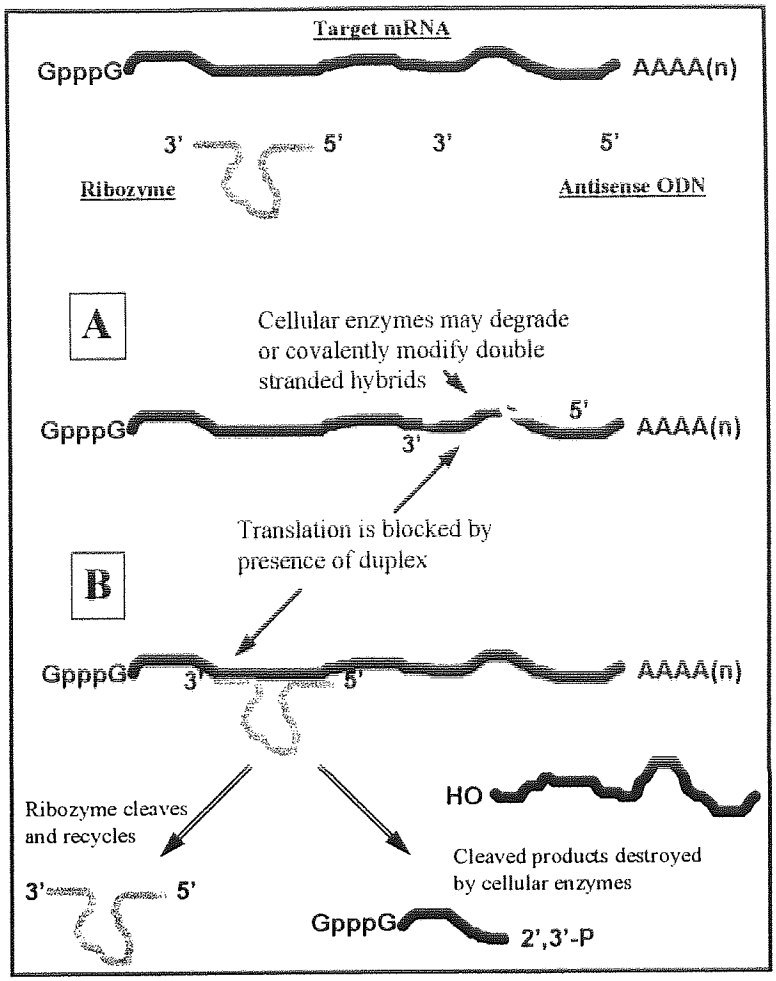

Since it is possible that ribozymes can elicit an 'antisense effect', whenever an inhibitory effect is observed with a ribozyme, the question arises as to whether or not this is due to target cleavage or merely the binding of the ribozyme to the target (Birikh et al, 1997b). Fortunately, the degree of 'antisense effect' can usually be determined by the use of a catalytically inactive ribozyme control. Inactive controls can be prepared by changing the composition of certain bases within the catalytic core of the ribozyme (see Section 1.2.3.1). Where these controls have been used, several investigators have reported an increased inhibitory effect of active ribozymes compared with inactive controls (Tabler *et al*, 1994, Ge *et al*, 1995, Jarvis *et al*, 1996, Flory *et al*, 1996). For example, Flory et al (1996) demonstrated that an active hammerhead ribozyme was able to reduce stromyelsin mRNA levels *in vivo* by 60% following intra-articular injection. By comparison, an inactive control (containing the same binding arms but with two mutations within the catalytic core) did not produce any significant decrease in stromelysin mRNA levels (for further details of this study

see Section 1.4.2.2). This suggested that mRNA cleavage was the mechanism of action rather than an 'antisense effect'. However some researchers have observed no difference at all in the inhibitory abilities of long chain ribozymes and corresponding antisense ORNs (Denman *et al*, 1994).

The major disadvantage of hammerhead ribozymes appears to be their extremely poor stability in biological fluids (Heidenreich *et al*, 1996). Unlike antisense constructs, the nucleotides within ribozymes cannot be uniformly chemically modified without eradicating (catalytic) activity (Usman and Cedergren, 1992). Hence stabilising hammerhead constructs has proved problematic. Nevertheless, considerable advances have been made in this area in recent times (see Heidenreich *et al*, 1994, Beigelman *et al*, 1995 and Section 1.2.4). Overall, ribozyme-based strategies may offer several advantages over their antisense counterparts and these are summarised in Table 1.2.

Table 1.2. A Summary of the Main Potential Advantages and Disadvantages of Utilising Ribozyme-Based Strategies Instead of Antisense Strategies for the Inhibition of mRNA Expression.

Advantages of Ribozymes Based Strategies	Disadvantages of Ribozyme Based Strategies
Ribozymes directly cleave target mRNA molecules to inhibit protein translation.	RNA-based ribozymes are generally less nuclease stable than similar DNA-based oligonucleotides.
Multiple turnover catalysis can allow ribozymes to act upon multiple 'substrate' mRNA molecules.	Target mRNA sequences must contain a specific triplet of nucleotides to permit cleavage (e.g. GUC).
Targeting of smaller recognition sequences within substrate mRNA molecules can improve catalysis.	Uniform chemical modifications cannot be made to ribozymes if catalytic activity is to be preserved.
Specificity of action is dependant upon both substrate binding and cleavage.	Chemical Synthesis of RNA based molecules such as ribozymes is financially more expensive.
The mechanism of ribozyme action is independent of host cell enzyme concentrations (e.g. RNase H).	Host cell concentrations of 'free' divalent metal ions (e.g. Mg^{2+}) must be at 10mM or above for catalysis.

A further point to note, arising from *in vitro* mechanistic studies, is that ribozyme catalysis requires millimolar concentrations of divalent cations such as magnesium (see Section 1.2.3.2.4). It is generally assumed that intracellular concentrations of magnesium are approximately 30mM (Marschall *et al*, 1994). However some proportion of these magnesium ions may be bound to cellular components. Therefore, 'free' concentrations of magnesium within cells may not be at 10mM or above, which

is thought to be optimal for hammerhead activity (Dahm and Uhlenbeck, 1991). This is therefore a potential disadvantage of the hammerhead ribozyme-based strategy which could contribute to a lack of correlation between *in vitro* and *in vivo* results.

1.3.2. Target Site Selection within Messenger RNAs.

The results of *in vitro* kinetic studies using relatively short substrate RNAs have shown that the design of ribozymes is not as simple as it first appears (see Section 1.2.3). For example, alternative, non-binding secondary structures can form within both ribozyme and substrate RNA molecules which can prevent ribozyme / substrate complexes forming and diminish catalytic activity (Walstrum and Uhlenbeck, 1990).

Designing hammerhead ribozymes targeted to large mRNA molecules *in vivo* presents an even greater challenge. Messenger RNA targets will usually be considerably longer (perhaps several hundred times longer) than the small substrate sequences used in most kinetic studies to date. Furthermore they can adopt highly complex secondary and tertiary structures, making target sites potentially inaccessible to ribozymes (Marschall *et al*, 1994).

Computer-based folding algorithms such as MFOLD (Zuker *et al*, 1991) may be a useful aid for predicting some accessible sites within large RNA molecules. However programs such as MFOLD can only identify a small number of folded structures which demonstrate similar free energies. Messenger RNAs within cells probably adopt many different folded conformations, which could exist in a dynamic equilibrium. In fact, some studies have shown that the use of folding programs cannot always be relied upon to identify target sites which can be effectively targeted *in vivo* (Dropulic and Jeang, 1994).

Some success in identifying suitable target sites has been achieved by the use of *in vitro* selection methods. Two different approaches to *in vitro* target selection have been devised which attempt to predict the relative accessibility of sites within large mRNA transcripts *in vitro*: The first uses an antisense ODN based approach to identify accessible sites with mRNA transcripts by their susceptibility to RNase H directed cleavage (Jarvis *et al*, 1996b, Birikh *et al*, 1997a). For example, Birikh *et al* (1997a) synthesised a randomised library of antisense ODNs (10-mers) and incubated them with a full length mRNA transcript *in vitro*, in the presence of RNase H. After 15 minutes at 37°C, RNase H cleavage products were separated by electrophoresis

and compared with appropriate size markers. This information was used to identify sites which were accessible to ribozyme binding. The mRNA sequence was then examined for 'cleavable' nucleotide triplets (e.g. GUC), located close to these 'binding regions' and these were used as targets for ribozyme-mediated cleavage. The ribozymes designed using this technique were 150-fold more active in cleaving a mRNA transcript (*in vitro*) than ribozymes designed using the MFOLD program (Birikh *et al*, 1997a). However this strategy only gives an indication of accessible binding sites and does not necessarily allow sites containing cleavage triplets to be identified. A more direct (and expensive) approach has been described by Lieber and Strauss (1995). This involves the synthesis of an entire library of ribozymes directed against a particular target triplet (e.g. GUC). The ribozymes are screened for their ability to cleave a full length mRNA transcript *in vitro* and the main cleavage products are detected using a complex technique involving 'tailing' and 'PCR cloning'. The use of this technique has allowed precise cleavage sites within a human growth hormone mRNA transcript to be identified. Ribozymes directed against these sites strongly inhibited gene expression in cell culture (Lieber *et al*, 1995).

Despite the apparent success of the empirical approaches described above, these techniques are unlikely to be universally successful in predicting accessible sites within mRNAs *in vivo*. One reason for their possible failure is that mRNA molecules within living cells usually have a multitude of associated protein molecules, which can potentially shield a target site from a ribozyme (Alberts *et al*, 1989, Bratty *et al*, 1993, Marschall *et al*, 1994). These proteins would not necessarily be present *in vitro* unless added to the appropriate media. On the other hand, the presence of certain proteins *in vivo* (such as nuclear proteins) could be beneficial in facilitating ribozyme binding and product release (Tsuchihashi *et al*, 1993, Herschlag *et al*, 1995).

Looking to the field of antisense technology, many ODN constructs have simply been targeted to the AUG initiation codon or to splice-sites within the mRNA which are thought to be accessible (Liebhaber *et al*, 1992). However some studies with ribozymes have contradicted such an approach to site selection (L'Huillier, 1992) and it appears that there is no optimum region for cleavage that is generic to all mRNAs (Rossi, 1995). Perhaps the only all-encompassing approach to determining suitable mRNA target sites is to actually screen a large number of different ribozyme constructs for their ability to reduce mRNA expression in cell culture, or even in animal models. Such an approach has been used recently (in cell culture) to identify ribozymes which can specifically cleave stromelysin mRNA in cultured fibroblast cells (Jarvis *et al*, 1996). However this 'walk the gene' approach is both costly and time-

consuming, therefore the empirical methods discussed above do have some advantages.

1.4. CELLULAR DELIVERY OF HAMMERHEAD RIBOZYMES.

Cellular delivery of hammerhead ribozymes is of crucial importance for the successful inhibition of gene expression using this methodology (Marschall *et al*, 1994). The first major obstacle to the efficient cellular delivery of ribozymes is their nuclease sensitivity within biological fluids (Bratty *et al*, 1993). However several strategies have been devised which can endow ribozyme molecules with nuclease resistance, without significant impairment of catalytic activity (Usman *et al*, 1996). These strategies have been discussed in Sections 1.2.3 and 1.2.4 and some of the other factors involved in the design of hammerhead ribozymes for *in vivo* applications are discussed in Section 1.3.

To function as therapeutic agents, ribozymes must gain access to their target mRNAs within the appropriate cellular compartments, namely the nucleus and cytoplasm. The delivery process therefore encompasses the targeting of ribozymes to cells within specific tissues, their internalisation by these cells and their intracellular trafficking following cell entry.

Two broad strategies can be envisaged for the delivery of ribozymes to their target sites. The first is endogenous delivery (the 'gene therapy' approach, see Section 1.1) which involves the intracellular transcription of a ribozyme-encoding gene via an expression vector (Sokol and Gewirtz, 1996). The second approach, which is still in its infancy, is exogenous delivery, which involves the cellular uptake of pre-formed, synthesised ribozymes (Marschall *et al*, 1994).

1.4.1. Endogenous Delivery.

This report is mainly focused upon ribozyme-based therapeutic applications which employ exogenous delivery strategies for chemically synthesised ribozymes. However a description of the basic concepts of the endogenous delivery approach is included here. Several recent reviews have discussed endogenous delivery and gene therapy in much more detail, these include some discussion regarding the endogenous delivery of ribozymes (Dropulic and Jeang, 1994, Rossi, 1995, Smith, 1995, Bunnell and Morgan, 1996, Sokol and Gewirtz, 1996).

Endogenous delivery requires a vector, which contains the gene encoding the ribozyme along with a suitable promoter gene which will influence its expression once delivered. Viral vectors, such as retroviral vectors or those derived from adenovirus or adeno-associated virus, are by far the most widely used (Rossi, 1995). Non-viral vectors such as liposomes have been used less frequently to produce transient expression of gene products (Bunnell and Morgan, 1996).

Traditionally, retroviral vectors have been the most widely used in gene therapy applications. However the usefulness of retroviral vectors for ribozyme delivery may be limited because of their extremely low efficiency of transduction into non-dividing cells (Rossi, 1995). Perhaps the biggest drawback to the use of retroviral vectors *in vivo*, however, is the random integration of delivered genes into the host cell genome. This represents a potentially dangerous intervention into the genetic structure of the recipient (Marschall *et al*, 1994). This could lead to the unintended silencing of host genes (e.g. tumour suppressor genes) or could even induce the expression of undesirable host genes (e.g. proto-oncogenes) by the introduction of the promoter sequence (Sokol and Gewirtz, 1996). Nevertheless, almost all studies to date which have reported the successful endogenous delivery of ribozymes, have utilised retroviral vectors (Crisell *et al*, 1993, Yu *et al*, 1993, Zhou *et al*, 1994, Sullenger, 1995, Wei *et al*, 1995, Ohta *et al*, 1996a). For example, Zhou *et al* (1994) cloned hammerhead ribozymes, directed against the HIV-1 *tat* and *rev* genes, into a retroviral vector ('LTR-neomycin') under the transcriptional control of polymerase II and III promoters (see below). This vector system allowed the co-expression of the two ribozymes in human-T-lymphocytes. Cells co-expressing the ribozymes were resistant to HIV-1 infection for over 20 days in *ex vivo* studies. In contrast, cells expressing an inactive mutant ribozyme (control), delivered using the same vector system, supported replication of HIV-1. This indicated that the inhibitory effect was due to target cleavage by the ribozymes, rather than an antisense effect (Zhou *et al*, 1994).

Adenoviral vectors demonstrate improved efficiency of transduction into non-dividing cells, however their use is limited by the short duration of expression often seen following their use (Sokol and Gewirtz, 1996). In addition, they integrate randomly into the host genome and therefore there is also concern that constructs delivered by adenoviral vectors may be oncogenic (Bunnell and Morgan, 1996). Nevertheless some investigators have used adenoviral vectors to successfully deliver hammerhead ribozyme constructs in cell culture. For example, Feng *et al* (1995) constructed a recombinant adenovirus to encode an anti-*H-ras* hammerhead ribozyme. Adenoviral genes which were vital for replication, were replaced with genes encoding the *H-ras* ribozyme, along with a non-specific promoter sequence (see below) derived from the

human cytomegalovirus. Hence the recombinant adenovirus was replication defective. This adenoviral vector system allowed the expression of the anti-*ras* ribozyme in human bladder carcinoma cells. Expression of the ribozyme inhibited the growth of these cells, such that no viable cells were identified after 5 days. Growth inhibition was assumed to be a direct result of ribozyme-mediated cleavage of the *H-ras* mRNA (oncogene) because an adenoviral vector lacking the ribozyme gene did not exert any effect on cell growth. However the effects of inactive ribozymes or antisense controls were not measured. The authors also stated that the adenoviral vector system allowed more efficient delivery of the ribozyme encoding gene than other vectors, however, comparative studies were not performed using other viral vector systems in the same cell line.

Perhaps the most promising viral vector, which deserves more evaluation for ribozyme delivery, is the adeno-associated virus (Rossi, 1995). This shows a high transduction efficiency into dividing and non-dividing cells, it integrates specifically into chromosome 19 and the transient expression seen with the adenoviral vector is rarely observed (Sokol and Gewirtz, 1996). Although there are no published reports of the delivery of ribozyme-encoding genes using this vector, it has been used to transduce human hemopoietic cells with an antisense ORN construct targeted to the *TAR* sequence of HIV-1 (Chatterjee *et al*, 1992). Cells expressing the antisense ORN demonstrated over 99% reduction in infectious HIV-1 production following challenge with the virus, with no detectable cellular toxicity. The administration of a similar viral vector which did not express the antisense ORN had no effect on viral replication. However the effects of 'sense' or 'scrambled' (control) ORN sequences were not examined in this study, therefore, it is uncertain whether the inhibitory effect observed was truly an 'antisense' effect.

For the endogenous delivery of ribozymes, the selection of the promoter sequence is critical (for a more detailed review see Rossi, 1995). Promoters can basically be classified into three main types: Inducible promoters that allow the expression of transduced genes to be triggered by external events. For example, heat-inducible promoters have been utilised for ribozyme delivery in fruit flies (Zhao and Pick, 1993). Tissue specific promoters can be also be designed which attempt to restrict the expression of the transgene to a particular target organ. For example, a tyrosinase promoter has been used to achieve tissue specific expression of ribozymes in melanoma cells (Ohta *et al*, 1996a). However, the vast majority of studies involving ribozymes have utilised non-regulated promoters such as RNA Polymerase II or III (for review see Rossi, 1995). However, studies in transgenic mice (i.e. *in vivo* studies) have demonstrated that non-regulated promoters do not necessarily produce an even

expression of transduced ribozymes in all tissues, because preferential expression has been observed in the lungs (Zhou *et al*, 1994). Other factors such as the nature of the viral vector backbone and the precise location at which the promoters are situated within the gene construct, are also important considerations for endogenous delivery (for review see Rossi, 1995).

The main overall advantage of endogenous delivery strategies appears to be the continual (i.e. non-transient) expression which such strategies can produce. However this may not be applicable to all disease states. It could also be argued that the endogenous delivery strategy may be advantageous because the ribozymes produced are not chemically modified and are similar to naturally occurring RNA molecules. Therefore they would be metabolised via natural routes. By comparison, some chemically modified analogues, such as phosphorothioates, do not occur naturally and much less is known about their metabolism *in vivo* (Temsamani *et al*, 1997). Consequently it is possible that chemically modified analogues could generate toxic degradation products following metabolism *in vivo*.

In addition to delivering ribozymes for therapeutic purposes, the endogenous delivery strategy could also be useful for studying and modifying their intracellular transport (Rossi, 1995). There is evidence to suggest that regulatory mechanisms exist in cells, which control the transport of transcribed RNAs from the nucleus to specific compartments in the cytoplasm (Sullenger, 1995). Although these mechanisms have not yet been fully defined, it is thought that molecular 'localisation signals' within natural RNAs influence their trafficking to particular sites (Rossi, 1995). Therefore, it could be possible to attach 'localisation signals' to ribozymes during endogenous expression, which would allow the specific trafficking of high concentrations of ribozymes to the location of their target RNA substrates (Rossi, 1995, Akhtar and Rossi, 1996). Such a strategy would probably benefit the catalytic efficiency of ribozymes, since it has been demonstrated that the co-localisation of a ribozyme with its substrate, following endogenous expression, can considerably enhance ribozyme activity *in vivo* (Sullenger and Cech, 1992).

1.4.2. Exogenous Delivery.

Although a number of laboratories are investigating the delivery of chemically synthesised ribozymes to cells, this area of research remains in its infancy. Many of the strategies under investigation, for the exogenous delivery of chemically synthesised ribozymes, have been used previously to deliver antisense ODNs to cells. It is hoped

that the lessons learnt in improving the delivery of antisense ODNs can be applied to the delivery of ribozymes (Marschall *et al*, 1994 and Elkins and Rossi, 1995, Usman *et al*, 1996). Some investigators have suggested that ribozymes may enter cells via similar mechanisms to antisense ODNs (see below) following (direct) exogenous delivery, because they share many characteristics, such as size and anionic charge (see Section 1.1.1 and Marschall *et al*, 1994, Akhtar *et al*, 1995). Nevertheless, until this study (see also Fell *et al*, 1997) an exact mechanism for the cellular uptake of ribozymes has not yet been described in detail.

1.4.2.1. The Cellular Uptake and Intracellular Fate of Antisense Oligonucleotides.

Mechanism(s) have been described for the cellular uptake of antisense ODNs following exogenous delivery. (For detailed reviews see Akhtar and Juliano, 1992, Rojanasakul, 1996. Also see Section 4.1 for further discussion). Antisense ODNs are taken up poorly by cells following direct administration. (Akhtar and Juliano, 1992). Typically less than 10% of the total quantity added becomes cell associated, and consequently, high concentrations of ODNs are required for biological activity (Wickstrom *et al*, 1988, Wu-Pong *et al*, 1992). Experimental evidence suggests that the uptake of antisense ODNs is energy dependant (Loke *et al*, 1989, Wu-Pong *et al*, 1992) and saturable (Beltinger *et al*, 1995). Some reports suggest that antisense ODN uptake is largely sequence-independent (Yakubov *et al*, 1989, Rojanasakul, 1996). However, other investigators have reported that some ODN sequences, such as those containing 'G'-tetrads, become cell associated in greater quantities than other ODN sequences because they form distinct secondary structures (Hughes *et al*, 1994, Agrawal, 1996).

Passive diffusion is unlikely to account for the mechanism of antisense ODN uptake (Akhtar *et al*, 1991) and the majority of studies conclude that an endocytic mechanism is involved (Akhtar and Juliano, 1992, Rojanasakul, 1996). The existence of specific binding proteins for the uptake of antisense ODNs has been reported (Loke *et al*, 1989, Beltinger *et al*, 1995, Gewirtz *et al*, 1996) although a specific receptor has not yet been categorically defined. Other studies suggest that these antisense ODNs bind to a range of non-specific, cell-surface proteins or lipids (Yakubov *et al*, 1989, Shoji *et al*, 1991, Beck *et al*, 1996). Overall, mechanism(s) of receptor mediated (RME) and / or adsorptive endocytosis (AE) appear to be implicated (see Figure 1.10). Although fluid phase endocytosis (FPE) may predominate when these mechanisms become saturated (Beltinger *et al*, 1995).

Further evidence for an endocytic mechanism of cellular uptake is provided by ultrastructural studies which have shown that antisense ODNs become localised within endosomes following cell entry (Shoji *et al*, 1991, Wagner, 1994, Tonkinson and Stein, 1994, Tarrason *et al*, 1995, Beltinger *et al*, 1995). A small proportion of internalised ODNs appear able to depart endocytic vesicles and enter the nucleus or cytoplasm, although the mechanism for this process has not yet been defined (see Figure 1.10). However a significant proportion may be degraded by nucleases which accumulate within acidified endosomes (lysosomes), or exported from the cell (Loke *et al*, 1989, Wu-Pong *et al*, 1992, Stein *et al*, 1993, Tonkinson and Stein, 1994, Hudson *et al*, 1996a).

Figure 1.10. Schematic Diagram Demonstrating the Cellular Uptake of Oligonucleotides by Endocytosis, Adapted from Akhtar and Juliano, 1992. [Receptor mediated endocytosis (RME), adsorptive endocytosis (AE), fluid phase endocytosis (FPE), receptor (Y), antisense oligonucleotides (•)].

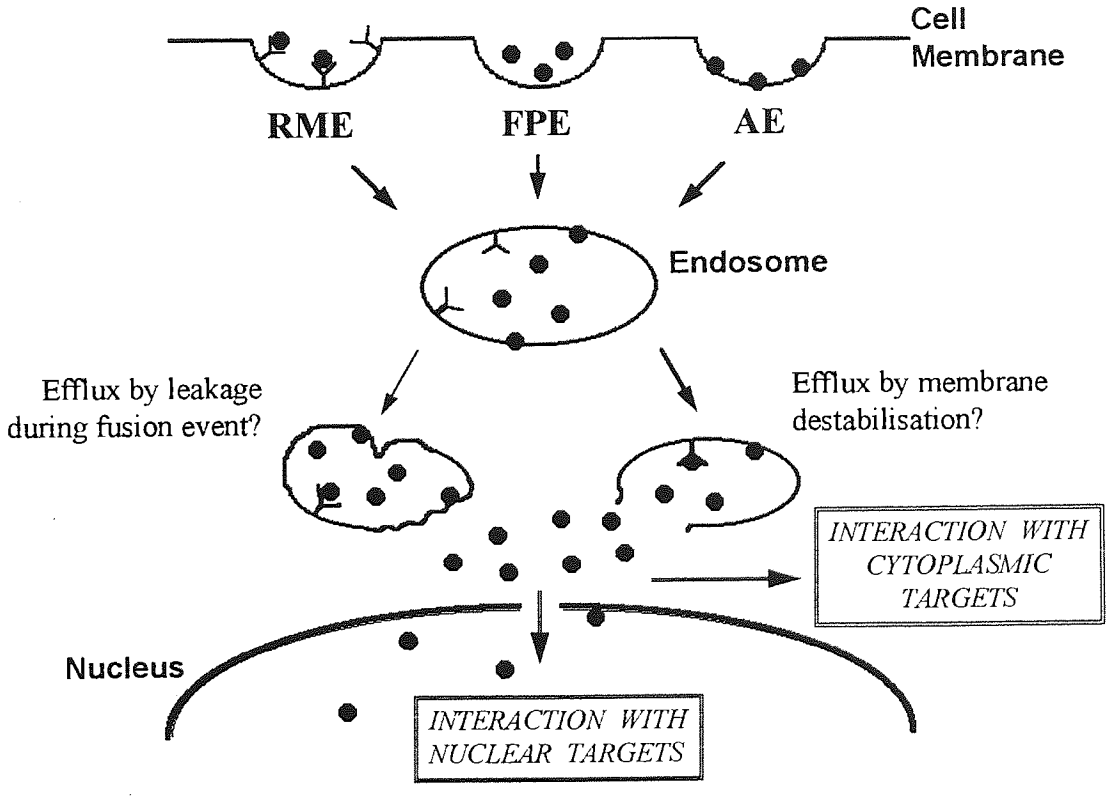

1.4.2.2. Direct Cellular Uptake of Ribozymes

Although not fully defined, the uptake characteristics of hammerhead ribozymes may be similar to those of antisense ODNs (see section 1.4.2.1). Therefore the efficiency of uptake following exogenous delivery is likely to be extremely low (Marschall *et al*,

1994). Nevertheless for diseases in which local or *ex vivo* application is possible, direct delivery of chemically stabilised hammerhead ribozymes may be sufficient (Usman and Stinchcomb, 1996). Indeed, efficacy studies utilising local, direct delivery of stabilised ribozymes are beginning to emerge. For example, two recent reports have described the use of exogenously delivered chimeric hammerhead ribozymes *in vivo*.

Directly delivered, hammerhead ribozymes have been investigated for their potential in reducing the expression of amelogenin, which is a major translation product in the development of tooth enamel (Lyngstadaas *et al*, 1995). New born mice received a single, sub-lingual injection (50μg in 5mL saline) of a chimeric (36-mer), anti-amelogenin mRNA hammerhead ribozyme. The ribozymes contained 2'-O-allyl modified nucleotides at all sites, except for five nucleotides within the catalytic core of the ribozyme which were unmodified. Ribozymes also contained PS linkages in the substrate binding arms. These modifications were designed to improve the stability of the ribozyme construct, however, stability was not actually measured *in vivo*. Levels of amelogenin mRNA expression were measured at various times post-injection. Administration of the ribozyme (50μg) completely eradicated amelogenin mRNA expression for 24 hours post-injection and it took a further 90 hours for levels of amelogenin to return to the levels observed in untreated animals. Other mice were injected with a similar dose of a catalytically inactive ribozyme, which produced 40% inhibition of amelogenin synthesis after 12 hours but normal levels of the protein were observed after 24 hours. An antisense ORN directed to the same binding site produced a similar effect to that of the inactive ribozyme, and a scrambled ORN sequence had no effect. This indicated that the most potent inhibition of mRNA expression could only be achieved via specific, ribozyme-mediated cleavage of the mRNA (Lyngstaadas *et al*, 1995). To further examine the effects of the active ribozyme, mice were sacrificed after five weeks and the molar teeth were examined by electron microscopy. In mice injected with the hammerhead ribozyme, the tooth enamel was found to be severely damaged compared with that of untreated animals. The nature of this damage was considered to reflect decreased levels of amelogenin resulting from ribozyme-mediated inhibition of mRNA expression (Sproat, 1996). However any other effects of the ribozyme, such as toxicity, were not studied in this report.

The expression of the mRNA encoding stromelysin, which is an inflammatory mediator involved in the progression of osteo-arthritis, has also been inhibited *in vivo* by a hammerhead ribozyme (Flory *et al*, 1996). Anti-stromelysin mRNA hammerheads used in this study were chimeric constructs containing 2'-O-methyl / 2'-amino modifications and terminal phosphorothioate linkages, as described by

Beigelman *et al* (1995). Flory *et al* (1996) administered these ribozymes to the synovial tissues in the knee of the rabbit by a single intra-articular injection. Doses ranging from 30ng to 300μg of ribozyme were administered in 0.5mL PBS. Radiolabelled ribozymes extracted from the synovial tissue remained 90% intact after 24 hours and trace quantities of intact ribozymes were observed 7 days after injection (following a 30ng dose). Twenty four hours post-injection, interleukin-1α was injected to the joint to induce stromelysin expression. Six hours later the synovial RNA was harvested from tissues and levels of stromelysin mRNA were detected by northern blot analysis (Flory *et al*, 1996). A dose dependant reduction in stromelysin mRNA expression was observed, 24 hours after administration of the ribozyme. Optimal inhibition was observed at a dose of 100μg, here, levels of stromelysin mRNA were reduced by 60% compared with 'vehicle only' treated animals. By comparison inactive (mutant) ribozymes with similar binding arms, and ribozymes with 'scrambled' binding arms, did not elicit any significant reduction in stromelysin mRNA levels when administered at the same dose. Therefore, the inhibitory effect was considered to be due to cleavage rather than binding alone (Flory *et al*, 1996).

Overall, these studies indicate that ribozymes are able to enter cells following exogenous delivery because they appear able to reach their intracellular substrates. However the mechanism and extent of cellular uptake was not examined and this subject warrants further study.

1.4.2.3. Polymer Devices for the Exogenous Delivery of Ribozymes.

A possible alternative to the direct administration of ribozymes in solution, is their entrapment within polymer devices. Such devices can maintain a reservoir of ribozyme in close proximity to a desired target site (Ayers *et al*, 1996) and can potentially protect the molecule from nucleases, as demonstrated with antisense ODNs (Lewis *et al*, 1995). Following release from the polymer device the 'free' ribozyme would be available for uptake by target cells.

Biodegradable polymer devices, such as poly-(L-lactic acid) (PLA) have been tested *in vitro* for their ability to provide antisense ODNs with nuclease protection. It also appears that formulations of this type can permit sustained release of antisense ODNs over periods of several weeks (Lewis *et al*, 1995). A similar approach has been investigated for using polymer entrapped hammerhead ribozymes *in vitro* (see Hudson *et al*, 1996b).

The polymer approach has also been utilised recently *in vivo* by Ayers *et al* (1996) who formulated chemically stabilised hammerhead ribozymes with poly-(acrylic acid) for ocular delivery in mice (N.B. The target sequence for these ribozymes was not identified in this study). A ribozyme / poly-(acrylic acid) gel was administered to mouse eyes and nuclease susceptibility and autoradiography were used to confirm that ribozymes were internalised within the cornea rather than simply adsorbed to the surface of the eye. Results indicated that 3 to 5% of the administered ribozyme became localised within the epithelial layers of the cornea following the administration of the gel formulation. In contrast, less than 1% was retained by the eye following the administration of the ribozyme in solution. Peak levels were observed in the eye after 30 minutes and ribozymes were also detected in the epithelial cells 3 hours post-administration when the gel formulation was used (Ayers *et al*, 1996).

1.4.2.4. The Potential for Improved Exogenous Delivery of Ribozymes Using Conjugates: Lessons from the Antisense Field.

Another potential option for the exogenous delivery of ribozymes is their attachment to carrier molecules which can enhance cellular uptake. Although very few published studies are available with regard to the application of such techniques to ribozyme technology, several investigators have already applied such strategies to the delivery of antisense molecules: For example, the covalent attachment of lipophillic molecules such as cholesterol (Letsinger *et al*, 1989, Boutorine and Kostina, 1993) and phospholipids (Shea *et al*, 1990) can increase cellular uptake and promote activity when attached to antisense ODNs. However these studies did not determine whether an endocytic mechanism was involved in the uptake of these conjugates.

Antisense ODNs have also been attached to avidin / biotin complexes via electrostatic attraction to poly-(L-lysine) linkers (Pardridge and Boado, 1990, Boado and Pardridge, 1996). Avidin is thought to enter cells via the adsorptive endocytosis pathway and the attachment of the avidin / biotin complex produced a 4-fold increase in cellular uptake *ex vivo* (Pardridge and Boado, 1990). Later studies also showed that conjugation could also improve transport of antisense ODNs across the blood brain barrier *in vivo* following carotid artery perfusion (Boado and Pardridge, 1996).

The conjugation of antisense ODNs to molecules which have a specific receptor has also been examined. This introduces the possibility of receptor mediated delivery which has the potential to increase the cellular uptake of antisense ODNs and also allow targeting to specific cell types, which express particular receptors (For reviews see Boado, 1995, Takaura and Hashida, 1996). For example, the transferrin receptor

is expressed by a variety of cell types and is involved in the intracellular transport of iron-bearing transferrin molecules by receptor mediated endocytosis (Friden, 1993). Conjugation of antisense ODNs to transferrin (the natural ligand) has been shown to improve the cellular uptake of antisense ODNs *ex vivo* (Citro *et al*, 1992). However, when administered *in vivo*, an antisense ODN / transferrin conjugate would theoretically compete with the natural ligand for receptor binding and this could compromise uptake. Therefore an alternative approach is to utilise monoclonal antibodies raised against the transferrin receptor antibody, which bind at a different site to the natural ligand (Friden, 1993). Antisense ODNs conjugated to an anti-transferrin receptor monoclonal antibody achieved a 3-fold increase in cellular uptake *ex vivo*, compared with an unconjugated antisense ODN (Walker *et al*, 1995). The possibility of using this strategy to enhance the exogenous delivery of ribozymes has also been investigated in this report (see Chapter 7).

Ideally a receptor mediated strategy would utilise a receptor, specific for a single cell type, to allow targeted delivery. An example of such a strategy is the targeting of mannose-specific lectins which mediate the cellular uptake of mannose by macrophage cells (Stahl *et al*, 1978). The possibility of hijacking this system to deliver antisense ODNs has been investigated (Akhtar *et al*, 1995b, Liang *et al*, 1996). The covalent attachment of a mannose conjugate to a radiolabelled antisense ODN during chemical synthesis resulted in a 4-fold increase in cellular uptake by macrophage cells *ex vivo* (Akhtar *et al*, 1995b), whereas the addition of mannosylated poly-(L-lysine), electrostatically linked to a fluorescent labelled ODN produced a 17-fold increase in cellular uptake *ex vivo* (Liang *et al*, 1996).

The main limitations to all carrier mediated systems are the escape of the conjugate from the endosomes following internalisation by RME, and the release of the carrier molecule from the antisense ODN (or ribozyme construct) following delivery. In an attempt to improve the release of antisense ODNs from endosomal vesicles following cellular uptake, a strategy involving the attachment of fusogenic peptides to antisense ODNs has been investigated (Bongartz *et al*, 1994). The covalent attachment of Influenza hemaglutinin envelope protein (a fusogenic peptide) to an antisense ODN via a disulphide linkage was shown to produce a 10-fold improvement in the efficacy of an antisense construct *ex vivo*. The presence of the fusogenic peptide was thought to destabilise endosomal membranes and therefore allow greater quantities of internalised ODN to escape from these vesicles and access their target sites (Bongartz *et al*, 1994).

Many of the carrier mediated strategies described above have yet to be evaluated for the delivery of ribozymes. Although the possibility of attaching receptor ligands to ribozymes via poly-(L-lysine) is under investigation. For example Leopold *et al* (1995) improved the cellular uptake of hammerhead ribozymes in leukemic cells by 7-10 fold using folate-conjugated poly-(L-lysine). The delivered ribozyme also produced a 3-fold greater reduction in the expression of *bcr / abl* mRNA expression than ribozymes delivered using the cationic lipid DOTMA (see Section 1.5.2.1.1). The increase in cellular uptake observed was thought to be due to the presence of the folate-conjugate because leukemic cells over-express the folate receptor (Leopold *et al*, 1995).

1.4.2.5. Liposomal Systems for the Exogenous Delivery of Ribozymes.

To date, liposome encapsulation has been the most widely used vehicle for the delivery of antisense ONs (for reviews see Akhtar and Juliano, 1992, Chonn and Cullis, 1995). Liposomes are small spheres of phospholipid bilayer which can either encapsulate nucleic acids within an aqueous core, or can form lipid / nucleic acid complexes due to opposing electrostatic charges. Broadly speaking liposomes can be classified as either cationic or non-cationic based upon the type of lipids used in the formulation (Elkins and Rossi, 1995).

The majority of investigators have utilised commercially available, cationic lipids for the delivery of antisense molecules (Bennett, 1995, Chonn and Cullis, 1995), probably because the inclusion of these positively charged lipids can increase encapsulation efficiency (Juliano and Akhtar, 1992). Cationic lipid formulations demonstrate several properties which are useful for the delivery of polynucleotides (Felgner *et al*, 1994): They spontaneously form complexes with polynucleotides upon mixing in aqueous solution by a condensation reaction (Felgner and Ringold, 1989, Eastman *et al*, 1997), therefore preparation can be relatively straightforward. Complexation with cationic liposomes usually protects polynucleotides from digestion by nuclease enzymes (Lappalainen *et al*, 1994, Bennett, 1995). Also the cationic charge increases the probability of interactions with negatively charged biological surfaces (e.g. cell membrane components) and this is thought to mediate an increase in the cellular uptake of lipid / nucleic acid complexes (Bennett *et al*, 1992).

Studies have shown that the efficiency of cellular uptake of cationic lipid / polynucleotide complexes is dependant upon the cell type (Juliano and Akhtar, 1992, Litzinger *et al*, 1996), the composition of the cationic lipid (Felgner *et al*, 1994) and

the surface charge characteristics of the lipid / polynucleotide complex (Lappalainen *et al*, 1994, Eastman *et al*, 1997).

Several investigators have also studied the mechanism(s) by which cationic liposomes interact with cell membranes. Some reports have suggested that cationic liposomes may fuse directly with the cell membrane (Bennett, 1995) but it appears much more likely that they are internalised by various endocytic or phagocytic processes (Juliano and Akhtar, 1992, Litzinger *et al*, 1996, Zelphati and Szoka, 1996). In the latter scenario, following endocytosis, cationic liposomes would become localised within endosomal vesicles. Some studies have reported that liposomally delivered polynucleotides can, eventually, gain access to sites within the cytoplasm following endocytosis (Felgner *et al*, 1987), while others have proposed that nuclear localisation can occur (Sioud *et al*, 1992). Therefore, it would appear that the exit of ODNs (or ODN / lipid complexes) from endosomal vesicles is possible. In a recent study Zelphati and Szoka (1996) used confocal fluoresence microscopy techniques to demonstrate that ODN / cationic lipid complexes actually become separated following internalisation by monkey kidney fibroblast cells. Three hours after administration to cells, fluorescein labelled ODNs were predominantly localised within cell nuclei, whereas cationic lipids (rhodamine-labelled DOTAP) remained within punctate structures in the cytoplasm. To study the mechanism by which the complexes were separated, anionic lipids (e.g. phosphatidylserine) were added to cationic lipid / ODN complexes *in vitro*. Anionic lipids displaced ODNs from cationic lipid complexes, with an optimal effect observed when the lipids were mixed at an equal (+ / -) charge ratio. On the basis of this finding the authors suggested that following internalisation, ODN / cationic lipid complexes (within endosomes) de-stabilise the endosomal membrane, causing anionic lipids (located mainly on the cytoplasmic face of the endosomal membrane) to 'flip-flop' with cationic lipids within the complex. The anionic lipids diffuse into the complex and form neutral pairs with the cationic lipid molecules. This eventually displaces the ODN from the complex, causing it to diffuse into the cytoplasm (Zelphati and Szoka, 1996). This proposed theory offers a feasible explanation for the mechanism by which ODNs are released from lipid complexes in endosomes. However, it does not explain why only endosomal membranes, and not the cell membrane, can be de-stabilised by ODN / lipid complexes. Therefore, this aspect of the mechanism requires further study, since the endosomal and cell membranes should be of a similar lipid composition.

Although a large number of investigators have utilised liposomes for the delivery of antisense ODNs (for reviews see Juliano and Akhtar, 1992, Chonn and Cullis, 1995, Bennett, 1995, Thierry and Takle, 1995, Rojanasakul, 1996) only a small number of

investigators have examined the use of these agents for ribozyme delivery: An initial study by Sioud *et al* (1992) examined the effects of an anti-tumour necrosis factor-α (TNF-α) ribozyme, delivered to human promyelocytic leukaemia cells via (undefined) cationic liposomes (see also section 1.5.2.2.1). Liposomes were capable of increasing the delivery of ribozymes, allowing 2 to 4% of the administered quantity to be taken up by target cells *ex vivo* when incubated in serum-free media. Furthermore ribozymes remained stable in the intracellular environment and were able to penetrate the nucleus. Both target mRNA and protein levels were reduced by up to 90%, following administration of the ribozyme (for further details of this study see Section 1.5.2.2.1). Taylor *et al* (1992) also reported that cationic liposome (Lipofectin®) mediated delivery of chimeric DNA / RNA ribozymes to human T-lymphocyte cells could improve both cellular uptake and intracellular stability following delivery in serum-free culture media. Experimental data showing the proportion of ribozyme which became cell associated, following cationic liposome mediated delivery, was not shown. However results did show that over 87% of chimeric ribozymes, delivered to T-cells using cationic liposomes, remained undegraded within cells for 6 hours after administration. By comparison, ribozymes which were directly administered, were degraded after 1 hour within cells.

Several subsequent studies have demonstrated that liposomal delivery can allow between 2 and 26% of administered hammerhead ribozymes to be delivered to cells *ex vivo*, following delivery in serum-containing media (Kariko *et al*, 1994, Lange *et al*, 1994, Kiehntopf *et al*, 1994, Jarvis *et al*, 1996). However the actual extent of cellular uptake which can be achieved is considered to be highly cell-type specific (Sullivan, 1993) probably because varying rates of endocytosis / phagocytosis exist between different cell types.

With regard to improving stability, a small number of studies have specifically examined the nuclease stability of ribozymes following liposomal complexation. For example, 30% of an unmodified hammerhead ribozyme remained intact for over 1 hour in 10% foetal bovine serum when complexed with a cationic liposome (DOTMA), whereas 'free' ribozyme was immediately degraded in the same media (Chonn and Cullis, 1995). Ribozymes complexed with cationic liposomes have also demonstrated improved stability when administered to cells in serum-containing culture media. For example Kariko *et al* (1994) observed very little degradation over a 22 hour period when an unmodified hammerhead ribozyme / cationic lipid (DOTMA) complex was administered to human osteosarcoma cells. By comparison, ribozymes which were not complexed with the liposome were degraded almost instantaneously in cell supernatants. Thierry and Takle (1995) also reported resistance

to serum nucleases when hammerhead ribozymes were complexed with non-cationic liposomes via a minimal volume entrapment method. In this study, unmodified ribozymes remained undegraded in 7% foetal calf serum for up to 24 hours when complexed with the liposome. By comparison 'free' ribozymes were instantaneously degraded in the same serum.

Some studies have briefly examined the intracellular fate of cationic liposome-delivered hammerhead ribozymes: Fluorescent localisation studies have indicated that cationic lipid (DOTAP) mediated delivery of hammerhead ribozymes results in a punctate subcellular distribution consistent with endosomal localisation (Lange *et al*, 1994). This indicates that lipid / ribozyme complexes enter cells via an endocytic process. Other studies report both cytoplasmic (Sullivan, 1993, Kariko *et al*, 1994) and nuclear (Sioud *et al*, 1992) penetration of ribozymes following liposomal delivery, thus indicating that ribozymes are able to depart endosomal vesicles when delivered via liposomes.

The fact that liposomal formulations can improve the stability and cellular uptake of synthesised ribozymes *in vitro* will undoubtedly prompt their widespread application to *in vivo* studies. Indeed, cationic liposomes have already been utilised for the exogenous delivery of chemically synthesised ribozymes. For example, Kisich *et al* (1995) and Sioud (1996) have reported the use of a cationic lipid formulations to deliver hammerhead ribozymes to murine peritoneal macrophages *in vivo* (see Section 1.5.2.2.1 and Table 1.3).

There are however some potentially major limitations to the use of cationic lipids as delivery systems for ribozymes and other drugs. At high concentrations, cationic lipids are known to be toxic to cells and therefore conditions must be carefully controlled and optimised (Felgner *et al*, 1994). Toxicity problems may be further compounded when repeated administration of cationic lipids is required (Bennett, 1995), as could be envisaged for many ribozyme applications. Another problem which may cause difficulties in the formulation of most liposomal delivery systems is that complexation with the ribozyme must occur in a serum free environment (Lascombe *et al*, 1996) and optimal cellular delivery only occurs in serum-free conditions (Lewis *et al*, 1996) However, novel lipid systems are under investigation which do not demonstrate this requirement (Lewis *et al*, 1996). The entrapment of foreign particles or drugs during the complexation process could pose further toxicity problems (Felgner *et al*, 1994).

Variations on the liposomal delivery strategy may also be available for ribozyme applications in future. For example liposomes could be targeted to specific cell types

by the attachment of antibodies or targeting ligands to the liposomal membrane, rather than attaching these molecules directly to the ribozyme itself. Antisense ODNs have already been targeted to specific cell types using liposomes bearing monoclonal antibodies (Leonetti *et al*, 1990).

1.5. BIOLOGICAL APPLICATIONS OF THE HAMMERHEAD RIBOZYME.

Since the discovery of ribozymes (see section 1.2.1) a number of investigators have explored the use of these agents in inhibiting the expression of undesirable genes in cells. Similarly, a great deal of effort has been applied to the use of antisense ON technologies for the manipulation of gene expression (see Section 1.1.1). The majority of ribozyme-based applications have focused upon the development of therapies which can either prevent the replication of HIV, or inhibit the expression of oncogenes involved in human cancers (Marschall *et al*, 1994) therefore these studies have received the most attention in this report.

1.5.1. The Efficacy of Endogenously Expressed Ribozymes.

To date, the majority of efficacy studies involving ribozymes have used endogenous expression systems to introduce these agents into various cell types (see section 1.3.1). The main focus of this report is on ribozyme-based therapeutic applications which employ exogenous delivery strategies for chemically synthesised ribozymes, therefore these are dealt with in the most detail in this section. Nevertheless, an overview of several important efficacy studies performed with endogenously expressed ribozymes is included here. For more detailed reviews on the efficacy of endogenously expressed ribozymes refer to Marschall *et al*, 1994, Akhtar and Rossi, 1996, Bertrand and Rossi, 1996.

1.5.1.1. Endogenous Expression of Ribozymes Directed Against HIV.

In principle, ribozymes can be targeted to any stage of the life cycle of human immunodeficiency virus (HIV) where single stranded viral RNAs containing highly conserved sequences are present (Akhtar and Rossi, 1996). HIV-1 target RNA sequences such as *gag*, *env*, *pol* (which encode structural proteins)or *tat* and *rev* (which encode regulatory proteins) have proved especially popular as potential sites for cleavage by ribozymes *in vivo* (Dropulic and Jeang, 1994).

The first demonstration of ribozyme activity (*ex vivo*) against HIV-1, involved the endogenous expression of an anti-*gag* hammerhead ribozyme within Hela CD4+ cells using a retroviral vector system (Sarver *et al*, 1990). Ribozyme-expressing cells were less susceptible to HIV-1 propagation than cells which did not possess the ribozyme, as measured by a 40-fold reduction in the release of the viral p24 antigen (Sarver *et al*, 1990). Later, a package of 'multi-target' ribozymes, targeted to nine different sites within the HIV-1 *env* gene was also expressed within Hela cells. This strategy proved to be highly effective in inhibiting viral replication (90% effective compared with controls), as measured by levels of p24 antigen production (Chen *et al*, 1992). However it is uncertain as to whether the effects observed in both these early studies were a result of specific, ribozyme-mediated cleavage of the target genes because neither 'inactive' nor 'antisense' controls were used.

Inhibition of HIV-1 replication, resulting from specific cleavage by hammerhead ribozymes, has subsequently been demonstrated following endogenous expression (via a retrovirus) in cultured T-lymphocytes (Crisell, 1993). In this study, an active ribozyme construct inhibited HIV-1 replication by up to 98%, 7 days after viral challenge. By comparison, an inactive ribozyme and antisense ORN controls, targeted to the same binding site, did not inhibit HIV-1 replication.

More recent studies, which utilised a novel retroviral expression system, demonstrated that cultured human-T-Lymphocytes could be rendered completely resistant to HIV-1 replication for over 20 days, when anti-*tat* and anti-*rev* hammerheads were co-expressed (for further details of this study see Section 1.4.1 and Zhou *et al*, 1994). The same group has since reported that a similar immunisation against HIV-1 infection can be achieved when the same ribozyme constructs are endogenously expressed in primary bone-marrow derived monocytes (Bertrand and Rossi, 1996).

In a recent article, it is reported that a group lead by Tom Cech is aiming to begin phase I clinical trials with multi-target hammerhead ribozymes directed against the HIV-1 *tat* and *rev* genes (see Coghlan, 1996). These trials will involve the endogenous expression of hammerhead ribozymes in CD34+ primordial blood cells derived from HIV-positive patients, using a retroviral vector system. Cech's group claim that preliminary results show CD34+ cells, and other blood cells descending from these, can express hammerhead ribozymes and resist HIV infection. Therefore, it is hoped that CD34+ cells can be modified and returned to HIV-positive patients in order to 're-stock' their immune systems with HIV-resistant cells (Coghlan, 1996). Similar trials are also being planned by another group (see Sun *et al*, 1997). These trials still require regulatory approval but their results are eagerly anticipated.

However, there is concern that the endogenous expression of ribozymes within CD34+ cells will prove problematic due to the fragility of these cells, hence, this may limit the success of human trials (see Coghlan, 1996).

In addition to the studies performed with the hammerhead, hairpin ribozymes have also shown promise with regard to the inhibition of HIV-1 replication, following endogenous expression. The studies involving the hairpin ribozyme are summarised in Section 1.2.2.3.

The endogenous delivery approach has also been used to study the effects of co-localising ribozymes with their intracellular targets. For example anti-HIV hammerhead ribozymes have been fused with a tRNA construct and expressed in human embryonic kidney cells (Westaway *et al*, 1995). The tRNA / ribozyme construct became bound to viral proteins (namely HIV reverse transcriptase) following expression, and hence, became packaged with viral components in the cytoplasm. This was thought to contribute to the 20-fold reduction in the infectivity of HIV-1 which was subsequently observed (Westaway *et al*, 1995).

1.5.1.2. Endogenous Expression of Ribozymes Directed Against Cancer and Other Targets.

Endogenously expressed ribozymes have also been developed which can decrease the expression of a variety of oncogenes in neoplastic cells. Inhibition of oncogenesis can potentially reduce proliferation or promote apoptosis ("programmed cell death") in cancer cells (Prochownik, 1993, Goyns, 1995). Ribozymes have the ability to distinguish mutated RNA transcripts which differ from the 'wild type' by only one nucleotide. Hence the opportunity exists to eliminate mutant gene expression without affecting that of normal host genes. For example, the expression of *c-fos* mRNA has been inhibited with endogenously expressed hammerhead ribozymes in an ovarian cancer cell line, selected for cisplatin resistance (Scanlon *et al*, 1991). The *fos* gene product has been implicated in several aspects of malignant cell growth and elevated levels appear to confer resistance to chemotherapeutic drugs such as cisplatin. Hammerhead ribozyme expression resulted in a 7-fold stronger suppression of *c-fos* than an inactive mutant ribozyme. In addition, the cisplatin resistant phenotype was reversed in ribozyme treated cells (Scanlon *et al*, 1991).

Koizumi *et al* (1992) expressed a variety of hammerhead ribozyme constructs targeted to *c-Ha-ras* mRNA (which contains a single GGU to GUU point mutation) in NIH3T3 cells. Ribozyme expression resulted in a 50% reduction in the number of

transformed cell foci and this effect was shown to be a result of catalytic cleavage rather than an antisense effect.

Cai *et al* (1995) have targeted mutated *p53* pre-mRNA with hammerhead ribozymes retrovirally expressed in a human lung cancer cell line. Mutations to the *p53* gene are the most common alterations identified in human cancer and are thought to be involved in the loss of tumour suppressor function. Catalytic cleavage of the mutant p53 mRNA, but not the 'normal' host p53 mRNA, was demonstrated *ex vivo* although this did not suppress tumour cell growth.

A number of reports by Scanlon and co-workers have described the use of several endogenous delivery strategies (including adenoviral and retroviral vectors with tissue specific promoters) to express hammerhead ribozymes targeted against mutated (oncogenic) *H-ras* mRNA. The suppression of malignant phenotypes in both human melanoma cells and human bladder carcinoma cells has been achieved using these strategies (Feng *et al*, 1995, Ohta *et al*, 1996a & 1996b).

With regard to other, non-cancer applications of endogenously expressed hammerhead ribozymes; a small number of studies have progressed to testing the efficacy of ribozymes *in vivo* in transgenic mice. For example Larsson *et al* (1994) demonstrated a 90% reduction in target mRNA levels when an anti-β-2-microglobulin hammerhead ribozyme was expressed in transgenic mice using a retroviral vector system. More recently, L'Huillier (1996) has described the use of hammerhead ribozymes targeted to bovine α-lactalbumin mRNA. Ribozymes were expressed in murine mammary tissue by the use of a vaccinia virus vector. Ribozyme activity produced a 40% reduction in mRNA expression *in vivo* using this technique.

1.5.2. Efficacy of Exogenously Delivered Ribozymes

Of the efficacy studies which have involved exogenous delivery; the majority have utilised ribozymes prepared by *in vitro* transcription techniques. However, recent improvements in the chemical synthesis of RNA (Wincott *et al*, 1995, Rao *et al*, 1995) have allowed site-specific chemical modifications to hammerhead ribozymes which can enhance the nuclease stability of these constructs (Usman *et al*, 1996). Hence a small number of efficacy studies have been reported which have utilised exogenously delivered, synthetic hammerhead ribozymes. These studies are described below and have also been summarised in Table 1.3.

1.5.2.1. Efficacy of Exogenously Delivered Ribozymes Directed Against Genes Involved in Cancer.

1.5.2.1.1. Ribozymes Targeting *bcr / abl* as Potential Therapies for CML.

The molecular event underlying the creation of the Philadelphia chromosome in chronic myelogenous leukemia (CML) involves a translocation between the *abl* and *bcr* genes on chromosomes 9 and 22. The resulting transcription and translation products, *bcr /abl* mRNA and p210 protein, are unique to malignant cells and represent a target for drug intervention. Selective inhibition of *bcr / abl* mRNA would be required in order to spare the wild type genes in normal cells, whilst purging the mutant genes in leukemic cells (Kronenwett *et al*, 1996). However targeting of the *bcr / abl* mRNA is somewhat more complex than the targeting of a gene bearing a point mutation because both normal and CML cells have the same mRNA sequence, but in CML cells the order of the two sequences is altered (James *et al*, 1996). Ribozymes show considerable potential in inhibiting *bcr / abl* expression because they owe their specificity to both mRNA binding and cleavage (Kronenwett *et al*, 1996). A number of different groups have used exogenously delivered hammerhead ribozymes to illustrate that several sites within the *bcr / abl* mRNA are susceptible to catalytic cleavage (Snyder *et al*, 1993, Lange *et al*, 1994, Leopold *et al*, 1995).

Snyder *et al* (1993) delivered chemically synthesised, chimeric DNA / RNA ribozymes to human myelogenous leukemia cells (bearing the *bcr / abl* translocation) using a commercially available cationic lipid formulation (Transfectam®). This resulted in a 49% reduction in *bcr / abl* mRNA levels, and a complete inhibition of p210 production by the leukemic cells after 72 hours. The ribozyme also inhibited cellular proliferation by 84% during this time period. By comparison, an antisense ODN control was shown to be less effective than the ribozyme in inhibiting *bcr / abl* expression, but this alone did not demonstrate specificity of *bcr / abl* mRNA cleavage.

Lange *et al* (1994) synthesised 5'-capped ribozymes using an *in vitro* transcription technique. These were exogenously delivered into a *bcr / abl* bearing cell line using the cationic lipid 'DOTAP'. Treatment with the ribozyme produced a 3 to 5-fold reduction in *bcr /abl* mRNA and reduced cell proliferation by 60 % after 72 hours. In this study, mismatched ribozymes and antisense RNA controls were also tested for efficacy and were found to be less than 50% as effective as the targeted ribozyme. Consequently the authors stated that this represented specific *ex vivo* cleavage of the *bcr / abl* mRNA, although wild type *abl* and *bcr* controls were not used.

Leopold *et al* (1995) used an *in vitro* transcription technique to produce RNA sequences bearing three hammerhead constructs, targeted to sites near to the *bcr / abl* junction. These were exogenously delivered to cells as a complex with folate conjugated poly-(L-lysine). The 'triple-unit' ribozyme reduced levels of *bcr / abl* mRNA by 1000-fold after 24 hours, and was more effective than the individual ribozymes alone. Furthermore, an inactive (control) ribozyme did not reduce levels of the *bcr / abl* mRNA. However, further experiments indicated that cleavage of *bcr / abl* mRNA by the active ribozyme was not specific because wild type *abl* and *bcr* mRNAs were also cleaved by the 'triple-unit' ribozyme (Leopold *et al*, 1995).

Recently, the focus appears to have shifted to improving the selectivity of hammerhead ribozymes directed against *bcr / abl* mRNA *in vitro*, before *ex vivo* studies proceed (James *et al*, 1996, Kronenwett *et al*, 1996). This should aid in the design of hammerhead constructs for future *ex vivo* studies, which must demonstrate specificity of action against *bcr / abl* and not the wild type genes. In addition it would be preferable if patient derived cell lines, rather than transformed cell lines were used in future *ex vivo* studies (Kronenwett *et al*, 1996).

1.5.2.1.2. Ribozymes Targeting *mdr*-1 To Reduce Drug Resistance in Cancer.

Multi-drug resistance (MDR) is one of the major impediments to the success of conventional cancer chemotherapy agents. The mechanism underlying this resistance involves the over-expression of a phosphoglycoprotein, coded by the *mdr*-1 mRNA, which functions as a drug efflux pump (for review see Endicott and Ling, 1989).

In an attempt to reduce the expression of *mdr*-1 mRNA; chimeric DNA / RNA hammerhead ribozymes were designed which contained deoxyribonucleotides within the substrate binding arms and 2'-fluoro modifications at all pyrimidine nucleotides within the catalytic core and Stem-Loop II (Kiehntopf *et al*, 1994). Such modifications have been shown to protect the molecule from nuclease digestion (see section 1.2.4). These chimeric hammerheads were exogenously delivered to drug resistant mesothelioma cells using the commercially available cationic lipid formulation 'Lipofectin®' (DOTMA). The administration of the ribozyme produced a 93% reduction in phosphoglycoprotein pump expression at the surface of chemo-resistant cells. In addition the resistance of these cells to doxorubicin and vindesine was reversed. Control experiments demonstrated that an all-RNA ribozyme had no effect on mRNA expression or drug resistance, presumably because of nuclease degradation of this molecule (Kiehntopf *et al*, 1994). An all-RNA inactive ribozyme (control) was also shown to be ineffective, however, this did not indicate specific

target cleavage by the (active) ribozyme because it is likely that the inactive construct was also unstable. Therefore, the use of a chemically stabilised (inactive) control would have been more suitable.

1.5.2.1.3. Ribozymes Targeting Mediators of Cancer Metastasis.

Glioblastomas (also see section 1.6) are highly invasive intracerebral tumours which are known to express the CD44 glycoprotein molecule, which is a mediator of cellular adhesion and invasion. Ge *et al* (1995) synthesised an all-RNA hammerhead ribozyme using an *in vitro* transcription technique, which was designed to cleave exon 2 of the CD44 mRNA and, therefore, reduce the expression of this glycoprotein. The ribozyme was exogenously delivered to human glioma cells using the cationic lipid formulation 'Lipofectamine®' (DOSPA). Immuno-fluorescent techniques were used to show that 20-30% of cells treated with the ribozyme had significantly decreased, or totally eliminated, expression of the CD44 glycoprotein at the cell surface, 48 hours after administration. By comparison, a catalytically inactive ribozyme (control), delivered to cells in a similar manner, had no effect on the expression of the CD44 glycoprotein. This indicated that the observed effect was due to ribozyme mediated-cleavage of the CD44 mRNA (Ge *et al*, 1995).

1.5.2.1.4. Ribozymes Targeting the RNA Component of Telomerase

Eukaryotic chromosomes are capped with repetitive telomeres which appear to be involved in maintaining chromosomal integrity and cellular proliferative capacity (Kanawa *et al*, 1996). In normal somatic cells each cycle of cell division results in the loss of telomeres, and hence, the lifespan of such cells is finite. Many malignant cells, however, do not show any net loss of telomeres following cell division because they posses telomerase, a ribonucleoprotein which directs the synthesis of new telomeric DNA repeats (Kanawa *et al*, 1996). Hence, telomerase itself, is a potential differential target for anti-cancer therapy and hammerhead ribozymes directed against the RNA component of this molecule are under investigation for this purpose. Hammerhead ribozymes prepared by an *in vitro* transcription technique have been shown to specifically cleave the RNA component of telomerase in extracts of hepatocarcinoma cells (Kanawa *et al*, 1996). The specific cleavage of the RNA component resulted in a 50-80% reduction in telomerase activity in cell extracts (Kanawa *et al*, 1996). However neither *ex vivo* or *in vivo* activity were demonstrated in this study. Nevertheless, ribozymes directed against telomerase have enormous potential as anti-cancer agents because they could be completely non-toxic to somatic cells which do

not possess the target molecule. Hence the use of ribozymes targeted against telomerase is an interesting prospect for future studies.

1.5.2.2. Efficacy of Exogenously Delivered Ribozymes Directed Against Other Targets.

Probably as a result of the advances which have been made in inhibiting HIV-1 replication using endogenously expressed ribozymes (see section 1.5.1.1), there has been little interest in using exogenously delivered ribozymes to inhibit HIV-1 replication in either *ex vivo* or *in vivo* efficacy studies. However several other potential therapeutic applications have received considerable interest:

1.5.2.2.1. Ribozymes Targeting Tumour Necrosis Factor-α.

Among the multiple factors released from mononuclear cells, the pro-inflammatory cytokine; tumour necrosis factor-α (TNF-α) has been shown to be responsible for auto-aggression by a variety of mechanisms. TNF-α is believed to play a key role as a mediator of septic shock, cancer cachexia, rheumatoid arthritis and other auto-immune diseases and the expression of this cytokine therefore represents a target for the treatment of these diseases (Sioud, 1996).

Anti-TNF-α hammerhead ribozymes were first synthesised using an *in vitro* transcription technique by Sioud *et al* (1992). These ribozymes were exogenously delivered to human myelomonocytic cells in culture, using an un-identified cationic lipid formulation. Treatment with these ribozymes reduced TNF-α mRNA levels by 80-90% and produced a 70-85% reduction in the secretion of TNF-α protein by these cells *ex vivo*. In subsequent studies (Sioud, 1996), the hammerhead ribozymes were modified to accommodate a protein binding region at the terminus of the molecule. These hammerheads again proved effective in inhibiting TNF-α mRNA expression when delivered *ex vivo* using (unspecified) cationic lipids. Consequently, they were complexed with cationic lipids and delivered to BALB/c mice by intra-peritoneal injection (total dose of ribozyme was 10 nanomoles), in order to assess *in vivo* efficacy. Fluorescent labelling of an ON marker, combined with flow cytometric analysis, indicated that approximately 60% of the administered dose was taken up by peritoneal cells *in vivo*. Moreover, the administration of the ribozyme resulted in a 50% reduction in TNF-α protein secretion by peritoneal cells when compared with control animals, which were dosed with an *E. coli* tRNA rather than the ribozyme (Sioud, 1996). However, an inactive ribozyme construct was not used as a control in

these studies, therefore, it is not clear whether the observed effect was due to catalytic cleavage by the ribozyme.

Kisich *et al* (1995) also demonstrated *in vivo* efficacy of anti-TNF-α hammerhead ribozymes when the cationic lipid 'DOSPA' was used to exogenously deliver ribozymes to peritoneal cells *in vivo*. Approximately 25% of an administered dose of hammerhead ribozymes accumulated within macrophages after 3 hours, when injected into the peritoneal cavity of mice. However the exact dose administered to the animals was not stated. To test the efficacy of the ribozyme, peritoneal macrophages were harvested from the mice and levels of TNF-α secretion were determined *ex vivo*. The active ribozyme inhibited TNF-α secretion by 85%, whereas a catalytically inactive control inhibited secretion by 45%. An addition (control) ribozyme with scrambled binding arms did not significantly inhibit TNF-α secretion. Thus indicating that efficient TNF-α suppression requires both binding and catalytic activity by hammerhead ribozymes (Kisich *et al*, 1995, Usman and Stinchcomb, 1996).

1.5.2.2.2. Ribozymes Targeting *c-myb*.

The proto-oncogene *c-myb* is thought to be a critical regulator of smooth muscle proliferation. The hyperproliferation of smooth muscle often occurs in coronary arteries following angioplasty treatment, therefore the inhibition of *c-myb* mRNA expression is a potential target in the prevention of artery restenosis following this type of surgery (Jarvis *et al*, 1996).

Chemically modified hammerhead ribozymes based on the stabilised constructs of Beigelman *et al* (1995) have recently been designed to target *c-myb* mRNA expression (Jarvis *et al*, 1996). Three different hammerheads were chemically synthesised and complexed with the cationic lipid 'DOSPA' for exogenous administration to rat aortic smooth muscle cells. The active hammerhead constructs reduced levels of *c-myb* mRNA expression by up to 80% relative to a catalytically inactive ribozyme control. Furthermore, the active ribozymes were at least twice as effective in inhibiting *c-myb* expression as a series of antisense PS-ODNs directed to the same target site. Thus indicating that ribozymes had superior efficacy and showed greater specificity than antisense ODNs (Jarvis *et al*, 1996).

1.5.2.2.3. Ribozymes Targeting Amelogenin mRNA

Chemically modified hammerhead ribozymes have been directed against amelogenin mRNA, which expresses a major translation product involved the development of-

tooth enamel (Lyngstadaas *et al*, 1995). 'Free' ribozymes, administered directly to new born mice via a single sub-lingual injection, have been shown to specifically reduce mRNA expression *in vivo* (Lyngstadaas *et al*, 1995 and Sproat, 1996). The details of this study are described in Section 1.4.2.2 (and summarised in Table 1.3), however, it is not discussed further here because there is no apparent therapeutic advantage in targeting this particular gene.

1.5.2.2.4. Ribozymes Targeting Stromelysin mRNA.

Excessive levels of stromelysin, a matrix metalloproteinase, are thought to be responsible for the degradation of cartilage in osteoarthritis. Flory *et al* (1996) have demonstrated that the expression of stromelysin mRNA can be inhibited with hammerhead ribozymes in vivo. This study is discussed in detail in Section 1.4.2.2. The authors concluded that hammerhead ribozymes could be useful in reducing the active joint degradation that occurs in patients with osteoarthritis (Flory *et al*, 1996) . This study perhaps best demonstrates the speed with which advances have been made in hammerhead ribozyme technology in recent years. The demonstration that chemically synthesised, exogenously delivered hammerhead ribozymes can be active *in vivo*, will undoubtedly prompt the initiation of human trials in the near future.

Table 1.3. Examples of *Ex Vivo* and *In Vivo* Inhibition of mRNA Expression by Exogenously Delivered Hammerhead Ribozymes (also see relevant Sections above for further details of these studies).

Genetic Target (reference)	Cleavage Triplet Targeted	Ribozyme Length and Type	Delivery Method	Cell Line / Animal Model	Comments (also see text)
bcr / abl mRNA (Snyder *et al*, 1993)	GUU	40-mer Chimeric DNA / RNA ribozyme	cationic lipid complex (Transfectam®)	EM-2 human myelogenous leukemia cells	49% decrease in *bcr/abl* mRNA. 84% decrease in cell proliferation after 72 hours.
bcr /abl mRNA (Lange *et al*, 1994)	GUU	50-mer all-RNA ribozyme	cationic lipid complex (DOTAP)	K562 human myelogenous leukemia cells	5-fold decrease in *bcr /abl* mRNA. 60% decrease in cell proliferation after 72 hours.
bcr / abl mRNA (Leopold *et al*, 1995)	GUC, GUU, and GUA	large all-RNA transcript bearing three ribozyme motifs	folic acid / polylysine carrier complex	Transformed 32D murine myeo-blastoma cells	1000-fold decrease in *bcr / abl* mRNA after 24 hours.
mdr-1 mRNA (Kiehntopf *et al*, 1994)	GUC	42-mer chimeric 2'-fluoro-modified ribozyme	cationic lipid complex (DOTMA)	PXF118 human pleural mesothelioma cells	93% Reduction in protein levels. Reverse of drug-resistant phenotype after 72 hours.
CD44 mRNA (Ge *et al*, 1995)	GUA	38-mer all-RNA ribozyme	cationic lipid complex (DOSPA)	SNB-19 human glioma cells	Expression of CD44 adhesion protein decreased in up to 30% of cells after 48 hours.
c-myb mRNA (Jarvis *et al* 1996)	AUC	36-mer chimeric 2'-O-Methyl / 2'-C-allyl ribozyme	cationic lipid complex (DOSPA)	Rat aortic smooth muscle cells (RASMC)	80% reduction in *c-myb* mRNA levels after 12 hours.
TNF-α mRNA (Kisich *et al*, 1995)	Not identified	36-mer all-RNA Ribozyme	i.p. injection of ribozyme / cationic lipid complex (DOSPA)	Mice (total dose not identified)	85 % reduction in TNF-α protein secretion by peritoneal macrophages
TNF-α mRNA (Sioud 1996)	GUC	45-mer 5'-capped RNA ribozyme	i.p. injection of ribozyme / cationic lipid complex	BALB/c mice (10 nmoles total dose of ribozyme)	50% reduction in TNF-α protein secretion by peritoneal macrophages
amelogenin mRNA (Lyngstaadas *et al*, 1995)	GUC	38-mer chimeric 2'-O-allyl-modified ribozyme	direct sub-mandibular injection	New-born BALB/c mice. (50μg total dose)	Eradication of protein synthesis for 24 hours. Alteration of tooth phenotype
Stromelysin mRNA (Flory *et al*, 1996)	CUC	36-mer chimeric 2'-O-Methyl / 2'-amino ribozyme	direct intra-articular injection to the knee joint	New Zealand male white rabbits (100μg total dose)	60% reduction in stromelysin mRNA levels.

1.6. RIBOZYMES AS POTENTIAL THERAPEUTIC AGENTS IN GLIOBLASTOMA MULTIFORME.

1.6.1. An Overview of Glioblastoma Multiforme and Its Treatment.

Malignant gliomas account for approximately 2.5% of all cancer deaths world-wide in any given year and are by far the most common form of primary tumour arising from the central nervous system (Louis and Seizinger, 1994). 'Glioma' is a general term which encompasses a range of neoplasms derived from several neuronal cell types which are both morphologically and biologically heterogeneous (Louis and Seizinger, 1994). Astrocytomas account for the majority (75-90%) of all gliomas, and these in turn can be further subdivided according to their histological features (Wong *et al*, 1994). The most malignant and frequently occurring subtype of astrocytoma can be classified as 'high grade' astrocytoma and this has been called 'glioblastoma multiforme' (Louis and Seizinger, 1994).

Glioblastoma multiforme (GBM) accounts for approximately one third of all brain tumours and the prognosis for sufferers is extremely poor (Petersdorf and Livingston, 1994). Despite a number of advances in the past decades in the treatment of other cancers, medicine is yet to make a significant impact on the treatment of GBM (Selby, 1994). Statistics demonstrate that the median survival rate following diagnosis is less than one year (Petersdorf and Livingston, 1994). Clinically, GBM is usually characterised by its highly invasive nature, its ability to metastasise widely whilst avoiding recognition by the immune system and its high recurrence rate following any form of existing treatment (Louis and Seizinger, 1994).

The cell type(s) from which GBM originates have not been categorically defined, although it is often assumed that astrocytes are the source because histological markers for these cells are frequently present within the cytoplasm of cells (Wong *et al*, 1994). The extremely varied histological morphology which often presents in cell biopsies has actually given rise to the term 'multiforme' (Wong *et al*, 1994).

The cornerstone of existing treatment for GBM usually involves a combination of surgery and radiotherapy (Petersdorf and Livingston, 1994). Depending on the location of the tumour site within the brain, surgical removal can often provide temporary relief for patients but rarely, if ever, provides a permanent cure (Selby, 1994). GBM generally exhibits a remarkable resistance to radiotherapy, and therefore, tumouricidal doses can rarely be administered without severely affecting surrounding

tissues. Nevertheless radiotherapy is often used following surgery in an attempt to limit the extent of tumour regression (Leibel *et al*, 1994).

Chemotherapy has generally been ineffective, even when used as an adjunct to other treatments (Petersdorf and Livingston, 1994). Despite the fact that several agents have demonstrated cytotoxicity *in vitro*, their *in vivo* efficacy is usually poor, probably as a result of their poor penetration of the blood brain barrier following administration (Chiang *et al*, 1995). High doses of the more lipid soluble agents, such as the nitrosureas (e.g. carmustine, lomustine, semustine and nimustine), are under investigation as an adjunct to surgery and have shown more promising effects (Petersdorf and Livingston, 1994). Although results do not indicate that these drugs will offer a potential cure.

As traditional therapies for GBM appear to have developed as far as possible (Selby, 1994) it is widely considered that any possible cure for this condition is likely to arise from an increased understanding of the molecular genetics of the disease. Therapies which can intervene in the genetic malfunctions which occur in GMB can potentially be much more effective and demonstrate fewer side effects than traditional drugs (Chiang *et al*, 1995).

1.6.2. The Molecular Genetic Basis of Glioblastoma Multiforme.

The transformation of normal cells to malignant tumours is often a complex, multi-stage process characterised by inappropriate cell proliferation relative to the rate of cell differentiation. The mutation of particular genes is usually involved and causes one cell to divide and grow at the expense of others. Furthermore, abnormal cells may metastasise from their site of origin and invade the territory of other cells (Modjtahedi and Dean, 1994).

Tumour promoting 'proto-oncogenes' are often amplified and can be converted into oncogenes whose products are over-expressed and / or mutated in some way. Alternatively 'tumour suppressor genes' may become inactivated or mutated and this can also play a major role in the development of many of cancers (Modjtahedi and Dean, 1994).

Many detailed cytogenetic studies have been performed in GBM and have revealed common genetic abnormalities amongst sufferers (for detailed reviews see Khaziaie *et al*, 1993, Louis and Seizinger, 1994, Wong *et al*, 1994, Grunt and Huber, 1994, Hoi-

Sang *et al*, 1995). In summary, it appears that allelic losses or mutations on chromosomes 17p and / or 10 are the most common alterations in GBM. Although a number of different oncogenes have been implicated in GBM (e.g. *c-myc*, *ros*-1, *c-myb* and *gli*), two specific genes appear to be implicated (often independently) in the vast majority of studies:

The tumour suppressor gene *p53* is located on chromosome 17p and is thought to be mutated or lost in approximately 50-80% of all GBM cases (Kordek *et al*, 1995). Mutations to the *p53* gene result in the expression of a mutant p53 protein which has been implicated in a variety of cancers (Louis and Seizinger, 1994). Mutations to *p53* occur with similar frequency in GBM to other types of astrocytoma, consequently GBMs with such an alteration may originate from other 'lower grade' astrocytoma which de-differentiate into GBM (Kordek *et al*, 1995).

Often independently of any mutation to the *p53* gene, the epidermal growth factor receptor (EGFr) gene is amplified or over-expressed in 30-60% of GBM cases (Kordek *et al*, 1995). This is thought to be directly correlated to mutations or allelic losses on chromosome 10, which are essentially restricted to GBM and are uncommon in other forms of astrocytoma (Modjtahedi and Dean, 1994). In approximately half of all cases, the amplification of the EGFr gene is accompanied by the co-expression of mRNA for at least one of its growth factor ligands (e.g. epidermal growth factor (EGF)). Hence it appears possible that an autocrine stimulatory loop can develop and this provides a mechanism by which the neoplastic cell escapes normal physiological control (Modjtahedi and Dean, 1994).

The fact that *p53* mutation and 17p loss appear to be alternative genetic events to EGFr amplification suggest that at least two distinct subsets of GBM may occur (for review see Loius and Seizinger, 1994). Studies have shown that GBMs with EGFr amplification usually occur in older adults (more commonly in males) and are associated with an extremely poor prognosis. Whereas GBMs with *p53* mutations usually occur in younger adults (more commonly in females) and although they too are almost always fatal, the progress of the disease is often less aggressive (Modjtahedi and Dean, 1994).

Strategies which can inhibit the production of mutated *p53* proteins and / or reduce the expression of EGFr mRNA would therefore appear to have considerable potential in reducing the progression of GBM and could even result in a cure. Ribozymes have the potential to inhibit gene expression in a highly specific manner consequently if they can be effectively directed against mutated *p53* mRNA and / or EGFr mRNA they

could be effective therapies for GBM. In fact, the prospect of reducing the expression of mutated *p53* pre-mRNA with ribozymes, whilst maintaining the expression of the 'wild type' gene, has already been investigated in *ex vivo* studies (Cai *et al*, 1995 also see Section 1.5.1.2).

During this thesis, the possibility of reducing EGFr mRNA expression with hammerhead ribozymes has been the main goal and hence this strategy is discussed in more detail below.

1.6.3. The Epidermal Growth Factor Receptor mRNA as a Target for Hammerhead Ribozymes.

The epidermal growth factor receptor (EGFr) is one of a family of *c-erb*B receptors which are becoming increasingly recognised as an important cross-connected signal transduction system that controls normal cell development (for review see Grunt and Huber, 1994). The EGFr mRNA (known as *c-erb*B1) encodes the precursor of the 170kDa glycoprotein receptor consisting of 3 major domains: A heavily glycosylated extracellular domain for ligand recognition, a hydrophobic transmembrane domain and an intracellular domain which is associated with a C-terminal tyrosine kinase (Grunt and Huber, 1994). A variety of growth factor ligands for this receptor have been identified including the epidermal growth factor (EGF) itself, transforming growth factor (TGF-α), amphiregulin, heparin-binding EGF, β-regulin and a several viral growth factors (for review see Grunt and Huber, 1994). The binding of these growth factor ligands to the EGFr results in the transmission of a signal from the external ligand binding domain, across the plasma membrane, to the intracellular domain. Here the associated tyrosine kinase becomes activated and this in turn triggers a cascade of enzymatic and biological events which ultimately lead to DNA synthesis and cell proliferation (Modjtahedi and Dean, 1994).

The level of EGFr expression varies considerably amongst the normal tissues of the human body, however these variations are minor in comparison to the gross amplification and over-expression of EGFr observed in several cancer cells (for review see Modjtahedi and Dean, 1994). Indeed the EGF receptor and its ligands, or the production of mutated forms of these, appear to play a pivotal role in both the initiation (Hoi-Sang *et al*, 1995) and progression (Khazaie *et al*, 1993) of glioblastoma multiforme.

Commonly in GBM, the 'wild-type' EGFr mRNA is amplified or over-expressed, although occasionally the amplified gene is mutated or rearranged and this is associated with abnormal protein (receptor) production (Wong *et al*, 1994). The most common mutation of the EGF-receptor observed in GBM (seen in approximately 17% of cases involving EGFr over-expression) results in the deletion of a 267 amino acid region from the ligand binding domain (Modjtahedi and Dean, 1994). The significance of this receptor mutation in GBM has not been determined and is currently under investigation. However, any deletion or mutation to EGFr mRNA may have implications for the design of ribozymes directed against this target because complementary base sequences are required for target recognition and cleavage by ribozymes. Although it may be possible to inhibit EGFr mRNA expression using single ribozyme constructs, it would appear therefore that strategies employing 'multi-target ribozymes' may have a greater probability of *in vivo* efficacy because of the possibility of target mutations and target site inaccessibility (see section 1.3.2).

The 5532 base sequence of the 'wild type' human *c-erb*B1 (EGFr mRNA) gene has already been determined and the biological functions of several different regions of this mRNA have been identified are demonstrated in Table 1.4. Therefore in this report hammerhead ribozymes, directed against a variety of sites within the 'wild type' gene, have been designed and studied. The ultimate future aim of this approach is to use these constructs to effectively reduce the expression of EGFr mRNA in tumour cells and therefore provide a potential therapy for glioblastoma multiforme.

Table 1.4. Characteristics of the Human EGFr mRNA Showing the Coding Functions of Different Sequence Regions (as defined by Ullrich *et al*, 1984).

Base Numbers	Characteristics of mRNA sequence site:
0 to 186	5'-untranslated sequence (UTR)
187 to 189	site of the 'AUG' initiation codon
259 to 2127	sequence encoding the EGFr extra-cellular domain
2128 to 2190	sequence encoding the EGFr trans-membrane region
2191 to 3816	sequence encoding the EGFr cytoplasmic domain
3817 to 5511	3'-untranslated region (UTR)
5512 to 5517	polyadenylation signal
5532	polyadenylation site

1.7 AIMS AND OBJECTIVES.

The initial aim of this report was to design trans-acting hammerhead ribozyme constructs to cleave target sites within the human EGFr mRNA molecule. These ribozymes could ultimately be used to inhibit expression of this gene, which is involved in the progression of glioblastoma multiforme.

The introduction of specific chemical modifications into hammerhead molecules via automated synthesis, was investigated as a means to enhance the stability of these RNA-based molecules towards nucleases present in biological media, whilst maintaining their catalytic activity.

Stability enhancement would permit the application of ribozyme constructs to *ex vivo* studies, designed to assess the cellular association and ultrastructural localisation of ribozymes following administration to cells. These studies would be the main focus during this thesis and would aim to provide information regarding the exact mechanism of cellular uptake of ribozymes and their intracellular fate following cell entry.

Furthermore, the *in vivo* distribution of these ribozymes could be assessed following localised delivery to the brain, which would be the target organ for glioblastoma directed therapies.

Finally methods to enhance the exogenous cellular delivery and / or cellular uptake of stabilised ribozymes would be investigated using different strategies. This could possibly identify strategies to improve the access of ribozymes to their target sites within cells, and hence, improve their activity in future studies designed to demonstrate their biological efficacy.

CHAPTER TWO

GENERAL MATERIALS AND METHODS

The general methods and materials are described in this chapter. Details regarding specific variations and additions to the standard procedures outlined here are described in the relevant chapters.

2.1 MATERIALS

All chemical reagents used were molecular biology grade or alternatively the highest grade available from Sigma Chemical Company (Poole, UK) unless otherwise indicated.

Cell culture reagents and media were purchased from Life Technologies Inc. (Paisley, UK). Tissue culture flasks , multi-well tissue culture plates , 15mL and 50mL polypropylene tubes were purchased from Beckton Dickinson and Company (Plymouth, UK). Disposable pipettes, microcentrifuge tubes, Finnpipette tips and 2mL Biofreeze vials were purchased from Starstedt (Leicester, UK). Thermanox® cover slips (BDH Laboratory Supplies) were purchased from The Microscopy Department, Biochemistry Building, Birmingham University, UK.

2.2 GENERAL METHODS

2.2.1 Precautions to Avoid Ribonuclease Contamination

To minimise the risk of ribonuclease contamination from the skin and laboratory surfaces, disposable plastic gloves were worn at all times and changed frequently. (Gait *et al,* 1991). All water used was sterile (double distilled, de-ionised) which was prepared by autoclaving at 120°C for 30 minutes at 15 pounds per square inch above atmospheric pressure. Sterile double distilled water was rendered ribonuclease (RNase) free by the addition of 0.1% v/v diethyl pyrocarbon (DEPC), which is a ribonuclease inhibitor. The DEPC treated water was incubated at 37°C for 8 hours and then autoclaved under the above conditions to achieve sterility and to inactivate

the thermo-labile DEPC. All heat-stable aqueous solutions, which were not certified to be RNase free upon purchase, were also treated with 0.1% DEPC. Treated aqueous solutions were incubated at 37°C for 8 hours prior to autoclaving. Solutions containing amines were not treated with DEPC due to the possible formation of precipitates (Sambrook *et al*, 1989).

Also, wherever possible sterile disposable plastic tubes and pipette tips were used for storage and handling of oligoribonucleotide (ORN) solutions. Where glassware and metal spatulas were required these were rinsed with RNase free water and then baked overnight in a dry oven at 90°C. Glass cuvettes used for UV spectroscopy were soaked for 10 minutes in a 1:1 mixture of methanol and concentrated sulphuric acid. Cuvettes were then rinsed thoroughly with RNase free water and allowed to dry before use (Berger *et al*, 1987).

Electrophoresis tanks were decontaminated prior to use by soaking in 3% hydrogen peroxide followed by rinsing with copious quantities of RNase free water (Sambrook *et al*, 1989).

2.2.2 Polyacrylamide Gel Electrophoresis

Polyacrylamide gels were prepared and polymerised as described by Sambrook *et al* (1989) and Gait *et al* (1991). Biorad Protean II electrophoresis systems and Power Sources (Biorad, Hemel Hempstead, UK) were used throughout and were assembled and run according to the manufacturer's instructions.

1000mL stock solutions of native polyacrylamide gel mixtures were prepared. In general a 20% gel was used (200g acrylamide, 6.6g bis-acrylamide, 200mL 5 × TBE (54g tris base, 27.5g boric acid, 20mL 0.5M EDTA (pH8) to 1000mL with sterile water)) for oligonucleotides (ONs) up to 20 base residues in length,. For ON sequences of more than 20 base residues a 15% gel was used (150g acrylamide, 5.0g bis-acrylamide, 200mL TBE × 5). Gel mixtures were filtered and de-gassed and stored at 4°C in amber glass bottles. Denaturing gels were prepared by the addition of 8M urea (480g) to the native gel mixtures.

To prepare individual gels for electrophoresis, the polymerisation reaction was initiated by the addition of 0.6mL ammonium persulphate (10% w/v) and 40µl N,N,N',N'-tertraethylethylenediamine (TEMED) to 50mL aliquots of the stock gel mixture. The polymerising mixture was poured between two glass plates (200mm × 200mm and 220mm × 200mm) with 1mm spacers (Biorad). A 1mm wide comb with

20mm slots was inserted between the plates to form sample wells. Gels were allowed to polymerise for 30 minutes at room temperature before use.

Samples to be run on native gels were diluted with a non-denaturing loading buffer (10mg xylene cyanole, 10mg bromophenol blue, 10% v/v glycerol in 10mL 1 × TBE). Samples to be run on denaturing gels were diluted with a standard loading buffer (8mL formamide, 100µl 0.5M EDTA, 10mg bromophenol blue made up to 10mL with sterile water). TBE was used as the running buffer for electrophoresis and was diluted from a 5 × stock solution. Gels were run for 2 to 3 hours at 25 watts and were cooled throughout to 10°C using a thermostat controlled water circulator (Sarver Instruments, UK).

2.2.3 Autoradiography

Following separation of radioactive samples by PAGE, the 220mm × 200mm plate was carefully removed from the tank with the intact gel on the upper surface. The gel was covered with a single layer of Saran wrap and stored in a Hypercassette (Amersham Life Sciences, Amersham, UK) fitted with an intensifying screen. Under dark room conditions gels were exposed to Kodak HP autoradiograph film and stored at -70°C for the required exposure time. Films were developed using freshly prepared Kodak photographic reagents.

2.2.4. Scanning and Analysis of Autoradiograph Images.

Digitised images of autoradiograph films were obtained by scanning, using a UVP Transilluminator with multi-focus camera attachment, linked to an IBM PC486 computer running 'UVP Gel-Works®' (Synoptics Ltd. Upland, USA). Images were displayed using 'Grab-It®' software (Synoptics Ltd.) and the relative intensities of bands on the autoradiograph images were determined using the 'UVP Gel-Works®' analysis software. The software allowed for variations in background intensity ('noise') on the autoradiograph images. This allowed the relative quantities of test species to be determined and compared with controls. Autoradiograph images presented in this report were printed using a Hewlett Packard Deskjet 600 printer.

2.2.5. Liquid Scintillation Counting

The specific activities of radiolabelled nucleic acid sequences were determined using a Packard 1900TR Scintillation Counter. Samples of known volume were added to 10mL of Optiphase Hi-Safe 3 (Pharmacia-Wallac, St. Albans, UK) and counted for 5

minutes using an appropriate program for the detection of ^{32}P isotope activity. Counts were compared with background values and the half life and reference date of the ^{32}P radionucleotides were used to account for decay during the experimental period. Specific activities were calculated as cpm / µl and were typically in the region of 200,000 cpm / µl for recently radiolabelled sequences.

2.3. SYNTHESIS AND PURIFICATION OF OLIGODEOXY-RIBONUCLEOTIDES (ODNs) AND ANALOGUES.

2.3.1 Preparation of the Automated DNA / RNA Synthesiser

The ODNs used in this thesis were synthesised on an automated DNA / RNA synthesiser (Model 392, Applied Biosystems (ABI), Warrington, UK). Synthesis reagents, columns and nucleoside phosphoramidites were supplied by Cruachem Ltd, Glasgow, UK unless otherwise stated and were stored under argon at 4°C when not in use.

Before synthesis commenced the reagent lines on the synthesiser were purged with DNA grade acetonitrile. Reagent bottles containing acetonitrile were added to the machine in the positions normally reserved for synthesis reagents and a 'dummy' synthesis was performed as described by Brown and Brown (1991). The bottles containing acetonitrile were then replaced with the required synthesis reagents in their designated positions.

2.3.2 Oligodeoxynucleotide (ODN) Synthesis.

Automated synthesis of ODNs has become an established technique over the past decade. Various solid phase phosphoramidite techniques have been developed (For reviews see Caruthers, 1989, Brown and Brown, 1991). The standard method used to synthesise ODNs and other analogues employs 2-cyanoethyl chemistry and is illustrated schematically in Figure 2.1. The chemistry involved in this synthesis cycle is used for the automated synthesis of all nucleic acid analogues used in this thesis. However certain reagents and step times were varied according to the type of nucleic acid sequence synthesised. These variations are noted in Sections 2.3.3, 2.3.4, 2.3.5, 2.4.1 and 2.4.2.

Figure 2.1. A Schematic Representation of the Phosphoramidite Technique of Oligodeoxynucleotide Synthesis. (Adapted from Brown and Brown (1991) and Applied Biosystems User Manual Number 69 (1992)). [Nu = nucleoside. Large white circles represents the controlled pore glass (CPG) column material].

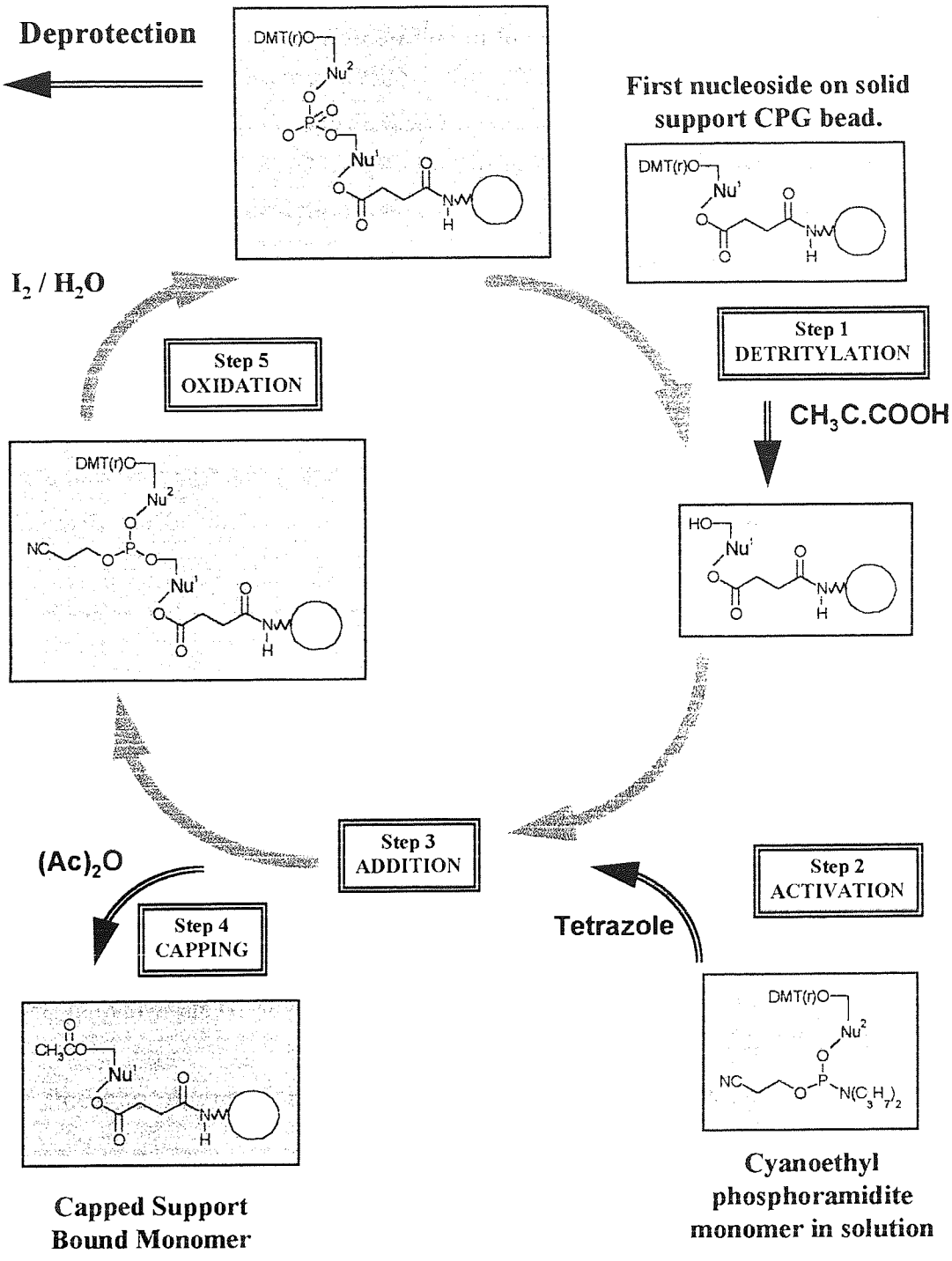

The nucleosides at the 3'-terminus were attached by means of a succinamide linker to borosilicate CPG support beads, housed inside a polypropylene column. In the first synthesis step, the support-bound nucleosides were detritylated with 2% trichloroacetic acid (TCA). This removed the DMT(r) protecting groups, thus providing free 5'-hydroxyl groups for attachment of the second nucleotide.

Quantification of the released DMT(r) groups was used to indicate the step-wise coupling efficiency and overall yield (See Section 2.3.6). In the second step an excess of the second nucleoside, protected at the 5'-hydroxyl position to prevent self-polymerisation, was activated by tetrazole which acted as a catalyst in the protonation of the N,N-diisopropyl phosphoramidite group. In the subsequent addition step, the protonated amino group was displaced due to nucleophilic attack by the 5'-hydroxyl group of the support bound nucleoside. This addition step formed support bound dimers, bearing 5'-DMT(r) groups which prevented further nucleoside additions. In the capping step any unreacted 5'-hydroxyl groups were rendered inert to further nucleoside addition by acetylation with acetic anhydride and 1-methylimidazole, thus minimising the chain length of any impurities (i.e. failure sequences). In the oxidation step the successfully dimerised sequences were oxidised with aqueous iodine (iodine-water-pyridine in basic tetrahydrofuran) to convert the phosphite triester into a more stable pentavalent phosphate triester. After this stage the fully protected phophotriester dimers on the solid support material were ready to enter further cycles of base addition. Synthesis cycles were repeated until the ODNs reached the required chain length.

2.3.3 Phosphodiester Oligodeoxynucleotide (PO ODN) Synthesis.

The standard pre-programmed 'CE Cycle' was used on the DNA / RNA synthesiser to produce phosphodiester (PO) ODNs used in this thesis. This cycle is identical to that described in section 2.3.2. The coupling time for each base addition was 30 seconds with the duration of a complete synthesis cycle being approximately 12 minutes. Following synthesis the solid support material bearing the synthesised PO was manually removed from the column. The PO was cleaved from the solid support material and the base protecting groups removed by treatment with concentrated ammonium hydroxide (d=0.88) at 55°C for 5 hours.

2.3.4 Phosphorothioate Oligodeoxynucleotide (PS ODN) Synthesis.

The pre-programmed 'sulfur' cycle was used for the synthesis of phosphorothioate (PS) ODNs on the DNA / RNA synthesiser. This cycle was a modified version of the 2-cyanoethyl phosphoramidite cycle outlined in Section 2.3.2. The key feature of this cycle was the presence of a sulphurisation step using triethylthiuram disulphide (TETD) prior to the capping step (Zon and Stec, 1991). In addition no final oxidation step is required as the sulphurisation step converts the phosphite triester into a sulphurised phosphate triester linkage. Coupling times remained unaltered, however the net result of the addition of the sulphurisation step (900 seconds) and the removal

of the final oxidation step was a total cycle time of approximately 18 minutes. Following synthesis the solid support material bearing the synthesised PS ODN was manually removed from the column. The PS ODN was cleaved from the solid support material and the base protecting groups removed by treatment with concentrated ammonium hydroxide (d=0.88) at 55°C for 12 hours.

2.3.5 Synthesis of 2'-O-Methylated Oligoribonucleotides.

2'-O-methylated ORNs have a methyl moiety at the 2'-sugar position on the nucleotide bases. Although the actual preparation of 2'-O-methylated phosphoramidites is somewhat more complex than for the standard phosphoramidites, the synthesis of ONs from these 2'-O-methylated monomers is relatively straight forward (For review see Sproat and Lamond, 1991). 2'-O-Me ORNs were routinely synthesised using the cyanoethyl phosphoramidite method outlined in Section 2.3.2. Alternatively, where sulphurised phosphate linkages were required, these were introduced into 2-O-Me ORNs by using the synthesis cycle described in Section 2.3.4 for phosphorothioate ODNs. (N.B. Chimeric sequences containing both 2'-O-methylated ORNs and unmodified ORNs were synthesised using a custom synthesis designed for RNA containing sequences, this is described in Section 2.4.2).

2.3.6 Calculation of Coupling Efficiency and Overall Yield of Oligonucleotide Synthesis.

A stock solution of 0.1M *p*-toluene sulphonic acid (19.2g in 1000mL acetonitrile) was prepared. For a 0.2μM scale synthesis the contents of the collecting tubes containing the orange effluent from each detritylation were made up to 25mL with the *p*-toluene sulphonic acid solution. The absorbance of the these solutions was measured in a 1cm cuvette in a UV visible spectrophotometer (Jenway Scientific Instruments, Basingstoke, UK) at 485nm.

The coupling efficiency and overall yield were calculated as follows, using the method described by Brown and Brown (1991):

Overall yield = y/x

% Overall yield = overall yield X 100

% Stepwise Yield (coupling efficiency) = 100 (overall yield)$^{(1/y-x)}$

Where y = OD_{495nm} final or lowest trityl effluent collected
and x = OD_{495nm} second or highest trityl effluent collected

The coupling efficiency was typically 98% for PO and PS ODNs with overall yields in the region of 70% for 36-mer sequences. Coupling efficiencies were slightly lower for 2-O-Me ORNs with typical values of 96% and overall yields of approximately 60% for 36-mer sequences.

2.3.7 Purification of Oligodeoxynucleotides and 2'-O-Me Oligoribonucleotides.

After protection ONs were purified through DNA Grade Sephadex G-25 Columns (Nap-10 columns, Pharmacia Biotech, St.Albans, UK). Columns were washed with 3 × 5mL sterile RNase free water before the application of the ON solution (1mL) to the top of the column. A further 1.5mL of RNase free water was added to the column and the eluted fraction containing the purified ON was collected in microcentrifuge tubes. The eluted samples were dried by vacuum centrifugation using a Savant DNA Speed Vac (Savant, UK) and stored at -70°C. This purification procedure removed salts and other impurities such as failed sequences less than 10 bases in length. ODNs were further purified by PAGE if required (See Section 2.2.1).

2.3.8. Quantification of Oligonucleotides.

ON samples were quantified by UV spectroscopy at 260nm (Jenway Scientific Instruments, UK).The method used to calculate the quantities of ON in samples from OD_{260nm} measurements was adapted from that of Brown and Brown (1991):

2.3.8.1. Estimation of the Molecular Weight of ONs (Brown and Brown, 1991):

$$\text{Mol. wt} = \{(251 \times nA) + (245 \times nT) + (267 \times nG) + (230 \times nC) + (61 \times n\text{-}1) + (54 \times n) + (17 \times n\text{-}1) + 2\}$$

Where; (i) nA — the number of adenine bases in the ODN sequence, etc.
(ii) n — is the total number of bases.
(ii) (61 × n-1) — accounts for the molecular weight of phosphate groups (this adjustment should be (78 × n-1) for PS ODNs).
(iv) (54 × n) — accounts for the hydration of 3 water molecules per base.
(v) (17 × n-1) — accounts for ammonium cations associated with the phosphate groups.

For 2'-O-Me ORNs a total of (n × 14) should be added to the calculated molecular weight. For unmodified ORNs a total of (n × 16) should be added to the calculated molecular weight.

2.3.8.2. Estimation of the Molecular Extinction Coefficient (ε) (Brown and Brown, 1991):

$$\varepsilon = \{(8.8 \times nT) + (7.3 \times nC) + (11.7 \times nC) + (15.4 \times nA)\} \times 0.9$$

2.3.8.3. Conversion of OD_{260nm} units into milligrams (Brown and Brown, 1991):

$$1mg \approx \varepsilon / (Mol.wt/1000) \quad OD_{260nm} \text{ units}$$

$$\therefore 1\ OD_{260nm} \text{ unit} \approx (Mol.wt/1000) / \varepsilon \quad \text{milligrams}$$

2.4 OLIGORIBONUCLEOTIDE SYNTHESIS, DEPROTECTION AND PURIFICATION.

Prior to synthesis the lines on the DNA / RNA synthesiser were purged as described in Section 2.3.1.

2.4.1 Synthesis of Oligoribonucleotides (ORNs) and Ribozymes.

Although automated assembly of ODNs has been established for some time. The introduction of automated ORN synthesis has been slower, due to problems in finding compatible protecting groups for the ribonucleoside 2'- and 5'- hydroxyl groups. In addition, coupling of ORN phosphoramidites is generally less efficient, and once deprotected, ORN sequences are highly susceptible to degradation by RNases which are ubiquitous and difficult to remove (Gait *et al*, 1991). The solid phase strategy used for synthesis of ORNs in this thesis was similar to the cyanoethyl phosphoramidite technique employed in the preparation of ODNs (See Section 2.3.2). However, several modifications to the standard method were implemented to ensure an adequate yield and to remove the additional protecting groups.

Developments in the 1990's led to the availability of two main types of ribonucleoside phosphoramidites for solid phase ORN synthesis. The major difference between these is the use of different protecting groups for the 2'-hydroxyl position: The 2'-O-t-butyldimethylsilyl (TBDMS) protecting group, which can be removed post-synthesis using tetra-*n*-butyl-ammonium fluoride, is marketed by several companies including Applied Biosystems in the UK. A wide range of modified phosphoramidite derivatives using this chemistry have also been described (Wahl *et al*, 1996). TBDMS protected

chemistry is perhaps the most widely used and the technique has recently been optimised to improve yields and synthesis time (Wincott *et al*, 1995). The use of TBDMS does, at present, appear to demonstrate marginal advantages over rival chemistries, in terms of slightly higher product yields and shorter synthesis times. However these advantages are offset by the increased purchase cost for these reagents. Consequently, they were not used during this thesis.

The main alternative to TBDMS protected chemistry is the use of 1-(2-fluorophenyl)-4-methoxypiperidin-1-yl (Fpmp) acetal protected ribonucleosides, originally developed by Professor Collin Reese (Reese *et al*, 1991) and marketed in the UK by Cruachem Ltd. A crucial property of the 2'-O-Fpmp protecting group is that its rate of hydrolysis hardly changes under the harshly acidic conditions (pKa=0.66) required for detritylation. Consequently, unlike the TBDMS group, it shows no tendency to undergo 2' - 3' migration during this synthesis step. (Rao, 1994 and Cruachem Technical Bulletin No.037).

A custom synthesis cycle was designed for use with 5'-O-(DMT(r))-2'-O-(Fpmp)-protected ribonucleoside phosphoramidites (a gift from Cruachem Ltd.) on the ABI 392 DNA/ RNA Synthesiser. The full synthesis cycle is listed in Appendix I. This cycle is based on the cyanoethyl phosphoramidite technique (See Section 2.3.1), the alterations made to this for ORN synthesis are described in Table 2.1.

Table 2.1. The Key Differences Between the Custom Synthesis Cycle designed For the Production of Oligoribonucleotides and the Standard Cyanoethyl Phosphoramidite Technique Described in Section 2.3.2.

Synthesis Step	Changes to Standard CE Cycle	Reason for Change
Detritylation	Use of RNA Grade Deblock solution instead of standard reagent	Anhydrous 2% TCA reduces risk of 2'-Fpmp group hydrolysis
Addition	Double addition of phosphoramidite monomer to columns. Increased wait time.	Increased coupling time to allow for reduced coupling efficiency with ribonucleosides
Oxidation	No wait step following addition of I_2 / H_2O solution	Reduced exposure of 2'-Fpmp group to hydrolytic conditions.
Capping	Additional capping step included after the oxidation step	Decreased risk of further base additions to failed sequences

The method used for ORN synthesis was designed in conjunction with Cruachem Ltd and the design reflects their experience in producing ORNs and the improvements to the synthetic protocol described by Rao and MacFarlane, 1995. All ORNs and all-RNA ribozymes were synthesised without the removal of the DMT(r) group from the final base in the sequence and were deprotected and purified as described in Section 2.4.3. Stepwise coupling efficiency and overall yields can be calculated as described in Section 2.3.6.

2.4.2 Synthesis of Chimeric Ribozymes Containing Oligoribonucleotides.

To synthesise 'mixed sequences' containing ORNs and other oligodeoxynucleoside analogues, the method described in Section 2.4.1 was used. Where DNA or 2'-O-Me phosphoramidites were required the custom cycle designed for the addition of 5'-O-(DMT(r))-2'-O-(Fpmp)-protected ribonucleoside phosphoramidites continued to be used (i.e. If the sequence to be synthesised contained even a single RNA base, the custom RNA cycle was used throughout). This involved increased cycle times and the use of increased quantities of ancillary reagents compared with the synthesis cycles optimised for the preparation of non-ribonucleoside sequences. However, the importance of using a cycle which created an environment with less potential for hydrolysis of the 2'-Fpmp protecting groups on the ribonucleoside bases had to be preserved throughout. Chimeric sequences were synthesised without the removal of the 5'-O-DMT(r) group and were deprotected and purified as described in Section 2.4.3.

2.4.3 Deprotection of Oligoribonucleotides and Chimeric Ribozymes.

The complete deprotection of ORNs is a two step process as described by Rao and MacFarlane (1995) and Cruachem Technical Bulletin No.010. Following synthesis the CPG support bound 5'-O-DMT(r)-2'-O-Fpmp ORNs were removed from the column housing and transferred to sterile microcentrifuge tubes. Concentrated aqueous ammonia (d=0.88) in triethylamine was added according to the synthesis scale (0.5mL for 0.2μM scale, 1.0mL for 1.0μM scale). The tubes were sealed with parafilm, vortexed briefly, and incubated at 55°C overnight or at 70°C for 5 hours. Following incubation, samples were cooled to room temperature and centrifuged at 3000 rpm for 2 mins. The ammoniacal solution was transferred to a sterile microcentrifuge tube and dried by vacuum centrifugation using a Savant DNA Speed-Vac. At this stage the base protecting groups had been removed, although the 5'-O-DMT(r) and the 2'-O-Fpmp groups remained. The presence of the 2'-O-Fpmp group protected the ORN against RNase degradation. Consequently these protected ORNs were either stored

for prolonged periods at -20°C or alternatively, the protected ORNs were purified at this stage by reverse phase HPLC (See Section 2.4.4) or by PAGE (See Section 2.2.2).

For removal of the 5'-O-DMT(r) and 2'-O-Fpmp groups; 500μL of 0.5M sodium acetate buffer (pH 3.25) was added to the dried pellet of the protected ORN in the microcentrifuge tube. The solution was vortexed for 2 minutes and incubated at 30°C for 36 hours. The acidic solution was neutralised with 3.0M Tris-base (100μL) and centrifuged at 10,000 rpm for 3 minutes. The supernatant solution was transferred to a separate, sterile microcentrifuge tube and three times the volume of Analar grade ethanol (Fisons Laboratory Supplies, Loughborough, UK) was added. The solution was placed at -70°C (dry ice / isopropanol) for 30 minutes and then centrifuged at 10,000 rpm for a further 5 minutes. The supernatant solution was discarded without disturbing the solid pellet and a further 900μL of Analar grade ethanol was added. The tube was vortexed briefly and centrifuged for a further 5 minutes at 10,000 rpm. The supernatant was again discarded and the deprotected, desalted ORN pellet was dried by vacuum centrifugation.

Following re-suspension in sterile RNase free water the ORN can be quantified by UV absorbance as described in Section 2.3.8. Due to the loss of the chromophoric 2'-O-Fpmp groups a typical reduction of 50% in OD_{260nm} was noted following the second deprotection step. Where further purification was required this was performed by PAGE (See Section 2.2.2).

2.4.4 Reverse Phase HPLC Purification of 5'-O-DMT(r)-2'-O-Fpmp Protected Oligoribonucleotides.

Protected ORNs were purified using a Jones Apex ODS 5 micron column on a gradient HPLC system with UV detection at Cruachem Limited (West of Scotland Science Park, Glasgow, UK). A linear gradient of acetonitrile in 0.1M triethylammonium acetate buffer (pH 7.0) was used as the mobile phase. The initial acetonitrile concentration of 25% was gradually increased to 65% after 40 minutes using a flow rate of 1.5mL/minute. Following an initial analytical separation of the crude reaction mixture the main peak representing the ORN was identified. Samples of the purified ORN were collected at the correct elution time on subsequent preparative runs. Collection of the fraction was stopped when the absorbance fell below about 20% of the peak value. ORNs were collected in microcentrifuge tubes and evaporated to dryness by vacuum centrifugation.

2.5. LABELLING OF SYNTHESISED NUCLEIC ACIDS.

2.5.1 5'-End [^{32}P]-Radiolabelling

ODNs, ORNs and chimeric sequences were separately 5'-end labelled with [^{32}P]-γ-dATP (Supplied by Amersham Life Sciences, DuPont NEN and ICN Biomedicals, UK), with a specific activity designated to be greater than 185 TBq / mmol at the reference date. The method used is described by Sambrook *et al* (1989), using bacteriophage T4 polynucleotide kinase (Life Technologies and Bioline, UK) in 5 × reaction buffer (100mM Tris, pH 7.5, 20mM $MgCl_2$, 10mM DTT, 0.2mM spermidine and 0.2mM EDTA) at 37°C for 45 minutes. Approximately 50 picomoles of nucleic acid were labelled in 20μL reaction buffer containing 20 units of T4 kinase and 5μL of [^{32}P]-γ-dATP. Where radiolabelled ONs of a higher specific activity were required, the quantity of nucleic acid was reduced to 10 picomoles and the amount of [^{32}P]-γ-dATP was increased 3-fold. (Sambrook *et al*, 1989). 5'-labelled nucleic acids were purified by PAGE (See Sections 2.6.1 and 2.2.2) or by Nensorb-20® column purification (See Section 2.6.2.).

2.5.2 3'-End Labelling of ODNs with [^{32}P]-α-ddATP and ddCTP

ODNs were labelled at the 3'-end with an additional dideoxynucleotide using calf thymus terminal deoxynucleotidyl transferase (Boehringer Mannheim, Germany) according to the manufacturer's protocol. To 1nanomole of a dried sample of nucleic acid, 10μL of the supplied reaction buffer (1M potassium cacodylate, 125mM Tris-HCl, 1.25mg/mL BSA, 25mM cobalt chloride) and 5μL cobalt chloride (100mM) was added. Where a radiolabel was required at the 3'-terminus of the ODN; 5μL of [^{32}P]-α-ddATP (ICN Biomedicals Ltd, UK) with a specific activity at reference of 650 Curies per mmol was added to the reaction mixture. Where the addition of a non-radioactive dideoxynucleotide was required, 2.5μL of ddCTP (1.0mM molecular biology grade solution, Sigma, Poole, UK) was added to the reaction mixture. The reaction mixture was made up to 48μL with sterile RNase free water and finally, 2μL terminal deoxynucleotidyl transferase was added and the reaction mixture was incubated at 37°C for 60 minutes. 3'-end labelled nucleic acids were purified by PAGE (See Sections 2.6.1 and 2.2.2) or by column purification (See Section 2.6.2.).

2.5.3 Preparation of Internally Radiolabelled Chimeric Oligoribonucleotides.

A technique was developed for the synthesis of internally radiolabelled ribozymes using T4 RNA Ligase. This enzyme catalyses the ATP-dependant formation of a phosphodiester bond between a 5'-terminal phosphate (of a 'donor' ORN) and a 3'-terminal hydroxyl (of an 'acceptor' ORN) (Romaniuk and Uhlenbeck, 1983, Maunders, 1993).

The minimum size of the 5'-terminal moiety on the 'donor' ORN is a 3',5'-*bis* phosphate (i.e. 5'-P-base-P-3'). The minimum size of the 3'-terminal moiety on the 'acceptor' ORN is a trinucleoside *bis*-phosphate (i.e. 5'-base-P-base-P-base-OH-3'). Ribonuceloside, deoxynucleoside or 2'-O-methylated nucleosides at the 3'-terminus of the 'acceptor' ORN will undergo the ligation reaction. (Tessier *et al*, 1986, Maunders, 1993). However, if the 3'-terminal nucleoside is modified with a 3'-phosphate or 2',3'-dideoxy moiety, the ORN is no longer a substrate for the ligation reaction (Uhlenbeck and Gumport, 1982, Tessier *et al*, 1986).

Following synthesis (See Sections 2.3 and 2.4) ORNs possess a 3'-terminal hydroxyl group but do not possess a 5'-terminal phosphate. Therefore synthesised ORNs could be used in the ligation reaction as 'acceptor' sequences without further modification. In contrast, ORNs required the addition of a 5'-terminal phosphate before they could be used in the ligation reaction as 'donor' sequences. Furthermore, to prevent the formation of circular or multimeric products, the 3'-terminal hydroxyl group on the 'donor' sequence also required modification or deletion in order to prevent the 'donor' from participating in the ligation reaction (Middleton *et al*, 1985, Tessier *et al*, 1986). (i.e. A 'blocking group' which would not undergo ligation had to be added to the 3'-terminus of the 'donor' to render it incapable of acting as an 'acceptor' itself. and thus. forming circular or multimeric products)

2.5.3.1 Preparation of the 'Donor' Oligoribonucleotide for Internal Radiolabelling.

The method of internal radiolabelling used in this thesis uses T4 polynucleotide kinase, which demonstrates 3'-phosphatase activity, and is capable of removing a 3'-phosphate 'blocking group' (Uhlenbeck and Gumport, 1982). As an alternative to a 3'-phosphate blocking group, the 'donor' sequences used in this report were 'blocked' at the 3'-terminus by the addition of a 2',3'-dideoxy CTP residue, as previously described by Tessier *et al*, (1986). However attachment of this blocking group to 'donor' ORNs, required the prior addition of a 3-mer sequence of ODNs to the 3'-terminus of the 'donor' ORN during automated synthesis. The addition of the 3'-terminal ODN

sequence (3-mer) was required to allow 'donor' sequences to be substrates for terminal transferase. Non-radiolabelled ddCTP blocking groups were added to attached to 'donor' ORNs bearing 3'-terminal ODNs (100μM) using terminal transferase as described in Section 2.5.2. The 'donor' sequences, blocked at the 3'-end with ddCTP, were column purified as described in Section 2.6.2.

Following column purification of the 3'-blocked 'donor' ORN, a radioactive 5'-phosphate group was added to the 'donor' using [^{32}P]-γ-dATP and T4 polynucleotide kinase as described in Section 2.5.1. The 3'-blocked, 5'-phosphorylated 'donor' ORNs were column purified as described in Section 2.6.2.

2.5.3.2 Internal Radiolabelling Using T4 RNA Ligase.

Following purification the radiolabelled 'donor' ORN was reconstituted in 20μL ligation reaction buffer (50mM HEPES pH 8.3, 10mM $MgCl_2$, 10ug/mL BSA, 10% v / v DMSO and 100μM ATP). This reaction buffer was found to give an optimal yield of ligated product, although the quantities of DMSO and ATP were varied in some experiments (in the range 1μM to 1mM). The ATP concentration in particular has been reported to be critical for the ligation of some ORNs (Romaniuk and Uhlenbeck, 1983, Tessier *et al*, 1986, Maunders, 1993).

A 5:1 concentration ratio of donor:acceptor was used in the ligation reaction. Typically a 50μM solution of the 'donor' would be used and this was mixed with the 'acceptor' ORN reconstituted in 18μL ligation reaction buffer. 2μL of T4 RNA Ligase (Pharmacia Biotech, 180μg/mL) was added to the microcentrifuge tube and the reaction was incubated at 15°C for 12 hours (Tessier *et al*, 1986). The ligated, internally radiolabelled ORN was separated from unreacted ORNs by PAGE as described in Sections 2.6.1 and 2.2.2.

2.5.4 5' End Fluorescein Labelling.

A fluorescent label was attached to the 5'-end of ODNs and ORNs during automated synthesis. Fluorescein cyanoethyl phosphoramidite (Cruachem, See Figure 2.2) was reconstituted in DNA grade acetonitrile to a concentration of 0.1M and attached to a spare monomer position on the DNA / RNA synthesiser. The Custom synthesis cycle designed for use with ribonucleoside phosphoramidites was used for the addition of the fluorescein phosphoramidite because of the longer coupling time which this cycle allowed. The synthesis was performed without a final detritylation step because the fluorescein phosphoramidite monomer bears no DMT(r) group and is only suitable for

addition to the 5'-terminus of a synthesised ON. 5'-FITC labelled ONs were deprotected according to the protocol for the type of ON synthesised. The FITC label was not degraded during the protocol for ORN deprotection (See Section 2.4.3).

Figure 2.2. The Structure of the Fluorescein -CE Phosphoramidite (Adapted from Cruachem Technical Bulletin No. 015)

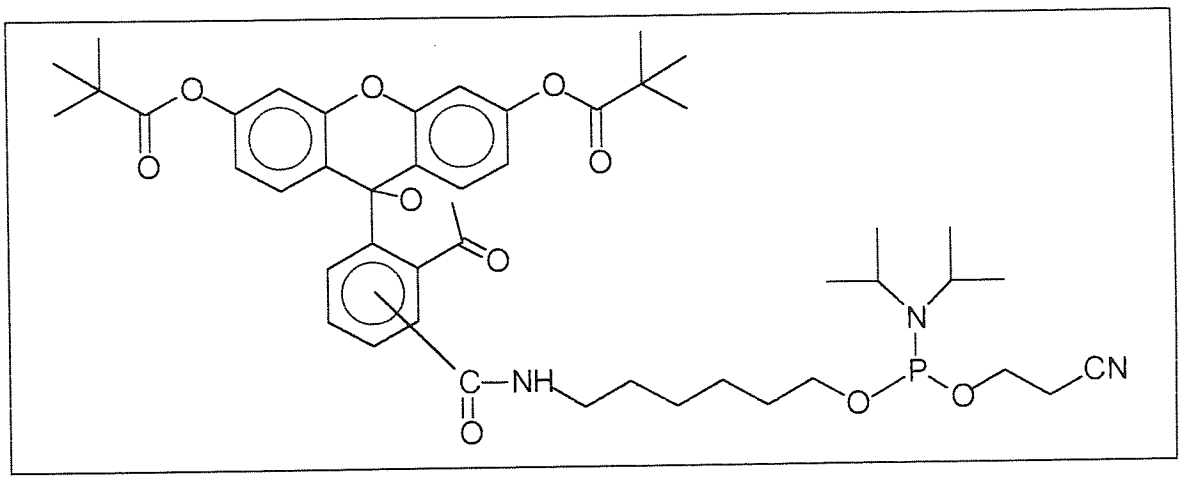

2.5.5 5'-Biotinylation of Oligonucleotides.

Both ORNs and PS ODNs were 5'-biotinylated during automated synthesis. Biotin cyanoethyl phosphoramidite (Cruachem, See Figure 2.3) was reconstituted in DNA grade acetonitrile to a concentration of 0.1M and added to a spare monomer position on the DNA / RNA synthesiser.

Figure 2.3. The Structure of the Biotin -CE Phosphoramidite (Adapted from Cruachem Technical Bulletin No.003).

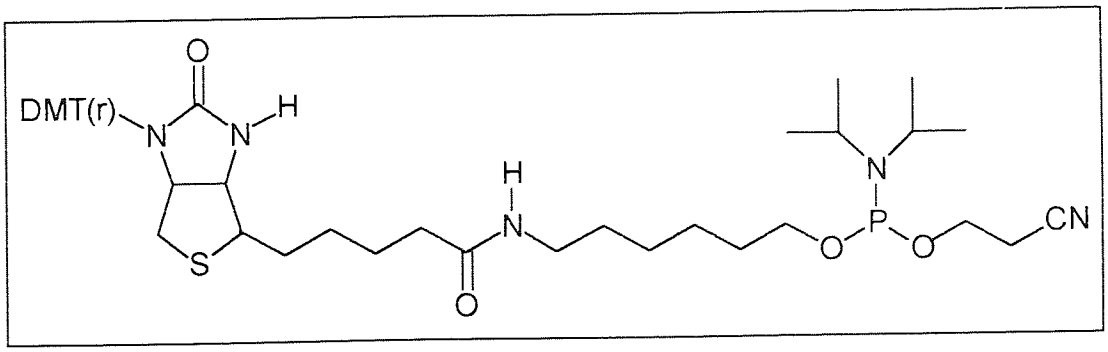

The Custom synthesis cycle designed for use with ribonucleoside phosphoramidites was used for the addition of the biotin phosphoramidite because of the longer coupling time which this cycle allowed. Where ODNs were 5'-biotinylated a final detritylation step was included in the synthesis cycle to remove the 5'-DMT(r) from the biotin moiety. Where ORNs and chimeric ORNs were 5'-biotinylated the final detritylation step was omitted because 5'-DMT (r) was subsequently removed during

deprotection of ORN containing sequences. Both 5'-biotinylated ODNs and ORNs were purified by column purification. (See Section 2.6.2).

2.5.6 Attachment of the 5'-Thiol Modifier C_6 Group

The 5'-Thiol Modifier C_6 group was attached to both and ODNs and 2'-O-Me ODNs using C_6 thiol modifier cyanoethyl phosphoramidite monomers (Cruachem, See Figure 2.4). The phosphoramidite was reconstituted in DNA grade acetonitrile to a concentration of 0.1M and added to a spare monomer position on the DNA / RNA synthesiser. The Custom cycle designed for the synthesis of ORNs (See Appendix II) was used for the addition of the thiol modifier phosphoramidite because of the longer coupling time which this cycle allowed. The final detritylation step was omitted (i.e. 'Trityl ON' synthesis) because the 5'-O-DMT(r) group was removed during subsequent use in conjugation reactions. Thiol modified ODNs were purified by column purification when required. (See Section 2.6.2).

Figure 2.4. The Structure of the C_6 Thiol modifier-CE Phosphoramidite (Adapted from Cruachem Technical Bulletin No.014).

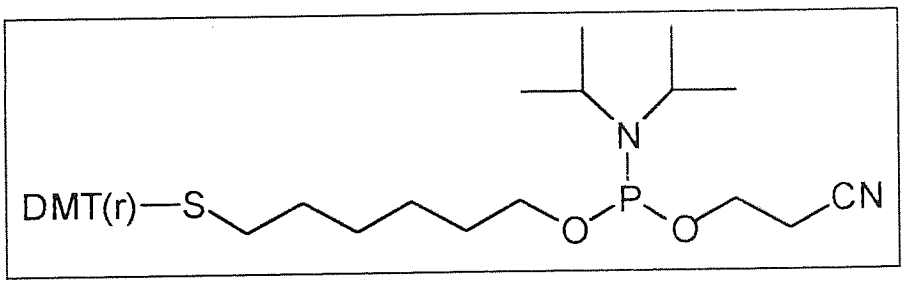

2.6 PURIFICATION OF LABELLED NUCLEIC ACIDS

2.6.1 Polyacrylamide Gel Electrophoresis

PAGE was performed as described in Section 2.2.2. Radiolabelled ONs were mixed with an equal volume of non-denaturing loading buffer (10mg xylene cyanole, 10mg bromophenol blue, 10% v/v glycerol in 10mL TBE). For purification of radiolabelled ON sequences containing up to 20 nucleotide bases, 20% native polyacrylamide gels were used. Where ON sequences contained more than 20 bases, 15% native gels were used to improve the molecular weight separation during purification as described by Maniatis *et al* (1975) and Gait *et al* (1991). The position of the purified radiolabelled product within the gel was visualised by autoradiography as described in Section 2.2.3. For PAGE purification of non-radiolabelled nucleotides, samples were loaded

onto gels as described above. However, additional samples of radiolabelled ON markers of known chain length were added to adjacent wells on the gel to allow location of the purified, unlabelled product band by autoradiography. Appropriate gel bands containing the purified products were excised and transferred, to sterile microcentrifuge tubes containing 5M ammonium acetate, 1mM EDTA and 0.5% SDS (Gait *et al*, 1991). Excised bands were incubated in the elution buffer overnight at room temperature. The supernatant solution was removed and dried by vacuum centrifugation. Alternatively, ODNs were first desalted, using DNA Grade Sephadex G-25 Columns (Nap-10 columns, Pharmacia Biotech, St. Albans, UK) as described in Section 2.3.7. Dried ONs were stored at -70°C until required, with particular attention paid to handling techniques for samples containing ORNs (See Section 2.2.1).

2.6.2 Column Purification.

As an alternative to PAGE, both labelled and unlabelled ONs were purified using Nensorb-20® chromatographic cartridge columns (DuPont NEN Research products, Boston, USA) as described by Johnson *et al* (1990). Using this technique, salts and failure sequences of less than 10 nucleotide bases in length are washed through the column and removed. ONs (containing 10 or more nucleotide bases) remain bound to the column material. Purified ON samples can be eluted from the column using short chain alcohols, which release only the bound ON from the column material if used at low concentration. The manufacturers state that this technique is approximately 95% effective in removing impurities, including proteins, from synthesised ON samples. (Johnson *et al*, 1990). The capacity of each cartridge was 20µg combined of nucleic acid and protein since the two compete for the same binding sites on the column material.

Dried ONs were reconstituted in 5mL of 'reagent A buffer' (0.1M Tris HCl, 1mM EDTA pH 7.4, triethylamine 14µL/10mL). Nensorb-20® columns were initially washed with 2mL of Analar grade methanol (100%) and pre-equilibrated with 5mL of 'Reagent A Buffer'. For these and all subsequent wash steps a 20mL syringe was used to push solvents through the column drop-wise. The sample in 'reagent A buffer' was pipetted onto the resin bed of the column and pushed into the resin using the syringe. The column was then washed with 10mL of 'reagent A buffer' followed by 5mL sterile RNase free water to remove salts and other impurities. The column bound ONs were eluted with 15% Analar grade methanol (in sterile RNase free water) and dried by vacuum centrifugation.

2.7. CELL LINES AND CULTURE TECHNIQUES.

2.7.1 Long Term Storage of Cells

All cell lines were prepared for long term storage by trypsinising a semi-confluent 75 cm^2 flask with 2mL trypsin (2% v/v) in PBS / EDTA (0.2% w/v EDTA in PBS, pH 7.2) and neutralising with 10mL DMEM. The cells were pelletted by centrifugation at 1,000 rpm for 3 minutes (Mistral 3000 I centrifuge, Sanyo MSE, Leicester, UK). The supernatant media was removed and the cell pellet was re-suspended in 1mL 'freezing media' containing 90% v/v FCS and 10% v/v DMSO (as a cryoprotectant) in a 2mL screw capped cryo-vial (Costar, Cambridge, USA). The cells were frozen slowly at -70°C before transfer to a liquid nitrogen storage vessel at -196°C. Cells were recovered by rapid thawing at 37°C and gradual dilution with maintenance media appropriate to the cell line being recovered (See Sections 2.7.4 to 2.7.8).

2.7.2 Determination of Cell Number.

Cell density was determined using the counting chamber of a Neubauer haemocytometer (Weber Scientific International Ltd, UK). Cells were removed from culture flasks with 2mL trypsin (2% v/v) in PBS / EDTA (0.2% w/v EDTA in PBS, pH 7.2) and diluted to 10mL with PBS in a sterile 15mL tube. Cells were immediately pelleted by centrifugation at 1,000 rpm for 3 minutes (Mistral 3000 I centrifuge). The supernatant was removed and the cell pellet was re-suspended in 10mL of the relevant culture media. The counting chamber of the haemocytometer was filled with a small aliquot of the cell suspension and this was counted using a light microscope. Cell number was determined by obtaining the mean count per large square on the haemocytometer. This mean count value indicated the number of cells $\times 10^4$ present in the sample per mL.

2.7.3. Determination of Viable Cell Number By Trypan Blue Exclusion Assay

Cell viability was measured by haemocytometry using a trypan blue exclusion assay. Cells were washed with PBS and 100µL of trypan blue (4mg/mL) was mixed with 400µL of re-suspended, trypsinised cells and counted as described in Section 2.7.2. Living cells exclude trypan blue, however non-viable cells are stained by this agent and can be identified when viewed under the microscope.

The mean total count of viable cells per square and the mean total cell count (viable + non-viable) can be used to calculate the number of viable cells per mL and the percentage of viable cells:

Viable cells per mL = mean viable count per square $\times 10^4 \times 1.25$ (dilution factor)
% Viable cells = mean viable cell count / total cell count $\times 100$

2.7.4 A431 Cell Line

A431 epithelial cells, derived from a vulval carcinoma (Freshney, 1973), were a gift from Dr. P.L. Nicklin (Ciba, Horsham, UK). A431 cells express the epidermal growth factor receptor (EGFr) at levels 10 to 50 fold higher than is seen in other cell lines (Ullrich *et al*, 1984) and, like most transformed cell lines, also express the human transferrin receptor (Gherardi, 1996). A431 cells were maintained at 37°C, in a 5% CO_2 atmosphere, in Dulbecco's Modified Eagle's medium (DMEM) containing 10% v/v mycoplasma-screened FCS, 1% v/v penicillin / streptomycin and 2mM *L*-glutamine (All supplied by Life Technologies Inc, UK). Cells were maintained in 75 cm^2 flasks (Falcon, UK) with a 30mL volume of maintenance media. Cells were passaged every 2 days by diluting 1 to 5 with fresh maintenance media. To passage, the cells were washed with sterile PBS and trypsinised with 2% trypsin in PBS / EDTA (0.2% EDTA in PBS, pH 7.2).

Where A431 cells were grown on cell culture plates, the cell number was determined using a Neubauer haemocytometer as described in Section 2.7.2. Cells were diluted to the appropriate number per millilitre using maintenance media. A431 cells were seeded at 7.5×10^4 cells per well in 24 well plates (Costar, Cambridge, USA) when used for cell association studies, unless otherwise stated. This dilution produced approximately 70% confluent cell cultures after 24 hours, after which cells were used in association studies.

Where A431 cells were grown on Thermanox® cover slips, these were cut to size (approximate circular diameter 1.5 cm) and sterilised by immersion in 100% Analar grade ethanol for 5 minutes. The Thermanox® cover slips were then air dried and placed inside 12 well plates (Sterilin, Hounslow, UK). A431 cells were seeded at 1.5×10^5 cells per well on the cover slips inside the 12 well plates. Any air trapped beneath the cover slips was gently pressed out using a sterile pipette tip. This produced approximately 90% confluent cell cultures on the cover slips after 24 hours.

2.7.5 U87-MG Cell Line

U87-MG human glioblastoma cells, derived from a grade 3 malignant glioma by explant technique (Ponten and McIntyre, 1968), were obtained from the European Collection of Animal and Cell Cultures (ECACC), Porton Down, UK. U87-MG cells were maintained at 37°C, in a 5% CO_2 humidified atmosphere, in DMEM containing 10% v/v mycoplasma-screened FCS, 1% v/v penicillin / streptomycin and 1mM *L*-glutamine (All supplied by Life Technologies Inc, UK). Cells were maintained in 75cm^2 flasks (Falcon, UK) with a 30mL volume of maintenance media. Cells were passaged every 4 days by diluting 1 to 5 with fresh maintenance media. To passage, the cells were washed with sterile PBS and trypsinised with 2% trypsin in PBS / EDTA.

Where U87-MG cells were grown on cell culture plates, the cell number was first determined as described in Section 2.7.2. Cells were diluted to the appropriate count per millilitre using maintenance media. U87-MG cells were seeded at 5.0×10^4 cells per well in 24 well plates when used for cell association studies, unless otherwise noted. This produced 70-80% confluent cell cultures after 24 hours, when cells were used for association studies.

2.7.6 RAW 264.7 Cell Line

Murine macrophages, RAW 264.7, were obtained from the ECACC. These cells were established from the ascites of a tumour induced in a male mouse by the intraperitoneal injection of Abelson leukaemia virus (Raschke *et al*, 1978). Raw 264.7 cells were maintained as described for U87-MG cells in Section 2.7.3. Cells were passaged every 2 days by diluting 1 to 5 with fresh maintenance media. To passage, the cells were washed with sterile PBS and trypsinised with 2% v/v trypsin in PBS / EDTA. For cell association studies RAW 264.7 cells were grown on 24 well culture plates. Cells were seeded as described for U87-MG cells in Section 2.7.4 and were used in cell association studies 24 hours post seeding.

2.7.7 Caco-2 Cell Line

Caco-2 intestinal epithelial cells, derived from a human colonic adenocarcinoma, were kindly donated by Dr. V.Moore (Aston University). Two types of media were prepared for the culture of Caco-2 cells at 37°C, in a humidified atmosphere of 10% CO_2 in air: Maintenance media comprised of DMEM containing 10% v/v mycoplasma-screened FCS, 1% v/v non-essential amino acids and 1% v/v *L*-glutamine

(All supplied by Life Technologies Inc, UK) was used for routine maintenance culture. Cells were maintained in 150cm^2 flasks (Falcon, UK) with 40mL maintenance media, which was replenished every 2 days. Cells were passaged weekly by diluting 1 in 10 with fresh maintenance media. To passage, the cells were washed with sterile PBS and trypsinised with 2% trypsin in PBS / EDTA. Where Caco-2 cells were grown on cell culture plates, a plating medium composed of maintenance medium supplemented to a final concentration of 1% v/v penicillin / streptomycin was prepared. Caco-2 monolayers used for cell association studies were grown on 24 well plates. Two to three day post-confluent cultures were trypsinised, re-suspended in plating medium and the cell number determined as described in Section 2.7.2. Cells were diluted with plating media and seeded at 2.0×10^4 cells per well. The 24 well plates were incubated at 37°C in a humidified atmosphere of 10% CO_2 in air. The plating media was replenished every two days and the monolayers were used for cell association studies 7 days after seeding.

2.7.8 ECV304 Cell Line

ECV304 endothelial cells, derived from transformed human umbilical cord, were obtained from the ECACC. ECV304 cells were maintained at 37°C, in a 5% CO_2 atmosphere, in DMEM containing 10% v/v heat inactivated FCS and 1% v/v penicillin / streptomycin (All supplied by Life Technologies Inc, UK). ECV304 were maintained in 75cm^2 flasks (Falcon, UK) with a 30mL volume of maintenance media. Cells were passaged every 2 days by diluting 1 to 10 with fresh maintenance media. To passage, the cells were washed with sterile PBS and trypsinised with 2% v/v trypsin in PBS / EDTA (0.2% w/v EDTA in PBS, pH 7.2).

Where ECV304 cells were grown on cell culture plates, the cell number was determined as described in Section 2.7.2. Cells were diluted using maintenance media and seeded at 7.5×10^4 cells per well in 24 well plates (Costar) and used for cell association studies 24 hours post seeding.

2.8. CELL ASSOCIATION STUDIES.

Methods for cell association studies used throughout this thesis are detailed below. Details of amendments and additional methods used are described in the relevant chapters

2.8.1 Cell Association of Oligonucleotides (and Ribozymes).

Radiolabelled ONs (and ribozymes) were diluted to a final concentration 0.8μM in media, unless otherwise stated. Cells were seeded in 24 well plates as described in Sections 2.7.4 to 2.7.8. Unless otherwise stated, culture media used in cell association studies was of the same composition as that used during the maintenance of each cell line with the exception that FCS was not included in the media (i.e. all culture media used in cell association studies was serum-free). The use of serum free media reduced the potential for enzymatic degradation of nucleic acids.

After the required incubation period cells were washed twice with 1mL sterile PBS (warmed to 37°C) per well. The PBS was aspirated and the nucleic acids added to wells in warmed serum free culture media. Cells were incubated for the required time period at 37°C, unless otherwise stated. Following incubation the apical serum-free media was removed from the cells and collected. Cells were then washed 4 times with ice cold PBS / azide (0.05% w/v sodium azide in PBS) and the washings collected. Cell monolayers were solubilised by the addition of 1mL triton-X100 (3% in distilled water) for 2 hours at 37°C. The cell suspension was harvested and the wells washed twice more with 1mL triton-X100 to remove any remaining cells. The cell suspension and final triton-X100 washings were pooled and collected.

Quantities of radiolabelled nucleic acids in each of the three fractions (apical supernatant media + PBS washes + cell suspensions) were assessed by liquid scintillation counting using a Packard 1900TR Scintillation Counter. Fractions were added to 10mL of Optiphase Hi-Safe 3 (Pharmacia-Wallac, St. Albans, UK) and counted for 5 minutes using an appropriate program for the detection of ^{32}P isotope activity. Counts per minute were recorded and background values were subtracted to give counts per minute. The half life and reference date of the ^{32}P radionucleotides were used to account for decay during the experimental period.

2.8.2 Assay To Determine The Effect of PBS / Azide Washes.

To assess the number of PBS / azide washes required to remove loosely bound ON from A431 cell surfaces, a cell association study using a radiolabelled ODN was initiated as described in Section 2.8.1. Following incubation, apical supernatants were removed as described in Section 2.8.1. However, a total of seven PBS / azide (0.05% w/v sodium azide in sterile PBS) washes were performed and each was collected in a separate vial of scintillant. The cell association study was then completed as described in Section 2.8.1. However the quantity of radiolabelled ODN

in each of the PBS / azide wash samples was detected separately to allow an estimate of the number of washes required to remove loosely bound ODN to be determined.

2.8.3 Cell Association of Radiolabelled Mannitol.

Mannitol is one of a group of polysaccharides which enter cells by the process of fluid phase endocytosis (Cohn and Ehrenreich, 1969, Luby-Phelps, 1989). Therefore *D*-[1-^{14}C] Mannitol (Amersham Life Sciences, Amersham, UK) was used as a radiolabelled marker for this process, as demonstrated by Wu-Pong *et al* (1992) and Levis *et al* (1995) with radiolabelled sucrose. To assess the cell association of the *D*-[1-^{14}C] Mannitol marker, cell association studies were performed as described in Section 2.8.1. However, ONs were replaced with *D*-[1-^{14}C] Mannitol. Two experiments were performed separately using two different final concentrations of *D*-[1-^{14}C] Mannitol (0.8μM and 8.0μM) in culture media. Quantities of *D*-[1-^{14}C] Mannitol in each of the three fractions collected during these studies (apical media + PBS washes + cell suspensions) were assessed by liquid scintillation counting. Fractions were added to 10mL of Optiphase Hi-Safe 3 (Pharmacia-Wallac, St. Albans, UK) and counted for 10 minutes using an appropriate program for the detection of ^{14}Carbon.

2.8.4. Assessment of the Effect of Temperature on Cell Association of Nucleic Acids.

To assess the effect of temperature on cell association of nucleic acids, studies were performed as described in Section 2.8.1 at 37°C, in parallel with additional experiments at 4°C. For the low temperature experiments the method was amended as follows: After the required growth period, cells in 24 well plates were washed twice with 1mL sterile PBS (at 4°C). The PBS was aspirated and cells were incubated in serum free culture media (at 4°C) for 15 minutes in the refrigerator. The media was removed and radiolabelled nucleic acid in serum free media (at 4°C) was added to each well and incubated for the required time period at 4°C.

2.8.5. Assessment of the Effect of Metabolic Inhibitors on Cell Association of Nucleic Acids.

To assess the effect of metabolic inhibition on the cell association of nucleic acids, cells were pre-treated with sodium azide and 2'-deoxy-glucose, which reduce cellular ATP production by more than 60%, as described by Wu-Pong *et al*, 1992. Serum free media containing 10mM sodium azide and 50mM 2'-deoxy-glucose was prepared and

warmed to 37°C. Following initial washing of the cells with sterile PBS as described in Section 2.8.1 cells were pre-treated for 30 minutes at 37°C with media containing the metabolic inhibitors. The media was removed and radiolabelled nucleic acid in the serum free media containing inhibitors was added to the wells and the cell association experiments were continued as described in Section 2.8.1.

2.8.6. Assessment of the Effect of Competitors on the Cell Association of Nucleic Acids.

In self-competition studies the uptake of a radiolabelled nucleic acid was assessed in the presence of an excess of unlabelled material of the same type. In competition studies an excess of PS or PO ODN was used to compete with radiolabelled nucleic acid for association with cells. Experiments were performed as described in Section 2.8.1 with the following additions: Following initial washing of the cells with sterile PBS as described in Section 2.8.1 cells were pre-treated for 15 minutes at 37°C with media containing the unlabelled, competing nucleic acid. The media was removed and radiolabelled nucleic acid in serum free media containing an excess of the unlabelled competitor was added to the cells. In the above competition studies a 10 to 100-fold excess of the competitor was used with respect to the radiolabelled nucleic acid. Cells were incubated at 37°C and studies were completed as described in Section 2.8.1.

2.8.7 Cellular Localisation of Fluorescent Labelled Nucleic Acids and Dextrans.

2.8.7.1 Preparation of Fluorescent Labelled Probes for Localisation studies.

Rhodamine B isothiocyanate-dextran (0.002-0.01 moles RITC per mole of glucose, approximate Mol. wt. 10,000) was obtained from Sigma and purified through DNA Grade Sephadex G-25 Columns (Nap-10 columns, Pharmacia Biotech) as described in Section 2.3.7 to remove any free rhodamine present. Fluorescent labelled dextrans are well characterised markers of fluid phase endocytosis and are known to reside in endosomal / lysosomal vesicles following cell entry (Berlin and Oliver, 1980). Unlike dextrans labelled with fluorescein, dextrans labelled with other fluorophores such as rhodamine demonstrate significantly less bleaching when exposed to light (Swanson, 1989). 5'-FITC labelled nucleic acids were synthesised and purified as described in Section 2.5.4. Fluorescein (free acid crystals) and free FITC (mixed isomers, HPLC purified) were obtained from Sigma.

2.8.7.2. Cell Association of Fluorescent Labelled Probes.

Cells were seeded onto 8 well plastic chamber slides (Nunc-Gibco, Paisley, UK) and incubated for 24 hours. A431 cells were seeded at a density of 3×10^4 cells per well, U87-MG cells were seeded at a density of 2×10^4 cells per well. Following incubation cells were washed with sterile PBS at 37°C.

5'-FITC labelled nucleic acids were diluted to a concentration of 5μM in serum free culture media. Where co-localisation studies were to be performed, the media containing the fluorescein labelled nucleic acids was supplemented with 5μM RITC-dextran. The media was added to the cells which were incubated for the required period. In control experiments, cells were incubated with 5μM of free FITC or free fluorescein and incubated for the same period of time as test samples. Following incubation cells, were washed six times with sterile PBS to remove traces of non-cell associated fluorophores. Cells were fixed 2% v/v glutaraldehyde (freshly prepared in PBS) for 30 minutes on ice. The fixative was removed and the cells and the plastic chamber gasket was separated from the slide. Slides were mounted in glycerol (50%) in PBS containing 1% v/v DABCO as an anti-fading agent (Johnson *et al*, 1982) and a cover slip added.

2.8.7.3 Fluorescent Microscopy.

A Jenamed fluorescence microscope (Jena Instruments, Oberkochen, Germany) and a high pressure mercury HBO-50 light source (C-Z Scientific, Basingstoke, UK) were used to visualise cell associated fluorophores.

The excitation and emission spectra of fluorescein and rhodamine B overlap to a small degree (Lansing-Taylor and Salmon, 1989), therefore narrow band-pass filters were required to distinguish between the fluorophores. A 510nm wavelength blocking filter was used for detection of fluorescein and FITC labelled probes. With reference to the UV emission spectra of fluorescein and rhodamine (Lansing-Taylor and Salmon, 1989), the use of the 510nm narrow band blocking filter should totally prevent any cross-over excitation from rhodamine. For the detection of rhodamine dextran, a 590nm wavelength narrow band blocking filter was used as recommended for the differential detection of this fluorophore (Holz, 1982). The filter sets were mounted in a mechanical cube positioned above the objective lens of the microscope to permit rapid switching of the filters and allow images of the fluoresence from multiple probes in the same specimen.

Cells were photographed using an Olympus camera with Jenamed adapter and Kodak Gold (colour), Konika (colour) or Ilford FP4 (black and white) film (minimum ISO 200).

2.9 STATISTICS

Unpaired students t-tests, 95% confidence intervals and two-sided P values were calculated using the Instat 2 Statistical Software package (Graph Pad Software, San Diego, USA). Tests were performed on cell association data from different experimental populations to determine statistically significant differences between mean values obtained in experiments.

Low P values indicated that experimental populations were unlikely to be sampled from populations with equal mean values. Data sets were assumed to be significantly different when P values below 0.05 were calculated. Unpaired t-tests assumed that data were randomly sampled, that each value was obtained independent of the others, that the populations were scattered according to a Gaussian distribution and that the standard deviations (SD) of the two populations tested were not significantly different. The software package was used to perform F-tests which indicated whether or not the standard deviations of two experimental populations were significantly different.

Where standard deviations were significantly different (i.e. where the SDs of two data populations varied widely), a Welch t-test was used. The Welch t-test is a modification of the unpaired t-test that does not assume that two populations have equal standard deviations, although this test continues to assume that data follow a Gaussian distribution. The P values obtained using Welch's t-test tend to be more conservative than those obtained using the standard unpaired t-test, which generally result in higher P values and a wider confidence interval.

CHAPTER THREE

DESIGN, *IN VITRO* ACTIVITY AND BIOLOGICAL STABILITY OF HAMMERHEAD RIBOZYMES

3.1. INTRODUCTION.

A comprehensive characterisation of a *trans*-acting hammerhead ribozyme used for the inhibition of mRNA expression would appear to consist of the following steps: cleavage of a short, synthetic substrate *in vitro*; cleavage of a transcript of the target mRNA *in vitro*; ribozyme function in cells (*ex vivo*), then in an animal model (*in vivo*) and finally, in humans (Birikh *et al*, 1997b).

Despite the fact that the general sequence and structural requirements for hammerhead ribozyme catalysis are well defined (see Section 1.2.3), kinetic studies have demonstrated that the design of ribozymes which can efficiently cleave short, synthetic substrates *in vitro* can be problematic (see Section 1.2.3.4). For example, the length of the 'substrate binding sequences' is critical for efficient, multiple-turnover catalysis. Furthermore, certain ribozyme and substrate sequences can form alternative, non-binding secondary structures which can prevent the proper formation of ribozyme-substrate complexes, and hence, diminish catalytic activity (Walstrum and Uhlenbeck, 1990, Clouet-D'Orval and Uhlenbeck, 1996).

The use of RNA folding algorithms can be useful for identifying some secondary structures within relatively small RNA molecules, such as *trans*-acting hammerhead ribozymes (Denman, 1993). This can allow potentially inactive ribozymes to be eliminated from consideration prior to *in vitro* screening. Indeed, a folding algorithm has been utilised in this report for this purpose. However, establishing that any given ribozyme is catalytically active *in vitro* is only the first step in designing a ribozyme construct for the inhibition of mRNA expression. Even ribozymes which demonstrate potent catalytic activity *in vitro* cannot, necessarily, be assumed to show a similar level of activity *ex vivo* (or even *in vivo*) because there are many additional factors inside cells which can influence activity (see Section 1.3.2). This is demonstrated by the fact that some ribozymes, capable of cleaving short substrates *in vitro*, have proved ineffective at cleaving mRNAs within cells (Crisell *et al*, 1993, Tsuchihashi *et al*, 1993, Rossi et al, 1994, Heidenreich *et al*, 1994, Beck and Nassal, 1995). The

inaccessibility of target sites within large mRNAs, which have highly complex secondary and tertiary structures, is considered to be the main reason for the lack of correlation between *in vitro* and *ex vivo* data which has sometimes been observed (Marschall *et al*, 1994, Birikh *et al*, 1997b).

Several strategies have been devised for targeting accessible binding sites within mRNAs: For example, many antisense ODN constructs were originally targeted to sites in the proximity of the AUG initiation codon, or to splice-sites within mRNAs, because these sites were thought to be accessible to binding (Van Der Krol *et al*, 1988, Liebhaber *et al*, 1992). A similar approach was initially used in this report when designing ribozymes. However, studies by other workers have cast doubt upon this approach to site selection (L'Huillier, 1992 & 1996) and it is now thought that there is probably no optimum region for cleavage that is generic to all mRNAs (Rossi, 1995). Computer folding algorithms, such as MFOLD (Zuker *et al*, 1991) may be useful for predicting some accessible sites within the complex secondary structures of large RNA molecules. This technique has also been used in this report to study ribozyme target sites within the epidermal growth factor receptor (EGFr) mRNA. However, this method has several limitations (see Section 1.3.2.2) and, therefore, the use of empirical (*in vitro*) techniques, such as RNase H mapping (Birikh *et al*, 1997a), may have several advantages. The benefits of some of these recently developed techniques are discussed in Section 1.3.2.2, but they were not used in this study.

A major obstacle to the exogenous administration of ribozymes to cells is the instability of these RNA-based molecules in biological fluids (see Section 1.2.4.1). When this study was initiated, several investigators had applied site specific chemical modifications to the hammerhead ribozyme motif in order to examine its function and improve biological stability (for examples see Ruffner and Uhlenbeck, 1990 & 1991, Perreault *et al*, 1990, Pieken *et al*, 1991, Taylor *et al*, 1992, Williams *et al*, 1992, Bratty *et al*, 1993). In general, chemical modifications had been shown to have beneficial effects upon ribozyme stability but also reduced the catalytic activity of ribozymes (Usman and Cedergren, 1992). Chemical modifications at several sites within the catalytic core of the ribozyme often resulted in a pronounced loss of catalytic activity (see Section 1.2.4)

In an attempt to produce catalytically active, yet biologically stable hammerhead constructs, a variety of site-specific chemical modifications were introduced into hammerhead ribozyme molecules during this report. Initially, ribozyme constructs were prepared which contained phosphorothioate (PS) inter-nucleotide linkages at all sites, except for those within the 'catalytic core' of the ribozyme. These modifications

were combined with the introduction of ODNs in the 'substrate binding arms' of the ribozyme. However, during the preparation of this report, a number of other investigators were able to identify functional groups within the 'catalytic core' of the hammerhead which could accept chemical modifications, without severely disrupting catalysis (see Section 1.2.4 and Figure 1.8). In some instances this allowed biologically stable hammerhead constructs to be prepared which retained almost 'wild type' levels of catalytic activity (see Sections 1.2.4.2 to 1.2.4.4). In the light of these discoveries, further modifications to hammerhead ribozymes were investigated in the present study. These modifications involved the introduction of 2'-O-methylated nucleosides into hammerhead constructs, which were constructed with only 5 unmodified ribonucleotides within the 'catalytic core' of the molecule.

The serum half-life of modified ribozymes and / or antisense ODNs is often used to compare relative biological stability. Probably because the determination of serum half-life offers a basic indication of the (extra-cellular) stability of these molecules *in vivo*. Hence, the stability of chemically synthesised constructs was examined in human serum. Ribozyme stability was also examined in a mixture of lysosomal enzymes. The lysosomes represent a major site of intra-cellular degradation (Alberts *et al*, 1989), especially for molecules which enter cells via endocytosis (see Hudson *et al*, 1996a). Therefore, the stability of ribozymes incubated in lysosomal extract was used to give an indication of intra-cellular stability. In addition to the studies reported in this chapter, the stability of unmodified (all-RNA) ribozymes and antisense ODNs was also examined in the lysosomal enzyme mixture and in a variety of animal tissue extracts. These studies are described in Appendix II (see also Hudson *et al*, 1996a).

In summary, *trans*-acting hammerhead ribozymes directed against proto-oncogene targets have been designed and evaluated in this chapter. Initial studies describe the design of ribozymes directed against the *c-myc* (proto-oncogene) mRNA, which was selected because the research group had previous experience in developing antisense ODNs directed against this target (see Section 2.2.1). However, the main focus of attention in this chapter (and subsequently throughout this thesis) has been the design and exogenous delivery of ribozymes directed against the epidermal growth factor receptor (EGFr) mRNA (see Section 1.6.3). The immediate aim was to produce chemically stabilised, yet catalytically active ribozyme constructs, which could remain stable in cell-containing media for several hours. This would allow the cellular uptake characteristics of the ribozyme constructs to be examined in subsequent studies.

3.2. MATERIALS AND METHODS.

The 'Wisconsin Package' of computer programs, (Version 8.1-Unix, Genetics Computer Group, Madison, USA) was used in this report to obtain mRNA sequences and for folding analyses. These programs were accessed 'on-line' via the Unix system at Daresbury Laboratories, UK. For purposes of copyright the following acknowledgement is cited as requested by the program authors: Program Manual for the Wisconsin Package, Version 8, Genetics Computer Group, Madison, USA and the Program Manual for the EGCG Package, Hinxton Hall, Cambridge, UK.

3.2.1. Design of Hammerhead Ribozymes Directed Against *c-myc* mRNA

In initial studies, hammerhead ribozymes directed against exon 2 of the human *c-myc* mRNA (Gazin *et al*, 1984. Genbank accession code; D90467) were designed. Previous studies, by other investigators in the laboratory had utilised antisense ODNs which were directed against the 'AUG' initiation codon site (located at bases 4495-4498) on exon 2 of this mRNA. Preliminary data indicated that these antisense ODNs were capable of inhibiting p64 *myc* protein expression *ex vivo* (unpublished data; Dr. Kolya Bellov, formerly of Aston University). Hence, it was thought that sites in the proximity of the 'AUG' codon could be accessible targets for hammerhead ribozymes. All 'GUC' triplet codons within the mRNA sequence, located at sites close to the AUG initiation codon, were identified using the Wisconsin package. 'GUC' was selected as the target cleavage triplet because most 'wild-type' hammerhead ribozymes cleave RNA molecules after this triplet of nucleotides (see Section 1.2.1) and kinetic studies had generally indicated that this sequence could be cleaved *in vitro* by most *trans*-acting hammerheads (Bratty *et al*, 1993). Hammerhead constructs, based on the catalytic motif described by Tuschl and Eckstein (1993) were designed against sites containing the 'GUC' cleavage triplet. Hammerheads were constructed with 5 base pairing nucleotides in each of Stems I and III, since this was generally considered to be the minimum number of bases required for proper substrate binding (Usman *et al*, 1996). Any ribozyme construct containing a tetrad of guanine (G) bases was not used because ODNs containing 'G'-tetrads had been shown to elicit non-sequence specific effects when administered *in vivo* (Yaswen *et al*, 1992).

The site closest to the AUG initiation codon, which fulfilled the above criteria, was selected for synthesis. The hammerhead ribozyme chosen (5'-GGU GUC UGA UGA GGC CGU UAG GCC GAA ACC GC-3', see Figure 3.1), was designed to cleave the *c-myc* mRNA after a GUC triplet at position 4727. This ribozyme was synthesised as described in Section 3.2.3. A 27-mer sequence of the *c-myc* mRNA target (5'-UCC

UAC GUU GCG *GUC* ACA CCC UUC CUC-3', see Figure 3.1) was also synthesised, in order to allow the *in vitro* activity of the ribozyme construct to be tested. (N.B. The ribozyme and substrate sequences were synthesised and purified by reverse phase HPLC as described in Section 2.4.4 by Cruachem Ltd, Glasgow).

Figure 3.1. Diagram Showing the Two-Dimensional Structure of the 32-mer *c-myc* Hammerhead Ribozyme and the 27-mer Substrate Sequence. (The arrow indicates the predicted site of catalytic cleavage. The numbering system of Hertel *et al*, 1992 has been used to identify nucleotides within the catalytic core).

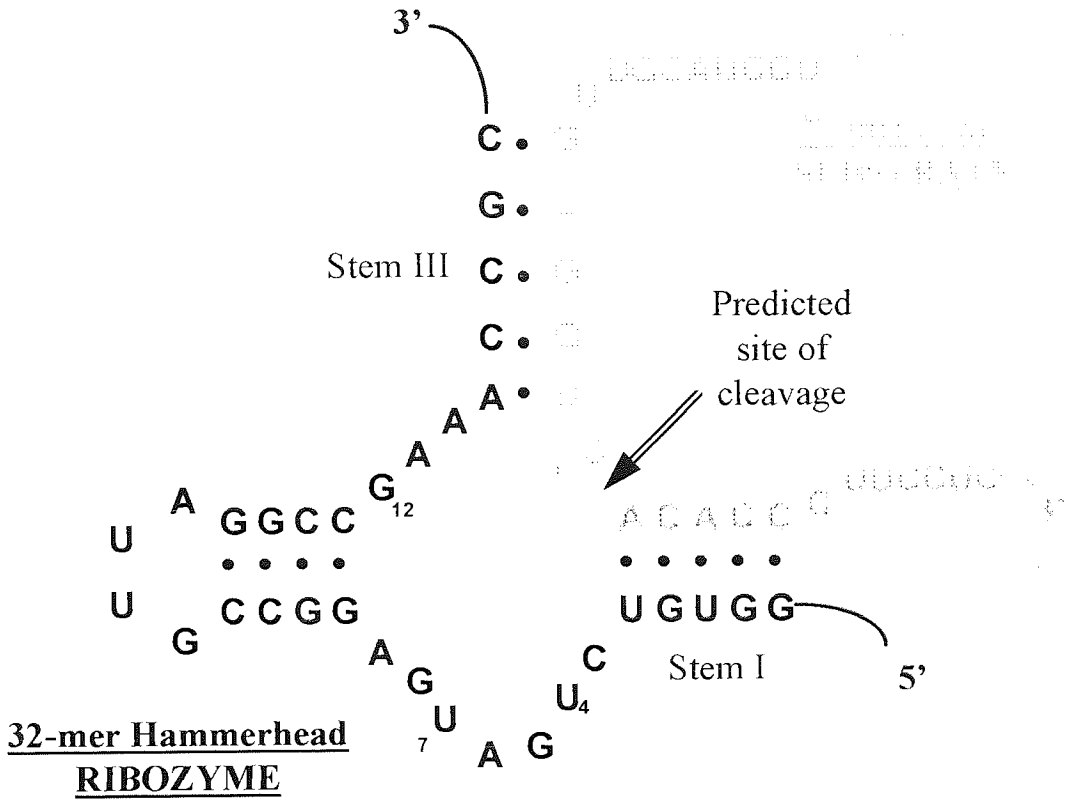

3.2.2. The Design of Hammerhead Ribozymes Directed Against Epidermal Growth Factor Receptor (EGFr) mRNA.

The sequence of the 'wild type' human *c-erb*B1 (the EGFr precursor mRNA) gene described by Ullrich *et al* (1984) (Genbank accession code; X00588) was obtained using the Wisconsin package. All 'GUC' triplets within the mRNA sequence were identified as potential targets for ribozyme cleavage. Ribozymes were designed with 7 base pairing nucleotides in stems I and III, since kinetic studies predicted that ribozymes with similar length base-pairing arms usually demonstrated efficient multiple turnover catalysis *in vitro* (see Section 1.2.3.4 and Hertel *et al*, 1994). The catalytic core of the hammerhead ribozymes was based on that described by Werner

and Uhlenbeck (1995). Unlike the catalytic core structure used for the *c-myc* ribozyme (see Figure 3.1); the terminal loop on stem II of this motif did not contain any uridine (U) bases, which were replaced by adenine (A) bases. Purine bases such as adenine are considered to be less susceptible to endonucleases than pyrimidine bases (Beigelman *et al*, 1995), hence, this slight alteration to the sequence could potentially improve stability. Again, any ribozyme construct which contained a quartet of guanine (G) bases within its structure was eliminated from consideration (see Section 3.2.1).

3.2.2.1. Identifying Self-Complementary Structures within Hammerhead Ribozyme Molecules.

In order to identify any degree of self-complementary base-pairing within designed hammerhead constructs; Sequences were folded into their lowest energy conformations using the RNAFOLD program (Wisconsin EGCG package). This program graphically depicts the predicted secondary structure of small RNA molecules in their lowest energy state. The program also gives an indication of the energy required for Watson-Crick base-pair formation (ΔG) within a particular structure, expressed in units of kcal / mol. Very low (negative) values of ΔG are an indication of stable base-pair formation (and stable secondary structure formation) within the lowest energy structure. Ribozyme sequences folding into a 'correct' hammerhead structure demonstrated ΔG values of -3.3 kcal / mol. This reflected the formation of stable base pairs in Stem II of the ribozyme (see Figure 1.4). Where ΔG values below -3.3 kcal / mol were obtained, this indicated the potential for the formation of stable, self-complementary base-pairs within other areas of the ribozyme structure. This could potentially prevent substrate binding, hence, these constructs were eliminated from further consideration.

3.2.2.2. Using RNAFOLD to Predict the Biological Activity of anti-EGFr mRNA Hammerhead Ribozymes.

To determine the potential reactivity of ribozyme / substrate complexes (*in vitro*) the RNAFOLD program was used in accordance with the method of Denman (1993). Only single RNA species can be folded using the RNAFOLD program. Hence, the determinations were made by folding *cis*-acting forms of the ribozyme / substrate complexes. The method used is outlined in schematic form in Figure 3.2. Briefly, short substrate sequences of the mRNA target, and ribozymes directed against them, were joined at the end of either stem I or stem III with a 5-base loop of adenine (A) or uridine (U) residues, thus forming 4 different *cis*-acting ribozyme structures. Each of these was then folded into its lowest energy structure using RNAFOLD. The

percentage of *cis*-constructs which adopted the hammerhead secondary structure was noted and ΔG for the lowest energy structures was scored. Ribozyme / substrate complexes which did not form hammerhead structures in all 4 (100%) of the *cis*-acting files were eliminated from further consideration. Previous studies have shown that such constructs usually demonstrate poor substrate cleavage *in vitro* because they form non-hammerhead secondary structures (Denman, 1993).

Figure 3.2. Diagram Showing the Procedure used to Examine the Folding Characteristics of Different Ribozyme / Substrate Complexes.

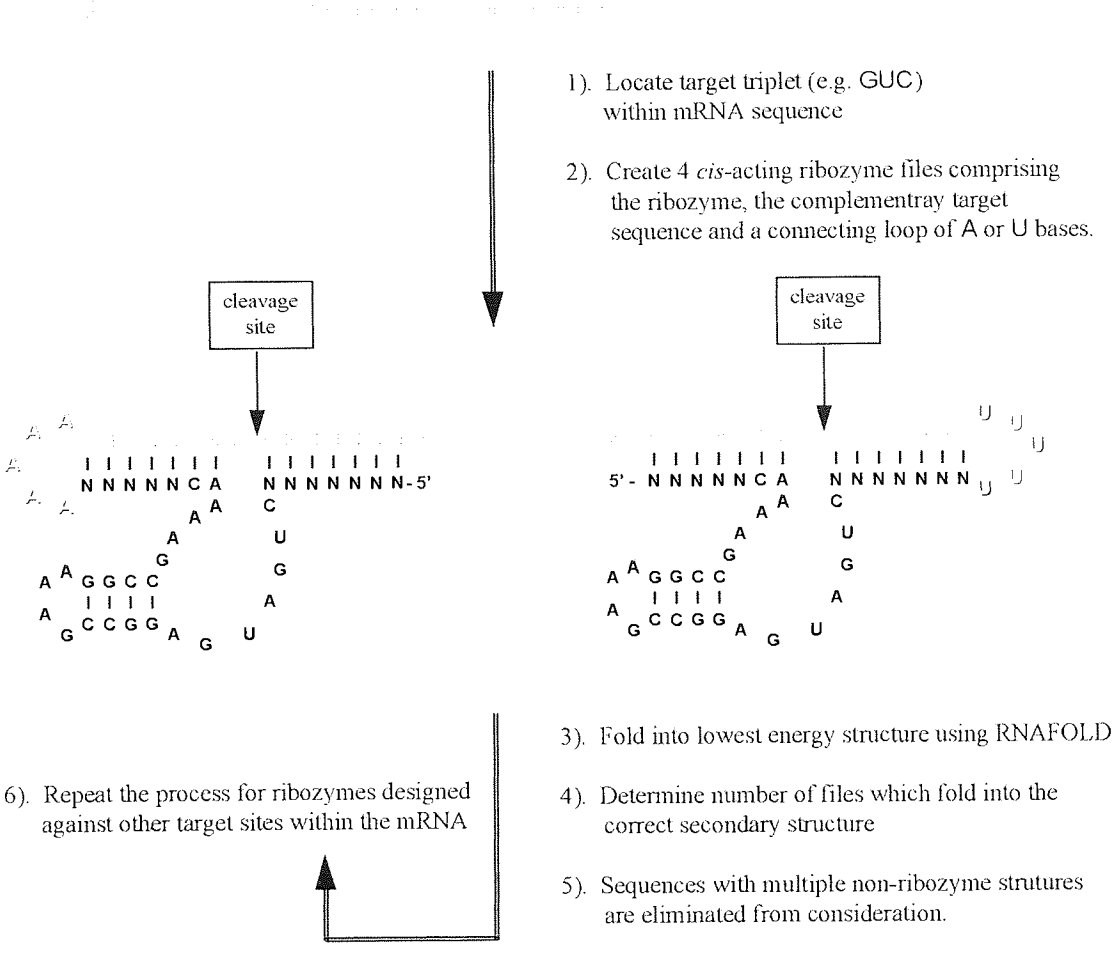

3.2.2.3. Using MFOLD to Predict the Accessibility of Target Sequences within the Epidermal Growth Factor Receptor (EGFr) mRNA.

To predict the accessibility of target sites within the EGFr mRNA, large sections of the mRNA sequence were folded using the MFOLD program, which is part of the Wisconsin EGCG package. The Unix system at the Daresbury Laboratory allowed RNA sequences of up to 500 bases to be analysed using the MFOLD program. The EGFr mRNA sequence totalled 5532 bases, and hence, the entire mRNA sequence could not be folded as a single data file. Therefore, the accessibility of target

sequences was analysed within 500 base sequences of the EGFr mRNA. Sequences were folded into the lowest energy structure and two energetically sub-optimal structures using the MFOLD program. Graphic representations of folded structures were obtained as 'squiggle' plots using the Ghost-View for Windows® program (courtesy of Dr. Peter Lambert, Aston University). Target sites within the folded structures were then identified and examined for their apparent accessibility to ribozyme binding. Target sites at or near single stranded regions (e.g. within loop regions), and / or sites containing distorted double-stranded regions which were free of complex secondary structure, were considered to be the most favourable targets for ribozyme cleavage.

3.2.3. Synthesis, Radiolabelling and Chemical Modification of Hammerhead Ribozymes.

All-RNA hammerhead ribozymes and substrate sequences were synthesised as described in Section 2.4.1 and deprotected as described in Section 2.4.3. Unless otherwise stated, all-RNA ribozymes and substrates were purified by PAGE as described in Section 2.6.1.

Figure 3.3. Diagram Showing the Structure of The Chimeric DNA / RNA Hammerhead Ribozymes Directed Against the *c-myc* mRNA. [The numbering system of Hertel *et al*, 1992 has been. Bases shown in bold type are unmodified ORNs, other bases are ODNs. The symbol '•' denotes the position of phosphorothioated linkages].

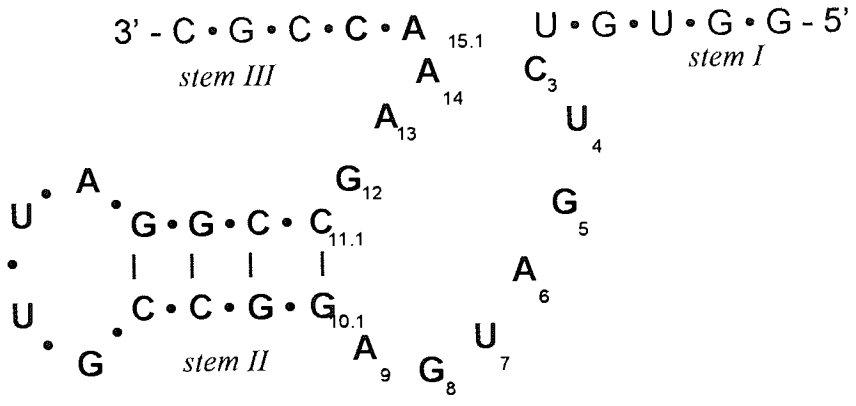

In an attempt to improve the stability of hammerhead ribozyme constructs; a variety of chemically modified, chimeric ribozyme constructs were synthesised during the preparation of this thesis (see sections 3.1. and 1.2.4): Initial modifications involved the synthesis of chimeric *c-myc* ribozymes containing ODNs within stems I and III (i.e. within the substrate binding arms), at all sites except for the nucleotides at positions $A_{15.1}$ and $C_{15.2}$ which were retained as ORNs (see Figure 3.3 and for

nomenclature see Figure 1.4). Furthermore, all inter-nucleotide linkages within stem I, stem-loop II and stem III of the molecule were phosphorothioated (see Section 1.2.4.2). Unmodified phosphodiester linkages were retained at sites which were 5' to bases C_3 to $G_{10.1}$, and at all sites which were 5' to bases G_{12} to $A_{15.1}$ (i.e. at all sites within the catalytic core, see Figure 3.3). These chimeric DNA / RNA ribozymes were synthesised as described in Sections 2.4.1, deprotected as described in Section 2.4.3 and purified by non-denaturing PAGE as described in Section 2.6.1.

Ribozymes directed against the EGFr mRNA were synthesised which contained a variety of site-specific chemical modifications (see Figure 3.4). These were synthesised in a two step process as described in Section 2.4.2. In the first step, a 3-mer ODN 'starter' sequence containing PS inter-nucleotide linkages was synthesised. This would comprise the 3'-terminus of the 36-mer ribozyme molecule. In the second step, the relevant reagents were changed on the automated synthesiser and the remainder of the ribozyme sequence was added to the 3-mer 'starter' sequence. The remaining nucleotides were all 2'-O-methylated, with the exception of 5 specific bases within the catalytic core (i.e. bases G_5, A_6, G_8, G_{12} and $A_{15.1}$) which were retained as unmodified ORNs (see Figure 3.4).

Figure 3.4. Diagram Showing the Structure of The Chimeric, Partially 2'-O-Methylated, Hammerhead Ribozyme Motif Directed Against the EGFr mRNA. [The numbering system of Hertel *et al*, 1992 has been used. Bases shown in bold and underlined represent unmodified RNA bases, boxed bases represent oligodeoxynucleotides (DNA bases. All other nucleotide bases are 2'-O-methylated. The symbol '•' denotes the position of phosphorothioate linkages].

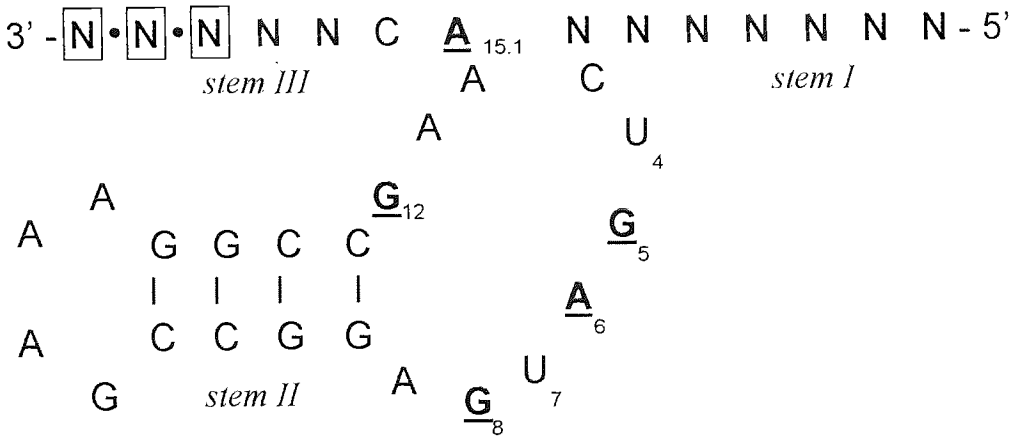

These chimeric sequences were deprotected as described in Section 2.4.3 and were purified by non-denaturing PAGE as described in Section 2.6.1. Both modified and unmodified ribozymes and ODNs were 5'-end labelled using T4 kinase as described in

Section 2.5.1. Following 5'-end radio-labelling, nucleic acid sequences were separated from 'free' radiolabel by PAGE as described in Section 2.6.1 and were column purified as described in Section 2.6.2.

For internal radio-labelling of chimeric ribozymes; the sequence was first synthesised in two halves (see Section 2.5.3 and Figure 4.1), which were ligated using T4 RNA ligase as described in Section 2.5.3.2. Internally radiolabelled ribozymes were separated from non-ligated sequences by PAGE as described in Section 2.6.1 and were column purified as described in Section 2.6.2.

3.2.4. *In Vitro* Catalytic Activity Assays.

A 'standard' buffer solution was prepared for all cleavage reactions (50mM Tris-HCl (pH 7.5), 10mM $MgCl_2$ (molecular biology grade, Sigma) in sterile double distilled water) which was autoclaved prior to use. This 'standard' reaction buffer solution has been used by a variety of other groups to demonstrate hammerhead ribozyme-mediated cleavage of RNAs *in vitro* (for example see Fedor and Uhlenbeck, 1992, Tuschl and Eckstein, 1993, Beigelman et al, 1995). Ribozyme and substrate samples of known concentration were evaporated to dryness under reduced pressure and reconstituted at the required concentration in a 50μL volume of the 'standard' reaction buffer. To disrupt any aggregates of RNA molecules which formed during storage, reconstituted ribozyme and substrate samples were separately heated to 90°C for 1 minute in a water bath and were allowed to cool on ice to 37°C.

To initiate the cleavage reaction, the required volumes of ribozyme and substrate solutions were mixed with vortexing. Reactions were carried out under conditions of both ribozyme excess (single turnover conditions) and substrate excess (multiple turnover conditions). To assess the degree of substrate cleavage aliquots of the reaction mixture were removed after timed intervals and quenched with a 'stop' buffer (8M urea, 50mM EDTA and 0.1% w/v of the dyes bromophenol blue and xylene cyanole, both obtained from Sigma, UK). Radiolabelled substrates and any products were separated by 15% denaturing PAGE (8M urea) as described in Section 2.6.1 and were visualised by autoradiography as described in Section 2.2.3. Autoradiograph band intensities were quantified as described in Section 2.2.4. Where catalytic activity was examined under single-turnover conditions (excess ribozyme); the fraction of substrate remaining was plotted as a function of time and fitted to a double exponential function using MicroCal Origin (MicroCal Software, Northampton, Massachusetts, USA). The 'fast' (first exponential) portion of the double exponential

curve was used to determine activity half-times and observed reaction rates (from semi-natural log (ln) plots).

Where catalytic activity was examined under multiple-turnover conditions (excess substrate conditions), more detailed kinetic analyses were performed. Initial reaction rates were measured in several experiments, where a range of different ribozyme:substrate ratios had been used. The substrate concentration in these experiments was kept at least 10-fold higher than the (fixed) ribozyme concentration (10nM). Therefore, in theory, reactions would be described by Michaelis-Menton equation (for review see Ferscht, 1977). Initial reaction rates were plotted as a function of the substrate concentration, which allowed any deviation from Michaelis-Menton kinetics to be examined. Eadie-Hoftsee plots were then prepared as described by Ferscht (1977). The Eadie-Hoftsee plot is basically a linear, graphical representation of the Michaelis-Menton equation (Ferscht, 1977). Data were fitted to a linear function on these plots using a least squares ('best linear fit') analysis method (MicroCal Origin software). The parameters V_{max}, K_m and k_{cat} were then estimated from Eadie-Hoftsee plots as described by Ferscht (1977): V_{max} (the maximum reaction rate) was determined from the intercept of the Eadie-Hoftsee Plot with the y-axis (x=0). K_m (the Michaelis constant; equal to the substrate concentration at which the reaction rate is half its maximum value) was determined from the gradient of the Eadie-Hoftsee plot. The rate constant; k_{cat} (the maximum number of molecules cleaved in unit time or 'the turnover number'), was determined using the equation; ($k_{cat}=V_{max}$ /Ribozyme (enzyme) concentration), as described by Ferscht (1977).

3.2.5. Stability Studies

The stability of radio-labelled ODNs and ribozyme constructs was examined in human serum obtained from blood samples provided by healthy volunteers (kindly supplied by Dr. M. Coleman, Aston University). Stability was also examined in an extract of rat lysosomal enzymes (prepared as described in Appendix II), which has been shown to contain levels of proteolytic enzymes very similar to those present within lysosomes *in vivo* (Seymour *et al*, 1994). Dried samples of radiolabelled ribozyme (approximately 10 nanomoles) were reconstituted in 20μL of the extract or sera under examination. The reaction mixture was then incubated at 37°C. After fixed time intervals; aliquots (1μL) of the mixture were removed, quenched with 'stop' buffer (8M urea, 50mM EDTA) and stored at -70°c until all subsequent samples had been collected. Intact radio-labelled ribozymes were separated from degradation products by 20% denaturing PAGE (8M urea). Relative quantities of intact species and

degradation products were estimated by analysis of autoradiograph images (see Section 2.2.4).

In order to examine the stability of ribozyme constructs in cell-containing media (cell supernatants); A431 cells were seeded at 7.5×10^4 cells per well in 24 well plates and incubated for 24 hours in serum-containing media (as described in section 2.7.4). The cells were washed four times with 1mL sterile PBS (warmed to 37°C) per well, which was then aspirated. Stability studies were initiated via the addition of the radio-labelled ribozyme (10 nanomoles per mL) to the apical surface of the cells in (200μL) serum-free DMEM media. Following the required incubation period, the apical media was removed and added to an equal volume of 'stop' buffer (9:1 v / v formamide: TBE (Sigma)). Intact radio-labelled polynucleotides were separated from degradation products by 20% denaturing PAGE (8M urea) as described above.

3.3. RESULTS.

3.3.1. All-RNA Hammerhead Ribozymes Directed Against Human *c-myc* mRNA.

3.3.1.1. *In Vitro* Catalytic Activity of an All-RNA *c-myc* Ribozyme

In order to examine the activity of the 32-mer ribozyme against the 27-mer substrate sequence *in vitro*, experiments were performed as described in Section 3.2.4. In theory, ribozyme mediated cleavage of the 5'-end labelled substrate would be expected to yield two RNA products: A detectable 15-mer 2',3'-cyclic phosphodiester product and an unlabelled 12-mer 5'-hydroxyl sequence which would not be detectable by autoradiography.

The *in vitro* reaction was performed using an excess of unlabelled ribozyme (40nM ribozyme: 1nM substrate) in order to ensure that initial reaction rates obeyed first order kinetics (Ferscht, 1997). Under these conditions, the appearance of the radiolabelled cleavage product on autoradiographs suggested that the ribozyme was able to cleave the substrate in the predicted manner (see Figure 3.5). In order to quantify the extent of substrate cleavage and to allow the activity half life to be determined, the intensity of autoradiograph bands was measured as described in Section 2.2.4. A profile of the cleavage reaction was obtained by plotting the percentage of intact substrate as a function of time (see Figure 3.6). The reaction profile indicated that the rate of cleavage was more rapid at time points up to 8 hours.

However, it appeared that a steady state was reached at reaction times beyond 8 hours. A semi-log plot of reaction profile (see Figure 3.6. (inset)) during the initial 8 hours was linear. This suggested that the reaction proceeded via first order, or pseudo first order, kinetics during the initial 8 hours. Using the method of Ferscht (1977) the activity half life ($t\frac{1}{2}$) was estimated from the semi-log plot using the equation; $t\frac{1}{2} = 0.693 / k$, where k is the observed rate of reaction (obtained from the gradient of the linear semi-log plot).

Figure 3.5. Autoradiograph Demonstrating the *In Vitro* Cleavage of a 27-mer RNA Substrate Sequence by the *c-myc* Hammerhead Ribozyme Under Single Turnover Conditions at 37°C. [Lane **A**; unreacted substrate control (time zero), Lanes **B to G** show progressive cleavage of the substrate as a function of time: Lane **B**; time zero. Lane **C**; time = 2 hours. Lane **D**; time = 4 hours. Lane **E**; time = 8 hours. Lane **F**; time = 18 hours. Lane **G**; time =25 hours. Lane **H**; unreacted substrate (control) incubated in reaction buffer for 25 hours at 37°C].

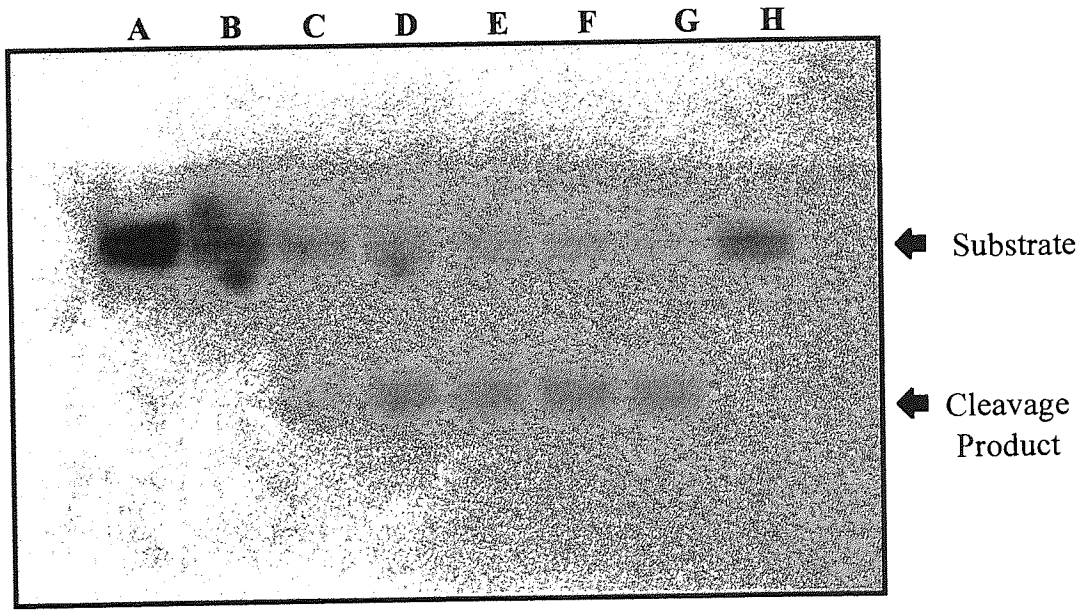

The estimated activity half life was 354 minutes (5.9 hours). This was somewhat inferior to the activity half-lives observed for hammerhead ribozymes described by other investigators: For example, several reports have described all-RNA hammerhead constructs of similar size, which demonstrate activity half lives *in vitro* of less than 5 minutes (for examples see Fedor and Uhlenbeck, 1992, Tuschl and Eckstein, 1993, Hertel *et al*, 1994, Beigelman *et al*, 1995).

The reason for the poor activity demonstrated by the *c-myc* ribozyme was unclear from the above results. This could possibly have been due to the formation of self-complimentary structures within ribozyme molecules. Such a phenomenon could

prevent substrate binding by ribozymes (i.e. this could reduce the population of ribozymes able to bind to substrate molecules). Alternatively this could reflect the formation of alternative, non-cleaving ribozyme / substrate complexes. The formation of such complexes has been highlighted by other investigators (Hertel *et al*, 1996) as a potential reason for the surprisingly poor catalytic cleavage observed with some hammerhead constructs. Ribozymes 'locked' in thermodynamically stable, non-hammerhead conformations with substrate molecules could potentially be rendered inactive. Therefore, the folding characteristics of the ribozyme were examined in subsequent studies (see Section 3.3.1.4).

Figure 3.6. *In Vitro* Activity Profile of 32-mer *c-myc* Hammerhead Ribozyme. (The percentage of intact substrate remaining, in the presence of a 40-fold excess ribozyme, was plotted as a function of time. [INSET: A semi-natural log (ln) plot of the same data is shown].

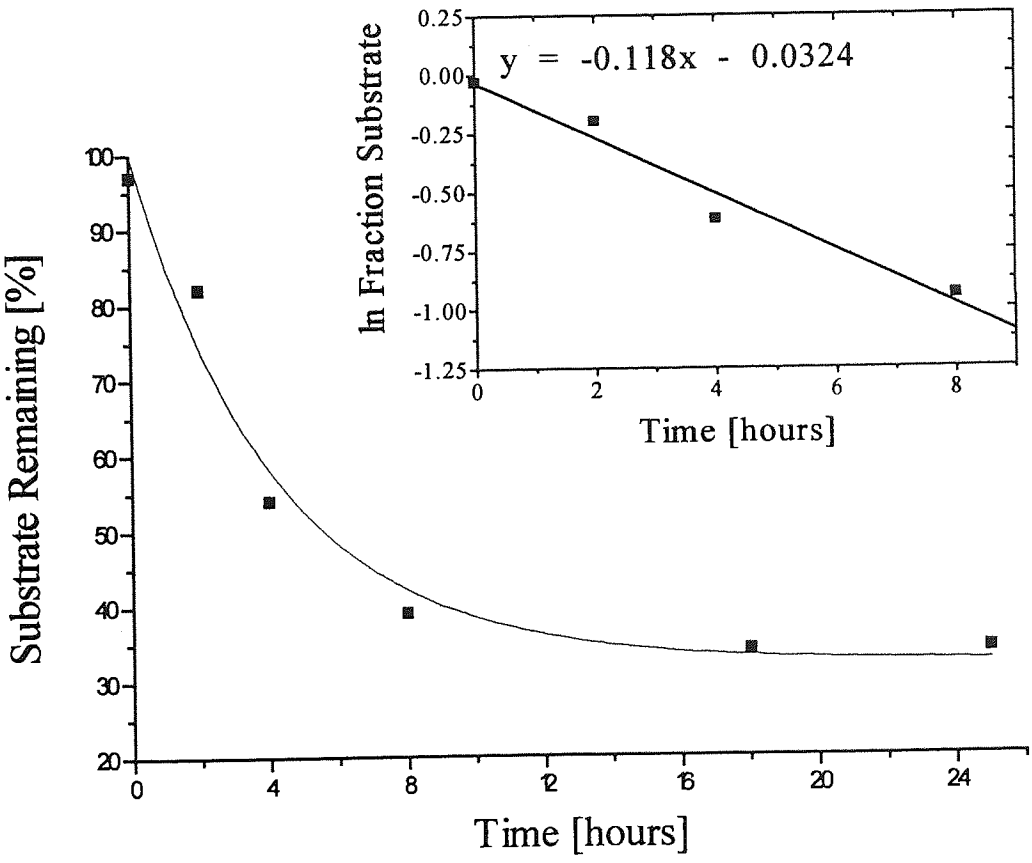

3.3.1.2. Specificity of Substrate Cleavage by the *c-myc* Hammerhead Ribozyme.

In order to demonstrate that the observed cleavage of the 27-mer substrate sequence was specific; an *in vitro* catalytic assay was performed using a non-complementary substrate sequence (5'-CAG CTC GCC CAA *GUC* CTG CGC CTC GCA -3') relating to another potential target site along the human *c-myc* mRNA. The

hammerhead ribozyme would not be expected to bind and cleave a non-complimentary sequence, despite the fact that it contained a 'GUC' nucleotide triplet. The cleavage assay was again performed under conditions of ribozyme excess (40-fold), at 37°C, as described in Section 3.2.4. As a positive control, an *in vitro* catalytic assay was performed using the ('correct') corresponding substrate under the same reaction conditions for a period of 8 hours.

Figure 3.7. Autoradiograph Demonstrating the Inability of a 32-mer *c-myc* Hammerhead Ribozyme in Cleaving a Non-Complimentary RNA Substrate Sequence *In Vitro*. (Lane **A**; unreacted 'scrambled' RNA (control). Lanes **B to H** show non-complimentary substrate incubated with (unlabelled) ribozyme for increasing time periods: Lane **B**; time = zero. Lane **C**; time = 2 hours. Lane **D**; time = 4 hours. Lane **E**; time = 8 hours. Lane **F**; time =18 hours. Lane **G**; time = 25 hours. Lane **H**; time =48 hours. Lane **I**; complementary target substrate reacted with ribozyme for 8 hours (positive control). Lane **J**; complementary substrate (control)].

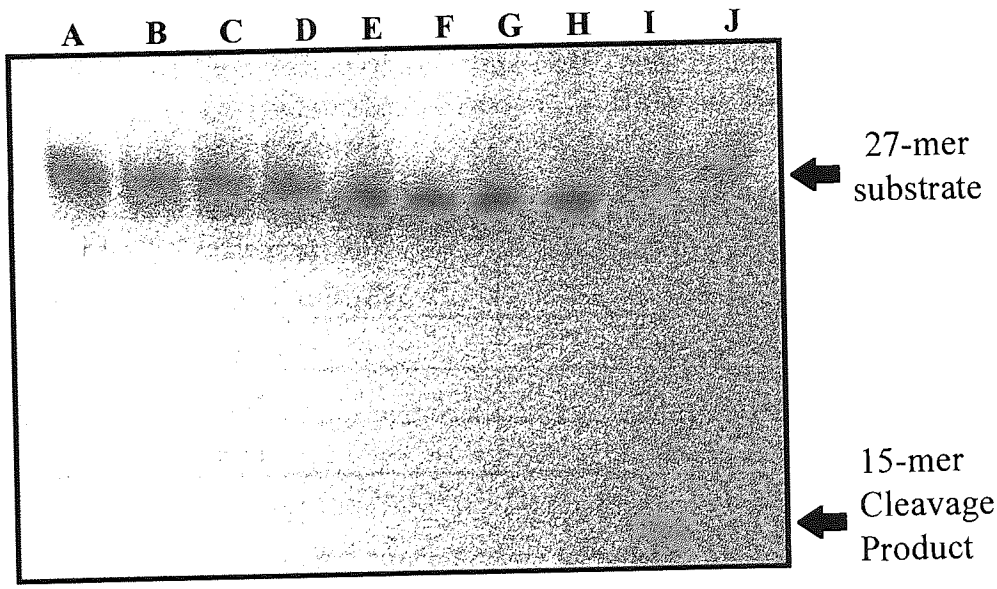

Samples were separated by 20% denaturing PAGE for a similar period of time (3.5 hours, at 10 watts constant power) to that used in the previous study (see Section 3.3.1.1). Results are demonstrated in Figure 3.7. The lack of any bands migrating below the level of the radiolabelled non-complimentary sequence (see Figure 3.7), suggested that the ribozyme was unable to cleave the non-complimentary RNA under the conditions tested. In the test samples (lanes B to H), no bands were observed which migrated at a similar rate to the 15-mer cleavage product, demonstrated in the positive control sample (Lane I).

Therefore, this indicated that substrate cleavage by the *c-myc* hammerhead ribozyme was sequence-specific because the ribozyme was only able to cleave the its corresponding (antisense) substrate sequence. This validated the results observed in the previous study (see Section 3.3.1.1) in which the ribozyme was reacted with its complementary substrate sequence.

3.3.1.3. The Effect of the Magnesium Ion Concentration on the *In Vitro* Catalytic Activity of the *c-myc* Hammerhead Ribozyme.

In order to assess the requirement for magnesium ions in the catalytic reaction, *in vitro* catalytic activity assays were performed as described in Section 3.2.4. However, in these assays the concentration of magnesium ions (in the form of nuclease-free, molecular biology grade $MgCl_2$) present in the catalytic reaction buffer was varied: *In vitro* catalytic assays were performed using 2mM, 10mM ('standard' concentration) and 20 mM $MgCl_2$. Substrate half-lives were estimated from autoradiographs as described in Sections 2.2.4 and 3.2.4. Results are demonstrated in Table 3.1.

Table 3.1. A Comparison of Substrate Half Times Following Cleavage by the *c-myc* Hammerhead Ribozyme at Different Magnesium ion Concentrations.

$MgCl_2$ Concentration in Catalytic Reaction Buffer	Activity Half-Life *In Vitro* (hours)
2mM	19.0
10mM	5.9
20mM	5.7

Increasing the magnesium ion concentration above that used in the 'standard' reaction buffer did not produce any significant reduction ($P>0.05$) in the activity half time of the *c-myc* ribozyme. However, a 5-fold reduction in the concentration of $MgCl_2$ produced more than a 3-fold increase in the activity half-time. This indicated that optimal catalytic activity was dependant upon the presence of a minimum concentration of magnesium ions. Other investigators have observed a similar dependency on the concentration of divalent metal ions in the hammerhead ribozyme reaction (see Section 1.1.3.2.4). For example, Dahm and Uhlenbeck (1991) concluded that a magnesium ion concentration of at least 10mM was required for the optimal catalytic activity of a series of hammerhead ribozyme constructs *in vitro*. The dependency on the magnesium ion concentration provided further evidence to suggest

that substrate cleavage observed during *in vitro* activity assays (see section 3.3.1) was a result of hammerhead ribozyme-mediated catalysis.

3.3.1.4. Analysis of the Folding Characteristics of the *c-myc* Hammerhead Ribozyme.

In an attempt to explain the relatively poor catalytic activity of the *c-myc* hammerhead ribozyme, observed during *in vitro* catalytic assays, folding analyses were performed as described in Sections 3.2.2.1 and 3.2.2.2. The *c-myc* hammerhead ribozyme molecule was folded into the lowest energy structure and two energetically sub-optimal structures using the RNAFOLD algorithm. The ('correct') hammerhead structure was predicted to be one of the energetically sub-optimal conformations, with a free energy (ΔG) of -3.3 kcal / mol, resulting from the formation of four stable base pairs in Stem II of the molecule. The formation of this structure would be desirable for catalytic activity. However, an alternative structure was predicted by the algorithm to be the lowest energy conformation (i.e. the most stable conformation) and this was calculated to have a free energy of -4.1 kcal / mol. Within the alternative structure, stable base-pairs formed between nucleotides in the substrate binding arms (stems I and III) and nucleotides (G_{12} and A_{13}) within the catalytic core of the ribozyme motif (see Figure 3.9). This could potentially prevent the stem nucleotides from binding to the complementary substrate sequence. The fact that the 'alternative' structure demonstrated a lower free energy than the 'hammerhead' structure suggests that the formation of the 'alternative' structure would be thermodynamically favoured in solution. On the other hand, the 'alternative' conformation could be in rapid exchange with the hammerhead conformation. In either case, the formation of the alternative, self-complimentary conformation could limit substrate binding, and hence, could reduce the catalytic efficiency of this ribozyme construct.

In order to examine the characteristics of the complex formed between the ribozyme and its substrate; folding analyses were performed as described in Section 3.2.2.2. Four *cis*-acting ribozyme / substrate constructs were designed and folded using the RNAFOLD program. Three of the four *cis*-acting files (75%) adopted the predicted hammerhead structure, with a calculated free energy (ΔG) of -13.4 kcal /mol. These conformations would be expected to represent catalytically active ribozyme / substrate complexes. However, one of the files folded into an alternative non-hammerhead conformation, with a free energy (ΔG) of -14.8 kcal /mol. In this folded structure, base-pairing between the substrate sequence and bases U_4, G_5 and A_6 within the catalytic core of the ribozyme prevented the formation of the 'correct' hammerhead

structure. Studies by other investigators (Denman, 1993) have shown that ribozyme / substrate complexes which adopt non-hammerhead conformations when folded using this method, usually demonstrate poor catalytic activity *in vitro*. Hence, the formation of inactive ribozyme / substrate complexes offers a further possible explanation for the poor activity observed with the *c-myc* hammerhead ribozyme *in vitro*. (see section 3.3.1.1).

Figure 3.8. RNAFOLD Analysis of the *c-myc* Hammerhead Ribozyme Showing Lowest Energy Conformations.

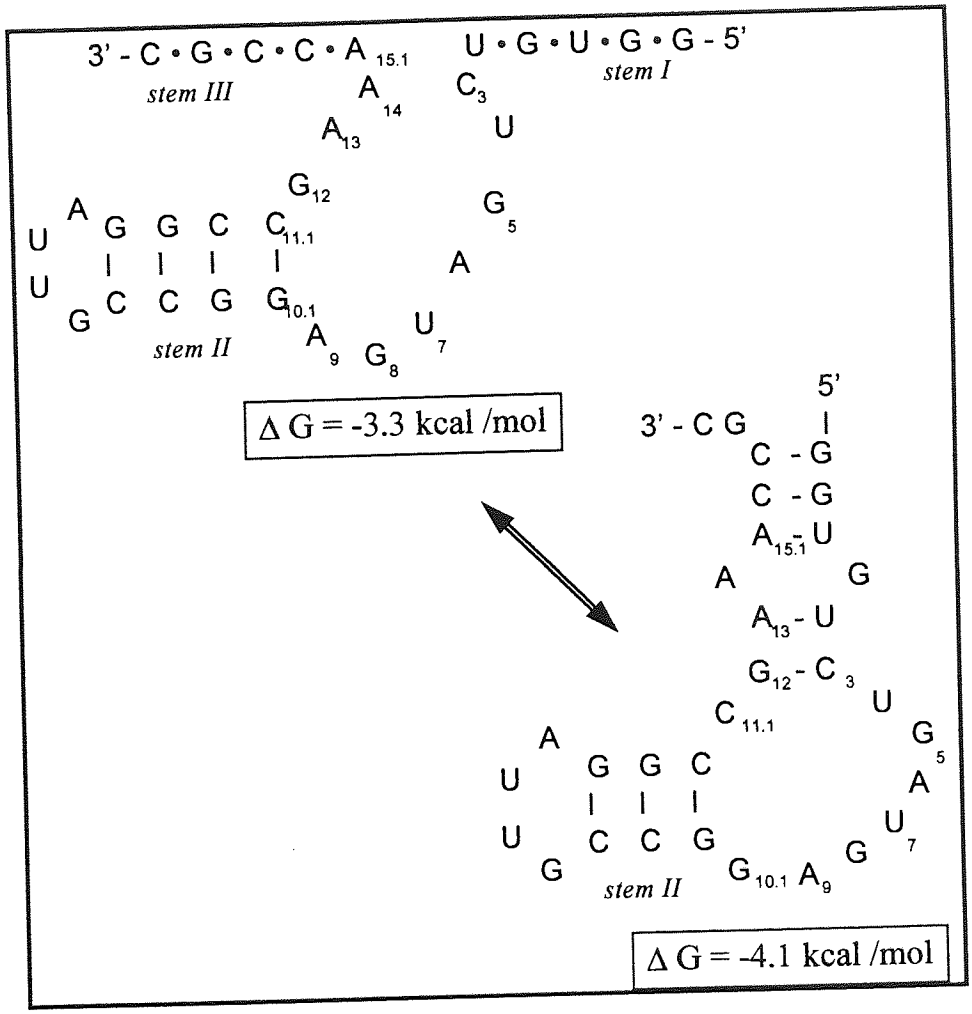

3.3.2. *In Vitro* Activity and Stability of A Chemically Modified *c-myc* Hammerhead Ribozymes Containing Deoxyribonucleotides and Phosphorothioate Linkages.

Stability studies indicated that unmodified (all-RNA) *c-myc* ribozymes were extremely unstable in human serum and other biological media, and hence, this would severely limit the cellular uptake of the intact molecule (see Appendix II). By comparison, ODNs, especially those containing PS inter-nucleotide linkages were more biologically stable. Probably because these molecules were less efficient substrates for

nucleases and ribonucleases present in biological media. Therefore, the possibility of introducing site-specific ODN and PS modifications, into the *c-myc* hammerhead ribozyme structure was investigated as a means of improving biological stability.

At the time that this study was initiated, the introduction of PS linkages into the hammerhead ribozyme structure had been mainly confined to kinetic studies (Ruffner and Uhlenbeck, 1990, Buzayan et al, 1990, Ruffner and Uhlenbeck, 1991, Slim and gait, 1991) which aimed to describe the details of the hammerhead catalytic reaction mechanism (see sections 1.2.3 and 1.2.4). As a consequence, little information was available with regard to the effects of partial PS modification on the biological stability of hammerhead constructs. Consequently, in an attempt to produce a more nuclease-stable, active hammerhead construct: *c-myc* hammerhead ribozymes were chemically synthesised which contained oligodeoxynucleotides (DNA) and PS inter-nucleotide linkages. These were introduced at sites within the substrate binding arms and within stem-loop II, to produce the chimeric motif demonstrated in Figure 3.4. Kinetic studies predicted that modifications at these sites would be unlikely to affect the catalytic efficiency of the ribozyme construct (see Section 1.2.4).

3.3.2.1. *In Vitro* Activity of Chemically Modified *c-myc* Ribozymes.

In order to examine whether or not the partial chemical modifications had any effect upon the catalytic activity of the ribozyme construct; *in vitro* catalytic assays were performed under single-turnover conditions as described in section 3.2.4. An all-RNA 27-mer sequence of the mRNA, identical to that used in previous assays (see Section 3.3.1.1), was used as the target substrate molecule. Both the ribozyme and substrate sequences were 5'-end radiolabelled prior to use in these studies.

The partially modified DNA / RNA *c-myc* hammerhead was able to cleave the 27-mer substrate sequence in the predicted manner, as indicated by the appearance of a radiolabelled band corresponding to the expected 15-mer cleavage product (see Figure 3.9). The activity half life of the modified construct was estimated to be 5.4 hours. This was similar to the activity half life (5.9 hours) determined for the all-RNA ribozyme construct of the same base sequence which was used in previous studies (see Section 3.3.1). Therefore, it would appear that the introduction of the selective chemical modifications into the stems of the ribozyme did not have a detrimental upon catalytic activity. This finding correlates with that of Shimayama *et al* (1993), who investigated the properties of a number of different chimeric ribozymes, containing ODNs and PS linkages within the stem regions. These investigators found that chimeric constructs generally exhibited catalytic activities which were comparable to

'wild-type' all-RNA ribozymes. However, some chimeric constructs actually demonstrated K_{cat} values which were up to 7-fold higher than 'wild-type' ribozymes (Shimayama *et al*, 1993).

Figure 3.9. Autoradiograph Demonstrating the *In Vitro* Cleavage of a 27-mer *c-myc* RNA Substrate by a Chimeric DNA / RNA Hammerhead Ribozyme Under Single-Turnover Conditions. [Lane **A**; radio-labelled ribozyme and radiolabelled substrate (control) incubated in the absence of magnesium ions for 10 hours, Lane **B** unreacted substrate at time zero (control). Lanes **R1 to R5** show progressive cleavage of the substrate as a function of time: Lane **R1**; time = 1 hour. Lane **R2**; time = 2 hours. Lane **R4**; time = 4 hours. Lane **R6**; time = 6 hours. Lane **R10**; time = 10 hours. Lanes **C1 to C10** show unreacted substrate (controls) incubated for similar time periods in the reaction buffer (i.e. 1 to 10 hours)].

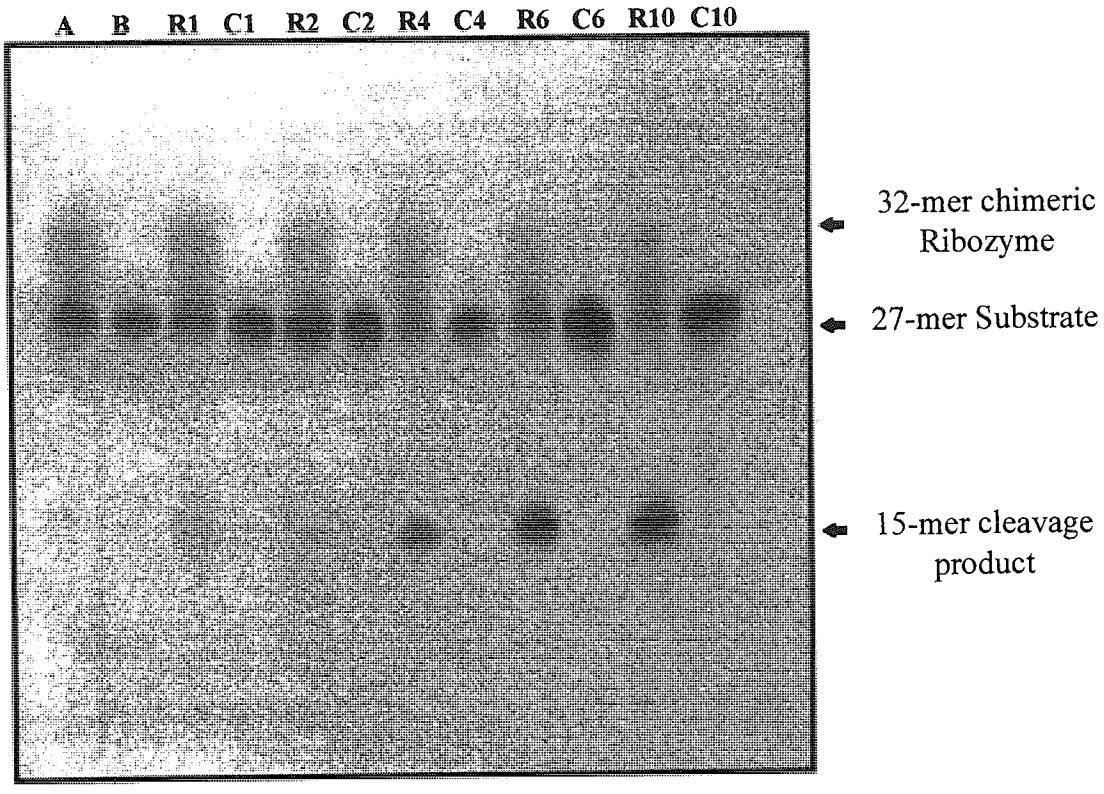

Despite the fact that the catalytic efficiency of the chimeric *c-myc* ribozyme used in these studies was similar to that of the unmodified (all-RNA) construct *in vitro*, it must be reiterated that the catalytic activity of both constructs used was poor in comparison to that of hammerhead constructs designed by other investigators. Possible reasons for this have been discussed in section 3.3.1.4.

3.3.2.2.. Stability of Modified DNA / RNA *c-myc* Ribozymes in Cell-Containing Media and Serum.

The stability profile of the modified construct in human serum is demonstrated in Figure 3.10. Results indicated that the introduction of chemical modifications was unable to render the molecule stable towards the nuclease (and ribonuclease) enzymes present within human serum. Only trace quantities of the intact ribozyme were observed on autoradiographs after 60 minutes incubation. Analysis of band intensities indicated that this fraction of intact ribozyme constituted less than 4% of the total quantity incubated in the serum. Therefore, the selective modifications gave rise to very little improvement in the nuclease stability of the intact ribozyme when compared with the unmodified all-RNA construct (see Appendix II, Figure A2.1).

Figure 3.10. Autoradiograph Demonstrating the Stability Profile of the Chimeric DNA / RNA *c-myc* Ribozyme (10 nanomoles) in Human Serum as a Function of Time. [Lane **C**; Chimeric ribozyme incubated in sterile PBS (control). Other lanes (**5 to 60**) demonstrate the incubation of the chimeric ribozyme with undiluted human serum for increasing reaction times (in minutes)]

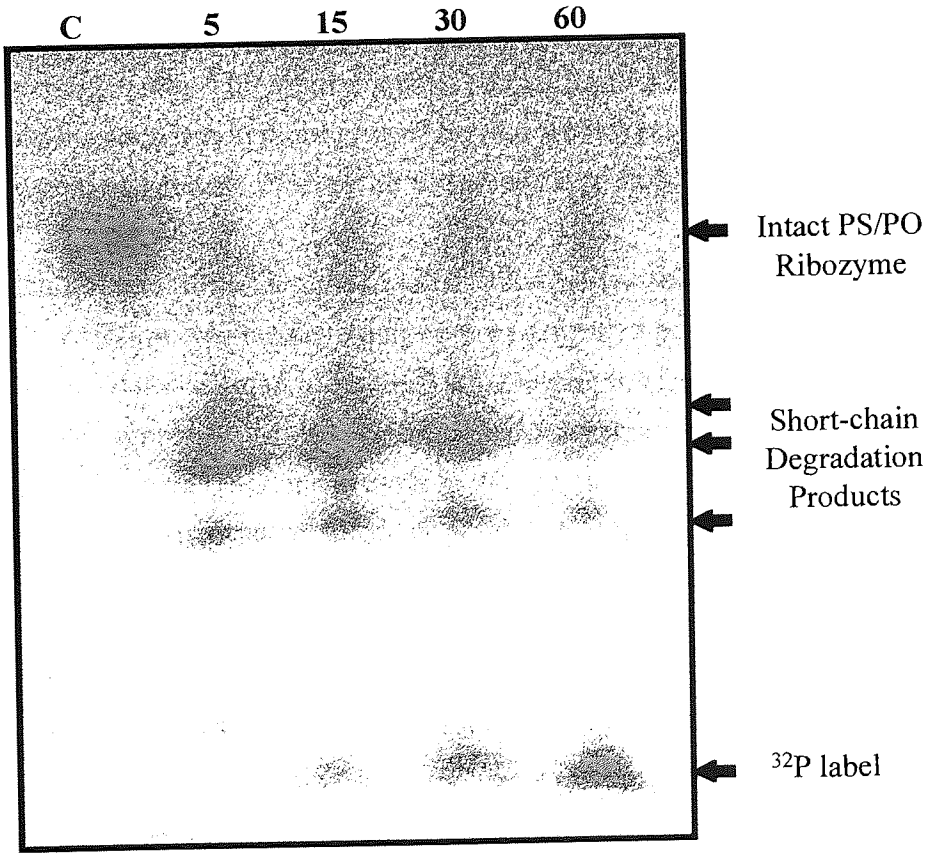

However, the degradation products observed with the modified construct (Figure 3.10) appeared to be different to those resulting from serum degradation of the all-

RNA construct (Figure A2.1). A number of bands corresponding to short chain degradation products were observed when the modified construct was exposed to human serum. This could indicate that the modified construct was mainly degraded by endonucleases, which cleave RNA molecules at sites which are 3' to pyrimidine (U or C) bases (see Section 1.2.4.1). Only four sites within the catalytic core of the modified *c-myc* ribozyme (at positions $C_{11.1}$, U_7, U_4 and C_3), contained pyrimidine nucleotides with 3'-unmodified PO linkages. Other sites which were 3' to pyrimidines had been modified with PS linkages and this may have reduced their susceptibility to cleavage by pyrimidine-specific endonucleases. Other investigators (Shimayama *et al*, 1993) have reported endonuclease-specific degradation of ribozyme constructs containing ODN and PS modifications in the stem regions of the molecule (see Section 1.2.4.1).

The results observed here indicate that the introduction of ODNs and PS linkages into stems I and III of the *c-myc* ribozyme can protect the molecule from the action of exonucleases to some extent. However, the modifications used were unable to improve the overall stability of the ribozyme molecule in human serum because of the action of pyrimidine-specific endonucleases. Despite the instability of the chimeric *c-myc* ribozyme in human serum, the short term objective of the studies described in this chapter was to produce a ribozyme construct which could remain stable in A431 cell-containing media. The cellular uptake properties of a 'cell-stable' construct could potentially be examined in (subsequent) *ex vivo* studies (since it is not always essential to supplement cell culture media with serum during cellular uptake studies).

To test the stability of the modified *c-myc* ribozyme construct when incubated with A431 cells in serum-free media; studies were performed as described in Section 3.2.5 and results are demonstrated in Figure 3.11. Despite the fact that the DMEM culture media was not supplemented with any serum during these studies, the quantity of intact 5'-radiolabelled ribozyme present in the apical media was gradually depleted, as a function of time. Analysis of autoradiograph band intensities indicated that less than 20% of the radiolabelled ribozyme remained within the apical media after 15 minutes. However, it was only possible to speculate with regard to the exact nature of this degradation, since the only degradation products observed were those corresponding to the migration of the free phosphate radiolabel (see Figure 3.14). Therefore, the degradation observed could have been the result of ribozyme digestion by exonucleases, or alternatively, the removal of the 5'-end radiolabel by phosphatase enzymes.

Figure 3.11. Autoradiograph Demonstrating the Stability of the Chimeric DNA / RNA *c-myc* Ribozyme Following Incubation with A431 cells in Serum-Free DMEM Culture Media. [Lane **C**; Control sample of ribozyme incubated in serum-free DMEM (only) for 240 minutes. Other lanes (**15 to 240**) demonstrate the incubation of the chimeric ribozyme in the apical media of A431 cell cultures for increasing incubation times (in minutes)]

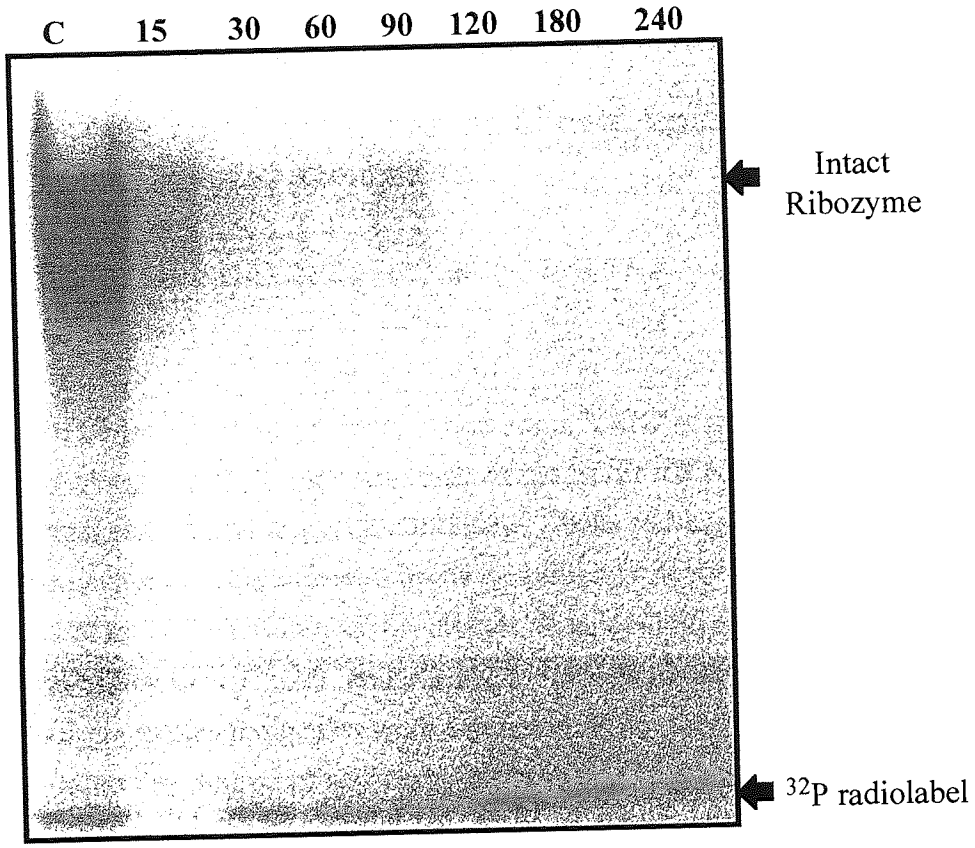

Nevertheless, regardless of the mechanism of degradation, the stability profile suggested that the association of the radio-labelled ribozyme could not be monitored in A431 cells for time periods in excess of 15 minutes. This was because the detection of any cell-associated ribozyme would be dependant upon the [^{32}P] radiolabel remaining attached to the ribozyme molecule during such studies. It was also noted that some degradation was observed in the control sample which was incubated with serum-free DMEM media, in wells which did not contain A431 cells. This suggested that the culture media itself contained low levels of phosphatase and / or nuclease enzymes. Nevertheless the level of degradation observed in the control sample was much less than that observed when ribozymes were incubated in the presence of A431 cells for similar time periods.

Overall, the degradation studies suggest that the site-specific chemical modifications introduced into the *c-myc* ribozyme were unable to render the molecule stable towards nucleases present within human serum. Furthermore the chimeric ribozymes

were unstable in the presence of A431 cells, possibly as a result of degradation by nuclease enzymes exported by these cells. Therefore, alternative chemical modifications would probably be required to improve the stability of ribozyme constructs, if studies involving their exogenous administration to cells were to be performed. However, the degradation observed in the cell studies could have reflected the removal of 5'-end radiolabels via the action of phosphatase enzymes. Hence, the use of an alternative labelling method, which did not involve end-labelling, would also be desirable if cell association studies were to be performed.

3.3.3.. Chimeric Hammerhead Ribozymes Directed Against the Human Epidermal Growth Factor Receptor mRNA.

3.3.3.1. Computer Aided Design of Anti-EGFr mRNA Hammerhead Ribozymes.

A total of 65 potential target sites, containing a 'GUC' triplets of nucleotides were identified along the 5532 base sequence of the EGFr mRNA sequence. Consequently, 65 hammerhead ribozymes, each containing 7 base-pairing nucleotides in stems I and III, were designed against these sites as described in Section 3.2.2. Prior to the synthesis of any EGFr-ribozyme constructs, folding analyses were performed as described in Sections 3.2.2.2. and 3.2.2.2.3. Initially the folding characteristics of the individual ribozymes molecules were examined. Ribozyme constructs which demonstrated any degree of self-complimentary binding (except for the formation of the stem II structure) when folded into their lowest energy conformations were eliminated from further consideration. As a rule of thumb, any construct which demonstrated a free energy (ΔG) of less than -3.3 kcal / mol when folded into its lowest energy conformation demonstrated some degree of self-complimentary binding (N.B. The free-energy of the stem-loop II region of the ribozyme motif demonstrated a free energy of -3.3 kcal / mol when individually folded into its lowest energy conformation). Of the 65 hammerhead designs which were folded using the RNAFOLD algorithm; 13 motifs did not appear to demonstrate any degree of self-complimentary binding when folded into the lowest energy conformation (see Table 3.2). The free energy (ΔG) of all these motifs was determined to be -3.3 kcal / mol, as a result of the formation of the stem-loop II structure within the catalytic motif. This was considered to be favourable for ribozyme activity.

Table 3.2. Hammerhead Ribozymes Designed Against Different Target Regions Along the Human Epidermal Growth Factor Receptor mRNA which Demonstrated Favourable Folding Characteristics. (Designs were based on the hammerhead motif in Figure 3.4).

Sequence Name	**Stem I** (7 'antisense' bases)	**Catalytic Core** (including stem-loop II).	**Stem III** (7 'antisense' bases)
EGFR-02	5'- GGACGCC	CUGAUGAGGCCGAAAGGCCGAA	ACGAGGU -3'
EGFR-04	5'- AGGCGGG	CUGAUGAGGCCGAAAGGCCGAA	ACUCGGG -3'
EGFR-07	5'- UCCCAAG	CUGAUGAGGCCGAAAGGCCGAA	ACCACCU -3'
EGFR-09	5'- UAGAUAA	CUGAUGAGGCCGAAAGGCCGAA	ACUGCUA -3'
EGFR-10	5'- CACUGCU	CUGAUGAGGCCGAAAGGCCGAA	ACUAUGU -3'
EGFR-24	5'- CUCCCAU	CUGAUGAGGCCGAAAGGCCGAA	ACUCCUG -3'
EGFR-37	5'- CCUGAAU	CUGAUGAGGCCGAAAGGCCGAA	ACAAGGU -3'
EGFR-49	5'- CAAUAGC	CUGAUGAGGCCGAAAGGCCGAA	ACAAUGA -3'
EGFR-50	5'- UCUGGAA	CUGAUGAGGCCGAAAGGCCGAA	ACUUGUG -3'
EGFR-51	5'- CUGCCAU	CUGAUGAGGCCGAAAGGCCGAA	ACUUGAU -3'
EGFR-58	5'- CCCAAAG	CUGAUGAGGCCGAAAGGCCGAA	ACCUGAU -3'
EGFR-61	5'- AGGCAGA	CUGAUGAGGCCGAAAGGCCGAA	ACACUUU -3'
EGFR-65	5'- UGUGUGU	CUGAUGAGGCCGAAAGGCCGAA	ACUGAAC -3'

In order to examine the folding characteristics of the complex formed between these ribozymes and their corresponding substrate sequences, the method of Denman (1993) was used, as demonstrated in Figure 3.2. All of the *cis*-acting files, constructed using 11 of the 13 EGFr-ribozyme motifs shown in Table 3.2, adopted a hammerhead secondary structure when folded into the lowest energy conformation using RNAFOLD (i.e. all 4 *cis*-acting files for any given ribozyme / substrate complex adopted a hammerhead secondary structure). The substrate sequences for these ribozyme constructs and the predicted site of cleavage within the mRNA are demonstrated in Table 3.3.

With regard to the remaining 2 ribozyme motifs: Only 50% of the *cis*-acting files based on ribozymes EGFR-37 and EGFR-49; adopted a hammerhead structure when folded into the lowest energy conformation. The *cis*-acting files which did not adopt the hammerhead structure, demonstrated Watson-Crick base-pairing between the relevant substrate and bases within the catalytic core of ribozymes EGFR-39 and EGFR-49. The formation of these base-pairs within ribozyme / substrate complexes (*in vitro*) would potentially prevent substrate cleavage. Since the free energy values

(ΔG) predicted for these 'alternative' structures were lower than those predicted for the 'correct' hammerhead structures, the formation of the alternative conformations would be thermodynamically favoured *in vitro*. Hence, these motifs (EGFR-39 and EGFR-49) were eliminated from further consideration.

Table 3.3. Target Substrate Sequences for Hammerhead Ribozyme Motifs Designed Using the Analysis Method of Denman, (1993). [The abbreviation 'UTR' represents 'untranslated' sequence].

Ribozyme Sequence Name	Designed to cleave mRNA 3' to base:	mRNA Substrate Sequence (predicted site of cleavage indicated by arrow (↓))	Location of Target Substrate Sequence
EGFR-02	73	5'- ACCUCGUC↓GGCGUCC-3'	5'-UTR
EGFR-04	89	5'- CCCGAGUC↓CCCGCCU-3'	5'-UTR
EGFR-07	369	5'- AGGUGGUC↓CUUGGGA-3'	coding region
EGFR-09	549	5'- UAGCAGUC↓UUAUCUA-3'	coding region
EGFR-10	690	5'- ACAUAGUC↓AGCAGUG-3'	coding region
EGFR-24	1983	5'- CAGGAGUC↓AUGGGAG-3'	coding region
EGFR-50	4280	5'- CACAAGUC↓UUCCAGA-3'	3'-UTR
EGFR-51	4394	5'- AUCAAGUC↓AUGGCAG-3'	3'-UTR
EGFR-58	4793	5'- AUCAGGUC↓CUUUGGG-3'	3'-UTR
EGFR-61	5008	5'- AAAGUGUC↓UCUGCCU-3'	3'-UTR
EGFR-65	5401	5'- GUUCAGUC↓ACACACA-3'	3'-UTR

In summary, RNAFOLD analysis of EGFr-ribozyme sequences and *cis*-acting motifs predicted that 11 EGFr-ribozyme constructs (based on the design shown in figure 3.5) would demonstrate favourable folding characteristics *in vitro*. Hence, these ribozyme constructs would be less likely to adopt inactive conformations when reacted with substrate RNA molecules *in vitro*. These constructs were designed to cleave the EGFr mRNA at a various, specific sites throughout the molecule. These substrate sites are shown in Table 3.3.

In an attempt to identify mRNA target sites which would be accessible to hybridisation by ribozymes; the folding characteristics of large sequences of the EGFr mRNA were examined using the MFOLD algorithm as described in Section 3.2.2.3. Squiggle plots (for example see Figure 3.12) were obtained which demonstrated the secondary structure of regions of the EGFr mRNA. Target substrate sequences were then identified within the folded mRNA structures.

Unfortunately, none of the target sites within the substrate appeared to be located within single stranded regions (such as loop structures, see Figure 3.12), which were considered to be the most favourable targets for ribozyme cleavage. However five of the ribozyme target sites (targeted by ribozymes; EGFR-02, EGFR-50, EGFR-51, EGFR-58 and EGFR-65 (shown in Figure 3.12)), appeared to be located at distorted double-stranded regions which were free of complex secondary structure. These sites were considered to be the most favourable for ribozyme binding.

Figure 3.12. Squiggle Plot Showing the Secondary Structure of the 3'-end of the Human EGFr mRNA Sequence (*c-erb*B1), Folded Using the MFOLD Algorithm. (The positions of numbered bases along the mRNA sequence are indicated. The large arrow indicates the predicted site of *trans*-cleavage by ribozyme construct EGFR-65 which is demonstrated in Table 3.3).

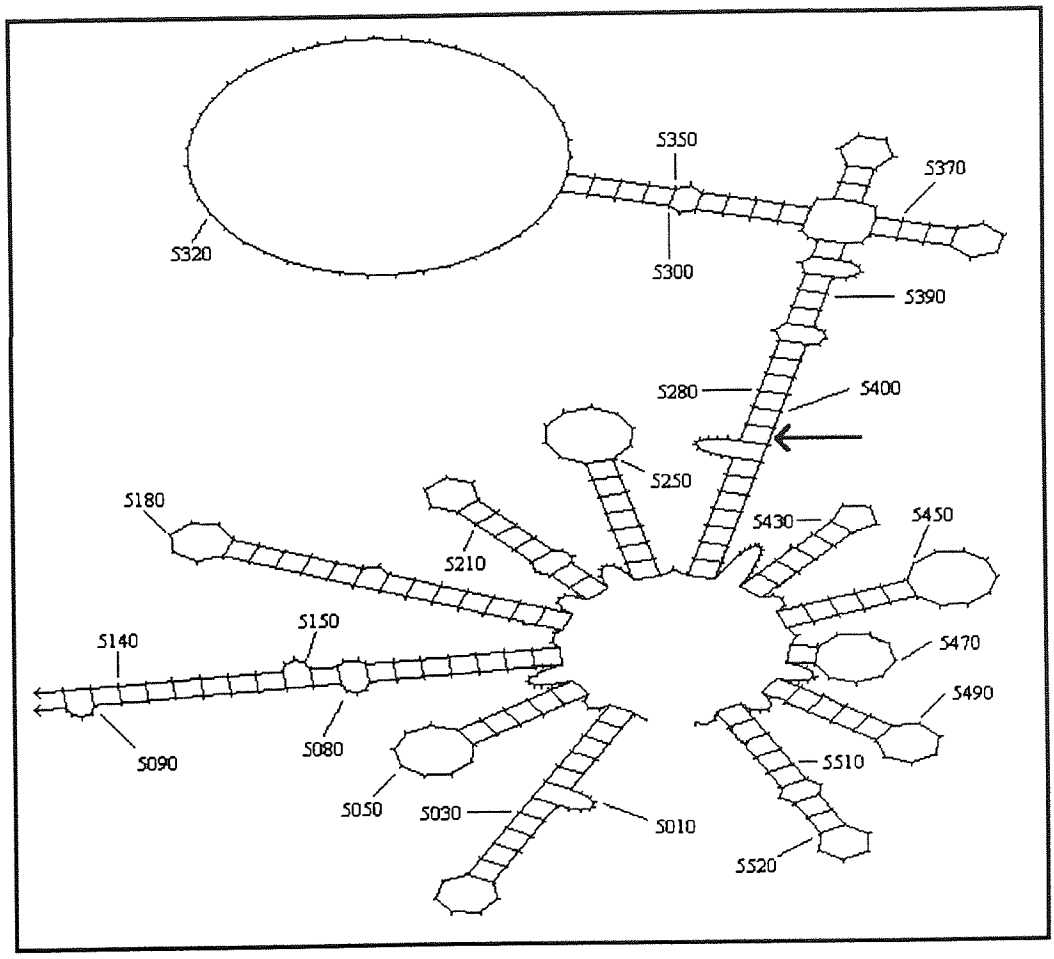

Resources were only available to synthesise a small number of the candidate ribozyme structures from the 'shortlist' of designs shown in Table 3.3. Therefore ribozymes EGFR-02 and EGFR-65 were chosen for synthesis, since these were directed against different functional regions of the mRNA (the 3'-UTR and 5'-UTR, respectively (see Table 3.3)) and their target sites appeared to be accessible, as predicted by MFOLD analyses. In addition, EGFR-24 was also chosen for synthesis because, unlike the

other ribozymes, it was directed to a coding region of the mRNA molecule. Therefore, the synthesis of this ribozyme could possibly allow the targeting of different functional regions of the mRNA to be examined in future studies.

3.3.3.2. Catalytic Activity of Chimeric Hammerhead Ribozymes Directed Against EGFr mRNA Substrates *In Vitro*.

Three hammerhead ribozyme sequences (EGFR-04, EGFR-24 and EGFR-65, see Tables 3.2. and 3.3) directed against the EGFr mRNA, were chemically synthesised in order to assess their relative catalytic activities *in vitro*. These ribozymes were synthesised as chimeric, chemically modified constructs based on the design shown in Figure 3.4. In addition an 'all-RNA' version of ribozyme EGFR-65 was synthesised for use in these studies. Short complementary sequences of the target mRNA substrates (15-mer sequences) were also synthesised and 5'-end radiolabelled.

In vitro catalytic assays were performed under single-turnover conditions (40nM ribozyme:1nM substrate) as described in Section 3.2.4. In theory, ribozyme mediated cleavage of the 5'-end labelled substrates would be expected to yield two RNA products: A detectable 8-mer 2',3'-cyclic phosphodiester product and an unlabelled 7-mer 5'-hydroxyl sequence which would not be detectable by autoradiography. In order to quantify the extent of substrate cleavage; the intensity of auto-radiograph bands was measured as described in Section 3.3.6. Fractions of substrate remaining were plotted as a function of time (semi-logarithmic plot) and activity half-times were estimated as described in section 3.2.4.

The results of the *in vitro* catalytic assays indicated a considerable variation in the relative catalytic rates of the three chemically modified ribozymes (see Figure 3.13). EGFR-65 demonstrated the shortest activity half time of the modified constructs (see Table 3.4 and Figure 3.14), under single turnover conditions. The activity half-time determined for EGFR-24 was slightly higher but was of a similar order of magnitude to that of EGFR-65.

The activity half times for both of these constructs were of a similar order of magnitude to those observed by other investigators with hammerhead ribozymes containing similar 2'-modifications (Beigelman *et al*, 1995). For example, Beigelman *et al* (1995) demonstrated that a partially 2'-O-methylated construct had an activity half time of 4 minutes under single turnover conditions *in vitro*. Moreover the activity half-times demonstrated by EGFR-24 and EGFR-65 were 20 to 30-fold lower than

those observed with the all-RNA *c-myc* hammerhead ribozymes described in previous studies (see Section 3.3.1.1).

Figure 3.13. *In Vitro* Activity Profiles for Chimeric Hammerhead Ribozymes Directed Against EGFr mRNA Targets, Under Single Turnover Conditions.

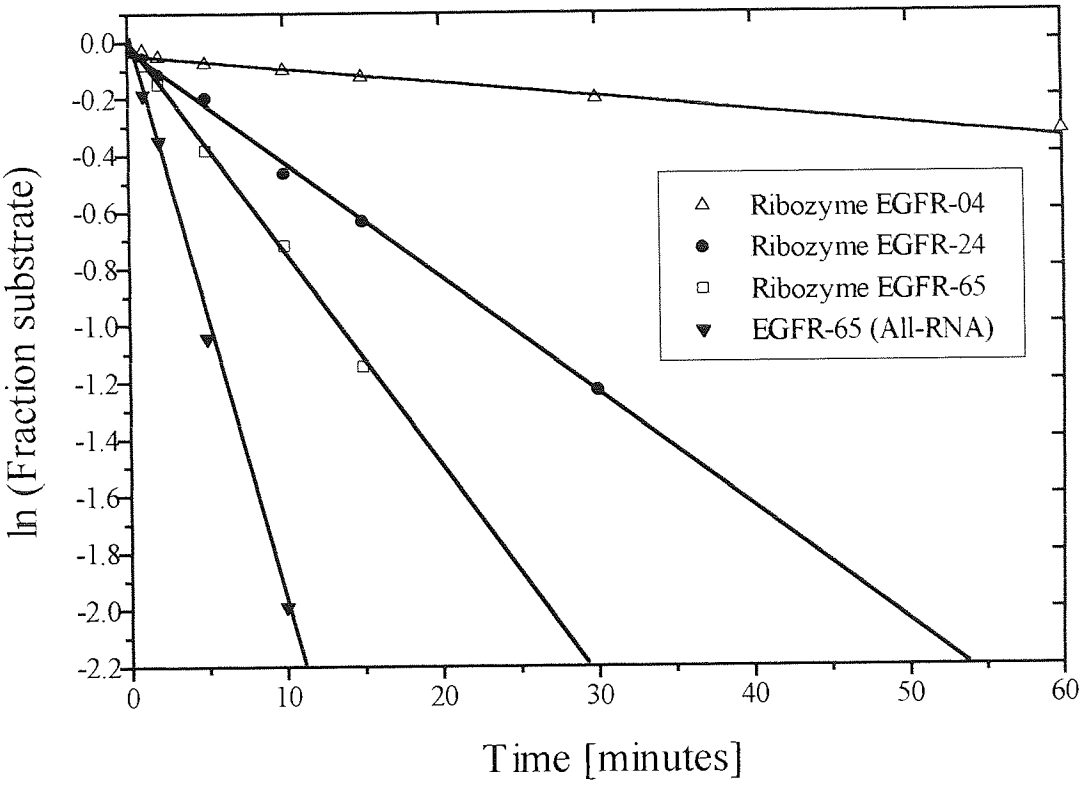

Table 3.4. Estimated Activity Half Times for Different EGFr-Ribozymes Under Single-Turnover Conditions.

Ribozyme Sequence	Activity Half-Life ($t_{\frac{1}{2}}$) (minutes)
Modified EGFR-02	139.5
Modified EGFR-24	17.2
Modified EGFR-65	9.2
'All-RNA' EGFR-65	3.4

However, the reaction rate observed with ribozyme EGFR-02 was inferior to that observed with the other modified constructs. This resulted in an activity half-life in excess of 2 hours for EGFR-02 (see Table 3.4). The reason for the poor catalytic activity demonstrated by this construct was unclear from these studies since this construct had demonstrated favourable folding characteristics in previous studies (see Section 3.3.3). The *in vitro* assay was repeated using samples of EGFR-02 and its corresponding substrate which were obtained from separate (additional) synthesis

batches. However, similar results were observed, indicating that an error in the synthesis of EGFR-02 or its substrate was unlikely to account for the lack of catalytic activity observed.

Figure 3.14. A Representative Autoradiograph, Demonstrating the *In Vitro* Cleavage of a 15-mer RNA Substrate by the Chemically Modified Ribozyme; EGFR-65, Under Single-Turnover Conditions. [Lane **C1**; unreacted substrate control (time zero). Lanes **1 to 60** show progressive cleavage of the substrate as a function of time (in minutes). Lane **C2**; unreacted substrate control after 60 minutes incubation at 37°C. Lane **F**; [^{32}P]-γ-dATP radiolabel (control)].

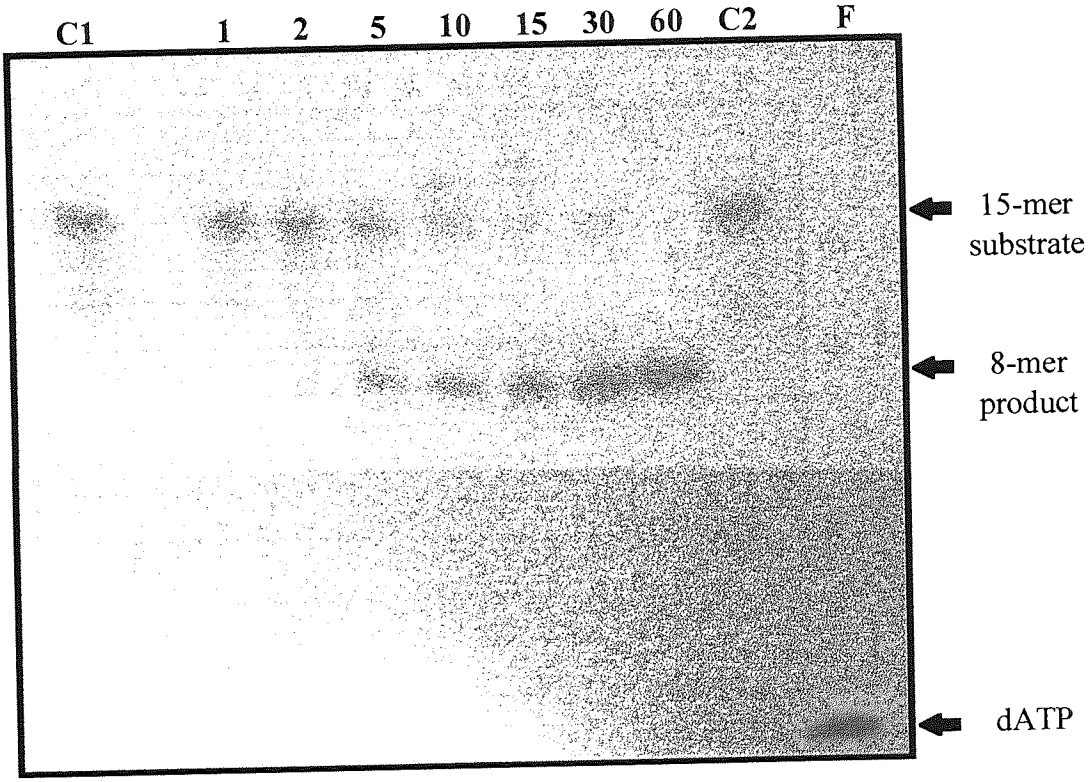

In order to examine any effect which the selective chemical modifications had on the *in vitro* activity of the ribozyme constructs; the activity of an 'all-RNA' version of EGFR-65, was examined (see Figure 3.15). The activity half time demonstrated by the unmodified (all-RNA) construct was almost 3-fold lower than that observed with the modified construct of the same base sequence (see Table 3.4). However, in terms of biological activity in cells, the observed deterioration in catalytic ability could potentially be balanced by an improvement in the biological stability of the modified construct.

Other investigators have reported similar decreases in catalytic efficiency when 2'-modifications were introduced into hammerhead ribozymes at specific sites (Paolella *et al*, 1992). However, other groups have since designed hammerhead constructs

containing specific 2'-modifications, which demonstrate catalytic activities equivalent to those of unmodified (all-RNA) constructs (Heidenreich *et al*, 1994, Beigelman *et al*, 1995, Usman *et al*, 1996). These studies have been discussed in more detail in Section 1.2.4.3.

Figure 3.15. A Representative Autoradiograph, Demonstrating the *In Vitro* Cleavage of a 15-mer RNA Substrate by an Unmodified (All-RNA) Ribozyme; EGFR-65, Under Single-Turnover Conditions. [Lane **C1**; unreacted substrate control (time zero). Lanes **1 to 60** show progressive cleavage of the substrate as a function of time (in minutes). Lane **C2**; unreacted substrate control after 60 minutes incubation at 37°C. Lane **F**; [^{32}P]-γ-dATP radiolabel (control)].

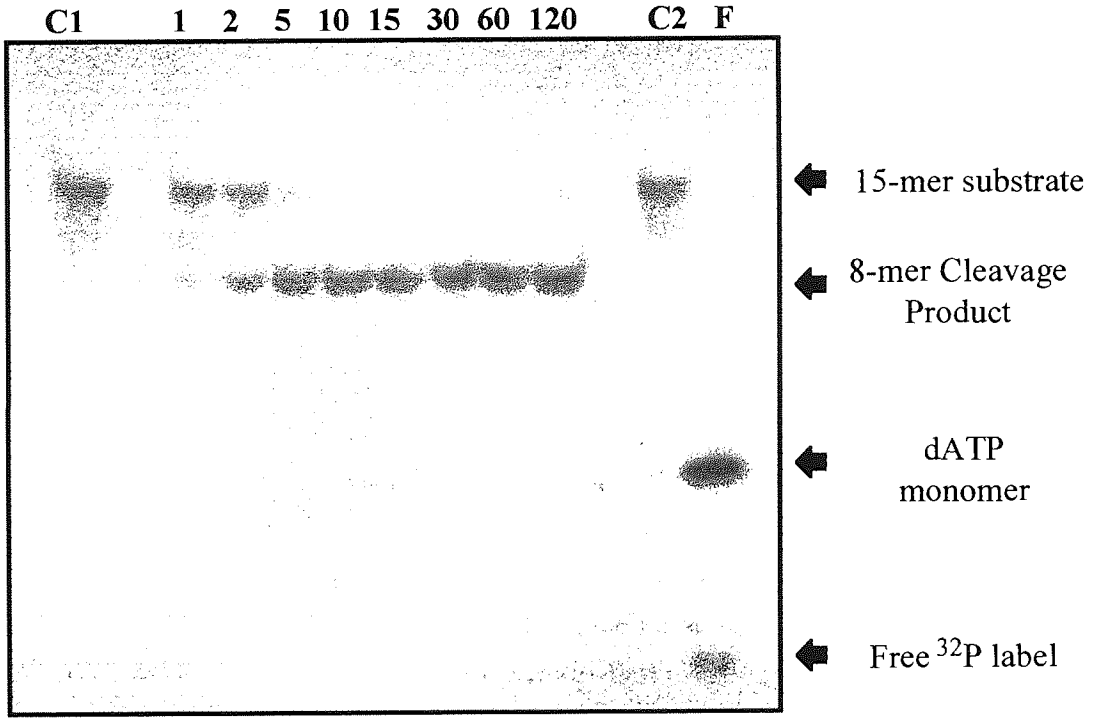

To further characterise the catalytic properties of the (most active) modified EGFR-65 construct, its *in vitro* catalytic activity was examined under multiple-turnover (excess substrate) conditions. The aim was to determine the kinetic parameters K_m and K_{cat} for the EGFR-65 ribozyme, thus allowing this construct to be compared with ribozyme constructs designed by other investigators. To examine multiple turnover catalysis, a series of *in vitro* catalytic assays were performed, in which a variety of different ribozyme:substrate concentration ratios were used. The concentration of the modified EGFR-65 ribozyme was fixed (at 10nM) and the substrate concentration was varied in the range from 100nM (1:10 ratio) to 800nM (1:80 ratio) in these experiments. Representative autoradiographs obtained in two of these assays are demonstrated in Figures 3.16 and 3.17.

Figure 3.16. Representative Autoradiograph, Demonstrating the *In Vitro* Cleavage of a 15-mer RNA Substrate (**100nM**) by Ribozyme EGFR-65 (**10nM**) as a Function of Time. [Lane **C1**; unreacted substrate control (time zero). Lanes **0 to 60** show progressive cleavage of the substrate as a function of time (in minutes). Lane **C2**; unreacted substrate control after 60 minutes incubation at 37°C. Lane **F**; [^{32}P]-γ-dATP radiolabel (control)].

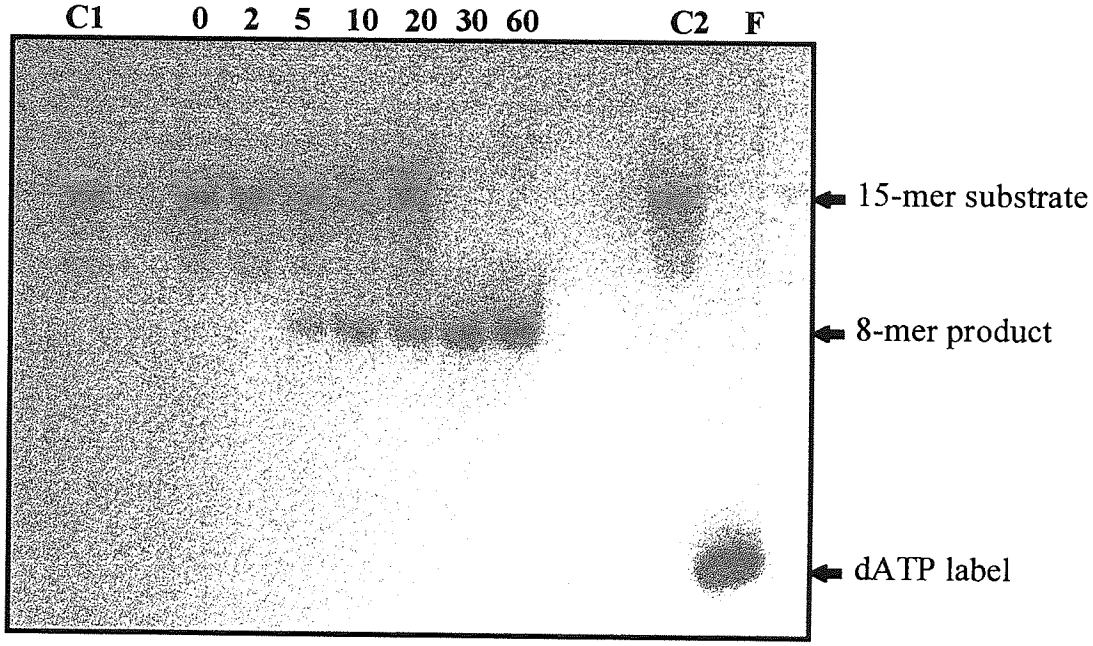

Initial reaction velocities were determined via analysis of autoradiograph band intensities as described in Sections 2.2.4 & 3.2.4. Reaction velocities were plotted as a function of the substrate concentration (see Figure 3.18). The catalytic reaction appeared to obey Michaelis-Menton kinetics (see Ferscht, 1977) because reaction rates were initially linear (first order or pseudo-first order) at low substrate concentrations. However, saturation appeared to occur when higher concentrations of substrate were used. Therefore, the catalytic cleavage reaction appeared to be truly catalytic (i.e. the ribozyme appeared to exhibit multiple turnover catalysis similar to that exhibited by a 'traditional' protein enzyme).

An Eadie-Hoftsee plot was produced using the method of Ferscht (1977). This plot is demonstrated in Figure 3.20. Michaelis-Menton parameters were estimated from the Eadie-Hoftsee plot as described in Section 3.2.4: The chimeric ribozyme (EGFR-65) exhibited a K_m value of 126 nM, this figure represents the substrate concentration at which the reaction rate was at half its maximum value. V_{max} (the maximum reaction rate) was estimated to be 14.6 nM min^{-1} . Finally, k_{cat} (the turnover number) was determined to be 1.46 min^{-1} .

Figure 3.17. Representative Autoradiograph, Demonstrating the *In Vitro* Cleavage of a 15-mer RNA Substrate (**400nM**) by Ribozyme EGFR-65 (**10nM**) as a Function of Time. [Lane **C1**; unreacted substrate control (time zero). Lanes **0 to 60** show progressive cleavage of the substrate as a function of time (in minutes). Lane **C2**; unreacted substrate control after 60 minutes incubation at 37°C. Lane **F**; [^{32}P]-γ-dATP radiolabel (control)]

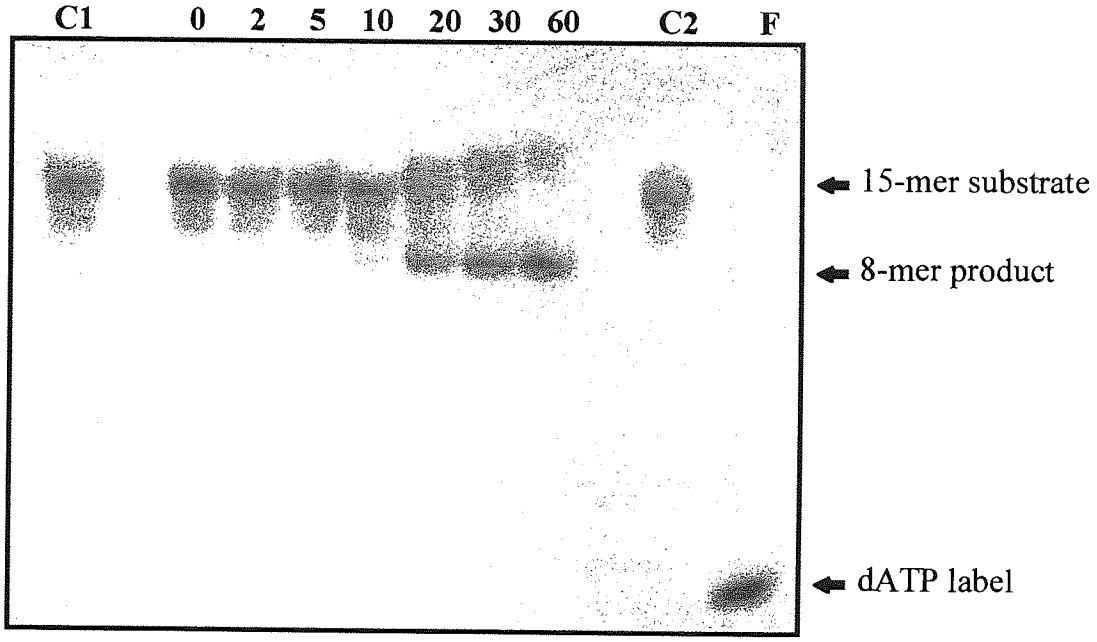

The kinetic parameters obtained with the modified ribozyme EGFR-65 are of a similar order of magnitude to those calculated for a variety of other (partially) 2'-modified hammerhead ribozymes, designed by other investigators (Pieken *et al*, 1991, Beigelman *et al*, 1995, Heidenreich *et al* 1994 & 1996). For example, Pieken *et al* (1991) determined kinetic constants (under similar conditions to those used here) for a variety of hammerhead ribozymes which contained 2'-amino or 2'-fluoro modifications at specific pyrimidine nucleotides: K_m values, determined for these constructs, ranged from 62nM to 321nM. Whereas k_{cat} values ranged from 0.1 min^{-1} to 4.8 min^{-1}. However, several groups have described all-RNA hammerhead constructs which demonstrate k_{cat} values *in vitro* which are up to 6-fold higher than that exhibited by EGFR-65 (Hendry *et al*, 1992, Tuschl and Eckstein, 1993, Hertel *et al*, 1996).

Another point to note is that the kinetic parameters exhibited by EGFR-65, and indeed by all other trans-acting hammerheads described to date, are outside the range observed with protein enzymes. For example, the protein enzyme Ribonuclease A (which also has RNA substrates) exhibits a K_m value of 4.0 mM, and a k_{cat} of 14400 min-1 (Cech and Bass, 1986).

Figure 3.18. Initial Reaction Velocities Plotted as a Function of Substrate Concentration, for a Series of *In Vitro* Catalytic Reactions Involving the Cleavage of a 15-mer radiolabelled RNA Substrate by the Chimeric Ribozyme; EGFR-65, Under Multiple-Turnover Conditions.

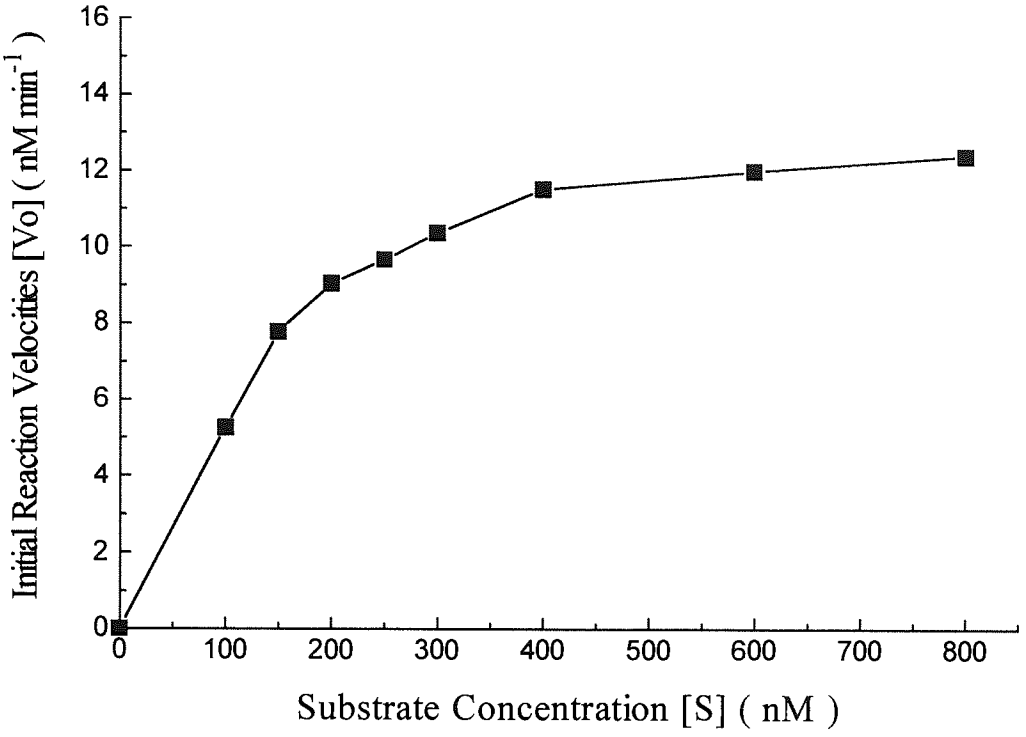

Figure 3.19. Eadie-Hoftsee Plot for The Catalytic Cleavage of the 15-mer RNA Substrate Molecule By The Chimeric Ribozyme; EGFR-65 (Vo represents the initial reaction velocity, [S] represents the nanomolar substrate concentration)

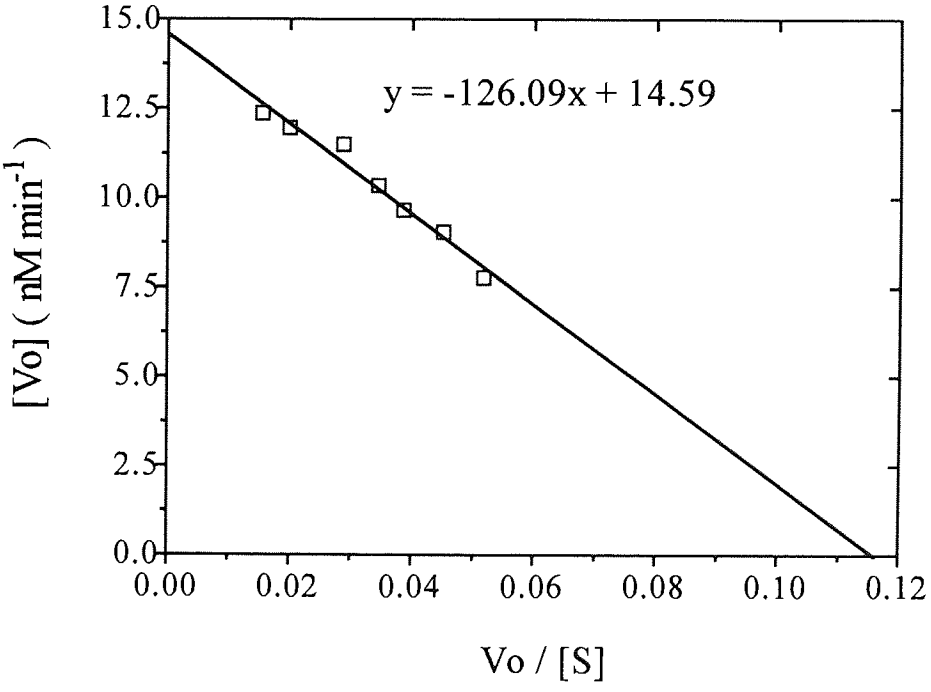

3.3.3.3. Biological Stability of EGFr-Ribozymes Containing 2'-Modified Nucleosides and Phosphorothioates.

In this section, the biological stability of the modified ribozyme construct EGFR-65 was examined *in vitro*. An internal radiolabel was incorporated into the ribozyme structure using the method described in Section 3.2.2 and Figure 4.1. The incorporation of the internal radiolabel was intended to reduce the potential for degradation (removal of the [^{32}P] radiolabel) by phosphatases which are frequently present within biological fluids. The stability of the internally radiolabelled, chimeric construct was examined in human serum and rat tritosomal extract as described in Section 3.2.5. In addition the stability of EGFR-65 was also examined in A431 cell supernatants as described in Section 3.2.5. Representative autoradiographs demonstrating the results of these studies are demonstrated in Figures 3.20 to 3.22.

The chimeric ribozyme (EGFR-65) appeared to remain stable in human serum for up to 2 hours at 37°C. Since unmodified ribozymes were degraded in the same serum in less than 10 seconds (see Figure A2.1, Appendix II), the serum stability of EGFR-65 appeared to be have been improved more than 500-fold compared with an unmodified construct. After incubation periods in excess of 2 hours, degradation occurred, although the pattern of degradation was also distinctly different to that observed with all-RNA (see Figure A2.1), and PS ODN modified ribozymes (see Figure 3.10). Degradation of EGFR-65 appeared to occur via the loss of monomer nucleotides, probably from the 3'-terminus of the molecule. The residues at the 3'-terminus of the molecule were deoxynucleotides, linked by inter-nucleotide phosphorothiotes (see Figure 3.4). These terminal deoxynucleotides were not 2'-O-methylated, and hence, they were probably more susceptible to exonuclease degradation than the other nucleotides within the construct. Therefore, cleavage of these nucleotides by 3'-specific exonucleases offers a likely explanation for the degradation observed.

The purpose of the ODNs incorporated into the ribozyme at the 3'-terminus was to allow a terminal blocking group to be attached for internal radiolabelling (see Section 2.5.3.1 and Figure 4.1) rather than to improve the overall stability of the construct. Therefore, the replacement of these terminal ODNs with 2'-O-methylated nucleotides (in an unlabelled construct) would possibly improve the stability of the intact ribozyme. The primary degradation product, thought to consist of the intact ribozyme minus the terminal deoxynucleotides, was observed in human serum after 20 hours, thus indicating that the 2'-modified portion of the ribozyme was much more resistant to further degradation by exonucleases.

Figure 3.20. Autoradiograph Demonstrating the Degradation of the Chimeric Ribozyme EGFR-65 in Human Serum As a Function of Time. [Lane **C**; Ribozyme (control), incubated in sterile PBS for 20 hours. Lanes **0.5 to 20**; demonstrate the incubation of the chimeric ribozyme in human serum for increasing incubation times (in hours) Lane F; [^{32}P]-γ-dATP radiolabel (control)]

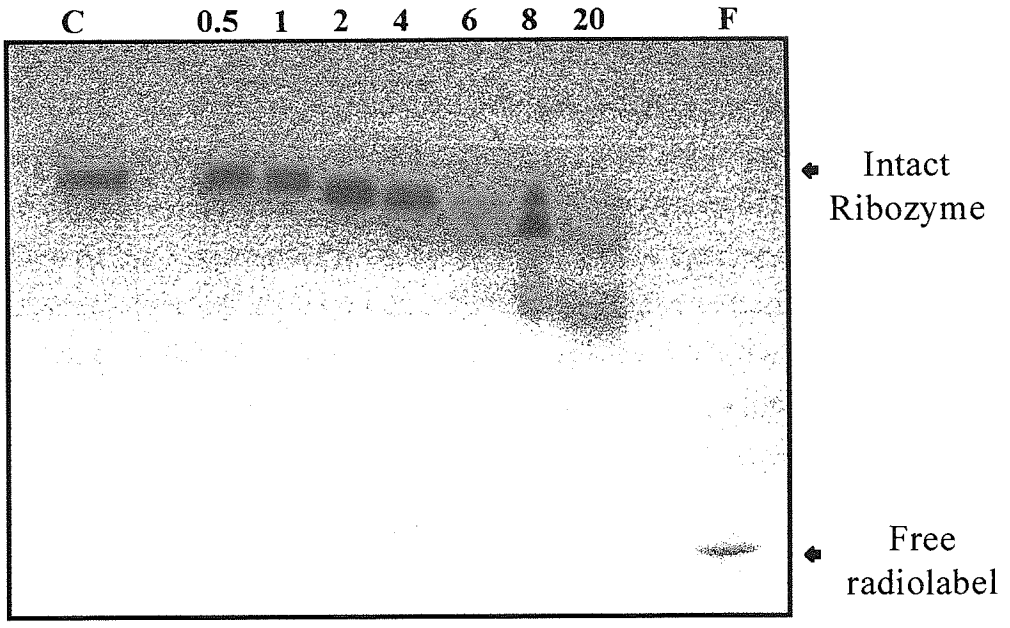

Figure 3.21. Autoradiograph Demonstrating the Degradation of the Chimeric Ribozyme EGFR-65 in Rat Tritosomal Extract As a Function of Time. [Lane **C**; Ribozyme (control), incubated in sterile PBS for 20 hours. Lanes **0.5 to 20**; demonstrate the incubation of the chimeric ribozyme in tritosomal extract for increasing incubation times (in hours) Lane **F**; [^{32}P]-γ-dATP radiolabel (control)].

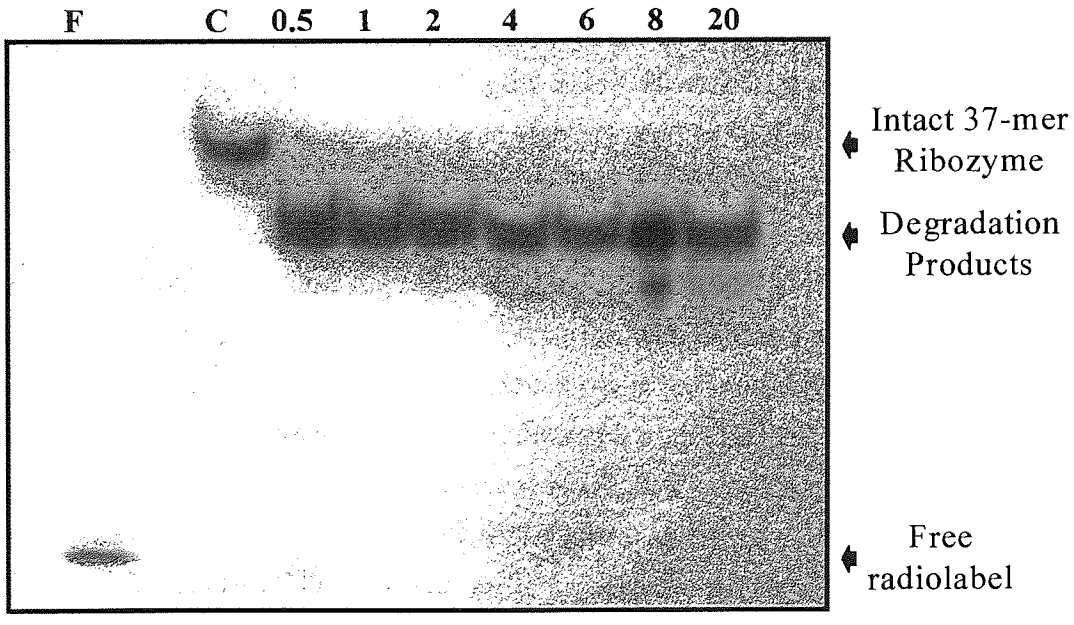

Other investigators, most notably Heidenreich *et al* (1994 & 1996) and Beigelman *et al* (1995), have observed similar improvements in serum stability, following the incorporation of 2'-modified nucleotides (including 2'-O-methyl nucleotides) into hammerhead ribozymes. These studies are discussed in more detail in Section 1.1.4.

Degradation of EGFR-65 in the rat tritosomal extract was more rapid, with only a fraction of the intact ribozyme molecule remaining after 30 minutes incubation (see Figure 3.21). The primary degradation product, observed on the autoradiographs, migrated at a similar rate to the degradation product observed in human serum (see Figure 3.23). Again this suggested that the primary source of degradation was the digestion of the 3'-terminal PS ODNs by exonuclease enzymes. The increased rate of degradation observed, could potentially reflect a higher concentration of 3'-specific exonucleases within the tritosomal extract. Further evidence to support the proposed degradation mechanism is provided by other studies in this report, (see Appendix II), which demonstrated that PS ODNs are susceptible to extensive degradation in tritosomal extract within 60 minutes.

Again the primary degradation product persisted in the tritosomal extract for up to 20 hours. This suggested that the 2'-modified portion of the ribozyme molecule was relatively stable in this extract. Studies by other investigators appear to indicate that the composition of the tritosomal extract is similar to that of lysosomal vesicles *in vivo*. (Seymour *et al*, 1994). Hence, results indicate that 2'-modified ribozymes may remain stable within endosomal vesicles for several hours.

Ribozyme EGFR-65 appeared to remain relatively stable in A431 cell supernatants: No degradation products or free radiolabel were observed on autoradiographs at incubation times up to 8 hours (see Figure 3.25). However, it must be reiterated that the DMEM culture media used in these stability studies was not supplemented with any serum. Nevertheless, the lack of any radiolabelled degradation products would appear to indicate that the presence of the labelled ribozyme could be monitored in cell culture studies because the radio-label remained attached to the intact ribozyme in the presence of the A431 cells. This observation was considered to be particularly encouraging, since the stability enhancement observed would allow cellular association studies to be performed. Heidenreich *et al* (1994 & 1996) have also demonstrated the stability of a fluorescent labelled, 2'-modified ribozyme constructs in cell culture supernatants (of human lymphoblastic leukemia cells) and in extracts of cell nuclei. Whereas, an unmodified (all-RNA) ribozyme described by the same group, was rapidly degraded when exposed to cells.

Figure 3.22. Autoradiograph Demonstrating the Stability of Chimeric Ribozyme EGFR-65 in A431 Cell Supernatants, Containing Serum-Free DMEM Culture Media. [Lane **C1**; Ribozyme (control), incubated in DMEM (only) for 8 hours. Lanes **1 to 8**; demonstrate the incubation of the chimeric ribozyme in A431 cell supernatants for increasing incubation times (in hours) Lane **F**; [^{32}P]-γ-dATP radiolabel (control). Lane **C2**; positive control, Ribozyme incubated in DMEM media supplemented with 20% foetal calf serum for 20 hours]. N.B. In this figure two different areas of the same autoradiograph have been aligned.

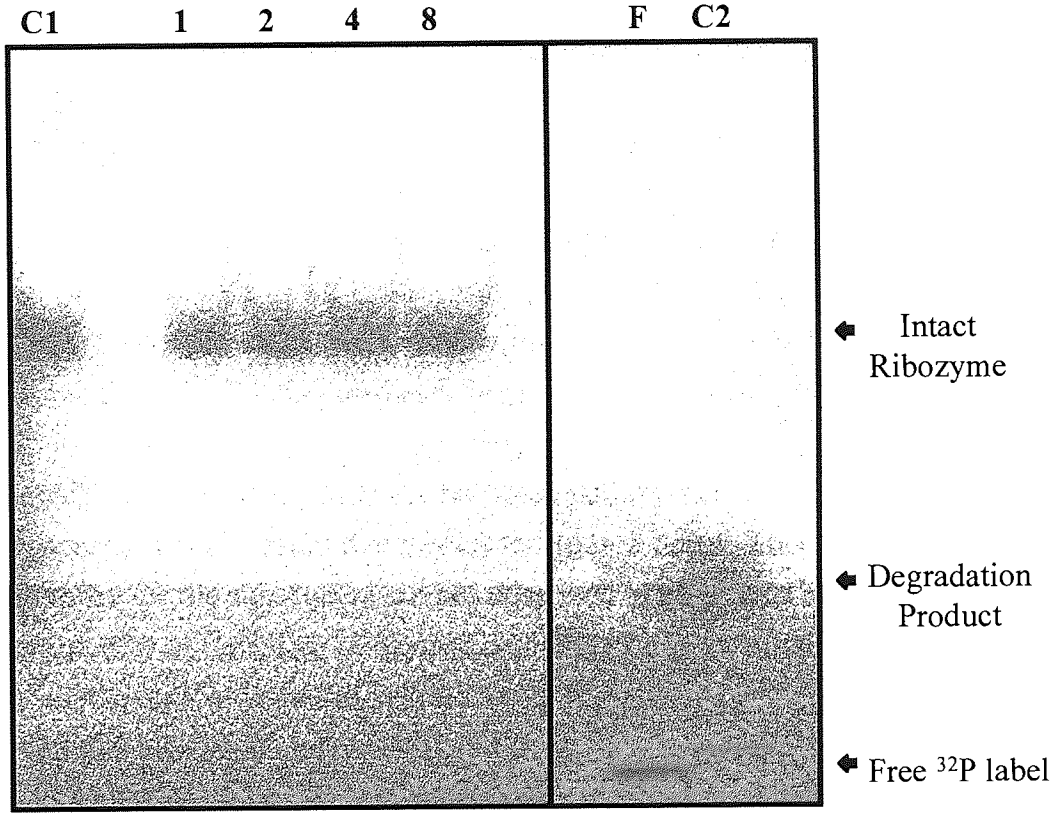

3.4. CONCLUDING REMARKS.

In this chapter, *trans*-acting hammerhead ribozymes, designed to cleave *c-myc* and EGFr mRNA targets, have been studied. These ribozymes were capable of cleaving short RNA substrates *in vitro*, in a specific manner, with varying degrees of efficiency.

The value of using RNA folding programs to design small hammerhead ribozymes was highlighted, since a folding program (RNAFOLD) was able to predict the formation of inactive structures within some ribozymes and ribozyme / substrate complexes. This allowed ribozyme motifs with unfavourable secondary structures to be identified and eliminated, prior to chemical synthesis. However, the predictive value of other folding programs (such as MFOLD) in identifying accessible target sites within large mRNAs seems limited because only a small number of the possible

RNA secondary structures can be examined. Therefore, recently developed empirical techniques, such as RNase H mapping, may prove to be more useful in predicting accessible sites for ribozyme mediated cleavage of mRNAs, such as the EGFr mRNA (see Section 1.3.2)

Unmodified ribozymes were degraded almost instantaneously in several biological fluids including human serum (see Appendix II). Therefore, site-selective chemical modifications were introduced into hammerhead ribozymes to improve their stability. Studies showed that chimeric 2'-O-methylated hammerheads, containing only 5 unmodified ORNs within the catalytic core (at sites G_5, A_6, G_8, G_{12} and $A_{15.1}$), remained intact in human serum for up to 2 hours. Moreover, a (radiolabelled) degradation product, thought to consist of the ribozyme sequence, minus a short terminal ODN sequence, remained stable in both serum and lysosomal enzymes for up to 20 hours. The *in vitro* activity of the modified ribozyme was impaired (3-fold), when compared with an 'all-RNA' counterpart. However, the kinetic parameters (K_m and K_{cat}) calculated for the chimeric construct (EGFR-65) were within the range expected for an active hammerhead ribozyme (Birikh *et al*, 1997b).

Internally radiolabelled, chimeric ribozymes also remained completely stable in A431 cell supernatants (in serum free media) for up to 8 hours. This was of particular importance for the subsequent studies described in this thesis because it indicated that the properties of (labelled) ribozymes could be examined in cell culture studies. Overall, the results described in this chapter suggest that active ribozymes can be stabilised in biological environments via site-selective chemical modifications. Therefore, it may be possible to deliver them exogenously (*in vivo*) for therapeutic purposes.

CHAPTER FOUR

CELL ASSOCIATION OF EXOGENOUSLY DELIVERED CHIMERIC RIBOZYMES.

4.1 INTRODUCTION.

For ribozymes to fulfil their potential in the treatment of diseases caused by undesirable gene expression, it is essential to deliver them to their intracellular target sites (mRNAs) within the cell nucleus and / or cytoplasm. For exogenous delivery, problems associated with the poor biological stability of ribozymes in the extracellular environment must first be addressed. Strategies to enhance ribozyme stability have been examined in Chapter 3 and are also discussed in Section 1.2.4. The next logical step is to decipher the cell entry mechanism(s) of stabilised ribozymes to assist in the design of delivery strategies which can enhance pharmacological efficacy. However, until this study (see also Fell *et al*, 1997) an exact mechanism for the cellular uptake of ribozymes has not been described in detail.

Several groups have investigated the mechanisms of cellular uptake of antisense ODNs, which share several properties with ribozymes (see Sections 1.1.1 & 1.4.2.1), and a number of mechanisms have been proposed (for reviews see Akhtar and Juliano, 1992, Rojanasakul, 1996). Cellular uptake of antisense ODNs is an energy dependant process which can be inhibited at low temperature and also by metabolic inhibitors. (Loke *et al*, 1989, Wu-Pong *et al*, 1992). Studies on ODN interaction with phospholipid membranes (Akhtar *et al*, 1991) indicate that passive diffusion is highly unlikely to be involved in the mechanism of ODN uptake and suggest the involvement of an endocytic process.

Some studies indicate that PO ODNs bind to a specific surface protein and enter cells by receptor mediated endocytosis (RME) (Loke *et al*, 1989). Although other workers have reported concentration dependant binding to a wide range of cell surface proteins or lipids, which is non-specific and thought to involve ionic interactions between the anionic ODNs and surface proteins (Yakubov *et al*, 1989, Shoji *et al*, 1991, Beck *et al*, 1996). These studies may indicate a non-specific uptake mechanism of adsorptive endocytosis

(AE) at low ODN concentrations with fluid phase endocytosis (FPE) predominating at higher PO ODN concentrations when the AE mechanism becomes saturated.

PS ODNs can competitively inhibit PO ODN uptake (Stein *et al*, 1988, Beck *et al* 1996) and some studies suggest that they share specific binding proteins for cell entry via RME (Loke *et al*, 1989). The exact identity of these proteins is not known but could represent epitopes of the fibrinogen receptor because both fibrinogen and heparin have been shown to inhibit surface binding of PS ODNs (Gewirtz *et al*, 1996). However other workers report uptake of PS ODN to be non-saturatable (Hughes *et al*, 1995), or to be mediated by a range of cell surface proteins (Beltinger *et al*, 1995). Thus indicating that cell association of PS ODNs is not solely due to a specific receptor but rather to non-specific protein binding, with cell entry via a combination of RME and AE at low PS ODN concentration, with FPE predominating when these mechanisms become saturated (Beltinger *et al*, 1995). Evidence for non-specific protein binding, as a result of the anionic character of both PO and PS ODNs, is further supported by studies demonstrating that cell association is pH dependant and can be inhibited by the action of protease enzymes (Beck *et al*, 1996). No specific uptake receptor has been categorically defined as yet and it may be that cell entry occurs via preferential adsorption, or binding, to a range of proteins, followed by endocytosis.

Cell association of antisense ODNs modified at the 2' ribose sugar position, with lipophillic alkyl groups such as the 2'-O-methyl group, has been less widely studied. It has been proposed that 2'-O-alkylated ODNs (such as 2'-O-methyl, 2'-O-propyl and 2'-O-nonyl ODNs) enter cells by an endocytic process, in a similar manner to other ODNs (Hughes *et al*, 1995). The introduction of 2'-O-alkyl groups has been shown to increase cell association: For example, the association of 2'-O-methyl PS ODNs in hamster ovary (CHO) cells at 37°C, was 2-fold higher than that of PS ODNs which were not 2'-modified. Furthermore, increasing the size of the 2'-alkyl substituent (and hence increasing the lipophilicity of the ODN molecule), increased the level of cellular association (Hughes *et al*, 1996). However, this effect was thought to be due to increased binding to cell phospholipid membranes by the more lipophillic analogues, rather than an actual increase in the cell entry of these molecules (Hughes *et al*, 1995).

Unmodified oligoribonucleotides (ORNs) are destroyed quickly by nucleases present in serum and consequently cellular uptake is extremely poor (Elkins and Rossi, 1995). Despite the fact that chemical modifications can now largely overcome stability problems

(Usman and Stinchcomb, 1996), very little information is available regarding the exact mechanism by which chemically modified ribozymes enter cells after exogenous administration (Akhtar *et al*, 1995). Since they share many characteristics, such as size and anionic charge, with their antisense ODN counterparts (see Section 1.1.1), ribozymes have been anticipated to enter cells by similar endocytic mechanisms (Akhtar *et al*, 1995). Although subtle differences in cell association characteristics could arise from the requirement for partial chemical modification and the maintenance of a distinct secondary structure within ribozymes, capable of permitting catalytic activity.

Due to the lack of published information regarding cellular uptake of ribozymes, the aim of studies described in this chapter was to describe the mechanism(s) of cellular association of a biologically stable ribozyme construct following exogenous delivery. Mechanistic studies would be performed using the same cell line for all assays; the A431 epithelial cell line, which would require initial characterisation and toxicity testing. This cell line has been reported to express 10 to 50-fold higher levels of the epidermal growth factor receptor (EGFr) than other cell lines (Ullrich *et al*, 1984, Coulson *et al*, 1996). This could be a useful property in subsequent studies because the ribozyme used in these studies is targeted against the EGFr mRNA.

Cellular association studies would also provide quantitative information on the overall proportion of delivered ribozyme which became cell associated, giving an indication as to whether any effects could be expected if 'free' ribozymes were (directly) exogenously administered to A431 cells during *ex vivo* efficacy studies.

4.2 MATERIALS AND METHODS.

General materials and methods used are outlined in Chapter 2. Ribozyme and ODN synthesis, purification and labelling and cell culture techniques are all described in detail in Chapter 2, alterations and additions to the methods are outlined in relevant sections below.

4.2.1 Preparation of Nucleic Acid Sequences.

A 37-mer chimeric ribozyme (Sequence EGFR-65, see Section 3.3.4), was synthesised and internally radiolabelled as described in Section 2.5.3. The majority of nucleosides within the ribozyme were 2'-O-methylated with PO inter-nucleoside linkages, with the

exception of five unmodified ribonucleotide bases within the catalytic core, which were preserved in order to retain catalytic activity. Two nucleotides at the 3'-terminus of the molecule were unmodified deoxyribonucleotides, joined by PS linkages. (See Figure 4.1 for a schematic representation of the synthesis and composition of the chimeric ribozyme used in cell association studies).

Unmodified 37-mer PO and PS ODNs were of the same base sequence as the chimeric ribozyme used in these studies and contained unmodified deoxyribonucleotide bases throughout.

4.2.2. General Cell Culture Techniques.

Cells were maintained and seeded for cell association studies as described in Section 2.7. Where A431 cells were seeded for a 48 hour incubation period prior to experimental assay, cells were seeded at a density of 4.0×10^4 cells per well (24 well plates), rather than 7.5×10^4 cells per well as was the case in all other experiments. In all cell association studies additional wells were seeded with cells and counted during experiments using a haemocytometer as described in Section 2.7.2 to allow data to be normalised to cell number when required.

4.2.3. Cell Association Studies.

Cell association studies were performed as outlined in Sections 2.8.1 to 2.8.6. Additional experiments particular to this chapter are described below:

4.2.3.1. Assessment of the Effect of pH on Cell Association of Chimeric Ribozyme and Oligodeoxynucleotides.

To assess the effect of pH on cell association of ribozymes and ODNs, serum free DMEM media (pH 7.3) which was routinely used in cell association studies was replaced with Hanks' balanced salt solution (HBSS), buffered to a set pH. HBSS (9.8g / L) containing 0.01% w/v phenol red and 5mM D-glucose was buffered with either 25mM HEPES (pH 7.0 and pH 8.0) or 25mM MES (pH 5.0 and 6.0). The pH adjusted media were filter sterilised using 0.2μM cellulose acetate bottle filters (Costar) and stored at 4°C prior to use in cell association studies. Cell association studies were then performed as described in Section 2.8.1 using the serum free, pH adjusted HBSS media.

Figure 4.1. A Schematic Representation of the Synthesis of the Internally Radiolabelled Chimeric Ribozyme used in Cell Association Studies.

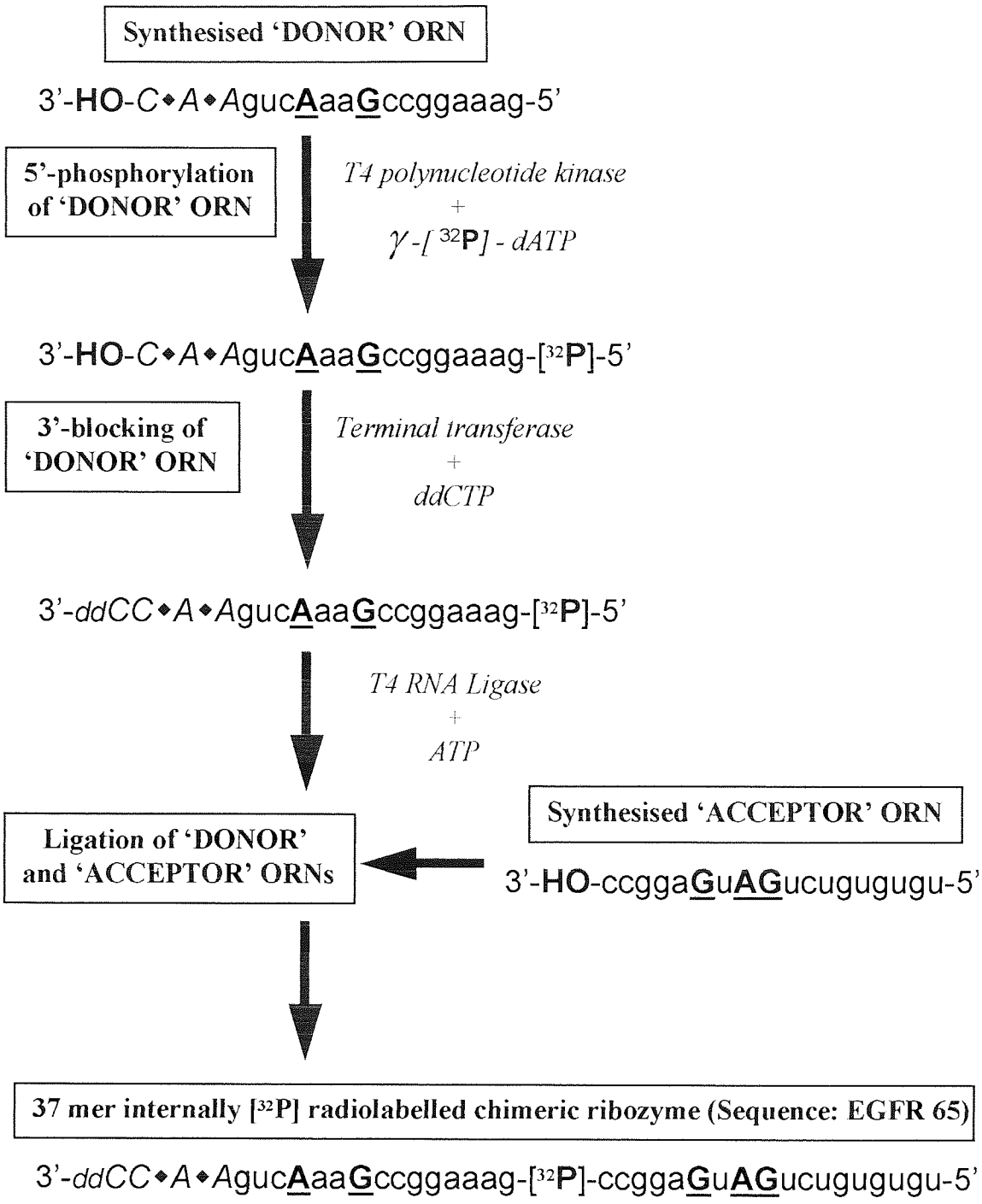

[Bases shown in bold underlined capitals represent unmodified ribonucleotides, bases shown in capital italics represent deoxyribonucleotides and bases shown in lower case represent 2'-O-methylated ribonucleotides. The symbol '♦' indicates a phosphorothioate linkage between bases. 'HO-' represents a 3'-hydroxyl group. ORN; oligoribonucleotide, ddCTP; .2',3'-dideoxy cytosine triphosphate].

4.2.3.2. The Effect of Pronase® on Cell Associated Ribozyme.

Pronase® is the name given to a group of proteolytic enzymes, with broad specificity, that are produced in the culture supernatant of *Streptomyces griseus* K-1 (Narahashi and Yanagita, 1967). To assess the effect of Pronase® on cell associated ribozymes, studies were initiated as described in Section 2.8.1. Following incubation (for various time periods) with ribozyme, the apical serum-free DMEM media was removed from the cells and collected. Cells were washed 4 times with ice cold PBS / azide (0.05% w/v sodium azide in PBS) and the washings collected. Cells were treated with 0.25% w/v nuclease-free Pronase® (Calbiochem, Nottingham, UK) in HBSS (pH 7.2 and 4°C) for 15 minutes. (This incubation period was chosen because viable cell numbers were unaffected by Pronase® administration after 15 minutes, as determined by dye exclusion assay (see Section 2.7.3). Incubation with Pronase® for time periods in excess of 40 minutes caused a slight reduction in A431 cell viability). Alternatively, control cell populations were treated with HBSS buffer alone for the same time period at 4°C. Following Pronase® treatment, A431 cells were not solubilised, instead the Pronase-containing media was removed and collected in 10mL scintillant (Optiphase Hi-Safe 3). Cells were then solubilised by the addition of 1mL Triton-X100 (3% v/v in distilled water) for 2 hours at 37°C and harvested as described in Section 2.8.1. Quantities of radiolabelled ribozyme in each of the four fractions (i.e. apical DMEM media + PBS washes + Pronase / HBSS wash + cell suspensions) were assessed by scintillation counting (see Section 2.8.1).

4.2.3.3. Competition Studies with Nucleic Acids and Other Polyanions.

The effect of competition with PO and PS ODNs on cell association of ribozyme was determined as described in Section 2.8.6. In order to assess the effect of competition with other nucleic acids such as long chain DNA (obtained from salmon testes) and dATP (nucleotide monomer) as well as other high molecular weight polyanions, the method described in Section 2.8.6 was adapted as follows: Salmon testes DNA (molecular biology grade, D-9156), dATP (molecular biology grade), dextran sulphate (approximate molecular weight 10,000), and heparin (sodium salt, Grade I-A, cell culture tested), were obtained from Sigma. Following initial washing of the cells with sterile PBS as described in Section 2.8.1 cells were pre-treated for 15 minutes at 37°C with serum free media containing the competing agent (10μM). The media containing the competing agent was removed and radiolabelled ribozyme in serum free media, containing additional competing agent (10μM), was added to the cells. The concentration of the competing agent

represented a 12.5 fold excess compared with the concentration (0.8μM) of the radiolabelled ribozyme. Cells were incubated at 37°C for the required time period. The extent of ribozyme cell association in the presence of the competing agents was determined as described in Section 2.8.1.

4.3 RESULTS.

4.3.1 Toxicity Testing and Characterisation of Cells.

To assess cell viability during experiments, the toxicity of ribozymes on A431 cells was tested at concentrations used during cell association and trafficking studies (See Chapter 5). In addition, the A431 cell line was further characterised to determine cell growth rates, to identify any variability in cell association using cells incubated for different time periods prior to use and to establish a protocol for removal of loosely associated material by PBS washing.

To assess the cellular toxicity of the chimeric ribozyme (EGFR-65, See Figure 4.1) on A431 cells, studies were initiated as described in section 2.8.1 using a range of concentrations of chimeric ribozyme (0.4μM to 40μM). Cells were incubated for 4 hours in serum free media containing ribozymes, the media was removed and the cells washed with PBS as described in Section 2.8.1. Cells were trypsinised and the total cell count and percentage of viable cells remaining were immediately determined by trypan blue exclusion assay as described in Section 2.7.3. Control cell samples were incubated for the same time period in serum-containing media alone.

Figure 4.2 demonstrates the effect of various concentrations of ribozyme on A431 cell viability after 4 hours at 37°C, compared to the control population. At ribozyme concentrations in the range 0.4μM to 10.0μM, the percentage of viable cells remaining after 4 hours was not significantly different ($P>0.05$) to that of control samples. However, at higher concentrations of 20μM and 40μM, viable cell number was significantly reduced compared with the control sample (20μM; $P<0.05$ and 40μM; $P<0.01$) indicating a toxic effect at higher concentrations (see Figure 4.2). The precise mechanism of cytotoxicity is unclear from this data and there is a lack of published information regarding the toxicity of 2'-O-methylated nucleotides either *ex vivo* or *in vivo* (see Sproat, 1996). It is likely, however, that the loss of cell viability observed here

represents non-specific toxicity of chemically modified ribozymes at high concentrations, which is not related to any predicted pharmacological action of the ribozyme.

Figure 4.2. Graph of The Percentage of Viable A431 Cells Remaining After Treatment with Various Concentrations of Chimeric Ribozyme for 4 hours at 37°C Compared with Control (n=6 ± SD. except for 40μM; n=3 ± SD).

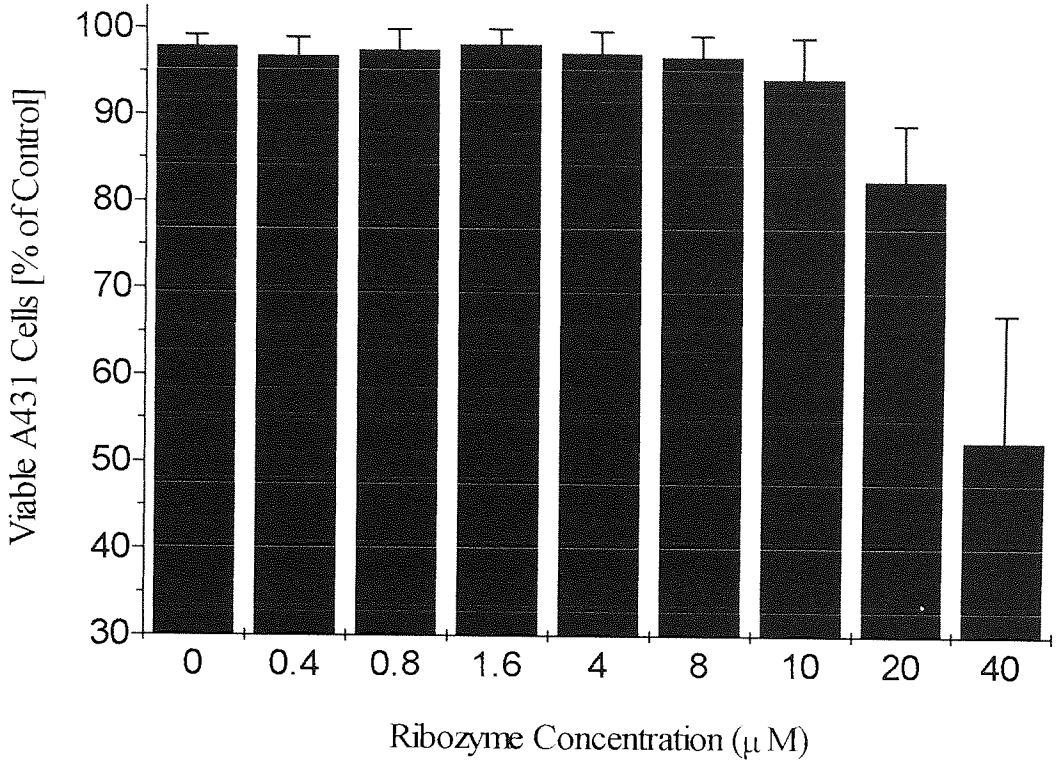

The total viable count of cells incubated in serum free media for 4 hours, in the absence of ribozyme, was not significantly different to that of the control sample grown in serum containing media. Greater than 96% of this cell population remained viable during the experiment indicating that cell viability was not significantly affected during the 4 hour time period by the absence of serum derived growth factors (Griffiths, 1992).

With reference to the growth curve obtained for A431 Cells (See Figure 4.3), the cell doubling time was in excess of 4 hours. Therefore a cytotoxic rather than anti-proliferative effect would appear to offer the most likely explanation of the reduction in cell number following exposure to high ribozyme concentrations. (i.e. high concentrations of ribozyme did not inhibit cell division but were directly toxic to the A431 cells). However, the aim at this stage was to establish the maximum, non-toxic concentration of ribozyme which could be adminsitered during cell association studies, rather than to establish the mechanism of toxicity. The data indicates that ribozyme concentrations of up

to 10μM did not have a significant effect on viable A431 cell population over a 4 hour time period and could, therefore, be used to assess cell association.

To further characterise the A431 cell line, a growth curve was calculated in serum containing media. To calculate the growth curve, cells were seeded as described in Section 2.7.4 for various time periods at 37°C. Cells were trypsinised and viable cell counts were calculated by trypan blue exclusion assay as described in Section 2.7.3.

The growth curve (See Figure 4.3) indicates that following seeding, A431 cells enter a lag period of at least 12 hours, followed by a period of exponential growth. Cell number increased by a mean value of 44% after 24 hours. The cell doubling time during the exponential growth phase, estimated using the method of Griffiths (1992), was approximately 34 hours. This doubling time was within the range expected for this cell line (Gherardi, 1996). If cell association studies were performed 24 hours post-seeding, then cells would probably have entered an exponential period of growth.

Figure 4.3. Standard Growth Curve for A431 Cells Calculated from a Seeding Concentration of 7.5×10^4 Cells / mL at 37°C. (n=6 ± SD)

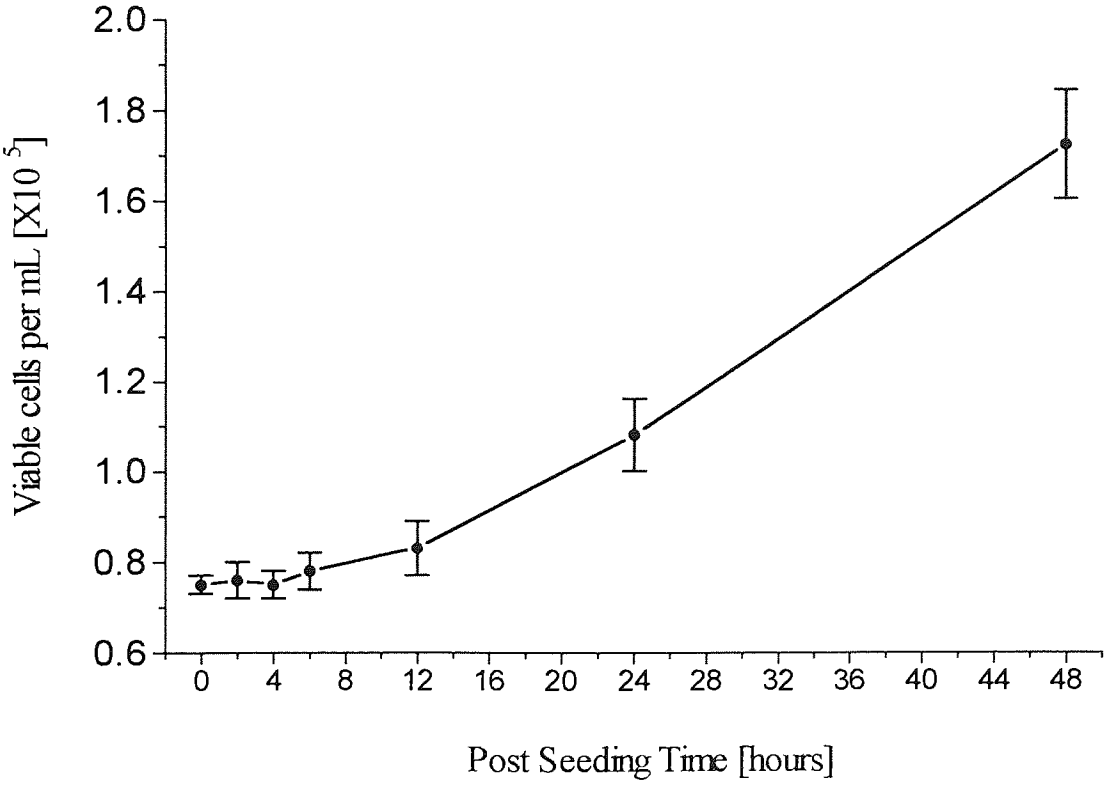

4.3.2 Optimisation of Cell Association Studies

To standardise the protocol for cell association studies, A431 cells were seeded at 7.5×10^4 cells / mL for 24 hours and also at 4.0×10^4 cells / mL for 48 hours on 24 well plates prior to use in preliminary experiments. Preliminary cell association studies were performed as described in Section 2.8.1. Additional wells were also seeded at the appropriate density, incubated for the same period and cell counts were determined as described in Section 2.7.2. These counts were used to normalise cell association data to cell number (1×10^5 cells / mL).

In the preliminary studies, over a 4 hour incubation period, no significant difference ($P=0.326$) was detected in the mean percentage of 0.8μM radioactive ribozyme which became associated with the cells seeded for 24 hours (1.14% ± 0.09) and 48 hours (1.20% ± 0.07) respectively (All results normalised to 1×10^5 cells / mL, n=4 ± SD). Indicating that post-seeding incubation time had little effect on cell association over the incubation period tested. Possibly because cells would be in the exponential growth phase at both 24 and 48 hours post-seeding, which was supported by the fact that both cell cultures appeared to be sub-confluent when seeded at these densities.

Table 4.1. The Percentage of Non-Cell Associated Ribozyme Removed from The Surface of A431 Cells by Consecutive PBS / azide Washes.

1mL PBS / azide wash number.	Mean % of non-cell associated radioactivity in each PBS / azide wash (n=4).	Mean Cumulative % of non-cell associated radioactivity removed in consecutive washes.
1st	87.48	87.48
2nd	8.97	96.45
3rd	2.39	98.84
4th	0.94	99.78
5th	0.19	99.97
6th	0.03	100
7th	0.00	100

To establish the number of PBS / azide washes required to remove loosely bound or non-cell associated radioactive ribozyme from the cell surface, assays were performed as

detailed in Section 2.8.2. The percentage of non-cell associated ribozyme which was removed after 4 hours, by each of seven PBS /azide washes was calculated and the results indicated in Table 4.1. When the amount of radioactivity in samples was reduced to the background level, as detected by scintillation counting, it was assumed that all non-cell associated radioactivity had been removed by washing.

The results indicate that over 99.5% of non-cell associated radioactivity, which can be removed from cells by apical washing, is removed by four (1mL) PBS / azide washes. Hence, in subsequent cell association studies cells a four step washing protocol was used to remove non-bound or loosely cell associated radioactive material. Any remaining radioactivity in the experimental protocol (See Section 2.8.1) would be assumed to be cell associated.

In summary, the preliminary experiments detailed in this section showed that ribozymes could be added to A431 cells in concentrations up to 10μM without causing significant toxicity. The growth curve indicates that A431 cells would be in an exponential phase of growth at 24 to 48 hours post seeding. When normalised to cell number, there was no significant difference in the percentage of ribozyme which became associated with cells grown for 24 and 48 hours. Therefore if cells were seeded for 24 hours prior to association experiments they would produce results representative of cells in the exponential growth phase. In cell association studies a four step PBS / azide wash protocol (described in Section 2.8.1) could be used to remove non-cell associated radioactive material.

4.3.3 Time Profile of Cell Association of Chimeric Ribozyme Compared with a Phosphorothioated ODN and Markers For Fluid Phase Endocytosis.

To investigate the cellular association of internally radiolabelled ribozyme (EGFR-65, See Figure 4.1) over a 6 hour time period in A431 cells, the protocol described in Section 2.8.1 was used. A time profile of the cell association of 0.8μM chimeric ribozyme was obtained and compared to that of *D*-[1-^{14}C] mannitol which enters cells exclusively by fluid phase endocytosis and can therefore be used as a marker for this process (see Besterman *et al*, 1981, Levis *et al*, 1995). Cell association of *D*-[1-^{14}C] mannitol was investigated as described in Section 2.8.3. Experiments were performed using a final concentration of 0.8μM.

Ribozyme cell association was also compared with PS ODNs which are generally considered to enter cells by a process of adsorptive and / or receptor mediated endocytosis as discussed in Section 4.1. Cell association of a 20-mer, internally radiolabelled PS ODN (5'-GGA GG*G TCG CAT CGC-3', [^{32}P]-radiolabelled at the position indicated (*) via the ligation of two ODNs with DNA ligase; a gift from Dr. Nadia Normand, Aston University), was tested in A431 cells as described in Section 2.8.1 using a 0.8μM concentration of PS ODN.

The results of these studies are illustrated in Figure 4.4. At all time points examined over a 4 hour period, the percentage cell association of the internally [^{32}P] radiolabelled ribozyme was significantly higher ($P<0.001$) than that of *D*-[1-^{14}C] mannitol. The increased proportion of ribozyme entering A431 cells suggests it is unlikely that ribozyme cell entry occurred exclusively via the fluid phase endocytic pathway under the conditions tested. This pattern is consistent with the findings of other workers examining antisense ODN uptake, where cell association was noted to be significantly higher than that of radiolabelled sucrose, which is an alternative fluid phase marker (Beltinger et al, 1995, Levis *et al*, 1995). These authors concluded a mechanism of adsorptive or receptor mediated process was likely to explain the increased levels of cell association.

Cell association of the internally radiolabelled PS ODN was likewise significantly higher ($P<0.001$) than that of *D*-[1-^{14}C] mannitol. This proportionate increase agrees with the findings of Beltinger *et al* (1995) at the PS ODN concentration used. However the actual percentage of PS ODN which became cell associated here in A431 cells, was lower than that demonstrated with K562 cells (Beltinger *et al*, 1995) and with Caco-2 cells (Beck *et al*, 1996). This was not unexpected because cellular association of PS ODNs is known to be cell-type specific (see Section 4.3.1.1)

By comparison with cell association of the chimeric ribozyme, the percentage of internally radiolabelled PS ODN which became cell associated was significantly higher ($P<0.0024$, determined by Welch's t-test) at all times points tested over a six hour period. This correlates with differences which have been observed when cell association of PS and PO antisense ODNs has been compared by other workers (Agrawal *et al*, 1992, Shoji *et al*, 1996, Beck *et al*, 1996). The proportion of PS ODN which became cell associated was shown to be significantly higher than for PO ODNs although this effect may be cell type specific (Rojanasakul, 1996). The chimeric ribozyme used in these studies contained

predominantly PO linkages between bases (only two of the inter-nucleotide linkages were PS) and this may explain the differences observed.

Figure 4.4. Graph Showing % Cell Association Against Time for Internally Radiolabelled Chimeric Ribozyme in A431 Cells Compared with % Cell Association of *D*-[1-^{14}C] mannitol and PS ODN (mean ± SD).

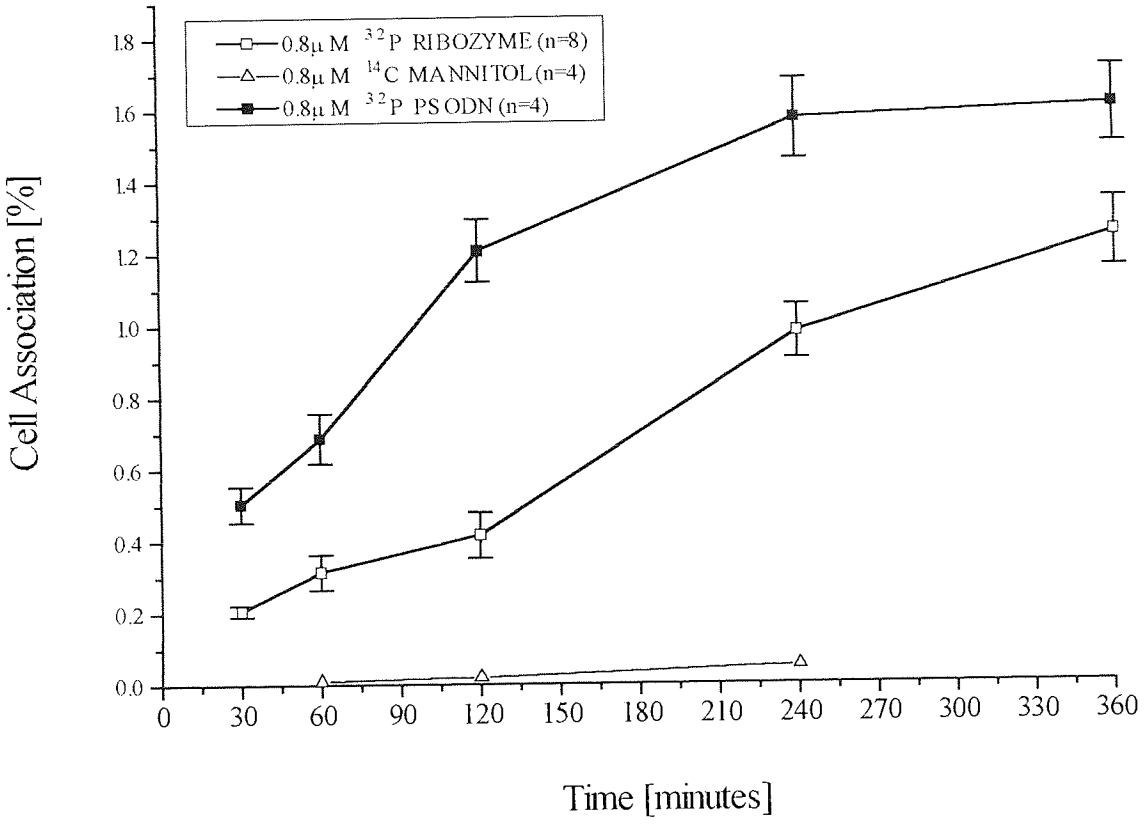

Although the PS ODN (20-mer) used in these studies was 17 nucleotides shorter in length than the chimeric ribozyme (37-mer), this is unlikely to have accounted for the increased cell association observed with the PS ODN, since studies by other investigators (Beck *et al*, 1996) have demonstrated that increasing the length of a given ODN can actually increase cellular association.

4.3.4 The Effects of Temperature and Metabolic Inhibition on the Cell Association of Chimeric Ribozyme in A431 Cells.

To investigate the effect of temperature and metabolic inhibitors on the cellular association of internally radiolabelled ribozyme (EGFR-65, See Figure 4.1), cell association was tested over a 4 hour time period in A431 cells as described in Sections

2.8.4 and 2.8.5. The results of these experiments are demonstrated in Figure 4.5 which shows the percentage of added ribozyme which became associated with cells, which were incubated either at 4°C throughout, or were treated with sodium azide and 2-deoxy glucose and incubated at 37°C, compared with control. The control sample represents the percentage of chimeric ribozyme which became cell associated with A431 cells which were incubated at 37°C throughout and were not treated with any metabolic inhibitor.

Figure 4.5. Graph Showing the Effect of Reduced Temperature and Metabolic Inhibition on the % Cell Association of Chimeric Ribozyme in A431 Cells as a Function of Time, Compared with Control. (n=6, mean values ± SD)

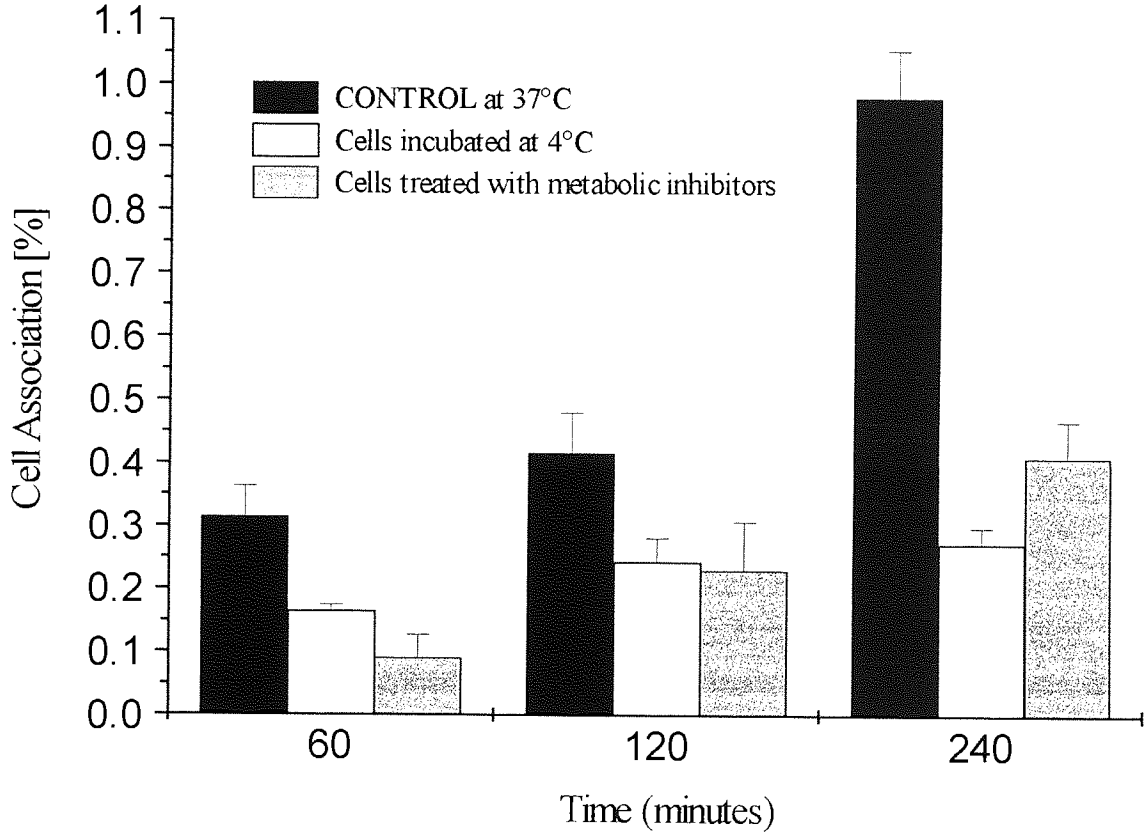

Cell association of ribozyme was reduced but not completely inhibited at low temperature (4°C) at all time points tested ($P<0.006$, considered extremely significant). This effect became more pronounced with time, with a maximal effect noticed after 4 hours at which time cell association was inhibited by over 70%. A similar effect has been noted for both PO and PS ODNs by other workers (Wu-Pong *et al*, 1992, Deshpande *et al*, 1996, Shoji *et al*, 1996). Although there is evidence that reduced temperature has little effect on PS ODN cell association up to 15 minutes after administration to Caco-2 cells (Beck *et al*, 1996) suggesting an initial phase of cell association which is non-energy dependant.

Metabolic inhibition also reduced the extent of ribozyme cell association compared with control at all time points tested ($P<0.0012$, considered very significant). Metabolic inhibition reduced cell association by almost 60% after 4 hours and this effect was similar to that of a reduction in temperature. A similar effect of metabolic inhibitors on cell association of antisense ODNs has been noted in other cell lines (Loke et al, 1989, Wu-Pong *et al*, 1992, Beck *et al*, 1996). Although in some cases, the initial cellular uptake of PS ODNs was unaffected by metabolic inhibition suggesting that cell association of PS ODNs was unlikely to be an energy dependant during the initial 15 minutes of incubation (Beck *et al*, 1996).

The reduced cell association at low temperatures and in the presence of metabolic inhibitors indicates that a considerable degree of the association involves cellular energy. The requirement for cellular energy could potentially arise directly from the demands of an active transport process (for example RME), or alternatively it could be indirectly due to effects on a secondary active transport processes (for example FPE) or the maintenance of cell membrane potential, structure or integrity. The lack of complete inhibition of cell association could be due to energy-independent surface binding of ribozymes in the absence of internalisation. Alternatively, in the case of the metabolic inhibitors, it could be due to incomplete ATP depletion by the sodium azide / 2-deoxyglucose combination.

4.3.5 The Effect of Ribozyme Concentration on Cell Association.

In order to assess the effect of the apical ribozyme concentration on cell association, studies were performed as described in Section 2.8.1. However a range of concentrations of internally radiolabelled ribozyme (Sequence EGFR-65, See Figure 4.1) were used in serum free culture media instead of the standard 0.8μM preparation. The concentrations tested were in the range 0.4μM to 5μM, which represented concentrations from 50% below the standard level (0.8μM) used in other experiments, up to a 6.25 fold higher concentration, which was the highest concentration available for use prior to the experiment. The various concentrations of ribozyme were prepared by adding the relevant quantity of unlabelled ('cold') ribozyme to a 0.4μM radiolabelled sample of the ribozyme.

The effect of concentration of *D*-[1-^{14}C] mannitol on cell association was also tested to allow comparisons to be made. *D*-[1-^{14}C] mannitol uptake occurs exclusively by the fluid phase endocytic mechanism and therefore would not be expected to be saturable.

Experiments were performed as described in Section 2.8.3 using various concentrations of *D*-[1-^{14}C] mannitol prepared in serum free media.

Results are demonstrated in Figure 4.6. Cell association of the chimeric ribozyme appeared to be concentration dependant over the range tested, after 4 hours. At a concentration of 0.4μM the percentage of ribozyme which became cell associated was significantly greater ($P<0.001$),than when administered at higher concentrations. Percent cell association was not significantly different ($P>0.05$) in the range between 0.8μM and 1.0μM but was significantly higher ($P<0.01$) than the percentage of ribozyme which became cell associated when concentrations between 2μM and 5μM were administered. The percentage of added ribozyme which became cell associated was not significantly reduced ($P>0.05$) when concentrations were increased above 2μM, possibly indicating some saturation of the cellular uptake process above this concentration.

Figure 4.6. Graph Showing the Effect of Concentration on the Cellular Association of Internally Radiolabelled Chimeric Ribozyme compared with *D*-[1-^{14}C] mannitol in A431 Cells after 4 hours at 37°C. (n=4, mean ± SD)

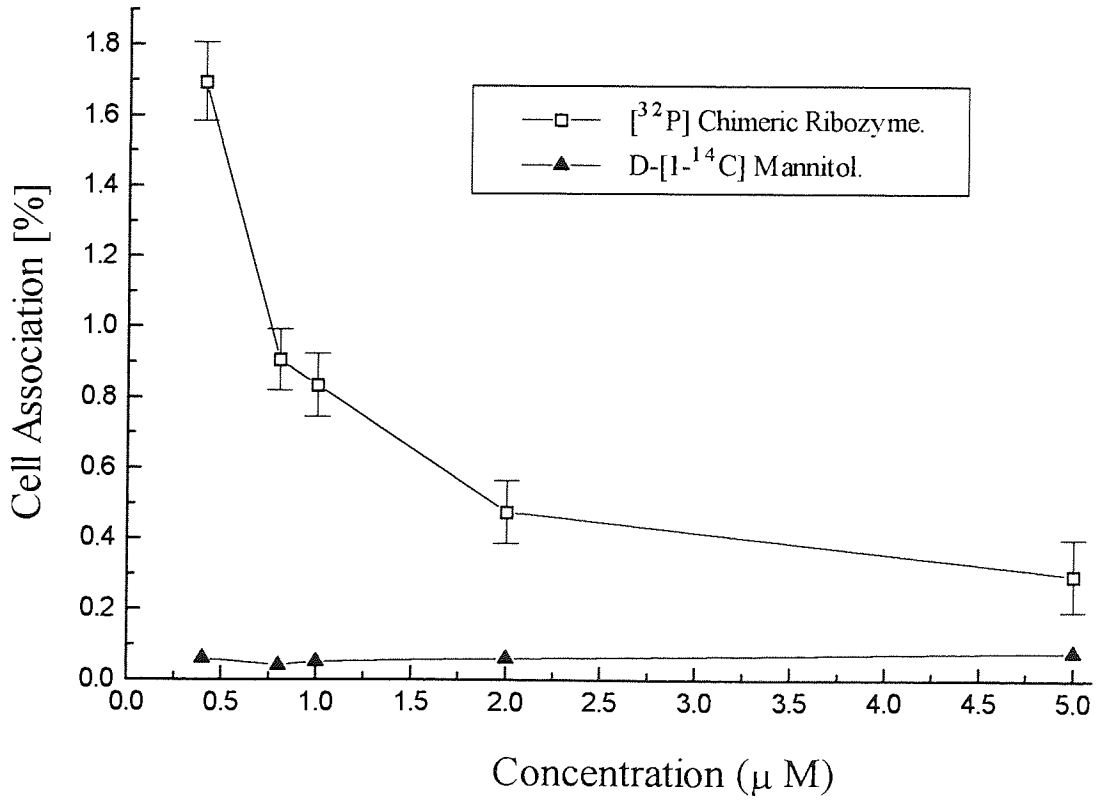

There was no significant difference ($P>0.05$) in the percentage of *D*-[1-^{14}C] mannitol which became cell associated, over the range of concentrations examined. This indicated

that the mechanism by which *D*-[1-^{14}C] mannitol became cell associated was not saturable. Cell association of ribozyme was significantly higher ($P<0.024$) than *D*-[1-^{14}C] mannitol at all concentrations tested. However differences between the two were more marked at lower concentrations.

In terms of the actual amount of ribozyme which became cell associated (See Table 4.2), expressed as nanomoles of ribozyme associated per 10^5 cells, there was some increase in the amount of ribozyme which became cell associated as the ribozyme concentration was increased. Differences between the amount of cell associated ribozyme when added at 0.4μM to 0.8μM were significantly different ($P<0.05$) compared with levels recorded when ribozyme was added at a concentration of 5.0μM. A possible explanation for this could be that not enough ribozyme was added to saturate binding sites at the lowest concentrations used. Therefore, when higher concentrations were added the remaining 'spare capacity' allowed more ribozyme to become cell associated. However, the increase in the amount cell associated was not statistically significant ($P>0.05$, determined by Welch's test) in the concentration range from 1.0μM to 5.0μM, indicating that the process had already become saturated in this concentration range.

Table 4.2. Total Quantities of ribozyme which became Cell Associated after 4 hours Incubation with A431 Cells at Varying Concentrations.

Ribozyme Concentration [μM]	Mean amount of cell associated ribozyme [nmoles / 10^5 cells]	Standard Deviation
0.4	6.52	0.43
0.8	6.98	0.66
1.0	8.03	0.86
2.0	9.17	1.71
5.0	14.33	4.90

Overall these results indicate that cellular uptake of ribozymes is much more efficient than that of mannitol when administered at concentrations below 2μM. Therefore it is extremely unlikely that ribozymes enter cells exclusively by fluid phase endocytosis when administered at low concentrations. However, when ribozyme concentrations are increased, there is a progressive reduction in the relative efficiency of cellular uptake, possibly indicating the saturation of a particular uptake process. The extent of ribozyme

uptake remains higher than that of the fluid phase marker up to a concentration of 5μM, although differences become more marginal as the ribozyme concentration is increased. It is feasible that cellular uptake of ribozymes proceeds primarily via the fluid phase endocytic mechanism at high concentrations, when the more efficient uptake process becomes saturated.

A similar concentration dependency has been noted for PS antisense ODNs when administered to other cell lines (Beltinger *et al*, 1995, Zhao *et al*, 1993) with the authors concluding that the saturable and concentration dependant nature of PS ODN cell association was indicative of a specific cell surface binding mechanism such as RME. However, a similar uptake profile would also result if uptake were mediated via adsorptive endocytosis. There appears to be conflicting evidence with regard to the concentration dependency of PO ODNs: Beck *et al* (1996) suggested that PO ODN uptake was not concentration dependant in Caco-2 cells after 15 minutes, whereas Wu-Pong *et al* (1992) demonstrated concentration dependency, but not saturation of PO ODN uptake, in Rauscher Red cells at concentrations up to 10μM after 2 hours. However differences in cell association characteristics between the chimeric ribozyme and unmodified PO ODNs could arise from the chemical modifications to nucleotide bases or the presence of PS linkages at the 5' terminal of the ribozyme molecule. Alternatively this effect could be cell line specific.

4.3.6. The Effect of Oligonucleotide Competition on Cell Association of Chimeric Ribozyme.

To assess the effects of various oligonucleotide (ON) analogues on the cell association of ribozyme, the method described in Section 2.8.6 was used. Experiments were designed to demonstrate 'self'-competition via the addition of an excess of unlabelled ribozyme both prior to, and during cell association studies. In addition, competition was investigated by incubating cells with excess concentrations of both PO and PS ODNs prior to, and during, ribozyme cell association studies. The results (demonstrated in Figure 4.7) were obtained after 4 hours incubation with 0.8μM radiolabelled ribozyme and / or excess competing agent at 37°c. The control represents cell association of 0.8μM radiolabelled ribozyme with no competing agent present.

The addition of a 12.5-fold excess of unlabelled ribozyme significantly reduced ($p<0.001$) the percentage of radiolabelled ribozyme which became cell associated after 4 hours. This

indicated that the radiolabelled ribozyme was competing with the excess unlabelled ribozyme for cell association, probably by competing for the same uptake or surface binding mechanism. Saturable and self-competitive cellular association has also been demonstrated for PO and PS ODNs and is indicative of a specific cell surface binding mechanism which could possibly be mediated by surface proteins or lipids. (Loke *et al*, 1989, Wu-Pong *et al*, 1992, Zhao *et al*, 1993, Beltinger *et al*, 1995, Shoji *et al*, 1996).

Cell association of ribozyme was significantly reduced in the presence of excess quantities of both PO and PS ODNs ($P<0.001$). This suggests the presence of competition between the ribozyme and ODNs for cellular uptake and / or binding. As ODNs, in particular PS ODNs, are widely considered to enter cells by either AE or RME (See Section 4.1) the ribozyme may be competing for cellular uptake via one or both of these processes.

Figure 4.7. Graph Showing Percent Cell Association of Chimeric Ribozyme with A431 cells in the Presence of Excess Concentrations of Oligonucleotide Analogues. (n=4, except for control where n=8, values are mean ± SD)

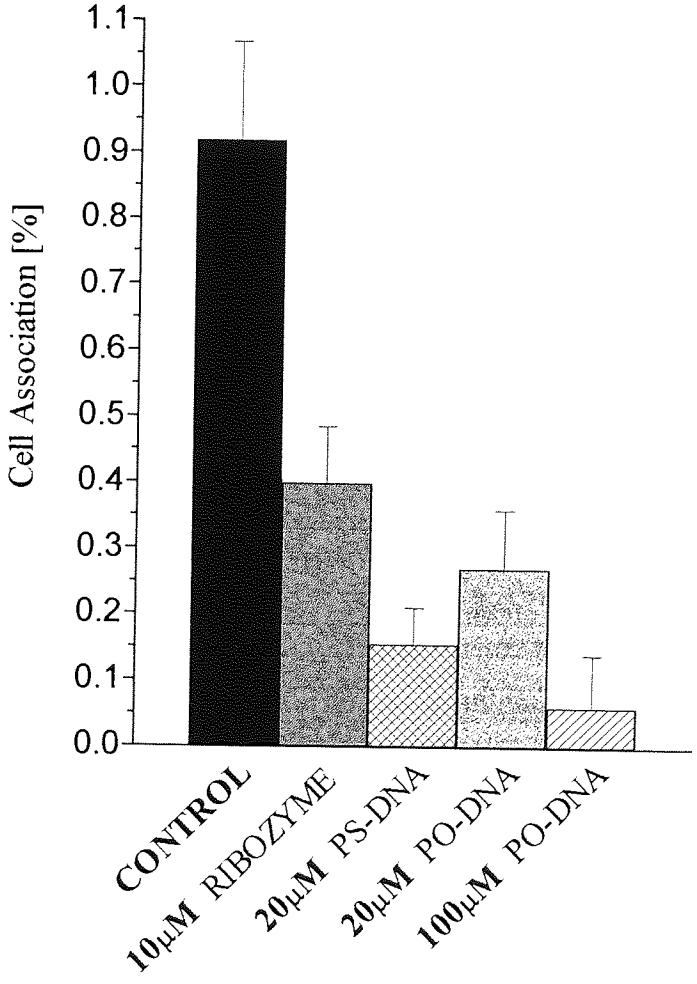

The most potent 'competing' agent was the PS ODN which reduced ribozyme cell association by 84 % after 4 hours when added to A431 cells at a concentration of 20μM. However this level of inhibition was not significantly different (P=0.0703) to that which resulted from the addition of PO ODN (20μM). The increased inhibition by the PS ODNs could be due to the increased anionic character of these molecules. Indeed PS ODNs have been shown to be more potent competitive inhibitors than their PO ODN counterparts, in studies comparing cellular association of different antisense ODN chemistries (Zhao *et al*, 1993, Beck *et al*, 1996).

The effect of higher ODN concentration on ribozyme cell association was only tested with the PO ODNs, due to availability. Inhibition of ribozyme cell association was significantly greater (P=0.0182, determined by Welch's test) when cells were incubated with 100μM PO ODN than when treated with 20μM PO ODN. Therefore competition between the ribozyme and the PO ODN would appear to be concentration dependant.

4.3.7. The Effect of 'Competitor' Chain Length on Cell Association of Ribozymes.

In an attempt to identify any effect of ODN chain length on ribozyme cell association, competition studies were performed (See Sections 2.8.6 and 4.3.5.) using 20μM of salmon testes DNA and 20μM dATP respectively, as the competing agents. The salmon testes DNA (587-831 base pairs, Sigma D-9156) was used to demonstrate the effect of 'cross' competition with a long chain DNA sequence, which would possess a much greater number of anionic charges than the PO ODN used in previous studies (See Section 4.3.5.) The dATP (Sigma D-4788) was used to demonstrate the effect of 'cross' competition with a single base monomer. The results of these studies are demonstrated in Figure 4.8.

Results were recorded after 4 hours incubation with 0.8μM radiolabelled ribozyme, both without (control), and with, excess competing agent at 37°c. Cell association of ribozyme was significantly reduced in the presence of excess quantities of both salmon testes DNA and dATP (P<0.001). Again this indicates competition between the ribozyme and these nucleic acids for cellular uptake and / or binding. The inhibitory ('competitive') effect of these agents on cell association has also been demonstrated with PO ODNs (Wu-Pong *et al*, 1996), although dATP had little effect on cellular uptake of both PO and PS ODNs

when administered to Caco-2 cells (Beck *et al*, 1996) suggesting that the effect of dATP could be cell line specific.

Figure 4.8. Graph Showing Percent Association of Chimeric Ribozyme with A431 Cells in the Presence of Excess Concentrations of Salmon Testes DNA and dATP after 4 hours. (mean ± SD).

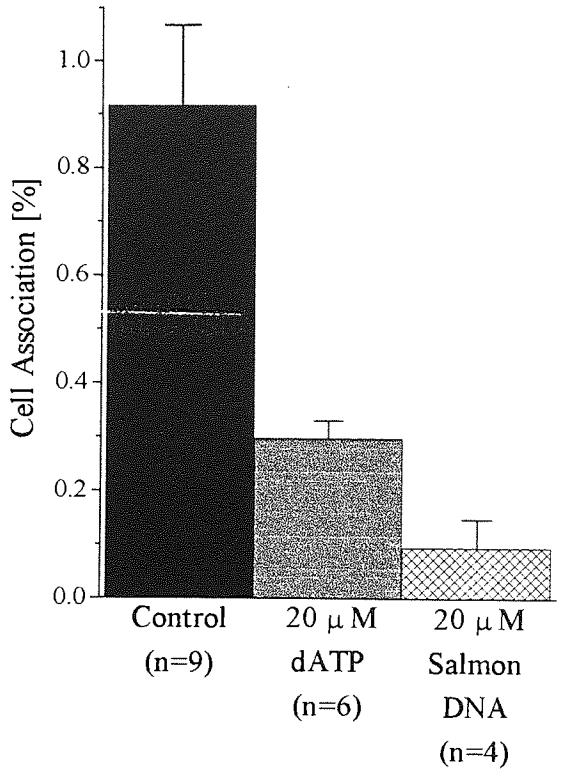

Competitive inhibition by salmon testes DNA (20μM) was significantly greater (P<.0146) than that produced by 36-mer PO ODN (20μM, see Section 4.3.5) and also 20μM dATP. Indicating that increasing the nucleotide chain length, and therefore increasing both the size and anionic charge of the competing agent, may increase inhibition of ribozyme cell association. However the extent of competitive inhibition seen with the 36-mer PO ODN was not significantly greater (P=0.576) than that produced by dATP.

Increasing the length of antisense ODNs has been shown to lead to greater cellular association and this effect is thought to be mediated by the increase in the anionic character of the ODN allowing greater ionic interaction with cell surface proteins (Beck *et al*, 1996). Therefore, the more potent inhibition of ribozyme cell association produced

by pre-incubation with salmon DNA could arise from increased blocking of protein binding sites by the longer chain salmon testes DNA molecule.

4.3.8. The Effect of High Molecular Weight Polyanions on Cellular Association of Chimeric Ribozymes.

To examine the competitive effect of non-nucleic acid polyanions on cellular association of ribozymes, studies were performed as described in Section 4.2.3.3. Heparin and dextran sulphate are polyanionic compounds which could potentially compete with ribozymes for cellular association, if the process were mediated by ionic interactions with cell surface structures such as proteins.

The results (demonstrated in Figure 4.9) represent cell association of 0.8μM radiolabelled ribozyme in the presence of a competing polyanion. The control sample represents cell association of 0.8μM radiolabelled ribozyme in the absence of any competing polyanion. Cell association of ribozyme was significantly reduced ($P<0.0001$) in the presence of both polyanions. Heparin was the most potent competitor, reducing the percentage of ribozyme which became cell associated by over 80% after 4 hours.

Figure 4.9. Graph Showing Percent Association of Chimeric Ribozyme with A431 Cells in the Presence of Excess Concentrations of Polyanions after 4 hours Incubation at 37°C. (mean ± SD).

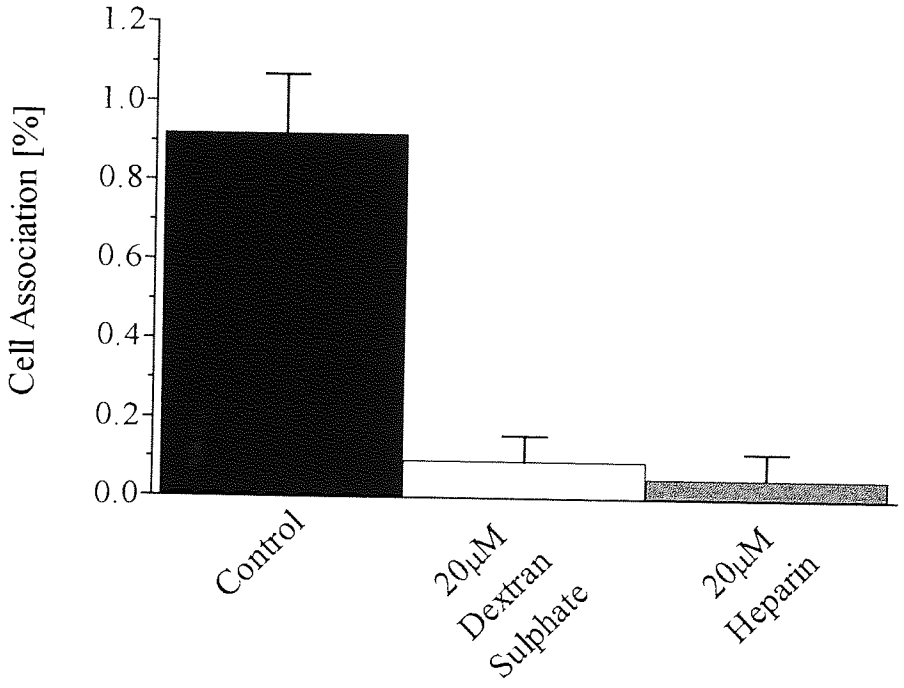

Both dextran sulphate (Wu-Pong *et al*, 1992) and heparin (Gewirtz *et al*, 1996) have been shown to competitively inhibit cellular association of antisense ODNs *in vitro* and from these results it would appear that they exert a similar effect on ribozyme cell association. Dextran sulphate (Kajio *et al*, 1992) and heparin (Ishai-Michaeli, *et al*, 1992) have also been shown to prevent basic fibroblast growth factors from binding to their specific receptor sites on the cell surface. Indeed, they are especially effective at preventing growth factor ligands from binding to low affinity receptor subtypes (Guvakova *et al*, 1995). Therefore, the inhibition of cellular association of both ribozymes and ODNs by dextran sulphate and heparin does not totally rule out the existence of a specific receptor mediated process for the cell association of these nucleic acids. Although if such a receptor did exist it is seems unlikely that it would demonstrate a high degree of specificity for its nucleic acid ligand(s), because these anionic molecules, which are not chemically related to ribozymes, are able to compete very effectively for this cellular association process. Another possible explanation for the above results could be that ribozymes were themselves interacting with the heparin and other anions in the culture media and this prevented cell binding. In order to provide further evidence of ribozyme interactions with cell surface proteins additional experiments were performed.

4.3.9 The Influence of pH on Ribozyme Cellular Association.

Studies were performed as described in Section 4.2.3.1 to assess the effect of pH on cellular association of 0.8μM internally radiolabelled ribozyme over a 4 hours. As the pH of the extracellular environment was reduced, cell surface proteins would become protonated and would probably become more attractive to negatively charged molecules such as ribozymes or ODNs. Therefore, if some degree of protein binding were involved in the cellular association of ribozymes it would be likely that the level of cell association would increase as the pH of the culture media became more acidic.

For purposes of comparison with antisense ODNs, studies were also performed over a 30 minute incubation period. In these experiments the cell association of internally radiolabelled ribozyme was compared with that of 5'-[^{32}P]-end labelled (see Section 2.5.1) PO and PS ODNs of the same base sequence. The shorter time period was selected for these experiments in order to ensure the stability of the 5'-end labelled ODNs towards nuclease and phosphatase enzymes present in cell containing media (See Chapter 3). The results of these experiments are demonstrated in Figure 4.10.

With reference to Figure 4.10 it seems clear that cellular association of the ribozyme is markedly increased in A431 cells as the extracellular environment becomes more acidic. Differences in cellular association were significantly different ($P<0.003$) at each media pH value tested. (i.e. a single 'point' rise in the pH of the media caused a significant reduction in the percentage of ribozyme which became cell associated). At pH 5.0 the level of cell association was increased more than 5-fold when compared with that typical levels recorded in other experiments detailed in this chapter where a standard culture medium at pH 7.25 was used (see Section 2.7.4) under similar conditions, (for example see Figure 4.4).

Figure 4.10. A Comparison of the Influence of Media pH on the Cellular Association of Chimeric Ribozyme, PO and PS Oligodeoxynucleotides after 30 minutes Incubation at 37°C (n=4, values are mean ± SD). INSET: The Influence of Media pH on the Cellular Association of Internally Radio-Labelled Ribozyme with A431 cells after 4 hours at 37°C. (n=4, mean ± SD).

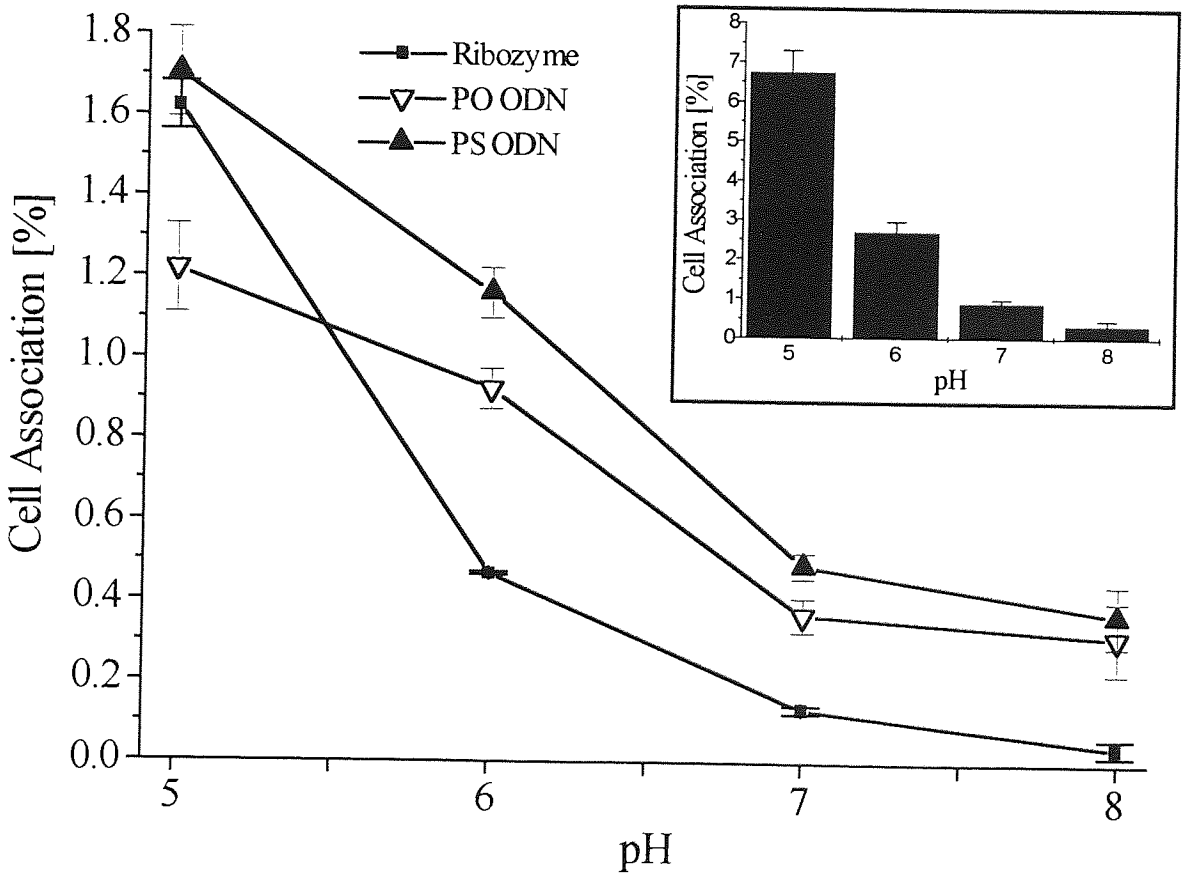

Cell morphology and viable cell counts were not affected by the changes in media type and pH. Therefore it seems unlikely that the marked increase in cell association could be explained by loss of cell membrane viability at lower pH.

Other workers have demonstrated the influence of extracellular pH on the association of antisense ODNs with various cell types *in vitro* (Goodarzi *et al*, 1991, Kitajima *et al*, 1992, Beck *et al*, 1996). The results obtained here with ribozymes appear to mirror these findings, in that a decrease in the pH of the extracellular environment produces an increase in the amount of material which becomes cell associated. Figure 4.10 demonstrates the results of comparative studies, which indicate the relative influence of pH on cellular association of ribozymes, PO and PS ODNs after a 30 minute incubation period. After 30 minutes at pH 5, cellular association of both ribozymes and ODNs was significantly higher ($P<0.01$) than when administered in higher pH environments. The cell association data for all three types of nucleotide after 30 minutes appears to show a similar trend to that obtained after 4 hours for ribozymes (see Figure 4.10 [inset]), in that a rise in the extracellular pH reduces the percentage of cell associated nucleotide.

There was no significant difference ($P=0.240$) between the percentages of ribozyme and PS ODN which became cell associated at pH 5, although both were significantly higher ($P<0.008$) than the percentage of PO ODN which became cell associated. From pH 6 to pH 7 percent association was significantly higher ($P<0.0035$) in the order PS > PO > ribozyme. At pH 8 there was no significant difference ($P=0.399$) between the percentages of PO and PS ODN which became cell associated, although the percentage association of both types of ODN was significantly higher at pH 8 ($P<0.01$) than that of associated ribozyme.

Studies in other cell lines (Beck *et al*, 1996) have shown that the percentage of PS ODN which becomes cell associated is higher than that of PO ODN at low pH, but only marginal differences exist above pH 5. A similar trend is noticed here in that differences between PO and PS ODNs association are much more pronounced at lower pH. Nevertheless, the differences in PO and PS association are significantly different at all pH conditions tested. In comparison with ribozymes, cellular association of both PS and PO ODNs appears to be higher than that of ribozymes at pH 6 and above. (However, some of the increased cellular association seen with 5'- end labelled ODNs could potentially be a result of the removal of the phosphate radiolabel by phosphatases, although this was not

examined here). However at pH 5; PS ODNs and ribozymes show similar, higher levels of cellular association.

Overall, the influence of pH on the cellular association of ribozymes with A431 cells appears to give support to the theory that interaction with cell surface proteins is involved in the cellular binding / uptake process because proteins become protonated at lower pH. However, many cell surface proteins with high pKa values would be fully protonated across the pH range tested in these experiments. In theory, only amino acids with lower pKa values, for example histidine with a pKa of 6.5, would demonstrate dramatic changes in the level of protonation over the pH range tested here (Blackburn and Gait, 1990). Nevertheless, other proteins could still be affected to some degree by protonation of carboxylic acid residues which would reduce repulsion of anionic molecules such as ribozymes and ODNs. Another possibility which cannot be excluded here is of interaction with cell surface lipids, which could potentially demonstrate pH dependency (Akhtar and Juliano, 1992(b)).

4.3.10. Assessment of Cell Surface Protein Binding By Chimeric Ribozymes.

To estimate the protein bound component of ribozyme cell association, the method described in Section 4.2.3.2 was used. After incubation with internally radiolabelled ribozyme for a fixed time period (60, 120 or 240 minutes) A431 cells were washed with Pronase® at 4°C, in order to remove the fraction bound to cell surface proteins. The results of these studies are demonstrated in Figure 4.11 compared with control experiments in which cells were washed with buffer solution alone at 4°C.

Cell associated ribozyme was highly sensitive to the action of Pronase® following incubation at 37°C. The maximal effect of Pronase® treatment was seen when cells were incubated for 60 minutes prior to Pronase treatment. In this case, almost 60% of the cell associated ribozyme was removed by Pronase when compared with the control sample. Where cells were incubated with ribozymes for longer periods, slightly less cell associated material was removed. However, statistically significant ($P<0.05$) differences were only obtained when the 60 minute and 240 minute data were compared. Between 6% and 8% of the cell associated ribozyme was removed from control samples by washing with HBSS buffer for 15 minutes. However this proportion was significantly less ($P<0.0001$) than that removed by the action of Pronase®. The difference between the HBSS control

and Pronase treated samples is quite pronounced, indicating that a substantial proportion of the total cell-associated ribozyme is bound to cell surface proteins.

Figure 4.11. Graph Showing the Percentage of Cell Associated Ribozyme Following Treatment with Pronase Enzyme Compared with Control Samples Treated with HBSS Buffer Solution Alone. (n=4, Values are mean ± SD)

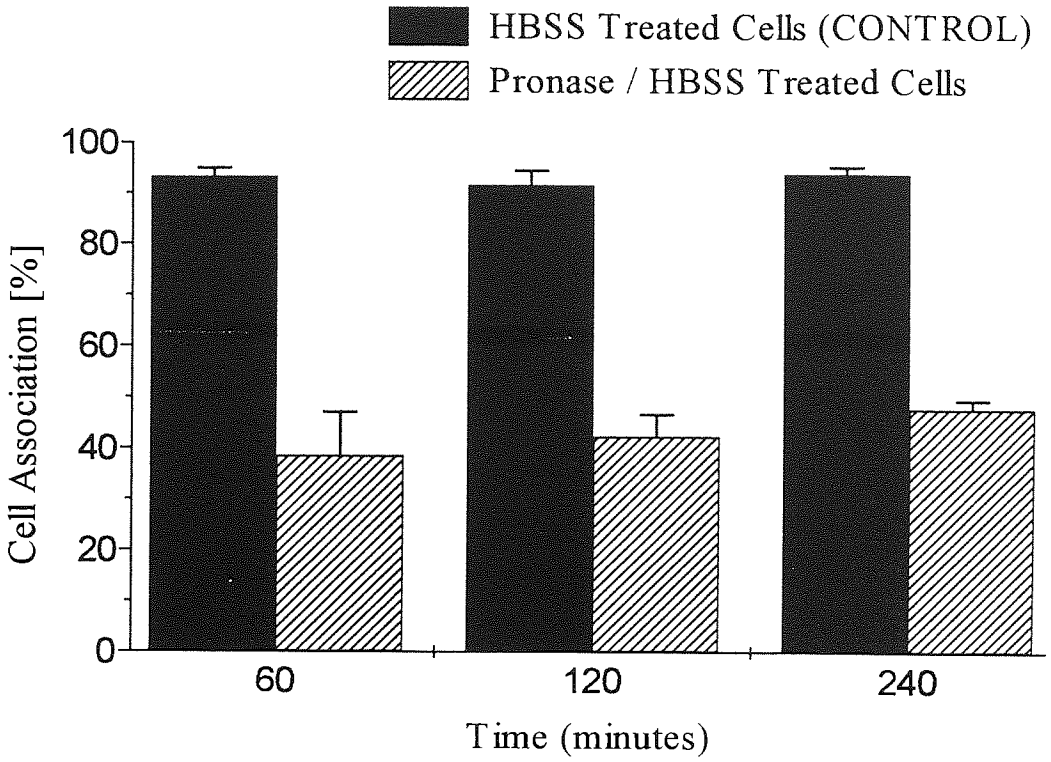

The possibility that some of the radiolabelled material, present in the Pronase® and control washes, could have been exported from cells by some form of exocytic process ('efflux') was not excluded. However, the efflux of cell associated ribozymes, following incubation with A431 cells (for 4 hours) has been examined elsewhere in this report (Section 5.3.3). Results indicated that less than 17% of cell associated ribozymes were exported from A431 cells to the supernatant media within 15 minutes at 37°C. Therefore, it would appear that the proportion of ribozyme present in the HBSS control washes (less than 8%) could possibly reflect the proportion of ribozyme lost from cells via efflux during this 15 minute 'wash step' at 4°C (i.e. at the lower temperature used). However, efflux of ribozymes from A431 cells is unlikely to account for the substantial reduction in cell associated ribozyme which was observed when cells were treated with Pronase® for 15 minutes at 37°C. The reduction in the percentage of cell associated ribozyme as a result of efflux (<17%) after 15 minutes (see Section 5.3.3) was significantly lower ($P<0.001$) than the reduction in cell associated ribozyme observed when cells were

treated with Pronase® (>52%) for the same period of time. Therefore, this indicates that Pronase® removes a greater proportion of cell-associated ribozyme than would be predicted by efflux alone. The likely reason for this is that Pronase specifically removes ribozymes which are bound to cell-surface proteins.

The proportion of cell associated ribozyme which was not Pronase sensitive could have been internalised, tightly bound to glycoproteins resistant to Pronase treatment (Sweeny and Walker, 1993), or even bound to cell surface lipids (Akhtar *et al*, 1991, Akhtar and Juliano, 1992(b)). Various protease enzymes have also been demonstrated to remove a significant proportion of cell associated PO and PS ODNs from other cell lines (Wu-Pong *et al*, 1992, Beck *et al*, 1996). Thus demonstrating further similarity in the binding characteristics of ribozymes and antisense ODNs.

4.3.11. Comparison of Ribozyme Cell Association in A431 cells with that in Other Cell Lines.

To allow the level of ribozyme association observed in A431 cells to be compared with that in other cell lines; experiments were performed using the cell lines described in Section 2.7. Cell association experiments were performed using the method outlined in Section 2.8.1 using A431 (vulval) epithelial cells, U87-MG (glial) cells, Raw 264.7 (macrophages), Caco-2 (colonic) cells and ECV304 (umbilical cord) endothelial cells.

The results of these studies, which are normalised to cell number, are demonstrated in Figure 4.12. The normalised percentage cell association was not significantly different ($P>0.05$) in A431 cells compared with that in ECV304 cells. However the normalised level of cellular association was significantly higher ($P<0.001$) in the other cell lines tested, with the greatest amount of cell association seen in the Raw 264.7 macrophage cells. In this macrophage cell line the percentage of ribozyme which became cell associated was approximately 3-fold higher than in A431 cells. It is unlikely that this difference is due to any phagocytic ability of this cell line because such activity would be absent without the addition of specific chemotactic factors to the culture medium.

These experiments highlight the difficulty in comparing results obtained using different cultured cell lines, even within the same laboratory. Nevertheless, overall trends in cellular association characteristics may be similar in unrelated cell lines, even if the absolute levels of cellular association may differ. Mechanistic studies performed in a

specific cell line can often highlight overall trends in a variety of cell types. For example, much of the evidence for the proposed mechanism(s) of ODN cellular association has been derived from trends identified in experiments using different, cell lines (For review see Rojanasakul, 1996).

Figure 4.12. A Comparison of the Cellular Association of Internally Radiolabelled Ribozyme Range in Various Cell Lines. (n=4, values represent mean Percentage cell associated ribozyme adjusted to 10^5 cells ± SD).

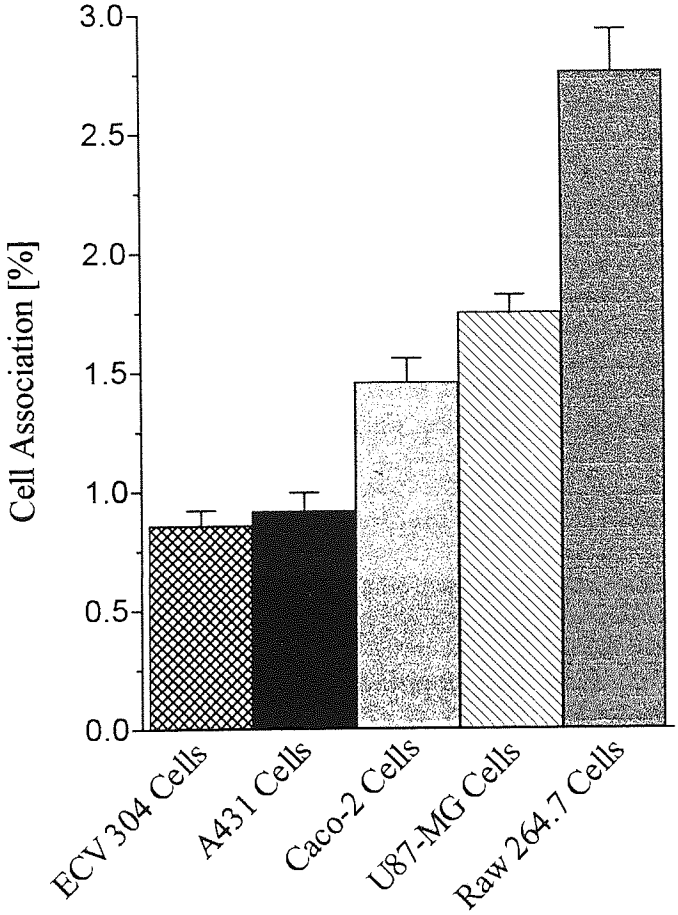

The uptake and binding characteristics of PO and PS ODNs are known to differ when experiments are performed using different cell lines *in vitro* (Noonberg *et al*, 1993, Akhtar and Rossi, 1996). Therefore a similar variation in cellular association characteristics between cell lines could be expected for ribozymes because each cell line varies, for example, in shape, size, morphology and cell surface characteristics.

4.4. CONCLUDING REMARKS.

Cellular association of exogenously delivered, chemically stabilised ribozymes *in vitro* has been studied in this chapter, in order to provide evidence for the mechanism(s) of ribozyme cell entry. The hammerhead ribozymes were chemically modified to increase their biological stability (also see Chapter 3) and also internally radiolabelled to reduce experimental inaccuracy arising from the removal of end radiolabels by phosphatase enzymes. However, the assumption was made in all studies that the levels of radioactivity present in experimental samples, represented the presence of intact radiolabelled ribozymes or ODNs.

When added directly to A431 cells, ribozyme association was inefficient with only around 1% of the added quantity becoming cell associated after 4 hours. However, the level of cellular association was significantly higher that of radiolabelled mannitol, a marker of fluid phase endocytosis (FPE), thereby indicating that ribozymes were unlikely to enter cells via FPE alone. In addition, cellular association was significantly reduced at low temperature and in the presence of metabolic inhibitors. This would appear to discount the possibility of ribozymes entering cells via passive diffusion alone, as was originally proposed for some types of ODNs by Agris *et al*, 1986.

Cellular association of ribozymes was demonstrated to be both concentration dependant and saturable. Other studies indicated that cellular association could be competed by unlabelled ('cold') ribozyme (i.e. association was 'self-competitive'). These characteristics are considered to be indicative of a specific cell surface binding mechanism, such as receptor mediated endocytosis (RME) or adsorptive endocytosis (AE) (Loke *et al*, 1989, Beltinger *et al*, 1995).

Competition studies with PO and PS ODNs, indicated that there may be some overlap in their mechanism(s) of cell association because both were able to strongly compete with ribozymes for cellular association. However, polyanions such as dextran sulphate and heparin also competed with ribozymes for association with A431 cells. Since these polyanions are chemically unrelated to ribozymes, this would appear to cast doubt over the existence of a specific receptor for ribozyme uptake. At the very least it suggests that if specific binding proteins exist, they exhibit low levels of affinity for their ribozyme ligands.

Evidence to suggest the involvement of cell surface proteins in the cellular association of ribozymes was also obtained. Firstly, the cell association of ribozymes was increased at reduced extracellular pH. This reduction in pH would protonate cell surface proteins, making them more attractive to anionic molecules such as ribozymes. Furthermore, a proteolytic enzyme was able to remove over 50% of cell associated ribozymes. This suggests that protein binding has a significant role in the cellular association of ribozymes. It also demonstrates that only a fraction of the ribozymes added to A431 cells actually become internalised, even if protein binding to the cell surface takes place.

Overall, these findings tend to suggest that a process of RME and / or AE would offer the most likely explanation of the predominant mechanism by which chimeric ribozymes enter cells. This is probably mediated by binding to a range of cell surface proteins and possibly other surface components. It must be noted, however, that association of ribozymes was cell-line specific, therefore, difficulties could arise in drawing direct comparisons between the results obtained in A431 cells and those obtained in other cell lines.

Further studies, which examine the intracellular fate of ribozymes following exogenous delivery to A431 cells (see Chapter 5) have provided additional evidence regarding the mechanism(s) of ribozyme cell entry.

CHAPTER FIVE

UPTAKE AND INTRACELLULAR TRAFFICKING OF CHIMERIC HAMMERHEAD RIBOZYMES

5.1. INTRODUCTION.

An appreciation of the uptake mechanism(s) and intracellular trafficking of exogenously delivered hammerhead ribozymes could facilitate the use of these agents for therapeutic and experimental purposes. In Chapter 4, cellular association and binding characteristics of chemically stabilised chimeric ribozymes were examined. The cellular association of ribozymes was a concentration and energy dependant process, which was self-competitive. Cellular association versus time profiles were similar to those demonstrated for antisense ODNs and were largely consistent with mechanism(s) of receptor mediated and / or adsorptive endocytosis. Binding to cell surface proteins was also observed. Nevertheless, the information regarding the binding and cellular association of ribozymes cannot, on its own, predict the final intracellular destination(s) of exogenously delivered ribozymes. Consequently, it is only possible to speculate with regard to the final concentrations of ribozyme which will arrive at the desired target sites within cells.

In order to modulate gene expression, ribozymes would almost certainly have to be co-localised with their mRNA (or pre-mRNA) targets at specific intracellular sites. Yet if the assumption were made that ribozymes enter cells via an endocytic process, it would be expected that the majority of internalised ribozymes would be localised within acidified endosomal vesicles following cell entry (Hopkins, 1985, Smythe and Warren, 1991). Therefore, ribozymes would have to exit these endocytic vesicles in order to exert a biological effect. Otherwise, they could be released from cells via exocytosis, or alternatively they could be degraded by nucleases which can accumulate within these vesicular structures (Akhtar *et al*, 1995).

In this chapter, the parameters of cellular trafficking of ribozymes have been examined using several techniques: Intracellular compartmentalisation of fluorescein-labelled ribozymes was examined and compared with that of antisense ODNs and endosomal markers labelled with different fluorophores. In addition, by utilising the rapidly developing technique of immuno-electron microscopy, the trafficking of biotinylated

ribozymes and PS ODNs within A431 cells was examined. This technique allowed more precise, higher-resolution results to be obtained, providing a better understanding of the sites at which ribozymes are likely to come into contact with their targets. Finally the extent of ribozyme efflux from A431 cells was investigated to provide an indication of the proportion of internalised ribozyme which was exported from cells over given time periods. Ribozymes rapidly exported from cells via exocytosis would probably not have had the opportunity to exert any biological effect.

Although there is a lack of published information with regard to the intracellular trafficking of exogenously delivered ribozymes, several groups have examined the intracellular distribution of antisense ODNs. Most of the studies reported to date have utilised fluorescent labelling, often in combination with isotope labelling, to indicate the sites of intracellular localisation of antisense ODNs (Stein *et al*, 1988, Loke *et al*, 1989, Yakubov *et al*, 1989, Shoji *et al*, 1991, Bennett *et al*, 1992, Iverson *et al*, 1992, Iwanga and Ferriola, 1993, Tönkinson and Stein, 1994, Zamecnik *et al*, 1994, Zani *et al*, 1995). In the majority of fluorescence studies a punctate, subcellular distribution of fluorescent-labelled ODNs is described following exogenous delivery (Wagner, 1994). This pattern of distribution is indicative of localisation within endosomal or lysosomal vesicles (Rojanasakul, 1996).

Comparative studies, using both modified and unmodified fluorescein-labelled ODNs have produced some interesting results. Early studies indicated comparable levels of internalisation of both PO and PS ODNs following exogenous delivery (Marti *et al*, 1989). Fluorescent-labelled ODNs, modified with methylphosphonate linkages, exhibited similar punctate patterns of distribution to those observed with PO and PS ODNs (Shoji *et al*, 1991). The findings of a quantitative study, utilising both confocal microscopy and flow cytometry, indicated that both fluorescein-labelled PO and PS ODNs reside in vesicular structures following cell entry. However, fluorescein-labelled PS ODNs were detected at higher intensities compared with PO ODNs, when endosomes or vacuoles within HL60 cells were acidified by treatment with monensin (Tonkinson and Stein, 1994). The extinction coefficient of fluorescein varies with changes in pH. Therefore, the authors concluded that PS ODNs were localised within acidic environments because the intensity of fluorescence was increased following monensin treatment. Indicating that PS ODNs were mainly sequestered in endosomes or lysosomes. However, results indicated that PO ODNs did not predominantly reside in acidic compartments and could have been located in the cytoplasm, nucleus, or in non-acidified pinosomes which were quickly exported from cells via an efflux cycle. Overall, this study highlights the potential differences in the way(s) that different ODN analogues could be compartmentalised within cells.

A small number of studies have examined the ultrastructural localisation of PS ODNs within cells using immuno-labelling and electron microscopy: Tarrason *et al* (1995) used a combination of fluorescent and immuno-labelling techniques to study the intracellular localisation of PS ODNs in human B-cells. Fluorescent microscopy indicated that both fluorescein and digoxigenin-labelled PS ODNs accumulated within similar perinuclear-nuclear vesicles. Using double immuno-fluoresence techniques, some degree of crossover in the localisation of PS ODNs and an immunoglobulin specific for lysosomal proteins was demonstrated, thus indicating an accumulation of PS ODNs in lysosomes. In parallel studies, a variety of fixatives and immunogold labelling methods (involving the use of anti-digoxigenin antibodies) were used to detect digoxigenin-labelled PS ODNs within cells by electron microscopy. Some gold particles were sparsely distributed in the cytoplasm and nucleus of cells. Although the majority of gold particles were considered to be restricted to electron-dense structures with a lysosome-like appearance, thus confirming the results of the fluorescence studies (Tarrason *et al*, 1995).

However, a potential criticism of this work is that increased levels of immuno-labelling intensity were seen in cells which were exposed to higher levels of aldehyde-based fixatives. Harsher fixation protocols (i.e. those involving the use of higher concentrations of aldehyde-based fixatives) would be expected to reduce the specificity of immunogold labelling. Therefore, some degree of non-specific labelling may have occurred in these studies, especially where higher levels of fixation were used (personal communication; Dr. P. Monaghan, CRC Laboratories, Sutton, UK).

Immunoelectron microscopy was also utilised by Beltinger *et al* (1995), in order to demonstrate cellular binding and trafficking of PS ODNs. A pre-embedding labelling technique, using streptavidin-gold, was used to visualise biotinylated PS ODNs which had been cross-linked to cell surface proteins. In separate studies, biotinylated PS ODNs were detected within intracellular compartments. Here, post-embedding techniques were used that employed a 'double antibody' labelling process in which cells were first treated with a primary 'anti-biotin' antibody, followed by detection of this primary antibody with Protein-A gold.

When biotinylated PS ODNs were cross-linked to cell surface proteins, gold particles were visualised bound to cell surface components and also within structures thought to be clathirin coated pits, forming at the cell surface (Beltinger *et al*, 1995). Where the post-embedding technique was used to examine intracellular distribution; gold particles were visualised within, or at the periphery of, clear vesicles which were thought to be endosomes. Gold particles were also visualised within electron dense

lysosome-like structures, free within the cytoplasm and within the nucleus. In the latter structure, particles were reported to preferentially localised to the euchromatin / heterochromatin surface (Beltinger *et al*, 1995).

Free biotin is known to enter cells in very small quantities in a concentration (Cohen and Thomas, 1982) and energy dependant manner (Ma *et al*, 1994, Said *et al*, 1994). Therefore, where biotin is used to label ODNs or ribozymes in localisation studies, control experiments must be carefully selected. One approach is to add free biotin to a control sample of cells, to confirm that the biotin moiety itself does not contribute to any observations made. When control samples of this type were processed by Beltinger *et al* (1995) only a few randomly distributed gold particles were detected on the electron micrographs. In addition, in cells processed in the absence of any added agent, gold particles were rarely detected, indicating very low levels of (detectable) endogenous biotin in the K562 cell line. Nevertheless, similar controls would be required in the experiments detailed in this chapter in order to examine detectable levels of 'endogenous' and 'added' biotin in the A431 cell line.

Finally, with regard to the efflux of internalised ribozymes from cells, once again there is a lack of published information available. However, some proportion of antisense ODNs which become internalised within cells are known to be exported to the extracellular environment (Loke *et al*, 1989). Initial attempts to quantify the extent of efflux suggested that up to 50% of PO ODNs rapidly dissociated from Rauscher cells when these cells were re-suspended in fresh culture medium. However, the levels of cell associated PO ODNs then stabilised indicating that at least some PO ODN was able to remain internalised (Wu-Pong *et al*, 1992).

More recent studies have examined the efflux of both PO and PS ODNs from HL60 cells in more detail (Stein *et al*, 1993, Tonkinson *et al*, 1994, Tonkinson and Stein, 1994). In these studies, efflux of fluorescent-labelled ODNs was measured after steady state accumulation within cells had been achieved (3 to 6 hours load time). Results were described by a double exponential function, with two distinct mathematical 'compartments' being identified, in line with the findings of other studies involving pinocytosed molecules (Besterman *et al*, 1981). Exocytosis of ODNs from each of these 'compartments' was calculated. The turnover of ODNs in each compartment occurred at different rates and this was indicated by a half-life value. Some authors describe these mathematical compartments as 'shallow' and 'deep' compartments within cells, however, these compartments have not yet been defined physiologically (Tonkinson and Stein, 1994).

Interestingly, PS ODNs were retained within HL60 cells for relatively long periods of time, with over 70% of internalised PS ODNs residing in the 'deep' compartment with a turn-over half life of approximately 4 hours. In contrast, PO ODNs appeared to be effluxed more rapidly, with over 60% residing within the 'shallow' compartment, with a turn-over half-life of 10 to 15 minutes (Tonkinson *et al*, 1994, Tonkinson and Stein, 1994). However, some proportion of effluxed PO ODNs were demonstrated to be partially degraded, whereas, PS ODNs were stated to demonstrate 'much greater stability' in HL60 cells (although this was not confirmed experimentally in this study). Therefore, the different biological stabilities of radiolabelled PS and PO ODN could have influenced results to some extent.

The observed rate constants for the efflux of various molecules from the two mathematical 'compartments' are fairly similar in most reports (Besterman *et al*, 1981, Stein *et al*, 1993, Tonkinson *et al*, 1994, Tonkinson and Stein, 1994). However, the relative amount of material residing in each compartment is dependant upon the cell type and the loading time (Tonkinson and Stein, 1994), as well as the chemistry of the molecule examined (e.g. PS or PO ODN, see above). For example, when cellular trafficking of ^{14}C-sucrose was examined, the relative amounts detected in each compartment varied considerably with loading time. With almost 90% of the sucrose found to reside in the compartment with slower turnover when loading times in excess of 3 hours were used (Besterman *et al*, 1981). Other authors have commented upon the inappropriate extrapolation of efflux study data between different cell lines (Tonkinson and Stein, 1994). Therefore, in the studies detailed in this chapter comparisons have been made between efflux of both chimeric ribozymes and PS ODNs in the A431 cell line, under similar conditions, in order to allow trends to be compared.

Despite the fact that several studies have examined the intracellular localisation, trafficking and efflux of antisense ODNs, there is clearly a need for further information in these areas with regard to exogenously delivered ribozymes. The overall aim of the present studies was to allow a better understanding of these characteristics. This could indicate whether or not exogenously delivered ribozymes were able to access their intracellular target sites and, therefore, possibly exert biological effects. Furthermore, these studies could give an indication of any requirement for additional delivery system(s) and aid in the design of such strategies.

5.2. METHODS.

5.2.1. Preparation of Nucleic Acid Sequences.

A 36-mer partially modified, chimeric ribozyme (Sequence EGFR-65, see below), targeted against an untranslated region of the human EGFr mRNA, was synthesised as described in Section 2.4.2:

5'-ugugugucu**GA**u**G**aggccgaaaggcc**G**aa**A**cug*A*♦*A*♦*C*-3'

The majority of nucleotides within the ribozyme were 2'-O-methylated and joined by phosphodiester linkages, with the exception of five unmodified ribonucleotide bases within the catalytic core (shown above as bold, underlined bases), which were preserved in order to retain catalytic activity. Three nucleotides at the 3'-terminus of the molecule were unmodified deoxyribonucleotides (shown above in capital *italics* at the 3' terminus), joined by PS inter-nucleotide linkages (signified by '♦' symbols above). The three deoxyribonucleotides were retained in order to preserve a similar structure to that examined in the cellular association studies outlined in Chapter 4. Unmodified 36-mer PO ODNs, and PS ODNs, of the same base sequence were also synthesised, as described in Sections 2.3.3 and 2.3.4.

5.2.2. Labelling of Nucleic Acids.

Fluorescein (FITC) labels were added to the 5' end of both chimeric ribozymes, PO and PS ODNs during automated synthesis as outlined in Section 2.5.4. Chimeric ribozymes and PS ODNs were 5'-biotinylated during automated synthesis (see Section 2.5.5). Labelled nucleic acids were stored at -70°C and protected from light prior to use.

5.2.3. Cellular Localisation of Fluorescent-Labelled Probes.

In order to assess the cellular distribution of fluorescent-labelled compounds, experiments were performed as described in Section 2.8.7.2. In all studies, additional wells were seeded with cells and viable counts were determined, after incubation with the test solutions, using a haemocytometer as described in Section 2.7.2.

Following incubation with fluorescent compounds, cells were routinely washed and fixed as described in section 2.8.7.2. However, some cells were simply washed with sterile PBS to removed traces of non-cell associated fluorophores and immediately

viewed under the microscope in the absence of any fixative treatment. This allowed the extent of artefacts caused by the fixation process to be assessed. However, it was not possible to routinely perform detailed examinations, over longer time periods, with non-fixed cells because the condition of such cells deteriorated rapidly. Cell associated fluorophores were visualised using a Jenamed fluorescence microscope as described in Section 2.8.7.3.

5.2.4. Ultrastructural Localisation of Biotinylated Ribozymes and ODNs.

The technique of immunocytochemistry was used to detect biotin and biotinylated compounds within sections of A431 cells. The detection method involved the use of monoclonal antibodies raised against biotin, which specifically bind to their biotin antigen within cells, provided that the antigen has not changed its structure. Monoclonal antibodies can be labelled with gold particles to permit detection.

When cells are prepared for electron microscopy, some form of cross-linking fixation protocol is required to preserve cellular morphology. In addition, cells must be dehydrated, embedded within a support material and cut into extremely thin sections. However, chemical fixatives generally have a detrimental effect on immuno-reactivity because antigen structure can be chemically destroyed. In addition, the access of antibodies to their antigens is hindered by extensive protein cross linking within thin cell sections (Griffiths *et al*, 1993). Therefore, a justifiable compromise has to be found between preservation of cellular morphology and the maintenance of immuno-reactivity (Monaghan and Moss, 1995).

Several approaches have been used here in an attempt to limit the damage to the biotin antigen whilst maintaining cellular morphology as far as possible. Fixation damage was minimised in several ways: Cell samples were fixed for a shorter time period (20-30 minutes) than would be routinely used if preservation of cellular morphology were the sole aim. In addition, the fixative solution contained very low levels of glutaraldehyde, which was substituted with paraformaldehyde; a less potent cross linker. Dehydration was performed at low temperatures in order to reduce the extraction of cellular components by dehydrating solvents. This technique is termed the progressive lowering of temperature (PLT) method and was followed by a low temperature embedding stage, into a resin which has a low viscosity even at very low temperatures. The combination of these measures would be expected to significantly reduce damage to the biotin antigen within cell preparations (Monaghan and Moss, 1995).

5.2.4.1. Incubation of Cells for Immunocytochemical Studies.

For electron microscopy, cells were grown on Thermanox® cover slips as described in Section 2.7.4. Following a 24 hour growth period the cells were incubated with either 10μM 5'-biotinylated chimeric ribozyme or 10μM 5'-biotinylated ODN (See Section 5.2.1) in serum-free cell culture media at 37°C for 4 to 6 hours. Control samples were prepared in parallel, where cells were incubated with either 10μM d-biotin (Sigma, molecular biology grade) in serum free media or in the absence of any biotinylated agent for the same time period. These cells served as a control of the labelling specificity of biotinylated nucleic acids, as opposed to endogenous or added biotin.

5.2.4.2. Fixation for Immunoelectron Microscopy.

Cell preparations for immunocytochemical studies were fixed for 20-30 minutes in freshly prepared fixative solutions containing paraformaldehyde 1.5% v/v (Sigma, microscopy grade [P-6148]), 0.05% v/v glutaraldehyde (Sigma, Grade I), 0.2% w/v picric acid (donated by Birmingham Medical School) in 0.1M phosphate buffer. Picric acid was added as this is known to stabilise cellular proteins in immuno-labelling studies (Mercer and Birbeck, 1972) and has been used successfully in previous studies requiring the immuno-detection of biotin (Beltinger *et al*, 1995).

Some of the control cell samples, which had not been incubated in the presence of any biotinylated agent were subjected to a much higher level of fixation (2.5% v/v glutaraldehyde in 0.1M phosphate buffer). These cells were subsequently processed via the same PLT method, however, the greatly increased level of cross linking fixative permitted greater preservation of cellular morphology. These cell preparations were not immuno-labelled, but were viewed under the electron microscope to assess the morphological characteristics of the A431 cell line.

5.2.4.3. Dehydration of Fixed Cells By The Progressive Lowering of Temperature (PLT) Method.

Following fixation, cells were dehydrated by the PLT method which involves stepwise reduction in temperature as the concentration of the dehydrating agent is increased (Armbruster *et al*, 1982). Fixed A431 cells on Thermanox® cover slips were placed inside drilled chambers in sterile aluminium blocks containing ascending concentrations of ethanol for 30 minute periods at progressively lower temperatures as indicated in Table 5.1.

Table 5.1. Conditions for Dehydration of Fixed Cells by the PLT Method

Ethanol Concentration	Temperature	Location / Equipment
30%	0°C	on ice
55%	-15°C	refrigerator ice box
70%	-30°C	cryostat chamber
100%	-50°C	Reichert CS Auto
100%	-50°C	Reichert CS Auto

5.2.4.4. Embedding and Sectioning of Dehydrated Cells in Acrylic Resin.

The purpose of the infiltration and embedding steps was to prepare the cells within a solid medium which would have sufficient strength to allow thin sections to be cut using a microtome. Lowicryl HM20 (Polysciences Europe, Eppelheim, Germany) was polymerised with 'Initiator C solution' (Polysciences Europe) for a short period of time with very gentle mixing to prevent foaming. Cells were infiltrated with the Lowicryl resin inside the Reichert CS Auto at -50°C. Initially cells were exposed to a 2:1 mixture of ethanol:resin for 1 hour, followed by exposure to a 1:2 mixture of ethanol:resin for a further 1 hour period. Cells were then infiltrated with 100% Lowicryl resin inside the CS Auto for a 20 hour period at -50°C. The resin solution was replenished several times throughout this period.

Cells were embedded following the addition of fresh Lowicryl resin which was polymerised at -50°C with UV light for 48 hours in the Reichert CS Auto. The Thermanox® cover slips were broken away from the resin material leaving resin embedded cells. These were allowed to equilibrate to room temperature for a further 24 hours prior to sectioning. Thin cell sections (<0.1μm) were cut from the resin blocks (pyramids) using a diamond knife microtome and these sections were collected on the dull side of Formvar-coated nickel grids (Amersham, UK).

5.2.4.5. Immunocytochemical Labelling of Biotin Antigens within Cell Sections.

Four separate methods were available for the detection of biotin antigens within the prepared sections of A431 cells. Each detection method relies upon the visualisation of colloidal gold particles by electron microscopy. Gold particles are highly electron dense and appear on electron micrographs as a dark dot against the cell structure if properly contrasted by the use of staining techniques (See Section 5.2.4.6). Indirect labelling methods combine the use of a primary antibody raised against biotin, which

is subsequently detected with a secondary gold labelled agent (See methods C and D in Figure 5.1). Indirect methods are more time consuming than direct methods and require a greater number of controls than for direct labelling methods in order to confirm labelling specificity. There is also a greater potential for non-specific reactions, especially where Protein A:gold is used as this binds indiscriminately to all antibodies. Indirect methods are more widely used because primary antibody gold conjugates are often unavailable (Griffiths *et al*, 1993).

Figure 5.1. A Schematic Representation of Possible Labelling Strategies For the Immuno-detection of Biotin Antigens within Cell Sections.

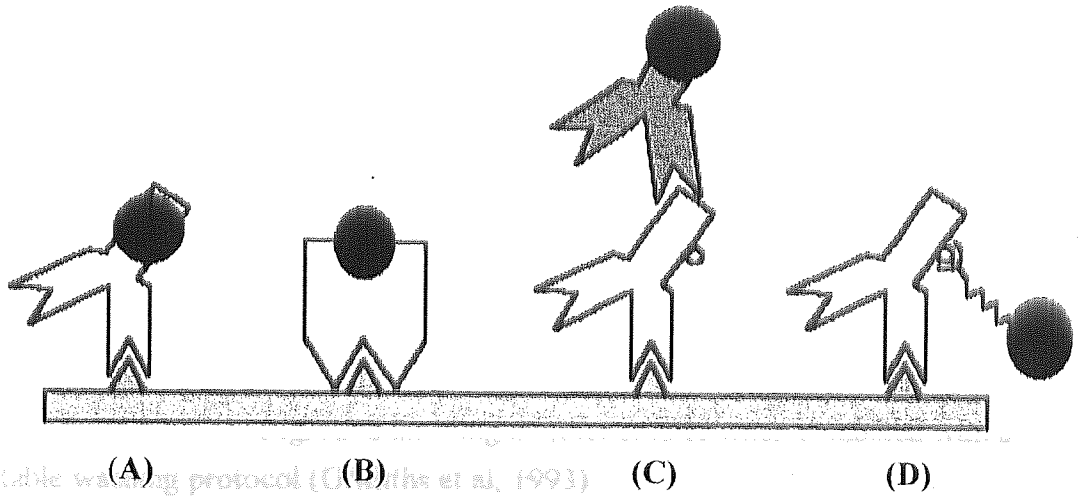

[In all cases shaded triangles represent biotin antigens. Large black circles represent colloidal gold particles. In (A) biotin antigens are detected by the use of a Primary Ab:gold conjugate. In (B) biotin antigens are detected by a streptavidin:gold conjugate. In (C) biotin antigens are detected by a primary Ab. The primary Ab is subsequently bound by a secondary Ab fragment which is labelled with colloidal gold. In (D) biotin antigens are detected by a primary Ab. This primary Ab is subsequently labelled by the addition of Protein A:gold which binds indiscriminately to the Fc region of all antibody molecules.]

However, direct labelling options are commercially available for the immuno-detection of biotin within cell preparations. Historically streptavidin has been the most frequently used 'direct' detector for biotin. Streptavidin is an antibiotic compound derived from the fungus *Streptomyces* which has a very high affinity constant for binding to biotin (Wilchek and Bayer, 1989). When conjugated with colloidal gold it has been used successfully to detect a variety of biotinylated molecules within cells (Griffiths *et al*, 1993) including cell surface bound PS ODNs (Beltinger *et al*, 1995). However, recent studies indicate that a primary anti-biotin Ab: gold conjugate

demonstrates a higher level of sensitivity in the detection of biotin compared with streptavidin (Technical Bulletin & Catalogue (1995), British BioCell International, Cardiff, UK). Fewer controls are required with direct labelling methods to ensure labelling specificity because only a single labelling step is necessary. Direct labelling methods are also less time consuming and the overall cost of the labelling reagents is less than that with indirect methods.

In the present studies, a primary goat anti-biotin Ab, conjugated to 5nm colloidal gold was used. This primary antibody preparation has only recently become available and allowed a direct, one-step labelling protocol to be used in these studies. This is in contrast to previous studies where the intracellular localisation of antisense ODNs was assessed using an indirect labelling protocol (Beltinger *et al*, 1995).

Before the cell sections were exposed to the immuno-gold label, they were first exposed to a blocking buffer. The cell sections on nickel grids were carefully placed onto 30μL droplets of blocking buffer (0.2% w/v BSA, 0.5% w/v purified fish gelatin in sterile PBS) for 45 minutes at room temperature. The buffer was a general purpose protein solution which would bind to sites on the sections which had an affinity for proteins (Behnke, 1986, Birrell *et al*, 1987). Similar buffers have been shown to significantly reduce background labelling in other studies when combined with a suitable washing protocol (Griffiths et al, 1993).

Before the immuno-gold labelling solution was applied, cell sections were briefly washed by placing the nickel grids onto a droplet of 0.2% BSA in PBS. The goat anti-biotin antibody:gold conjugate (5nm gold [EM-GAB5], British BioCell International, Cardiff, UK) was diluted 1 in 60 with sterile 0.2% BSA in PBS. In preliminary studies, this dilution was found to give optimal labelling with very low levels of background / non-specific labelling (i.e. this dilution produced the best 'signal to noise ratio'). The cell sections on nickel grids were placed onto 30μL droplets of the diluted immuno-labelling solution and incubated overnight in a humidified atmosphere at 4°C.

Following immuno-labelling, a thorough washing protocol was required in order to remove non-specifically bound antibody:gold particles from the cell sections. The nickel grids were first floated on droplets of 0.2% BSA in PBS for 5 minutes. This process was repeated four times using fresh droplets of buffer. Grids were then floated on droplets of sterile water for the same time period and the process was, again, repeated four times with a fresh droplet of water.

5.2.4.6. Cell Staining and Examination by Electron Microscopy.

Two stains were used in these studies in order to provide contrasted images of the cell sections: Uranyl acetate stain (2% v/v uranyl acetate in 70% v/v acetone) and Reynolds lead citrate stain (0.0133g lead nitrate, 0.0176g sodium citrate, 0.08mL 1N sodium hydroxide in 50mL sterile water) were (separately) applied to the grids for 15-30 minutes. (Mercer and Birbeck, 1972). Following the application of each stain, the nickel grids were rinsed with sterile water. All cell sections were examined using a JEOL 200X Transmission Electron Microscope, micrographs were taken using Amersham EM photographic media.

5.2.5. Cellular Efflux Studies.

In order to assess the efflux of labelled nucleic acids from A431 cells, a similar method to that of Tonkinson and Stein (1994) was used. Studies were initiated as described in Section 2.8.1. Cells were incubated with either 1μM internally radiolabelled chimeric ribozyme (sequence EGFR-65, see section 4.2.1), 1μM internally radiolabelled PS ODN, or 1μM *D*-[1-^{14}C] Mannitol (Amersham Life Sciences, UK) for 4 hours at 37°C. Following cell loading, the culture plates were placed on ice and the apical media was removed and collected in scintillant (Optiphase HiSafe 3). Cells were washed six times with ice cold PBS and these washings were added to the apical media in the scintillant. Cells were then re-suspended in pre-warmed serum-free media and incubated for the stated efflux times (5 minutes to 4 hours). Following efflux, the apical media was removed and the cells were quickly washed three times with ice cold PBS. Efflux samples (apical media + PBS washings) were collected in scintillant. Mean levels of radioactive material in each sample were determined by liquid scintillation counting as described in section 2.2.5.

5.2.5.1. Curve Fitting for Efflux Data

The efflux data, obtained as described in section 5.2.5, were fitted to an exponential function using MicroCal Origin (MicroCal Software, Northampton, Massachusetts, USA). Each curve was assumed to represent a double exponential function of the form; $C_T = Ae^{(-\alpha t)} + Be^{(-\beta t)}$, where A and B represent the proportion of ribozyme or PS ODN in each compartment at t=0, and α and β are the rate constants for the loss of ribozyme or PS ODN from each compartment.

5.2.5.2. Stability of Efflux Products.

In order to demonstrate that the export of the [^{32}P] radiolabel from cells correlated with the loss of intact ribozyme, studies were performed to examine the efflux product(s). In these studies, cells were initially loaded with internally radiolabelled ribozymes for 4 hours and processed as described in Section 5.2.5. Cells were then re-suspended in pre-warmed serum-free media and incubated for the stated efflux times (5 minutes to 4 hours). Following incubation, the apical media was removed and a 40μL aliquot of this media was added to an equal volume of 'stop' buffer (9:1 v / v formamide in 1 × TBE). Intact radio-labelled radiolabelled ribozymes were separated from any degradation products by 15% denaturing PAGE (8M urea) as described in Section 2.2.2. Autoradiography (performed over a period of 17 days due to the low levels of radioactivity present in the efflux samples) was performed as described in Section 2.2.3 and digitised images of autoradiographs were obtained as described in Section 2.2.4.

5.3. RESULTS.

5.3.1 Fluorescent Localisation Studies.

5.3.1.1 Preliminary Studies

A431 cells grown on chamber slides, as described in section 2.8.7.2, were incubated for 4 hours in serum free media and viewed under the fluorescent microscope. No auto-fluoresence was observed which indicated that fluorescence detected in subsequent studies would be due to the presence of exogenously delivered fluorophores. Furthermore, phase contrast microscopy of untreated cells indicated that the appearance and morphology of these cells was similar to that of cells which were incubated with either 5μM FITC-labelled chimeric ribozymes, FITC-ODNs, RITC-dextran or free flourescein. (For example see Figure 5.2).

Viable cell counts indicated that treatment with 5μM FITC ribozyme, FITC-ODNs and free fluorescein had no effect on viable cell numbers when compared with control samples of cells which were not exposed to fluorescent compounds. Incubation with 5μM RITC-dextran (rhodamine-dextran) did produce a 10% (average) reduction in viable cell numbers compared with untreated controls, possibly indicating some toxicity. However, the reduction in viable cell numbers in the RITC-dextran treated samples, relative to the control samples, was not statistically significant ($P=0.069$).

Figure 5.2. Phase Contrast Images of A431 cells Incubated for 4 hours in Serum Free media: **[A]** In the Absence of any Fluorescent Compound and **[B]** In the Presence of 5μM FITC-labelled ribozyme (Cells were fixed as described in 2.8.7.2, Magnification × 12.5).

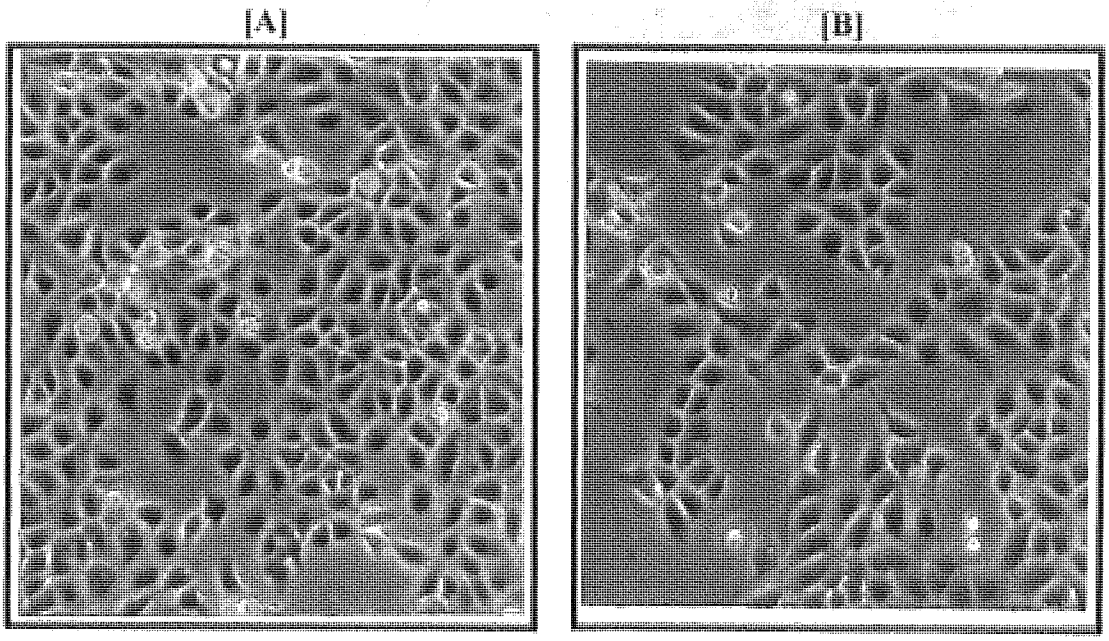

5.3.1.2. Cellular Uptake and Distribution of FITC-Labelled Ribozymes Compared With Free fluorescein Label and Free FITC.

The cellular uptake and distribution of FITC-labelled ribozymes was compared to that of both free fluorescein and free FITC in A431 cells. Ribozymes or 'free label' were incubated with A431 cells at the same concentration (5μM) for 4 hours as described in section 2.8.7. However, cells were not fixed after incubation, instead they were washed with PBS and immediately viewed and photographed. The aim of these studies was to provide a control of labelling specificity.

Incubation with both the 'free' fluorescein and 'free' FITC label produced an intense fluoresence within A431 cells. Patterns of fluoresence distribution were identical following incubation with either fluorescein or FITC (for example see photograph of FITC distribution, Figure 5.3). Fluoresence was widely distributed throughout the cells with a considerable degree of intra-nuclear localisation apparent. This widespread pattern of fluoresence was largely expected, because both molecules have been shown to diffuse freely across biological membranes, and thus, penetrate diverse regions of living cells (Lansing-Taylor and Salmon, 1989).

Figure 5.3. Fluoresence Detection of 'Free' FITC Label Associated with A431 Cells. (Magnification × 50, Ilford FP4 black & white film).

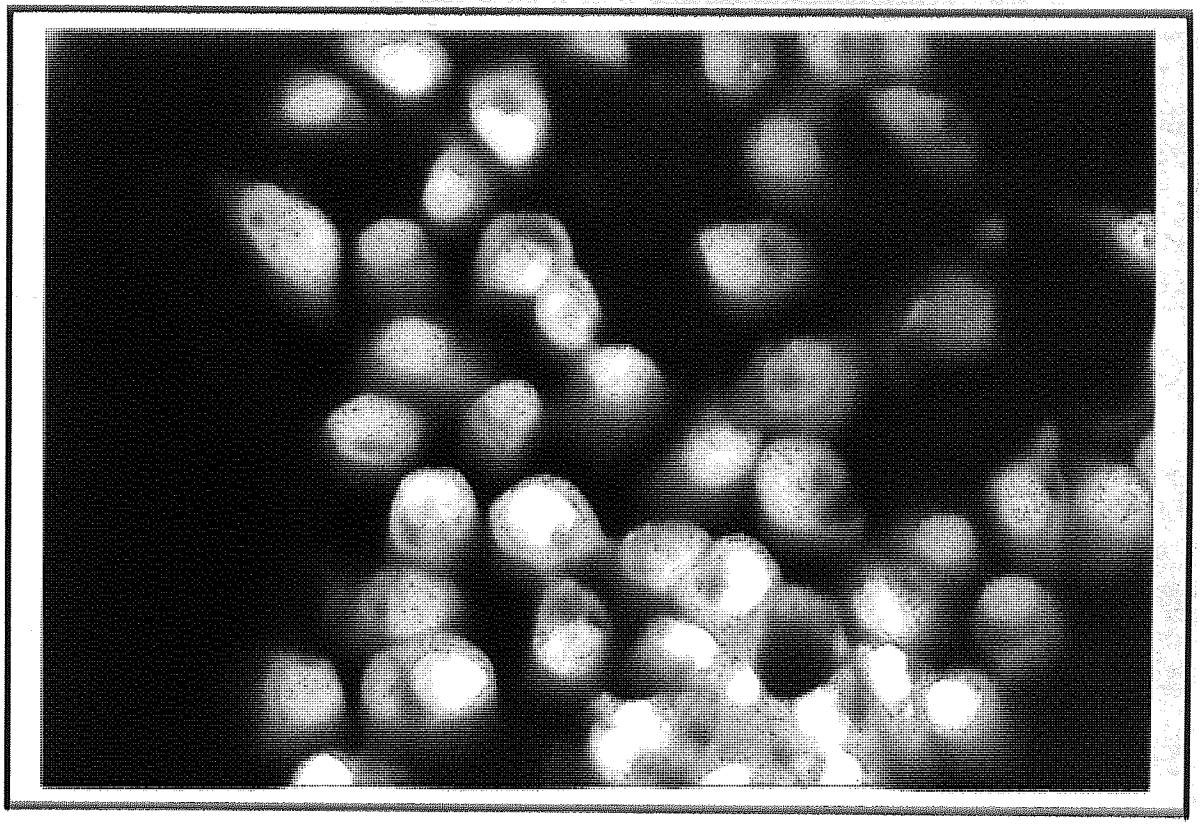

By contrast, the cellular distribution of the FITC-labelled ribozyme was distinctly different to that of the free fluorescent labels (See Figure 5.4). The intensity of cell associated fluoresence appeared to be considerably lower than that observed with the free fluorescent labels, although actual intensity levels were not directly measured. The majority of fluoresence was localised at the periphery of cells, probably within the cytoplasm. In addition, the punctate pattern of distribution observed would be consistent with a predominantly endosomal localisation of the FITC-ribozyme.

The clear differences in cellular localisation patterns of the FITC-ribozyme and free fluorophores indicated that the FITC label remained attached to the ribozyme in the intracellular environment for at least 4 hours and could, therefore, be used as a specific label for fluoresence localisation studies. Although the actual integrity of the fluorescent labelled ribozyme was not examined further (by PAGE for example), other studies in this report have indicated that the chimeric ribozyme (without the FITC label) can remain stable in serum-free cell supernatants (see Figure 3.22) and within the intra-cellular environment (see Figure 5.25) for the time period examined in these experiments.

Figure 5.4. Fluoresence Detection of FITC-Ribozyme Associated with A431 Cells. (Magnification × 50, Ilford FP4 black & white film).

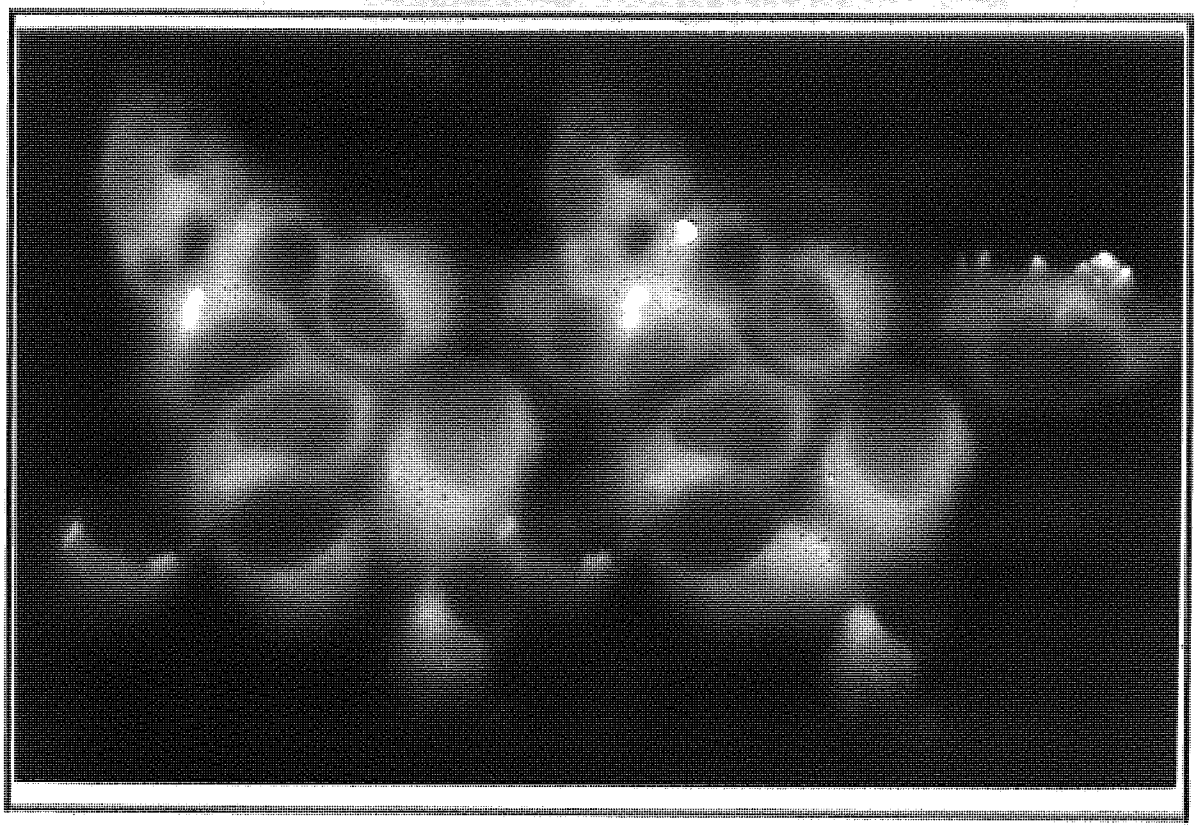

5.3.1.3 Comparative Cellular Uptake of FITC-Labelled Ribozymes, PS ODNs and PO ODNs into A431 Cells.

The cellular uptake and distribution of FITC-labelled ribozymes (5μM) was compared qualitatively with that of FITC-labelled PS ODNs (5μM) of the same nucleotide base sequence. These concentrations were within the range used in previous studies by other investigators which examined the subcellular distribution of fluorescent-labelled ODN analogues (for examples see Tonkinson and Stein, 1994, Tarrason *et al*, 1995, Shoji *et al* 1991 & 1996). Studies were performed as described in section 2.8.7 using cells which were fixed with 2% v/v glutaraldehyde.

The intensity of fluoresence within cells which were incubated with FITC-ribozymes appeared to be slightly lower than that observed in cells incubated with FITC-PS ODNs, although the exact difference was not measured quantitatively. This difference was not entirely unexpected because FITC-PS ODNs have been shown to produce increased fluorescent signals relative to FITC-PO analogues, when administered to other cell lines (for example see Agrawal et al, 1992). The FITC-ribozyme used in the present studies contained mainly PO inter-nucleotide linkages (see Section 5.2.1).

Figure 5.5. Fluoresence Detection of FITC Ribozymes and ODNs in A431 Cells After 4 hours Incubation. **[A]** FITC Ribozyme (Mag. ×20), **[B]** FITC-Ribozyme (Mag ×100), **[C]** FITC-PS ODN (Mag ×20), **[D]** FITC-PS ODN (Mag × 100). (Kodak colour photographic film).

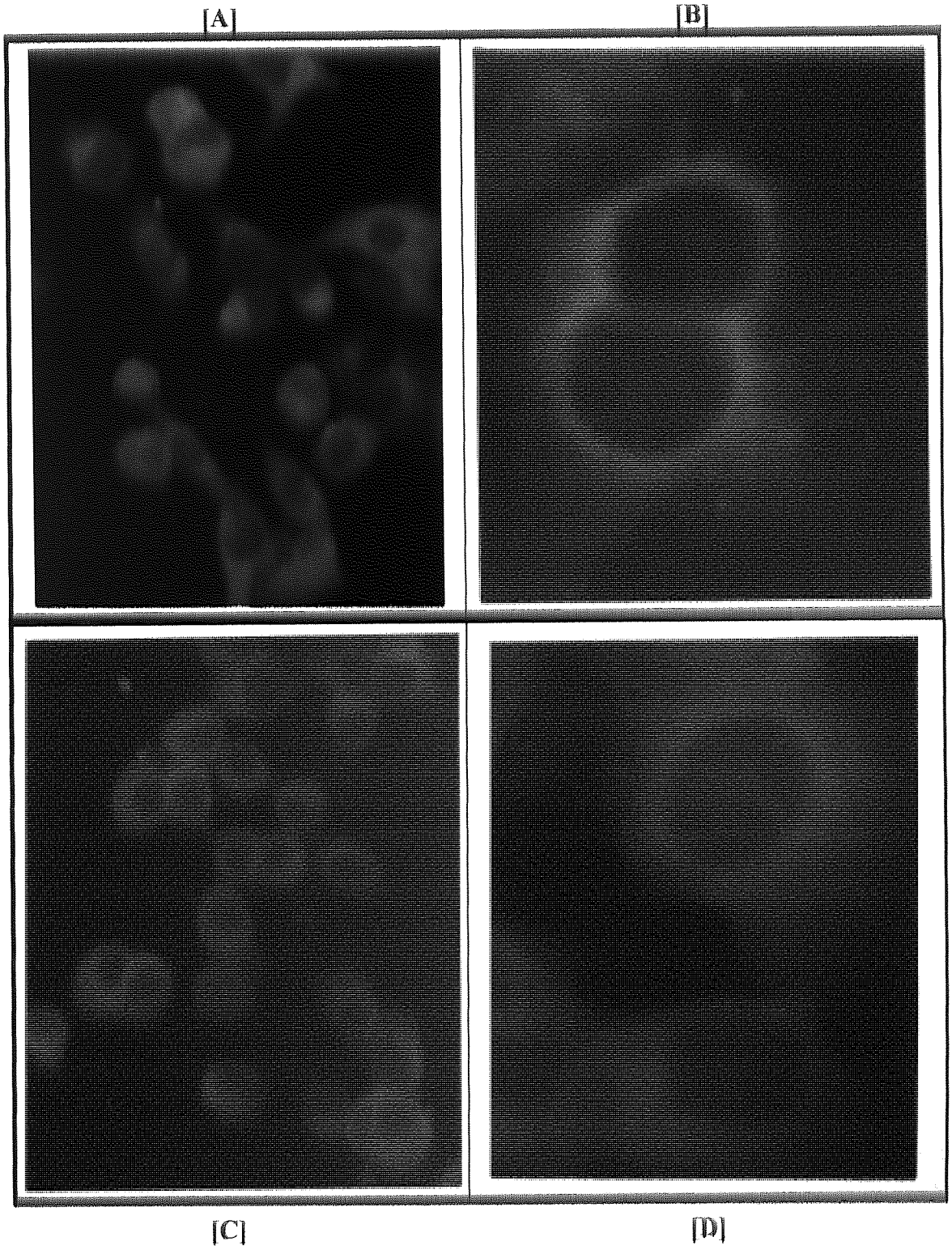

Similar patterns of subcellular localisation were observed when FITC-ribozymes or FITC-PS ODNs were incubated with cells for 1-4 hours (See Figure 5.5). In line with the observations made in previous studies (See Figure 5.4), in which cells were

viewed without chemical fixation, the fluoresence was mainly observed at the periphery of A431 cells, close to the cell membrane. This suggests that the fixation conditions did not alter the distribution of FITC-ribozymes in A431 cells. At higher magnification a punctate pattern of distribution was observed (See Figure 5.5 (B & D)) with both the FITC-ribozyme and FITC PS ODNs. Similar punctate distribution patterns have been described by other workers examining the subcellular distribution of fluorescent-labelled ODNs (Wagner, 1994) and this is considered to be indicative of localisation within endosomal / lysosomal vesicles. (Rojanasakul, 1996).

5.3.1.4. Subcellular Localisation of FITC-Labelled Ribozymes and PS ODNs Compared with Fluorescent Endosomal Markers in A431 Cells.

Fluorescently labelled dextrans are known to reside in endocytic vesicles of various types following cell entry (Berlin and Oliver, 1980). In this study, A431 cells were incubated with rhodamine-labelled dextrans and also FITC-labelled ribozymes or PS ODNs, in order to ascertain their relative subcellular localisation's. Experiments were performed as described in section 2.8.7 but cells were not exposed to chemical fixatives prior to microscopy.

The excitation and emission spectra of fluorescein and rhodamine overlap to a small degree (Lansing-Taylor and Salmon, 1989), therefore, narrow band blocking filters were required (See Section 2.8.7.3) to differentiate between the two fluorophores during detection by microscopy. As a control procedure, some cells were incubated with only RITC-dextran, or only FITC-ribozyme (i.e. with only one type of fluorophore). These cells were viewed using both types of blocking filter. No overlapping fluorescence was observed from either fluorophore when they were viewed using filters designed to block emissions at their particular wavelength (i.e. Emissions from either fluorophore were only observed when the 'correct' narrow band blocking filter was used). This indicated that the narrow band filters would permit each fluorophore to be detected separately within cells.

When A431 cells were incubated with either FITC-ribozymes or FITC-PS ODNs, for 4 hours at 37°C, similar patterns of subcellular distribution were observed (See Figure 5.6[A] and Figure 5.7[A]). Both of the FITC-labelled nucleotides exhibited a punctate pattern of intracellular localisation, similar to that observed by other workers examining the localisation of fluorescent-labelled antisense ODNs in other cell lines (Agrawal *et al*, 1992, Stein *et al*, 1994, Wagner, 1994).

Figure 5.6. Fluoresence Detection of FITC-Ribozyme and RITC-dextran in A431 Cells After 4 hours Incubation at 37°C. **[A]** FITC-Ribozyme Photographed Using a 510nm blocking filter (Mag. ×50) and **[B]** RITC-dextran, photographed using a 590nm filter (Mag. ×50).

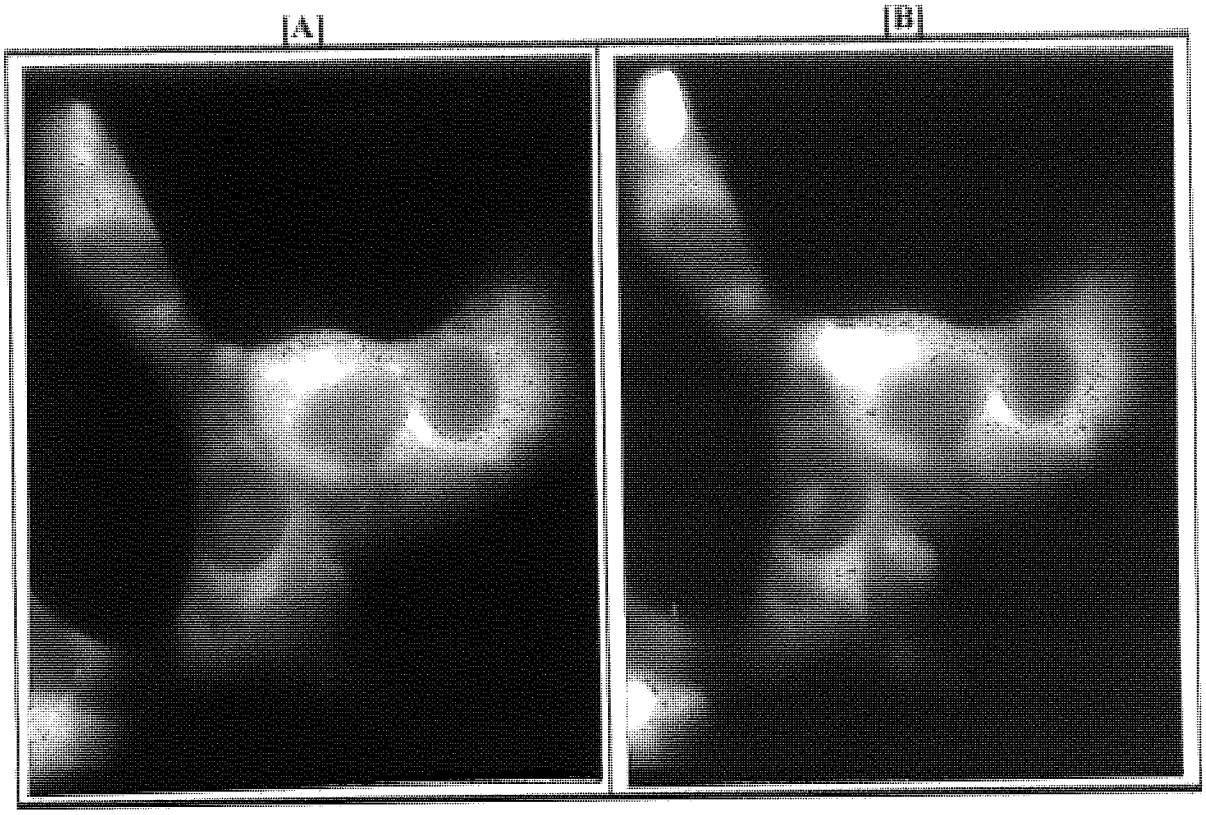

When the subcellular localisation of rhodamine-dextran was compared with that of the FITC-labelled ribozyme and PS ODN, in the same cells, a considerable degree of co-localisation was observed (See Figures 5.6[B] and Figure 5.7[B]). This indicated that the majority of FITC-labelled ribozymes, FITC-PS ODNs and RITC-dextran were present within similar intracellular regions following cell entry and / or binding.

The punctate pattern of subcellular distribution, combined with the considerable degree of co-localisation with an endosomal marker (RITC-dextran), suggested that ribozymes were mainly sequestered into endosomal vesicles following cell entry. However, these observations alone, provided little further information regarding the exact nature of the cellular uptake mechanism, other than that it appeared to be mediated by an endocytic process. Molecules entering cells by either FPE, AE or RME would become localised within some type of endosomal vesicle following cell entry. Hence, similar patterns of subcellular localisation would be expected if any of these mechanisms were involved in the cellular uptake of ribozymes. However, the mechanistic studies described in Chapter 4 indicated that ribozymes and PS ODNs were unlikely to enter cells via FPE alone. Furthermore, the fluorescent studies described here, and the mechanistic studies described in Chapter 4, demonstrated

several similarities in the cellular association characteristics and subcellular distribution of ribozymes and PS ODNs in A431 cells. Since it is widely considered that PS ODNs enter cells via a process of AE and / or RME (Rojanasakul, 1996), these similarities suggest that ribozymes also enter cells by AE or RME.

Figure 5.7. Fluoresence Detection of FITC-PS ODN and RITC-dextran in A431 Cells After 4 hours Incubation at 37°C. **[A]** FITC-PS ODN Photographed Using a 510nm blocking filter (Mag. ×25) and **[B]** RITC-dextran, photographed using a 590nm filter (Mag. ×25).

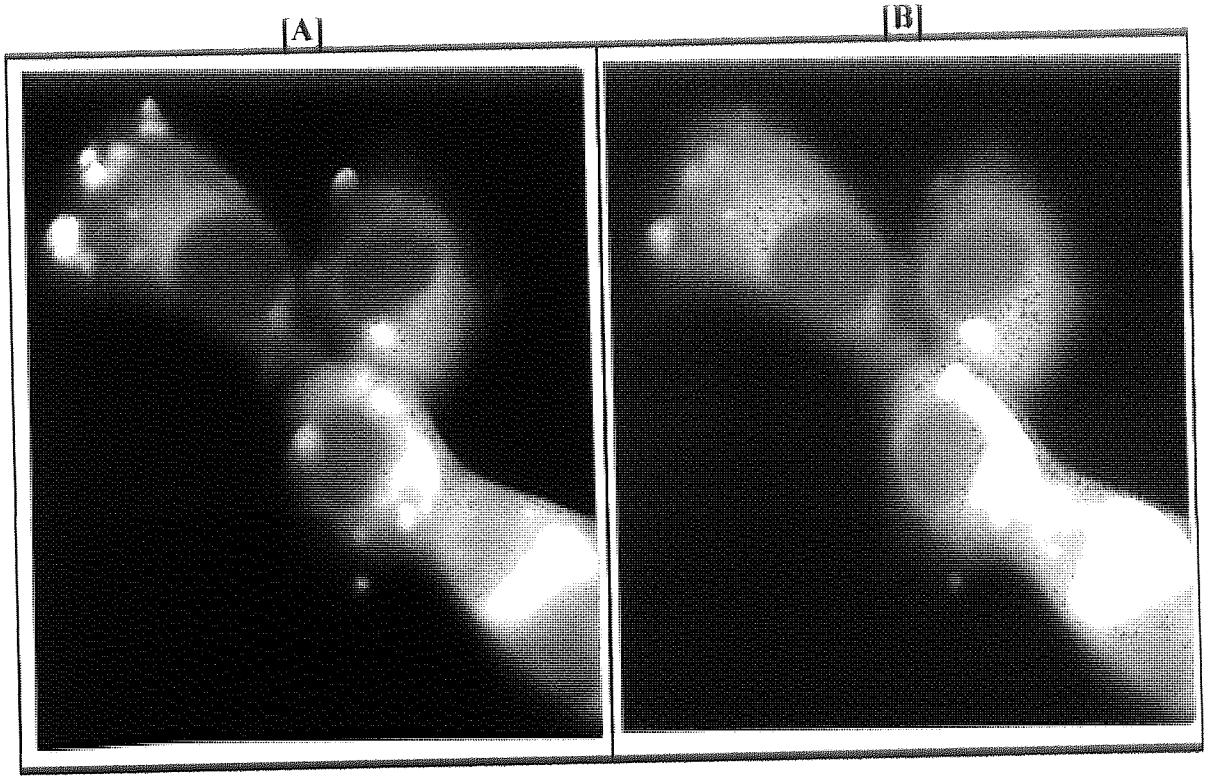

However, if ribozymes and PS ODNs share similar endocytic uptake mechanisms, they would also share similar obstacles in reaching their intracellular targets following internalisation. Endosomes are membrane bound structures which become acidified and often accumulate nucleases (Hopkins, 1985, Smythe and Warren, 1991, Akhtar *et al*, 1995). Therefore, ribozymes, like antisense ODNs, must exit the harsh environment of the endosome in order to exert a biological effect in the nucleus or cytoplasm. Potential mechanisms for the release of ODNs and other molecules from endosomal vesicles have been discussed (Akhtar and Juliano, 1992), however, the fate of ODNs and ribozymes following escape from endosomes remains a matter of debate. Therefore, ultrastructural studies, using the higher resolution technique of electron microscopy, were performed in an attempt shed further light on the fate of ribozymes and PS ODNs following cell entry.

5.3.2. Ultrastructural Studies.

5.3.2.1 Electron Microscopy

Eukaryotic cells vary in shape and structure and are differentiated according to their specific functions in various tissues and organs (Bubel and Fitzsimmons, 1989). Therefore, to gain an understanding of the particular ultrastructural features of the A431 cell line, cells were examined by electron microscopy following exposure to high levels of chemical fixation. Identical staining techniques were used to those which would be utilised in subsequent immunocytochemical studies. Therefore, the identification of organelles and structural features within the highly preserved cells would be a useful aid for locating similar structures in less well preserved cells, exposed to much lower levels of chemical fixation.

Figure 5.8 Electron Micrograph of an A431 Cell Preserved Using a Standard Fixation Protocol, Showing Several Ultrastructural Features. (×15,000, plasma membrane (pm), cell nucleus (nu), nuclear envelope (ne), mitochondria (mt), cytoplasm (cy), endoplasmic reticulum (er), small arrows indicate structures consistent with endosomal / pinosomal vesicles)). [Bar = 500nm].

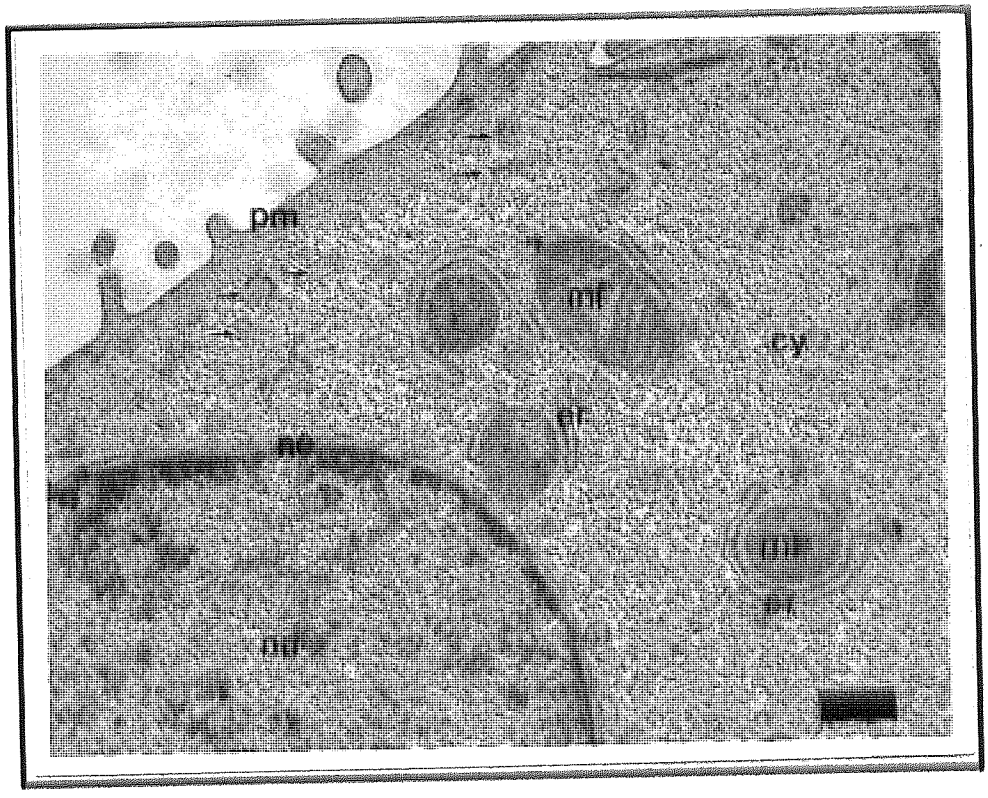

Intracellular structures were identified by comparison with reference manuals (Baker, 1966, Bubel and Fitzsimmons, 1989, Alberts *et al*, 1989, Griffiths *et al*, 1993) and

published ultrastructural data from studies with A431 cells (Parton, 1994). The assistance of Leslie Tompkins (Electron Microscopist, Birmingham University, UK) is also gratefully acknowledged.

Ultrastructural features were clearly visible within cells even at relatively low magnification (See Figures 5.8 and 5.9). For example, the cell nuclei and mitochondria were particularly well contrasted with respect to other organelles. Both plasma and nuclear membranes remained intact during preparation and were clearly defined (See Figure 5.8). Certain structures considered to be 'delicate' with respect to their preservation during the dehydration process (Mercer and Birbeck, 1976) were also visible. For example, the golgi complex and endoplasmic reticulum were well preserved (See Figure 5.9). However, these cells, treated with high levels of chemical fixatives, probably demonstrated the optimum level of ultrastructural preservation which could be achieved.

Figure 5.9. Electron Micrograph of A431 Cell, Showing Ultrastructural Features in the Proximity of the Cell Nucleus. (×25,000, cell nucleus (Nu), nuclear envelope (Ne), mitochondria (mt), golgi complex (gc), endoplasmic reticulum (er)). [Bar = 200nm].

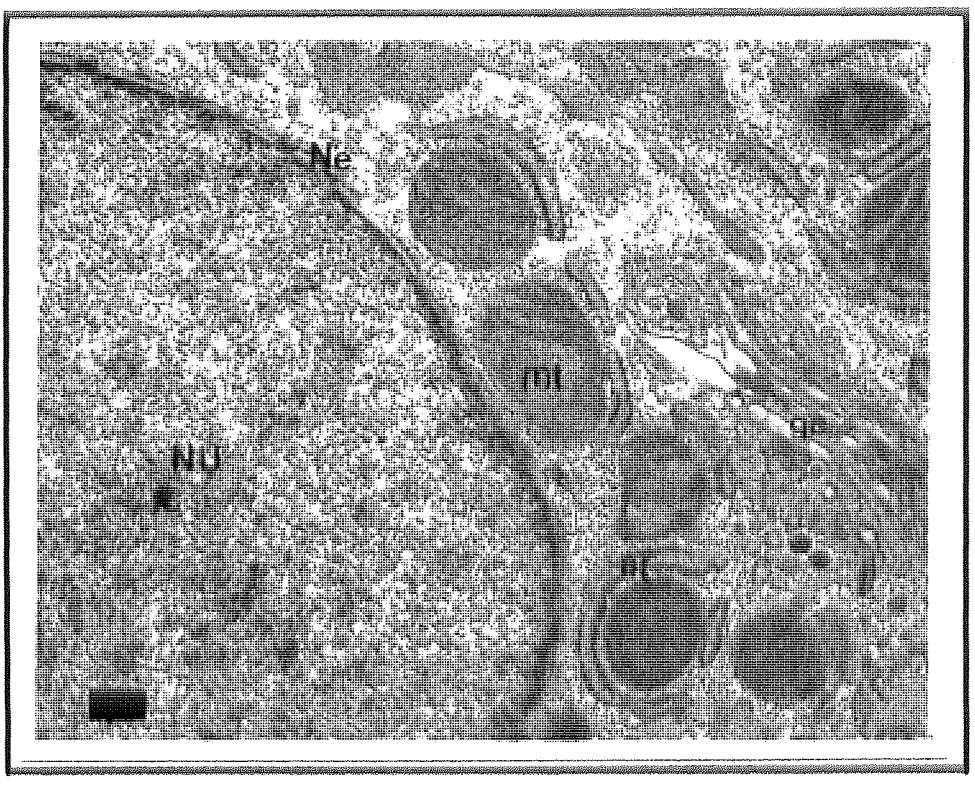

Figure 5.10. Electron Micrograph of an A431 Cell Showing Mitochondria. (×40,000, Mitochondria (mt)).[Bar = 200nm].

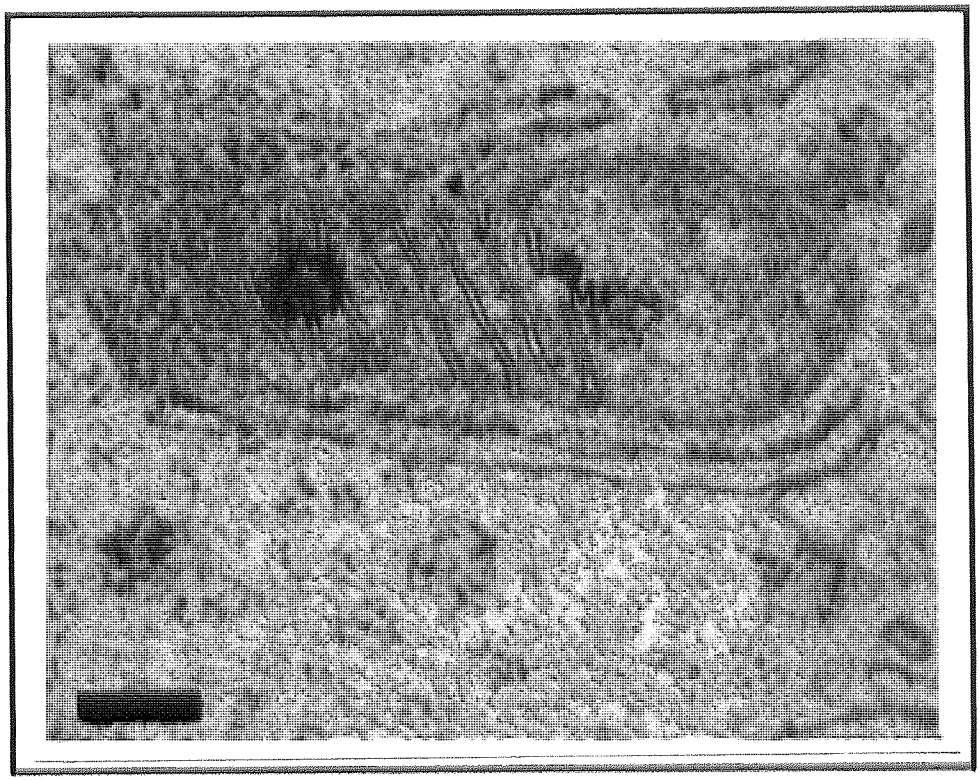

Figure 5.11. Electron Micrograph of an A431 Cell Showing Multi-Vesicular Bodies (mvb) within the Cytoplasm. (×40,000) [Bar = 200nm].

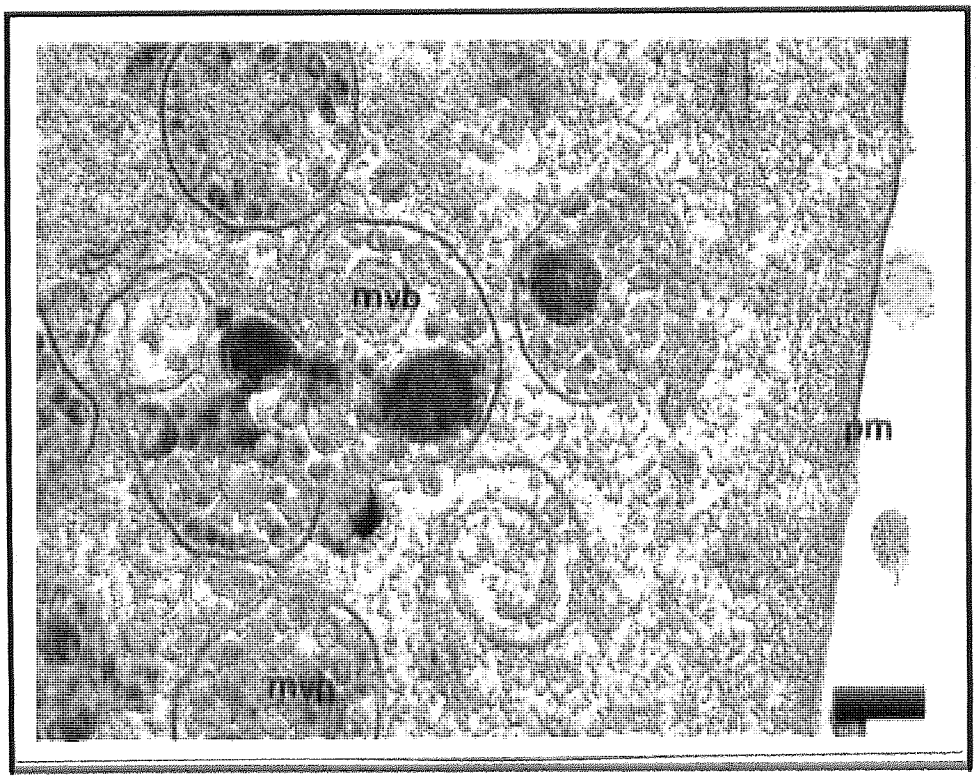

At slightly higher magnification more detailed images of the mitochondria (See Figure 5.10) were observed with clearly visible cristae. In general, the mitochondria appeared to accumulate preferentially around the nucleus and were associated with the endoplasmic reticulum. However, some mitochondria were visible in the peripheral cytoplasm. The size of the mitochondria was consistent with those recorded in other cell lines, where typical dimensions of approximately 500nm × 2000nm have been recorded (Baker, 1966, Alberts *et al*, 1989).

In addition, more detailed images of multi-vesicular bodies were obtained (See Figure 5.11) at higher magnification. These structures were particularly abundant in the A431 vulval cell line and were similar in appearance to those observed in rat ovarian cells by other workers (Bubel and Fitzsimmons, 1989). Multi-vesicular bodies (mvb's), also referred to as secondary lysosomes, are formed when primary lysosomes fuse with endosomes or phagosomes. Mvb's are membrane bound vesicles, thought to be involved in the digestion and disposal of unwanted cytoplasmic components and foreign particles (Bubel and Fitzsimmons, 1989).

Figure 5.12. Electron Micrograph of an A431 Cell Showing an Endosomal-Type Vesicle within the Cytoplasm (cy) (The large arrow indicates the endosomal / pinosomal vesicle (×60,000) [Bar=100nm]

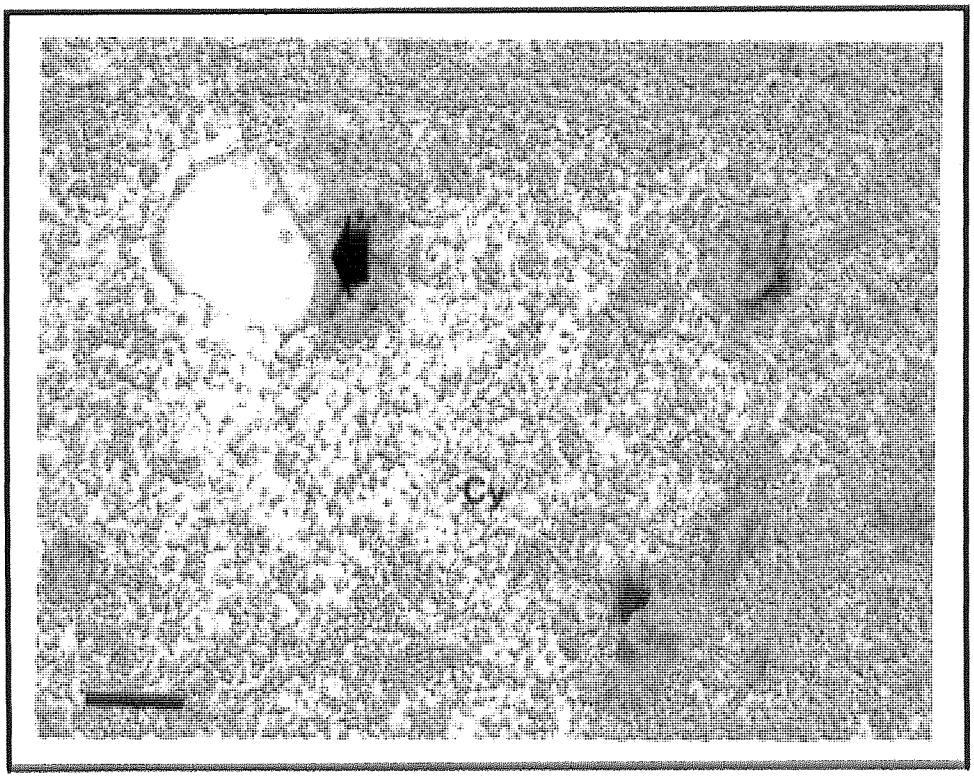

Endosomal vesicles (pinosomes) appeared to be less abundant than multi-vesicular bodies within the A431 cells, although this could be because they were less well preserved during the dehydration and embedding protocol. Endosomes forming from invaginations of the plasma membrane usually range in size from approximately 50nm to 150nm (Hopkins, 1985), although they can become enlarged by fusing together (Bubel and Fitzsimmons, 1989). Endosomes are membrane bound and can be coated with proteins such as clathirin, or uncoated (Hopkins, 1985).

In several studies endosomes have been identified on electron micrographs as clear vesicles close to the cell surface (Beltinger *et al*, 1995) in contrast to other vesicles such as primary lysosomes, which are generally described as dark-staining, electron dense structures. (Tarrason *et al*, 1995, Beltinger *et al*, 1995). Cytoplasmic vesicles consistent with those described in the above studies were observed within A431 cells (For example Figure 5.12 demonstrates an endosome which was located approximately 800nm from the cell membrane).

5.3.2.2 Immunocytochemical Studies of Intracellular Trafficking.

Considerably lower levels of chemical fixation were used to prepare cells for immunocytochemical studies (See Section 5.2.4.2). Hence, the preservation of cellular morphology was somewhat compromised, in order to permit immuno-labelling of the biotin antigen used. Electron micrographs obtained in these studies were less well contrasted in comparison to those depicted in Section 5.3.2.1 and generally higher levels of magnification were required in order to identify gold particles within cells.

5.3.2.2.1. Controls for Immunocytochemical Experiments.

Initially, A431 cells were processed for preliminary labelling studies to determine the optimal level of dilution for the primary antibody:gold conjugate. At dilution factors of 1 in 40 and above, no gold particles were evident on the Formvar coating of the nickel grids and only occasional gold particles, at constant frequency, were visible within cell sections. Indicating that the blocking / washing procedures were adequate in the removal of excess antibody:gold conjugate when used at this concentration. However, at lower dilution factors (1 in 20 and below) increasing numbers of gold particles were evident both within cell sections and on the Formvar coating of the nickel grids. This labelling was almost certainly non-specific, therefore, in subsequent immunochemical studies the gold conjugate was used at a minimum dilution of 1 in 60 (See section 5.2.4.5) to ensure labelling specificity.

A431 cells incubated either with 10μM *d*-biotin (See section 5.2.4.1), or alone, were processed and immuno-labelled as described in Section 5.2.4. Cells incubated with *d*-biotin served as a control of labelling specificity of biotinylated ribozymes and PS ODNs, as opposed to endogenous or added biotin. Similar controls of labelling specificity have been used by other workers in assessing the trafficking of biotinylated nucleotides (Beltinger *et al*, 1995).

In cells incubated in the absence of any biotinylated agent, very few, or more often, no gold particles were detected within cell sections after extensive searching. Any gold particles present appeared to be randomly distributed and did not preferentially localise at any intracellular location. For example, no particles were observed within clear vesicles, consistent with endosomes (See Figure 5.13).

Figure 5.13. Electron Micrograph of an Immuno Gold Labelled A431 Cell Incubated in the Absence of Exogenous Biotin. (×75,000, Clear vesicles consistent with endosomes were evident, although no gold particles were observed within this cell). [Bar =100nm].

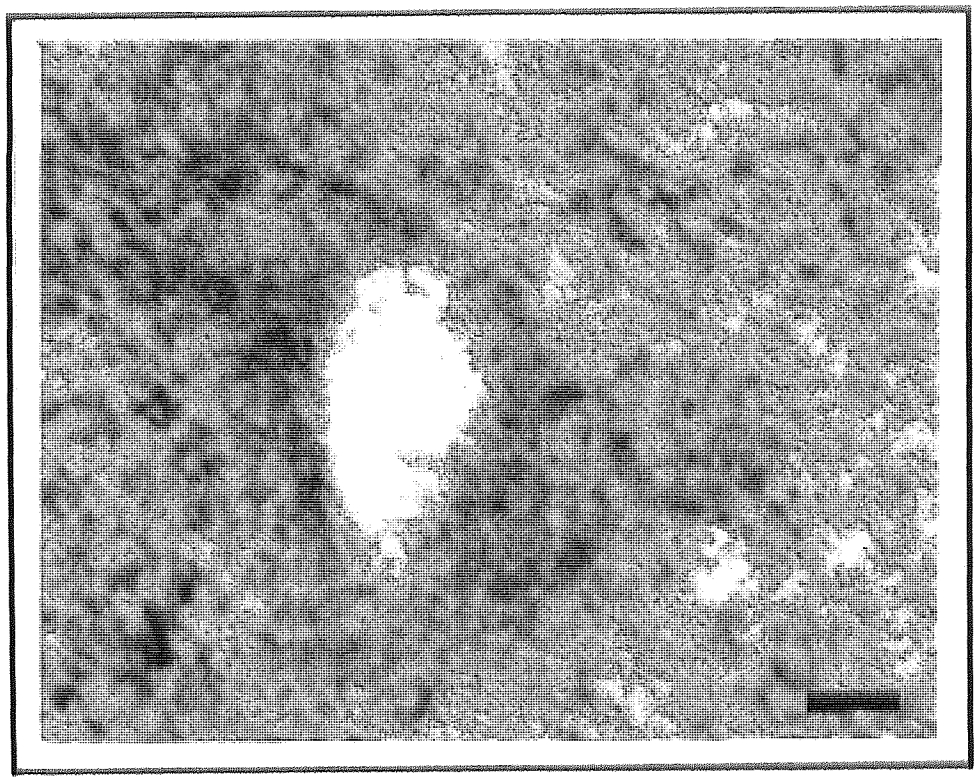

In *d*-biotin treated cells, levels of immunogold labelling appeared to be marginally higher, although typically less than 5 gold particles were counted in each cell. Individual gold particles were identified within the cytoplasm and also within both clear and electron dense vesicular structures (See Figures 5.14 and 5.15). However,

the gold particles did not appear to preferentially localise at any intracellular location and the overall distribution of gold particles appeared to be random.

Overall, observations of a large number of cell sections indicated extremely low levels of immuno-labelling of both endogenous biotin and exogenously delivered *d*-biotin within the A431 cells. This could be considered surprising, since biotin is an essential co-enzyme involved in key biosynthetic reactions, and is often widely distributed throughout cells (Sweetman and Nyhan, 1986, Alberts *et al*, 1989). However, biotin is known to occur mainly in a protein bound form within cells (Griffiths *et al*, 1993), and therefore, in its 'free' form it could be inaccessible to binding by the antibody:gold conjugate. Although endogenous biotin is present in most tissues, it only occurs at relatively high concentrations within hepatic, renal and pancreatic cell types (Griffiths *et al*, 1993). Therefore, biotin may only be present at low concentrations within A431 (vulval) cells, which could also explain the low levels of immuno-labelling observed.

Figure 5.14. Electron Micrograph of an Immuno-Gold Labelled A431 Cell Incubated with 10μM *d*-Biotin for 4 hours. (×100,000, The small arrow indicates a single gold particle within the cytoplasm (cy) approximately 400nm from the nucleus (Nu)) [Bar =100nm].

Radiolabelled biotin has been shown to enter cultured hepatic cells via a receptor mediated type process (Said *et al*, 1994). However, in ultrastructural studies the tagging of biotin routinely involves an extracellular labelling protocol (Griffiths *et al*,

1993). This involves initial binding of 'free' biotin to the cell surface at low temperatures (0-4°C), followed by tagging with a streptavidin:gold conjugate. The temperature is then increased to permit the cellular uptake of the pre-labelled biotin / streptavidin complex. The trafficking of the 'pre-labelled' molecule can then be monitored by electron microscopy (Busch *et al*, 1989). (i.e. The biotin molecule requires labelling prior to cell entry for efficient detection by immunochemistry).

Other workers assessing the trafficking of biotinylated antisense ODNs in K562 cells have used similar controls of labelling specificity to those selected here (Beltinger *et al*, 1995). K562 cells incubated in the absence of biotinylated ODNs showed few, randomly distributed gold particles when labelled with a streptavidin gold conjugate. By comparison, significantly increased levels of gold labelling were observed in cells incubated with biotinylated-ODNs (Beltinger *et al*, 1995). Similarly, the control experiments performed in the present study, indicated that both endogenous and exogenously delivered 'free' biotin were not detected at significant levels in A431 cells, using the method described in section 5.2.4.5. A significantly increased level of immuno-gold labelling in cells incubated with either biotinylated ribozymes or PS ODNs could, therefore, be a specific indicator for the presence of these molecules within A431 cell sections.

5.3.2.2.2. Immunocytochemical Localisation of Biotinylated Ribozymes within A431 Cells.

In cells incubated in the presence of biotinylated ribozymes, the number of gold particles which remained within cells following the immuno-labelling / washing protocols was considerably increased, when compared with particle counts recorded in the control samples: Typically over 50 gold particles per cell were observed, equivalent to more than a 10-fold (minimum) increase in the frequency of immuno-gold labelling detection compared with the controls for labelling specificity (See section 5.3.2.2.1). No particles were seen on other areas of the nickel grids, such as the Formvar coating, which gave a further indication that washing protocols were adequate in the removal of any non-bound antibody:gold conjugate.

Extensive searches of cell ultrastructure using the electron microscope (see section 5.2.4.6), indicated that a large proportion of the gold particles were localised in close proximity to clear vesicles, thought to be endosomes or pinosomes (see Beltinger *et al*, 1995) (See Figures 5.15). Occasionally, these clear vesicles were observed close to the plasma membrane (See Figure 5.16), but more commonly, they were widely distributed throughout the cytoplasm (Figure 5.15).

Figure 5.15. Electron Micrograph Showing The Apparent Localisation of biotinylated-ribozymes at the periphery of clear vesicles consistent with endosomes (En) (indicated by arrowheads). Gold particles were also visualised within electron dense regions consistent with lysosomes (indicated by larger arrows). (×75,000, [Bar =100nm].

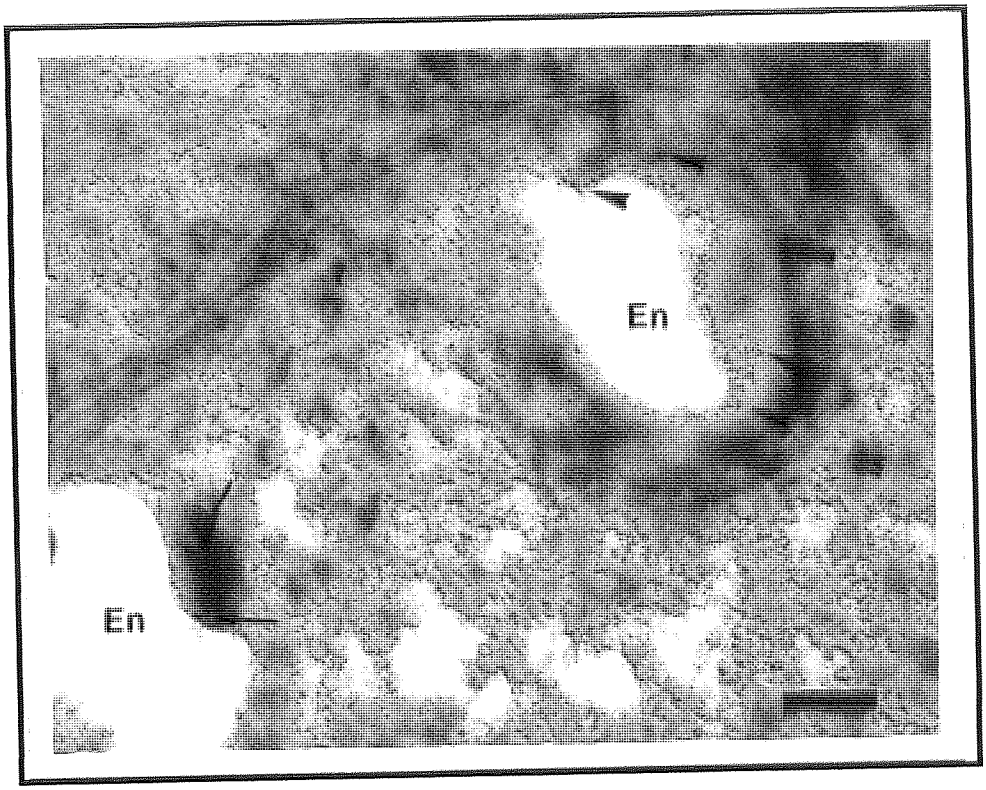

Gold particles were also visualised within electron dense regions, which were often in close proximity to the endosomal vesicles (See Figure 5.15). Such regions would be consistent with lysosomal-type vesicles, also observed by other workers (Tarrason *et al*, 1995, Beltinger *et al*, 1995). In general, when localised within clear vesicles, biotinylated-ribozymes appeared to be distributed towards the periphery of these structures, which could perhaps indicate that they were associated with endosomal membranes (Fig 5.15 and 5.16).

Figure 5.16. Electron Micrograph Showing Apparent Localisation of biotinylated-ribozymes (indicated by small arrows) at the periphery of clear vesicles close to the plasma membrane (pm).(×100,000, (cy) cytoplasm, (Ecf) Extracellular area / Formvar. [Bar =50nm].

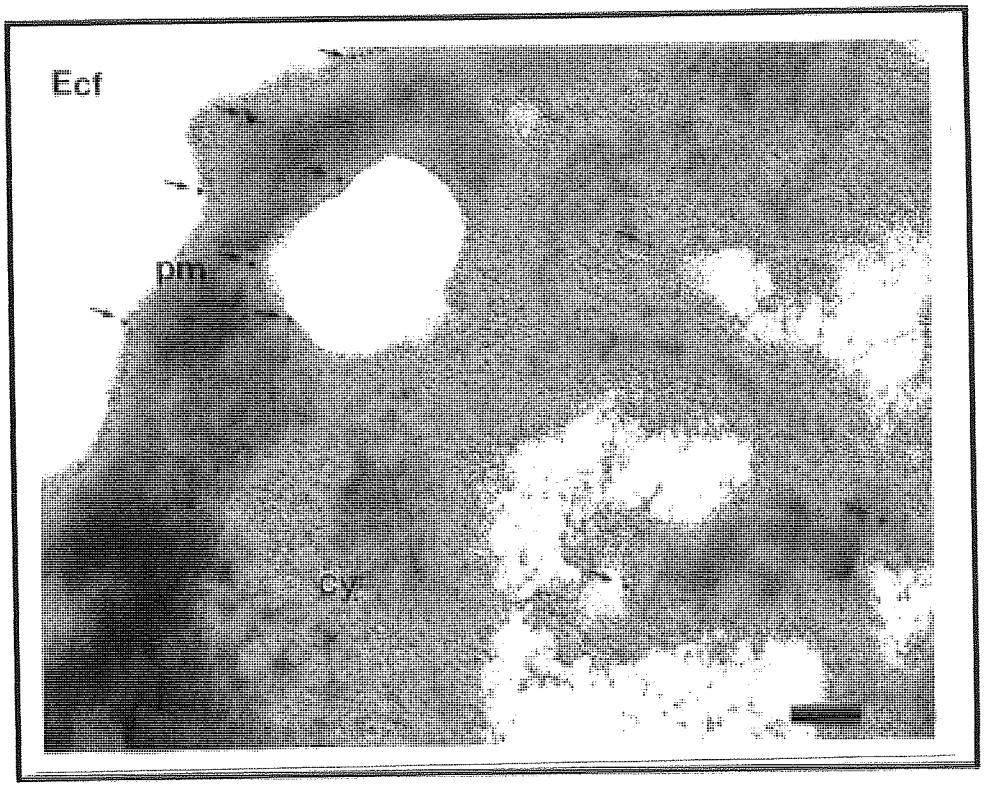

Again multi-vesicular bodies (mvb's) appeared to be well preserved within cell sections despite the relatively low concentrations of chemical fixative used here (See Figure 5.11 for comparison with highly fixed cells). Biotinylated ribozymes were commonly present within these structures (See Figure 5.17). Mvb's, or secondary lysosomes as they are also known, are formed when primary lysosomes fuse with endosomes or phagosomes (Bubel and Fitzsimmons, 1989). Therefore, the identification of gold particles within these vesicles provided further evidence to suggest that ribozymes had been present within endosomal or lysosomal vesicles at some stage following cell entry.

Generally, it was estimated that around 70% of all gold particles observed within cells appeared to be localised at close proximity to some type of vesicular structure within the cytoplasm. Similar patterns of localisation have been noted in other studies where trafficking of antisense ODNs has been examined (Beltinger *et al*, 1995, Tarrason *et al*, 1995). However, biotinylated-ribozymes were occasionally visualised both free within the cytoplasm and within other organelles:

Figure 5.17. Electron Micrograph Showing Localisation of biotinylated-ribozymes within a multi-vesicular body (mvb). These vesicles were distributed throughout the cytoplasm (cy) (×75,000). [Bar=100nm].

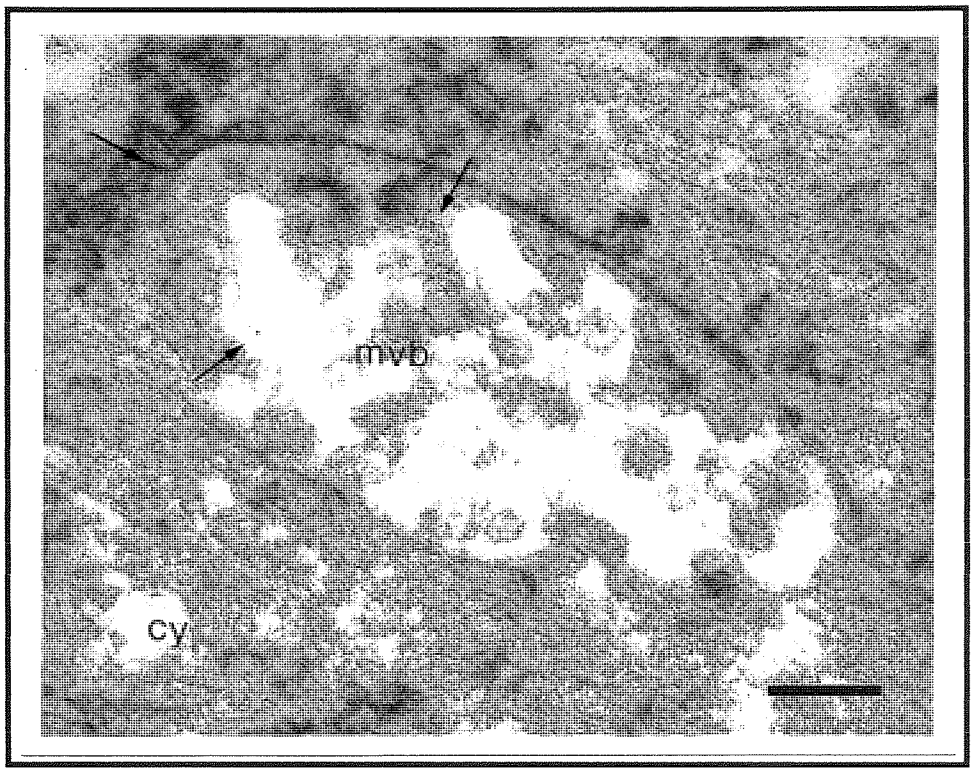

Figure 5.18. Electron Micrograph Demonstrating Penetration of Biotinylated-Ribozymes to the Cell Nucleus (Nu), as Indicated by small arrow heads. (×60,000. Gold particles were also evident close to the nuclear membrane (Nm) indicated by larger arrows). [Bar=100nm].

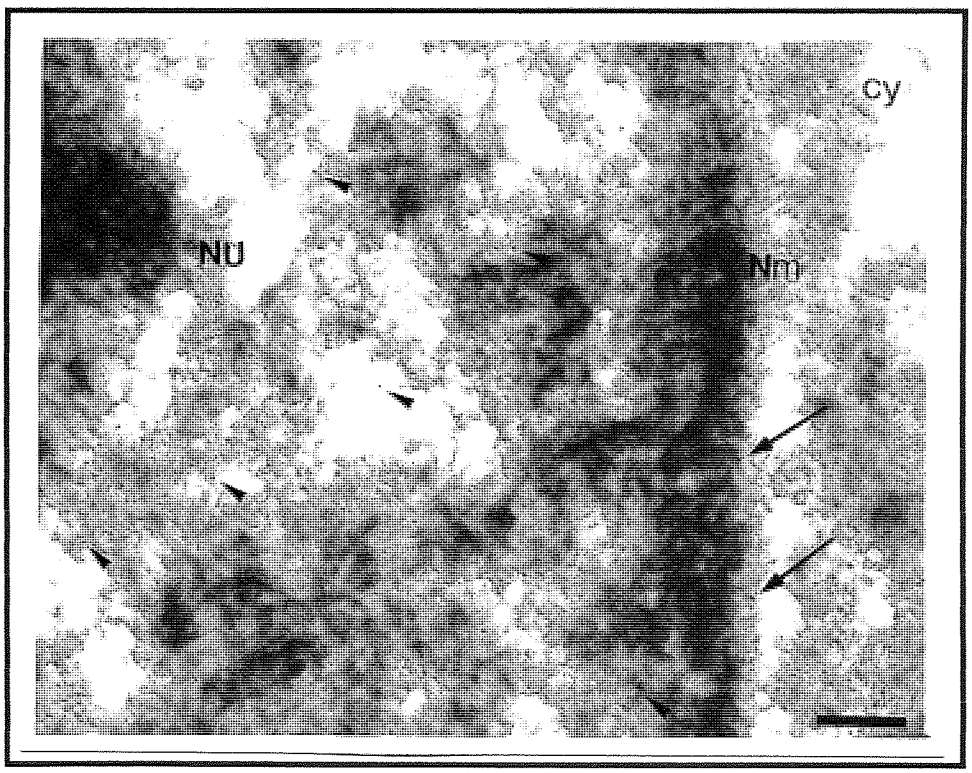

Frequently small numbers of gold particles (typically around 10 particles per cell) could be observed actually within cell nuclei. Alternatively, they were present in areas close to the nuclear membrane / envelope (See Figure 5.18). However, the level of morphological preservation in these cell sections was not of sufficient quality to permit structures such as the nuclear pores, or the nucleolus, to be specifically identified. Nevertheless, it would appear that at least some proportion of internalised ribozymes were able to penetrate the nucleus. The ability of biotinylated-PS ODNs in reaching the nucleus has been noted in K562 cells (Beltinger *et al*, 1995), where PS ODNs appeared to be localised to the euchromatin / heterochromatin interface. Penetration of the nucleus by PS ODNs has also been noted in the present study, in A431 cells (See Figure 5.22).

Interestingly, an extensive examination of the ultrastructural data revealed the presence of a small number of biotinylated-ribozymes within mitochondria (See Figure 5.19). Gold particles were not frequently observed within the mitochondria and they did not appear to be a significant site of intracellular localisation. Nevertheless, in certain cell sections, low numbers of gold particles (usually less than 5 particles per cell) were identified within these structures. Possibly indicating some penetration of these organelles by the biotinylated-ribozymes.

Figure 5.19. Electron Micrograph Demonstrating Low Levels of Biotinylated-Ribozymes Detected Within the Mitochondria (Mit). (×100,000. Gold particles indicated by arrows, (cy; cytoplasm)). [Bar=50nm].

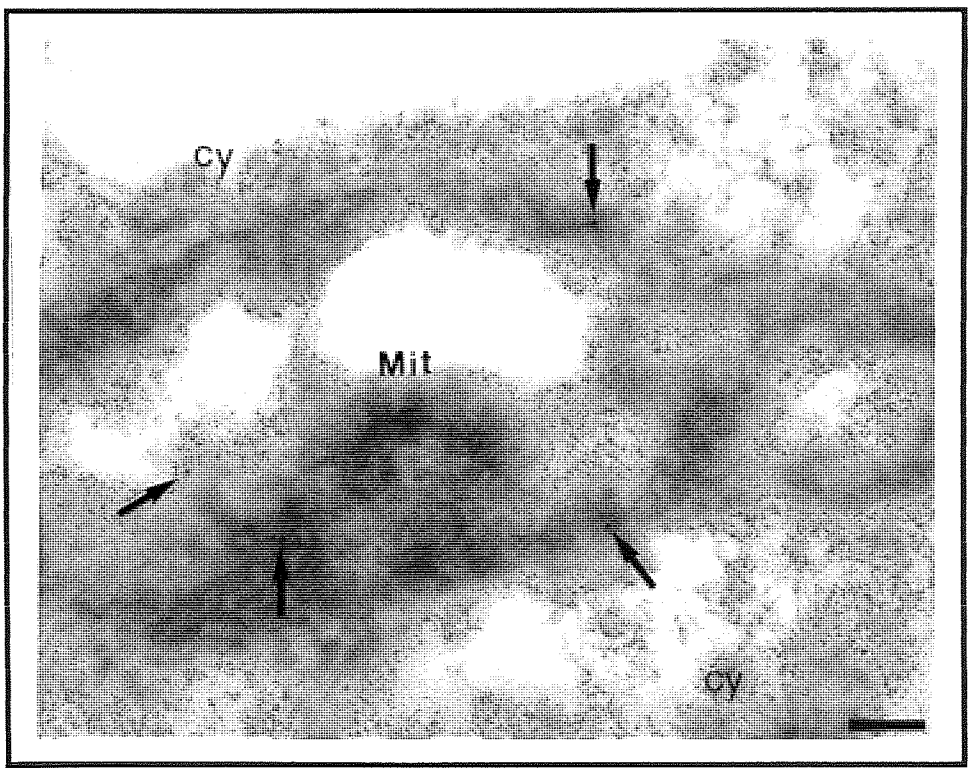

This finding has not been previously reported in ultrastructural studies examining the localisation of antisense ODNs (Beltinger *et al*, 1995, Tarrason *et al*, 1995), where no mention was made of observations in the mitochondria. The mitochondria contain their own genomic DNA and machinery for protein synthesis, however, they are also known to import specific proteins and phospholipids from the cytosol (for a more detailed description of these uptake processes see Alberts *et al*, 1989). Therefore, since ribozymes have been demonstrated to bind to cell surface proteins (see Section 4.3.9), it is possible that they could also bind to specific proteins, or even phospholipids, which are imported by the mitochondria. However, further studies are required to confirm this possibility.

The morphological preservation of the golgi complex within cells processed for immuno-studies, was not of the quality seen in cells exposed to higher levels of chemical fixation (See Figure 5.9). However, structures consistent with golgi were observed in some cell sections in areas around the nucleus (See Figure 5.19). The golgi usually presents as a series of layered cisternae on an electron micrograph, which appear as flattened sacs, often with secretory vesicles either attached or situated close to their margins (Bubel and Fitzsimmons, 1989).

Figure 5.20. Electron Micrograph Indicating the Localisation of Biotinylated-Ribozymes to Structures Consistent with the golgi complex (Gc). (×25,000. Gold particles are indicated by arrowheads. Vesicles (V) were situated close to the cisternae of the golgi) [Bar=200nm].

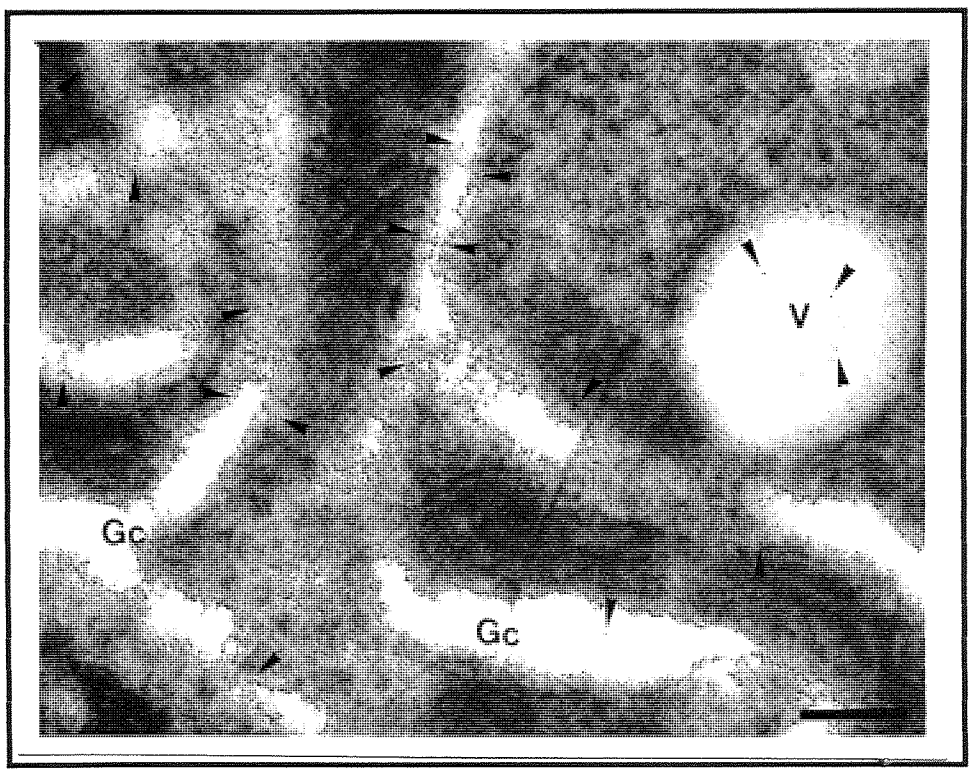

The appearance of golgi-type structures within the cell sections could potentially have been confused with that of the endoplasmic reticulum (ER). However, in previous studies where A431 morphology was well preserved, the ER appeared as two flat cisternae surrounding a mitochondria (See Figure 5.9), as they do in many other cell types (Bubel and Fitzsimmons, 1989). Therefore, the lack of associated mitochondria with these structures, the apparently multi-layered cisternae and the presence of closely situated vesicles (See Figure 5.20) implied that these structures were consistent with the remnants of the golgi complex. In most cell sections where the golgi complex could be identified, gold particles were observed, occasionally at relatively high frequency, within the cisternae and also within nearby vesicles. Figure 5.20 demonstrates a cell section with a particularly high degree of immuno-labelling in this region.

There is evidence to suggest that following the export of secretory vesicles from the golgi to the cell membrane, some components of secretory vesicle membranes can be 'recycled' back to the golgi, probably via endosomes (Alberts *et al*, 1989). The presence of this type of recycling mechanism in A431 cells could, in theory, explain the presence of the biotinylated ribozymes within the golgi complex because ribozymes may bind to golgi components at the cell membrane and become internalised along with them. Ribozymes, bound to golgi components could then be 'recycled' back to the cell membrane in secretory vesicles, or alternatively, they could be transported to the lysosomes (Alberts *et al*, 1989).The possible involvement of 'golgi recycling' in the cellular transport of ribozymes is supported by the fact that a considerable proportion of cell-associated ribozymes appear to be exported from cells after internalisation (see Section 5.3.3). The export of ribozymes from cells could involve their exocytosis in secretory vesicles originating from the golgi. However, other studies in this report have demonstrated that ribozymes do not accumulate within cells when golgi transport is inhibited (see Section 7.3.1.2.4). This was demonstrated by pre-treating cells with monensin, which is known to inhibit the transport of secretory vesicles from the golgi to the cell membrane, causing the vesicles (and their contents) to accumulate within the cytoplasm. 'Free' ribozymes did not (significantly) accumulate within cells following monensin treatment, which would appear to cast doubt upon the direct involvement of the 'golgi' in the cellular export of ribozymes.

5.3.2.2.3. Immunocytochemical Localisation of Biotinylated-Phosphorothioate Oligodeoxynucleotides (PS ODN) in A431 Cells.

Experiments designed to assess the intracellular localisation of biotinylated PS ODNs were performed in parallel to those assessing the localisation of ribozymes.
Cells were incubated with 10μM biotinylated PS ODN, of the same chain length and nucleotide base sequence as the ribozyme used in parallel studies (Section 5.2).
In cells incubated in the presence of biotinylated PS ODNs, the level of immuno-gold labelling was considerably increased compared with particle counts recorded in the control samples (See section 5.3.2.2.1): Typically, over 50 gold particles per cell were counted indicating the presence of PS ODNs and considerably higher levels of labelling observed in some cell sections. Cellular penetration of PS ODNs has been specifically confirmed in previous ultra-structural studies (Zamecnik *et al*, 1994, Beltinger *et al* 1995, Tarrason *et al*, 1995).

Figure 5.21. Electron Micrograph Showing The Apparent Localisation of biotinylated-PS ODN within clear vesicles consistent with endosomes / pinosomes (×100,000 Arrowheads indicate the position of immuno-gold particles). [Bar =50nm].

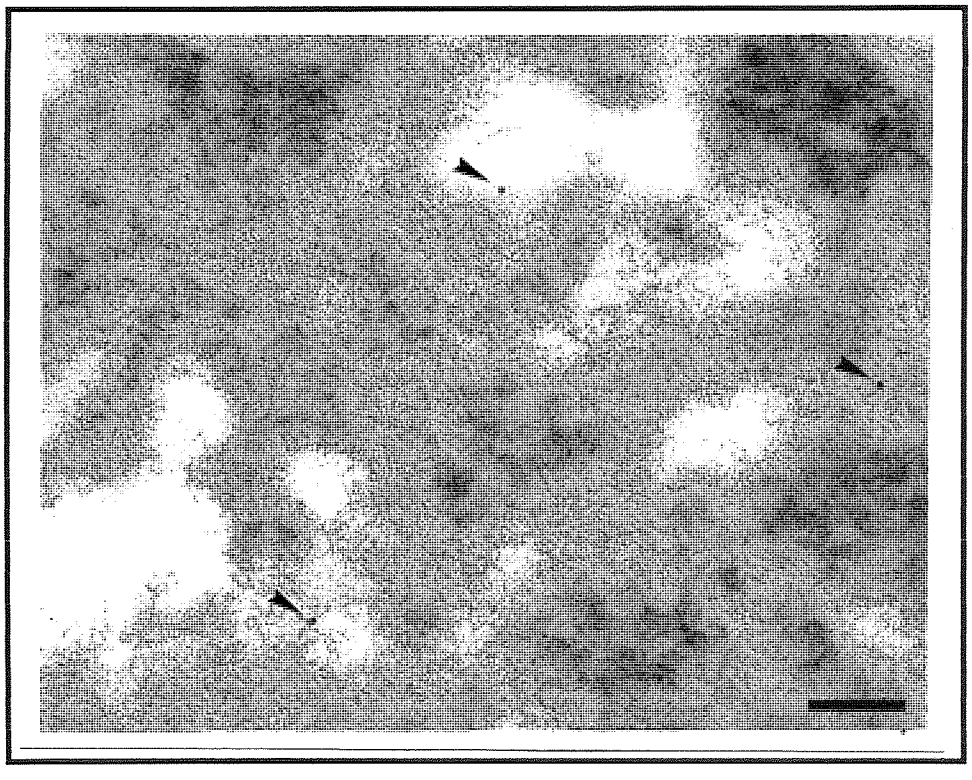

Levels of immuno-detection appeared similar to those seen in cells incubated with the biotinylated-ribozymes. Extensive searches of cell ultrastructure also revealed many similarities in the subcellular distribution of PS ODNs within A431 cell sections, when

compared with sections incubated with biotinylated ribozymes. The majority of gold particles (>70%) again appeared to be associated with either clear vesicles or, less frequently, with more electron-dense vesicular structures (See Figure 5.21).

Similar patterns of PS ODN subcellular distribution have been observed in other cell lines and reflect endosomal or lysosomal localisation (Beltinger *et al*, 1995, Tarrason *et al*, 1995) (See Figure 5.21). The similarity in the subcellular distribution of biotinylated ribozymes and PS ODNs would appear to suggest that they are processed in a similar manner by A431 cells and could share similar mechanisms for cell entry and trafficking.

Figure 5.22. Electron Micrograph Showing Penetration of the Nucleus (Nu) by Biotinylated-PS ODNs (×75,000. Arrowheads indicate immuno-gold particles within the nucleus). [Bar =100nm].

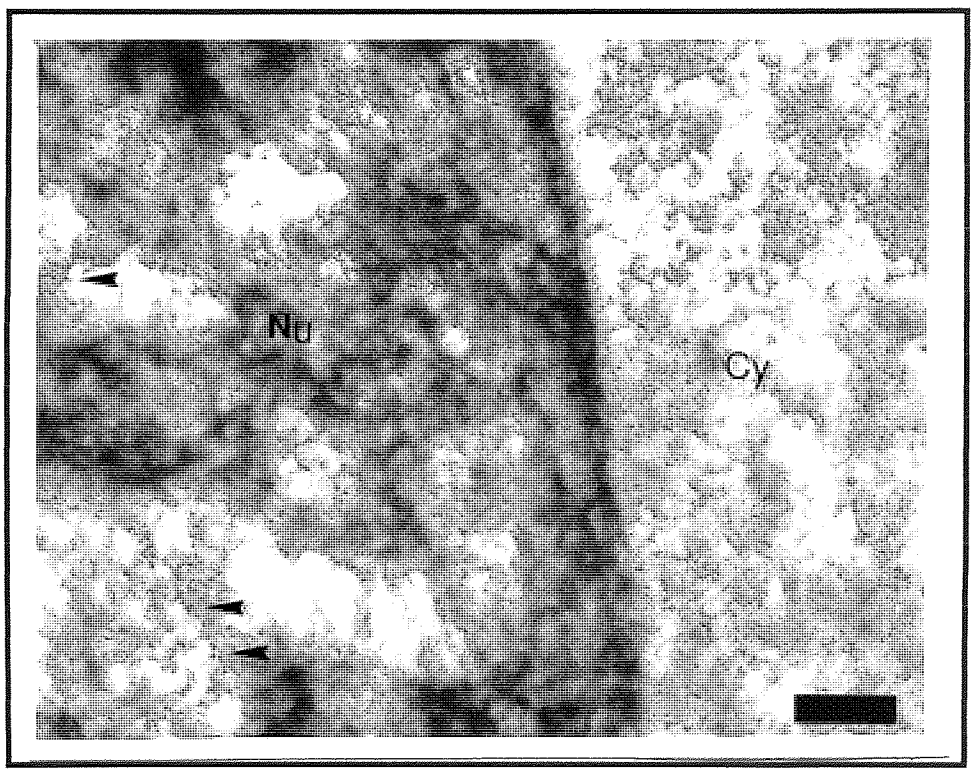

The ability of PS ODNs in penetrating the cell nucleus following exogenous delivery has been reported in one other study, in which it was concluded that PS ODNs entered the nucleus by passive diffusion via the nuclear pores (Beltinger *et al*, 1995). Although the level of structural preservation observed here was not sufficient to define the nuclear pores, the ability of PS ODNs in accessing the nucleus was confirmed (See Figure 5.22). Often a significant proportion of the PS ODNs detected within the cell (up to 30 gold particles) were observed within nuclei (See Figure

5.23). Alternatively PS ODNs were present in close proximity to the nucleus, possibly associated with the nuclear membrane / pores (See Figure 5.23). The level of nuclear penetration by PS ODNs appeared to be marginally greater than that seen with biotinylated-ribozymes, however, precise levels of immuno-detection were not measured in these qualitative studies.

Figure 5.23. Electron Micrograph Showing Localisation of Biotinylated-PS ODNs to the Cell Nucleus and Golgi (×40,000. Arrows indicate PS ODNs within the nucleus, or associated with the nuclear membrane. Arrowheads indicate PS ODNs associated with the remnants of the golgi complex (gc)). [Bar =200nm].

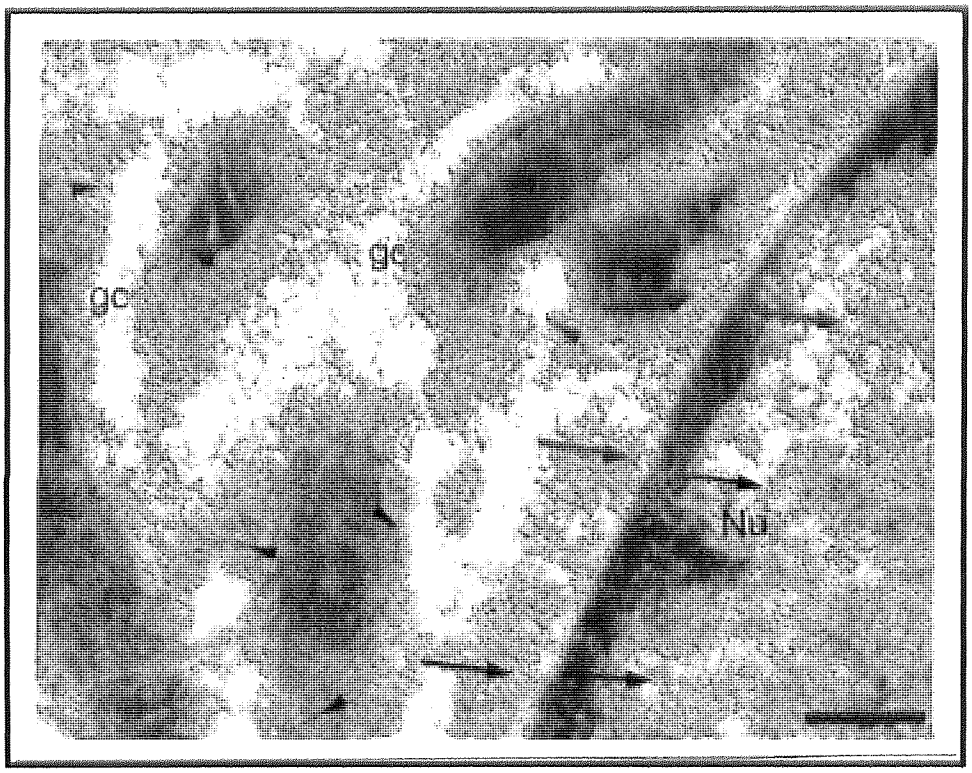

The morphological preservation of the golgi complex was again poor when compared with that seen in cells exposed to high levels of chemical fixatives (See Figure 5.9). However, structures similar to those seen in cells incubated with ribozymes (See Figure 5.19), and thought to be consistent with the remnants of the golgi complex, were observed (see section 5.3.2.2.2). PS ODNs were observed within these golgi-type structures, when they could be located, in close proximity to the nucleus. Levels of PS ODNs were relatively modest in these areas (usually around 5 particles per cell) compared with levels of ribozyme, although in some cell sections levels of immuno-detection within these structures were somewhat higher (See Figure 5.23).

Despite repeated observations of the mitochondria within the cell sections, PS ODNs were not detected within these organelles. This was in contrast to the observations made with biotinylated-ribozymes, which were detected within mitochondria, albeit at relatively low frequency. It is therefore possible that only the biotinylated-ribozymes had the ability to penetrate these organelles. A possible explanation for this could be that only the chimeric ribozymes were able to bind to specific proteins, internalised by the mitochondria. Although the mechanism of protein uptake by the mitochondria has not been categorically defined, it is thought that only proteins bearing a terminal 'signal peptide' can be imported by these organelles (see Alberts *et al*, 1989). Therefore, differences in the ability of ribozymes and PS ODNs in binding to these specific proteins could explain the apparent difference in their ability to penetrate the mitochondria.

5.3.3. Efflux of Ribozymes from A431 Cells.

Studies assessing the cellular association of antisense ODNs have indicated that some proportion of ODNs which become internalised within cells are later exported to the extracellular environment (see Section 5.1 and also; Loke *et al*, 1989, Wu-Pong *et al*, 1992, Stein *et al*, 1993, Tonkinson *et al*, 1994, Tonkinson and Stein, 1994, Agrawal and Akhtar, 1995). The method described in section 5.2.5 was used to measure the efflux of chimeric ribozymes, PS ODNs and *D*-[1-^{14}C] Mannitol after steady state accumulation in A431 cells had been achieved (after 4 hours). A representative plot of the rate of loss of these radiolabelled compounds from A431 cells as function of time is shown in Figure 5.24. Mean efflux data were fitted to a double exponential function of the form; $C_T = Ae^{(-\alpha t)} + Be^{(-\beta t)}$, where A and B represent the proportion of ribozyme or PS ODN in each compartment after 4 hours incubation. The exponential terms α and β represent rate constants (h^{-1}) for the loss of the molecules from the cells. Similar mathematical functions have been utilised by other groups to describe trends in the efflux rates of various molecules (Besterman *et al*, 1981, Tonkinson and Stein, 1994) and these are further discussed in the introduction to this chapter (See Section 5.1). Calculated 'best-fit' parameters for the bi-exponential loss of compounds from A431 cells are demonstrated in Table 5.2.

A significant proportion of internalised ribozyme was exported from A431 cells in a bi-phasic manner following steady state accumulation (See Figure 5.24). Efflux data were fitted to a bi-exponential function (see above) which indicated that approximately 23% of the internalised ribozymes were in the 'A' compartment at steady state. This is often referred to as the 'shallow' compartment (Agrawal and

Akhtar, 1995) from which efflux is relatively rapid. Approximately 72% of the ribozyme was found in the deeper 'B' compartment from which efflux is slower.

Figure 5.24. Graph Demonstrating The Rate of Loss of Radiolabelled Compounds from A431 cells as Function of Time.

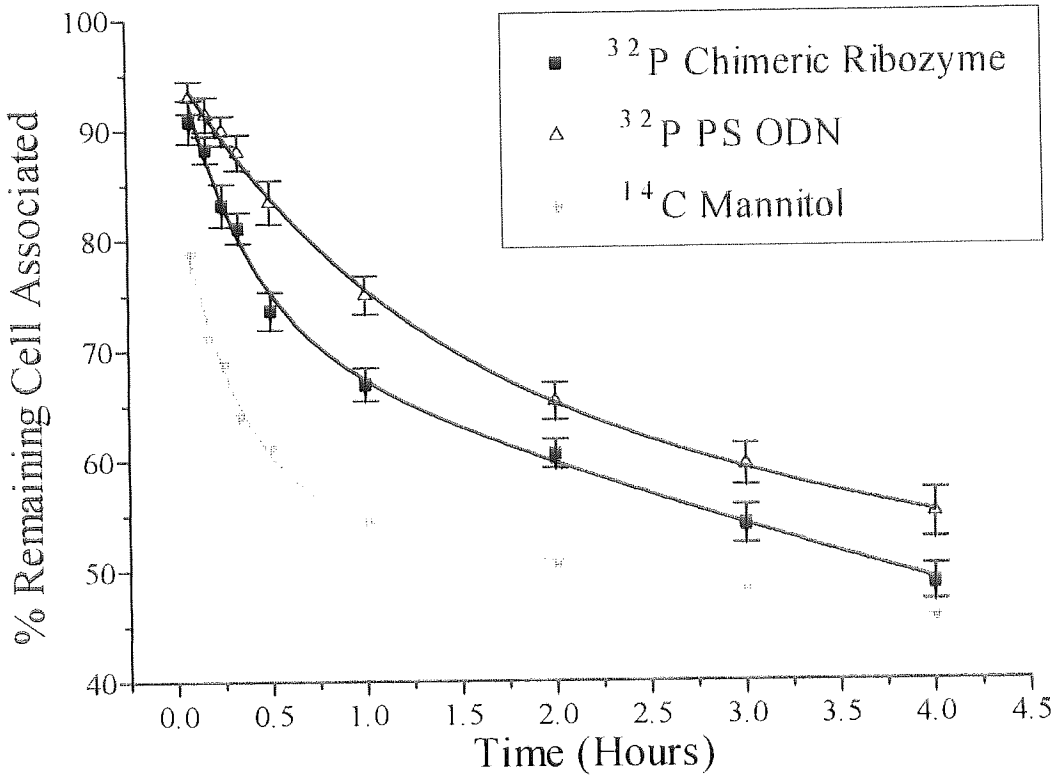

Table 5.2. The Parameters for The Bi-Exponential Loss of Radiolabelled Ribozymes, PS ODNs and Mannitol From A431 Cells Following Steady State Accumulation at 37°C.

Compound	**A** [%]	**α** [hour^{-1}]	**B** [%]	**β** [hour^{-1}]
Internally Radiolabelled Ribozyme	23.618 (+/- 2.44)	2.57 (+/- 0.75)	72.54 (+/-1.31)	0.23 (+/- 0.09)
Internally Radiolabelled PS ODN	32.78 (+/- 1.21)	1.06 (+/- 0.44)	65.38 (+/- 1.97)	0.17 (+/- 0.04)
D-[1-^{14}C] Mannitol	45.567 (+/- 5.86)	3.773 (+/- 1.45)	52.26 (+/- 6.87)	0.11 (+/- 0.11)

Data from studies monitoring PS ODN efflux were also fitted to a bi-exponential function. Results indicated that approximately 33% of the PS ODN was found to reside in the shallow 'A' compartment at steady state and approximately 65% was found in the deeper 'B' compartment. Therefore, within the limits of experimental error, very similar proportions of the both ribozymes and PS ODNs appeared to reside in each compartment after a load time of 4 hours.

With regard to the cellular efflux of *D*-[1-^{14}C] Mannitol, it must be stressed that Figure 5.24 is representative of the overall rate of loss of mannitol from A431 cells. The actual quantity of mannitol lost from A431 cells was much lower than that of the two nucleotides tested in this study. This was because mannitol was present within cells at much lower levels at steady state. (i.e. At the start of efflux measurement, the total intracellular concentration of mannitol which could be exported from the cells was considerably lower (approximately 200-fold less) than the equivalent concentration of ribozyme or PS ODN). Nevertheless the aim of this study was to obtain information regarding rates of cellular efflux, as this information can be used to describe exocytosis from particular compartments (Tonkinson and Stein, 1994).

Mannitol appeared to be distributed fairly evenly between the 'shallow' and 'deep' compartments following a load time of 4 hours. However, relative amounts of fluid phase markers residing in each of the two compartments are known to vary considerably according to the load time used (Besterman *et al*, 1981). The proportion of mannitol residing in the 'shallow' compartment after 4 hours was somewhat higher than that observed for both the ribozyme and PS ODN. However, other studies suggest that the proportion of mannitol in this 'shallow' compartment could be increased significantly if a shorter load time were used (Besterman *et al*, 1981).

With reference to all of the calculated rate constants, the initial rate of efflux (α) appeared to increase slightly in the order; PS ODN > ribozyme > mannitol, although all were of the same order of magnitude. Rate constants representing losses from the 'deeper' compartment were very similar throughout, with a turnover half life of around 180-210 minutes.

The observed rate constants for efflux from each mathematical compartment were of the same order of magnitude as those recorded in other studies (Besterman *et al*, 1981, Tonkinson and Stein *et al*, 1994). Although it is often invalid to compare efflux data obtained in different cell lines (Stein *et al*, 1993), results obtained with the ribozyme and PS ODN show some similarity to efflux profiles observed for PS ODNs in HL60 cells (Tonkinson and Stein, 1994), where PS ODNs were shown to reside

predominantly within 'deep' compartments, whereas PO ODNs were mainly (>60%) within the 'shallow' compartments (Agrawal and Akhtar, 1995).

Figure 5.25. Autoradiograph Image Demonstrating the Stability of Chimeric Ribozymes Exported by A431 Cells after Various Incubation Periods. [Lane ***C***; Ribozyme (control) incubated in serum-free DMEM (only) for 4 hours. Lanes ***5*** to ***240***; demonstrate radiolabelled products exported from A431 cells after increasing incubation periods (in minutes) Lane ***F***; [^{32}P]-γ-dATP radiolabel (control)]

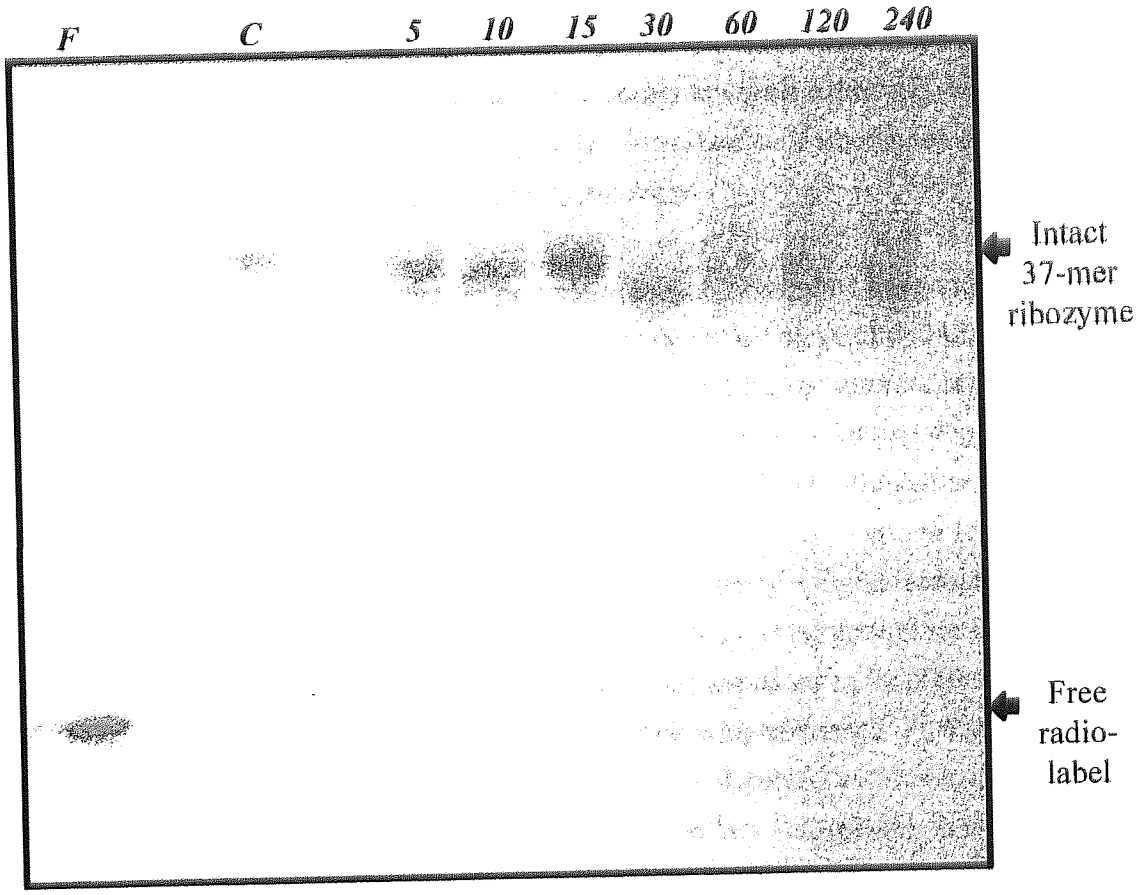

In order to confirm that the export of the [^{32}P] radiolabel from cells correlated with the loss of intact ribozyme, stability studies (see Section 5.2.5.2) were performed to examine the integrity of ribozyme efflux product(s). Examination of the efflux products indicated that significant amounts of the undegraded ribozyme were exported from cells at various post-loading times. No autoradiograph bands corresponding to the export of the free radiolabel were observed, which indicated that the [^{32}P] radiolabel remained attached to the ribozyme molecule throughout the duration of the experiment. This confirmed that efflux of the [^{32}P] radiolabel could be correlated with the export of the ribozyme from cells. In efflux samples obtained 5 to 15 minutes post-loading, the ribozyme appeared to be completely intact. However, at 30 to 240 minutes post-loading, shorter chain products were evident. These products were thought to represent the intact ribozyme molecule, minus the terminal

oligodeoxynucleotides, which were probably digested by 3'-exonucleases (see Section 3.3.3.3). The integrity of the radiolabelled PS ODN was not examined in this report, however, other investigators have reported that PS ODNs can remain stable within intracellular environments for the time period examined in the present studies (Tonkinson and Stein, 1994).

5.4. CONCLUDING REMARKS.

Previous studies in this report (see Chapter 4) have indicated that chimeric ribozymes enter cells via an inefficient process, which is consistent with either AE or RME. Either of these mechanisms would result in the localisation of ribozymes within endosomal or lysosomal vesicles following cell entry.

The studies described in this chapter provide evidence to support the proposed mechanism(s) of cellular uptake because ribozymes were observed within structures consistent with endosomal / lysosomal vesicles, when different microscopic techniques were employed. Fluorescent microscopy demonstrated a considerable degree of cell-surface binding by FITC-labelled ribozymes. In addition, FITC-ribozymes demonstrated a punctate pattern of subcellular distribution and were co-localised with fluorescent endosomal markers following uptake. By using a higher resolution technique, involving immuno-electron microscopy, the ultrastructural localisation of biotin-labelled ribozymes was examined. Ribozymes appeared to be predominantly localised within clear, endosomal-type vesicles following cell entry. Furthermore, a significant proportion of internalised ribozymes were detected within (electron-dense) primary lysosomes and multi-vesicular bodies (secondary lysosomes). Overall, the subcellular distribution of ribozymes appeared to be similar to that of biotin-labelled PS ODNs (also see Tarrason *et al*, 1995, Beltinger *et al*, 1995), giving further evidence to support a cellular uptake mechanism involving AE or RME.

However, ribozymes would be required to exit endosomal / lysosomal vesicles in order to exert their desired biological effects. Entrapment within these vesicles would probably result in the rapid export of ribozymes from cells, or their degradation by nucleases (Akhtar *et al*, 1995). Indeed, the export of ribozymes from cells was confirmed in cellular efflux studies, which indicated that around 50% of cell-associated ribozymes were exported from cells within 4 hours. However, ultrastructural studies did provide evidence to suggest that a small proportion of internalised ribozymes were able depart the endosomal vesicles. For example, ribozymes appeared able to penetrate the nucleus in small quantities and were also

observed in close proximity to the nuclear membrane / envelope. In addition, some ribozymes were detected 'free' within the cytoplasm. These findings were encouraging, since these intracellular regions broadly represent the target sites for ribozyme activity. Interestingly, a small proportion of internalised ribozymes were also observed within the mitochondria, and in association with the golgi complex. Nevertheless, it would appear likely that some form of additional delivery system, perhaps capable of promoting the release of ribozymes from endosomes, would improve their overall bioavailability.

Finally, it must be noted that in all electron microscopy studies, which must be performed under a vacuum and require fixation of cells, findings are dependant upon the assumption that the observed cellular morphology is representative of the true structure of the living cell (Griffiths *et al*, 1993). Furthermore, the validity of the immuno-labelling protocol was dependant on the assumption that biotin itself, did not contribute to the observations made. However, this assumption was verified to a large extent because endogenous biotin within cells, and biotin added exogenously, were not significantly detected within cells using the immuno-labelling protocol.

CHAPTER SIX

ASSOCIATION OF CHIMERIC HAMMERHEAD RIBOZYMES WITH GLIAL CELLS *IN VITRO* AND *IN VIVO*

6.1. INTRODUCTION

In Chapters 4 and 5, the cellular uptake characteristics of chimeric ribozymes were examined in the A431 vulval (epithelial) cell line. This cell line is known to over-express the epidermal growth factor receptor (EGFr) mRNA (Ullrich *et al*, 1984), which is the target molecule for the ribozymes studied during this thesis. The A431 cell line, therefore, offers a potentially useful model for assessing the efficacy of these ribozymes *ex vivo*. However, the ultimate goal of the research group is to design therapeutic agents which can be used to treat glioblastoma multiforme (GBM) (see Section 1.5). Ribozymes designed to treat GBM would require delivery to glial cells *in vivo*. Therefore, specific information regarding the association of ribozymes with glial cells would be desirable because cellular association characteristics are often cell line dependant (Noonberg *et al*, 1993, Akhtar and Rossi, 1996). Indeed, the studies described in Section 4.3.10 (Chapter 4) confirmed that levels of ribozyme association vary between different cell types *in vitro*. For example, the association of ribozymes with U87-MG (glial) cells was approximately 2-fold higher ($P<0.001$) than that observed with A431 (vulval) cells after 4 hours. Consequently, it would be unwise to simply extrapolate the findings observed in the vulval (A431) cell line to the situation in glial cells.

The U87-MG human glioblastoma astrocytoma cell line, derived from a malignant glioma (Ponten and McIntyre, 1968), was selected as a model for examining the cellular association of radiolabelled ribozymes with glial cells *in vitro*. The subcellular distribution of fluorescent (FITC) labelled ribozymes was also examined in these cells using fluorescent microscopy techniques. The aim of these studies was to give an insight into the mechanism(s) and extent of cellular uptake of ribozymes by glial cells (*ex vivo*), and to allow comparisons to be made with the uptake trends observed in the A431 cell line (See Chapters 4 & 5).

In addition to the *ex vivo* studies performed using the glial cell line, *in vivo* studies were also performed in an animal model. These studies involved the direct

introduction of FITC-labelled ribozymes into the cerebral ventricles of anaesthetised laboratory mice. The aim of the *in vivo* studies was to assess levels of uptake and the pattern of distribution of FITC-ribozymes following direct delivery to the brain. In addition, any degree of cellular localisation, perhaps consistent with localisation within glial cells, could be assessed.

A direct delivery technique was considered to be necessary because pharmacokinetic studies by other investigators indicated that penetration of the brain by ribozymes is extremely poor following systemic delivery (Desjardins *et al*, 1996). In these studies 2'-O-allyl modified ribozymes, which were administered to rats via a single intra-venous injection (25mg per animal), became predominantly bound to serum albumin and the tissue distribution of ribozymes was primarily to the liver (6%) and kidneys (1.6%). Overall, less than 0.1% of the administered dose of ribozymes was detected within the brain (Desjardins *et al*, 1996). Poor penetration of the brain can potentially be obviated by direct delivery techniques, such as intra-cerebroventricular (ICV) injection. In theory, this technique should permit much higher local concentrations of ribozymes to be achieved within the brain than would be possible following systemic delivery. Therefore, in the studies described in this chapter, ICV injection was used to administer ribozymes to mice.

Pharmacokinetic studies have also demonstrated that PS ODNs penetrate the brain poorly following systemic delivery (Agrawal *et al*, 1991, Srinivasan and Iversen, 1995, Agrawal *et al*, 1995). ICV injection has been used to overcome this problem in a recent study, which examined the fate of FITC-labelled PS ODNs within the mouse brain (Zhang *et al*, 1996). In this study, FITC-labelled PS ODNs were rapidly taken up into the brain substance following ICV injection. After several minutes PS ODNs became widely, but not uniformly, distributed to diverse regions of the brain. For example, strong fluoresence signals were detected in areas such as the forebrain nuclei, the corpus striatum, the hippocampus and the cerebral cortex. Initially, the fluorescent signal demonstrated a 'punctuated' pattern of distribution, which was indicative of localisation within cell bodies and dendritic processes (Piwinca-Worms, 1994, Zhang *et al*, 1996). However, at later time points (>24 hours) the fluorescent signal appeared to be granular and was thought to represent degraded material (Zhang *et al*, 1996). Overall, it was concluded that PS ODNs were able to penetrate cells within the brain following ICV injection and were preferentially distributed to certain cell-types. Consequently, the findings appeared to correlate with those of *in vitro* studies which demonstrated that uptake of PS ODNs was cell-type specific (Noonberg *et al*, 1993, Meeker *et al*, 1995, Akhtar and Rossi, 1996).

Further evidence to suggest that antisense ODNs can penetrate cells within the brain is provided by *in vivo* efficacy studies, in which antisense ODNs have been administered to animals by ICV injection (for a recent review see Ogawa and Pfaff, 1996). Antisense ODNs directed against a variety of mRNAs, encoding neurotransmitter receptors (for example the 'neuropeptide Y' mRNA, see Wahlestedt *et al*, 1993) and other proteins (for example *c-fos*, see Chiasson *et al*, 1992), have elucidated specific and predictable biological effects. These have included changes in levels of protein expression and changes in animal behaviour (Ogawa and Pfaff, 1996). Therefore, it appears likely that at least some proportion of ICV delivered ODNs are able penetrate intracellular sites and interact with target mRNAs.

Until this study however, the *in vivo* distribution and / or efficacy of ribozymes delivered to the brain has not been examined in detail. Therefore, an investigation into the distribution of chimeric ribozymes within the brain could be useful to the development of future therapies for gliomas and other neuronal disorders.

6.2. METHODS.

General materials and methods used in this chapter are outlined in Chapter 2. Ribozyme and ODN synthesis, purification and labelling and cell culture techniques are all described in detail in Section 2. Any alterations or additions to these methods are outlined in the relevant sections below.

6.2.1 Preparation of Radiolabelled Nucleic Acid Sequences.

A 37-mer chimeric ribozyme (Sequence EGFR-65, See Chapter 3), targeted against an untranslated region close to the 3' end of the human EGFr mRNA, was synthesised and internally radiolabelled as described in Section 4.2.1 (Also see Figure 4.1) Unmodified 37-mer PO and PS ODNs of the same base sequence as the chimeric ribozyme were also synthesised for use in these studies. However, PO and PS ODN sequences were not radiolabelled.

6.2.2. Preparation of Fluorescent Labelled Nucleic Acids.

A 36-mer partially modified ribozyme (Sequence EGFR-65, see Chapter 3), targeted against an untranslated region of the human EGFr mRNA, was synthesised as described in Section 5.2.1. An unmodified 36-mer PS ODNs of the same base sequence as the chimeric ribozyme was also synthesised. FITC labels were added to

the 5'-end of both chimeric ribozymes and PS ODNs during automated synthesis as outlined in Section 2.5.4. Fluorescent labelled nucleic acids were protected from light and stored at -70°C prior to use.

For *in vitro* localisation studies, samples of FITC-labelled ribozymes and PS ODNs were prepared as described in Section 2.8.7.2. For *in vivo* studies, FITC-labelled ribozymes and PS ODNs (see Section 5.2.2) were prepared at a concentration of 25μM in sterile 0.1% saline (Baxter Healthcare, Thetford, UK). This concentration was approximately half that administered in a recently published study which examined the *in vivo* distribution of PS ODNs following ICV injection to the mouse brain (Zhang *et al*, 1996).

6.2.3. *In Vitro* Cell Association Studies with U87-MG Cells.

U87-MG cells were maintained and seeded for cell association studies as described in Section 2.7.5. In all cell association studies additional wells were seeded with cells and counted during experiments using a haemocytometer as described in Section 2.7.2. This allowed data to be normalised to cell number when required. A variety of cell association studies were performed as outlined in Section 2.8.

With regard to EGFr mRNA expression within U87-MG cells; studies by other investigators in the laboratory demonstrated that levels of EGFr expression in U87-MG cells were up-regulated (3-fold) relative to normal human astrocytes. By comparison, the level of EGFr expression in U87-MG cells was only 15% of that in A431 cells (Coulson *et al*, 1996).

6.2.4. Cellular Localisation of Fluorescent Labelled Probes *In Vitro*.

In order to assess the cellular distribution of fluorescent labelled compounds *in vitro*, experiments were initiated as described in Section 2.8.7.2. Following incubation with fluorescent compounds, cells were routinely washed and fixed as described in section 2.8.7.2. However, some cells were simply washed with sterile PBS to remove traces of non-cell associated fluorophores and immediately viewed under the microscope in the absence of any fixative treatment. This allowed any effects of the fixation process to be assessed. However, it was not possible to routinely perform examinations over longer time periods (>1 hour) with non-fixed cells because the condition of such cells deteriorated rapidly. Cell associated fluorophores were visualised using a Jenamed fluorescence microscope as described in Section 2.8.7.3.

6.2.5. Animals

Male albino mice (weighing approximately 25g) were obtained from The Pharmacology Research Section, Aston University, UK and were used throughout these studies. The mice were housed in pairs in plastic cages with wood-chip bedding and were provided with free access to food and water throughout the experimental period. All mice were housed in humidity controlled areas at ambient temperature (20-25°C).

6.2.6. Intracerebroventricular Injection of Fluorescent Labelled Probes.

The method used was essentially that described by Brittain and Handley (1967). However, in the present studies the mice were briefly anaesthetised with Halothane / Oxygen in order to immobilise them during the actual injection procedure. The animals were held firmly onto the bench by extending the skin on either side of the neck with the thumb and forefinger. The site of injection was within 1mm of the midline and a line joining the anterior bases of both ears. Injections were made using a 22 gauge needle (0.32cm long) attached to a 0.1mL syringe. Injections (total volume 20μL) were made slowly over a period of approximately 30 seconds, through the skull and into the brain of the animal at a perpendicular angle. To provide a control of labelling specificity, similar volumes of fluorescein (25μM) were prepared (see Section 2.8.7.1) in the same buffer solution. 'Free' fluorescein was injected into 'control' animals using the same procedure as described above.

6.2.7 Preparation of Cerebral Tissue for Microscopy.

Four hours post-injection, mice were decapitated and skull was very carefully cut away to reveal the brain. The intact brain was removed and partially frozen by the application of 'Cryo-Jet Freezing Spray' (BDH Laboratory Supplies). The brain was carefully positioned in the correct orientation, on a 2cm wide droplet of partially frozen OCT Compound (BDH Laboratory Supplies), on an aluminium cryostat chuck. The brain and OCT compound were kept partially frozen during manipulations with the aid of the 'Cryo-Jet' freezing spray. The partially frozen brain on the chuck was submerged in liquid nitrogen for 2 seconds until the OCT Compound became opaque and firm, thus holding the mouse brain in the correct position for sectioning on the surface of the chuck. Brains were sectioned (either transverse or sagittally) at thicknesses of 10-20μm using a cryostat (Model OTF, Bright Instruments, UK) maintained at constant temperature (-24°C). Sequential cryosections were collected

on coated glass microscope slides ('Superfrost Plus' slides, 25mm × 75mm, BDH Laboratory Supplies) and the slides were numbered in the order of sectioning.

Cryosections that were to be stained (see Section 6.2.8), or stored for several days to permit repeated examination, were fixed in acetone at 4°C for 30 seconds. Other cryosections were immediately viewed using the microscope and photographed without exposure to any chemical fixative. The quality of cryosections which were not chemically fixed generally deteriorated within 1 hour. Cryosections which were fixed in acetone as described above were allowed to air dry for 2-3 minutes and were then either stained (see Section 6.2.8) or mounted in glycerol (50%) in PBS containing 1% v/v DABCO as an anti-fading agent (Johnson *et al*, 1982) and a cover slip added. Tissue sections were examined as described in Section 2.8.7.3 using a Jenamed fluorescence microscope (Jena Instruments, Oberkochen, Germany) and high pressure mercury HBO-50 light source (C-Z Scientific, Basingstoke, UK). A Weiss Phase Contrast Microscope was also used for low magnification phase contrast microscopy. Careful records were kept of the slide numbers to permit the identification of anatomical features in sequential sections through the brain. Photographs were taken using an Olympus camera with Jenamed adapter and Kodak Gold colour film (ISO 200).

6.2.8 Staining of Tissue Sections for Microscopy.

With reference to a stereotaxic atlas (Pellegrino *et al*, 1967), structures within sequential cryosections can be identified, if the sections are suitably stained. Pellegrino *et al* (1967) stained paraffin embedded brain sections for myelin and cell bodies when preparing their stereotaxic atlas. This atlas catalogues the appearance of structural features in sequential sections of the rat brain (which is anatomically similar to the mouse brain). In order to use this atlas as an anatomical guide, chemical stains for myelin and cell bodies (which were suitable for cryosections) were used in this report. Advice on suitable staining techniques was kindly provided by Dr. Glynn Woodward, Histopathologist, Dudley Road Hospital, Birmingham, UK. To allow anatomical regions of the brain to be more easily identified, one in every eight cryosections collected was chemically stained to highlight structural features. Solochrome cyanine was used to stain myelin fibres and eosin was used to stain cell bodies. The presence of any fluorescence within stained cell sections was not measured because of potential artefacts arising during the staining process.

6.2.8.1 The Solochrome Cyanine Technique for Myelin.

Fixed cryosections were air dried and exposed to the filtered solochrome cyanine stain (solochrome cyanine 0.2g, distilled water 96mL, iron alum (10%w/v) 4mL, concentrated sulphuric acid 0.5mL) for 10 minutes at room temperature. The stain was washed from the sections with running water and the stained sections were differentiated by immersion in 10% w/v iron alum solution for approximately 5 minutes. Cryosections were briefly examined to ensure suitable staining density had been achieved. Finally sections were thoroughly washed with distilled water and counter-stained as described below.

6.2.8.2 Eosin Staining For Cell Bodies.

Cryosections stained for the presence of myelin were counter-stained by the addition of 0.3% v/v eosin (in 0.3% w/v calcium chloride solution) for approximately 20 seconds at room temperature. The eosin stain was washed from the sections with distilled water and the sections were dehydrated in an ascending series of ethanols (95%, 98%, 99% and 100%). Finally sections were dehydrated in 100% xylene, mounted using Pirtex (supplied by Dudley Road Hospital) and a cover slip added.

6.3. RESULTS.

6.3.1 Time Profile for the Cellular Association of Chimeric Ribozymes with U87-MG Cells *In Vitro*, Compared with a Fluid Phase Marker.

A time profile for the cellular association of 0.8μM chimeric ribozyme in U87-MG cells (at 37°C) was obtained as described in section 2.8 and compared to that of *D*-[1-^{14}C] mannitol (0.8μM) (see Section 2.8.3). Mannitol is thought to enter cells exclusively by fluid phase endocytosis (FPE) and can, therefore, be used as a molecular marker for this process (See Besterman *et al*, 1981, Levis *et al*, 1995). The results of these studies are shown in Figure 6.1 and have been compared with the results observed in the A431 cell line (see Figure 4.4).

Only a relatively small proportion of ribozymes added to the apical media became associated with the U87-MG cells. For example, less than 1.9% of the added quantity became cell associated after 6 hours. However, the percentage of ribozyme associated with U87-MG cells was, on average, around 45% higher than the corresponding percentage which became associated with A431 cells in previous studies (see Section

4.3.3 and Table 6.1). The time profile of ribozyme cell association appeared to be biphasic in the U87-MG cell line. An initially more rapid phase of cellular association occurred in the first 2 hours and this was followed by a slower phase of association. In fact, the percentage of cell associated ribozyme increased only marginally from 4 to 6 hours post-administration and this increase was not statistically significant (P=0.075). A similar biphasic association profile was observed when the ribozyme construct was incubated with A431 cells, however, in these cells the level of cell association continued to increased significantly (P<0.001) from 4 to 6 hours post-administration. (See Section 4.3.3 & Table 6.1).

Figure 6.1. Graph Showing % Cell Association Against Time for Internally Radiolabelled Chimeric Ribozyme in U87-MG Cells, Compared with % Cell Association of *D*-[1-^{14}C] mannitol. (n=6, mean ± SD)

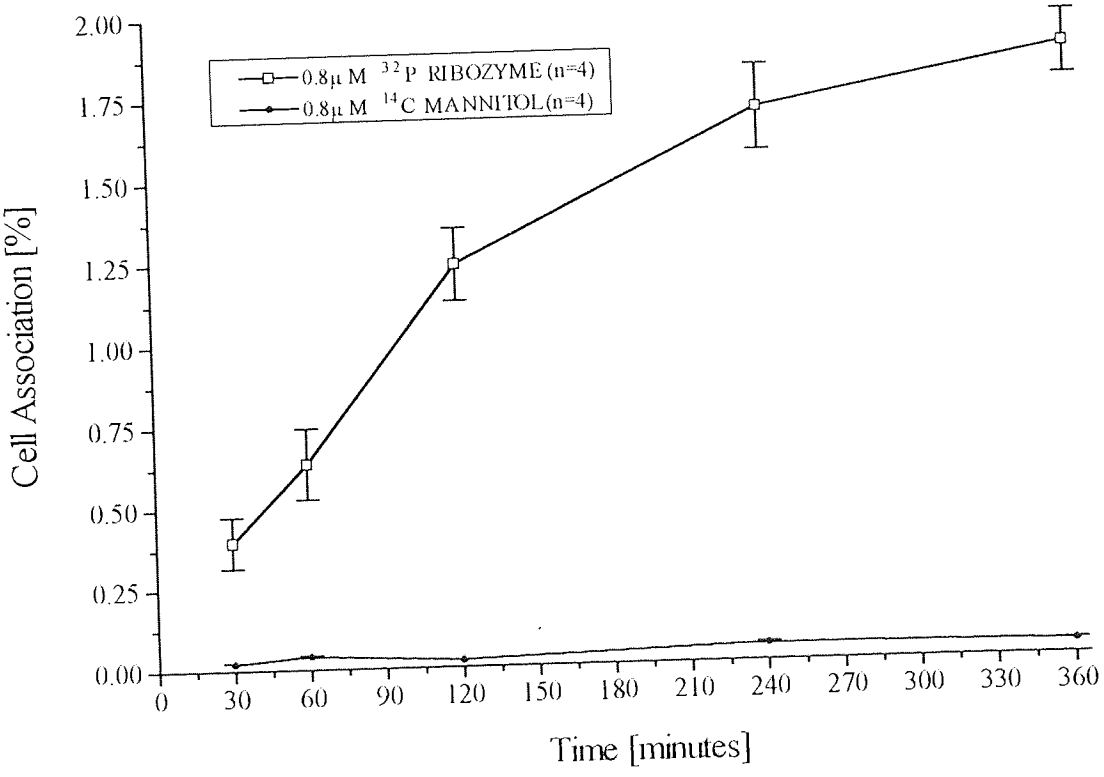

The quantity of cell associated *D*-[1-^{14}C] mannitol remained relatively stable in U87-MG cells throughout the experiment and did not significantly increase (P>0.05) above the level observed after 30 minutes. At all time points examined, the percentage of the internally [^{32}P]-radiolabelled ribozyme which became associated with U87-MG cells was significantly higher (P<0.001) than that of *D*-[1-^{14}C] mannitol. After 30 minutes, the mean quantity of cell associated ribozyme was 20-fold higher than the fluid phase (FPE) marker. After 6 hours, mean quantities of cell associated ribozyme were almost 50-fold higher than the fluid phase marker. The increased quantity of cell associated ribozyme relative to the fluid phase marker, suggested that it was unlikely that

ribozymes entered U87-MG cells exclusively via the FPE pathway. The relative difference seen between the ribozyme and fluid phase marker, is consistent with the findings of other studies which have examined the association of antisense ODN analogues in other cell lines (Beltinger *et al*, 1995, Levis *et al*, 1995). It is also consistent with the studies described in Section 4.3.3 which examined the cellular association of the same ribozyme molecule in A431 cells (see Table 6.1).

6.3.2. The Effects of Temperature and Metabolic Inhibition on the Cell Association of Chimeric Ribozyme in U87-MG Cells.

To investigate the effect of reduced temperature and metabolic inhibition on the cellular association of ribozymes with U87-MG cells, experiments were performed as described in Sections 2.8.4 and 2.8.5. The results of these experiments are demonstrated in Figure 6.2. This shows the percentage of ribozymes associated with cells, which were either incubated at 4°C throughout, or were pre-treated with sodium azide and 2-deoxy glucose and incubated at 37°C. The control sample represents the percentage of ribozymes associated with U87-MG cells which were incubated at 37°C throughout and were not treated with any metabolic inhibitors.

Cell association of ribozymes was reduced by approximately 70%, but not completely inhibited at low temperature (4°C), at all time points tested ($P<0.001$). The reduction in cell association remained relatively constant throughout the experimental period. Metabolic inhibition also reduced the extent of ribozyme cell association compared with controls at all time points tested ($P<0.001$). Maximal inhibition was seen after 4 hours, at which time the percentage of ribozyme associated with the metabolically inhibited cells was only 20% of the control value. The percentage of ribozymes associated with the metabolically inhibited cells did not significantly increase ($P>0.05$) during the 4 hour period examined. However, during the same time period (1 to 4 hours) the percentage of cell associated ribozymes increased ($P<0.001$) more than 3-fold in control samples.

The reduction in the percentage of cell associated ribozyme indicated some involvement of cellular energy in the mechanism of association. The requirement for cellular energy could potentially arise directly from the demands of an active transport process (for example RME). Alternatively it could be indirectly due to effects on secondary active transport processes (for example FPE), or the maintenance of cell membrane potential, structure or integrity. The lack of complete inhibition of cell association could be due to surface binding of ribozymes, in the absence of internalisation. This certainly appears to be the case in U87-MG cells exposed to

metabolic inhibitors because no significant increase (P>0.05) in cell associated ribozyme was detected after an initial 'binding' period. Alternatively, in the case of the metabolic inhibitors the effect could be due to incomplete ATP depletion.

Figure 6.2. Graph Showing the Effect of Reduced Temperature and Metabolic Inhibition on the % Cell Association of Chimeric Ribozyme in U87-MG Cells as a Function of Time, Compared with Control. (n=4, mean values ± SD).

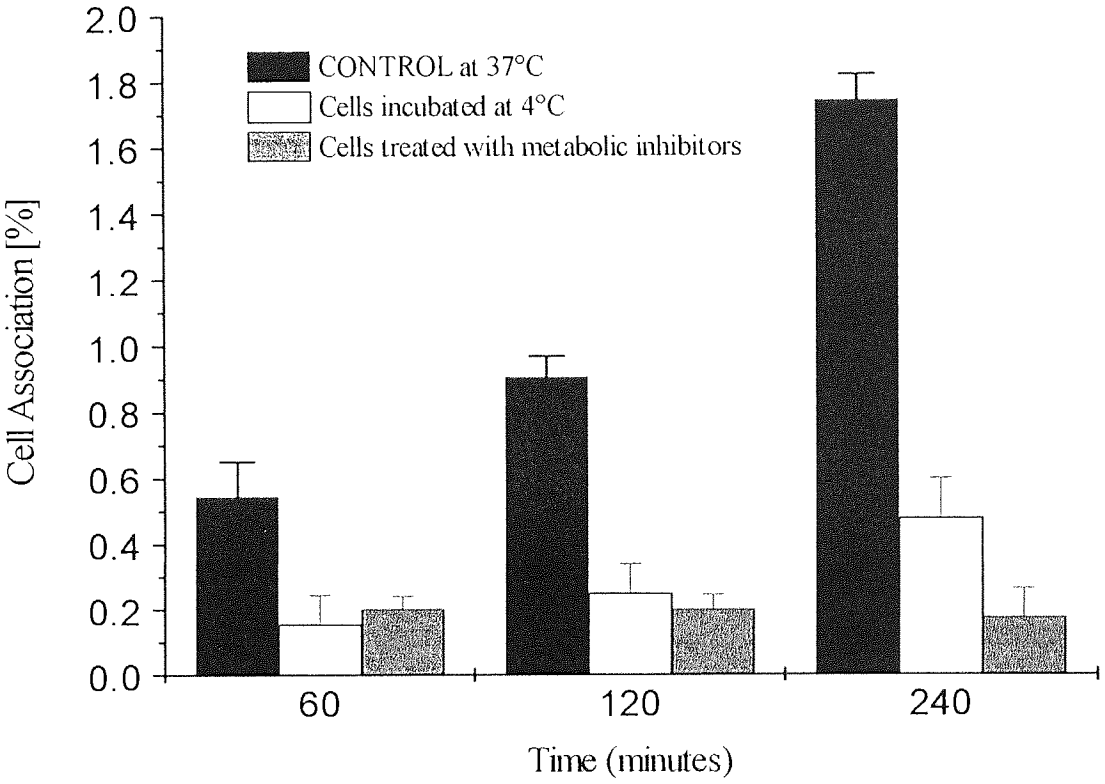

The (partial) inhibitory effect of reduced temperature and metabolic inhibitors on cell association has been observed with antisense ODNs in other cell lines (Wu-Pong *et al*, 1992, Deshpande *et al*, 1996, Shoji *et al*, 1996) and has been observed with the same ribozyme molecule in A431 cells (See Section 4.3.4). However, it was noted that the inhibitory effect of reduced temperature and metabolic inhibitors on ribozyme association was more pronounced in U87-MG cells than in A431 cells (see Table 6.1). This suggested that cell association of ribozymes showed a greater degree of energy dependency in U87-MG cells than in A431 cells. Furthermore, the actual quantities of cell associated ribozyme observed in U87-MG cells and in A431 cells, at 4°C or in the presence of metabolic inhibitors, were relatively similar. For example, the quantity of ribozyme associated with both cell types at 4°C, or in the presence of metabolic inhibitors, was not significantly different (P>0.05) after 120 minutes. This was in stark contrast to the quantities of cell associated ribozyme observed in control samples, where cellular association of ribozymes in U87-MG cells was significantly increased (P<0.01) relative to that in A431 cells. This suggests that when energy

dependant processes were inhibited, cellular association of ribozymes was similar in both U87-MG cells and A431 cells. However, when energy dependant processes, such as endocytosis, were not inhibited, a greater quantity of ribozyme became associated with U87-MG cells. A possible explanation for this could be that U87-MG cells demonstrate faster rates of endocytosis than A431 cells when cellular energy is not limited, and hence, U87-MG cells were able to internalise ribozymes more efficiently than A431 cells via endocytic processes.

6.3.3 The Effect of Ribozyme Concentration on Cellular Association in U87-MG Cells

In order to assess the effect of the apical ribozyme concentration on cell association, the method described in Section 2.8.1 was slightly modified. A range of concentrations of ribozyme were prepared in serum-free culture media, instead of the standard 0.8μM preparation (N.B. different concentrations were prepared by diluting 0.4μM internally radiolabelled ribozyme with the required quantity of unlabelled ribozyme). The concentrations tested were in the range 0.4μM to 4μM, which represented concentrations from 50% below the standard level (0.8μM) used in other experiments, up to a 5 fold higher concentration. The effect of *D*-[1-^{14}C] mannitol concentration on cell association was also tested under similar concentrations to allow comparisons to be made.

Results are demonstrated in Figure 6.3. Cell association of the chimeric ribozyme appeared to be concentration dependant over the range tested. As the ribozyme concentration was increased stepwise (0.4μM, 0.8μM, etc.), the percentage of cell associated ribozyme decreased significantly ($P<0.05$) with each corresponding increase in concentration. However, in the concentration range between 2μM and 4μM the percentage decrease was not statistically significant ($P>0.05$). The actual quantity of ribozyme which became cell associated when increasing concentrations were added (in terms of nanomoles of ribozyme associated per cell) was also examined. Quantities of cell associated ribozyme increased when higher apical concentrations were administered to U87-MG cells. However, when ribozymes were administered at concentrations of 0.8μM and above, the increase in the total quantity of cell associated ribozyme was not statistically significant ($P>0.0614$, determined by Welch's test), possibly indicating saturation of a cellular uptake process at concentrations above 0.8μM.

Figure 6.3. Graph Showing the Effect of Concentration on the Cellular Association of Internally Radiolabelled Chimeric Ribozyme Compared with *D*-[1-^{14}C] mannitol in U87-MG Cells after 4 hours at 37 °C. (mean ± SD).

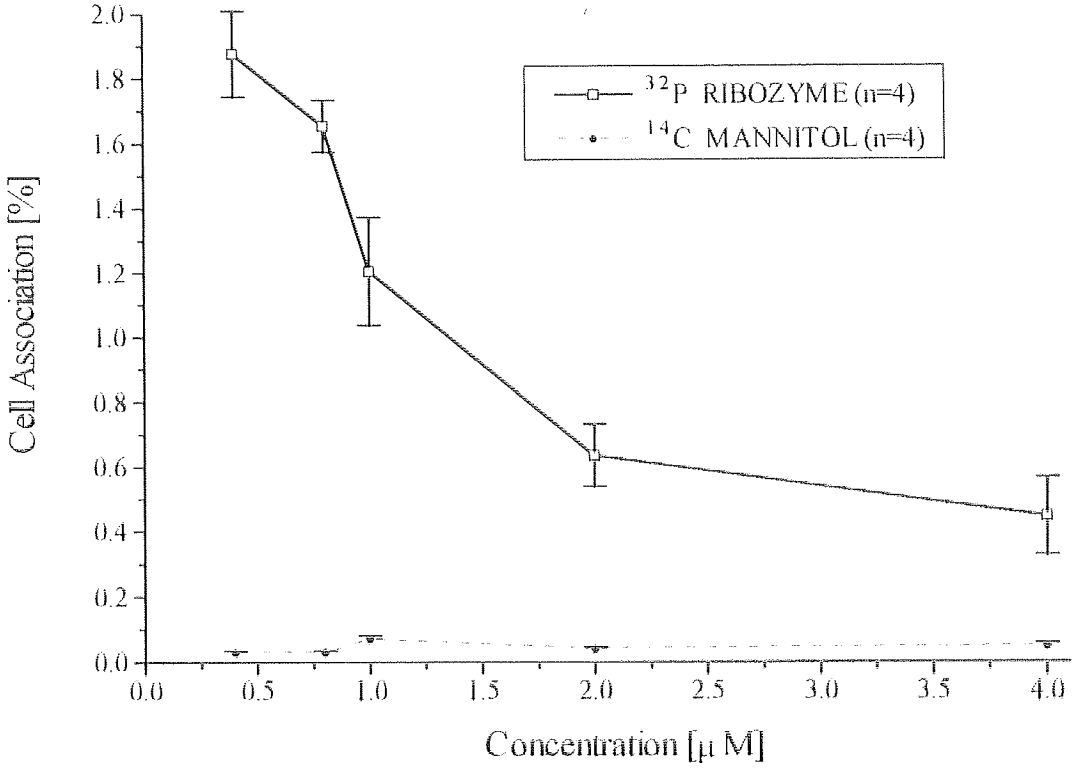

Previous studies in this report showed that cellular association of the ribozyme was also concentration dependant in A431 cells (See Section 4.3.5). However, studies in A431 cells indicated that saturation did not occur until cells were exposed to slightly higher apical ribozyme concentrations (1.0μM and above). A possible explanation for this slight difference between the two cell lines could be a variation in the availability of binding sites for ribozymes on the surface of cells. For example, the A431 cell line may express slightly higher levels of surface proteins or lipids which ribozymes can bind, therefore, saturation does not occur until all of these sites are occupied. Overall, the saturable and concentration dependant nature of ribozyme cell association indicates the involvement of a cell surface binding mechanism such as RME or AE.

There was no significant difference ($P>0.05$) in the percentage of *D*-[1-^{14}C] mannitol which became cell associated, over the range of concentrations examined. This indicated that the mechanism by which *D*-[1-^{14}C] mannitol became cell associated was not saturable. Cell association of ribozymes was significantly higher ($P<0.001$) than *D*-[1-^{14}C] mannitol at all concentrations tested. However, differences between the two were more pronounced when lower concentrations were administered. Although the extent of ribozyme uptake remained significantly higher than that of the fluid

phase marker at all concentrations tested (up to 4μM), the differences became more marginal as concentrations were increased. It is feasible, therefore, that cellular uptake of ribozymes proceeds via the fluid phase endocytic mechanism when more efficient uptake processes become saturated.

6.3.4. The Effect of Oligonucleotide Competition on Cell Association of Chimeric Ribozyme.

To assess the effects of competitors on the cellular association of ribozymes in U87-MG cells, the methods described in Section 2.8.6 were used. Experiments were designed to demonstrate competition by an excess of either unlabelled ribozyme (10μM) or PS ODN (10μM, of the same base sequence as the ribozyme). The results (demonstrated in Figure 6.4) were obtained after 4 hours incubation with 0.8μM radiolabelled ribozyme in the presence of excess unlabelled competing agents at 37°c. The control represents cell association of 0.8μM radiolabelled ribozyme with no competing agent present.

Figure 6.4. Graph Showing Percent Cell Association of Chimeric Ribozyme with U87-MG cells after 4 hours, in the Presence of Excess Concentrations of Either Unlabelled Ribozyme or PS ODN Compared with Control (n=4, mean ± SD).

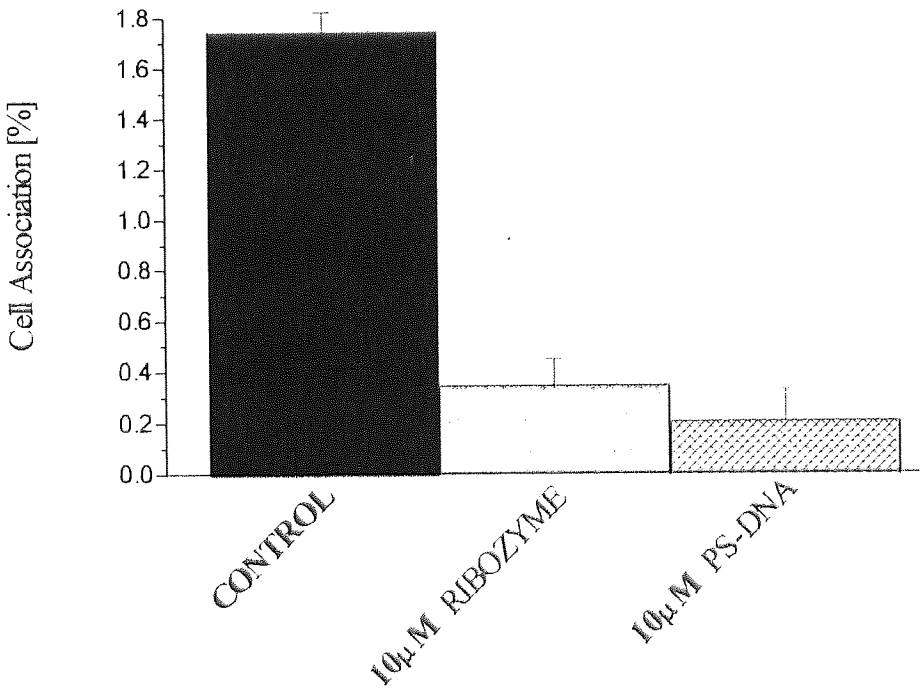

The addition of a 12.5 fold excess of unlabelled ribozyme reduced the percentage of radiolabelled ribozyme which became cell associated by over 80% ($p<0.0001$) after 4

hours. This indicated that the radiolabelled ribozyme was competing with the excess unlabelled ribozyme for cell association, probably by competing for the same uptake or surface binding mechanism. Co-incubation with an excess of PS ODN reduced the percentage of cell associated ribozyme by almost 90% ($P<0.001$). This suggested the presence of competition between the ribozyme and PS ODNs for cellular uptake and / or binding.

Competitive cellular association is considered to be indicative of a specific cell surface binding mechanism (Beltinger *et al*, 1995), which could possibly be mediated by surface proteins or lipids. Since PS ODNs are widely considered to enter cells by either AE or RME (See Section 4.1), the chimeric ribozymes used in these studies may be competing for cellular uptake via one or both of these processes. In previous studies (see Section 4.6.5) PS ODNs were also shown to compete with ribozymes for uptake in A431 cells. However, slightly higher concentrations of the competing PS ODN were used in these previous studies and, therefore, direct comparisons of the competitive effect in the two cell lines cannot be drawn. In U87-MG cells the competitive effect mediated by excess PS ODNs appeared to be slightly more pronounced than the 'self' competitive effect of excess ribozyme addition. However, the actual difference in the extent of inhibition by these competing agents was not significantly different ($P=0.1229$).

6.3.5. *In Vitro* Fluorescence Localisation Studies in U87-MG Cells.

6.3.5.1 Preliminary Studies

U87-MG cells grown on chamber slides as described in section 2.8.7.2 were incubated for 4 hours in serum free media and viewed under the fluorescent microscope. No auto-fluoresence was observed which indicated that fluorescence detected in subsequent studies would be due to the presence of exogenously delivered fluorophores.

Phase contrast microscopy of untreated cells indicated that the appearance and morphology of cells, was similar to that of cells which were incubated with either 5μM FITC labelled chimeric ribozymes, FITC-PS ODNs, 'free' flourescein or FITC. (For example see Figure 6.5). In addition, viable cell counts indicated that treatment with 5μM FITC ribozyme, FITC-ODNs and free fluorescein did not significantly affect viable cell numbers ($P>0.05$) compared with a control sample of cells which were not exposed to fluorescent compounds.

Figure 6.5. Phase Contrast Images of U87-MG cells Incubated for 4 hours in Serum Free media: **[A]** In the Absence of any Fluorescent Compound and **[B]** In the Presence of 5μM FITC-labelled ribozyme (Cells were fixed as described in 2.8.7.2, Magnification × 12.5).

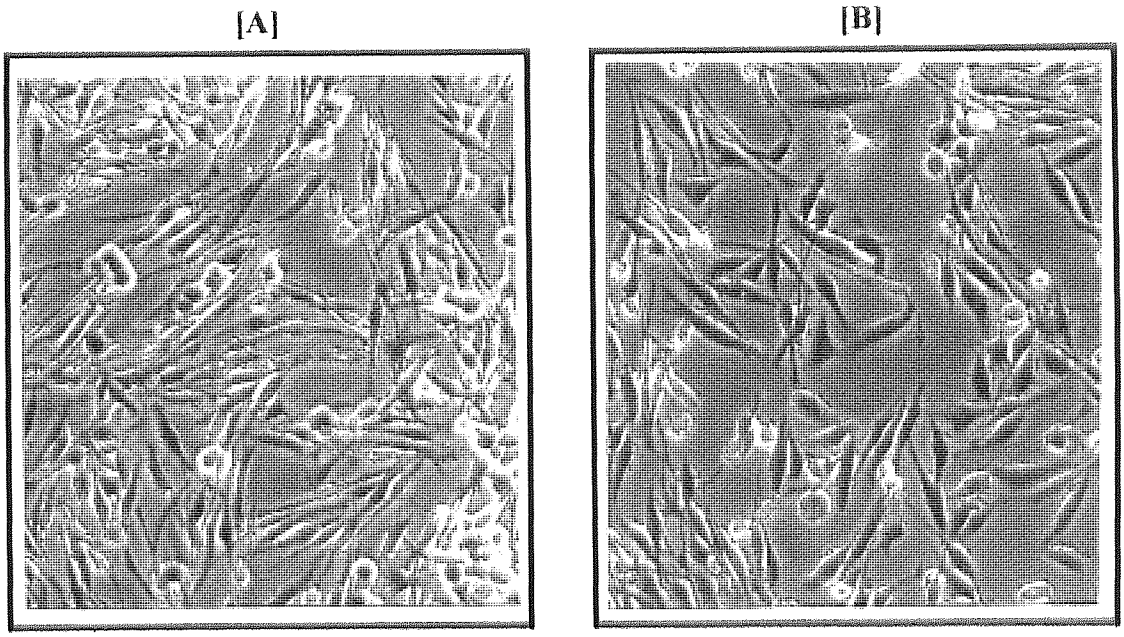

6.3.5.2 Cellular Uptake and Distribution of FITC Labelled Ribozymes and PS ODNs in U87-MG Cells, Compared With Free FITC Label and Free Fluorescein.

The cellular uptake and distribution of FITC labelled ribozymes was compared to that of both free fluorescein and free FITC in U87-MG cells, to provide a control of labelling specificity. Ribozymes or 'free label' were incubated with U87-MG cells at the same concentration (5μM) for 4 hours as described in section 2.8.7. The localisation of an FITC-labelled PS ODN (5μM), of the same nucleotide base sequence, was also assessed using the same method and compared to that of the FITC-labelled ribozyme. In these studies, cells were not fixed after incubation with each agent, but instead they were washed with PBS and immediately viewed and photographed.

Incubation with both the free fluorescein and free FITC label produced an intense fluoresence within U87-MG cells. Patterns of fluoresence distribution were similar following incubation with either fluorescein or FITC (for example, see the photograph of fluorescein distribution; Figure 6.6). Fluoresence was widely distributed throughout the cells and both 'free' labels appeared able to easily penetrate the cytoplasm. A considerable degree of intra-nuclear localisation was also apparent. This pattern of fluoresence was largely expected since these molecules have been shown to diffuse

freely across biological membranes, and thus, penetrate diverse regions of living cells (Lansing-Taylor and Salmon, 1989).

Figure 6.6 Fluoresence Detection of 'Free' Fluorescein Associated with U87-MG Cells. (Magnification × 50, Ilford FP4 black & white film).

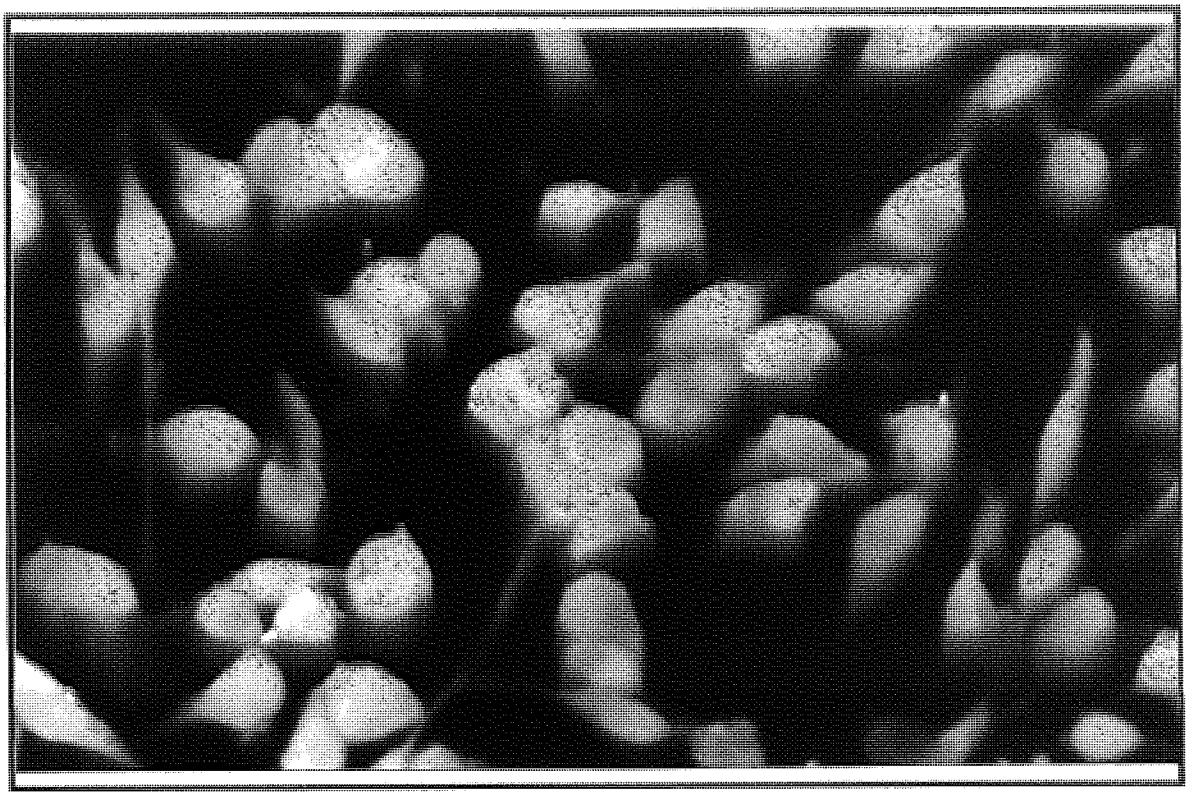

By contrast, the cellular distribution of both FITC-labelled ribozymes (Figure 6.7) and FITC labelled PS ODNs (Figure 6.8) was distinctly different to that of the free fluorescent labels (See Figures 6.6). When U87-MG cells were incubated with identical concentrations of either FITC-ribozymes or FITC-PS ODNs, the majority of fluoresence was localised at the periphery of cells, close to the cell membrane. In addition, a punctate pattern of fluoresence distribution was observed within the cell cytoplasm and this was considered to be indicative of localisation within endosomes (see Section 5.3.1). A similar pattern of subcellular distribution was also observed when FITC-ribozymes were administered to A431 cells (see Figure 5.3).

The intensity of cell associated fluoresence appeared to be considerably lower in cells exposed to FITC-labelled nucleic acids than in cells incubated with the free fluorescent labels. However, the actual levels of fluoresence were not measured quantitatively. Nevertheless, there were clear differences in the cellular localisation patterns of FITC-ribozymes and free fluorophores and this indicated that FITC labels remained attached to ribozymes (and PS ODNs) in the intracellular environment for at least 4 hours.

Figure 6.7. Fluoresence Detection of FITC-Ribozyme Associated with U87-MG Cells *In Vitro*. (Magnification × 50, Ilford FP4 B & W film).

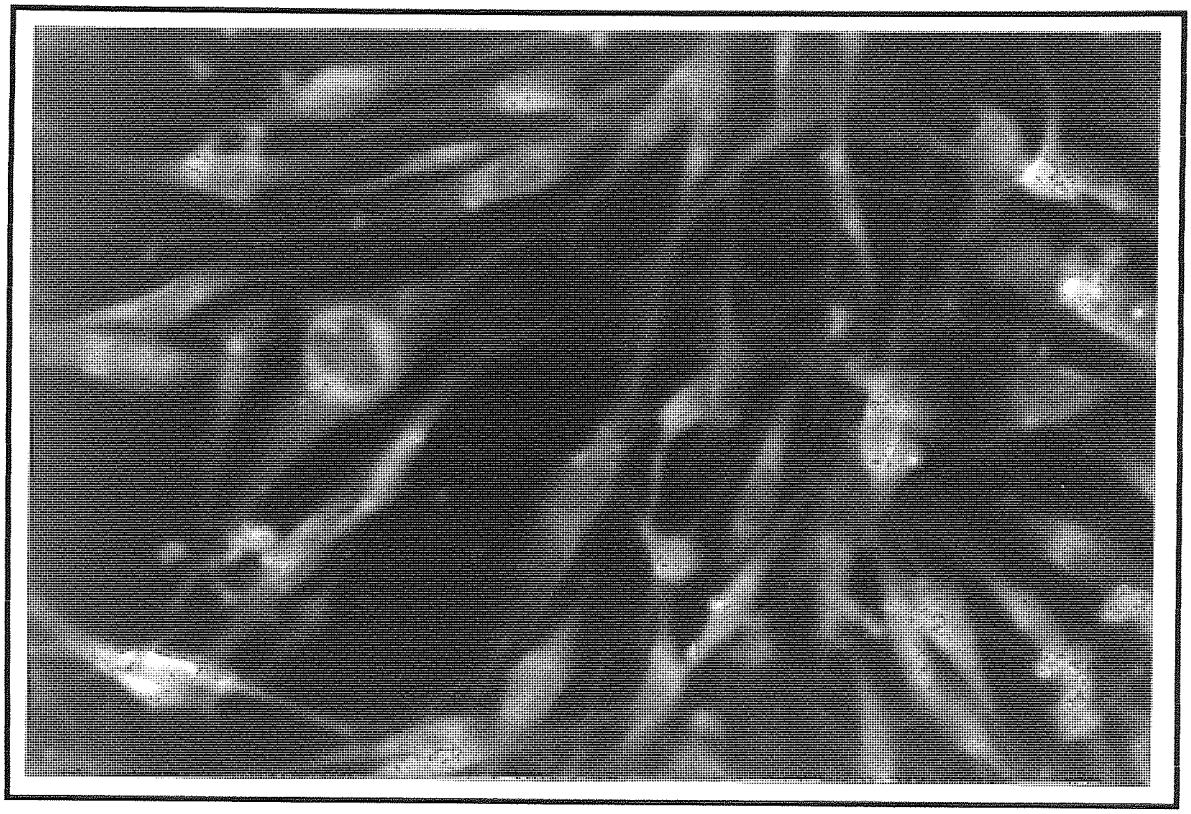

In summary, the *in vitro* studies described so far in this chapter have demonstrated that ribozymes associate with U87-MG cells via an active process, thus making cell entry via passive diffusion an unlikely prospect. The level of ribozyme cell association was significantly higher than that of known markers for FPE, and therefore, it seems unlikely that ribozymes enter U87-MG cells via this mechanism alone. The self-competitive, concentration-dependant and saturable nature of ribozyme association was indicative of a specific cell surface binding mechanism (Beltinger *et al*, 1995). Furthermore, since PS ODNs were able to strongly compete with ribozymes for association in U87-MG cells, a cellular uptake mechanism such as AE or RME was implicated. However, it is possible that the less efficient process of FPE may predominate when more efficient cellular uptake processes become saturated. Fluorescent studies indicated that following uptake, ribozymes demonstrate a punctate pattern of subcellular localisation in U87-MG cells and this is indicative of localisation within endosomes. Localisation within endosomal vesicles would be expected if ribozymes entered U87-MG cells via an endocytic process.

Figure 6.8. Fluoresence Detection of FITC-PS ODN Associated with U87-MG Cells *In Vitro*. (Magnification × 50, Ilford FP4 B & W film).

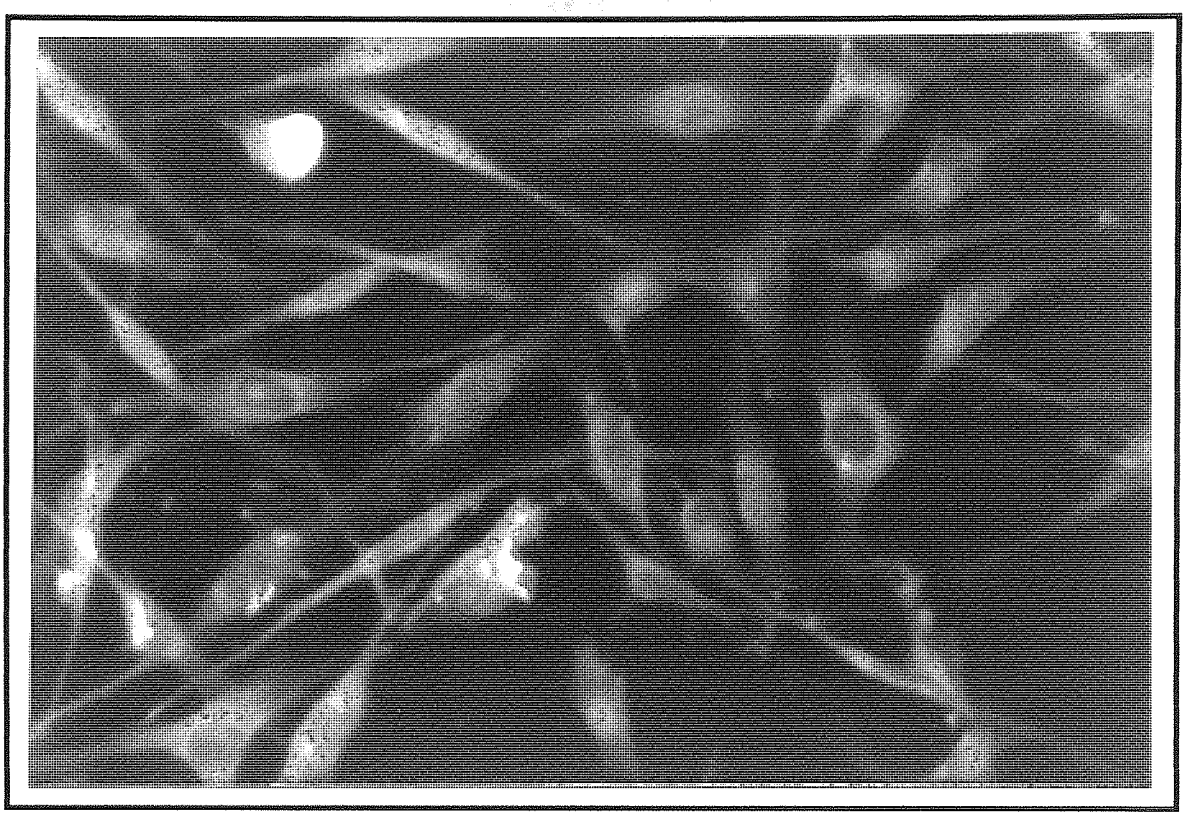

There appear to be many similarities in the mechanism(s) by which stabilised ribozymes and PS ODNs enter both U87-MG cells and A431 cells (see Table 6.1). However, the actual quantities of ribozyme able to enter these cells did appear to be cell line specific (see Section 4.3.10). The differences in association in the two cell lines could reflect variations in the availability of binding sites on the surface of these cells. Alternatively the different levels of cellular association could reflect differences in the intrinsic rate of endocytosis in these cell lines.

Overall, a process of RME and / or AE would offer the most likely explanation of the predominant mechanism by which chimeric ribozymes enter glial cells *in vitro*. Ribozymes appear to share similar uptake characteristics with PS ODNs in these cells and these molecules are also widely considered to enter cells via a process of AE or RME *in vitro* (Rojanasakul, 1996).

Table 6.1. A Comparison of the Cellular Association Characteristics of Chimeric Ribozymes Following Administration to A431 and U87-MG Cells.

Characteristic	A431 Cells	U87-MG Cells
Overall efficiency of cellular association.	Less than 1% of ribozyme was cell associated after 4 hours at 37°C. On average, levels of cell association were 48% lower than in U87-MG cells.	Approximately 1.7% of ribozyme was cell associated after 4 hours at 37°C. Levels of cell association were significantly higher ($P<0.05$) than in A431 cells.
Time profile of ribozyme cell association.	Biphasic profile. The percentage of cell associated ribozyme continued to increase significantly up to 6 hours post-administration.	Biphasic profile. Levels of cell associated ribozyme did not significantly increase after 4 hours post-administration.
Level of cell association compared with fluid phase marker.	Association of ribozymes was 20 to 30-fold higher ($P<0.001$) than that of fluid phase markers at all time points tested.	Association of ribozymes was 20 to 50-fold higher ($P<0.001$) than that of fluid phase markers at all time points tested.
Effect of reduced temperature	Average 54% reduction in levels of cell associated ribozyme at 4°C.	Average 73% reduction in levels of cell associated ribozyme at 4°C.
Effect of metabolic inhibition	Levels of cell associated ribozyme reduced by 58% (on average) in metabolically inhibited cells	Levels of cell associated ribozyme reduced by 77% (on average) in metabolically inhibited cells
Effect of competition by excess PS ODN of the same base sequence	88% reduction in ribozyme association in the presence of a 25-fold excess of PS ODN.	83% reduction in ribozyme association in the presence of 12.5-fold excess of PS ODN.
Concentration dependency of ribozyme cell association	Some saturation of cell association observed when ribozyme concentrations above 1μM were administered.	Saturation of cell association observed at ribozyme concentrations above 0.8μM
Subcellular distribution of fluorescent labelled ribozyme	Punctate pattern of subcellular distribution indicative of endosomal localisation	Punctate pattern of subcellular distribution, again indicating endosomal localisation

6.3.6 *In Vivo* Fluorescent Localisation Studies.

The studies described previously in this chapter provide a useful insight into the mechanism(s) of cellular uptake of ribozymes into glial cells *in vitro*. However, if the ultimate goal of producing a therapy for gliomas is to be achieved, the extent to which ribozymes are able localised to these target cells *in vivo* requires assessment. Using the methods described in Sections 6.2.6 and 6.2.7, FITC-labelled ribozymes were administered to the mouse brain via ICV injection and both sagittal and transverse cryosections were prepared. As a control procedure, free fluorescein label was independently administered to animals and cryosections were prepared in the same manner.

Initial observation of cryosections revealed fluoresence in diffuse areas of the brain, 4 hours post-injection with FITC-labelled ribozymes. This wide distribution of the fluorescent signal was not entirely uniform because fluorescence was mainly confined to non-myelinated fibres throughout the brain (For example see Figures 6.9 & 6.10 which show sagittal sections of the cerebellum). Fluorescence was absent within the myelinated 'white' fibres (which stain dark blue with solochrome cyanine, see Figure 6.10). The lack of penetration of myelinated fibres could possibly be related to the highly lipophillic nature of these regions.

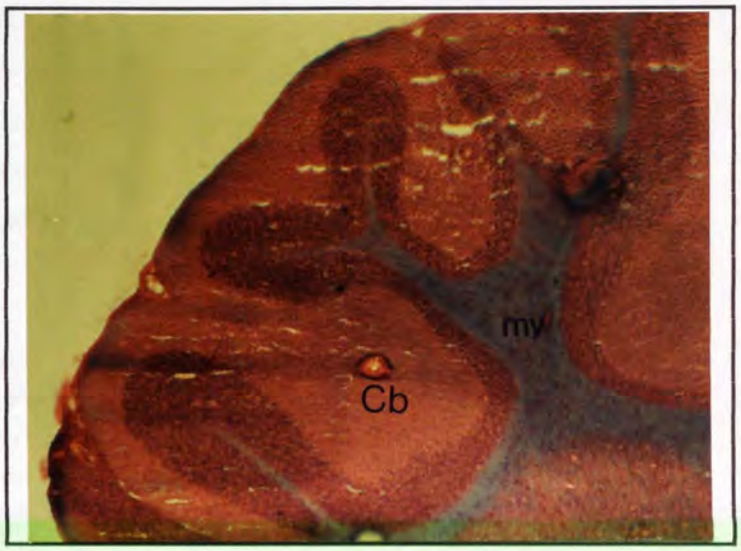

Figure 6.9.
Light Microscope Photograph of a sagittal section of the mouse brain showing the cerebellum. The section is stained for cell bodies (red) and myelin (blue) as described in Section 6.2.8. (Key; myelin (my), cerebellum (Cb) Magnification × 6.25)

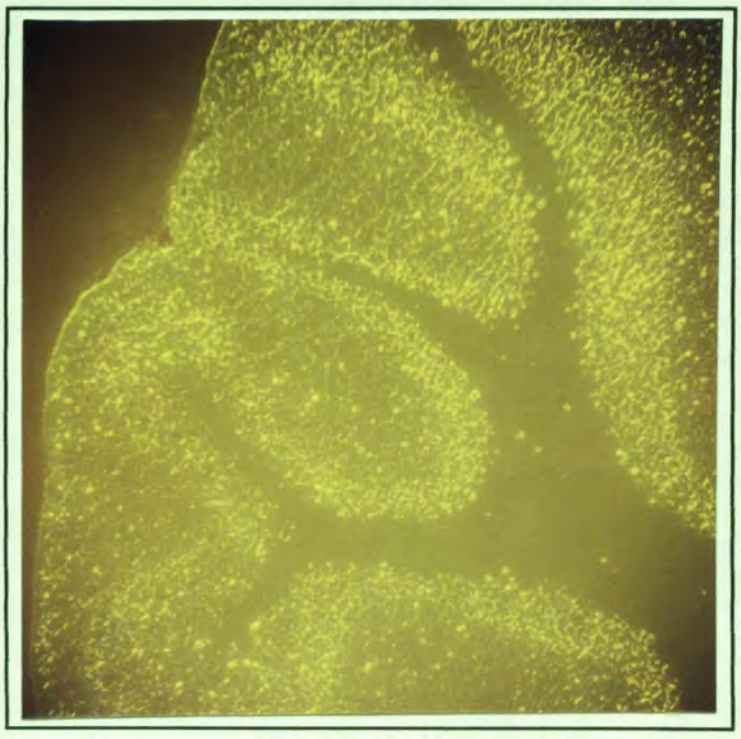

Figure 6.10.
Fluorescent Photo-micrograph of a Sagittal Section of the Mouse Brain showing the Cerebellum.
The cryosection was obtained 4 hours post-injection with FITC-labelled ribozyme and fixed after sectioning with acetone as described in Section 6.2.7. (Magnification × 8.5)

However, in brain sections injected with 'free' fluorescein alone, some 'background' fluoresence could also be detected throughout the brain in non-myelinated fibres, albeit at much lower intensity than that seen in FITC-ribozyme treated cryosections. Therefore, it is only possible to speculate as to whether or not the very generalised distribution of the fluorescent signal, seen in cryosections exposed to FITC-ribozymes, specifically indicated an extensive penetration of the brain by labelled ribozymes.

In a recent study examining the fate of FITC-PS ODNs after ICV injection to the brain a wide, non-uniform distribution of fluoresence was also reported (Zhang *et al*, 1996). In addition, PS ODNs appeared to preferentially localise to non-myelinated regions. In this report, which was conducted over a longer time period (24 hours), it was remarked that the 'background' fluorescence, seen in sections exposed to 'free' fluorescent label, "disappeared" when incubation times in excess of 24 hours were used (Zhang *et al*, 1996).

Figure 6.11. Light Microscope Photograph of a Transverse Cryosection of the Left Cerebral Hemisphere of the Mouse Brain. The cortex and Left Lateral Ventricle (V), with the choroid plexus within (cp) , are Clearly Defined. (Other structures; striatum (str), corpus collossum (cc), lateral septal nucleus (ls)). (Magnification ×6.25).

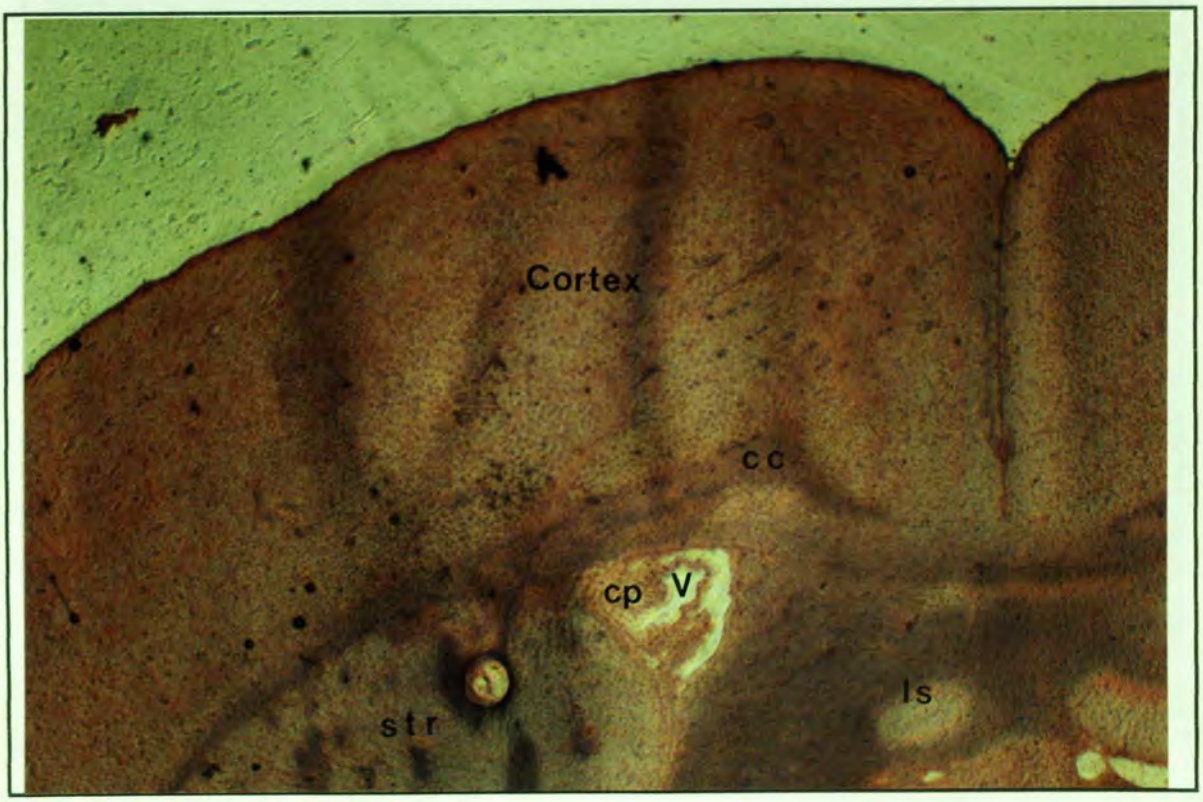

However, in the present study, when the cryosections were viewed at higher magnification, a number of distinct differences became evident when FITC-ribozyme treated samples were compared with 'free' label controls. These are discussed in more detail below and were considered to be indicative of specific ribozyme labelling. For example, the cerebral ventricles (i.e. the site of injection) were identified within cryosections by comparison with sequentially sectioned, stained cryosections. Figure 6.11 demonstrates a phase contrast photomicrograph of a transverse section of the left hemisphere of the brain, which clearly shows the lateral cerebral ventricle.

In cryosections obtained from FITC-ribozyme treated mice, a high intensity of fluoresence was frequently observed within the choroid plexus, situated within these ventricles (See Figure 6.12). The choroid plexus is the term used to describe blood capillaries within the ventricles of the brain. Interestingly, certain types of glia, such as astrocytes, are frequently associated with the choroid plexus (Ford, 1975, Nauta and Feirtag, 1986).

Figure 6.12. Fluorescent Photomicrograph of the Left Lateral Ventricle of the Mouse Brain, 4 hours after the Administration of FITC-Ribozyme by Intracerebroventricular Injection. (Magnification x 25)

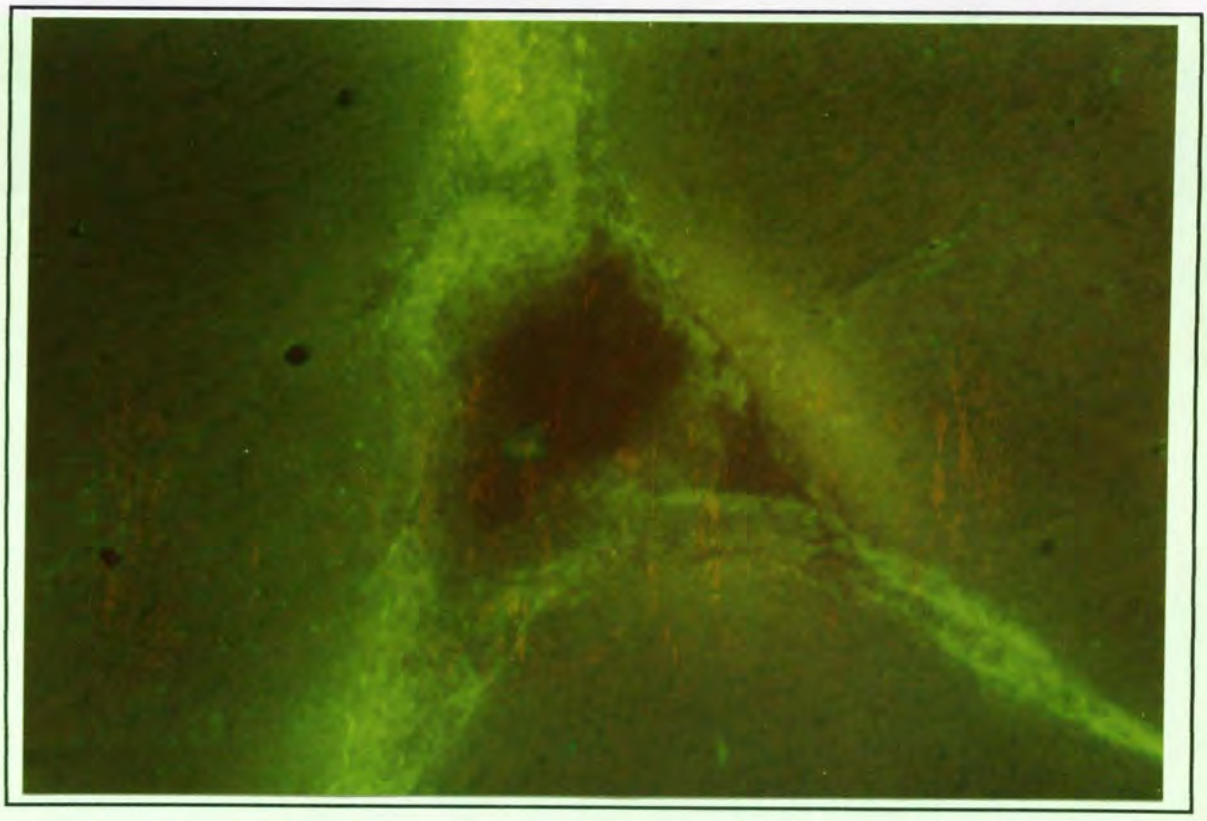

By comparison, an examination of the choroid plexus / ventricles of cryosections obtained from brains injected with free fluorescein alone, did not show any particular increase in the fluorescent signal in these regions (See Figure 6.13).

Figure 6.13. Fluorescent Photomicrograph of the Left Lateral Ventricle of the Mouse Brain, 4 hours after the Administration of Free Fluorescein by Intracerebroventricular Injection. (Magnification x 12.5)

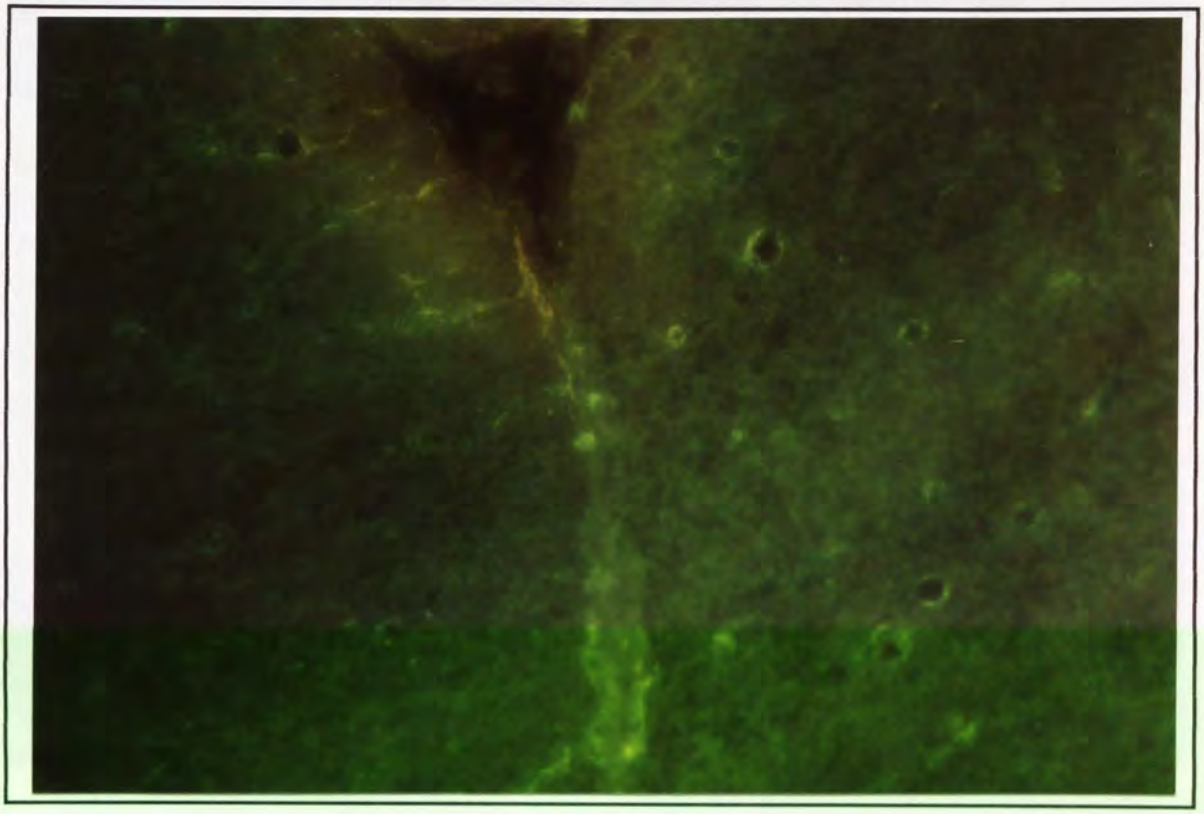

A high signal intensity associated with the choroid plexus alone, would not indicate that FITC-ribozymes injected into the ventricles were able to depart these structures and reach other areas of the brain. However, further examination of the areas surrounding the lateral ventricles revealed that, in certain areas of the cortex in particular, high signal intensities were present. In addition, the fluoresence in these areas demonstrated a highly punctuated pattern of distribution (See Figure 6.14).

Other investigators have noted similar patterns of distribution when fluorescent labelled PS ODNs have been injected into the cerebral ventricles and have concluded that this pattern of distribution is consistent with localisation within cell bodies and dendritic processes (Piwinca-Worms, 1994, Zhang *et al*, 1996). Other investigators have concluded that antisense ODNs are taken up by a wide variety of cell types including neurons, macrophages and glial cells (astrocytes) (Yee *et al*, 1994).

Figure 6.14. Photomicrographs of an area of the Striatum and Cerebral Cortex Close to the Left Lateral Ventricle, 4 hours after the Administration of FITC-labelled Ribozyme. **[A]** Fluorescent Photomicrograph Showing Punctuated Pattern of Distribution. **[B]** Phase Contrast Photomicrograph of the same Section with Striatum (str) and Cortex labelled. (Magnification x 25)

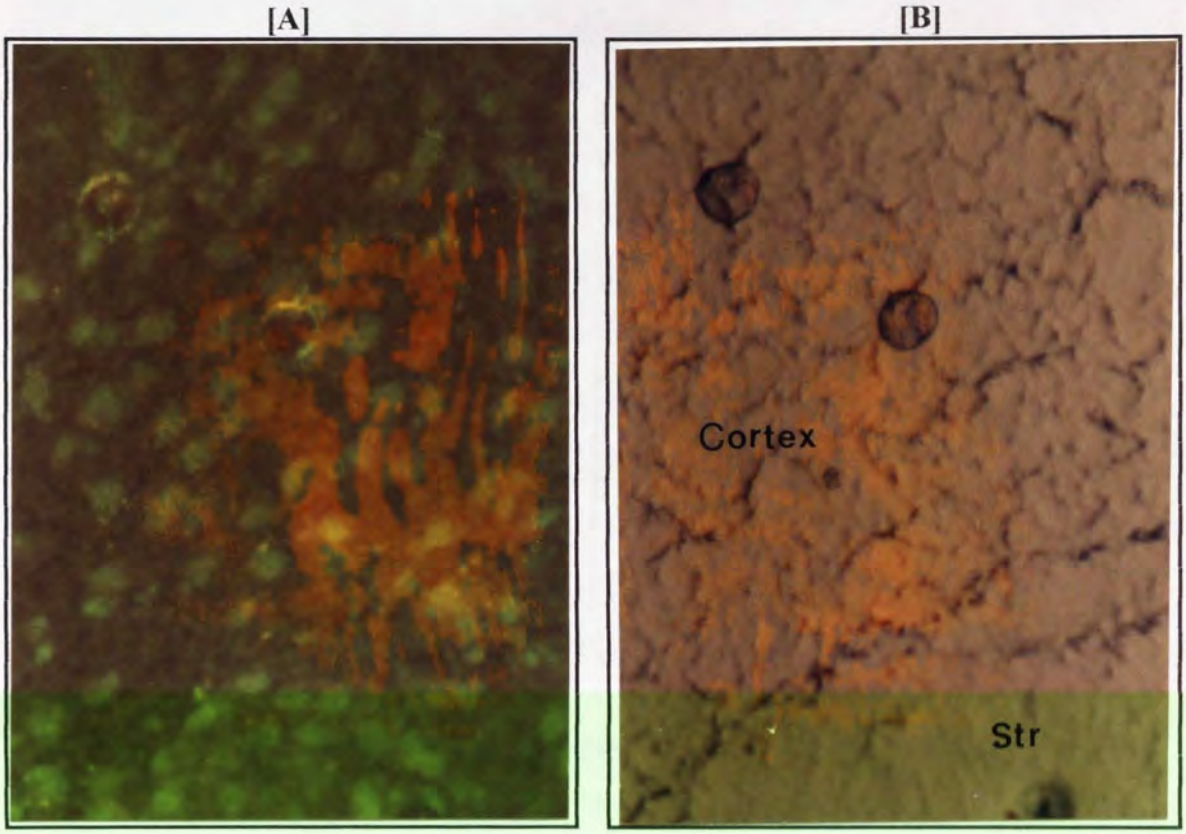

In some cryosections, the punctuated pattern of fluoresence appeared to radiate from the lateral ventricles into the cortex for several millimetres, but appeared unable to penetrate the outermost layers of the cortex close to the surface of the brain (for example see Figure 6.15).

The anatomical structure of the cortex is made up of highly distinct layers, of different cell types (Nauta and Feirtag, 1986). Therefore, the lack of penetration to the outer layers could be due to poor penetration of particular cell types. For example, the outermost layer of the cortex , the plexiform layer, is usually made up of closely packed dendrites and axons, with neuronal cell bodies more or less absent (Nauta and Feirtag, 1986). Another possible explanation could be that the extent of the penetration seen, represented the limit to which FITC-ribozymes were able to migrate from the ventricles within 4 hours.

Figure 6.15. Fluorescent Photomicrograph of the Cerebral Cortex close to the surface of the brain, 4 hours after the Administration of FITC-Labelled Ribozyme by ICV Injection. (Magnification x 25)

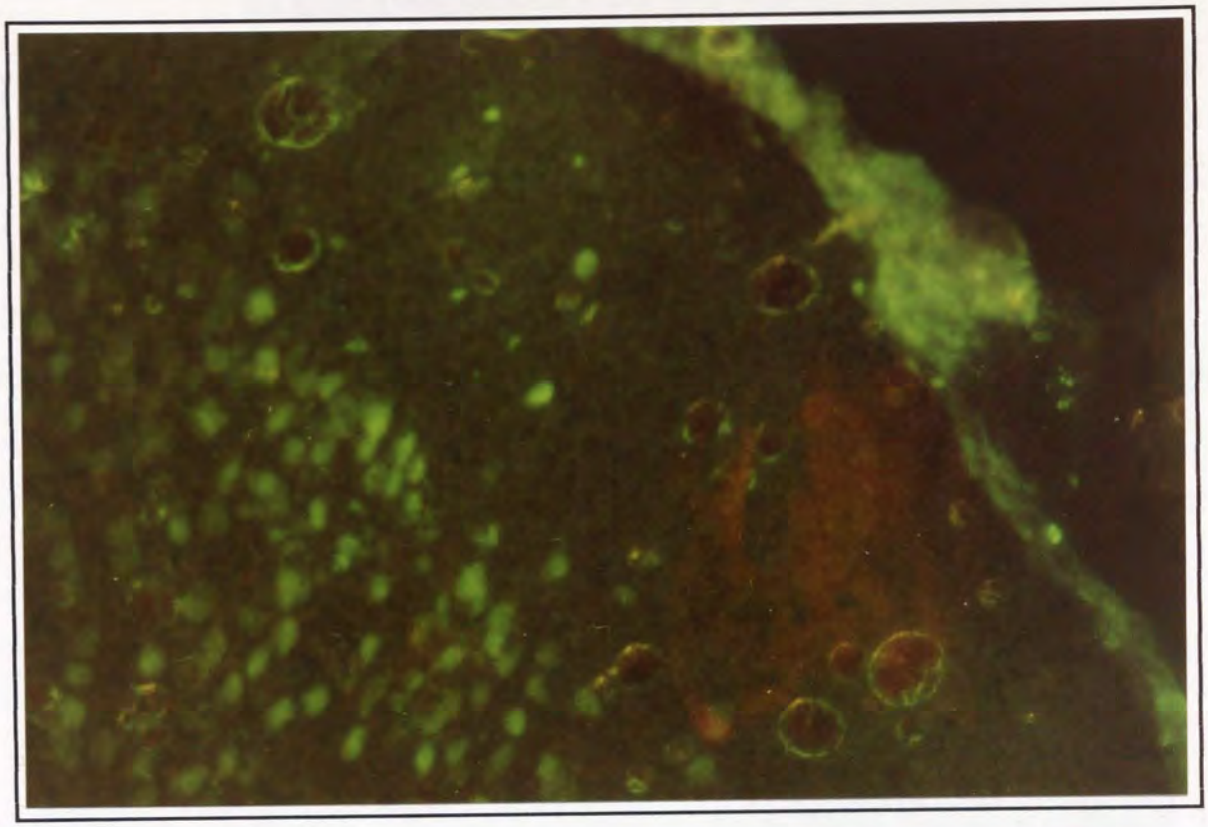

In some cryosections the outer surface of the cerebral hemispheres demonstrated a strong fluorescent signal (see Figure 6.16). This probably represented FITC-labelled ribozyme which had flowed around the brain in the subarachnoid space. The subarachnoid space is continuous with the ventricles and contains cerebro-spinal fluid (CSF), which coats the outer surface of the brain (Sherwood, 1989). The surface of the brain itself, beneath the sub-arachnoid space, is encapsulated by the pial-glial membrane. This, as its name suggests, is a continuous limiting membrane which has associated glial cells (Nauta and Feirtag, 1986). FITC-labelled ribozymes which were associated with the outer surface of the brain, perhaps with the pial-glial membrane, seemed able to penetrate the cerebral cortex beneath, as demonstrated in Figure 6.16. The punctuated pattern of distribution, thought to represent association with cell bodies, was evident in the outer layers of the cerebral cortex just beneath the surface in these cryosections.

Figure 6.16. Fluorescent Photomicrograph Showing the Surface of the Left Cerebral Hemisphere, 4 hours after ICV Injection of FITC-Labelled Ribozyme. Note the Intensity of Fluoresence at the Outer Surface of the Brain. (Magnification × 25).

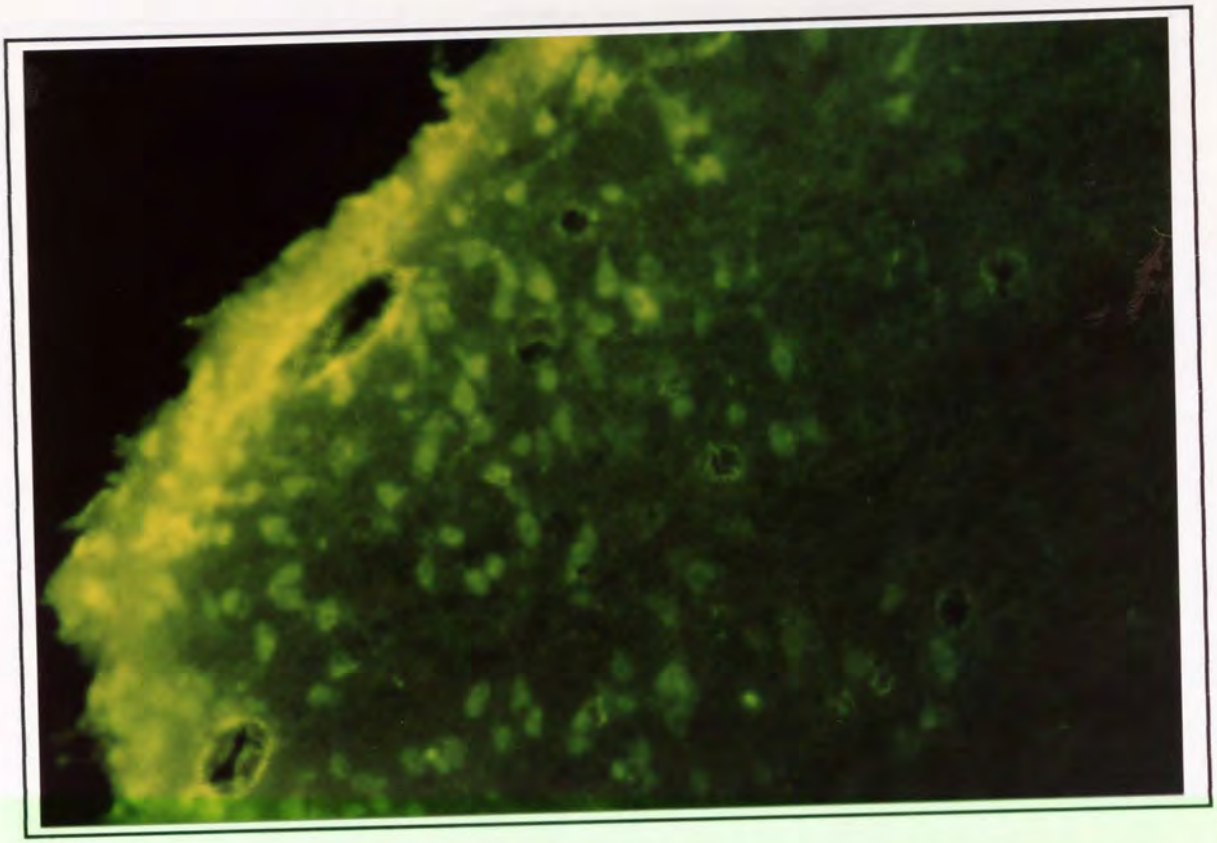

In contrast, cryosections obtained from the brains injected with 'free' fluorescein alone, did not demonstrate any increased fluoresence intensity within regions such as the cerebral cortex or the striatum. Moreover there was no evidence of the punctuated pattern of distribution (see Figure 6.17). The fluorescent signal did appear to be slightly more intense at the outer surface of the brain in some of the control cryosections, although there was no evidence of any punctuated pattern of distribution beneath the surface of the brain.

Darker patches representing the myelinated fibres within the striatum can be seen with careful viewing in Figure 6.17. However, there is no evidence of the apparently cellular distribution, seen in the FITC-ribozyme treated samples. Overall, this would appear to indicate that specific labelling of ribozymes was observed in cryosections where the punctuated pattern of distribution was seen.

Figure 6.17. Fluorescent Photomicrograph of the Left Cerebral Hemisphere of the Mouse Brain, 4 hours after the Administration of Free Fluorescein by Intracerebroventricular Injection. (Magnification x 12.5)

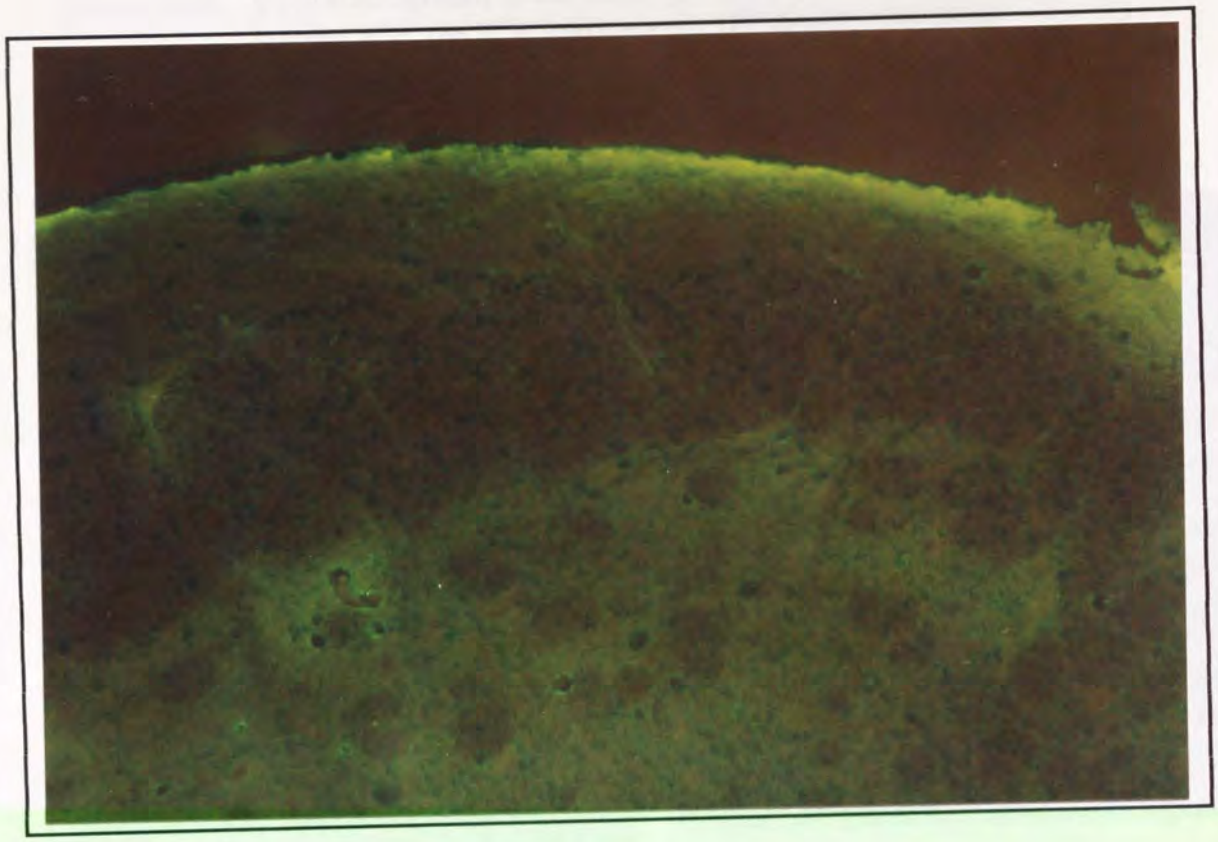

A small number of cryosections were prepared from the brains of mice injected with FITC-labelled PS ODNs of the same base sequence as the ribozyme (see Section 6.2.1). During microscopy, particular attention was focused upon the cerebral cortex and striatum, in regions close to lateral cerebral ventricles. Again, punctuated patterns of fluoresence distribution were evident in these areas following administration of the FITC-PS ODN (See Figure 6.18). Patterns of distribution were similar to those observed in the animals injected with the FITC-ribozyme and appeared to demonstrate localisation within cell bodies. In addition, there appeared to be no fluorescent signal within myelinated fibres. Other investigators have observed these punctuated patterns of distribution when the fate of fluorescent labelled PS ODNs has been examined *in vivo,* following ICV injection to the mouse brain (Zhang *et al*, 1996).

When compared with the control samples, obtained from brains injected only with the free fluorescent label, it would appear that specific labelling of both FITC-ribozymes and PS ODNs was observed within punctuated, cellular structures in the brain. This indicates that following the injection of ribozymes to the cerebral ventricles, ribozymes are able to penetrate the surrounding tissue and become associated with

specific cell types. However, the exact identity of these cell types is uncertain from these results.

Figure 6.18. Photomicrographs of the Cerebral Cortex of the Mouse Brain, 4 hours after the ICV Injection of FITC-labelled PS ODN. **[A]** Close to the lateral ventricle. **[B]** The outer layers of the pre-frontal cerebral cortex. (Magnification x 25)

[A] **[B]**

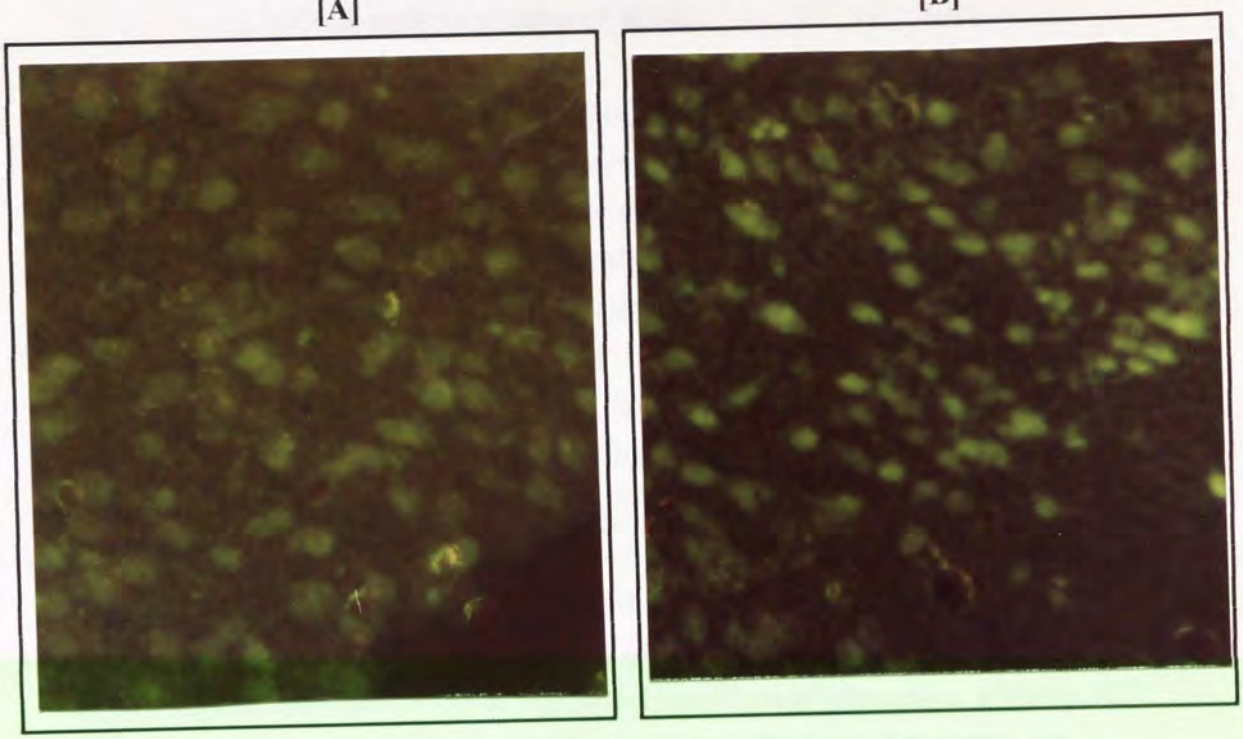

For the purposes of this research, evidence of specific localisation within the glia would be desirable. The glia are the supporting cells of the entire central nervous system (the term glia actually means 'glue') and are thought to be 10 times more numerate than neurons (Nauta and Feirtag, 1986). Therefore, ribozymes are almost certainly able to access areas of the brain where these cells are present, even though the apparently cellular localisation observed may not be within glial cells. In addition, strong fluorescent signals were observed in regions such as the choroid plexus and pial-glial membrane, which are known to have associated populations of glial cells.

6.4. CONCLUDING REMARKS.

In the studies outlined in this chapter, the cellular association of ribozymes with glial cells was examined, both in cell culture and in an animal model. The U87-MG (human glioblastoma) cell line was used to characterise the association of ribozymes with glial cells *ex vivo*. Overall, the mechanistic trends appeared to mirror those observed previously in this report, when chimeric ribozymes were administered to A431 cells

(see Chapters 4 & 5). This implied that ribozymes entered both cell types via similar mechanisms, which were consistent with AE or RME. However, the relative efficiency of these uptake processes appeared to cell-line specific, since a greater proportion of added ribozymes associated with U87-MG cells per unit time. This could reflect differences in the intrinsic rates of endocytosis present in each cell type. Alternatively, it could be due to differences in the availability of particular binding sites on the cell surface, such as proteins or lipids.

Subcellular localisation studies with FITC-labelled ribozymes and PS ODNs indicated a punctate pattern of subcellular distribution in U87-MG cells, which is considered to be indicative of localisation within endosomal vesicles (Rojanasakul, 1996). Again this correlated with the findings of fluorescent microscopy and immuno-electron microscopy studies performed in the A431 cell line (see Chapter 5).

Following ICV injection of FITC-labelled ribozymes to the mouse brain, a fluorescent signal could be detected in diverse areas of the brain substance, although fluorescence was absent within myelinated 'white' fibres. The most intense fluorescent signals were detected at the choroid plexus within the cerebral ventricles (i.e. at the site of administration). However, closer examination revealed strong fluorescent signals within areas of tissue adjacent to the cerebral ventricles, such as the striatum and the cerebral cortex. This indicated that significant quantities of ribozymes, administered via ICV injection, were able to depart the cerebral ventricles and penetrate the surrounding tissue. Moreover, a highly punctuated pattern of distribution was observed within the striatum and cortex, which appeared to represent cellular localisation of FITC-labelled ribozymes in these tissues. This pattern of distribution could represent localisation within cell bodies and dendritic processes (Piwinca-Worms, 1994, Zhang *et al*, 1996). However, the exact identity of the cell-types to which ribozymes became localised was uncertain. With regard to the glia, these cells are 10 times more numerate within the brain than neurons and are considered to be the supporting elements of the entire central nervous system (Nauta and Feirtag, 1986). Therefore, it would appear that ribozymes are almost certainly able to access areas of the brain where the glia are present, even though the patterns of localisation seen, may not specifically indicate uptake by the glia. Overall, the results of the *in vivo* studies outlined in this chapter indicate that locally administered ribozymes may be capable of penetrating target cells within the brain. Especially if these cells are present within the tissue surrounding the site of administration. Therefore it may be possible to use anti-oncogene ribozymes as an adjunct to surgery, in order to limit tumour regression in glioblastoma multiforme (see Section 1.6).

CHAPTER SEVEN

STRATEGIES TO ENHANCE THE CELLULAR DELIVERY OF HAMMERHEAD RIBOZYMES

7.1. INTRODUCTION.

As a consequence of the poor cellular uptake and inappropriate localisation of modified ribozyme constructs, it would appear that either high concentrations must be administered to cells, or alternatively strategies which can enhance delivery will be required, if ribozymes are to fulfil their potential as therapeutic agents. The former option may be viable for some therapeutic applications, especially those involving localised administration. Nevertheless, for many clinical conditions the repeated localised administration of high concentrations of ribozyme is not a viable prospect and, therefore, strategies to enhance cellular delivery are required.

In this chapter, two methods of improving the cellular delivery of hammerhead constructs have been investigated. The first technique which was investigated for the exogenous delivery of ribozymes, was their attachment to a carrier molecule which could potentially enhance cellular targeting and uptake via receptor mediated endocytosis (see Section 1.4.2.4). The transferrin receptor (for review see Friden, 1993), which transports iron-bearing transferrin into cells via receptor mediated endocytosis, was investigated as a potential carrier system by which ribozymes could be delivered to cells. This receptor, a 180 kDa dimeric transmembrane glycoprotein, has been reported to efficiently internalise low molecular weight drugs and antisense ODNs when complexed with the natural transferrin ligand (Citro *et al*, 1992, Wagner *et al*, 1994) or when conjugated to anti-transferrin receptor antibodies (Boado, 1995, Walker *et al*, 1995). In this report, chemically-stabilised ribozymes have been conjugated to the human monoclonal transferrin receptor-antibody (RVS-10) in an attempt to improve cellular association *ex vivo*.

An alternative approach was also investigated, using two commercially available cationic liposome formulations (see Section 1.4.2.5), which were evaluated for their ability to improve the delivery of chimeric ribozymes *ex vivo*. Cationic liposomes demonstrate several properties which are useful for the delivery of polynucleotides (for discussion see Section 1.4.2.5. and also Felgner *et al*, 1994, Zelphati and Szoka,

1996). The immediate aim of using cationic lipids in this report was to devise a method of delivering ribozymes to A431 cells at relatively high concentrations which was non-toxic and reproducible. Such a method could be subsequently used during *ex vivo* efficacy studies, which would probably require the delivery of high concentrations of ribozymes to cells.

Most cationic lipid preparations are formulated as lipososmes containing two lipid species; a cationic amphiphile and a neutral phospholipid such as dioleoyl-phosphatidylethanolamine (DOPE) (Felgner *et al*, 1994). To allow ease of reproducibility in future studies, commercially available cationic liposome formulations have been used; Lipofectin® (a 1:1 (w/w) formulation of DOTMA and DOPE, Life Technologies Ltd.) and Lipofectamine® (a 3:1 w/w formulation of DOSPA and DOPE, Life Technologies Ltd.). These formulations were chosen because they have been used previously by other workers to successfully deliver antisense ODNs to cultured cells (see Life Technologies Technical Bulletins Numbers 27 & 28).

Ribozymes were complexed with these liposome formulations at a variety of different cation:anion charge ratios. The cellular uptake of these complexes was examined in A431 cells and the ability of these formulations to protect hammerhead ribozymes from nuclease digestion was also examined. In addition the particle size of these formulations was measured in an attempt to describe the optimal particle size and charge ratio required for ribozyme delivery to A431 cells.

7.2. MATERIALS AND METHODS.

General materials and methods used in this chapter are outlined in Chapter 2. Ribozyme and ODN synthesis, purification and labelling, polyacrylamide gel electrophoresis and cell culture techniques are all described in detail in Chapter 2. Any alterations or additions to these methods are noted in the sections below.

7.2.1 Preparation of Nucleic Acid Sequences.

Hammerhead ribozymes constructs based on a 37-mer sequence (EGFR-65, see Section 3.3.3.1), targeted against an untranslated region close to the 3' end of the human EGFr mRNA (see Section 4.2.1), were synthesised, internally radiolabelled and purified as described in Sections 2.5.3 & 4.2.1. Site-specific chemical modifications were introduced into the structure of chimeric hammerhead ribozymes

during synthesis, to produce the chimeric construct depicted in Section 5.2.1 and Figure 4.1.

Where the attachment of antibody molecules to the ribozyme was required, two different sections of this chemically modified ribozyme were synthesised separately, for use in the internal radiolabelling reaction (see Sections 2.5.3. and 4.2.1). An 8-mer, fully 2'-O-methylated section from the 5'-terminus of the ribozyme sequence (5'-UGUGUGUC-3') was synthesised (N.B. this 8-mer did not contain any unmodified ORNs). The 5'-end C_6 thiol modifier was then attached to this 8-mer section as described in Section 2.5.6. The 8-mer section bearing the C_6 thiol modifier could then be used as an 'acceptor' molecule in the internal radiolabelling reaction (see Figure 4.1). The 'donor' sequence for the internal radiolabelling reaction, comprised the remainder of the hammerhead molecule (i.e. 5'-u**GA** u**G**a ggc cga aag gcc **G**aa **A**cu g*AA C*-3', see Section 5.21 for nomenclature), which was synthesised as described in section 2.5.3.

Figure 7.1. Diagram Showing the Structure of the Thiol-Modified Chimeric Hammerhead Ribozyme Used for the Preparation of Ribozyme-Antibody Conjugates.

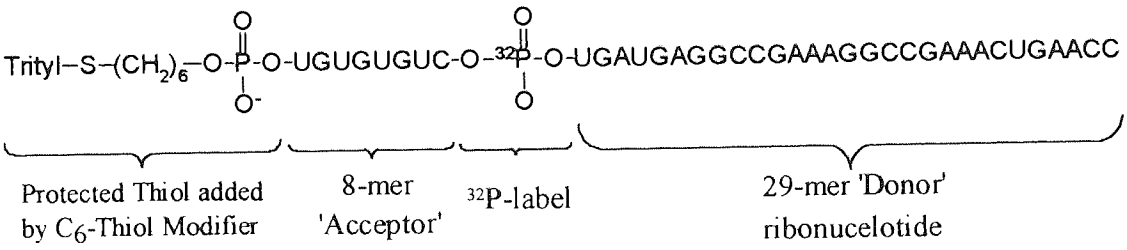

This 'donor' sequence and the 8-mer 'acceptor' sequence (bearing the 5'-end C_6 thiol modifier) were ligated as described in section 4.2.1 to produce a 37-mer internally radiolabelled hammerhead ribozyme bearing a C_6 thiol modifier group at the 5'-terminus (see Figure 7.1). This molecule was separated from unreacted sequences by 20% PAGE as described in Section 2.2.2 and was subsequently used in studies examining the attachment of antibody molecules to the ribozyme (see Section 7.2.3).

7.2.2. Cell Culture and Cell Association Studies.

A431 cells were maintained and seeded for cell association studies as described in Section 2.7. In all cell association studies, additional wells were seeded with cells and counted during experiments as described in Section 2.7.2 to allow data to be

normalised to cell number. Cell association studies were routinely performed as outlined in Section 2.8 but any variations to these methods are noted in the relevant sections below.

7.2.3. Preparation of Ribozyme-Antibody Conjugates.

Antibody molecules were conjugated to the synthesised thiol-modified ribozymes in a two step reaction which is demonstrated in Figure 7.2. The conjugation reactions and the subsequent characterisation of the conjugate (see Sections 7.2.3.1 to 7.2.3.3) were performed by Dr. Nadia Normand (Aston University), whose assistance is kindly acknowledged here. Ribozyme-antibody conjugates were then used in the cell association studies (see Section 7.2.3.4) described in this chapter.

7.2.3.1. Derivatisation of Monoclonal Antibodies with the Heterobifunctional Cross-Linker; SMCC.

Mouse-anti-human transferrin receptor antibody (Clone RVS-10 (IgG1 subclass), Biogenesis, UK) or a control mouse-anti-human IgG (2-4mg) (Sigma, UK) were diluted with 50mM phosphate buffer (pH 8.0) to a volume of 2.5mL. The heterobifunctional cross linker, succinimidyl 4-(maleimidomethyl) cyclohexane-1-carboxylate (SMCC) (0.05M) in dimethylformamide (DMF) solution was added to the antibody solutions. The reaction mixture was incubated for 90 minutes at room temperature in the dark. Excess SMCC was removed by gel filtration on Sephadex G-25 (3cm x 1cm column, Pharmacia Biotech Ltd) in 50mM phosphate buffer (pH 6.0), containing 0.1M NaCl and 5mM EDTA. The resulting concentration of antibodies was determined according to the method of Kuijpers *et al* (1993) by measuring UV absorbance at 280nm (1mg/mL = 1.4 OD units).

7.2.3.2. Conjugation of Thiol Modified Radiolabelled Ribozyme to SMCC-Modified Monoclonal Antibodies.

Deprotected 5'-end thiol modified internally [^{32}P] radiolabelled chimeric ribozymes were dissolved in 1mL of the reaction buffer at pH 7.0 (50mM phosphate buffer, 0.1M NaCl and 5mM EDTA) which had been thoroughly de-gassed with nitrogen and filtered using a 0.2μm syringe filter (Sartorius, UK). 750μg of the SMCC-derivatised monoclonal antibody (either transferrin receptor antibody or a control human IgG) was added to the ribozyme solution in 1mL of the same reaction buffer and left overnight at 4°C. Unreacted maleimide groups introduced by the SMCC on the antibody were blocked with 0.01M cysteamine for 2 hours at room temperature. The

conjugate was purified by gel filtration on sephadex G-25 (1.6cm x 20cm column, Pharmacia Biotech Ltd) and eluted in 50mM phosphate buffer (pH 7.4), containing 0.25M NaCl which had been filtered using a 0.2μm syringe filter (Sartorius, UK). The first 1-2mL fraction which was eluted from the column contained the purified conjugate.

Figure 7.2. Schematic Diagram Showing the Synthesis of Monoclonal Antibody-Ribozyme Conjugates

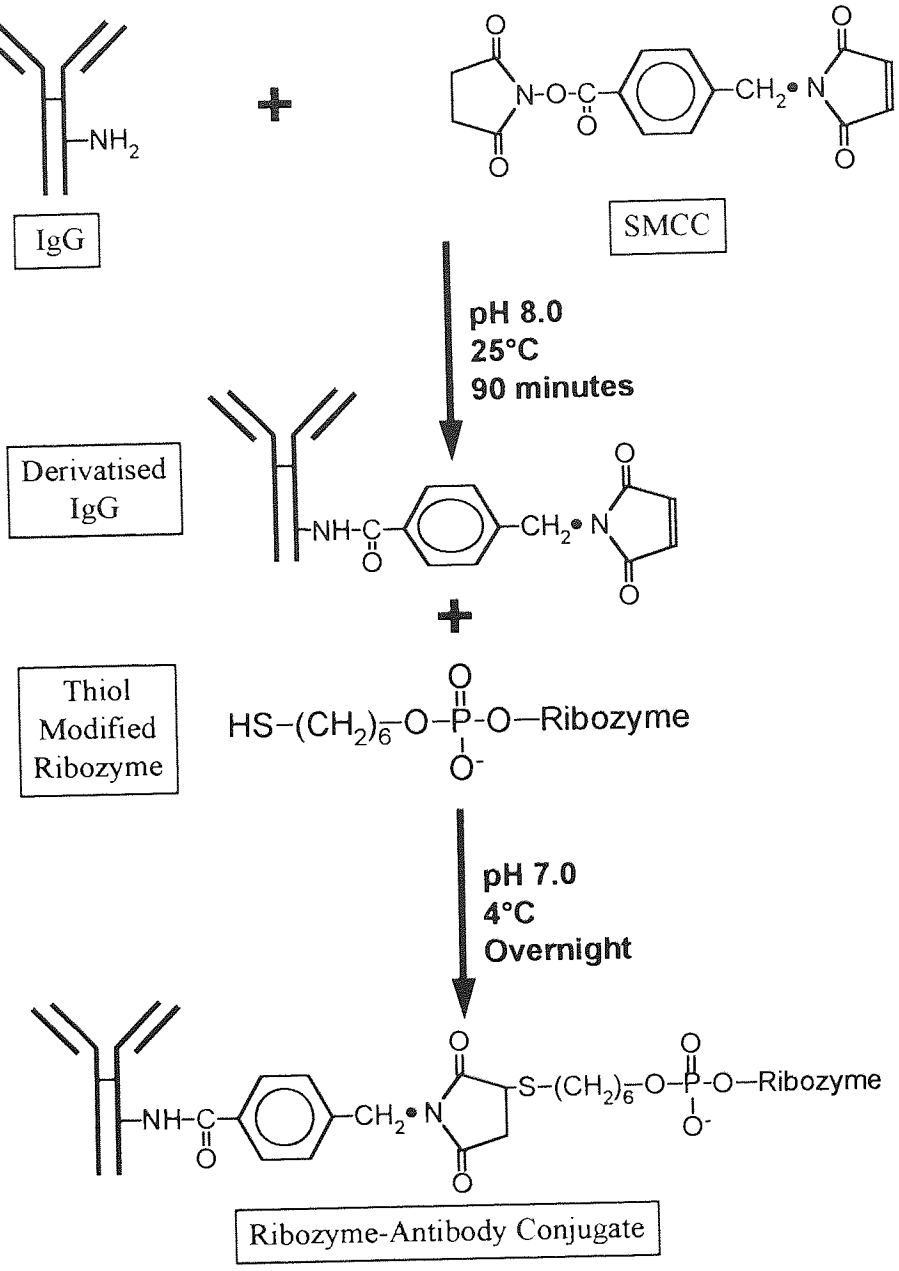

7.2.3.3. Characterisation of Ribozyme-Antibody Conjugates.

The number of ribozyme molecules conjugated to the transferrin receptor antibody was quantified spectrophotometrically by determination of the UV absorbance of the

conjugate at 260nm and at 280nm. The degree of conjugation was then derived from the A260 / A280 ratio using the method of Kuijpers *et al* (1993). To confirm the composition of the ribozyme-antibody conjugates (i.e. to confirm that the ribozyme was attached to the antibody), the purified samples were run on 10% SDS-PAGE gels for 3 hours according to the method of Sambrook *et al*, 1989. The relative mobility of conjugate samples was compared with that of unconjugated ribozyme and 'free' [^{32}P]-γ-dATP (ICN Biomedicals, UK). The relative mobility of conjugate samples incubated with Proteinase K (1.5 units / mL) for approximately 2 minutes at 37°C ([P-2308] molecular biology grade, Sigma Chemicals, UK), which is non-specific protease enzyme capable of digesting antibody molecules (Sambrook *et al*, 1993), was also assessed. Radioactive species were detected by autoradiography as described in Section 2.2.3. Scanned autoradiograph images were obtained using a UVP Transilluminator with multi-focus camera attachment, linked to an IBM PC486 computer running 'UVP Gel-Works' (Synoptics Ltd. Upland, USA) analysis and imaging software (see Section 2.2.4).

7.2.4. Cellular Uptake Studies Involving Ribozyme-Antibody Conjugates.

The cellular uptake properties of the transferrin receptor-ribozyme conjugate were evaluated in the A431 cell line, which expresses both the transferrin and EGFr receptors (see Section 2.7.4). For uptake experiments, cells were seeded as described in section 2.7.4 and incubated (24 hours post-seeding) with either the internally radiolabelled ribozyme-antibody conjugates or internally radiolabelled (unconjugated) ribozyme alone, in serum free media as described in Section 2.8.1.

For competition studies the non-derivatised anti-transferrin receptor antibody (RVS-10. Biogenesis, UK) was prepared at a 5-molar excess in serum-free media. Alternatively a 100μM solution (see Stein *et al*, 1984) of monensin (Sigma, UK [M-5273]) in serum-free media was prepared from a concentrated stock solution of monensin dissolved in Analar grade methanol (Fisons, UK). Competing antibody or monensin were pre-incubated with cells in ice-cold serum-free medium for 15 minutes, before re-warming to 37°C. Cellular association studies were then initiated using serum-free media, which was also supplemented with the relevant agent.

In all experiments, following the required incubation period, A431 cells were washed four times with 1mL PBS as described in Section 2.8.1. Cells were then lysed with 3% v/v Triton X-100 and cell associated radioactivity was determined by liquid scintillation counting as described in Section 2.2.4. Uptake studies were performed at either 4°C or at 37°C as described in Section 2.8.4.

7.2.5. Complexation of Hammerhead Ribozymes with Cationic Liposomes.

Lipofectin® reagent (a 1:1 (w/w) formulation of DOTMA and DOPE, equivalent to 0.474mg / mL of DOTMA) and Lipofectamine® reagent (a 3:1 w/w formulation of DOSPA and DOPE, equivalent to a 1.710mg / mL of DOSPA) were obtained from Life Technologies Ltd, Paisley, UK. These liposome formulations (stored at 0-4°C) were vortexed for 2 minutes, sonicated (twice) for 5 minutes and centrifuged for 1 minute at 2,000 r.p.m. in polypropylene microcentrifuge tubes prior to use (see Life Technologies Technical Bulletins Numbers 27 & 28). In all experiments, cationic:anionic (- / +) charge ratios were calculated on the basis that each molecule of the cationic lipid DOTMA carried a net charge of +1 (see Figure 7.3) and each molecule of the cationic lipid DOSPA carried a net charge of +5 (see Figure 7.4). The lipid DOPE was assumed to be neutral (Lewis *et al*, 1996).

Figure 7.3. The Chemical Structure of the Cationic Lipid DOTMA (Adapted from Felgner *et al*, 1987). [Molecular weight ≈ 669.5]

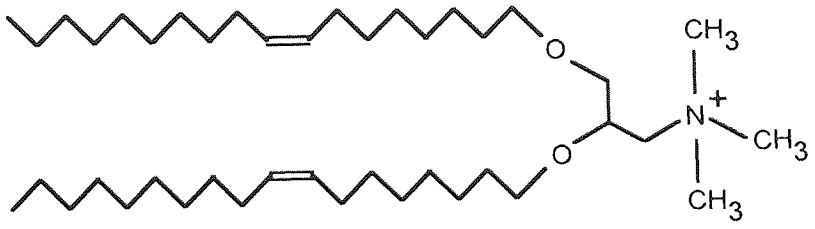

Figure 7.4. The Chemical Structure of the Cationic Lipid DOSPA. (Adapted from Life Technologies Bulletin No. 28, 1993). [Mol. wt. ≈1461].

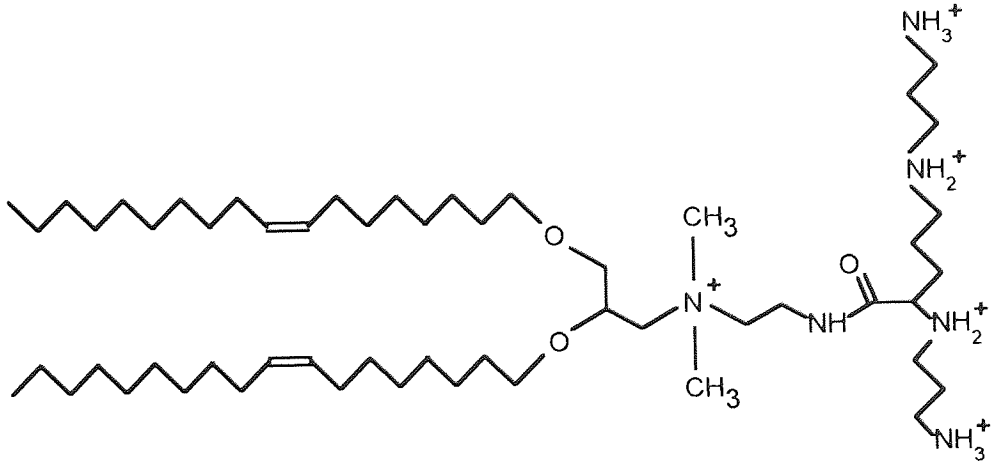

The anti-EGFr mRNA chimeric hammerhead ribozyme (see Section 7.2.1) was assumed to carry a net anionic charge equivalent to the number of inter-nucleotide

phosphate linkages contained within the molecule (i.e. the internally radiolabelled 37-mer was assumed to possess an overall charge of -36, whereas the unlabelled 36-mer was assumed to carry an overall charge of -35), in accordance with the method of Jaaskelainen *et al* (1994). All cationic:anionic (- / +) charge ratios were calculated by comparing the molar concentration of cationic lipid contained in a relevant liposome formulation (i.e. the concentration of either DOTMA or DOSPA), with the molar concentration of the ribozyme used.

For cellular association studies, cationic liposome / ribozyme complexes were prepared by diluting the cationic liposome formulation to the required concentration (see section 7.2.9.1) in 100μL of DMEM cell culture media (Life Technologies Inc, UK). The required concentration (see section 7.2.9.1) of the radiolabelled ribozyme was also diluted to 100μL with DMEM media in a separate microcentrifuge tube. The liposome and ribozyme solutions were combined, vortexed for 2 minutes and incubated for 30 minutes at 37°C to allow complexes to form.

For particle size distribution analyses quantities of each liposome formulation equivalent to a 10μM solution of the cationic lipid (either DOTMA or DOSPA) were prepared in 250μL sterile double-distilled water (i.e. the cationic lipid concentration was fixed in these studies). A separate solution containing the quantity of non-radiolabelled ribozyme required to produce a particular cationic:anionic charge ratio (from 0.25 to 10.0), was prepared in 250μL of sterile double-distilled water treated with DEPC (see Section 2.2.1). The liposome and ribozyme solutions were combined (producing a total volume of 0.5mL; the minimum volume required for particle size analysis), vortexed for 2 minutes and incubated for 30 minutes at 37°C to allow complexes to form. Immediately prior to particle size analyses the complexes were vortexed briefly and sonicated for 2 minutes.

7.2.5.1. Cellular Association Studies with Ribozyme / Cationic Liposome Complexes.

In order to examine the effects of Lipofectin® and Lipofectamine® on A431 cell viability, studies were performed to determine the maximum non-toxic dose of each reagent which could be administered to A431 cells. Cells were seeded on 24 well plates as described in Section 2.7.4. A range of cationic lipid concentrations (zero (control), 2μM, 5μM, 10μM, 15μM, 20μM and 25μM) were administered to A431 cells in a total volume of 200μL serum-free media (see Section 2.7.4) and incubated for 4 hours at 37°C. Following incubation, liposome-containing media was removed and cells were re-suspended in fresh serum-containing media for 30 minutes at 37°C.

Finally, viable cells counts were determined by trypan blue exclusion assay as described in Section 2.7.3 and the percentage of viable A431 cells was calculated.

For initial cell association studies, liposome / ribozyme complexes were prepared which contained final concentrations of 0.8μM radiolabelled ribozyme complexed with either 2μM DOTMA or 2μM DOSPA. Ribozyme concentrations of 0.8μM were routinely used in the studies described in Chapter 4, and hence, the same concentrations were used in these studies to allow comparisons to be made. Complexes were prepared in serum-free DMEM media which did not contain any additives (e.g. antibiotics) using the method described in Section 7.2.5. A431 cells were seeded on 24 well plates as described in Section 2.7.4 and liposome / ribozyme complexes were administered to cells in a total volume of 200μL of serum-free DMEM media. The percentage of complexed, radiolabelled ribozyme which became cell associated after fixed time intervals (zero to 4 hours) was determined as described in Section 2.8.1.

In subsequent studies, final concentrations of cationic lipids (DOTMA and DOSPA) were fixed at 10μM and the concentration of the radiolabelled ribozyme was varied in accordance with the method of Jaaskelainen *et al* (1994), to allow complexes with different cationic:anionic charge ratios to be produced. Ratios of ribozyme to cationic lipid were varied in the range from 0 to 10 (- / + charge ratio). Again complexes were prepared in a total volume of 200μL DMEM media as described in Section 7.2.9. A431 cells were seeded on 24 well plates as described in Section 2.7.4 and liposome / ribozyme complexes were administered to cells in a total volume of 200μL of serum-free DMEM media. The percentage of complexed, radiolabelled ribozyme which became cell associated after one hour was determined as described in Section 2.8.1.

7.2.5.2. The Serum Stability of Chimeric Ribozymes Complexed with Cationic Liposomes.

To investigate the serum stability of radiolabelled chimeric ribozymes when complexed with cationic liposomes; complexes were prepared in 200μL of DMEM as described in Section 7.2.9. The liposome / ribozyme complex was combined with 200μL of 60% v/v foetal bovine serum (Gibco, UK) in DMEM media and the mixture was incubated for up to 24 hours at 37°C. At fixed intervals, aliquots (5μL) of the reaction mixture were removed and added to 8M urea solution (35μL) in sterile DEPC treated water. After vortexing, the radiolabelled ribozyme and any degradation products in the mixture were separated by 15% PAGE as described in Section 2.2.2. and visualised by autoradiography as described in Section 2.2.3. Scanned

autoradiograph images were obtained using a UVP Trans-illuminator with multi-focus camera attachment, linked to an IBM PC486 computer running 'UVP Gel-Works' (Synoptics Ltd. Upland, USA) analysis and imaging software (see Section 2.2.4).

7.2.5.3. Particle Size Distribution Analysis.

The size distribution of the ribozyme / cationic liposome complexes was determined by quasi-electric laser light scattering using a Sematech submicron particle size analyser coupled to a Vale PC486 computer running the relevant 'Sematech RTG' detection and correlation software. The laser sampling time in all studies was fixed at 30 seconds. Mean particle sizes, based on a number-size distribution, were calculated from the size distribution data obtained.

7.3. RESULTS.

7.3.1. Cellular Delivery of Ribozyme / Anti-Transferrin Receptor Antibody Conjugates.

7.3.1.1. Conjugate Synthesis and Characterisation.

The number of ribozyme molecules conjugated to each anti-transferrin receptor antibody (TRA) molecule was quantified spectrophotometrically by Dr. Nadia Normand as described in Section 7.2.3.3. Analysis of three separately prepared batches of the TRA / ribozyme conjugate indicated that, on average, 5 or 6 ribozyme molecules were conjugated to each monoclonal antibody in the synthesis reaction. Previous studies have reported that approximately 10 molecules of a 20-mer PO ODN became conjugated with an anti-transferrin receptor antibody when a similar conjugation reaction was performed (Walker *et al*, 1995). The lower conjugation ratio observed in this report probably reflects the larger size of the 37-mer ribozyme compared with the 20-mer PO-ODN used in the previous study.

To confirm the constitution of TRA / ribozyme conjugates (i.e. to confirm that the ribozyme was actually linked to the antibody), purified samples were run on 10% SDS-PAGE gels as described in Section 7.2.3.3. Radiolabelled species were visualised by autoradiography and scanned images of autoradiographs were obtained as described in Section 2.2.4. The gel mobility of the antibody / ribozyme conjugate (see Figure 7.5, lane A) was markedly different to that of the unconjugated 37-mer ribozyme mixed with the non-derivatised antibody (see Figure 7.5, lane C).

Figure 7.5. Characterisation of the Anti-Transferrin Receptor Antibody / Ribozyme Conjugate. (10% SDS-PAGE analysis was performed by Dr. Nadia Normand, Aston University). **Lane A** is the ribozyme / anti-transferrin antibody conjugate, **Lane B** is the ribozyme / antibody conjugate incubated with Proteinase K as described In Section 7.2.7.3, **Lane C** is a physical mix of the 37-mer internally radiolabelled ribozyme and the non-derivatised antibody. **Lane D** is the free radiolabel ([^{32}P]-γ-dATP) used to internally label ribozyme molecules.

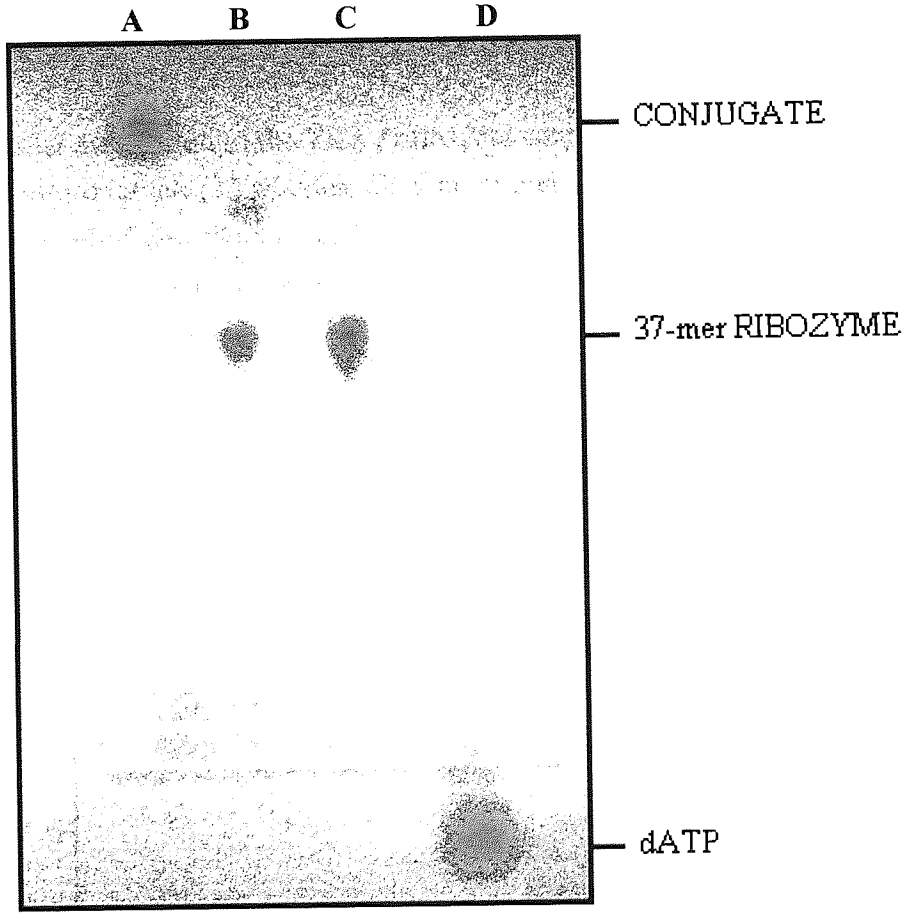

The incubation of the 'free' radiolabelled ribozyme with the non-derivatised TRA did not produce a shift in the mobility of the ribozyme construct (see Figure 7.5, lane C). This indicated that the ribozyme / antibody conjugate was not simply a result of the ribozyme adsorbing onto the antibody molecule and implied that covalent coupling of the ribozyme and antibody could be achieved using the reaction scheme described in Figure 7.2. To confirm the presence of the protein component (i.e. the non-radiolabelled antibody molecule) of the conjugate, partial digestion with Proteinase K was performed as described in Section 7.2.7.3. An intense band exhibiting mobility similar to that of the unconjugated 'free' ribozyme was observed (see Figure 7.5, lane B). Indicating the release of the radiolabelled ribozyme from the digested antibody molecule after Proteinase K treatment. Finally, the relative mobility of the 'free' [^{32}P]-γ-dATP radiolabel was noted to be markedly different to that of both the TRA / ribozyme conjugate and the unconjugated ribozyme molecule. No monomer bands

(i.e. bands with a similar mobility to that of the free label) were observed in any of the lanes containing conjugate samples, indicating that purified samples of the TRA / ribozyme conjugate did not contain degraded ribozyme fragments.

7.3.1.2. Cellular Association of Antibody / Ribozyme Conjugates.

7.3.1.2.1. Comparative Cellular Association of TRA / Ribozyme Conjugates and Unconjugated Ribozyme in A431 cells

The cellular association of the TRA / ribozyme conjugate was examined in A431 cells at fixed time intervals (30 minutes, 60 minutes and 120 minutes) in A431 cells at 37°C using the method described in Section 7.2.8. To compare the cellular association of the conjugate with that of the unconjugated ribozyme, parallel studies were performed to assess the association of the 'free' ribozyme under similar conditions (see Section 2.8.1) and results are shown in Figure 7.6.

Figure 7.6. Graph Showing Percentage Cell Association of TRA / Ribozyme Conjugate in A431 Cells as a Function of Time. Compared with an Unconjugated Ribozyme Control. (Experiments were performed at 37°C, n=4, values represent mean ± SD).

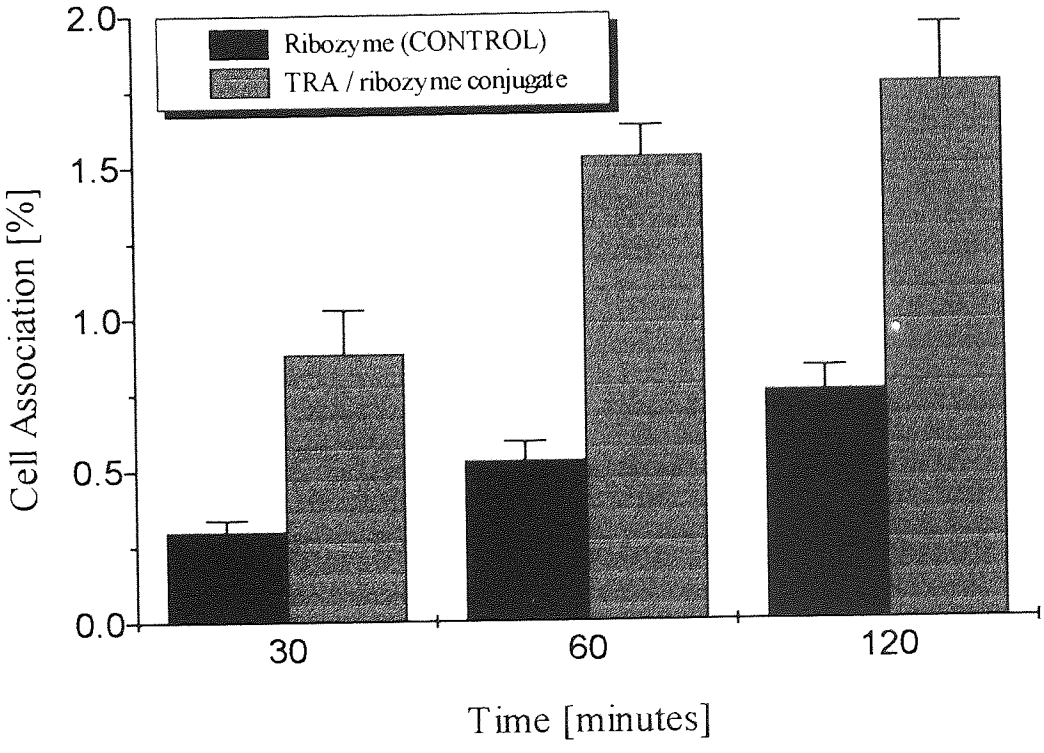

The cellular association of the TRA / ribozyme conjugate was approximately 3-fold higher than that of the unconjugated ribozyme after incubation periods up to 60 minutes. The level of association remained more than 2-fold higher than that of the

free ribozyme after 2 hours, despite the fact that the levels of cell associated conjugate did not significantly increase between 60 minutes and 120 minutes (P=0.069). The level of cell associated 'free' ribozyme continued to significantly increase (P<0.01) throughout the time period tested.

At all time points tested, differences between levels of cell associated conjugate and free ribozyme were statistically significant (P<0.001). Indicating that the attachment of the ribozyme to the anti-transferrin receptor antibody was able to increase levels of cell association in A431 cells. However, these studies alone did not give any indication as to whether this increase was specifically due to transferrin receptor mediated uptake.

7.3.1.2.2. Comparative Cellular Association of Ribozymes Conjugated to Non Specific and Anti-Transferrin Receptor Antibodies.

The cellular association of the TRA / ribozyme conjugate (at a concentration equivalent to 0.8μM ribozyme) was compared with that of the mouse anti-human IgG / ribozyme conjugate at similar concentrations in A431 cells. In addition, the cellular association of the unconjugated ribozyme was also determined as a control procedure. Cells were incubated with each agent for 1 hour in serum-free media at 37°C. Results are indicated in Figure 7.7.

Cellular association of the TRA / ribozyme conjugate was almost 3-fold higher (P<0.001) than that of the unconjugated ribozyme (control) after 60 minutes incubation. Furthermore, the association of the TRA / ribozyme conjugate was almost 2-fold higher (P<0.001) than that of the mouse anti-human IgG / ribozyme conjugate. The cellular association of the anti-human IgG / ribozyme conjugate was slightly higher than that observed for the free ribozyme. However, the difference between mean levels of cellular association was not statistically significant (P=0.0951) after 1 hour.

These results indicated that conjugation of the ribozyme to the anti-transferrin receptor antibody could increase cellular uptake via a mechanism which was specifically related to the presence of the TRA. By comparison the non-specific IgG molecule (the mouse anti-human IgG) did not significantly increase ribozyme uptake. This suggests that non-specific adsorption of conjugated antibody molecules to cellular components was unlikely to account for the increase in cellular association observed with the TRA / ribozyme conjugate. Nevertheless additional studies were required to provide further evidence that TRA-conjugated ribozymes were able to

enter cells via receptor mediated endocytosis (RME) as a result of binding to the transferrin receptor (see Sections 7.3.1.2.3 and 7.3.1.2.4).

Figure 7.7. Graph Showing Percentage Cellular Association of Chimeric Ribozymes When Conjugated to Antibody Molecules, Compared with an Unconjugated Control. (n=4, mean values ± SD).

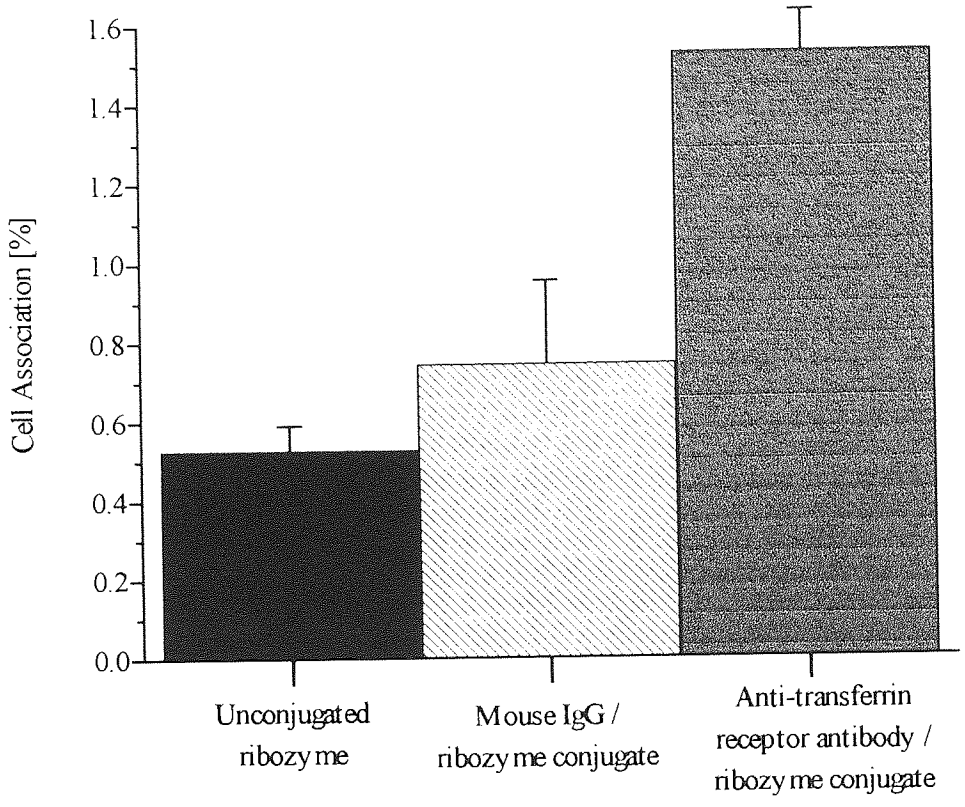

7.3.1.2.3. The Influence of Temperature and Competitors on the Cellular Association of the TRA / Ribozyme Conjugate.

To further confirm that TRA-conjugated ribozymes were able to enter cells via receptor mediated endocytosis (RME), as a result of transferrin receptor mediated uptake, further mechanistic studies were performed. RME is an energy dependant process which is usually inhibited at reduced temperature. Therefore, cellular association of the TRA / ribozyme conjugate was compared in A431 cells incubated at both 37°C and 4°C using the method described in Section 2.8.4. In addition, competition studies were performed in which the non-derivatised antibody was added to the culture media as a competing agent, in accordance with the method described in Section 2.8.6. The non-derivatised antibody was used at a 5-fold molar excess, compared with the concentration of ribozyme-conjugated antibody. The anti-transferrin antibody was used as the competing agent, rather than the transferrin ligand, because the ligand binds to the receptor at a different site to the antibody and,

therefore, would not necessarily be able to prevent binding by the TRA / ribozyme conjugate.

Results indicated that the mechanism of cellular uptake of the TRA / ribozyme conjugate was highly temperature dependant (see Figure 7.8). The percentage of TRA-conjugated ribozyme which became cell associated was reduced more than 5-fold (P=0.003) at 4°C, when compared with results observed at 37°C. This indicated that the TRA / ribozyme conjugates were internalised via an energy-dependant process, such as RME.

Figure 7.8. Graph Showing the Percentage Cell Association of TRA-Conjugated Ribozymes at 4°C and in the Presence of a 5-fold Excess of Unconjugated TRA. Results are Compared with a Control Showing Percent Cell Association after 1 Hour at 37°C in the Absence of Any Competing Agent (n=4, mean values ± SD).

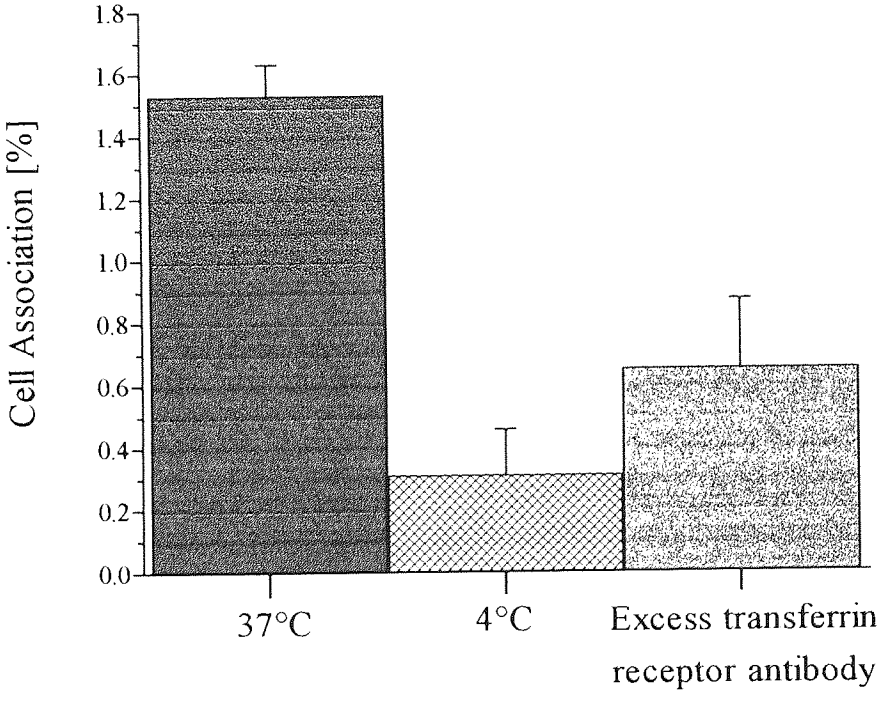

The cellular association of the TRA-conjugated ribozyme was inhibited by almost 60% (P=0.0034) in the presence of a 5-fold molar excess of the (unlabelled) non-derivatised antibody molecule. This result suggested that the TRA / ribozyme conjugate and the free TRA were competing for binding sites on the transferrin receptor to some extent. Therefore, this implied the specific involvement of the transferrin receptor in the cellular uptake of the TRA / antibody conjugate. The partial inhibition observed could be due to a lack of binding site saturation by the competing antibody or alternatively this could also indicate that cellular uptake of TRA / antibody conjugates did not occur exclusively via transferrin receptor mediated endocytosis. The latter explanation would appear to be the most valid because

ribozymes conjugated to the non-specific IgG were able to enter cells to some extent (see Figure 7.7), despite the fact that they would not be predicted to bind to any specific receptor on the surface of the A431 cells.

7.3.1.2.4. The Effect of Monensin on the Cellular Association of TRA / Ribozyme Conjugates with A431 Cells.

The physiological role of the transferrin receptor is to provide an efficient mechanism for the cellular uptake of iron-transferrin complexes (for a detailed review of this mechanism see Friden, 1993). Briefly, this process involves the internalisation of the receptor into endosomal vesicles following the binding of an iron-transferrin complex. The endosomes become acidified, causing the iron to dissociate from the transferrin molecule. The ('apo-') transferrin molecule remains bound to the transferrin receptor which is then recycled to the cell surface via the golgi complex. Upon reaching the cell surface the apo-transferrin molecule is released, thus allowing the binding of further iron-transferrin complexes to the receptor.

The carboxylic acid ionophore; monensin, has been shown to specifically inhibit the recycling of transferrin (the natural ligand) and the transferrin receptor (Stein *et al*, 1984). Although monensin is known to raise the pH of endosomes (Mollenhauer *et al*, 1990), this is not thought to be the mechanism by which the recycling process is inhibited. Instead, the exact mechanism has been shown to involve disruption to the transport of vesicles (containing transferrin and its receptor) from the golgi complex to the plasma membrane. This causes transferrin and its receptor to accumulate within bloated, intracellular vesicles (Stein *et al*, 1984). In light of these findings, monensin was investigated for its ability to increase intracellular concentrations of the ribozyme-antibody conjugate via a reduction in the cellular export of these conjugates when bound to the transferrin receptor. Cells were incubated with 100μM monensin in serum-free media both prior to and during the administration of TRA / ribozyme conjugates or 'free' ribozymes as described in Section 7.2.8. Results of these studies are shown in Figure 7.9.

The addition of monensin to the cell culture media increased the percentage of cell associated TRA / ribozyme conjugate by almost 40% (P=0.0049) in A431 cells after 30 minutes incubation. Monensin treatment also appeared to produce a slight increase (less than 20% increase) in the percentage of unconjugated ribozyme which became cell associated. This was interesting because ultrastructural studies had indicated some localisation of ribozymes within the golgi complex and associated vesicles. However, the observed increase was not statistically significant (P=0.0681). Therefore, despite

the fact that this may have indicated some ribozyme accumulation within cells as a result of reduced golgi transport or a rise in endosomal pH, this effect could also have been due to experimental variation.

Figure 7.9. Graph Showing the Effect of Monensin on the Cellular Association of TRA-Conjugated Ribozyme after 30 Minute Incubation at 37°C. Compared with the Effect of Monensin on the Cellular Association of an Unconjugated Ribozyme Control. (For monensin treated samples n=3, for other samples n=4, values are mean ± SD).

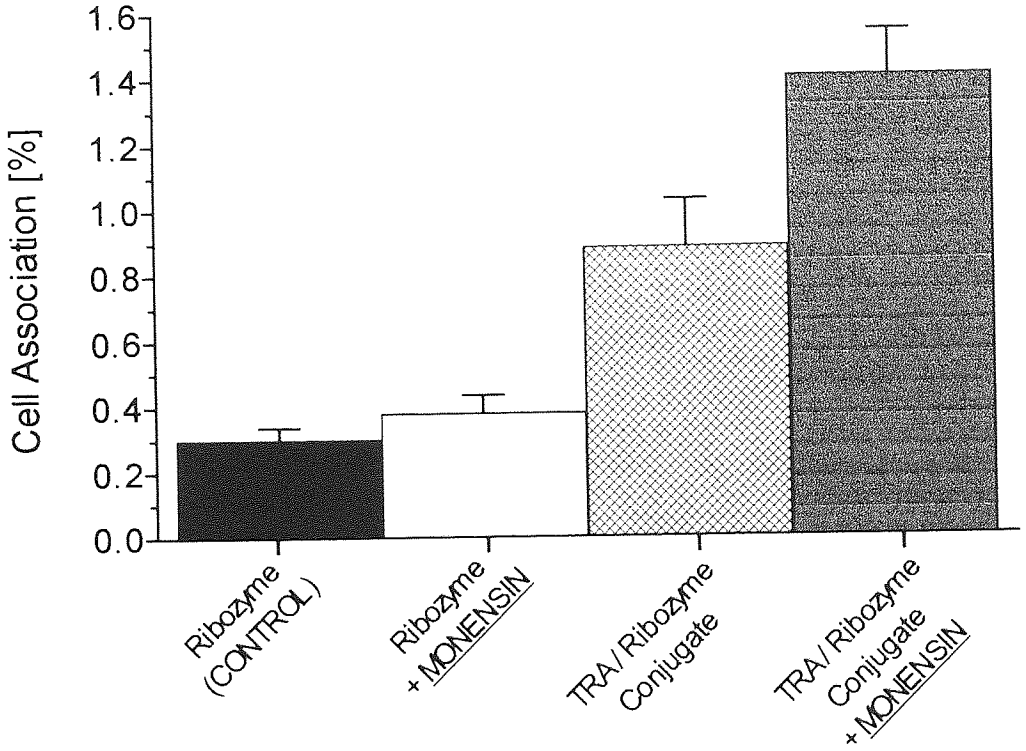

Previous results in this chapter indicated that TRA / ribozyme conjugates became cell associated via a specific mechanism (section 7.3.2.2.2), which was energy dependant and subject to competition by anti-transferrin antibody (section 7.3.2.2.3). In the light of these findings, the accumulation of TRA / ribozyme conjugates within cells after monensin treatment, provided further evidence to suggest that these conjugates entered cells via RME through an interaction with the transferrin receptor.

There are few other published reports of receptor-mediated delivery of ribozymes to cells by any mechanism, despite the fact that several studies have demonstrated the benefit of such techniques in delivering antisense molecules to cells (see Section 1.4.2.4). The data obtained here with the TRA / ribozyme conjugates correlate well with studies which have utilised transferrin receptor mediated delivery for ODNs and low molecular weight drugs (Citro *et al*, 1992, Wagner *et al*, 1994, Boado, 1995, Walker *et al*, 1995), where similar increases in cellular uptake have been reported.

Overall it would appear that conjugation of ribozymes to TRA has potential for the delivery of ribozymes to cells which express high levels of the transferrin receptor, such as those which comprise the blood brain barrier (Friden, 1993).

7.3.2. Cationic Liposome Mediated Delivery of Chimeric Ribozymes.

7.3.2.1. The Effect of Cationic Liposomes on Cell Viability.

To determine concentrations at which Lipofectin® and Lipofectamine® could be administered to A431 cells without significant toxicity, studies were performed as described in Section 7.2.9.1. The percentage of A431 cells which remained viable following treatment with a variety of concentrations of cationic liposomes was calculated and results are shown in Figure 7.10.

Figure 7.10. Graph Showing the Percentage of Viable A431 Cells Following Incubation with Various Concentrations of Cationic Lipid Formulations for 4 hours at 37°C (n=6, values are mean ± SD).

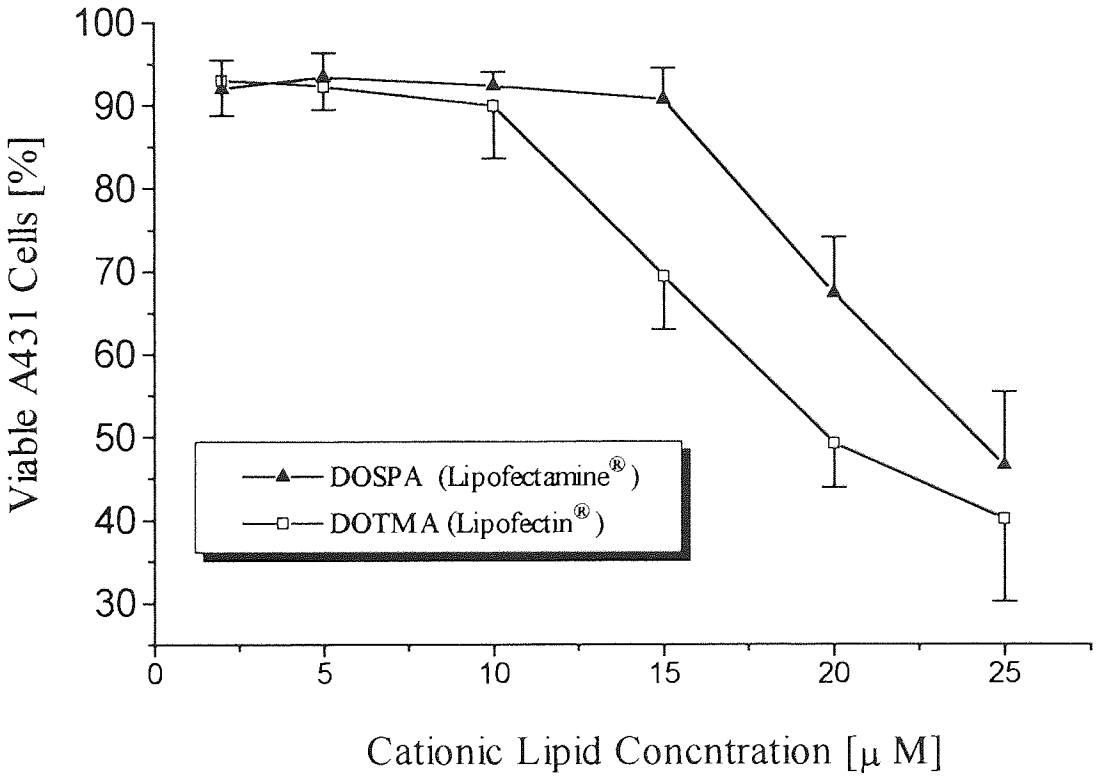

Results indicated that on average 97.6% (± 1.7%) of control cells, which were not treated with any liposome formulation, remained viable after 4 hours when incubated in serum-free media. This indicated that A431 cells were relatively unaffected by serum depravation over the time period tested.

Treatment with cationic liposomes reduced the mean percentage of viable cells when administered to A431 cells at all concentrations tested. However, the reduction in percentage cell viability was only marginally significant ($P \approx 0.05$) compared with the control, when DOTMA (in the form of Lipofectin®) and DOSPA (in the form of Lipofectamine®) were administered to A431 cells at concentrations in the range 2μM to 10μM. When concentrations of 15μM and above of either lipid were administered, the percentage of viable cells was markedly reduced.

The Lipofectin® (DOTMA) formulation appeared to cause a more pronounced reduction in cell viability than Lipofectamine® (DOSPA) in the concentration range from 15μM to 20μM. This effect could possibly have been due to the greater proportion (w/w ratio) of the neutral lipid DOPE present in the Lipofectin® formulation. Where concentrations were increased to 25μM, the reduction in cell viability produced by the two formulations was not significantly different ($P>0.05$). Overall, these results appear to indicate that the use of Lipofectin® or Lipofectamine® causes some toxicity when administered to cells at all cationic lipid concentrations tested. However, this toxicity is not pronounced (i.e. loss of cell viability is <10%) when concentrations in the range 2μM to 10μM of cationic lipid are administered to A431 cells. Concentrations in this range are recommended in the manufacturer's protocols for the use of these liposomes in other cell types (See Life Technologies Technical Bulletins Numbers 27 & 28). Therefore, concentrations in this range were used in subsequent studies in A431 cells.

7.3.2.2. Comparative Cellular Association of Ribozymes Complexed with Similar Concentrations of DOTMA and DOSPA.

For initial association studies, the ability of a 2μM solution of DOTMA or DOSPA to deliver 0.8μM chimeric ribozyme was examined in A431 cells after various time intervals as described in Section 7.2.9.1. The main aim of these studies was to determine which liposome formulation was the most efficient in delivering ribozymes to A431 cells. This formulation could then be used in future to deliver ribozymes in *ex vivo* efficacy studies. Results are indicated in Figure 7.11.

At all time points, both cationic lipid formulations significantly increased ($P<0.001$) the percentage of chimeric ribozyme which became cell associated when compared with the 'free' ribozyme control. Lipofectamine® mediated delivery resulted in an almost 28-fold increase in the quantity of cell associated ribozyme after 4 hours, whereas Lipofectin® mediated delivery produced a 12-fold increase after the same time period. The cationic lipid DOSPA (+5) carries a greater cationic charge than

DOTMA (+1), therefore, differences in the surface charge characteristics of the liposome / ribozyme complexes could offer a potential explanation for the differences observed between the two liposome formulations.

Figure 7.11. Graph Showing the Percentage Cellular Association of Chimeric Ribozymes As A Function of Time When Complexed with the Cationic Lipids DOTMA and DOSPA. (n=4, values represent mean ± SD. Data are normalised to 1×10^5 cells / mL).

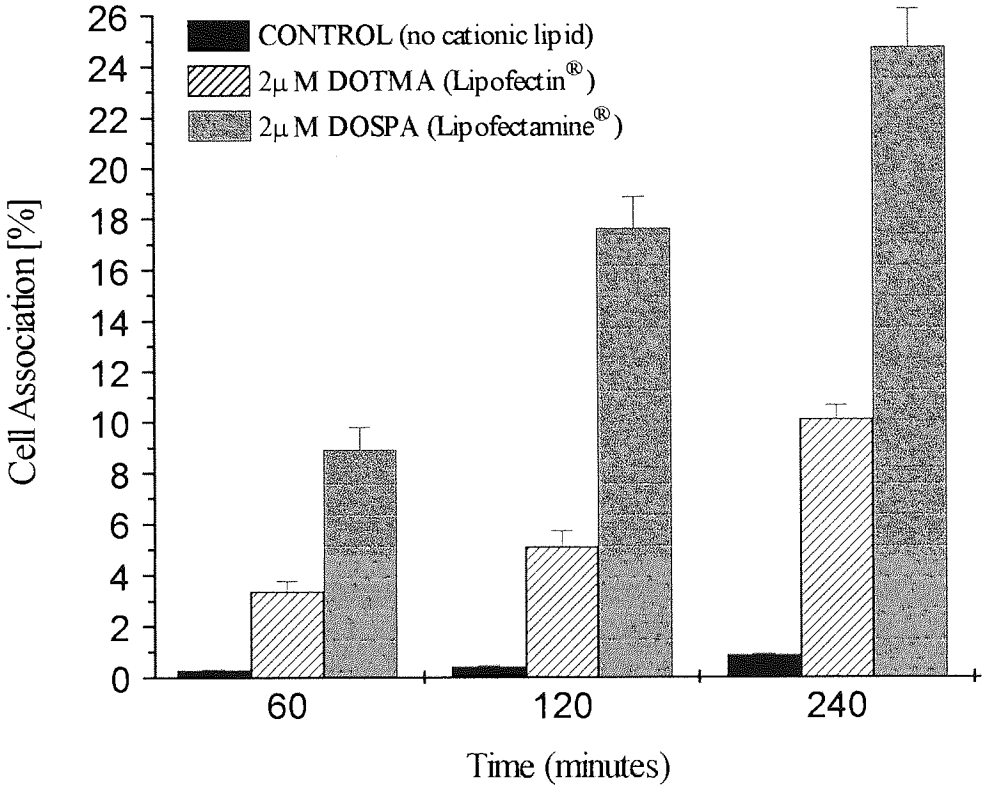

The increases in ribozyme cell association, resulting from cationic lipid complexation, correlate well with the findings of studies which have utilised DOTMA and DOSPA for the delivery of antisense ODNs. 5 to 80- fold increases in cellular association have been observed (depending on the cell line investigated) when a variety concentrations of these cationic lipids have been used (Felgner *et al*, 1987, Felgner and Ringold, 1989, Lappalainen *et al*, 1994, Chonn and Cullis, 1995). For example, a recent report by Lewis *et al* (1996) indicated that when Lipofectin® and Lipofectamine® were complexed (at similar concentrations to those used here) with a 15-mer PS ODN (250nM), approximately 80% and 50% respectively, became associated with monkey kidney epithelial cells after 4 hours. However, it is noticeable that Lipofectin® was shown to be the more effective agent for delivering PS ODNs in this study. This particular finding contradicts the results observed in this report because

Lipofectamine® was more effective in delivering ribozymes to A431 cells. This could reflect the differences in the ratio of cationic:anionic charge within the polyanion / lipid complexes used. Such differences have been shown to influence to the efficiency of ODN delivery by liposomes (see Jaaskelainen *et al*, 1994, Lappalainen *et al*, 1994, Eastman *et al*, 1997). However, other factors such as the composition of polar 'head' group of the cationic lipid (Felgner *et al*, 1994, Bennet, 1995) and the cell type used (Juliano and Akhtar, 1992, Sullivan, 1993, Litzinger *et al*, 1996), have also been shown to influence cellular association.

Despite the fact that similar cationic lipid concentrations were compared in this experiment, the actual cationic:anionic ratios within the liposome / ribozyme complexes were markedly different because of the different cationic charges of the lipids in each formulation. The (- / +) charge ratios used were 14.0 for DOTMA / ribozyme complexes and 2.8 for DOSPA / ribozyme complexes. Therefore, a situation which favoured the use of the Lipofectamine® formulation could have been produced under the conditions tested, since optimal formulations often possess a near equal ratio of cationic:anionic charges (Bennett, 1995).

Consequently, to further investigate possible reasons for the differences observed here and to compare Lipofectin® and Lipofectamine® under similar charge ratio conditions. Studies were performed to evaluate the cellular association of complexes with similar cationic:anionic charge ratios. The particle size of these complexes was also measured to identify any correlation between the size of the liposome / ribozyme complexes and levels of cellular association.

7.3.2.3. Cellular Association of Chimeric Ribozymes Complexed with Lipofectin® and Lipofectamine® at Various Charge Ratios.

Ribozyme / liposome complexes were prepared at various cationic:anionic charge ratios as described in Section 7.2.9. The concentration of cationic lipids was fixed at 10μM to allow association data to be compared with particle size data obtained in subsequent studies (a minimum concentration of 10μM was required for size analysis). Previous studies indicated that approximately 90% of cells would remain viable after 4 hours if a 10μM solution of either lipid formulation was administered to A431 cells (see Section 7.3.3.1).

Cellular association studies were performed as described in Section 7.2.9.1 and results are illustrated in Figure 7.12. Parallel studies were also performed to assess the cellular association of 'free' ribozymes in the same cells after 1 hour. Results indicated

a mean percentage cellular association of 0.47% (± 0.09) which was significantly lower ($P<0.001$) than the level of association observed at all charge ratios of liposome / ribozyme complexes.

Figure 7.12. Graph Showing Percentage Cell Association of Chimeric Ribozyme When Complexed with Cationic Lipid Formulations at Various Charge Ratios after One Hour. (n=3, values represent mean ± SD. DOSPA / ribozyme complexes at a charge ratio of 10 were not examined).

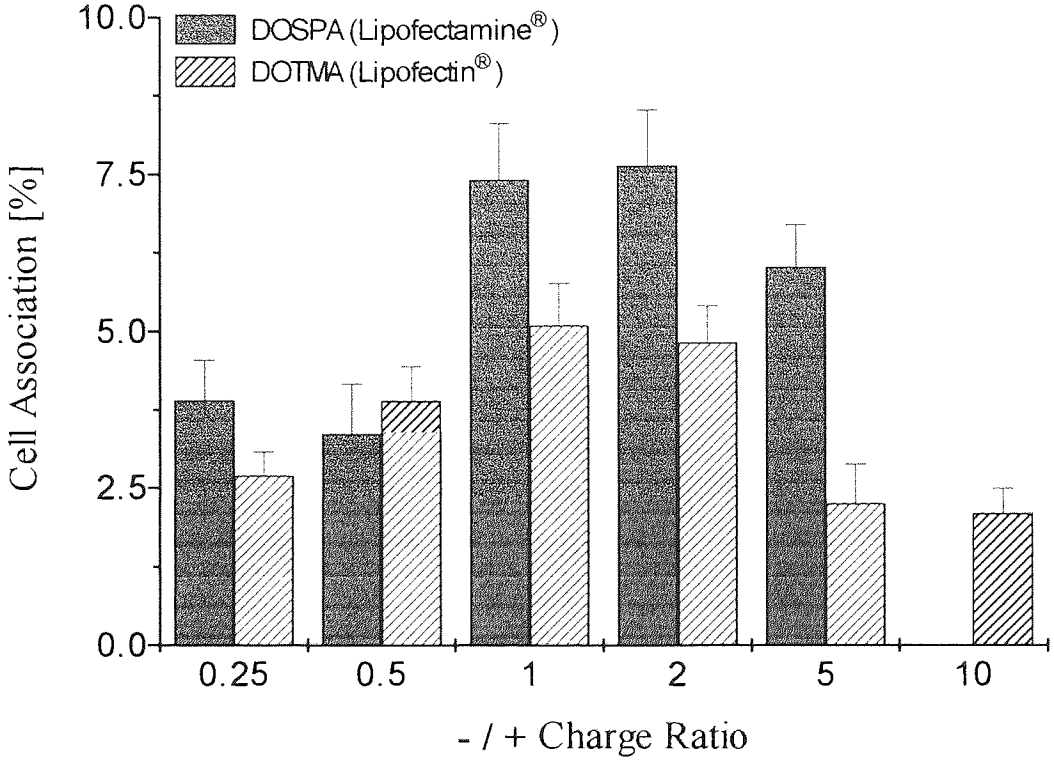

Results indicated that variations to the cationic:anionic charge ratio within cationic liposome / ribozyme complexes had a considerable effect upon the percentage of ribozyme which became associated with A431 cells after 1 hour. When complexes exhibited a net positive charge (at charge ratios of 0.25 and 0.5), similar percentages of complexed ribozyme became cell associated when either DOTMA or DOSPA were used. In general, these complexes were less effective in delivering ribozymes than complexes with a charge ratio of 1 or 2 (which appeared to be optimal). A possible explanation for this could be that the (net) positive charge of these complexes reduced the aggregation of liposome particles because of electrostatic repulsion. This phenomenon has been observed with ODN / lipid complexes (Jaaskelainen *et al*, 1994) and could result in an overall reduction in liposome particle size, which in turn could affect cellular association characteristics. Hence, particle size analyses were

performed in subsequent studies to further investigate this possibility (see Section 7.3.3.4).

Charge ratios of 1 and 2 appeared to be optimal for cellular association of both DOTMA and DOSPA complexes. Other investigators have observed that cationic lipid / polynucleotide complexes with approximately equal molar ratios of charged species, give optimal results in cell uptake studies (for review see Bennett, 1995). However, the percentage of ribozyme delivered by DOSPA complexes at these ratios was significantly higher ($P<0.0064$) than the percentage delivered by DOTMA complexes.

Percentages of cell associated ribozyme were not significantly reduced ($P>0.05$) when DOSPA / ribozyme complexes were prepared at a charge ratio of 5, when compared with results observed at charge ratios of 1 and 2. However, the percentage of cell associated ribozyme gradually declined when the charge ratio of DOTMA / ribozyme complexes was increased to 5 and above. This decrease could again reflect changes in particle size. Alternatively this effect could be due to a reduced level of interaction between these liposome complexes (which exhibited a (net) negative charge,) and negatively charged cell membrane components. Some investigators have suggested that such interactions are initially involved in the cellular uptake mechanism of liposome complexes (Felgner and Ringold, 1989).

Overall the results observed here indicated that the experimental conditions in the previous study (see Section 7.3.3.2) produced charge ratios within complexes which strongly favoured the use of the Lipofectamine formulation. Hence, this formulation appeared to be vastly superior to the Lipofectin formulation in delivering chimeric ribozymes to A431 cells. When ribozyme complexes were prepared with cationic liposomes at similar charge ratios, differences in proportions of ribozyme delivered by DOTMA (Lipofectin®) and DOSPA (Lipofecatmine®) were less pronounced but were, nevertheless, statistically significant. This could be reflect the larger size of the DOSPA molecule compared with DOTMA, or could be due to differences in the nature of the polar 'head' groups of these lipids.

7.3.2.4. Particle Size Analysis.

To further investigate the possibility that differences in the particle size of liposome / ribozyme complexes contributed to differences observed in cellular uptake properties of DOSPA and DOTMA complexes, studies were performed as described in Section 7.2.9.3. Figure 7.13 shows mean particle diameters of cationic liposome / ribozyme

complexes formulated at various cationic:anionic charge ratios. Size distributions were often highly variable and data obtained for ratios of 0.5 and 10 did not conform to a Gaussian (normal) distribution (distributions showed double peaks). The mean particle diameters of liposomes with no added ribozyme (- / + charge ratio of zero) were 48.8nm for DOSPA vesicles and 77.9nm for DOTMA vesicles, which represented a significant difference (P=0.0007) in the size of non-complexed liposomes.

Figure 7.13. Graph Showing Mean Particle Diameter of Various Cationic Liposome / Ribozyme Complexes as a Function of Cationic: Anionic Charge Ratio. (n=4, values represent mean ± SD).

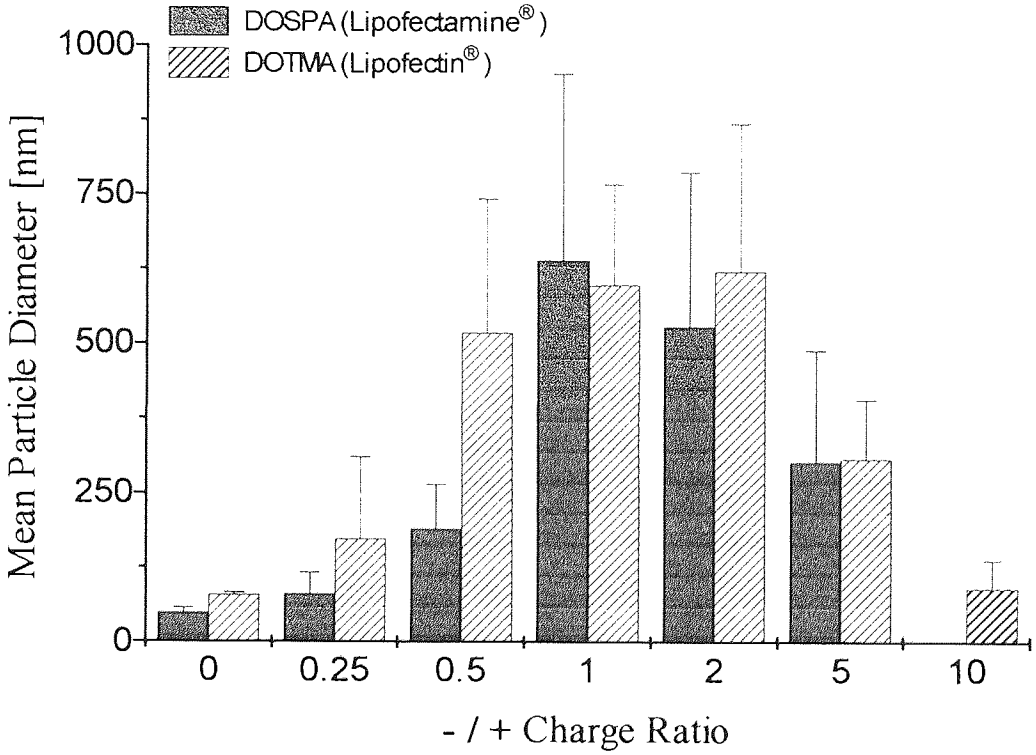

After the addition of chimeric ribozymes, mean particle diameters gradually increased as the (- / +) charge ratio was increased. For both lipid types, maximum (mean) particle diameters were observed at charge ratios in the range from 1 to 2.
As the (- / +) charge ratio was increased further, mean particle diameters appeared to be slightly reduced but these decreases in diameter were not statistically significant ($P>0.05$) at a charge ratio of 5. Overall, mean particle diameters observed, when both liposome formulations were complexed with ribozymes at equivalent (- / +) charge ratios, were not significantly different ($P>0.0699$). However, DOTMA liposomes appeared to increase in size at lower charge ratios than DOSPA liposomes.

There appeared to be some correlation between particle diameter data and cellular association data obtained in previous studies (see Section 7.3.3). Optimal cellular

association of liposome / ribozyme complexes occurred at (- / +) charge ratios of 1 to 2, which was also the ratio at which complexes demonstrated the largest particle sizes. These data suggest that the addition of ribozyme to cationic lipid complexes can increase the size of liposomal vesicles. This may occur via a reduction in the cationic surface charge of liposomal vesicles which consequently increases liposome aggregation. As the ratio of added ribozyme is increased to high (- / +) charge ratios, liposome particle diameters appear to fall slightly. This may indicate that liposome surfaces become predominantly negatively charged, which in turn blocks the aggregation of similarly charged liposome particles. Similar conclusions have been drawn when cationic lipid / ODN complexes have been examined in physicochemical studies (Jaaskelainen *et al*, 1994, Eastman *et al*, 1997). Nevertheless, the variations in particle size do not appear to explain the differences in cellular uptake efficiency which were observed when DOSPA and DOTMA complexes were compared for the delivery of chimeric ribozymes to A431 cells.

7.3.2.5. Stability of Liposome Complexed Ribozymes.

To investigate the serum stability of radiolabelled chimeric ribozymes complexed with 10μM DOSPA (Lipofectamine®) at a (- / +) charge ratio of 1.0, the stability of complexes was examined in 30% foetal bovine serum at various time intervals as described in Section 7.2.9.2. Results are shown in Figure 7.14. A control sample containing cationic liposome / ribozyme complexes incubated in sterile DEPC treated water for 24 hours at 37°C was also prepared (i.e. these samples were not exposed to serum). No signs of any degradation products migrating below the level of the intact ribozyme were observed in the control sample (see Figure 7.14, lane A).

Ribozymes complexed with Lipofectamine® reagent appeared to remain stable at all time points examined over a 24 hour period. No degradation products or free radiolabel (see Figure 7.14, Lane H), migrating below the level of the intact (control) ribozyme were evident at any time point (see Figure 7.14, Lanes B to G). This suggests that ribozymes complexed with the Lipofectamine® can remain stable in serum-containing media for periods of up to 24 hours.

Only a small number of studies have specifically examined the serum stability of ribozymes following complexation with cationic lipids (see Section 1.4.2.5). For example, 30% of an unmodified hammerhead ribozyme complexed with DOTMA, remained intact for 1 hour in 10% foetal bovine serum (Chonn and Cullis, 1995) and little degradation was observed over a 22 hour period when an unmodified

hammerhead ribozyme was complexed with DOTMA was incubated in human osteosarcoma cell supernatants (Kariko *et al*, 1994).

Figure 7.14. Stability of Internally Radiolabelled Chimeric Ribozyme Complexed with DOSPA Cationic Liposomes in 30% Foetal Bovine Serum At Various Time Intervals. Stability was analysed by PAGE (15%, 7M urea). [Lane **A**; control (see text), Lane **B**; time = zero, Lane **C**: time = 1 hour, Lane **D**; time = 2 hours, Lane **E**; time = 4 hours, Lane **F**; time = 6 hours, Lane **G**; time = 24 hours. Lane **H** is the free radiolabel ([^{32}P]-γ-dATP)].

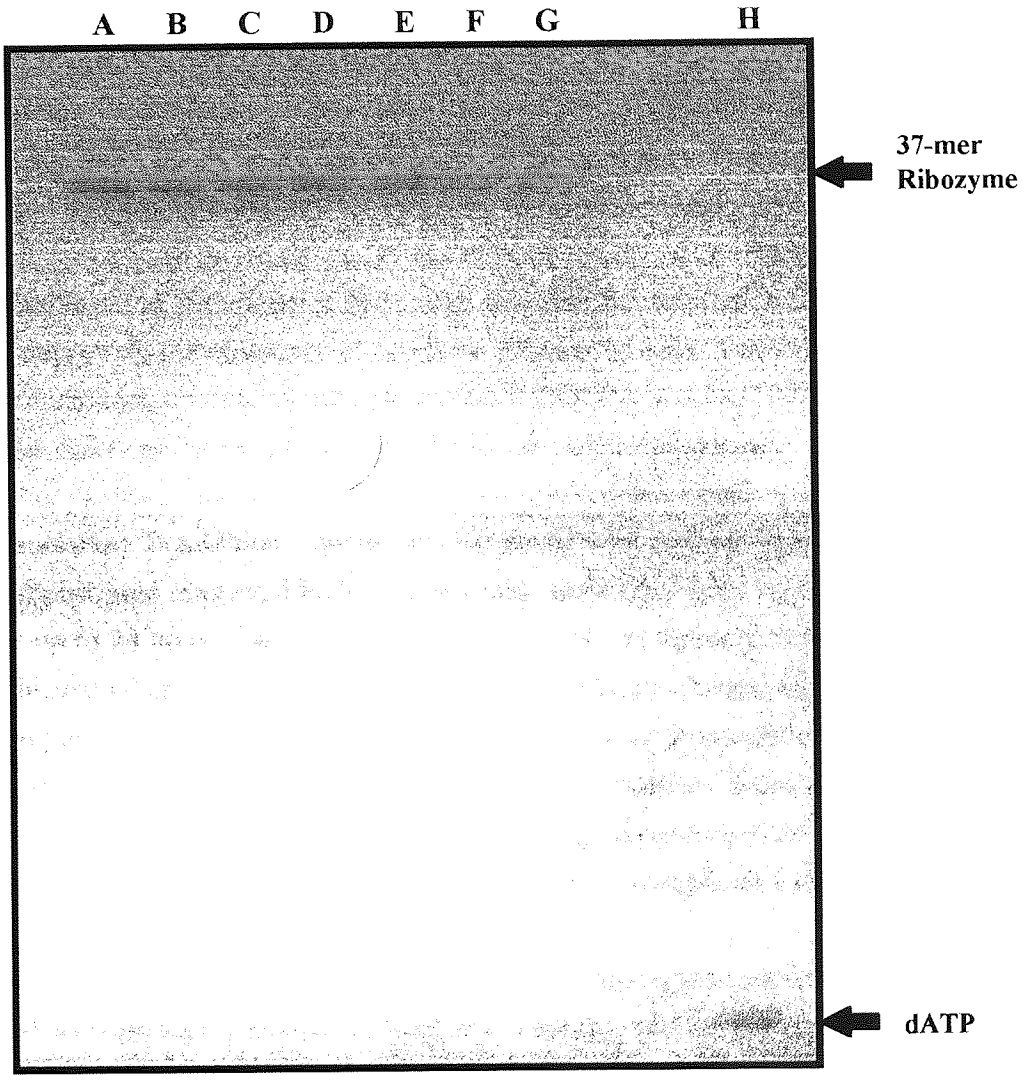

7.4. CONCLUDING REMARKS.

In this chapter, two separate strategies have been evaluated which can improve the cellular delivery of hammerhead ribozymes. The first strategy utilised transferrin receptor-mediated endocytosis to deliver chemically modified ribozymes to A431 cells. A 3-fold enhancement in cell-association was observed when ribozymes were conjugated to an anti-transferrin receptor antibody (TRA). Furthermore, studies

indicated that the increase in cell association observed with ribozyme-TRA conjugates was a result of a specific interaction with transferrin receptors. Levels of the cell associated conjugate could be further increased via the co-administration of monensin. This was probably due to an accumulation of receptor-bound conjugates within cells, since monensin is known to inhibit the intracellular trafficking of transferrin receptors (Molenhauer *et al*, 1990, Stein *et al*, 1995).

Eventually, it may be possible to use TRA-conjugates to target ribozymes to particular cells *in vivo* which express the transferrin receptor. Although many cell-types express the transferrin receptor (Shen and Shah, 1995), the capillary endothelial cells which comprise the blood brain barrier express particularly high concentrations (Friden, 1993). Furthermore, the expression of the receptor is usually increased when cells become malignant (Trowbridge and Omary, 1981). Therefore, TRA-conjugates could be particularly useful for targeting ribozymes to malignant cells within the brain.

Complexation with cationic liposomes was also investigated in this report as a means of improving the efficiency of ribozyme delivery to cells. Two commercially available formulations, containing the cationic lipids DOSPA and DOTMA, were evaluated for their ability to deliver chimeric ribozymes to A431 cells *ex vivo*. Complexation with either of these cationic lipid formulations resulted in a significant enhancement in cell association. In addition, ribozymes complexed with cationic lipids (DOSPA) demonstrated improved biological stability, since ribozymes remained stable in serum for up to 24 hours following complexation. Optimal delivery of ribozymes was achieved when the molar ratio of positive to negative charges within ribozyme / lipid complexes was approximately equal (i.e. when cationic:anionic charge ratios were around 1.0). The increased efficiency of these complexes (formulated at approximately equal charge ratios) in delivering ribozymes to cells, appeared to be related to the larger particle size (diameter) of the complexes formed.

In the short term, it was envisaged that cationic liposomes could be used as a means of delivering high concentrations of ribozymes to cells for the assessment of catalytic activity in A431 cells. Of the two formulations evaluated in this report, Lipofectamine® would appear to be the formulation of choice because higher proportionate increases in cell associated ribozyme were observed with this agent. However, both the DOSPA and DOTMA formulations reduced cell viability to some extent when administered to A431 cells for 4 hours at concentrations of 2μM and above. Toxicity could therefore be a limitation to the use of these cationic lipids in cell culture studies and *in vivo*.

DISCUSSION

The discovery of the *trans*-acting hammerhead ribozyme motif (see Section 1.2.1) introduced the possibility of specifically inhibiting gene expression via the catalytic cleavage of mRNA. In this report, hammerhead ribozymes directed against genetic targets involved in glioblastoma multiforme (GBM) have been evaluated. GBM is a malignant disease of the brain which has an extremely poor prognosis and currently has no effective treatment (Selby, 1994, Petersdorf and Livingston, 1994, Chiang *et al*, 1995). The epidermal growth factor receptor (EGFr) mRNA was selected for ribozyme targeting because there is a growing body of evidence to suggest that amplification or over-expression of EGFr is involved in the initiation and progression of GBM (see Section 1.6). Therefore, ribozymes which can inhibit EGFr expression, can potentially limit the progression of the disease.

An overall strategy to characterise a *trans*-acting hammerhead ribozyme for the inhibition of mRNA expression, would appear to consist of the following steps: cleavage of short, synthetic substrates *in vitro*; cleavage of a transcript of the mRNA *in vitro*; ribozyme efficacy within cells (*ex vivo*), then in an animal model (*in vivo*) and finally, in humans (Birikh *et al*, 1997b). However, considerable obstacles have to be overcome, to achieve even the initial steps in this overall strategy. The primary obstacles to ribozyme activity within cells are their poor biological stability and the inaccessibility of target sites within mRNA molecules (Gewirtz *et al*, 1996, Birikh *et al*, 1997a). In addition, their delivery to target sites within cells poses several problems (Elkins and Rossi, 1995).

Two broad strategies can be envisaged for the cellular delivery of ribozymes. The first involves the endogenous expression of ribozymes within cells and can be classified as a 'gene therapy' approach. This involves the permanent insertion of complete functional genes into cells and usually requires the use of viral vectors. The 'gene therapy' approach appears to have several limitations (see Section 1.4.1) and there is concern that the random integration of 'ribozyme expressing genes' into host cells could represent a dangerous intervention into the genetic structure of the recipient (Marschall *et al*, 1994). Furthermore, the irreversible nature of the 'gene therapy' approach makes it unsuitable for some therapeutic applications. Therefore, the exogenous delivery of synthetic ribozymes may be advantageous (Akhtar *et al*, 1995) and has been the focus of this report. The optimisation of appropriate exogenous

delivery strategies would require a fundamental understanding of the cellular uptake properties of synthetic ribozymes. Although the cellular mechanisms for the uptake of antisense ODNs have been widely studied (see Section 1.4.2.1 and for reviews see Akhtar and Juliano, 1992, Rojanasakul, 1996), until this report (see also Fell *et al*, 1997) the extent and mechanisms by which synthetic, chemically modified ribozymes penetrate cells has received little attention.

Unmodified, all-RNA ribozymes were degraded almost instantaneously following exposure to several biological extracts, including human serum and a mixture of lysosomal enzymes. This suggested that the cellular penetration of (exogenously delivered) all-RNA ribozymes would be almost negligible *in vivo*. By comparison PO and PS ODNs were slightly more stable in biological fluids (see Appendix II and Akhtar *et al*, 1991, Hudson *et al*, 1996a). Therefore, site-selective chemical modifications were examined as a means of improving the biological stability of active hammerhead ribozymes.

When these studies were initiated, reports by other investigators had suggested that the introduction of ODNs into the stem regions of hammerhead ribozymes could improve intracellular stability, without impairment of (*in vitro*) catalytic activity (Taylor *et al*, 1992). However, this claim was slightly misleading because intracellular stability was assessed following complexation with cationic lipids, which can, themselves, offer protection from nucleases (Kariko *et al*, 1994, Chonn and Cullis, 1995, Thierry and Takle, 1995). In the present study, the introduction of ODN and / or PS substitutions at specific sites within the stem regions of hammerhead ribozymes (see Figure 3.3) did not significantly improve the biological stability of ribozymes. This finding correlates with those of other investigators, who employed similar chemical modifications to stabilise hammerhead ribozymes without success (Shimayama *et al*, 1993). It was noted, however, that the main source of degradation in serum appeared to be endonuclease activity, which is considered to be pyrimidine-specific (Alberts *et al*, 1989). Therefore, site selective 2'-modifications at all pyrimidine residues, were introduced into hammerhead ribozymes in a further attempt to improve stability. Other sites for chemical modification were chosen on the basis of previous studies, these had identified functional groups within the hammerhead motif which could accept chemical modifications, without severe impairment of catalytic activity (see Yang *et al*, 1992, Paolella, *et al*, 1992, Heidenreich *et al*, 1994 and Figure 1.8). Modified constructs were synthesised which contained 2'-O-methyl substitutions at almost all sites, with the exception of 5 purine residues within the catalytic core, which were retained as unmodified oligoribonucleosides (see Figure 3.4). The *in vitro* catalytic activity exhibited by these chimeric ribozymes was slightly

impaired (activity half-life reduced 3-fold) relative to an unmodified (all-RNA) counterpart. However, the kinetic parameters determined for the most active construct (EGFR-65; k_{cat}=1.46min^{-1}, K_m=126nM) were within the range of typical values reported for hammerhead ribozymes by other investigators (k_{cat}≈1-2min^{-1}, K_m≈50-500nM; Birikh *et al*, 1997b). This demonstrated that the construct retained potent catalytic activity, however, it is difficult to draw direct comparisons with ribozymes designed by other investigators because many factors such as the length and sequence of ribozymes can influence these kinetic parameters (Hertel *et al*, 1994). The introduction of site specific 2'-O-methyl modifications significantly enhanced the stability of ribozyme constructs. Ribozymes remained completely intact in human serum for up to 2 hours and in (serum-free) cell supernatants for up to 8 hours. However, other investigators have observed even greater improvements in stability when a variety of 2'-modifications have been incorporated into ribozymes at similar sites (Heidenreich *et al*, 1994, Beigelman *et al*, 1995). For example, Beigelman *et al* (1995) demonstrated that partially 2'-O-methylated hammerheads, with 2'-amino substitutions at positions U_4 and U_7 (for nomenclature see Figure 1.4) and an 'inverted T' base at the 3'-terminus, retained almost 'wild-type' levels of catalytic activity and remained stable in serum for several days. The same group and others (Lyngstaadas *et al*, 1995, Flory *et al*, 1996, see also see Table 1.3) have since proceeded to test the efficacy of chimeric 2'-modified ribozymes *in vivo*. Results indicated that chimeric 2'-modified constructs remained stable and were active *in vivo* because specific gene inhibitory effects were observed following localised administration. Consequently, it has been claimed that site-selective chemical modifications can now largely overcome the stability problems of exogenously delivered ribozymes (Usman *et al*, 1996). However, neither of these *in vivo* studies involved the direct administration of ribozymes to the systemic circulation, and hence, ribozymes were not exposed to the nucleases present in serum.

Another factor which requires consideration when designing ribozymes is the physical accessibility of target sites within mRNA sequences. RNA folding analyses were used successfully, in the present study, to predict the relative activities of ribozymes directed to short, synthetic substrates *in vitro*. However, it is only possible to speculate with regard to the predictive value of the RNA folding program (MFOLD) which was used to identify accessible sites within the EGFr mRNA molecule, since only a small number of the possible secondary structures can be examined using this technique (Zuker *et al*, 1991). Indeed, some studies have shown MFOLD to be unreliable in identifying accessible sites within some large RNA molecules (Dropulic and Jeang, 1994, Birikh *et al*, 1997a). Therefore, the use of an empirical technique, (see Lieber and Strauss, 1995, Jarvis, 1996b, Birikh *et al*, 1997a), such as RNase H

mapping, would provide a better indication of accessible target sites within the EGFr mRNA. Nevertheless, target site accessibility was not an essential requirement for studying the cellular uptake properties of synthetic ribozymes, and hence, it was not studied further here.

In this report, the cellular association of exogenously delivered, chemically stabilised ribozymes was studied in cell culture models, in order to provide evidence for the mechanism(s) of ribozyme cell entry. Mechanistic studies were performed in two cell lines which were relevant to the application of anti-EGFr ribozymes. The A431 epithelial cell line was chosen because this cell line over-expresses EGFr (Ullrich *et al*, 1984, Coulson *et al*, 1996) and could, therefore, be used as a model for testing ribozyme efficacy in subsequent studies. In addition, the U87-MG human glioblastoma cell line was used because these cells share many phenotypic properties with the intended target cells *in vivo*.

Cellular association was highly inefficient in both cell types, with only 1-2% becoming associated after 6 hours. However, levels of cell association in U87-MG cells were approximately 2-fold higher than those observed in A431 cells at any given time point (see Table 6.1). Cellular association versus time profiles were biphasic in both cell types at 37°C; after an initially rapid phase during the first 2-3 hours, the rate of uptake began to level off (i.e. a 'plateau effect' was observed). Similar association profiles were demonstrated with PS ODNs and were consistent with those observed for a variety of ODN analogues (Yakubov *et al*, 1989, Iversen, 1992, Hughes *et al*, 1995, Levis, 1995).

At reduced temperature (4°C) and in the presence of metabolic inhibitors, cellular association was significantly reduced in both A431 and U87-MG cells. This would appear to discount the possibility of ribozymes entering cells via passive diffusion alone, as was originally proposed for some types of ODNs by Agris *et al*, 1986. The temperature and energy dependence of cellular association in both cell types suggested the involvement of endocytosis in the uptake of ribozymes and, again, similar phenomena have been observed with ODN analogues (Wu-Pong *et al*, 1994, Hughes *et al*, 1995, Shoji *et al* 1996). However, it would appear extremely unlikely that ribozymes entered cells exclusively via fluid phase endocytosis (FPE) because levels of cell associated ribozymes were considerably higher than those of mannitol, which is a marker of FPE (Cohn and Ehrenreich, 1969, Luby-Phelps, 1989). Cellular association of ribozymes was demonstrated to be concentration dependant and saturable. These characteristics have also been described for ODNs (Loke *et al*, 1989, Beltinger *et al*, 1995, Hawley and Gibson, 1996) and are considered to be indicative

of a specific cell-surface binding mechanism, possibly mediated by proteins. Consequently, the role of protein binding in the cellular association of ribozymes was investigated in the A431 cell line. A proteolytic enzyme (Pronase®) removed over 50% of cell associated ribozymes. Furthermore, levels of cell association were increased at low pH, which indicated that cellular binding sites were pH sensitive. Only proteins with relatively low pKa values would be susceptible to protonation over the pH range tested. However, protonation of carboxylic acid residues on other proteins could reduce the repulsion of anions by these groups, and this effect could offer an alternative explanation for the increase in cellular association seen here. Protein binding is also considered to play a role in the cellular association of ODNs (Loke *et al*, 1989, Beltinger *et al*, 1995, Beck *et al*, 1996, Hawley and Gibson, 1996, Rojanasakul, 1996) and a large number of proteins, and even specific receptors, have been implicated. These have included fibrinogen receptor epitopes (Gewirtz *et al*, 1996), ε-amino groups of lysine, guanidium groups of arginine, protonated imidazole groups of histidine (Blackburn and Gait, 1990) and sub-types of basic fibroblast growth factor receptors (Guvakova *et al*, 1995). The possibility that ribozymes bind to similar proteins cannot be discounted because PO and PS ODNs were able to strongly compete with ribozymes for cellular association in both A431 cells and U87-MG cells. This suggests that there may be a considerable degree of overlap in their mechanism(s) of cell entry. However, polyanions such as dextran sulphate and heparin were also able to compete with ribozymes for association in A431 cells and have been shown to compete with ODNs in other cell lines (Wu-Pong *et al*, 1992, Gewirtz *et al*, 1996). Since these polyanions are chemically unrelated to ribozymes, this casts doubt upon the existence of a specific protein receptor, responsible for the cellular uptake of ribozymes and / or ODNs. At the very least it suggests that if specific binding protein(s) exist, they exhibit low levels of affinity for their ribozyme ligands.

The overall trends in cellular association were similar in both A431 cells and U87-MG cells, although the actual level of cell association was greater in U87-MG cells than in A431 cells. Further studies, in a variety of unrelated cell lines, confirmed that the levels of cell association were cell-type dependent (when normalised to cell number). A similar cell-type dependency has also been observed for the association of ODNs (Loke *et al*, 1989, Noonberg *et al*, 1993, Yee *et al*, 1994, Beck *et al*, 1996, Akhtar and Rossi, 1996). Differences could reflect variations in the intrinsic rates of endocytosis between cell types. Alternatively, these differences could be related to the availability of binding sites, such as proteins, on cell surfaces. However, a variety of other factors, such as variations in cell size, gross morphology and varying stages in the cell cycle could have influenced levels of cell association. This highlights the fact

that it is difficult to draw quantitatively accurate comparisons between cell association studies performed in different cell-types.

It was evident in all of the mechanistic studies performed that the cellular uptake properties of chemically modified ribozymes showed many similar trends to those observed with antisense ODNs by other groups (for reviews see Akhtar and Juliano, 1992, Rojanasakul, 1996). ODNs are widely considered to enter cells via a process of receptor mediated endocytosis and / or adsorptive endocytosis and it would appear that chimeric ribozymes enter cells via similar mechanisms. The sequence requirements of hammerhead ribozymes, their partial chemical modification and their 'wishbone' secondary structure (Pley *et al*, 1994, Scott *et al*, 1995 & 1996) do not appear to alter the overall mechanism of uptake compared with the many ODN analogues which have been studied. The high molecular weight and polyanionic character of ribozymes appear to be the most important factors influencing their cellular uptake mechanism(s). However, some recent studies have indicated that cell association of ODNs can be sequence-specific in certain circumstances (Hughes *et al*, 1994, Agrawal *et al*, 1996, Devlin, 1996). For example, ODNs containing 'G'-quartets, become cell associated in greater quantities than other ODN sequences, even though they share the same mechanism of uptake, because they can form tetraplexes which have distinct secondary structures (Devlin, 1996). Therefore, it is possible that the secondary structure of ribozymes could also influence the overall magnitude of cell association.

An endocytic mechanism of cell entry would result in the localisation of ribozymes within endosomal or lysosomal vesicles following internalisation. Therefore, the intracellular fate of ribozymes was investigated using different techniques. Fluorescent microscopy indicated that FITC-labelled ribozymes became localised at the periphery of cells, close to the cell membrane, following exogenous delivery. FITC-ribozymes exhibited a punctate pattern of subcellular distribution, which is considered to be indicative of cell entry via endocytosis and subsequent localisation within vesicular compartments (Wagner, 1994, Rojanasakul, 1996). In addition, a considerable degree of co-localisation was observed between ribozymes and rhodamine-dextran, which has been characterised as an endosomal marker (Berlin and Oliver, 1980). Immuno-electron microscopy allowed a more detailed examination of the intracellular localisation of both biotin-labelled ribozymes and PS ODNs. Again, this indicated that ribozymes were predominantly found within endosomal vesicles following cell entry. These structures were identified as clear vesicles within the cytoplasm, in line with observations of ultrastructural morphology made by other workers (Bubel and Fitzsimmons, 1989, Griffiths *et al*, 1993, Beltinger *et al*, 1995). However, the lack of

a specific staining technique to highlight the endosomes made their identification difficult. The identity of the endosomal vesicles was somewhat confirmed by the fact that PS ODNs were also localised within these structures, and their predominant localisation within endosomes has been demonstrated in a previous ultrastructural study (Beltinger *et al*, 1995). In future studies, the co-incubation of ribozymes with an endosomal marker (such as horse radish peroxidase conjugated to larger gold particles), could further confirm the identity of the endosomal vesicles. However, gold-labelled endosomal markers would probably require in-house synthesis. In addition, the co-incubation of ribozymes with these compounds could potentially affect cellular association characteristics (e.g. by competition for binding sites). The number of control experiments required would also have to be multiplied in experiments involving the detection of multiple labels, and this would add to the heavy financial costs of such work.

Ribozymes were also observed in significant quantities within (electron-dense) primary lysosomal vesicles (see Tarrason *et al*, 1995, Beltinger *et al*, 1995) and within multi-vesicular bodies (secondary lysosomes). These are considered to be the principal sites of intracellular digestion (Alberts *et al*, 1989, Bubel and Fitzsimmons, 1989). Ribozymes sequestered in these vesicles would probably be exposed to high concentrations of nucleases (Hudson *et al*, 1996a) and would be rapidly exported from cells, via exocytosis, before they were able to exert a biological effect. To examine these possibilities, the extent of ribozyme export from cells and their intracellular stability was examined.

Cellular efflux studies, in A431 cells, confirmed that cell association of ribozymes was dynamic and represented both the uptake and efflux processes. The establishment of an equilibrium between cellular uptake and export offered a likely explanation for the 'plateau effect' which was observed after 2-3 hours in the initial cell association studies (see above). Efflux appeared to be bi-phasic with around 50% of cell associated ribozymes being exported from cells within 4 hours. Similar results were observed with PS ODNs in this report, and by other investigators (see Section 5.3.3 and see also Stein *et al*, 1993, Tonkinson and Stein, 1994). It has been suggested that the bi-phasic pattern of efflux could represent exocytosis from two (mathematically-derived) intracellular compartments (Tonkinson and Stein, 1994). Based on this assumption, efflux data were fitted to a double exponential function which indicated that approximately 23% of internalised ribozymes were rapidly exported ($t_{\frac{1}{2}} \approx 15$ minutes) from 'shallow' compartments which, in theory, could be situated at, or near, the cell surface. 'Shallow' compartments could represent cell-surface binding proteins (as predicted by the Pronase washing experiments) or primary endosomal vesicles (as

predicted by microscopy studies). By contrast, approximately 72% of ribozymes were thought to reside in 'deeper' compartments, from which efflux was somewhat slower ($t_{\frac{1}{2}} \approx 3$ hours). The 'deeper' compartments could represent late endosomes or lysosomes. Alternatively these 'deeper' compartments could represent intracellular vesicles which were processed via the golgi complex, since ultrastructural analyses indicated that ribozymes were present, in modest quantities, within the remnants of the golgi complex and its associated vesicles. It is possible, therefore, that the intracellular trafficking of ribozymes could involve transport to the golgi, within endosomes, as part of a membrane recycling system (see Alberts *et al*, 1989). After arriving at the golgi complex, ribozymes could be exported from the cell within secretory vesicles or transported to the lysosomes. However, subsequent studies in this report appeared to cast doubt upon the role of secretory (golgi) vesicles in the exocytosis of ribozymes because ribozymes did not accumulate within cells when the trafficking of these vesicles was inhibited. This was demonstrated by pre-treating cells with monensin, which is known to inhibit the transport of secretory vesicles from the golgi to the cell membrane, causing the vesicles (and their contents) to accumulate within the cytoplasm (see Stein *et al*, 1984). Since ribozymes did not (significantly) accumulate within cells following monensin treatment, this finding contradicts the proposed involvement of the golgi in the intracellular trafficking of ribozymes.

The composition of efflux products was examined in order to determine the extent of ribozyme degradation following cell association. Chimeric ribozymes present in efflux samples (after 4 hours) remained largely intact, which indicated that any exposure to the lysosomes did not result in significant degradation. This finding correlated with the stability of chimeric ribozymes following exposure to tritosomal (rat liver lysosome) extract *in vitro*. Therefore, the nuclease composition of the tritosomal extract could be similar to that of the lysosomes within cells, as proposed by other investigators (Seymour *et al*, 1994).

Regardless of the exact nature of their vesicular localisation, ribozymes would have to depart membrane bound compartments in order to exert biological effects within cells (Akhtar *et al*, 1995). Possible mechanisms for the release of ribozymes from endocytic vesicles include association with proteins, which can destabilise endosomal membranes, or leakage during fusion events (Akhtar and Juliano, 1992). Although the exact nature of endosomal release was not investigated in this report, an examination of the ultrastructural data suggested the existence of such a mechanism because biotinylated ribozymes and PS ODNs were visualised within the nucleus and 'free' within the cytoplasm. Nuclear penetration of PS ODNs has been observed in previous ultrastructural studies (Tarrason *et al*, 1995, Beltinger *et al*, 1995) and these authors

concluded that the nucleus was likely to be the main site at which antisense PS ODNs exert their biological effects. Other investigators have also suggested that the nucleus is the primary site for ribozyme activity within cells (Sioud, 1992, Crisell *et al*, 1993). The ultrastructural observations in this report would appear to support this hypothesis, since they provide direct physical evidence of nuclear penetration by ribozymes. Although the mechanism(s) by which ribozymes might enter nuclei have not been studied in detail, PS ODNs are thought to enter cell nuclei via diffusion through the nuclear pores (Clarenc *et al*, 1993), and therefore, ribozymes may gain access via a similar mechanism.

Since the ultimate goal of the research group was to apply the use of ribozymes and antisense ODNs to the treatment of malignant disease within the brain, the *in vivo* distribution of ribozymes was assessed following localised delivery to this organ. Fluorescent-labelled chimeric ribozymes were directly administered to the cerebral ventricles of mice via ICV injection and patterns of distribution were assessed by examination of cryosections. Following ICV injection, a fluorescent signal was detected in diverse areas of the brain but the most intense signals were detected at the choroid plexus, within the cerebral ventricles (i.e. at the site of administration). However, closer examination revealed strong fluorescent signals within areas of tissue which were adjacent to the cerebral ventricles, such as the striatum and the cerebral cortex. This indicated that significant quantities of ribozymes were able to depart the cerebral ventricles and penetrate the surrounding tissues. Moreover, a highly punctuated pattern of distribution was observed within the striatum and cortex, which was thought to represent cellular localisation of FITC-labelled ribozymes in these tissues. Similar patterns were noted when FITC-labelled PS ODNs were administered using a similar technique, both in the present study, and in experiments performed by other investigators (Piwinca-Worms, 1994, Zhang *et al*, 1996). These investigators suggested that the punctuated pattern of distribution represented localisation within cell bodies and dendritic processes. However, the specific identity of the cell types to which ribozymes became localised was uncertain in the present study. Localisation within glial cells would be ideal for therapies designed to treat GBM. Glial cells are known to be widely distributed throughout the brain and are present within the striatum and the cortex (Nauta and Feirtag, 1986). Therefore, it would appear that ribozymes are almost certainly able to access areas of the brain where the glia are present, even though the patterns of localisation seen may not specifically indicate uptake by the glia. A possible suggestion for future studies would be to assess the co-localisation of FITC-labelled ribozymes with a molecule capable of tagging the glia, such as an immuno-fluorescent marker, if such a compound became available. This could confirm whether or not localisation within the glia was observed in these

studies. Nevertheless, the penetration of the brain tissue by ribozymes and the apparently cellular localisation following ICV administration *in vivo*, demonstrates that ribozyme therapies have the potential to exert biological effects within the brain. However, it remains to be seen if ribozymes targeted to the brain, can, like there antisense counterparts (see Ogawa and Pfaff, 1996, Akhtar and Agrawal, 1997), demonstrate *in vivo* efficacy when delivered to this organ.

With regard to the treatment of GBM; surgery is currently the first line treatment but, at best, this merely prolongs the lifespan of patients because complete removal of the tumour mass is extremely difficult (Selby, 1994) and, therefore, tumour regression usually occurs. If the efficacy of ribozyme-based therapies could be established in animal models, it is possible that they could be used as an adjunct to surgery, in order to limit tumour regression in GBM. For example, it may be possible to administer ribozymes to tumour sites following surgical procedures, since it appears that locally administered ribozymes can penetrate cells in the tissues surrounding the site of administration. Ideally this would involve the use of a delivery vehicle which could release ribozymes at the tumour site over a prolonged period. The use of biodegradable polymer implants is, therefore, a potential delivery option for such an application. The entrapment of ribozymes within biodegradable polymer devices has been investigated (see Hudson *et al*, 1996b; Appendix III). Results indicated that biodegradable PLA films could release ribozymes over a sustained period *in vitro*. Furthermore, all-RNA ribozymes entrapped within biodegradable polymers retained their catalytic activity and were protected from degradation by nucleases. Hence, chemically stabilised hammerhead ribozymes (see Section 1.2.4.1) could potentially be released from polymer films after implantation *in vivo*. The studies described here suggest that ribozymes would be able to penetrate cells following release from polymer films, and hence, they could exert gene inhibitory effects within tumour cells.

Two further strategies were investigated for improving the cellular delivery of ribozymes. Ribozymes conjugated to an anti-transferrin receptor antibody (TRA) demonstrated increased levels of cell association in A431 cells. A 3-fold enhancement in cell-association was achieved using a TRA / ribozyme conjugate and this was demonstrated to be a result of a specific interaction with transferrin receptors. Further improvements in cellular delivery could be possible in cells which express particularly high levels of transferrin receptors. For example, many malignant cells express increased levels of the transferrin receptor (Shah and Shen, 1995) and this could allow them to be targeted *in vivo* by TRA / ribozyme conjugates. Furthermore, the capillary endothelial cells which comprise the blood brain barrier (BBB), express particularly high concentrations of the transferrin receptor (Friden, 1993). Therefore, strategies

which can exploit transferrin receptor-mediated delivery can potentially be used to deliver ribozymes and other molecules to the brain, via the BBB (Boado, 1995). Strategies to improve BBB transport would appear to be required if systemically delivered ribozymes were to be used for applications within the brain, since recent pharmacokinetic studies have shown that penetration of the brain by ribozymes is extremely poor following systemic delivery (Desjardins *et al*, 1996).

Further studies in this report have demonstrated that intracellular levels of TRA / conjugates can be increased via the co-administration of monensin. In fact, the co-administration of transferrin-drug conjugates (such as immunotoxin-TRA conjugates) and monensin is currently under investigation for cancer treatment (Shah and Shen, 1995). However, studies have shown that transferrin receptors remain entrapped within endocytic vesicles following internalisation, both in the presence and absence of monensin (Stein *et al*, 1995, Molenhauer *et al*, 1990). Therefore, TRA / ribozyme conjugates, like 'free' ribozymes, share a common obstacle because their escape from endosomal vesicles would be vital for catalytic activity within cells. Furthermore, the release of conjugated ribozymes from antibody complexes may also be required, in order to allow cleavage of target substrates. This could be a problem for the conjugates designed in this report because ribozymes were bound to antibodies via a thio-ether linkage, which would probably resist degradation *in vivo*. However, in future studies, the release of ribozymes from conjugates could be facilitated by using a cell-labile disulphide linkage.

Since 'free' ribozymes, and those delivered by carrier molecules, appear to become entrapped within endocytic vesicles following cell entry, it would appear that strategies which can facilitate the release of ribozymes from endosomes could improve their biological activity. Adjuvants which can facilitate the release of molecules from endosomal compartments are being investigated, and these include fusogenic peptides, pH-sensitive surfactants and polymeric dendrimers (see Hughes *et al*, 1996). In future, the application of these 'adjuvants' to the delivery of ribozymes could potentially improve their bioavailability. Perhaps the most widely studied agents for improving cytosolic penetration are, however, cationic liposomes. These agents are thought to facilitate the endosomal exit of ONs by a putative lipid exchange mechanism (see Section 1.4.2.5 and Zelphati and Szoka, 1996). Furthermore, they have been used successfully to deliver antisense ONs (for reviews see Juliano and Akhtar, 1992, Chonn and Cullis, 1995, Bennett, 1995, Thierry and Takle, 1995, Rojansakul, 1996) and ribozymes (see Table 1.3 and Kariko *et al*, 1994, Chonn and Cullis, 1995) to a variety of different cell-types. However, the efficiency of cellular uptake of cationic lipid / polynucleotide complexes is dependant upon the cell-type

(Juliano and Akhtar, 1992, Sullivan, 1993, Litzinger *et al*, 1996), the composition of the cationic lipid (Felgner *et al*, 1994) and the surface charge characteristics of the liposome / polynucleotide complex (Jaaskelainen *et al*, 1994, Lappalainen *et al*, 1994, Eastman *et al*, 1997). Therefore, the use of ribozyme / lipid complexes requires optimisation, on an individual basis, according to the cell-type and lipid formulation used (Felgner *et al*, 1994). In this report, two commercially available liposome formulations, containing the cationic lipids DOSPA and DOTMA, were evaluated for their ability to deliver ribozymes to A431 cells *ex vivo*. Complexation with either of these cationic lipid formulations resulted in a significant increase in levels of cell-associated ribozymes. Optimal delivery (to A431 cells) was achieved when the molar ratio of positive to negative charges within ribozyme / lipid complexes was approximately equal (i.e. when cationic:anionic charge ratios were around 1.0). The increased efficiency of these complexes (formulated at approximately equal charge ratios) in delivering ribozymes to cells, appeared to be related to their larger particle size (diameter).

In the short term, it was envisaged that cationic liposomes could be utilised as a means of delivering high concentrations of ribozymes to cells, in order to assess levels of catalytic activity in A431 cells. Of the two formulations evaluated in this report, Lipofectamine® (DOSPA) would appear to be the formulation of choice because higher proportionate increases in cell associated ribozyme were observed with this agent, when 'equi-toxic' concentrations were used. However, toxicity could be a potential barrier to the use of either formulation because both formulations reduced cell viability to some extent when administered to A431 cells for 4 hours at concentrations of 2μM and above. Efficacy studies would probably require incubation times to be extended beyond 4 hours, and hence, the toxic effects of these liposome formulations could be further potentiated in such studies.

In future, it would be desirable to use cationic lipids for the *in vivo* delivery of ribozymes. Despite the potential toxicity problems which can arise from the use of these agents, a small number of investigators have successfully utilised cationic liposomes to deliver ribozymes, both *ex vivo* and *in vivo* (see Table 1.3). However, in the *in vivo* studies performed to date (Kisich *et al*, 1995, Sioud, 1996), localised rather than systemic delivery of ribozymes has been the main aim. Systemically delivered, cationic liposomes appear to be taken up, almost exclusively, by the cells of the reticulo-endothelial system (i.e. mainly the spleen, liver and kidneys) (Litzinger *et al*, 1996). Therefore, therapeutic applications of systemically delivered cationic liposome complexes would probably be more effective in these organs.

Despite the many obstacles which still have to be overcome in designing efficient, exogenous delivery systems for ribozymes, their therapeutic potential is in little doubt. A great deal of research attention is currently being focused on strategies to improve the cytosolic penetration of ribozymes and ODNs following exogenous delivery. However, the studies described in this report suggest that ribozymes can gain access to target sites within the nucleus and cytoplasm, albeit in very small quantities, following 'direct' exogenous administration to cells. Moreover, the gene inhibitory effects reported in animal studies (Lyngstaadas *et al*, 1995 and Flory *et al*, 1996) suggest that chemically modified ribozymes can also penetrate cells, *in vivo*, in the absence of additional delivery systems. Recently, it has been reported that human clinical trials are planned, which aim to test the efficacy of exogenously delivered, chimeric ribozymes (see Coghlan, 1996). The ribozymes used in these trials will be directed against (as yet unspecified) mRNA targets which are involved in diabetic retinopathy. Furthermore, these ribozymes will be locally administered to the eyes, via intra-vitreal injection, without an additional delivery system (Coghlan, 1996). The results of these clinical trials are eagerly awaited. The outlook is bright, however, since a number of human trials with antisense ONs have already shown promise (for a recent review see Akhtar and Agrawal, 1997) and the studies reported here suggest that ribozymes and ONs share similar cellular uptake characteristics.

It is interesting to note that most examples of gene inhibitory effects with (exogenously delivered) ribozymes have been demonstrated following their administration to highly localised sites *in vivo* (see Table 1.3). Local delivery of ribozymes does not, necessarily, require an additional delivery system to target ribozymes to specific cell-types or organs. Furthermore, locally delivered ribozymes can potentially avoid the primary sites of *in vivo* metabolism (e.g. the liver) and may have improved safety profiles, since fewer organs would be exposed to them. Therefore, local administration may (currently) have advantages and could, as discussed above, allow ribozymes to be used as an adjunct to surgery, in order to limit tumour regression in GBM.

REFERENCES

Agrawal, S. (1996a) Antisense Oligonucleotides: Towards Clinical Trials. *Trends in Biotechnology*. 14, 376-387.

Agrawal, S. (1996b) Antisense Therapeutics. *Methods in Molecular Medicine*. Agrawal, S. (Ed.) Humana Press Incorporated. Totowa, New jersey, USA.

Agrawal, S. and Akhtar, S. (1995) Advances in Antisense Efficacy and Delivery. *Trends in Biotechnology*. 13, 197-199.

Agrawal, S. Iadarola, P.L., Temsamani, J., Zhao, Q. and Shaw, D.R. (1996) Effect of G-rich Sequences on the Synthesis, Purification, Hybridization, Cell Uptake and Haemolytic Activity of Oligonucleotides. *Biology and Medicinal Chemistry Letters*. 6, 2219-2224.

Agrawal, S., Temsamani, J., Galbraith, W., and Tang, J.Y. (1995) Pharmacokinetics of Antisense Oligonucleotides. *Clinical Pharmacokinetics*. 28, 7-16.

Agrawal, S., Sarin, P.S., Zamecnik, M. and Zamecnik, P. (1992) Cellular Uptake and Anti-HIV Activity of Oligonucleotides and their Analogs. In: *Gene Regulation. Biology of Antisense RNA and DNA*. Erickson, R.P. and Izant, J.G. (Eds.) Raven Press Ltd, New York USA

Agrawal, S., Temsamani, J. and Tang, J.Y. (1991) Pharmacokinetics, Biodistribution and Stability of Oligodeoxynucleotide Phosphorothioates in Mice. *The Proceedings of the National Academy of Sciences of The USA*. 88, 7595-7599.

Agris, C.H., Blake, K.R., Miller, P.S., Reddy, M.P. and Tso, P.O.P. (1986) Inhibition of Vesicular Stomatitis Virus Protein Synthesis and Infections With Sequence-Specific Oligodeoxyribonucleoside Methylphosphonates. *Biochemistry*. 25, 6228-6234

Akhtar, S. (1995) Delivery Strategies for Antisense Oligonucleotide Therapeutics. Akhtar, S. (Ed). CRC Press Inc, London, UK.

Akhtar, S. and Agrawal, S. (1997) In Vivo Studies with Antisense Oligonucleotides. *Trends in the Pharmaceutical Sciences*. 18, 12-18.

Akhtar, S., Basu, S., Wickstrom, E. and Juliano, R.L. (1991) Interactions of Antisense DNA Oligonucleotide Analogues with Phospholipid Membranes (Liposomes). *Nucleic Acids Research*. 19, 5551-5559.

Akhtar, S., James, H. and Gibson, I. (1995) Molecular DIY with Hairpins and Hammerheads. *Nature Medicine* 1, 300-302

Akhtar, S. and Juliano, R.L. (1991) Antisense Oligonucleotides as Potential Therapeutic Agents. *The Pharmaceutical Journal.* July 20th 1991.

Akhtar, S. and Juliano, R.L. (1992) Cellular Uptake and Intracellular Fate of Antisense Oligonucleotides. *Trends in Cell Biology.* 2, 139-143.

Akhtar, S. and Juliano, R.L (1992b) Liposome Delivery of Antisense Oligodeoxynucleotides: Adsorption and Efflux Characteristics of Phosphorothioates. *The Journal of Controlled Release.* 22, 47-56.

Akhtar, S. Kole, R., and Juliano, R.L. (1991b) Stability of Antisense DNA Oligodeoxynucleotide Analogs in Cellular Extracts and Sera. *Life Sciences.* 49, 1793-1801.

Akhtar, S. and Rossi, J.J. (1996) Anti-HIV Therapy with Antisense Oligonucleotides and Ribozymes: Realistic Approaches or Expensive Myths? *The Journal of Antimicrobial Chemotherapy.* 38, 159-165.

Akhtar, S., Routeledge, A., Patel, R. and Gardiner, J.M. (1995b) Synthesis of Mono- and Dimannoside Phosphoramidite Derivatives for Solid Phase Conjugation to Oligonucleotides. *Tetrahedron Letters.* 36, 7333-7336.

Akhtar, S., Shoji, Y. and Juliano, R.L. (1992) Pharmaceutical Aspects of The Biological Stability and Membrane Transport Characteristics of Antisense Oligonucleotides. In: *Gene Regulation. Biology of Antisense RNA and DNA.* Erickson, R.P. and Izant, J.G. (Eds) Raven Press Ltd, New York USA

Alberts, B., Bray, D., Lewis, J., Raff, M., Roberts, K., Watson, J.D. (1989) Intracellular Sorting and The Maintenance of Cellular Compartments. In: *The Molecular Biology of the Cell.* Garland Publishing, New York, USA.

Anderson, P., Monforte, J., Tritz, R., Nesbitt, S., Hearst, J., Hampel, A. (1994) Mutagenesis of the Hairpin Ribozyme. *Nucleic Acids Research.* 22, 1096-1100.

Armbruster, B.L., Carlemalm, E., Chiovetti, R., Garavito, R.M., Hobot, J.A., Kellenberger, E. and Villinger, W. (1982) Specimen preparation for Electron Microscopy Using Low Temperature Embedding Resins. *The Journal of Microscopy.* 126, 77-85.

Ayers, D., Cuthbertson, J.M., Schroyer, K. and Sullivan, S.M. (1996) Polyacrylic Acid Mediated Ocular delivery of Ribozymes. *The Journal of Controlled Release.* 38, 167-175.

Baker, J.R. (1966) Cytological Technique: The Principles Underlying Routine Methods. Chapman and Hall Publications, London, UK.

Beck, G.F., Irwin, W.J., Nicklin, P.L. and Akhtar, S. (1996) Interactions of Phosphodiester and Phosphorothioate Oligonucleotides with Intestinal Epithelial Caco-2 Cells. *Pharmaceutical Research.* 13, 1028-1037.

Beelman, C.A. and Parker, R. (1995) Degradation of mRNA in Eukaryotes. *Cell*. 81, 179-183.

Behnke, O. (1986) Non-Specific Binding of Protein-Stabilised Gold Solutions as a Source of Error in Immunochemistry. *The European Journal of Cell Biology*. 41, 326-338.

Beigelman, L., McSwiggen, J.A., Draper, K.G., Gonzalez, C., Jensen, K., Karpeisky, A.M., Modak, A.S., Matulic-Adamic, J., DiRenzo, A.B., Haerberli, P., Sweedler, D., Tracz, D., Grimm, S., Wincott, F.E., Thackray, V.G. and Usman, N. (1995) Chemical Modification of Hammerhead Ribozymes. *The Journal of Biological Chemistry*. 43, 25702-25708.

Beigelman, L., Karpeisky, K., Matulic-Adamic, J., Gonzalez, C. and Usman, N. (1995b) New Structural Motifs for Hammerhead Ribozymes. Catalytic Activity of Abasic Nucleotide Substituted Ribozymes. *Nucleosides and Nucleotides*. 14, 907-910.

Belikova, A.M., Zarytova, V.F. and Grineva, N.I. (1967) Synthesis of Ribonucleosides and Diribonuceloside Phosphates Containing 2-chloroethylamine and Nitrogen Mustard Residues. *Tetrahedron Letters*. 37, 3557-3562.

Beltinger, C., Saragovi, H.U., Smith, R.M., LeSauter, L., Shah, N., DeDionisio, L., Christensen, L., Raile, A., Jarett, L. and Gewirtz, A.M. (1995) Binding, Uptake and Intracellular Trafficking of Phosphorothioate-Modified Oligodeoxynucleotides. *The Journal of Clinical Investigation*. 95, 1814-1823.

Bennett, C.F. Chaing, M.Y., Chan, Y., Shoemaker, J.H.E. and Mirabelli, C.K. (1992) Cationic Lipids Enhance Cellular Uptake and Activity of Phosphorothioate Antisense Oligonucleotides. *Molecular Pharmacology*. 41, 1023.

Bennett, C.F. (1995) Intracellular Delivery of Oligonucleotides with Cationic Liposomes. In: *Delivery Strategies for Antisense oligonucleotide Therapeutics*. Akhtar, S. (Ed). CRC Press Inc, London, UK.

Bennett, R.M. (1993) As Nature Intended? The Uptake of DNA and Oligonucleotides By Eukaryotic Cells. *Antisense Research and Development*. 3, 235-241.

Bergan, R., Connell, Y., Fahmy, B., Kyle, E. and Neckers, L. (1994) Aptameric Inhibition of p210 *bcr-abl* Tyrosine Kinase Autophosphorylation by Oligodeoxynucleotides of Defined Sequence and Backbone Structure. *Nucleic Acids Research*. 22, 2150-2154.

Bergan, R., Kyle, E., Connell, Y. and Neckers, L (1995) Inhibition of Protein-Tyrosine Kinase Activity in Intact Cells by the Aptameric Action of Oligodeoxynucleotides. *Antisense Research and Development*. 5, 33-38.

Berger, S.L., Kimmel, A.R. (1987) A Guide to Molecular Cloning Techniques. In: *Methods in Enzymology*. Volume 152. Academic Press Inc Ltd. London, UK.

Berlin, R.D. and Oliver, J.M. (1980) Characterisation of FITC-Dextran As An Indicator of Fluid Phase Pinocytosis. *Journal of Cell Biology*. 85, 660-671.

Bertrand, E. and Rossi, J (1996) Anti-HIV Therapeutic Hammerhead Ribozymes: Targeting Strategies and Optimization of Intracellular Function. *Nucleic Acids and Molecular Biology*. 10, 301-313.

Bertrand, E., Pictet, R. and Grange, T. (1994) Can Ribozymes be Efficient Tools to Inactivate gene Function? *Nucleic Acids Research*. 22, 293-300.

Berzal-Herranz, A., Joseph, S., Chowrira, B.M., Butcher, S.E., Burke, J.M. (1993) Essential Nucleotide Sequences and Secondary Structure Elements of the Hairpin Ribozyme. *EMBO Journal*. 12, 2567-2574.

Besterman, J.M., Airhart, J.A., Woodworth, R.C., and Low, R.B. (1981) Endocytosis of Pinocytosed Fluid in Cultured Cells: Kinetic Evidence for Rapid Turnover and Compartmentation. *The Journal of Cell Biology*. 91, 716-727.

Birikh, K.R., Berlin, Y.A., Soreq, H., Eckstein, F. (1997a) Probing Accessible Sites for Ribozymes on Human Acetylcholinesterase RNA. *RNA*. 3, 429-437.

Birikh, K.R., Heaton, P.A. and Eckstein, F. (1997b) The Structure, Function and Application of the Hammerhead Ribozyme. *The European Journal of Biochemistry*. 245, 1-16.

Blackburn, G.M. and Gait, M.J. (1990) Antisense Oligonucleotide Technology (Chapter 9), 339-377. In: *Nucleic Acids in Chemistry and Biology*. IRL Press, Oxford, UK.

Boado, R.J. (1995) Antisense Delivery through the Blood Brain Barrier. *Advanced Drug Delivery Reviews*. 15, 73-107.

Boado, R.J. and Pardridge, W.M. (1996) Pharmacokinetics and Blood Brain Barrier Transport of [^{3}H]-Biotinylated Phosphorothioate Oligodeoxynucleotide Conjugated to a Vector mediated delivery System. *The Journal of Pharmacology and Experimental Therapeutics*. 276, 206-211/

Bongartz, J.P., Aubertin, A.M., Mihaud, P.G. and Lebleu, B. (1994) Improved Biological Activity of an Antisense Oligonucleotide Conjugated to a Fusogenic Peptide. *Nucleic Acids Research*. 22, 4681-4688.

Bouterine, A.S. and Kostina, E.V. (1993) Reversible Attachment of Cholesterol to oligodeoxyribonucleotides for Studies of the mechanisms of their Penetration into Eukaryotic Cells. *Biochimie*. 75, 35-41.

Bradley, M.O., Chrisey, L.A. and Hawkins, J.W. (1992) Antisense Therapeutics. In: *Gene Regulation. Biology of Antisense RNA and DNA*. Erickson, R.P. and Izant, J.G. (Eds) Raven Press Ltd, New York USA

Bratty, J., Chartrand, P., Ferbeyre, G., Cedergren, R. (1993) The Hammerhead RNA Domain, A Model Ribozyme. *Biochimica et Biophysica Acta*. 1216, 345-359.

Brittain, R.T. and Handley, S.L. (1967) Temperature Changes Produced By The Injection of Catecholamines and 5-Hydroxytryptamine into the Cerebral Ventricles of The Conscious Mouse. *The Journal of Physiology*. 192, 805-813.

Brown, T. and Brown, D.J.S. (1989) Modern Machine Aided Methods of Oligodeoxynucleotide Synthesis. In: *Oligonucleotides and Analogues*. Eckstein, F. (Ed).Oxford University Press. Oxford, UK.

Bubel, A and Fitzsimmons, C. (1989) , Electron Micrographs of Cell Ultrastructure. In: *Microstructure and Function of Cells*. Ellis Horwood Publications, Chichester, UK.

Bunnell, B.A. and Morgan, R.A. (1996) Gene Therapy for HIV Infection. *Drugs of Today*. 32, 209-224.

Burke, J.M. (1996) Hairpin Ribozyme: Current Status and Future Prospects. *Biochemical Society Transactions*. 24, 608-615.

Burke, J.M., Belfort, M., Cech, T.R., Davies, R.W., Schweyen, R.J., Shub, D.S., Szostak, J.W., Tabak, H.F. (1987) Structural Conventions for Group I Introns. *Nucleic Acids Research*. 15, 7217-7221.

Busch, G., Hoder, D., Reutter, W. and Tauber, R. (1989) Selective Isolation of Individual Cell Surface Proteins from Tissue Culture Cells by Cleavable Biotin Label. *The European Journal of Cell Biology*. 50, 257-262.

Buzayan, J.M., Gerlach, W.L., Bruening, G. (1986) Non-Enzymatic Cleavage and Ligation of RNAs Complementary to a Plant Virus Satellite RNA. *Nature*. 323, 349-353.

Buzayan, J.M., Van Tol, H., Feldstein, P.A. and Bruening, G. (1990) Identification of a Non-Junction Phophodiester That influences an Autolytic Processing reaction of RNA. *Nucleic Acids Research*. 18, 4447-4451.

Cai, D.W., Mukhopadhyay, T., Roth, J.A. (1995) Suppression of Lung cancer Cell growth by Ribozyme-Mediated Modification of p53 pre-mRNA. *Cancer Gene Therapy*. 2, 199-205.

Caruthers, M.H. (1989) Synthesis of Oligonucleotides and Oligonucleotide Analogues. In: Oligodeoxynucleotides - Antisense Inhibitors of Gene Expression. *Topics in Molecular and Structural Biology*. Volume 12. Cohen, J.S. (Ed). The Macmillan Press. London, UK.

Cech, T.R. (1992) Ribozyme Engineering. *Current Opinion in Structural Biology*. 2, 605-609.

Cech, T.R. (1993) The Efficacy and Versatility of Catalytic RNA: Implications for an RNA World. *Gene*. 135, 33-36.

Cech, T.R. and Bass, B.L. (1986) Biological catalysis by RNA. *Annual Reviews in Biochemistry*, 55, 599-644.

Cech, T.R., Zaug, A.J., Grabowski, P.J. (1981) *In Vitro* Splicing of the Ribosomal RNA Precursor of *Tetrahymena*: Involvement of a Guanosine Nucleotide in the Excision of the Intervening Sequence. *Cell*. 27, 487-496.

Cech, T.R. and Uhlenbeck, O.C. (1994) Hammerhead Nailed Down. *Nature*. 372, 39-41.

Chatterjee, S., Johnson, P.R. and Wong, K.K. (1992) Dual inhibition of HIV-1 In Vitro by means of an Adeno-Associated Virus Antisense Vector. *Science*. 258, 1485-1488.

Chen, C.J., Banerjea, A.C., Harmison, G.G., Haglund, K., Schubert, M. (1992) Mulit-target Ribozymes Directed to Cleave At Up To Nine Highly Conserved HIV-1 *env* RNA Regions Inhibits HIV-1 Replication. *Nucleic Acids Research*. 20, 4581-4589.

Chiang, L., Flores, E.P., Wen, D.Y., Hall, W.A. and Low, W.C. (1995) Gene Therapy for Neurodengenerative Disorders and Malignant Brain Tumours. *Behavioural and Brain Sciences*. 18, 52-53.

Chiasson, B.J., Hooper, M.L., Murphy, P.R. and Robertson, H.A. (1992) Antisense Oligonucleotide Eliminates *In Vivo* Expression of *c-fos* in Mammalian Brain. *The European Journal of Pharmacology*. 227, 451-453.

Chonn, A., and Cullis, P.R. (1995) Recent Advances in Liposomal Drug-Delivery Systems. *Current Opinion in Biotechnology*. 6, 698-708.

Chowrira, B.M., Berzal-Herranz, A., Burke, J.M. (1991) Novel Guanosine Requirement for Catalysis by the hairpin Ribozyme. *Nature*. 354, 320-322.

Chu, C.J., Dijkstra, J., Lai, M.Z., Hong, K. and Szoka, F.C. (1990) Efficiency of Cytoplasmic delivery by pH-Sensitive Liposomes in Cells in Culture. *Pharmaceutical Research*. 7, 824-834.

Clouet-D'Orval, B. and Uhlenbeck, O.C. (1996) Kinetic Characterisation of I/II Format Hammerhead Ribozymes. *RNA*. 2, 483-491.

Citro, G. Perrotti, D., Cucco, C., D'Angelo, I., Saachi, A., Zupi, G. and Calabretta, B. (1992) Inhibition of Leukemia Cell Proliferation by Receptor-Mediated Uptake of c-myb Antisense Oligonucleotides. *The Proceedings of the National Academy of Sciences of the USA*. 89, 7031-7035.

Clarenc, J.P., Lebleu, B., Leonetti, J.P. (1993) Characterisation of the Nuclear Binding Sites of Oligodeoxyribonucleotides and Their Analogues. *The Journal of Biological Chemistry*. 286, 3600-3604.

Coghlan, A. (1996) Can Gene Scissors Chop up HIV? *The New Scientist*. 152, 24.

Cohen, N.D. and Thomas, M. (1982) Biotin transport Into Fully Differentiated 3T3-L1 Cells. *Biochemical and Biophysical Research Communications*. 108, 1508-1516.

Cohen, J.S. (1993) Selective Anti-Gene Therapy for Cancer: Principles and Prospects. *The Journal of Experimental Medicine*. 168, 351-355.

Cohn, Z.A. and Ehrenreich, B.A. (1969) The Uptake, Storage and Intracellular Hydrolysis of Carbohydrates by Macrophages. *The Journal of Experimental Medicine*. 129, 201-225.

Collins, R.A., and Olive, J.E. (1992) Reaction Conditions and Kinetics of Self-Cleavage of a Ribozyme derived from Neurospora VS RNA. *Biochemistry*. 32, 2794-2799.

Coulson, J. M., Poyner, D.R., Chantry, A., Irwin, W.J. and Akhtar, S. (1996) A Non-antisense Sequence-Selective Effect of a Phosphorothioate Oligodeoxynucleotide Directed Against the Epidermal Growth Factor Receptor in A431 Cells. *Molecular Pharmacology*. 50, 314-325.

Crisell, P., Thompson, S. and James, W. (1993) Inhibition of HIV-1 Replication by Ribozymes that Show Poor Activity *In Vitro*. *Nucleic Acids Research*. 21, 5251-5255.

Dahm, S.C. and Uhlenbeck, O.C. (1991) The Role of Divalent Metal Ions in the Hammerhead RNA Cleavage Reaction. *Biochemistry*. 30, 9464-9469.

Dahm, S.C., Derrick, W.B. and Uhlenbeck, O.C. (1993) Evidence for the Role of a Solvated Metal Hydroxide in the Hammerhead Cleavage Mechanism. *Biochemistry*. 32, 13040-13045.

Denman, R.B. (1993) Using RNAFOLD to Predict the Activity of Small Catalytic RNAs. *BioTechniques*. 15, 1090-1094.

Denman, R.B., Smedman, M., Ju, W., Rubenstein, R., Potempska, A., Miller, D.L. (1994) Ribozyme Mediated Degradation of β-amyloid Peptide Precursor mRNA in COS-7 Cells. *Nucleic Acids Research*. 22, 2375-2382.

Deshpande, D., Toledo-Velasquez, D., Thakkar, D., Liang, W.W. and Rojanasakul, K. (1996) Enhanced Cellular Uptake of Oligonucleotides by EGF Receptor-Mediated Endocytosis in A549 Cells. *Pharmaceutical Research*, 13, 57-61.

Desjardins, J.P., Sproat, B.S., Beijer, B., Blaschke, M., Dunkel, M., Gerdes, W., Ludwig, J., Reither, V., Rupp, T., Iversen, P.L. (1996) Pharmacokinetics of a Synthetic, Chemically Modified Hammerhead Ribozyme Against the Rat Cytochrome P450 3A2 mRNA After Single Intravenous Injection. *The Journal of Pharmacology and Experimental Therapeutics*. 278, 1419-1427.

Devlin, T. Iver, R.P., Johnson, S. and Agrawal, S (1996) Mixed backbone Oligonucleotides Containing Internucleotide Primary Phosphoramidate Linkages. *Bio-organic and Medicinal Chemistry Letters*. 6, 2663-2668.

Dropulic, B. and Jeang, K.T. (1994) Intracellular Susceptibility to Ribozymes in a Tethered Substrate-Ribozyme Pro-Virus Model is Not Predicted by Secondary Structures of Human Immunodeficiency Virus Type I RNAs *In Vitro*. *Antisense Research and Development*. 4, 217-221.

Dropulic, B. and Jeang, K.T. (1994b) Gene Therapy for Immunodeficiency Virus Infection: Genetic Antiviral Strategies and Targets for Intervention. *Human Gene Therapy*. 5, 927-939.

Eastman, S.J., Siegel, C., Tousignant, J., Smith, A.E., Cheng, S.H. and Scheule, R.K. (1997) Biophysical Characterisation of Cationic Lipid: DNA Complexes. *Biochimica et Biophysica Acta*. 1325, 41-62.

Ebbinghaus, S.W., Gee, J.E., Rodu, B., Mayfield, C.A., Sanders, G. and Miller, D.M. (1993) Triplex Formation Inhibits HER-2 Transcription In Vitro. *The Journal of Clinical Investigation*. 92, 2433-2439.

Elkins, D.A. and Rossi, J.J. (1995) Cellular Delivery of Ribozymes. In: *Delivery Strategies for Antisense oligonucleotide Therapeutics*. Akhtar, S. (Ed). CRC Press Inc, London, UK.

Endicott, J.A. and Ling, V. (1989) The Biochemistry of P-glycoprotein- Mediated Drug Resistance. *Annual Reviews in Biochemistry*. 58, 137-171.

Epstein, L.M. and Gall, J.G. (1987) Self-Cleavage Transcripts of Satellite DNA from the Newt. *Cell*. 48, 535-543.

Erickson, R.P. and Izant, J.G. (1992) Gene Regulation. The Biology of Antisense RNA and DNA. Erickson, R.P. and Izant, J.G. (Eds.) Raven Press Ltd, New York USA.

Fedor, M.J. and Uhlenbeck, O.C. (1992) Kinetics of Intermolecular Cleavage by Hammerhead Ribozymes. *Biochemistry*. 31, 12042-12054.

Felgner, P.L., Gadek, T.R., Holm, M., Roman, R., Chan, H.W., Wenz, M., Northrop, J.P., Ringold, G.M. and Danielsen, M (1987) Lipofection: A Highly Efficient, Lipid mediated DNA-Transfection Procedure. *The Proceedings of the National Academy of Sciences of the USA*. 84, 7413-7417.

Felgner, P.L., and Ringold, G.M. (1989) Cationic Liposome-Mediated Transfection. *Nature*. 337, 387-388.

Felgner, J.H., Kumar, R., Sridnar, C.N., Wheeler, C.J., tsai, Y.J., Border, R., Ramsay, P., Martin, M. and Felgner, P.L. (1994) Enhanced Gene Delivery and Mechanism Studies with a Novel Series of Cationic Lipid Formulations. *The Journal of Biological Chemistry*. 269, 2550-2561.

Fell, P.L., Hudson, A.J., Reynolds, M.A., Usman, N. and Akhtar, S. (1997) Cellular Uptake Properties of a 2'-Amino / 2'-O-Methyl Modified Chimeric Hammerhead Ribozyme Targeted to the Epidermal Growth Factor Receptor mRNA. *Antisense and Nucleic Acid Drug Development.* (In Press).

Feng, M., Cabrera, G., Deshane, J., Scanlon, K.J., Curiel, D.T. (1995) Neoplastic Reversion Accomplished by High Efficiency Adenoviral-Mediated Delivery of an Anti-ras Ribozyme. *Cancer Research.* 55, 2024-2028.

Ferscht, A. (1977). The Basic Equations of Enzyme Kinetics. In: *Enzyme Structure and Mechanism*. Ferscht, A (Ed.), W.H. Freeman and Company, Belfast University Press, UK.

Flory, C.M., Pavco, P.A., Jarvis, T.C., Lesch, M.E., Wincott, F.E., Beigelman, L., Hunt, S.W. and Schrier, D.J. (1996) Nuclease-Resistant Ribozymes Decrease Stromelysin mRNA levels in Rabbit Synovium Following Exogenous Delivery to the Knee Joint. *The Proceedings of the National Academy of Sciences of the USA*. 93, 754-758.

Ford, D.H. (1975) *Anatomy of the Central Nervous System In Review*. Elsevier Scientific Publications, Amsterdam, Netherlands.

Forster, A.C. and Symons, R.H. (1987) Self Cleavage of Plus and Minus Strand RNAs of a Virusoid and a Structural Model for the Active Sites. *Cell.* 49, 211-220.

Freshney, M. (1973) *The Journal of the National Cancer Institute*. 51, 1417-1424.

Friden, P.M. (1993) Receptor mediated Transport of Peptides and Proteins Across the Blood-Brain Barrier. In: *The Blood-Brain Barrier, Cellular and Molecular Biology*. Pardridge, W.M. (Ed) Raven Press, New York, USA.

Frier, S.M., Lima, W.F., Sanghvi, Y.S., Vickers, T., Zounes, M., Cook, P.D. and Ecker, D.J. (1992) Thermodynamics of Antisense Oligonucleotide Hybridization. In: *Gene Regulation: Biology of Antisense RNA and DNA*. Erickson, R.P. and Izant, J.G. (Eds). Raven Press Ltd, New York, USA.

Gait, M.J., Pritchard, C., Slim, G. (1991) Oligoribonucleotide Synthesis. In: *Oligonucleotides and Analogues*. Eckstein, F. (Ed).Oxford University Press. Oxford, UK.

Gazin, C., De Dinechin, S.D., Hampe, A., Masson, J.M., Martin, P., Stehelin, D. and Galibert, F. (1984) The Nucleotide sequence of the Human *c-myc* Locus: Provocative Open reading frame within the First Locus. *The EMBO Journal.* 3, 383-387.

Ge, L., Resnick, N.M., Ernst, L.K., Salvucci, L.A., Asman, D.C. and Cooper, D.L. (1995) Gene therapeutic Approaches to Primary and Metastatic Brain Tumours: II. Ribozyme-Mediated Suppression of CD44 Expression. *The Journal of Neuro-Oncology*. 26, 251-257.

Gewirtz, A.M., Stein, C.A. and Glazer, P.M. (1996) Facilitating Oligonucleotide Delivery: Helping Antisense Deliver on Its Promise. *Proceedings of the National Academy of Sciences of the USA*. 93, 3161-3163

Gherardi, C. (1996) The Catalogue of Cell Cultures and Hybridomas. The European Collection of Animal Cell Cultures (ECACC), The Centre for Applied Microbiology and Research, Porton Down, Salisbury, UK. 7th Edition. Gherardi, C (Ed). Cerdic Publishing, Paris, France. Unpublished data on file also obtained from ECACC.

Gibson, I. (1994) Antisense DNA and RNA Strategies: New Approaches to Therapy. *The Journal of the Royal College of Physicians of London*. 28, 507-511.

Goodarzi, G., Watabe, M. and Watabe, K. (1991) Binding of Oligonucleotides to Cell Membranes at Acidic pH. *Biochemical and Biophysical Research Communications*. 181, 1343-1351.

Goodarzi, G., Watabe, M. and Watabe, K. (1992) Organ Distribution and Stability of Phosphorothioated Oligodeoxyribonucleotides in Mice. *Biopharmaceutics and Drug Disposition*. 13, 221-227.

Goyns, M.H. (1995) Apoptosis - The Key to Future Anti-cancer Therapy? *Drugs of the Future*. 20, 601-608.

Griffiths, B (1992) Scaling Up of Animal Cell Cultures. In: *Animal Cell Culture, A Practical Approach*. Freshney, R.I. (Ed). IRL Press, Oxford, UK.

Griffiths, G., Burke, B. and Lucocq, J. (1993) *Fine Structure Immuno-Cytochemistry*. Griffiths, G. (Ed.) Springer-Verlag Publications, Berlin, Germany.

Grunt, T.W. and Huber, H. (1994) The Family of *c-erb*B Genes: From Basic Research to Clinical Oncology. *Onkologie*. 17, 346-357.

Guerrier-Takada, C., Gardiner, K., Marsh, T., Pace, N., Altman, S. (1983) The RNA Moiety of Ribonuclease P is the Catalytic Subunit of the Enzyme. *Cell*. 35, 849-857.

Guerrier-Takada, C., Li, Y. and Altman, S. (1997) Artificial Regulation of Gene Expression in Escherichia coli by RNase P. *The Proceedings of the National Academy of Sciences of the USA*. 92, 11115-11119.

Guerrier-Takada, C., Salavati, R. and Altman, S. (1997) Phenotypic Conversion of Drug Resistant Bacteria to Drug Sensitivity. *The Proceedings of the National Academy of Sciences of the USA*. 94, 8468-8472.

Guvakova, M.A., Yakubov, L.A., Vlodavsky, I., Tonkinson, J.L., and Stein, C.A. (1995) Phosphorothioate Oligodeoxynucleotides Bind to Basic Fibroblast Growth Factor, Inhibit Its Binding to Cell Surface Receptors, and Remove It from Low Affinity Binding Sites on Extracellular Matrix. *The Journal of Biological Chemistry*. 270, 2620-2627.

Hampel, A. and Tritz, R. (1989) RNA Catalytic Properties of the Minimum Minus Strand of the Tobacco Ringspot Virus Satellite RNA Sequence. *Biochemistry*. 28, 4929-4933.

Haseloff, J. and Gerlach, W.L. (1988) Simple RNA Enzymes with New and Highly Specific Endoribonuclease Activities. *Nature*. 334, 585-591.

Hawley, P. and Gibson, I. (1996) Interaction of Oligodeoxynucleotides with Mammalian Cells. *Antisense and Nucleic Acid Drug Development*. 6, 185-195.

Hegg, L.A. and Fedor, M.J. (1995) Kinetics and Thermodynamics of Inter-Molecular Catalysis by Hairpin Ribozymes. *Biochemistry*. 34, 15813-15828.

Helene, C. and Toulme, J.J. (1990) Specific Regulation of Gene Expression by Antisense, Sense and Antigene Nucleic Acids. *Biochemica et Biophysica Acta*. 1049, 99-125.

Heidenreich, O., Benseler, F., Fahrenholz, A., Eckstein, F. (1994) High Activity and Stability of Hammerhead Ribozymes Containing 2'-modified Pyrimidine Nucleosides and Phosphorothioates. *The Journal of Biological Chemistry*. 267, 1904-1909.

Heidenreich, O., Xu, X., Swiderski, P., Rossi, J.J., Nerenberg, M. (1996) Correlation of Activity with Stability of Chemically Modified Ribozymes in Nuclei Suspension. *Antisense and Nucleic Acid Drug Development*. 6, 111-118.

Heller, J. (1993) Polymers for the Controlled Parenteral Delivery of Peptides and Proteins. *Advanced Drug Delivery Reviews*. 10, 163-204.

Hendry, P. and McCall, M. (1996) Unexpected Anistropy in Substrate Cleavage Rates by Asymmetric Hammerhead Ribozymes. *Nucleic Acids Research*. 23, 3922-3927.

Herschlag, D. (1995) RNA Chaperones and the RNA Folding Problem. *The Journal of Biological Chemistry*. 270, 20871-20874.

Hertel, K.J., Pardi, A., Uhlenbeck, O.C., Koizumi, M., Ohtsuka, E., Uesugi, S., Cedergren, R., Eckstein, F., Gerlach, W.L., Hodgson, R., and Symons, R.H. (1992) Numbering System for the Hammerhead. *Nucleic Acids Research*. 20, 3252 (only).

Hertel, K.J., Herschlag, D., Uhlenbeck, O.C. (1994) A Kinetic and Thermodynamic Framework for the Hammerhead Ribozyme reaction. *Biochemistry*. 33, 3374-3385.

Hertel, K.J., Herschlag, D., Uhlenbeck, O.C. (1996) Specificity of hammerhead Ribozyme Cleavage. *The EMBO Journal*. 15, 3751-3757.

Hoi-Sang, U., Espiritu, O.D., Kelly, P.Y., Klauber, M.R. and Hatton, J.D. (1995) The Role of the Epidermal Growth Factor Receptor in Human Gliomas: The Control of Cell Growth, The Control of Glial Process Extension and the Expression of Glial Fibrillary Acidic Protein. *The Journal of Neurosurgery*. 82, 847-857.

Holz, H.M. (1982) Worthwhile Facts About Fluorescence Microscopy: Filter Sets. 3rd Revised Edition. Carl-Zeiss Publications, Oberkochen, Germany.

Homann, M., Tabler, M., Tzortzakaki, S., Sczakiel, G. (1994) The Extension of Helix II of an Anti-HIV-1 Directed Hammerhead Ribozyme with Long Antisense Flanks Does Not Alter the Kinetic Parameters *In Vitro* but Causes Loss of Inhibitory Potential in Living Cells. *Nucleic Acids Research*. 22, 3951-3957.

Hopkins, C. (1985) Coated Pits and Their Role in Membrane Receptor Internalization. In: *Molecular Mechanisms of Transmembrane Signalling*. Cohen, J. and Housely, M. (Eds). Elsevier Science Publications, Dublin.

Hudson, A.J., Lee, W., Porter, J., Akhtar, J., Duncan, R. and Akhtar, S. (1996a) Stability of Antisense Oligonucleotides During Incubation with a Mixture of Isolated Lysosomal Enzymes. *The International Journal of Pharmaceutics*. 133, 257-263.

Hudson, A.J., Lewis, K.J., Rao, M.V. and Akhtar, S. (1996b) Biodegradable Polymer Matrices for the Sustained Exogenous Delivery of a Biologically Active *c-myc* Hammerhead Ribozyme. *The International Journal of Pharmaceutics*. 136, 23-29.

Hughes, J.A., Avrutskaya, A.V. and Juliano, R.L. (1994) The influence of Base Composition on Cellular Transport and Membrane Binding of Oligonucleotides. *Antisense Research and Development*. 4, 2111-216.

Hughes, J., Avroutskaya, A., Sasmor, H.M., Guinosso, C.J., Cook, P.D. and Juliano, R.L. (1995) Oligonucleotide Transport Across Membranes and Into Cells: Effects of Chemical Modifications. In: *Delivery Strategies For Antisense Oligonucleotide Therapeutics*. Akhtar, S. (Ed) CRC Press Inc, London, UK.

Hughes, J.A., Aronsohn, A.I., Avrutskaya, A.V. and Juliano, R.L. (1996) Evaluation of Adjuvants that Enhance the Effectiveness of Antisense Oligonucleotides. *Pharmaceutical Research*. 13, 404-410.

Hutchins, C.J., Rathjen, P.D., Forster, A.C. and Symons, R.H. (1986) Self Cleavage of Plus and Minus RNA Transcripts of Avocado Sunblotch Viroid. *Nucleic Acids Research*. 14, 3627-3640.

Ishai-Michaeli, R., Svahn, C., Weber, M., Chajek-Shaul, T., Korner, G., Ekre, H., and Vlodavsky, I. (1992) Displacement and Binding of Basic Fibroblast Growth Factors By Heparin, Heparinases and Other Glycosaminoglycans. *Biochemistry*. 31, 2080-2088.

Iversen, P.L. (1991) In Vivo Studies with Phosphorothioate Oligonucleotides: Pharmacokinetics Prologue. *Anti-Cancer Drug Design*. 6, 531-538.

Iversen, P.L., Zhu, S., Meyer, A. and Zon, G. (1992) Cellular Uptake and Subcellular Distribution of Phosphorothioate Oligonucleotides Into Cultured cells. *Antisense Research and Development*. 2, 211.

Iwanga, T. and Ferriola, P.C. (1993) Cellular Uptake of Phosphorothioate Oligodeoxynucleotides is Negatively Affected By Cell Density in Transformed Rat Tracheal Epithelial Cell Line. *Biochemical and Biophysical Research Communications*. 191, 1152.

James, H., Mills, K. and Gibson, I. (1996) Investigating and Improving the Specificity of Ribozymes Directed Against the bcr-abl Translocation. *Leukemia*. 10, 1054-1064.

Jaros, E., Perry, R.H., Adam, L., Kelly, P.J., Crawford, P.J., Kalbag, R.M., Mendelow, A.D., Sengupta, R.P. and Pearson, A.D.J. (1992) Prognostic Implications of p53 Protein, Epidermal Growth Factor Receptor and Ki-67 Labelling in Brain Tumours. *The British Journal of Cancer*. 66, 373-385.

Jarvis, T.J., Alby, L.J., Beaudry, A.A., Wincott, F.E., Beigelman, L., McSwiggen, J.A., Usman, N. and Stinchcomb, D.T. (1996) Inhibition of Vascular Smooth Muscle Cell Proliferation by Ribozymes that Cleave c-myb mRNA. *RNA*. 2, 419-428.

Jarvis, T.J., Wincott, F.E., Alby, L.J., McSwiggen, J.A., Beigelman, L., Gustofson, J., DiRenzo, A., Levy, K., Arthur, M., Matulic-Adamic, J., Karpiesky, A., Gonzalez, C., Woolf, T.M., Usman, N. and Stinchcomb, D.T. (1996b) Optimising the Cell Efficacy of Synthetic Ribozymes. *The Journal of Biological Chemistry*. 271, 29107-29112.

Jaaskelainen, I., Monkkonen, J. and Urtti, A. (1994) Oligonucleotide-Cationic Liposome Interactions. A Physicochemical Study. *Biochimica et Biophysica Acta*. 1195, 115-123.

Johnson , B.A., McClain, S.G., Doran, E.R., Tice, G. and Kirsch, M.A. (1990) Rapid purification of Synthetic Oligonucleotides: A Convernient Alternative to HPLC and Polyacrylamide Gel Electrophoresis. *Biotechniques*. 8, 424-429.

Johnson, G.D., Davidson, R.S., McNamee, K.C., Russell, G., Goodwin, D. and Holborow, E.J. (1982) Fading of Immunofluoresence During Microscopy: A Study of the Phenomenon and its Remedy. *Journal of Immunology Methods*. 55, 231-242.

Joseph, S. and Burke, J.M. (1993) Optimization of an Anti-HIV Hairpin Ribozyme by In Vitro Selection. *The Journal of Biological Chemistry*. 268, 24515-24518.

Juliano, R.L. and Akhtar, S. (1992) Liposomes as a drug Delivery System for Antisense Oligonucleotides. *Antisense Research and Development*. 2, 165-176.

Kajio, T., Kahahara, K. and Kato K. (1992) Factors Influencing the Affinity of Basic Fibroblast Growth Factors for High and Low Affinity Binding Sites. *FEBS Letters*. 306, 243-246.

Kanawa, Y., Ohkawa, K., Ueda, K., Mita, E., Takehara, T., Sasaki, Y., Kasahara, A. and Hayashi, N. (1996) Hammerhead Ribozyme-Mediated Inhibition of Telomerase Activity in Extracts of Human Hepatocellular Carcinoma Cells. *Biochemical and Biophysical Research Communications*. 225, 570-576.

Kariko, K., Megyeri, K., Xiao, Q. and Barnathan, E.S. (1994) Lipofectin-Mediated Cell Delivery of Ribozyme Targeted to Human Urokinase Receptor mRNA. *FEBS Letters*. 352, 41-44.

Karwan, R. (1993) RNase MRP / RNas P: A Structure-Function Relation Conserved in Evolution? *FEBS Letters*. 319, 1-4.

Kerr, S.M., Stark, G.R., Kerr, I.M. (1988) Excess Antisense RNA from Infectious Recombinant SV40 Fails to Inhibit Expression of a Transfected, Interferon Inducible Gene. *European Journal of Biochemistry*. 175, 65-72.

Khazaie, K., Schirrmacher, V. and Lichtner, R.B. (1993) EGF Receptor in Neoplasia and Metastasis. *Cancer and Metastasis Reviews*. 12, 255-274.

Kiehntopf, M., Brach, M.A., Licht, T., Petschauer, S., Karawajew, S., Kirschning, C. and Herrmann, F. (1994) Ribozyme Mediated Cleavage of MDR-1 Transcript Restores Chemosensitivity on previously Resistant Cancer Cells. *EMBO Journal*. 13, 4645-4652.

Kiehntopf, M., Esquivel, E.L., Brach, M.A., Herrmann, F. (1995) Ribozymes: Biology, Biochemistry and Implications for Clinical Medicine. *The Journal of Molecular Medicine*. 73, 65-71.

Kisich, K.O., Stecha, P.F., Harter, H.A. and Stinchcomb, D.T. (1995) Inhibition of TNF-α Secretion by Murine Macrophages Following *In Vivo* and *In Vitro* Ribozyme Treatment. *The Journal of Cellular Biochemistry*. 19A, 291.

Kitajima, I., Shinohara, T., Minor, T., Bibbs, L., Bilakovics, J. and Nerenberg, M. (1992) Human T-cell Leukaemia Virus Type-1 Tax Transformation is Associated with Increased Uptake of Oligodeoxynucleotides in vitro and in vivo. *The Journal of Biological Chemistry*. 267, 25881-25888.

Koizumi, M., Kamiya, H. and Ohtsuka, E. (1992) Ribozymes Designed to Inhibit Transformation of NIH3T3 Cells by Activated c-Ha-ras Gene. *Gene*. 117, 179-184.

Kole, R., Shukla, R.R. and Akhtar, S (1991) Pre-mRNA Splicing as a Target for Antisense Oligonucleotides. *Advanced Drug Delivery Reviews*. 6, 271-286.

Kordek, R., Biernat, W., Alwasiak, J., Yanagihara, R. and Liberski, P.P. (1995) Epidermal growth Factor Receptor and p53 Protein Expression in Human Glioblastomas. *The European Journal of Neurology*. 2, 487-491.

Kregnow, D., Ratajczak, M.Z. and Gewirtz, A.M. (1995) Disrupting the Flow of genetic information with Antisense Oligodeoxynucleotides: Research and therapeutic Applications. In: *Delivery Strategies for Antisense Therapeutics*. Akhtar, S. (Ed). CRC Press, London, UK.

Krieg, A.M. (1993) Uptake and Efficacy of Phosphodiester and Modified Oligonucleotides in Primary Cell Cultures. *Clinical Chemistry*. 39, 710-712.

Krieg, A.M. and Stein, C.A. (1995) Phosphorothioate Oligodeoxynucleotides: Antisense or Anti-Protein? *Antisense Research and Development*. 5, 241 (only).

Kronenwett, R., Haas, R. and Sczakiel, G. (1996) Kinetic Selectivity of Complementary Nucleic Acids: bcr-abl Directed Antisense RNA and Ribozymes. *The Journal of Molecular Biology*. 259, 632-644.

Krystal, G.W. (1992) Regulation of Eukaryotic Gene Expression by Naturally Occurring Antisense RNA. In: *Gene Regulation. Biology of Antisense RNA and DNA*. Erickson, R.P. and Izant, J.G. (Eds.) Raven Press Ltd, New York, USA.

Kuijpers, W.H.A., Bos, E.S., Kaspersen, F.M., Veeneman, G.H. and Van Boeckel, C.A.A. (1993) Specific recognition of Antibody-Oligonucleotide Conjugates by Radiolabelled Antisense Nucleotides: A Novel Approach for Two-Step Radio-Immunotherapy of Cancer. *Bioconjugate Chemistry*. 4, 94-102.

Lai, M.M.C. and Wu, H.N. (1991) The Molecular Biology of the Human Hepatitis Delta Virus. *The Journal of Biological Chemistry*. 15D, 55 (only).

Lamond, A.I. and Sproat, B.S. (1993) Antisense Oligonucleotides made of 2'-O-Alkyl RNA: Their Properties and Applications in RNA Biochemistry. *FEBS Letters*. 325, 123-127.

Lange, W., Cantin, E.M., Finke, J. and Dolken, G. (1994) In Vito and In Vivo Effects of Synthetic Ribozymes Targeted Against bcr / abl mRNA. *Leukemia*. 7, 1786-1794.

Lansing-Taylor, D. and Salmon, E.D. (1989) Basic Fluorescence Microscopy. In: *Methods in Cell Biology*. Volume 29. Wang, Y.L. and Taylor, D.L. (Eds). Academic Press Inc. San Diego, USA.

Lappalainen, K., Urtti, A., Soderling, E., Jaaskelainen, I., Syrjanen, K., Syrjanen, S. (1994) Cationic Liposomes Improve the Stability and Intracellular Delivery of Antisense Oligonucleotides into Caski Cells. *Biochimica et Biophysica Acta*. 1196, 201-208.

Larsson, S., Hotchkiss, G., Andang, M., Nyholm, T., Inzunza, J., Jansson, I., Ahrlund-Richter, L. (1994) Reduced β2-microglobulin mRNA Levels in Transgenic Mice Expressing a designed hammerhead Ribozyme. *Nucleic Acids Research*. 22, 2242-2248.

Lascombe, I., Mougin, P., Vuillermoz, C., Adessi, G.L. and Jouvenot, M. (1996) Gene Transfer into Sub-cultured Endometrial Cells Using Lipofection. *Biotechniques*. 20, 88-91.

Leavitt, M.C., Yu, M., Yamada, O., Kraus, G., Looney, D., Poeschla, E. and Wong-Staal, F. (1994) Transfer of an Anti-HIV-1 Ribozyme Gene into Primary Human Lymphocytes. *Human Gene Therapy*. 5, 1115-1120.

Lee, B.S., Wu, H.N., Huang, T.H. (1993) The Catalytic Domain of Human Hepatitis Delta Virus RNA. *FEBS Letters*. 324, 296-300.

Leibel, , S.A., Scott, C.B. and Loeffler, J.S. (1994) Contemporary Approaches to the Treatment of Malignant Gliomas with Radiation Therapy. *Seminars in Oncology*. 21, 198-219.

Leonetti, J.P., Machy, P., Degols, G., Lebleu, B. and Leserman, L. (1990) Antibody Targeted Liposomes Containing oligodeoxyribonucleotide Sequences Complementary to Viral RNA Selectivity Inhibit Viral Replication. *The Proceedings of the National Academy of Sciences of the USA*. 87, 2448-2451.

Leopold, L.H., Shore, S.K., Newkirk, T.A., Reddy, R.M. and Reddy, E.P. (1995) Multi-Unit Ribozyme Mediated Cleavage of bcr-abl mRNA in Myeloid Leukemias. *Blood*. 85, 2162-2170.

Letsinger, R.L., Zhang, G.R., Sun, D.K., Ikeuchi, T. and Sarin, P.S. (1989) Cholesterol Conjugated Oligonucleotides: Synthesis, Properties and Activity as Inhibitors of replication of Human Immunodeficiency virus in Cell Culture. *The Proceedings of the National Academy of Sciences of the USA*. 86, 6553-6556.

Levis, J.T., Butler, W.O., Tseng, B.Y. and Paul, O.P.T. (1995) Cellular Uptake of Oligodeoxyribonucleoside Methylphosphonates. *Antisense Research and Development*. 5, 251-259.

Lewis, K.J., Irwin, W.J. and Akhtar, S. (1995) Biodegradable Polymer devices for the Sustained Exogenous Delivery of Antisense Oligonucleotides. *The Journal of Controlled Release*. 37, 173-183.

Lewis, J.G., Lin, K.Y., Kothavale, A., Flanagan, W.M., Matteucci, M.D., De Prince, R.B., Mook, R.A., Hendren, R.W. and Wagner, R.W. (1996) A Serum-Resistant Cytofectin for Cellular delivery of Antisense Oligodeoxynucleotides and Plasmid DNA. *The Proceedings of the National Academy of Sciences of the USA*. 93, 3176-3181.

L,Huillier, P.J., Davis, S.R. and Bellamy, A.R. (1992) Cytoplasmic delivery of Ribozymes Leads to Efficient Reduction in α-Lactalbumin mRNA Levels in C1271 Mouse Cells. *EMBO Journal*. 11, 4411-4418.

Liang, W.W., Shi, X., Deshpande, D., Malange, C.J. and Rojanasakul, Y. (1996) Oligonucleotide Targeting to Alveolar Macrophages by Mannose Receptor-Mediated Endocytosis. *Biochimica et Biophysica Acta*. 1279, 227-234.

Lieber, A. and Strauss, M. (1995) Selection of Efficient Cleavage Sites in Target RNAs by Using a Ribozyme Expression Library. *Molecular Cell Biology*. 15, 540-551.

Litzinger, D.C., Brown, J.M., Wala, I., Kaufman, S.A., Van, G.Y., Farrell, C.L. and Collins, D. (1996) Fate of Cationic Lipososmes and Their Complex with Oligonucleotide *In Vivo*. *Biochimica et Biophysica Acta*. 1281, 139-149.

Liu, F.Y. and Altman, S. (1995) Inhibition of Viral Gene Expression by RNase P from *Escherichia coli*. *Genes and Development*. 9, 471-480.

Loke, S.L., Stein, C.A., Zhang, X.H., Mori, K., Makanishi, M., Subasinghe, C., Cohen, J.S. and Neckers, L.M. (1989) Characterisation of Oligonucleotide Transport into Living Cells. *Proceedings of the National Academy of Sciences of the USA*. 86, 3474-3478.

Louis, D.N. and Seizinger, B.R. (1994) The Genetic Basis of Neurological Tumours. *Clinical Neurology*. 3, 335-352.

Luby-Phelps, K. (1989) Preparation of Fluorescently Labelled Polysaccharides. In: *Methods in Cell Biology*. Volume 29. Wang, Y.L. and Taylor, D.L. (Eds). Academic Press Inc. San Diego, USA.

Lyngstadaas, S.P., Risnes, S., Sproat, B.S., Thrane, P.S., Prydz, H.P. (1995) A Synthetic, Chemically Modified Ribozyme Eliminates Amelogenin, The Major Translation Product in Developing Mouse Enamel In Vivo. *EMBO Journal*. 14, 5224-5229.

Maniatis, T., Jeffrey, A., and Van DeSande, H. (1975) Chain Length Determination of Small Double- and Single-Stranded DNA Molecules by Polyacrylamide Gel Electrophoresis. *Biochemistry*. 14, 3787-3794.

Marschall, P., Thomson, J.B. and Eckstein, F. (1994) Inhibition of Gene Expression with Ribozymes. *Cellular and Molecular Neurobiology*. 14, 523-538.

Maunders, M.J. (1993) DNA and RNA Ligases. In: *Methods in Molecular Biology*. Burell, M.M. (Ed). Volume 16. Humana Press Inc., Totowa, New Jersey, USA.

McKay, D.B. (1995) Three-Dimensional Structure of the Hammerhead Ribozyme. *Nucleic Acids and Molecular Biology*. 10, 161-172.

Meeker, R., LeGrand, G., Ramirez, J., Smith, T. and Shih, Y.H. (1995) Antisense vasopressin Oligonucleotides: Uptake, Turnover, Distribution , Toxicity and Behavioural Effects. *The Journal of Neuro-Endocrinology*. 7, 419-428.

Mercer, E.H. and Birbeck, M.S.C. (1972) Fixation, Washing and Dehydration. In: *Electron Microscopy*, A Handbook For Biologists. Blackwell Scientific Publications, Oxford, UK.

Mickisch, G. and Schroeder, F. (1994) From Laboratory Expertise to Clinical Practice: Multi Drug Resistance-Based Gene Therapy Becomes Available for Urologists. *The World Journal of Urology*. 12, 104-111.

Middleton, T., Herilhy, W.C., Schimmel, P.R. and Munro, H.N. (1985) Synthesis and Purification of Oligoribonucleotides Using T4 RNA Ligase and Reverse-Phase Chromatography. *Analytical Biochemistry*. 144, 110-117.

Miller,P.S., Braiterman, I.T. and Tso, P.O.P. (1977) Effects of a Trinucleotide Ethylphosphotriester, Gmp(Et)Gmp(Et)U, on Mammalian Cells in Culture. *Biochemistry*. 16, 1988-1996.

Miller, W.A., Hercus, T., Waterhouse, P.M., Gerlach, W.L. (1991) A Satellite RNA of Barley Yellow Dwarf Virus Contains a Novel Hammerhead Structure in the Self-Cleaving Domain. *Virology*. 183, 711-720.

Milligan, J.F.,Matteucci, M.D.and Martin, J.C. (1993) Current Concepts in Antisense Drug Design. *The Journal of Medicinal Chemistry*. 36, 1923-1931.

Modjtahedi, H. and Dean, C. (1994) The Receptor for EGF and Its Ligands: Expression, Prognostic Value and Target for Therapy in Cancer (Review). *The International Journal of Oncology*. 4, 277-296.

Mollenhauer, H.H., Morre, D.J. and Rowe, L.D. (1990) Alteration of Intracellular Traffic by Monensin; Mechanism, Specificity and Relationship to Toxicity. *Biochimica et Biophysica Acta*. 1031, 225-246.

Monaghan, P. and Moss, D. (1995) An Introduction to Immunocytochemistry. *Microscopy and Analysis*. 10, 17-19.

Narahashi, Y. and Yanagita, M. (1967) Studies on the Proteolytic enzymes (Pronase) of *Streptomyces griseus* k-1. Nature and Properties of the Proteolytic Enzyme System. *The Journal of Biochemistry*. 62, 633-641.

Nauta, W.J.H. and Feirtag, M. (1986) *Fundamental Neuroanatomy*. Freeman and Co. Publications, New York, USA.

Noller, H.F., Hoffarth, V., Zimniak, L. (1992) Unusual Resistance of Peptidyl Transferase to Protein Extraction Procedures. *Science*. 256, 1416-1419.

Noonberg, S.B., Garovoy, M.R. and Hunt, C.A. (1993) Characteristics of Oligonucleotide Uptake in Human Keratinocyte Cultures. *The Journal of Investigative Dermatology*. 101, 727-731

Ogawa, S. and Pfaff, D.W. (1996) Application of Antisense DNA Method for the Study of Molecular Basers of Brain Function and Behaviour. *Behaviour Genetics*. 26, 279-292.

Ohta, Y., Kijima, H., Ohkawa, T., Kashani-Sabet, M. and Scanlon, K.J. (1996a) Tissue-Specific Expression of an Anti-ras Ribozyme Inhibits Proliferation of Human Malignant Melanoma. *Nucleic Acids Research*. 24, 938-942.

Ohta, Y., Kijima, H., Kashani-Sabet, M. and Scanlon, K.J. (1996b) Suppression of Malignant Phenotype of melanoma Cells by Anti-Oncogene Ribozymes. *The Journal of Investigative Dermatology*. 106, 275-281.

Ojwang, J.O., Hampel, A., Looney, D.J., Wong-Staal, F. and Rappaport, J. (1992) Inhibition of Human Immunodeficiency Virus Type I Expression by a Hairpin Ribozyme. *The Proceedings of the National Academy of Sciences of the USA*. 89, 10802-10806.

Okada, T., Yamaguchi, K. and Yamashita, J. (1994) Triplex-Forming Oligonucleotide Binding Represses Transcription of the Human *c-erb*B Gene in Glioma. *Growth Factors*. 11, 259-270.

Paolella, G., Sproat, B. and Lamond, A. (1992) Nuclease-Resistant Ribozymes with high catalytic Activity. *The EMBO Journal*. 11, 1913-1919.

Pardridge, W.M. and Boado, R.J. (1990) Enhanced Cellular Uptake of Biotinylated Antisense Oligonucleotides or peptide mediated by Avidin, A Cationic Protein. *FEBS Letters*. 254, 129-132.

Parton, R. (1994) Ultrastructural Localization of Gangliosides; GM1 is Concentrated in Caveolae. *The Journal of Histochemistry and Biochemistry*. 42, 155-166.

Pellegrino, L.J., Pellegrino, A.S. and Cushman, A.J. (1967) *A Stereotaxic Atlas of The Rat Brain*. Plenum Press, New York, USA.

Perreault, J.P., Labuda, D., Usman, N., Yang, J.H. and Cedergren, R.J. (1991) Relationship Between 2'-Hydroxyls and Magnesium Binding in the Hammerhead RNA Domain: A Model for Ribozyme Catalysis. *Biochemistry*. 30, 4020-4025.

Petersdorf, S.H. and Livingston, R.B. (1994) High Dose Chemotherapy for the Treatment of Malignant Brain Tumours. *The Journal of Neuro-Oncology*. 20, 155-163.

Pieken, W.A., Olsen, D.B., Benseler, F., Aurup, H. and Eckstein, F. (1991) Kinetic Characterisation of Ribonuclease Resistant 2'-Modified Hammerhead Ribozymes. *Science*. 253, 314-317.

Pley, H.W., Flaherty, K.M., McKay, D.B. (1994) Three-Dimensional Structure of a Hammerhead Ribozyme. *Nature*. 372, 68-74.

Piwinca-Worms, D. (1994) Making Sense Out of Antisense: Challenges of Imaging Gene Translation with Radiolabelled Oligonucleotides. *The Journal of Nuclear Medicine*. 35, 1064-1066.

Ponten , J. and McIntyre, E.H. (1968) Long Term Culture of Normal and Neoplastic Human Glia. *Acta Pathology & Microbiology Scandanavia*. 74, 465-486.

Porumb, H., Gousset, H., Letellier, R., Salle, V., Braine, D., Vassy, J., Amor-Gueret, M., Israel, L. and Taillandier, E. (1996) Temporary *Ex Vivo* Inhibition of the Expression of the Human Oncogene *HER2* by a Triple Helix-Forming Oligonucleotide. *Cancer Research*. 56, 515-522.

Prochownik, E.V. (1992) Antisense Approaches to Assessing Oncogene Signalling Pathways. In: *Gene Regulation. Biology of Antisense RNA and DNA*. Erickson, R.P. and Izant, J.G. (Eds.) Raven Press Ltd, New York, USA.

Prody, G.A., Bakos, J.T., Buzayan, J.M., Schneider, I.R., Bruening, G. (1986) Autocatalytic Processing of Dimeric Plant Virus satellite RNA. *Science*. 231, 1577-1580.

Rao, M.V. (1994) The Use of Fpmp-Protected Chemistries for the Synthesis of Oligoribonucleotides. Seminar to The Drug Delivery Research Group, Aston University, Birmingham. March, 1995.

Rao, M.V. and Macfarlane, K. (1995) Improvements to the Chemical Synthesis of Biologically Active RNA using 2'-O-Fpmp Chemistry. *Nucleosides and Nucleotides*. 14, 911-913.

Raschke, W.C., Baird, S., Ralph, P. and Nakoinz, I. (1978) Functional macrophage Cell Lines Transformed by Abelson Leukemia Virus. *Cell*. 15, 261-267.

Raub, T.J. and Audus, K.L. (1990) Adsorptive Endocytosis and Membrane Recycling By Cultured Primary Bovine Brain Microvessel Endothelial Cell Monolayers. *The Journal of Cell Science*. 97, 127-138.

Reese, C.B., Rao, M.V., Serafinowska, H.T., Thompson, E.A., and Yu, P.S. (1991). Studies in the Solid Phase Synthesis of Oligoribonucleotides and Polyribonucleotides. *Nucleosides and Nucleotides*. 10, 81-97.

Rojanasakul, Y. (1996). Antisense Oligonucleotide Therapeutics: Drug Delivery and Targeting. *Advanced Drug Delivery Reviews*. 18, 115-131.

Romaniuk, P.J., and Uhlenbeck, O.C. (1983) Joining of RNA Molecules with RNA Ligase. In: *Methods in Enzymology*. Volume 100. Academic press Inc., New York, USA.

Rossi, J. J. (1994) Making Ribozymes work in Cells. *Current Biology*. 4, 469-471.

Rossi, J.J. (1995) Controlled, Targeted, Intracellular Expression of Ribozymes: Progress and Problems. *Trends in Biotechnology*. 13, 301-306.

Ruffner, D.E., Stormo, G.D. and Uhlenbeck, O.C. (1990) Sequence Requirements of the Hammerhead RNA Self-Cleavage Reaction. *Biochemistry*. 29, 10695-10702.

Ruffner, D.E. and Uhlenbeck, O.C. (1991) Thiophosphate Interference Experiments Locate Phosphates Important for the Hammerhead RNA Self-Cleavage Reaction. *Nucleic Acids Research*. 18, 6025-6029.

Said, H.M., Ma, T.Y. and Kamanna, V.S. (1994) Uptake of Biotin By Human Hepatoma Cell Line, Hep G2: A Carrier Mediated Process Similar to that of Normal Liver. *The Journal of Cellular Physiology*. 161, 483-489.

Saijo, Y., Perlaky, L., Wang, H. and Busch, H. (1994) Pharmacokinetics, Tissue Distribution and Stability of Antisense Oligodeoxynucleotide Phophorothioate ISIS 3466 in Mice. *Oncology Research*. 6, 243-249.

Sambrook, J., Fritsch, E.F. and Maniatis, T. (1989) *Molecular Cloning: A Laboratory Manual*. Volumes 1-3. (Second Edition). Cold Spring Harbour Laboratory Press. Cold Spring Harbour, NY, USA.

Sargueil, B., Pecchia, D.B., Burke, J.M. (1995) An Improved Version of the Hairpin Ribozyme Functions as a Ribonucleoprotein Complex. *Biochemistry*. 34, 7739-7748.

Sarver, N., Cantin, E.M., Chang, P.S., Zaia, J.A., Ladne, P.A., Stephens, D.A. and Rossi, J.J. (1990) Ribozymes as Potential Anti-HIV-1 Therapeutic Agents. *Science*. 247, 1222-1225.

Sawata, S., Shimayama, T., Komiyama, M., Kumar, P.K.R., Nishikawa, S. and Taira, K. (1993) Enhancement of Cleavage rates of DNA-Armed Hammerhead Ribozymes by various divalent Metal ions. *Nucleic Acids Research*. 21, 5656-5660.

Scaringe, S.A., Franklyn, C. and Usman, N. (1990) Chemical Synthesis of Biologically Active Oligoribonucleotides using β-cyanoethyl Protected Ribonucleoside Phosphoramidites. *Nucleic Acids Research*. 18, 5433-5441.

Scanlon, K.J., Jiao, L., Funato, T., Wang, W., Tone, T., Rossi, J.J. and Kashani-Sabet, M. (1991) Ribozyme Mediated Cleavage of c-fos mRNA Reduces Gene Expression of DNA Synthesis Enzymes and Metallothionien. *The Proceedings of the National Academy of Sciences of the USA*. 88, 10591-10595.

Scanlon, K.J., Ohta, Y., Ishida, H., Kijima, H., Ohkawa, T., Kaminski, A., Tsai, J., Horng, G. and Kashani-Sabet, M. (1995) Oligonucleotide-Mediated Modulation of Mammalian Gene Expression. *The FASEB Journal*. 9, 1288-1296.

Scott, W.G., Finch, J.T., Klug, A. (1995) The Crystal structure of an All-RNA Hammerhead Ribozyme: A Proposed Mechanism for Catalytic Cleavage. *Cell*. 81, 991-1002.

Scott, W.G., Murray, J.B., Arnold, J.R.P., Stoddard, B.L. and Klug, A. (1996) Capturing the Structure of a catalytic RNA Intermediate: The Hammerhead Ribozyme. *Science*. 274, 2065-2069.

Selby, R. (1994) The Surgical Treatment of Cerebral Glioblastoma Multiforme: An Historical Review. *The Journal of Neuro-Oncology*. 18, 175-182.

Seymour, L.W., Ulbrich, K., Styger, P.S., Brereton, M., Subr, V., Strohalm, J. and Duncan, R. (1994) Tumour Tropism and Anticancer Efficacy of Polymer-Based Doxorubicin Prodrugs in the Treatment of Subcutaneous Murine B16F10 Melanoma. *The British Journal of Cancer*. 70, 636-641.

Shah, D. and Shen , W.C. (1995) The Paradox of Transferrin Receptor-Mediated Drug Delivery-Intracellular Targeting or Transcellular Transport? *The Journal of Drug Targeting*. 3, 243-245.

Sharp, P.A. (1991) Five Easy pieces. *Science*. 254, 663 (only).

Shea, R.G., Marsters, J.C. and Bischofberger, N. (1990) Synthesis, Hybridisation Properties and Antiviral Activity of Lipid-Oligodeoxynucleotide Conjugates. *Nucelic Acids Research*. 18, 3777-3783.

Sheldon, C.C. and Symons, R.H. (1989) Mutagenesis Analysis of a Self-Cleaving RNA. *Nucleic Acids Research*. 17, 5679-5685.

Sherwood, L. (1989) The Central Nervous System. In: *Human Physiology, From Cells to Systems*. The West Publishing Company, St.Paul, Minnesota, USA.

Shimayama, T., Nishikawa, F., Nishikawa, S. and Taira, K. (1993) Nuclease Resistant Chimeric Ribozymes Containing Deoxyribonucleotides and Phosphorothioate Linkages. *Nucleic Acids Research*. 21, 2605-2611.

Shimayama, T., Nishikawa, S., Taira, K. (1995) Generality of the NUX Rule - Kinetic Analysis of the Results of Systematic Mutations in the Trinucleotide at the Cleavage Site of Hammerhead Ribozymes. *Biochemistry*. 34, 3649-3654.

Shoji, Y., Akhtar, S., Periasamy, A., Herman, B. and Juliano, R.L. (1991) Mechanism of Cellular Uptake of Modified Oligodeoxynucleotides Containing Methylphosphonate Linkages. *Nucleic Acids Research*. 19, 5543-

Shoji, Y., Shimada, J., Mizushima, Y., Iwasawa, A., Nakamura, Y., Inouye, K., Azuma, T., Sakurai, M. and Tateo, N. (1996) Cellular Uptake and Biological Effects of Antisense Oligodeoxynucleotide Analogs Targeted to Herpes Simplex Virus. *Antimicrobial Agents and Chemotherapy*. 40, 1670-1675.

Sioud, M., Natvig, J.B., Forre, O. (1992) Preformed Ribozymes Destroys Tumour Necrosis Factor mRNA in Human Cells. *The Journal of Molecular Biology*. 223, 831-835.

Sioud, M. (1996) Ribozyme Modulation of Lipopolysaccharide-Induced Tumour Necrosis Factor-α Production by Peritoneal Cells *In Vitro* and *In Vivo*. *The European Journal of Immunology*. 26, 1026-1031.

Slim, G. and Gait, M.J. (1991) Configurationally defined Phosphorothioate-Containing Oligoribonucleotides in the Study of the Mechanism of Cleavage of Hammerhead Ribozymes. *Nucleic Acids Research*. 19, 1183-1188.

Smith, A.E. (1995) Viral Vectors in Gene Therapy. *Annual Reviews in Microbiology*. 49, 807-838.

Smythe, E. and Warren, G. (1991) The Mechanism of Receptor-Mediated Endocytosis, A Review. *The European Journal of Biochemistry*. 202, 689-699.

Snyder, D.S., Wu, Y., Wang, J.L., Rossi, J.J., Swiderski, P., Kaplan, B.E. and Forman, S.J. (1993) Ribozyme Mediated Inhibition of bcr-abl Gene Expression in a Philadelphia Chromosome Positive Cell Line. *Blood*. 82, 600-605.

Sokol, D.L. and Gewirtz, A.M. (1996) Gene Therapy: Basic Concepts and Recent Advances. *Critical Reviews in Eukaryotic Gene Expression*. 6, 29-57.

Sproat, B.S. and Lamond, A.I. (1991) 2'-O-Methyloligoribonucleotides: Synthesis and Applications. In: *Oligonucleotides and Analogues*. Eckstein, F. (Ed).Oxford University Press. Oxford, UK.

Sproat, B.S. (1996) Synthetic Catalytic Oligonucleotides Based on the Hammerhead Ribozyme. *Nucleic Acids in Molecular Biology*. 10, 265-281.

Srinivasan, S.K. and Iversen, P.L. (1995) Review of *In Vivo* Pharmacokinetics and Toxicology of Phosphorothioate Oligonucleotides. *The Journal of Clinical Laboratory Analysis*. 9, 129-137.

Stein, B.S., Bensch, K.G. and Sussman, H.H. (1984) Complete Inhibition of Transferrin Recycling by Monensin in K562 Cells. *The Journal of Biological Chemistry*. 259, 14762-14772.

Stein, C.A., Mori, K., Loke, S.L., Subasinghe, C., Cohen, J.S. and Neckers, L.M. (1988) Phosphorothioate and Normal Oligodeoxyribonucleotides with 5'-linked Acridine: Characterisation and Preliminary Kinetics of Cellular Uptake. *Gene* 72, 333-341.

Stein, C.A. and Cheng, Y.C. (1993) Antisense Oligonucleotides as Therapeutic Agents-Is the Bullet Really Magical? *Science* 261, 1004-1008.

Stein, C.A., Tonkinson, J., Zhang, L.M., Yakubov, L., Gervasoni, J., Taub, R. and Rotenburg, S. (1993) Dynamics of Internalisation of Phosphodiester Oligodeoxynucleotides in HL60 cells. *Biochemistry*. 32, 4855-4861.

Sullenger, B.A. and Cech, T.R. (1993) Tethering Ribozymes to a Retroviral Packaging Signal for the Destruction of Viral RNA. *Science*. 262, 1566-1569.

Sullenger, B.A. (1995) Colocalizing Ribozymes with Substrate RNAs to Increase Their Efficacy as Gene Inhibitors. *Applied Biochemistry and Biotechnology*. 54, 57-61.

Sullivan, S.M. (1993) Liposome-Mediated delivery of Ribozymes. *Methods in Enzymology*. 5, 61-66.

Sun, J.S. and Helene, C. (1993) Oligonucleotide-Directed Triple Helix Formation. *Current Opinion in Structural Biology*. 3, 345-356.

Sun, L.Q., Warrilow, D., Wang, L., Witherington, C., Macpherson, J. and Symonds, G. (1994) Ribozyme-Mediated Suppression of Moloney Murine Leukemia Virus and human Immunodeficiency Virus Type I Replication in Permissive Cell Lines. *The Proceedings of the National Academy of Sciences of the USA*. 91, 9715-9719.

Sun, L.Q., Ely, J.A., Gerlach, W. and Symonds, G. (1997) Anti-HIV Ribozymes. *Molecular Biotechnology*. 7, 241-251.

Swanson, J. (1989) Fluorescent Labelling of Endocytic Compartments. In: *Methods in Cell Biology*. Volume 29. Wang, Y.L. and Taylor, D.L. (Eds). Academic Press Inc. San Diego, USA.

Sweeney, P.J. and Walker, J.M. (1993) Pronase Enzyme (EC3.4.24.4). In: *Methods in Molecular Biology*. Volume 16. Burrell, M.M. (Ed.) Humana Press Inc. Totowa, New Jersey, USA.

Sweetman, L. and Nyhan, W.L. (1986) Inheritable Biotin-treatable Disorders and Associated Phenomena. *Annual Reviews in Nutrition*. 6, 314-343.

Symons, R.H. (1992) Small Catalytic RNAs. *Annual Reviews in Biochemistry*. 61, 641-671.

Symons, R.H. (1994) Ribozymes. *Current Opinion in Structural Biology*. 4, 322-330.

Takagi, Y., and Taira, K. (1995) Temperature-Dependant Change in the Rate-Determining Step in a Reaction Catalyzed by a Hammerhead Ribozyme. *FEBS Letters*. 361, 273-276.

Takaura, Y. and Hashida, M. (1996) Macromolecular Carrier Systems for Drug delivery: Pharmacokinetic Considerations on Biodistribution. *Pharmaceutical Research*. 13, 820-831.

Tarrason, G., Bellido, D., Eritja, R., Vilaro, S., Piulats, J. (1995) Digoxigenin Labelled Phosphorothioate Oligonucleotides: A New Tool For The Study of Cellular Uptake. *Antisense Research and Development*. 5, 193-201.

Taylor, N.R., Kaplan, B.E., Swiderski, P., Li, H., Rossi, J.J. (1992) Chimeric DNA-RNA Hammerhead Ribozymes Have Enhanced In Vitro Catalytic Efficiency and Increased Stability *In Vivo*. *Nucleic Acids Research*. 20, 4559-4565.

Temsamani, J., Roskey, A., Chaix, C. and Agrawal, S. (1997) *In Vivo* Metabolic Profile of a Phophorothioate Oligodeoxyribonucleotide. *Antisense and Nucleic Acid Drug Development*. 7, 159-165.

Tessier, D.C., Brousseau, R. and Vernet, T. (1986) Ligation of Single-Stranded Oligodeoxyribonucleotides by T4 RNA Ligase. *Analytical Biochemistry*. 158, 171-178.

Thierry, A.R., and Takle, G.B. (1995) Liposomes as a Delivery System for Antisense and Ribozyme Compounds. In: *Delivery Strategies for Antisense oligonucleotide Therapeutics*. Akhtar, S. (Ed). CRC Press Inc, London, UK.

Thill, G., Vasseur, M., Tanner, N.K. (1993) Structural and sequence Elements Required for the Self-Cleaving Activity of the Hepatitis Delta Virus Ribozyme. *Biochemistry*. 32, 4254-4262.

Thompson, J.B., Tuschl, T. and Eckstein, F. (1993) Activity of Hammerhead Ribozymes Containing Non-Nucleotide Linkers. *Nucleic Acids Research*. 21, 5600-5603.

Thompson, J.D., Ayers, D.F., Malmstrom, T.A., McKenzie, T.L., Ganousis, L., Chowrira, B.M., Couture, L., Stinchcomb, D.T. (1995) Improved Accumulation and Activity of Ribozymes Expressed froma tRNA-based RNA polymerase III Promoter. *Nucleic Acids Research*. 23, 2259-2268.

Tidd, D.M. (1996) Ribonuclease-H Mediated Antisense Effects in Intact Human Leukaemia Cells. *Biochemical Society Transactions*. 24, 619-623.

Tonkinson, J.L. and Stein, C.A. (1994) Patterns of Intracellular Compartmentalisation, Trafficking and Acidification of 5'-Flourescein Labelled Phosphodiester and Phosphorothioate Oligodeoxynucleotides in HL60 Cells. *Nucleic Acids Research*. 22, 4268-4275.

Tonkinson, J.L., Guvakova, M., Khaled, Z., Lee, J., Yakubov, L., Marshall, W.S., Caruthers, M.H. and Stein, C.A. (1994) Cellular Pharmacology and Protein Binding of Phosphoromonothioate and Phosphorodithioate Oligodeoxynucleotides: A Comparative Study. *Antisense Research and Development*. 4, 269-278.

Trouet, A. (1974) Isolation of Modified Liver Lysosomes. In: *Methods in Enzymology*. 31, 323-329. Fleischer, S and Packer, L. (Eds.) The Academic Press, New York.

Trowbridge, I. and Omary, M. (1981) Human Cell Surface Glycoprotein Related to Cell Proliferation is the Receptor for Transferrin. *The Proceedings of the National Academy of Sciences of the USA*. 78, 3039-3043.

Tseng, B.Y. and Brown, K.D. (1994) Antisense Oligonucleotide Technology in the Development of Cancer Therapeutics. *Cancer Gene Therapy*. 1, 65-71.

Tsuchihashi, Z., Khosla, M. and Herschlag, D. (1993) Protein Enhancement of Hammerhead Ribozyme Catalysis. *Science*. 262, 99-102.

Tuschl, T. and Eckstein, F. (1993) Hammerhead Ribozymes: Importance of Stem-Loop II for Activity. *The Proceedings of the National Academy of Sciences of the USA*. 90, 6991-6994.

Tuschl, T., Thomson, J.B., and Eckstein, F. (1995) RNA Cleavage by Small Catalytic RNAs. *Current Opinion in Structural Biology*. 5, 296-302.

Uhlenbeck, O.C. (1987) A Small Catalytic Oligoribonucleotide. *Nature*. 328, 596-600.

Uhlenbeck, O.C. and Gumport, R.L. (1982) T4 RNA Ligase. In; *The Enzymes*. Volume XV. The Academic Press Inc., New York, USA.

Ullrich, A., Coussens, J.S., Hayflick, T.J., Dull, A., Tam, A.W., Lee, J., Yarden, Y., Libermann, T.A., Schlessinger, J., Downward, J., Mayes, E.L.V., Whittle, N., Waterfield, M.D. and Seeburg, P.H. (1984) Human Epidermal Growth Factor Receptor cDNA Sequence and Aberrant Expression of the Amplified Gene in A431 Epidermoid Carcinoma Cells. *Nature*. 309, 418-425.

Usman, N. and Cedergren, R. (1992) Exploiting the Chemical Synthesis of RNA. *Trends in the Biochemical Sciences*. 17, 334-339.

Usman, N. Beigelman, L. and McSwiggen, J.A. (1996) Hammerhead Ribozyme Engineering. *Current Opinion in Structural Biology*. 1, 527-533.

Usman, N. and McSwiggen, J.A. (1995) Catalytic RNA (Ribozymes) as Drugs. *Annual Reports in Medicinal Chemistry*. 30, 285-294.

Usman, N. and Stinchcomb, D.T. (1996) Design, Synthesis and Function of Therapeutic Hammerhead Ribozymes. *Nucleic Acids in Molecular Biology*. 10, 243-264.

Van Der Krol, A.R., Mol, J.N.M. and Stuitje, A.R. (1988) Modulation of Eukaryotic Gene Expression By Complementary RNA or DNA Sequences. *Biotechniques*. 6, 958-960.

Vlassov, V.V., Karamyshev, V.N., Yakubov, L.A. (1993) Penetration of Oligonucleotides into mouse Organism Through Mucosa and Skin. *FEBS* Letters. 327, 271-274.

Wagner, R.W. (1994) Gene Inhibition Using Antisense Oligodeoxynucleotides. *Nature*. 372, 333-335.

Wahl, M.C., Ramakrishnan, B., Ban, C., Chen, X., and Sundralingam, M. (1996) RNA - Synthesis, Purification and Crystallisation. *Acta Crystallographica*. 52, 668-675.

Wahlestedt, C., Pich, E.M., Koob, G.F., Yee, F. and Heilig, M. (1993) Modulation of Anxiety and Neuropeptide Y-Y1 receptors by Antisense Oligonucleotides. *Science*. 259, 528-531.

Walker, I., Irwin, W.J. and Akhtar, S. (1995) Improved Cellular delivery of Antisense Oligonucleotides Using Transferrin Receptor Antibody-Oligonucleotide Conjugates. *Pharmaceutical Research*. 12, 1548-1555.

Walstrum, S. and Uhlenbeck, O.C. (1990) The Self-Splicing RNA of Tetrahymena is Trapped in a Less Active Conformation by gel Purification. Biochemistry. 29, 10573-10576.

Werner, M. and Uhlenbeck, O.C. (1995) The Effect of Base Mismatches in the Substrate Recognition Helixes of Hammerhead Ribozymes on Binding and Catalysis. *Nucleic Acids Research*. 23, 2092-2096.

Westaway, S.K., Larson, G.P., Li, S., Zaia, J.A. and Rossi, J.J. (1995) A Chimeric tRNALys3-Ribozyme Inhibits HIV Replication Following Virion Assembly. *Nucleic Acids Symposium Series*. 33, 194-199.

Wickstrom, E. (1986) Oligodeoxynucleotide Stability in Subcellular Extracts and Culture Media. *The Journal of Biochemical and Biophysical Methods*. 13, 97-102.

Wickstrom, E. (1992) Neutral DNA Analogs and Their Stereochemistry. In: *Gene Regulation. Biology of Antisense RNA and DNA*. Erickson, R.P. and Izant, J.G. (Eds.) Raven Press Ltd, New York USA

Wickstrom, E. (1995) Nuclease-Resistant DNA Therapeutics. In: *Delivery Strategies for Antisense oligonucleotide Therapeutics*. Akhtar, S. (Ed). CRC Press Inc, London, UK.

Wickstrom, E.L., Bacon, T.A., Gonzalez, A., Freeman, D.L., Lyman, G.H. and Wickstrom, E. (1988) Human Promyelocytic Leukemia HL-60 Proliferation and c-myc Protein Expression are Inhibited by Antisense Pentadecadeoxynucleotide Targeted Against c-myc mRNA. *Proceedings of the National Academy of Sciences of the USA*. 85, 1028-1032.

Wickstrom, E., Bacon, T.A. and Wickstrom, E.L. (1992) Down-Regulation of c-MYC Antigene Expression in Symphocytes of Eμ-*c-myc* Transgenic Mice Treated with anti-*c-myc* DNA Methylphosphonates. *Cancer Research*. 52, 6741-6745.

Wilchek, M. and Bayer, E.A. (1989) Avidin-Biotin Technology Ten Years On: Has It Lived up to Its Expectations? *Trends in the Biochemical Sciences*. 14, 408-412.

Williams, D.M., Pieken, W.A., Eckstein, F. (1992) Function of Specific 2'-Hydroxyl Groups of Guanosines in a Hammerhead Ribozyme Probed by 2'-Modifications. *The Proceedings of the National Academy of Sciences of the USA*. 89, 918-921.

Wilson, A.P (1992) Cytotoxicity and Viability Tests. In: *Animal Cell Culture, A Practical Approach*. Freshney, R.I. (Ed). Oxford University Press, Oxford, UK.

Wincott, F. , DiRenzo, A., Shaffer, C., Grimm, S., Tracz, D., Workman, C., Sweedler, D., Gonzalez, C., Scaringe, S., and Usman, N. (1995) Synthesis, Deprotection, Analysis and Purification of RNA and Ribozymes. *Nucelic Acids Research*. 23, 2677-2684.

Wong, A.J., Zoltlick, P.W. and Moscatello, D.K. (1994) The Molecular Biology and Molecular Genetics of Astrocytic Neoplasms. *Seminars in Oncology*. 21, 139-148.

Woolf, T.M. (1995) To Cleave or Not To Cleave: Ribozymes and Antisense. *Antisense Research and Development*. 5, 227-232.

Wu, H.N., Lee, J.Y., Huang, H.W., Huang, Y.S., Hsueh, T.G. (1993) Mutagenesis Analysis of a Hepatitis Delta Virus Genomic Ribozyme. *Nucleic Acids Research*. 21, 4193-4199.

Wu-Pong, S., Weiss, T.L. and Hunt, C.A. (1992) Antisense c-myc Oligodeoxynucleotide Cellular Uptake. *Pharmaceutical Research.* 9, 1010-1017.

Wu-Pong, S. and Byron, P.R. (1996) Airway to Biophase Transfer of Inhaled Oligonucleotides. *Advanced Drug Delivery Reviews.* 19, 47-71.

Yakubov, L.A., Deeva, E.A., Zarytova, V.F., Ivanova, E.M., Ryte, A.S., Yurchenko, L.V. and Vlassov, V.V. (1989) Mechanism of Oligonucleotide Uptake by Cells: Involvement of Specific Receptors? *Proceedings of the National Academy of Sciences of The USA.* 86, 6454-6458.

Yamada, O., Yu, M., Yee, J.K., Kraus, G., Looney, D. and Wong-Staal, F. (1994) Intracellular Immunization of Human T-Cells with a Hairpin Ribozyme Against Human Immunodeficiency Virus Type 1. *Gene Therapy.* 1, 38-45.

Yang, J.H., Usman, N., Chartrand, P., Cedergren, R.J. (1992) Minimum Ribonucleotide Requirement for Catalysis by the RNA Hammerhead Domain. *Biochemistry.* 31, 5005-5009.

Yaswen, P., Stampfer, M. and Ghosh, K. (1992) Effects of Sequence of Phosphorothioated Oligonucleotides On Cultured Human Mammary Epithelial Cells. *Antisense Research and Development.* 3, 67-71.

Yee, F., Ericson, H., Reis, D.J., and Wahlestedt, C. (1994) Cellular Uptake of Intracerebroventricularly Administered Biotin- or Digoxigenin-labelled antisense Oligodeoxynucleotides in the Rat. *Cellular and Molecular Neurobiology.* 14, 475-486.

Young-Ah, S., Kumar, P.K.R., Kawakami, J., Nishikawa, F., Taira, K., Nishikawa, S. (1993) Systematic Substitution of Individual Bases in Two Important Single Stranded Regions of the HDV Ribozyme for Evaluation of the Role of Specific Bases. *FEBS Letters.* 326, 158-162.

Yu, M., Ojwang, J., Yamada, O., Hampel, A., Rapaport, J., Looney, D., Wong-Staal, F. (1993) A Hairpin Ribozyme Inhibits the Expression of Diverse Strains of Human Immunodeficiency Virus Type I. *The Proceedings of the National Academy of Sciences of the USA.* 90, 6340-6344.

Yu, M. Poeschla, E. and Wong-Staal, F. (1994) Progress Towards Gene Therapy for HIV Infection. *Gene Therapy.* 1, 13-26.

Yu, M., Leavitt, M.C., Maruyama, M., Yamada, O., Young, D., Ho, A.D. and Wong-Staal, F. (1995) *The Proceedings of the National Academy of Sciences of the USA.* 92, 699-703.

Zabner, J., Couture, L., Smith, A., Welsh, M. (1994) Correction of c-AMP Stimulated Fluid Secretion in Cystic Fibrosis Airway Epithelia: The Efficiency of Adenoviral Mediated Gene Transfer. *Human Gene Therapy.* 5, 585-593.

Zamecnik, P. and Stephenson, M. (1978) Inhibition of Rous Sarcoma Virus Replication and Cell Transformation by a Specific Oligodeoxynucleotide. *Proceedings of the National Academy of Sciences of The USA*. 75, 280-284.

Zamecnik, P., Aghajanlan, J., Zamecnik, M., Goodchild, J. and Witman, G. (1994) Electron Micrographic Studies of Transport of Oligodeoxynucleotides Across Eukaryotic Cell Membranes. *Proceedings of the National Academy of Sciences of The USA*. 91, 3156-3160.

Zani, M., Lavitrano, M., French, D., Lulli, V., Maione, B., Sperandio, S. and Spadafora, C. (1995) The Mechanism of Binding of Exogenous DNA to Sperm Cells: Factors Controlling DNA Uptake. *Experimental Cell Research*. 217, 57-64.

Zaug, A.J., Been, M.D. and Cech, T.R. (1986) The Tetrahymena Ribozyme Acts Like an RNA Restriction Endonuclease. *Nature*. 324, 429-433.

Zelphati, O. and Szoka, F.C. (1996) Mechanism of Oligonucleotide Release From Cationic Liposomes. *The Proceedings of the National Academy of Sciences of the USA*. 93, 11493-11498.

Zhang, S.P., Zhou, L.W., Morabito, M., Lin, R.C.S. and Weiss, B. (1996) Uptake and Distribution of Fluorescein-Labelled D_2 Dopamine Receptor Antisense Oligodeoxynucleotide in Mouse Brain. *The Journal of Molecular Neuroscience*. 7, 13-28.

Zhao, Q., Matson, S., Herrera, C.J., Fisher, E., Yu, H. and Kreig, A.M. (1993) Comparison of Cellular Binding and Uptake of Antisense Phosphodiester, Phosphorothioate, and Mixed Phosphorothioate and Methylphosphonate Oligonucleotides. *Antisense Research and Development*. 3, 53-66.

Zhao, J.J. and Pick, L. (1993) Generating Loss of Function Phenotypes of the *Fushi tarazau* Gene with a Targeted Ribozymes in Drosophila. *Nature*. 365, 448-451.

Zhou, C., Bahner, I.C., Larson, G.P., Zaia, J.A., Rossi, J.J. and Kohn, D.B. (1994) Inhibition of HIV-1 in Human T-Lymphocytes by Retrovirally Transduced anti-*tat* and *rev* Hammerhead Ribozymes. *Gene*. 149, 33-39.

Zon, G. and Stec, W. J. (1991) Phosphorothioate Oligonucleotides. In: *Oligonucleotides and Analogues*. Eckstein, F. (Ed).Oxford University Press. Oxford, UK.

Zoumadakis, M. and Tabler, M. (1995) Comparative Analysis of Cleavage Rates after Systematic Permutation of the NUX Consensus Target Motif for Hammerhead Ribozymes. *Nucleic Acids Research*. 23, 1192-1196.

Zuker, M., Jaeger, J. and Turner, D. (1991) A Comparison of Optimal and Sub-Optimal RNA Secondary Structures Predicted by free Energy Minimization with Structures Determined by Phylogenetic Comparison. *Nucleic Acids Research*. 19, 2707-2714.

APPENDIX I

Custom Cycle for the Synthesis of Oligoribonucleotides and Chimeric Oligoribonucleotide Containing Sequences.

The following custom synthesis cycle was designed for use on an automated Applied Biosystems 392 DNA / RNA Synthesiser. This cycle was used throughout this thesis for the synthesis of oligoribonucleotides (ORN) and chimeric sequences containing ORN bases. The format used is identical to that required for programming into the synthesiser memory. The cycle is designed for optimum use with 5'-O-(DMT(r))-2'-O-(Fpmp)-protected ribonucleoside phosphoramidites (Cruachem) and was developed in conjunction with The Research and Development team at Cruachem Ltd, Glasgow, UK.

Custom 0.2μM Scale RNA Synthesis Cycle:

Step #	Function #	Name	Step Time	Step Active for Bases A G C T 5	Safe Step
1	106	Begin			Yes
2	64	18 to waste	3.0		Yes
3	42	18 to column	10.0	yes yes yes yes yes	Yes
4	2	Reverse flush	8.0	yes yes yes yes yes	Yes
5	1	Block flush	4.0	yes yes yes yes yes	Yes
6	101	Phos prep	3.0		Yes
7	140	Column 1 on			Yes
8	111	Block vent	2.0	yes yes yes yes yes	Yes
9	58	Tet to waste	0.9		Yes
10	33	B+Tet to column	1.0	yes yes yes yes yes	Yes
11	34	Tet to column	0.5	yes yes yes yes yes	Yes
12	33	B+Tet to column	0.7	yes yes yes yes yes	Yes
13	43	Push to column			Yes
14	141	Column 1 off			Yes
15	142	Column 2 on			Yes
16	64	18 to waste	4.0		Yes
17	1	Block flush	3.0	yes yes yes yes yes	Yes
18	111	Block vent	2.0	yes yes yes yes yes	Yes
19	58	Tet to waste	0.9		Yes
20	33	B+Tet to column	1.0	yes yes yes yes yes	Yes
21	34	Tet to column	0.5	yes yes yes yes yes	Yes

Step #	Function #	Name	Step Time	Step Active for Bases A G C T 5	Safe Step
22	33	B+Tet to column	0.7	yes yes yes yes yes	Yes
23	43	Push to column			Yes
24	143	Column 2 off			Yes
25	103	Wait	300	yes yes yes yes yes	Yes
26	140	Column 1 on			Yes
27	111	Block vent	2.0	yes yes yes yes yes	Yes
28	58	Tet to waste	0.9		Yes
29	33	B+Tet to column	1.0	yes yes yes yes yes	Yes
30	34	Tet to column	0.5	yes yes yes yes yes	Yes
31	33	B+Tet to column	0.7	yes yes yes yes yes	Yes
32	43	Push to column			Yes
33	141	Column 1 off			Yes
34	142	Column 2 on			Yes
35	64	18 to waste	4.0		Yes
36	1	Block flush	3.0	yes yes yes yes yes	Yes
37	111	Bolck vent	2.0	yes yes yes yes yes	Yes
38	58	Tet to waste	0.9		Yes
39	33	B+Tet to column	1.0	yes yes yes yes yes	Yes
40	34	Tet to column	0.5	yes yes yes yes yes	Yes
41	33	B+Tet to column	0.7	yes yes yes yes yes	Yes
42	43	Push to column			Yes
43	143	Column 2 off			Yes
44	103	Wait	300	yes yes yes yes yes	Yes
45	102	Cap prep	3.0		Yes
46	64	18 to waste	4.0		Yes
47	2	Reverse flush	5.0	yes yes yes yes yes	Yes
48	1	Block flush	3.0	yes yes yes yes yes	Yes
49	39	Cap to column	10.0	yes yes yes yes yes	Yes
50	103	Wait	30.0	yes yes yes yes yes	Yes
51	64	18 to waste	4.0		Yes
52	2	Reverse flush	5.0	yes yes yes yes yes	Yes
53	1	Block flush	3.0	yes yes yes yes yes	Yes
54	41	15 to column	8.0	yes yes yes yes yes	Yes
55	64	18 to waste	4.0		Yes
56	1	Block flush	3.0	yes yes yes yes yes	Yes
57	2	Reverse flush	5.0	yes yes yes yes yes	Yes
58	64	18 to waste	4.0	yes yes yes yes yes	Yes
59	42	18 to column	10.0	yes yes yes yes yes	Yes
60	4	Flush to waste	4.0	yes yes yes yes yes	Yes
61	42	18 to column	10.0	yes yes yes yes yes	Yes
62	2	Reverse flush	5.0	yes yes yes yes yes	Yes
63	1	Block flush	3.0	yes yes yes yes yes	Yes
64	102	Cap prep	3.0		Yes
65	64	18 to waste	4.0		Yes
66	2	Reverse flush	5.0	yes yes yes yes yes	Yes
67	1	Block flush	3.0	yes yes yes yes yes	Yes
68	39	Cap to column	10.0	yes yes yes yes yes	Yes

Step #	Function #	Name	Step Time	Step Active for Bases A G C T 5	Safe Step
69	103	Wait	30	yes yes yes yes yes	Yes
70	42	18 to column	10.0	yes yes yes yes yes	Yes
71	2	Reverse flush	5.0	yes yes yes yes yes	Yes
72	42	18 to column	10.0	yes yes yes yes yes	Yes
73	2	Reverse flush	5.0	yes yes yes yes yes	Yes
74	1	Block flush	3.0	yes yes yes yes yes	Yes
75	105	Start detrityl			Yes
76	64	18 to waste	4.0		Yes
77	42	18 to column	10.0	yes yes yes yes yes	Yes
78	2	Reverse flush	5.0	yes yes yes yes yes	Yes
79	1	Block flush	3.0	yes yes yes yes yes	Yes
80	112	Trityl advance			Yes
81	109	Waste -port			Yes
82	120	Advance FC			Yes
83	120	Advance FC			Yes
84	120	Advance FC			Yes
85	120	Advance FC			Yes
86	113	End advance			Yes
87	40	14 to column	6.0	yes yes yes yes yes	No
88	3	Trityl flush	5.0	yes yes yes yes yes	No
89	40	14 to column	6.0	yes yes yes yes yes	No
90	103	Wait	5.0	yes yes yes yes yes	No
91	3	Trityl flush	5.0	yes yes yes yes yes	No
92	40	14 to column	6.0	yes yes yes yes yes	No
93	103	Wait	5.0	yes yes yes yes yes	No
94	3	Trityl flush	5.0	yes yes yes yes yes	No
95	40	14 to column	6.0	yes yes yes yes yes	No
96	103	Wait	5.0	yes yes yes yes yes	No
97	3	Trityl flush	5.0	yes yes yes yes yes	No
98	42	18 to column	10.0	yes yes yes yes yes	No
99	3	Trityl flush	8.0	yes yes yes yes yes	No
100	110	Waste-Bottle			Yes
101	42	18 to column	8.0	yes yes yes yes yes	Yes
102	2	Reverse flush	5.0	yes yes yes yes yes	Yes
103	1	Block flush	4.0	yes yes yes yes yes	Yes
104	107	End			

Total Time for 1 complete cycle: 962.4 seconds

Approximate synthesis times:

(10mer) 2hours 20 minutes.
(20mer) 4hours 40 minutes.
(36mer) 8hours 37 minutes.

APPENDIX II

Comparative Stability of All-RNA *c-myc* Hammerhead Ribozymes and Antisense Oligodeoxynucleotides In Biological Media.

A2.1 INTRODUCTION

Both ribozymes and antisense ODNs must remain stable in biological environments if they are to exert gene inhibitory effects within cells. Therefore knowledge regarding the stability of these molecules *in vivo* could aid in their design for therapeutic applications. Antisense ODNs delivered via certain non-invasive routes (such as the vaginal route) have been shown to degrade less rapidly *in vivo* than those delivered systemically (Vlassov *et al*, 1993). Therefore, it is possible that certain routes of administration may be favourable for the delivery of ribozymes or ODNs, since certain tissues may demonstrate low levels of innate nuclease activity.

In order to investigate the stability of antisense ODNs and all-RNA ribozymes in various tissues, the degradation of these molecules was examined in animal tissue extracts. In addition the stability of unmodified ribozymes and antisense ODN analogues was examined in human serum and an extract derived from rat liver lysosomes (tritosomes). Degradation profiles of ribozymes and ODNs in human serum would give an indication of their stability in the systemic circulation (i.e. in the extra-cellular environment). Whereas, exposure to lysosomal enzymes would provide an indication of the likely stability of these molecules in the intracellular environment, since the lysosomes are a major site of intracellular degradation for endocytosed molecules (Alberts *et al*, 1989)

A2.2. METHODS

A2.2.1. Synthesis and Radiolabelling of Nucleic Acid Sequences.

32-mer *c-myc* hammerhead ribozymes (see Figure 3.1) were synthesised as described in Section 3.2.3. For comparative stability studies, a 20-mer PS ODN (5' ACA CCC AAT TCT GAA AAT GG 3'), was synthesised as described in Section 2.3.4. This sequence was antisense to the 3 '-splice site of the HIV I *tat*-gene and was kindly donated by Dr. Ian Walker, Aston University. Ribozymes and PS ODNs were 5'-end radiolabelled using T4 polynucleotide kinase as described in Section 2.6.2. Following 5'-end radiolabelling, nucleic acid sequences were separated from 'free' radiolabel by 20% PAGE as described in Section 2.6.1 and were column purified as described in Section 2.6.2.

An internally radiolabelled 20-mer PO ODN, antisense to the HIV-RNA *tat* gene, was also synthesised, as described below: A 25-mer template PO ODN (5' TGA GTG TCC AGC TTC TTA CCA GCA T 3') and a 13-mer primer PO ODN (5' GG TAA GAA GCT GG 3'), designed to form a duplex seven nucleotides from the 5'-end of

the template, were synthesised as described in Section 2.3.3. The template and primer sequences were mixed in Tris (pH7.5), heated to 80°c and allowed to cool to room temperature overnight. The template and primer sequence mixture was incubated with 2.5 units of *Klenow* fragment (*Klenow* fragment of *E.coli* DNA Polymerase I, Sigma, UK) in a 20µl reaction mixture containing 50mM Tris pH 7.5, 10mM $MgCl_2$, 50µCi of α-[^{32}P]-dATP (Amersham), and 0.5mM dCTP, dTTP, dGTP for 1hour at 37°c. The reaction was then spiked with cold excess dATP for 15 minutes at 37°c. The duplex was denatured by heating to 80°c for 10 minutes in a loading dye solution containing 7M urea followed by snap cooling on ice. The resultant 20-mer, internally labelled oligodeoxynucleotide contained three radio-labelled adenine (**A**) residues; 5' GGT AAG AAG CTG G**A**C **A**CT C**A** 3' , (shown in bold and underlined). The internally labelled oligodeoxynucleotides were separated from shorter chain sequences by 20% PAGE and were column purified as described in Section 2.6.2.

A2.2.2. Stability Studies

Dried samples of radiolabelled ribozyme (approximately 10 nanomoles) were reconstituted in 20µL of the particular type of extract or sera under examination (see A2.2.3). The reaction mixture was then incubated at 37°C. After fixed time intervals; aliquots (1µL) of the mixture were removed, quenched with 'stop' buffer (8M urea, 50mM EDTA) and stored at -70°c until all subsequent samples had been collected. Intact radiolabelled ribozymes and ODNs were separated from degradation products by 20% denaturing PAGE (8M urea). Relative quantities of intact species and degradation products were estimated by analysis of autoradiograph band intensities (see Section 2.2.4). In some studies, the bands containing intact nucleic acids were excised from polyacrylamide gels and specific radioactivity of sequences within the gel pieces was determined by liquid scintillation counting as described in Section 2.2.5. The extent of degradation could then be estimated by comparison with the specific activity of control samples.

A2.2.3. Preparation of Biological Extracts and Sera.

All samples of rat origin used in this study were obtained from the Wistar out-breed strain of rat, all were females, weight approximately 200g, 7-8 weeks old and were not previously starved:

Rat gastric lavage fluid was obtained by injecting 8mL of 0.1% w / v saline into the stomach of the rat using a gavage needle and syringe. The saline solution was repeatedly withdrawn and re-introduced to the stomach for approximately 30 seconds until the final gastric lavage sample was collected.

Rat Vaginal Washings were obtained by injecting 3ml of saline into the vaginal cavity of using a Pasteur pipette. Again the saline solution was repeatedly withdrawn and reintroduced into the cavity until the final sample was collected.

To obtain a rat pulmonary and liver extracts; the relevant organ (lung or liver) was carefully dissected from the rat and placed in a glass test tube. The organ was homogenised (using a Silverson homogeniser) and 10mL of 0.1% w/v saline was added to the homogenate. The homogenate was vortexed briefly and centrifuged at

slow speed (1000 r.p.m.) for 1 minute. The supernatant was removed using a Pasteur pipette and was used in stability studies.

Human serum, obtained from blood samples provided by healthy volunteers was kindly supplied by Dr. M. Coleman, Aston University. Human saliva was obtained from a healthy volunteer and was used undiluted in stability studies. All biological extracts and sera were stored at -70°C prior to use.

A2.2.4. Preparation of Rat Liver Lysosome Mixture (Tritosomal Extract).

Tritosome extract was prepared according to the method of Trouet (1974) and was supplied by Dr. R. Duncan, School of Pharmacy, University of London. Lysosomes and mitochondria have approximately the same buoyant density and are therefore difficult to separate by density gradient centrifugation. Therefore in order to modify the size and density of the endosomal compartments in rat liver cells, the detergent Triton WR-1339 was administered. This detergent accumulates within the endosomes of cells and consequently reduces their equilibrium density. The 'tritosomes' (lysosomes) can then be separated from other sub-cellular organelles to produce a concentrated preparation of lysosomal enzymes. Rats were injected intra-peritoneally with Triton WR-1339 (1mL /100g body weight). Four days later the rats were killed after overnight fasting. The liver was quickly dissected and homogenised in ice cold 0.25M sucrose (5mL per gram of liver) using a Silverson homogensier. The homogenate was centrifuged at 1,650 r.p.m. for 10 minutes in a refrigerated centrifuge at 4°C. The supernatant was removed and kept, the sediment was re-homogenised in cold 0.25M sucrose before centrifugation at 1,400 r.p.m. for further 10 minutes. The supernatant was again removed and pooled with the supernatant solution already obtained. The supernatant was then made up to a volume of 10mL with 0.25M sucrose. This was centrifuged at 17,000 r.p.m. for 10 minutes. The supernatant was removed and discarded, leaving a pellet which contained the 'tritosomal' fraction.

However further purification was required to remove any other large cytoplasmic granules (e.g. mitochondria) which could be present. The pellet was re-suspended in ice cold 45% (w / v) sucrose and briefly homogenised. This solution was divided into 9mL aliquots, each in a separate 25mL centrifuge tube. 8mL of a 34.5% (w / v) sucrose solution was carefully pipetted onto the surface of the solution in each centrifuge tube. A carefully pipetted layer of 14.3% (w / v) sucrose was then added on top of this. The centrifuged tubes containing the layered solutions (density gradients) were then centrifuged for 2 hours at 17,500 r.p.m. The tritosomes (modified lysosomes) were recovered from the interface between the 34.5% and 14.3% sucrose solutions using a 25mL pipette fitted with a rubber aspirator. The tritosome extract was stored at -70°c until used.

A2.2.5. Determination of the Protein Content of Biological Extracts.

In order to estimate the approximate protein content of biological extracts, a colorimetric assay was performed using a reagent based on Coomassie blue. Initially, a calibration curve was prepared using fixed dilutions of bovine serum albumin (Sigma, UK) in double distilled water. Exactly 1mL of each fixed dilution of BSA was

added to 5mL of a 1 in 4 dilution of Biorad Protein Assay Reagent® (Biorad, UK) according to the manufacturer's protocol. The optical density of these dilutions was determined at 595nm using a scanning UV / visible spectrophotometer (Cecil Elegant Technology, UK). The mean UV absorbance of the calibration samples at 595nm was used to produce a calibration curve, which allowed UV absorbance measurements to be correlated with protein concentrations in micrograms per mL. In order to determine the approximate protein content of the biological extracts, samples were first diluted 1 in 100 with double distilled water. 1mL of the diluted samples was added to a 1 in 4 dilution of Biorad Protein Assay Reagent® and the UV absorbance was determined at 595nm. With reference to the calibration curve, UV absorbance measurements allowed the approximate protein content of each biological extract to be determined.

A3. RESULTS.

Initially the protein content of the biological extracts was estimated using the method described in A2.2.5 and results are shown in Table A2.1. Biological extracts were normalised to a protein concentration of 20μg / mL by the addition of sterile PBS, prior to use in stability studies. Although human serum and the extract of lysosomal enzymes (tritosomes) were used undiluted in stability studies.

Table A2.1 Estimated Protein Content of Biological Extracts Used in Stability Studies.

Biological Extract	Estimated Protein Content (μg / mL)
Human Saliva	20
Rat pulmonary extract	300
Rat liver extract	600
Rat gastric lavage fluid	80
Rat vaginal washings	30

Unmodified (all-RNA) ribozymes were degraded very rapidly in all of the biological extracts which were examined (see Table A2.2), even when samples were quenched with 'stop' buffer immediately after the addition of the ribozyme to the reaction media. In all studies, no intact 32-mer ribozyme was observed after incubation periods beyond 1 minute. Following incubation with the majority of the extracts; the only bands which were visible on autoradiographs were those corresponding to the migration of the 'free' [^{32}P] radiolabel. This degradation could possibly reflect the removal of the radiolabel by phosphatases which are often present in biological fluids. However, 5'-end labelled PS ODNs were not degraded at a similar rate to the all-RNA ribozyme. Therefore, a more likely explanation would be that the ribozyme was rapidly degraded to monomer nucleotides by the action of exonucleases and / or ribonucleases present in the extracts and sera (see Section 1.2.4.1). When ribozymes were incubated in human serum and the pulmonary extract, a shorter chain degradation product was observed on autoradiographs after incubation periods up to 5 minutes (see Figure A2.1). The shorter chain degradation product was then further degraded, such that only the free radiolabel band could be observed after incubation periods in excess of 5 minutes. Degradation via a (radiolabelled) short chain

degradation product could indicate that endonuclease digestion was initially responsible for the degradation of the ribozyme in human serum and pulmonary extract. Other investigators have also demonstrated extremely short half-lives for unmodified, all-RNA ribozymes in foetal bovine serum. For example Shimayama *et al* (1993) estimated that the half-life of an all-RNA ribozyme was less than 1 minute in 0.1% foetal bovine serum.

Table A2.2 Relative Stabilities of All-RNA Ribozymes, and Oligo-Deoxynucleotides in Various Biological Extracts and Sera.

Biological Extract or Serum	5'-labelled All-RNA *c-myc* Ribozyme 32-mer	5'-labelled PS ODN 20-mer	Internally (*Klenow*) labelled PO ODN 20-mer
Human serum (α)	-	++	+
Tritosomal extract (α)	-	+++	++
Human saliva	-	not determined	++
Rat Liver extract	-	+	- / +
Rat Pulmonary extract	- / +	++++	++++
Rat Gastric Lavage Fluid	-	+	+
Rat Vaginal Washings	- / +	++++	+++

Key:
(-) Instantaneous degradation; no bands corresponding to the intact nucleotide were detectable after 10 seconds incubation.
(- / +) Rapid degradation; less than 50% intact after 1 minute, complete degradation of the intact nucleotide within 5 minutes.
(+) Approximately 50% remained intact after 5 minutes, complete degradation of the intact nucleotide observed with 15-20 minutes
(++) Over 50% degradation after 15-30 minutes, complete degradation of the intact nucleotide within 60 minutes
(+++) 50% degradation of the intact nucleotide within 40-60 minutes. Complete degradation of the nucleotide takes longer than 60 minutes
(++++) Relatively little degradation observed; over 80% of the intact nucleotide was detectable after 3 hours incubation.
(α) Human serum and tritosomal extract were used un-diluted in these studies and were not normalised according to their protein content.

Overall, the extremely poor stability of the all-RNA ribozymes observed here suggests that they would be quickly degraded *in vivo* and the cellular uptake of the intact molecule would be negligible. Therefore, it is unlikely that unmodified ribozymes would demonstrate pharmacological effects in vivo following exogenous delivery. The

studies described here provide little information with regard to potentially favourable routes for the non-invasive delivery of these unmodified ribozymes (i.e. administration sites at which degradation would be less pronounced). Trace remnants of the intact ribozyme were visible on autoradiographs after 60 seconds incubation in pulmonary and vaginal extracts. However, degradation was complete within 2 to 5 minutes, hence, these could hardly be considered to be favourable routes for the delivery of all-RNA ribozymes.

Figure A2.1. Autoradiograph Demonstrating the Rapid Degradation of the 32-mer all-RNA *c-myc* Ribozyme (10 nanomoles) when Incubated with Human Serum at 37°C. [Lane **C**; All-RNA Ribozyme incubated in sterile PBS (control). Other lanes ($\frac{1}{6}$ **to 60**) demonstrate the incubation of the all-RNA ribozyme with undiluted human serum for increasing reaction times (in minutes)]

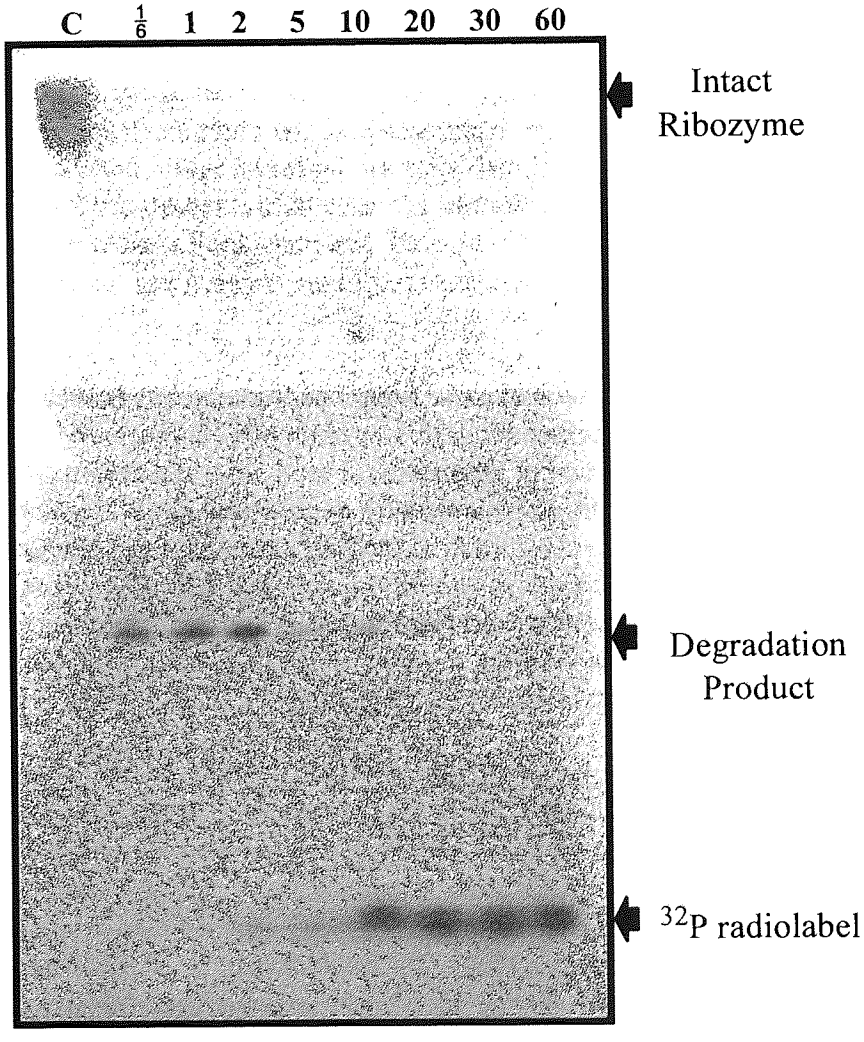

By comparison, the stability of both the unmodified PO and the PS oligo-deoxynucleotides varied widely in the different biological extracts which were examined: The half-lives observed in serum for both the PO (approximately 5 minutes) and PS ODNs (approximately 20 minutes) were slightly shorter than those previously observed with ODN constructs of similar length by other investigators (Wickstrom, 1986, Akhtar *et al*, 1991). This could reflect variations in nuclease activity between human serum samples obtained from different sources. Nevertheless,

the biological half-lives of both the modified and unmodified ODNs would be expected to be considerably greater than that of the all-RNA ribozyme in the extra-cellular environment *in vivo*.

Unmodified PO ODNs demonstrated a half life of approximately 30 minutes when incubated with the rat tritosomal extract. By comparison the observed half life for PS ODNs was approximately 50 minutes in the same extract. Thus indicating the improved resistance of the fully phosphorothioated construct towards the nuclease population present within the tritosomal extract. The exact enzyme composition of this extract has not yet been fully characterised. However levels of proteolytic enzymes contained within this extract are considered to be very similar to those present within lysosomes *in vivo* (Seymour *et al*, 1994). Hence there is some justification to suppose that the overall composition of the tritosomal extract is similar to that of lysosomes within cells.

Interestingly the degradation of both the PO and PS ODNs was much more rapid in the tritosomal extract than that observed when similar ODN sequences were incubated with a cytosolic extract (Akhtar et al, 1991). This indicates that degradation of ODNs is much more rapid within lysosomal compartments than in the cytoplasm of the cell. In addition, other investigators have demonstrated that intra-cellular digestion of antisense ODNs occurs within vesicular compartments leading to the exocytosis of degradation products (Tonkinson and Stein , 1994). Hence it would appear likely that lysosomal vesicles are a major site of intra-cellular degradation for antisense ODN molecules.

Both the modified and unmodified ODNs were rapidly degraded when incubated in diluted liver homogenate. The rapid rate of degradation observed in the liver extract was not unexpected since the liver is considered to be a major site for the metabolism (degradation) of ODNs following *in vivo* administration (Goodarzi *et al*, 1992). The rapid degradation of ODNs and ribozymes in the liver could represent a major problem for systemic, therapeutic applications of these molecules. Since pharmacokinetic studies have revealed that both ODNs and ribozymes become preferentially distributed to the liver shortly after intravenous administration (Goodarzi *et al*, 1992, Saijo *et al*, 1994, Desjardins *et al*, 1996).

The PO and PS ODNs were both completely degraded, after approximately 15-20 minutes, when incubated with gastric lavage fluid. The pH of the (diluted) gastric lavage sample was determined to be in the range pH 6 to 7 (using universal indicator). Therefore the (mild) acidity of this extract was unlikely to have influenced the rate of degradation observed because ODNs were undegraded in phosphate buffered saline at pH 7. The extent of degradation observed would appear to indicate that efficient oral delivery of ODNs would only be possible if a suitable delivery vehicle, which could protect from degradation in the gastric fluid, could be designed.

Compared with the extent of degradation observed in the other biological extracts, the PO and PS ODNs remained relatively stable when incubated with the rat vaginal washings. One study has reported that benzylamide / ODN conjugates, delivered via the vaginal route, demonstrate increased half-lives *in vivo* (Vlassov *et al*, 1993). However the exact reason for this improvement in stability was unclear from this study since radiolabelled ODNs, delivered via different routes, were all recovered

from the blood and pancreas of mice. Therefore it would appear that the recovered conjugate samples were all exposed to similar levels of serum nucleases (in the blood) regardless of their route of administration. Nevertheless this study suggests that the vaginal route of delivery may reduce the exposure of ODN molecules to high concentrations of nucleases at the site of administration. Hence, stability may be enhanced.

Little degradation was observed when either PO or PS ODNs were incubated with the pulmonary extract for a period of 3 hours (see Figure A2.2). Again this probably reflects the low concentrations of nuclease enzymes present within the pulmonary fluid. This was not entirely unexpected since DNAase enzymes have actually been administered to the lungs of cystic fibrosis patients in some cases in order to digest DNA from lysed cells which can accumulate (personal communication Dr. David Lacey, formerly of Aston University). Therefore, the innate nuclease activity within the lungs could be expected to be relatively low.

Figure A2.2. Autoradiograph Demonstrating the Stability of an Internally Radiolabelled 20-mer Phosphodiester Oligodeoxynucleotide (500 picomoles) Incubated in Rat Pulmonary Extract at 37°C.
[Lane **C**; Unreacted (control) incubated in sterile PBS. Other lanes (**5 to 180**) demonstrate the incubation of the PO ODN in pulmonary extract for increasing reaction times (in minutes)]

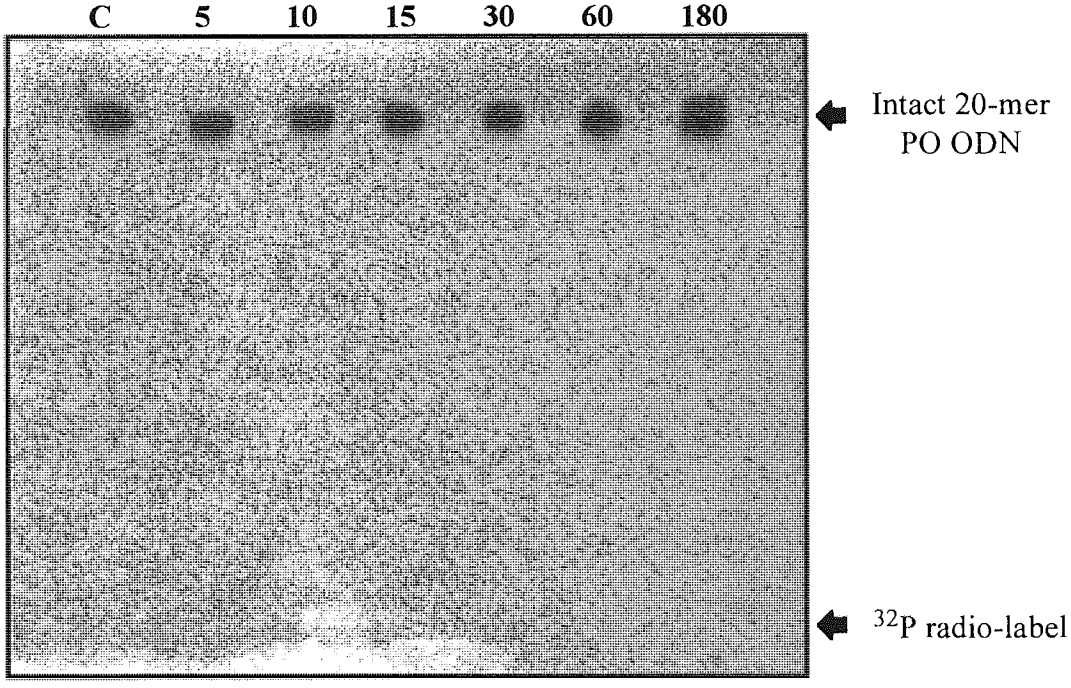

A4. CONCLUDING REMARKS.

These studies suggest that in terms of stability; the pulmonary and vaginal routes of delivery may be advantageous for the administration of ONs. Delivery via these routes could reduce the exposure of ODNs to high concentrations of nucleases which are present within the systemic circulation (in serum). For local applications within the lungs or (female) reproductive organs this could increase the bioavailability of ODNs by reducing their digestion. Indeed, the possibility of using ODN conjugates to treat pulmonary diseases has been reviewed recently (Wu-Pong and Byron, 1996).

APPENDIX III

Publications

A3.1. Stability of Antisense Oligonucleotides During Incubation with a Mixture of Isolated Lysosomal Enzymes.
Hudson, A.J., Lee, W., Porter, J., Akhtar, J., Duncan, R. and Akhtar, S.
The International Journal of Pharmaceutics. Volume 133, 257-263 (1996)

A3.2. Biodegradable Polymer Matrices for the Sustained Exogenous Delivery of a Biologically Active *c-myc* Hammerhead Ribozyme.
Hudson, A.J., Lewis, K.J., Rao, M.V. and Akhtar, S.
The International Journal of Pharmaceutics. Volume 136, 23-29 (1996)

A3.3. Cellular Uptake Properties of a 2'-Amino / 2'-O-Methyl Modified Chimeric Hammerhead Ribozyme Targeted to the Epidermal Growth Factor Receptor mRNA.
Fell, P.L., Hudson, A.J., Reynolds, M.A., Usman, N. and Akhtar, S.
Antisense and Nucleic Acid Drug Development. Volume 7, 319-326 (1997)